Transition Metal-Free Catalytic Systems for the Utilization of CO_2 to Achieve Valuable Chemicals

Dissertation

for the award of the degree

“Doctor rerum naturalium”

of the Georg August University Göttingen

GEORG-AUGUST-UNIVERSITÄT GÖTTINGEN

within the doctoral program of chemistry of the

Georg August University School of Science (GAUSS)

submitted by

Daniel Riemer

from Kyritz

Göttingen, 2020

Thesis Committee

Dr. Shoubhik Das, Institute of Organic and Biomolecular Chemistry, Georg August University Göttingen/Department of Chemistry, University of Antwerp (Belgium)

Prof. Dr. Manuel Alcarazo, Institute of Organic and Biomolecular Chemistry, Georg August University Göttingen

Prof. Dr. Lutz Ackermann, Institute of Organic and Biomolecular Chemistry, Georg August University Göttingen

Examination Board

Reviewer: Dr. Shoubhik Das, Institute of Organic and Biomolecular Chemistry, Georg August University Göttingen/Department of Chemistry, University of Antwerp (Belgium)

Second Reviewer: Prof. Dr. Manuel Alcarazo, Institute of Organic and Biomolecular Chemistry, Georg August University Göttingen

Further Members of the Examination Board

Prof. Dr. Konrad Koszinowski, Institute of Organic and Biomolecular Chemistry, Georg August University Göttingen

Dr. Michael John, Institute of Inorganic Chemistry, Georg August University Göttingen

Dr. Holm Frauendorf, Institute of Organic and Biomolecular Chemistry, Georg August University Göttingen

Date of the Oral Examination: 28.09.2020

Acknowledgement

First of all, I would like to express my sincerest gratitude to my doctoral thesis supervisor Prof. Dr. Shoubhik Das for giving me the opportunity to write this thesis in his working group and for his kind support during this thesis. As his first PhD student, I had the advantage of a very close supervision regarding scientific discussions and input.

Furthermore, I would like to thank my second and third supervisors within the GAUSS PhD program, Prof. Dr. Manuel Alcarazo and Prof. Dr. Lutz Ackermann, who also guided me through my thesis with their valuable scientific feedback and their critical questioning of my work, and to the members of the Examination Board Prof. Dr. Konrad Koszinowski, Dr. Michael John and Dr. Holm Frauendorf.

Great support was given to me by our collaborators for the EPR measurements and DFT calculations, namely Dr. Igor Tkach from the Max Planck Institute for Biophysical Chemistry Göttingen and Dr. Oldamur Hollóczki from the Mulliken Center for Theoretical Chemistry at the Rheinische Friedrich Wilhelm University Bonn and Dr. Samir Kumar Sakar and Dr. Markus Finger from the Institute of Inorganic Chemistry at the Georg August University Göttingen

Additionally, I am thankful to the analytical departments (namely mass spectrometry and NMR spectroscopy departments) of the faculty of chemistry for their fast and precise analyses and their patience in complicated cases. Especially the offered possibility to operate several analytical machines by myself (GC, GC-MS and NMR) sped up the output of my research projects. Moreover, I would like to thank the working group of Prof. Inke Siewert for measuring the *in situ* gas-phase GC spectra.

Many thanks go to all my labmates and group members during the past years, who made working here much more fun. Also our close collaboration in the lab during all our projects was very helpful to overcome all the difficulties. Thanks also for proofreading my texts and the feedback you gave me!

Moreover, I would like to thank Dr. Andrea Dietrich, Ralf Gerke and the team of numerous staff members of the glass blower, mechanical and electronic workshops, technical assistants and facility technicians for their very different and helpful support.

Contents

List of Abbreviations

aq	aqueous
Ar	aryl
atm	atmospheric pressure (101325 Pa)
BHT	3,5-di-*tert*-butyl-4-hydroxytoluene
bipy	bipyridine (derivative)
Bn	benzyl
BnBr	benzylbromide
Boc	*tert*-butyloxycarbonyl (protecting group)
calc.	calculated
Cbz	carboxybenzyl (protecting group)
CCS	carbon capture and storage
CCU	carbon capture and utilization
cf.	compare (*conferatur*)
Cy	cyclohexyl
δ	chemical shift
d	doublet
DABCO	1,4-diazabicyclo[2.2.2]octane
DBAD	di-*tert*-butyl azodicarboxylate
DBN	1,5-diazabicyclo[4.3.0]non-5-ene
DBU	1,8-diazabicyclo[5.4.0]undec-7-ene
DCM	dichloromethane
DDQ	2,3-dichloro-5,6-dicyano-1,4-benzoquinone
DFT	density functional theory
DIPEA	di-*iso*propyl-ethylamine (Hünig's base)
DMA	*N*,*N*-dimethylacetamide
DMAP	4-(dimethylamino)-pyridine
DMF	*N*,*N*-dimethylformamide
DMSO	dimethylsulfoxide
e.g.	for example (*exempli gratia*)
EA	ethyl acetate
ed.	editor, edition
EPR	electron paramagnetic resonance

eq	equivalents
ESI	electrospray ionization
et al.	and others (*et alii*)
Et	ethyl
EtI	ethyl iodide
Et_3N	triethylamine
EtOH	ethanol
FG	functional group
Fmoc	9-fluorenylmethoxycarbonyl (protecting group)
g	gram
gC_3N_4	graphitic carbon nitride
GC	gas chromatography
GC-MS	gas chromatography-coupled mass spectrometry
h	hour
hf	hyperfine
HMF	5-hydroxymethylfurfural
HOMO	highest occupied molecular orbital
HRMS	high resolution mass spectrometry
Hz	Hertz
i	*iso*
i.e.	that is (*id est*)
*i*PrOH	*iso*-propanol
ketoABNO	9-azabicyclo[3,3,1]nonan-3-one-9-oxyl
KO*t*Bu	potassium *tert*-butoxide
LC-ESI-HRMS	liquid chromatography-coupled electrospray ionization high resolution mass spectrometry
LED	light-emitting diode
LUMO	lowest unoccupied molecular orbital
m	*meta*
m	multiplet
M	molar [mol/L]
$[M^+]$	molecular ion peak
MB	methylene blue
Me	methyl

MeI	methyl iodide
MeOH	methanol
mg	milligram
MHz	megahertz
min	minute
mL	milliliter
mmol	millimole
MS	mass spectrometry
m/z	mass to charge ratio
n.r.	no reaction
Naph	2-naphthyl
NBS	*N*-bromosuccinimide
NHC	*N*-heterocyclic carbene
NMO	*N*-methylmorpholine *N*-oxide
NMR	nuclear magnetic resonance
o	*ortho*
p	*para*
p-TsOH	*para*-toluenesulfonic acid
PC	photocatalyst
Ph	phenyl
phen	1,10-phenanthroline
PMP	1,2,2,6,6-pentamethylpiperidine
ppm	parts per million
q	quartet
rt	room temperature
SET	single electron transfer
t	*tert*
t	triplet
T	temperature
TBD	1,5,7-triazabicyclo[4.4.0]dec-5-ene
*t*BuOOH	*tert*-butylhydroperoxide
TEMPO	2,2,6,6-tetramethylpiperidine-*N*-oxide
TEOA	triethanolamine
TFA	trifluoroacetic acid

THF	tetrahydrofurane
TLC	thin layer chromatography
UV	ultraviolet
vs SCE	*versus* saturated calomel electrode
w%	weight percent

1 Introduction

1.1 Green Chemistry

Green chemistry is an enormous research field. Among its subtopics, implementing the known greenhouse gas CO_2 in chemical research and industry is only one of many targets. During the last century, many developments have been achieved, which changed industrial processes toward greener production. The following section describes the basic principles of green chemistry. First, the major target is the solvent optimization applying for large-scale industrial processes. Ideally, no solvent should be necessary (so-called *neat* reaction conditions), but in most cases reaction kinetics are facilitated due to solvation effects and an increase of the molecule's mobility. Therefore, if the presence of a solvent is indispensable, it should be non-volatile for not polluting the environment *e.g.* as greenhouse gas, neither harmful or toxic nor corrosive. For instance, the use of the previously widely employed solvents benzene and CCl_4 is decreasing and simple water, alcohols and ketones are favored nowadays (and can ideally be obtained from biomass).[1]

Moreover, it is desirable that reactants are solubilized while products precipitate for an easy separation, thus enabling easy continuous reaction setups with the reactor design being one more important concept of green chemistry.[2] The solvation also favors the shift of the reaction equilibrium according to Le Chatelier's principle. Another target of green chemistry is the use of catalysts reducing the activation energy for transition states during a reaction, thus lowering the energy demand. Ideally, this catalyst should be cheap, non-toxic and stable. Especially non-toxicity is an important property when it comes to the production of fine chemicals and pharmaceuticals, which are usually not allowed to contain even traces of the usually utilized transition metals. Heterogeneous catalysts have the benefit of being easily separable from the reaction mixture. Yet, homogeneous catalysts are often much more selective and versatile. Reaction conditions should be generally mild, such as ambient pressure and room temperature in order to avoid additional heating or cooling. Nevertheless, industrial processes are preferred to be examined at slightly elevated temperature for an easier temperature control during exothermic reactions.[3]

But not only the already mentioned solvent molecules can act as greenhouse gases. The most prominent greenhouse gas is carbon dioxide, which is called to account for

the anthropogenic climate change. Albeit on the one hand CO_2 is non-toxic and ubiquitious in nature as part of the global carbon cycle and important for the growth of plants through photosynthesis at first glance, its major disadvantage is the absorption of light within the infrared spectrum emitted by the earth's surface on the other hand. Thus, it is responsible for retaining a part of the energy input from the sun on the earth leading to an average increase of the global temperature.[4]

In 2010, the CO_2 level in the atmosphere already reached 385 ppm and rose to 413 ppm in 2020, which is about 40% higher than compared to the pre-industrial age mainly caused by power generation, transportation, industry and agriculture. Moreover, the heating effect of CO_2 causes other known greenhouse gases to evolve. For instance, water evaporates from the oceans and methane (dissolved in greater waters) is released or ascends from permafrost or frozen deep-sea reservoirs in which it is stored as methane hydrates. Hence, it is evident that several different measures have to be considered by the society (by using renewable energy resources to an increasing extend), *via* application of green chemistry principles in the industry, but also through storage of the already emitted CO_2.[5]

This latter option of storing CO_2 is abbreviated as CCS for *carbon capture and storage* utilizing techniques for the sequestration of CO_2 from flue gas and others. However, similar problems compared to nuclear waste occur like finding suitable and safe repositories and the financial costs of such methods are quite prohibitive.[6] To circumvent treating CO_2 as an undesired waste product, the development of carbon capture and utilization (CCU) has been promoted. This technique is based on only temporary storage of CO_2 for a further utilization usually as C1 synthon. This approach offers the combination of reducing the emission of that greenhouse gas and converting CO_2 to valuable chemicals from a renewable and cheap resource. To date, only around 0.12 gigatons are annually utilized in contrast to the total anthropogenic CO_2 emissions of about 24 gigatons.[5b,7]

1.2 CO_2 Fixation Reactions

This CCU technology makes CO_2 an easily available and sustainable C1 synthon rather than a waste product and allows industrial processes to recycle it on larger scale.[7a,8] However, its high thermodynamic stability and high kinetic stability hinder wider applications. This ows to the fact that the carbon atom of CO_2 is in the highest possible oxidation state and thus only prone to reduction reactions. This also results in an exclusion of reactions with a transient oxidation of the carbon center like in oxidative additions to metal centers. Although CO_2 possesses two very polar bonds with an electronegativity difference of 0.9 between the electrophilic carbon and the nucleophilic oxygen, the molecule as a whole does not exhibit any dipole moment because of its linear structure. Hence, inducing reactivity might be accomplished by reducing its symmetry *via* addition to a catalyst or activator. Albeit high pressures are a major safety concern in industrial processes, using supercritical CO_2 for lowering kinetic barriers or applying high temperatures could help to overcome thermodynamic barriers.[7a–c,7e–h,9]

However, especially the approach of applying high temperature and pressure led to some early industrial processes utilizing CO_2, *e.g.* the Kolbe-Schmitt reaction, which was invented in 1874. During this reaction a phenolate is carboxylated under high pressure and temperature in *ortho* position and subsequently acidified to yield salicylic acid, which can undergo further acetylation toward aspirin.[10] Moreover, the synthesis of urea, an important fertilizer and intermediate in chemical industry from CO_2 and NH_3 at around 200 bar and 200 °C, was patented 100 years ago.[11]

Another large-scale CO_2 fixation process is the synthesis of carbonate polymers, in which CO_2 in the form of a carbonate monomer replaces the toxic and carcinogenic formaldehyde, which polycarbonates are usually made of. CO_2 reacts with an epoxide like oxirane (ethyleneoxide) to a cyclic carbonate, which is prone to ring-opening with methanol and further reaction with phenol to diphenylcarbonate. Excess phenol can be recovered during the later process. The so-produced diphenylcarbonate polymerizes with bisphenol A to polycarbonates providing about 15% of the worldwide produced carbonate-based polymers. Although a lead catalyst is used, this process can be considered a green chemistry example, since the catalyst is sufficiently separated by distillation, excess reactants are recycled and because of its inherent CO_2 fixation.[5a,11b,12]

Besides large industrial processes as exemplified above, a lot of research was also undertaken for CO_2 fixation on smaller scale with a plethora of reactive substrates activating CO_2. Examples are the already mentioned epoxides, but also organometallic reagents, alcohols, amines, alkynes and alkenes enable the formation of new C–O, C–N and C–C bonds, respectively.[13] Those reactions yielded several different valuable chemicals such as urea, formic acid, methanol, cyclic carbonates, lactones, carbamates and salicylic acid. Several of these reactions are conducted on industrial scale as well.[14] Moreover, synthesizing carboxylic acids using CO_2 as C1 synthon *via* C–H bond functionalizations or reactions with C–X bonds has also gained high interest within organic chemistry.[15]

During the last two decades, a plethora of transition metal catalysts along with transition metal-free homogeneous reactions was developed for CO_2 fixation reactions leading to sustainable syntheses of pharmaceutically active molecules and fine chemicals (**Scheme 1**).[7c–f,7h,13b–d,13g,15e–f,16]

For example, in 2004, García *et al.* developed a method for the cycloaddition of CO_2 to epoxides with an ionic liquid. Unfortunately, high amounts of base additive (4-(dimethylamino)-pyridine, DMAP) and a heavy metal complex as catalyst at high temperatures and CO_2 pressures were required while suffering from low conversions and by-product formation of phenylglycol.[16i] Three years later, Li and coworkers described the oxidative addition of CO_2 to terminal alkenes with alkyl and aromatic moieties. *N*-bromosuccinimide (NBS) was used as a catalytic bromide source facilitating the peroxide formation with overstoichiometric amounts of H_2O_2 *in situ*. Yet, NBS was used not in catalytic but stoichiometric amounts along with a basic additive (1,8-diazabicyclo[5.4.0]undec-7-ene, DBU) in even greater amounts.[3d]

In 2013, the research group of Leitner published a study about the reductive carboxylation of alicyclic and alkyl olefins (both terminal and internal ones) for the synthesis of alkyl carboxylic acids and directly reduced starting materials resulting in alkane by-products. This reaction was facilitated by high temperatures and gas pressures for both CO_2 and H_2, a rhenium catalyst, an acidic promotor and methyl iodide (MeI) as additive.[7f] Two years later Martin *et al.* disclosed their work about the hydrocarboxylation of alkynes yielding alkenyl carboxylic acids as *cis*-isomers exclusively. A nickel catalyst with a bipyridine ligand (bipy) was employed along with elemental manganese as reductant and *iso*-propanol (*i*PrOH) as hydrogen donor. Albeit this procedure lacks atom economy, it can be considered a green approach using almost only cheap catalysts

and additive materials with low toxicity (apart from the solvent *N*,*N*-dimethylformamide, DMF).[16f]

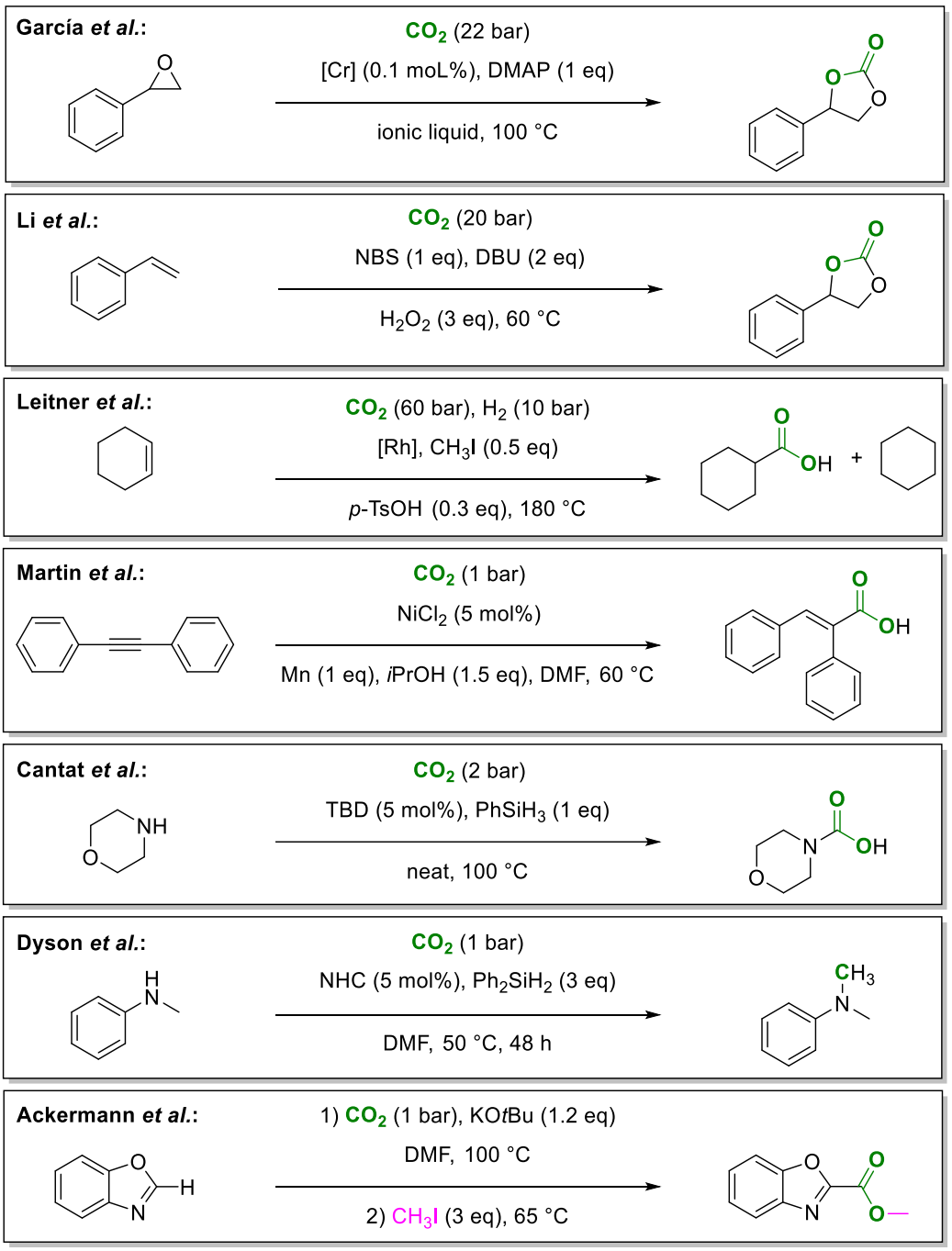

Scheme 1: Overview of different recent CO_2 fixation reactions.

The research group of Cantat showed the formylation of secondary amines to formamides with phenylsilane as hydrogen source and TBD (1,5,7-triazabicyclo[4.4.0]dec-5-ene) as organocatalyst. After first attempts with THF (tetrahydrofurane) as solvent they found that neat reaction conditions and increasing the temperature to 100 °C yielded higher formamide amounts.[13b] Later on, Dyson *et al.* took the same reaction yet broadening the scope of substrates and exchanging TBD by an NHC catalyst (*N*-

heterocyclic carbene). Here, the reaction temperature and CO_2 pressure were lower, but this was achieved by longer reaction times and the necessity of solvation by DMF.[13g] As a last example, Ackermann and Fenner presented the carboxylation of C–H bonds in heteroaromatics but without the use of a transition metal catalyst. CO_2 at atmospheric pressure in the presence of overstoichiometric amounts of the strong base KO*t*Bu (potassium *tert*-butoxide) provided the intermediate carboxylate at high temperature after overnight reaction in DMF. This intermediate was methylated with relatively high amounts of MeI yielding the heterocyclic carboxylic acid ester product.[16h]

1.3 CO_2-Catalyzed Reactions

Except for the fixation of CO_2 onto organic molecules as described above, its utilization also covers the use of CO_2 as a catalyst. Depending on the terminology used and its actual role within the mechanism, these reactions are also described as CO_2-mediated, CO_2-promoted or CO_2-assisted. In a narrower sense, CO_2 is considered a promoter or mediator when it is present besides the actual catalyst yet positively influencing the reaction *e.g.* by means of kinetics and selectivity. However, it can still fulfill the requirements as a catalyst through lowering the activation energy of the reaction while not being consumed itself. This was observed *e.g.* by Aresta *et al.* when ring-opening of THF was more efficient in the presence of a mixture of CO_2 and O_2 compared to O_2 alone.[17] Nevertheless, due to a lack of mechanistic insights those mentioned terms are usually used as synonyms yet.[18]

A patented application utilizing CO_2 as a catalyst was filed by the Shell Oil Company in 1968. Although acrolein is usually quite reactive, this method describes its selective reaction even under elevated pressure and temperature (up to 15 bar and 100 °C) with alcohols toward 3-alkoxypropanal derivatives. Consequently, when water is used instead of an alcohol, 3-hydroxypropanal is obtained. Instead of CO_2 other organic compounds could also catalyze this reaction. However, the inherent properties of CO_2 make it a good and cheap catalyst, which is easily separable from the reaction mixture in form of a gas while not further contaminating the product stream. Nevertheless, mechanistic considerations are not included.[19]

Besides this single early application, CO_2-catalyzed reactions are thriving fast recently because of their strong potential to replace toxic chemicals by a sustainable and renewable resource. In fact, by using the concept of CO_2 catalysis, the rearrangement of propargyl alcohols leading to enones or ketols, the reduction of sulfoxides to sulfides, the direct C–H allylation of ketones in *α*-position, the C–H arylation of amines and the dehydrogenation of glucose to 5-hydroxymethylfurfural (HMF) have been described already, among others.[20] Several dozens of those CO_2-catalyzed reaction methodologies have been described during the last 15 years, of which some even show interesting mechanistic implications. A publication by Yamada *et al.* describes the CO_2-catalyzed rearrangement of propargyl alcohols to enones in formamide as solvent with the byproducts being cyclic carbonates derived from the *reaction* of CO_2 with the substrate (**Scheme 2**). A base deprotonates the alcohol, which is attacking the electrophilic carbon center of CO_2 and a silver salt facilitates the activation of the triple bond by coordination. The following attack of the carboxylate moiety decides whether a cyclic carbonate is generated (*α*-position) or the rearrangement happens *via* a nucleophilic attack at the *β*-position. The rearrangement triggers CO_2 to be released from the allene intermediate and the formation of the enone product. Albeit the use of CO_2 as catalyst is convincing by means of green chemistry, this reaction relies on a harmful silver salt and produces a byproduct in higher amounts.[20a] Different products (namely *α*-hydroxy ketones) were obtained by Qi and coworkers from similar substrates, although a similar reaction system was used: The reaction system differed in a few details, namely the amount of DBU used, the counterion of the Ag^+ source, the CO_2 pressure and a water-acetonitrile mixture as solvent. More importantly, differing reaction temperatures triggered this event. These slight changes of the reaction initially led to the desired formation of cyclic carbonate intermediate, which was then ring-opened upon heating to form the actually desired *α*-hydroxy ketone. However, cyclic carbonates were also observed as byproducts.

The List group disclosed their work about the direct *α*-allylation of ketones in 2016. Albeit the mechanism was not clarified, they stated that a pre-equilibrium of an allylic alcohol with CO_2 yielded an intermediate carbonic acid hemiester as also independently proposed by Tunge *et al.* two years earlier.[21] This CO_2-activated intermediate transforms the hydroxyl group of the alcohol into a better leaving group thus facilitating its reaction with a cyclohexanone derivative after oxidative addition to a palla-

dium catalyst with phosphine ligands by water elimination. Addition of an (*S*)-configurated phosphoric acid derivative provided the products enantioselectively.[20e] Young and coworkers recently developed the palladium-catalyzed C–H arylation of amines exploiting the fact that CO_2 can form ammonium salts with 2 equivalents (eq) of amines. The authors hypothesized that this carbamate anion might serve as directing group although they admit that further studies would be necessary. Furthermore, the undertaken screening of different bases and especially the final choice of the rather seldomly used silver trifluoroacetate as basic additive, especially in overstoichiometric amounts, in combination with acetic acid as solvent were not further discussed.

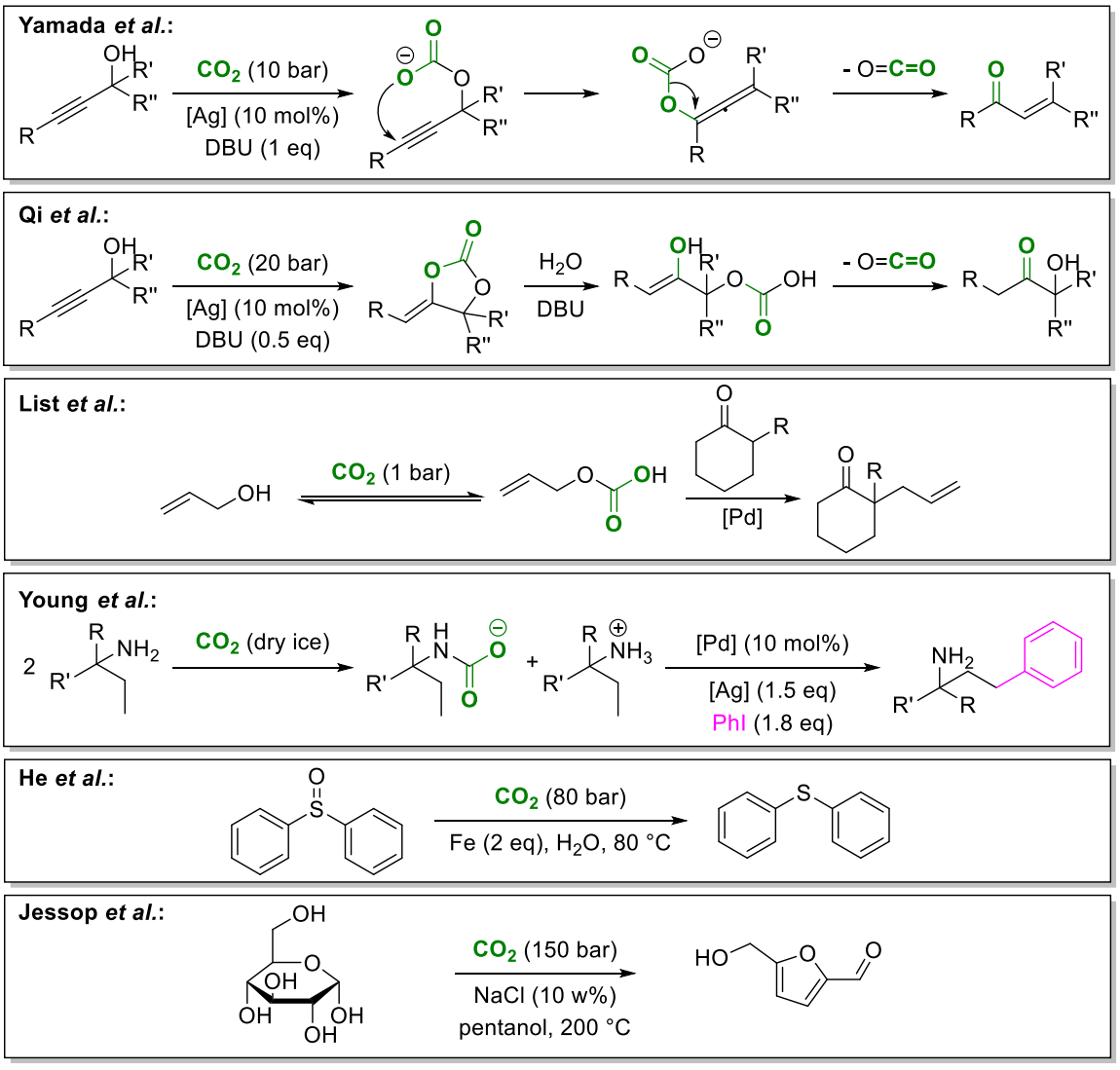

Scheme 2: Overview over recent CO_2-catalyzed reactions.

Recently, two differnet working groups proposed different yet rather simple procedures: First, He *et al.* published an interesting work about the green reduction of both aromatic and aliphatic sulfoxides to sulfides. Albeit elemental metals such as Fe were

used as reductants, water was the terminal hydrogen source since the reaction exploited the equilibrium of CO_2 and water forming carbonic acid thus facilitating the deprotonation of water. These protons are then expected to be reduced at the metal surface subsequently deoxygenating the sulfoxide substrates. The only drawback, apart from the overstoichiometric metal reductant, was the use of an autoclave for high pressure application, which was necessary in order to shift the already mentioned pre-equilibrium. However, mechanistic investigations were not undertaken.[20b] Second, Jessop *et al.* published their work about the above-mentioned dehydrogenation of potentially biomass-derived glucose or fructose with simple CO_2 as catalyst and simple NaCl as additive yielding HMF, which can also be derived from other types of biomass. Thus, it is a transformation of an alicyclic compound to a heteroaromatic one, which can be used as synthon much easier than the starting material. The resulting aqeous phase containing the salt additive could even be recycled without a loss of reactivity. Notably, in the same year Jessop's group also reported the further aldol condensation of HMF and acetone *via* CO_2 catalysis, leading to linear alkane chains over several steps. However, the sustainability of this reaction is tarnished by its high temperature and pressure and the use of pentanol as a non-natural alcoholic solvent.[20d,22] In summary, the mechanisms of those newly explored CO_2-catalyzed reactions are yet relatively ambiguous and worth further investigations.

1.4 Photochemistry

Most of the energy used on earth has its origin in sunlight. This energy is utilized on the one hand in nature, exemplified by photosynthesis, and on the other hand by the technical use of renewable energy sources, namely solar heat and photovoltaics. Chemistry and chemical processes usually rely on secondary energy sources and energy conversion techniques like generated electricity for heating. Because every step of such processes is accompanied by a loss of energy, the direct utilization of incident sunlight would be highly beneficial in sustainable chemistry and taking action against the climate change. Because of the high impact of this research direction, Ciamician published his visions of the replacement of coal by energy from sunlight more than 100 years ago.[23] However, only humble progress within the field of photochemistry was published during the following decades. An example is the Paternò-Büchi reaction describing the [2+2] cycloaddition of carbonyl compounds and alkenes under irradiation

of ultraviolet light (UV), although it is not widely used anymore.[24] Nevertheless, photochemistry gained new attention during the oil crisis of the 1970s accompanied by a more sustainable mindset and is steadily increasing due to the climate change and the expected depletion of fossil fuels in the near future.[25]

The first pioneering photocatalysts exhibited a heterogeneous semiconducting nature such as simple and harmless TiO_2. Since then, a plethora of applications was found *e.g.* for waste water treatment and functionalization of C–H bonds within aromatics.[26] More recently, graphitic carbon nitride (gC_3N_4) was examined as photocatalyst, which is a polyaromatic polymer material based on melamine or urea.[27] The drawback of such semiconductor materials is the high energy irradiation needed to overcome the valence-conduction band gap for electrons. Besides, heterogeneous catalysts are indeed easier to separate from the reaction mixture but usually also less selective and productive than homogeneous ones.

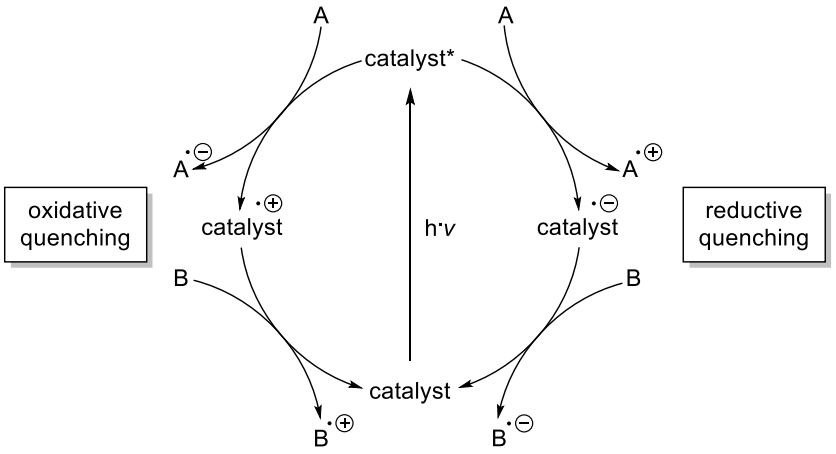

Scheme 3: General reaction scheme for photocatalytic reactions.

Hence, many transition metal-based photocatalysts are currently examined and even explored as homogeneous photocatalysts. Mechanistic investigations about their absorption spectra and redox potentials allow further tuning by modification of the metal, its oxidation state and the used ligands in order to adapt for specific reactions. The most widely used catalyst is a relatively simple ruthenium complex with bipyridine ligands, $Ru(bipy)_3Cl_2$, which is reported for cyclization, decarboxylation and activation of C–H bonds as well as oxidation and reduction reactions.[28] However, these homogeneous transition metal catalysts exhibit drawbacks such as the higher price of the metals and tedious syntheses of the ligands as well as the potential contamination of the product mixture with traces of heavy metals. Especially this contamination is prohibitive for the synthesis of pharmaceutically active drug molecules. In order to counter these

drawbacks, simple and less toxic organic molecules as photocatalysts – often used as dyes and stains – are an upcoming topic in photocatalysis. Because they combine non-toxicity with easier availability and are partially derived from plants and other biomass, they are an interesting alternative for green chemistry approaches. Some will be further discussed as they were applied as photocatalysts in this thesis as well.[29]

Since numerous reactions and reaction types are known using photocatalysis nowadays, only the general scheme of photocatalytic reactions is introduced here (**Scheme 3**). First, the photocatalyst is elevated to its excited state by irradiation of light. There are two possibilities of a photocatalyst's subsequent reactivity, which is either the reduction of a substrate (A) accompanied with the oxidation of the catalyst itself, thus called oxidative quenching, or the oxidation of a substrate (A) accompanied with the reduction of the catalyst, thus called reductive quenching. In both cases, single electron transfer (SET) occurs forming radical species as intermediates in contrast to common acid-base electron pair chemistry. Whether oxidative or reductive quenching occurs depends on the redox potential of both the catalyst species and the respective substrate as well as solvent, pH value and other parameters. After this quenching step, a second substrate (B) reacts with the catalyst releasing it to its energetic ground state and forming the second either positively or negatively charged radical species. It is self-evident that radical-radical recombination of those two contrarily charged radical substrate intermediates occurs fast forming the desired product. Since charged radicals are involved in photocatalytic as well as electrochemical processes, these reactions are more selective and mild compared to common methods involving neutral radicals such as free radical-mediated halogenation reactions. The beneficial reaction mechanics of this kind of reactions prompted us to design cheap and reliable reaction setups with the most commonly used blue light-emitting dioides (LEDs) described in **chapter 3.2.3**.[28a,29b,30]

1.5 Generation of Carbamates

While attention has been usually paid to CO_2 fixation through C–C bond formation, the formation of carbon-heteroatom bonds is a rather emerging topic in organic chemistry.[7m,13g,15e–f,16b–f,31] Especially the formation of C–N bonds using CO_2 as building block is a promising target aiming toward the synthesis of interesting natural products and drug molecules. In order to provide practical and widely applicable reaction protocols,

reaction conditions need to be milder, preferably at atmospheric pressure and low temperature.

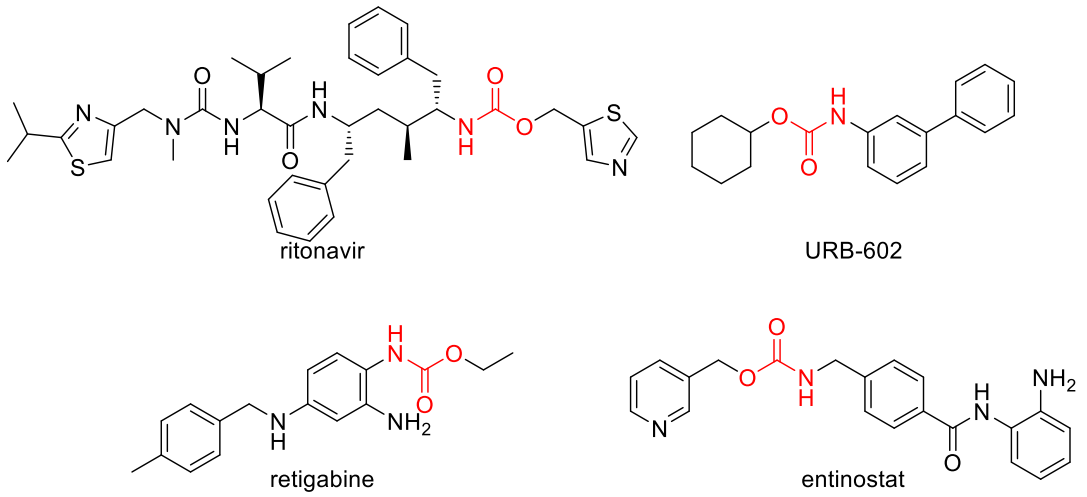

Figure 1: Important drugs with organic carbamate structures (marked in red).

For instance, C–N bond formation can be performed *via* formation of carbamates.[32] In general, organic carbamates with the general structural motif N–CO_2R (see **Figure 1**) are an important structural moiety in agricultural context and for the synthesis of drug molecules.[33] Several pharmaceuticals are characterized by a carbamate backbone, such as ritonavir, used for the treatment of hepatitis C and HIV and currently even subjected to clinical trials against the novel SARS-CoV-2,[34] the enzyme inhibitors entinostat[35] and URB-602 (the latter one will be discussed below) and the potassium channel regulator retigabine.[36] Carbamates also play an important role in synthetic organic chemistry, especially as intermediate structures for the protection of amino groups in peptide chemistry and as linkers in combinatorial chemistry.[37] Most common syntheses of organic carbamates need cumbersome and toxic reagents like phosgene or its derivatives or carbon monoxide leading to a higher operational complexity.[38] Thus, replacing these toxic reagents by CO_2 would be a highly sustainable and green approach.

Hence, it is not surprising that several homogeneous and heterogeneous metal catalysts based on Ru, Sn, Al and Au are already widely used for the conversion of amines and CO_2 to carbamates.[39] Additionally, macrocyclic polyether and potassium superoxide can be used to improve reaction conditions by enhancing the nucleophilicity of the oxygen atom within the carbamate anion through weakening the ion–ion interaction of the carbamate anion and the corresponding ammonium cation.[40] Additionally, some inorganic and organic base-catalyzed or -mediated transition metal-free systems have been developed recently.[41]

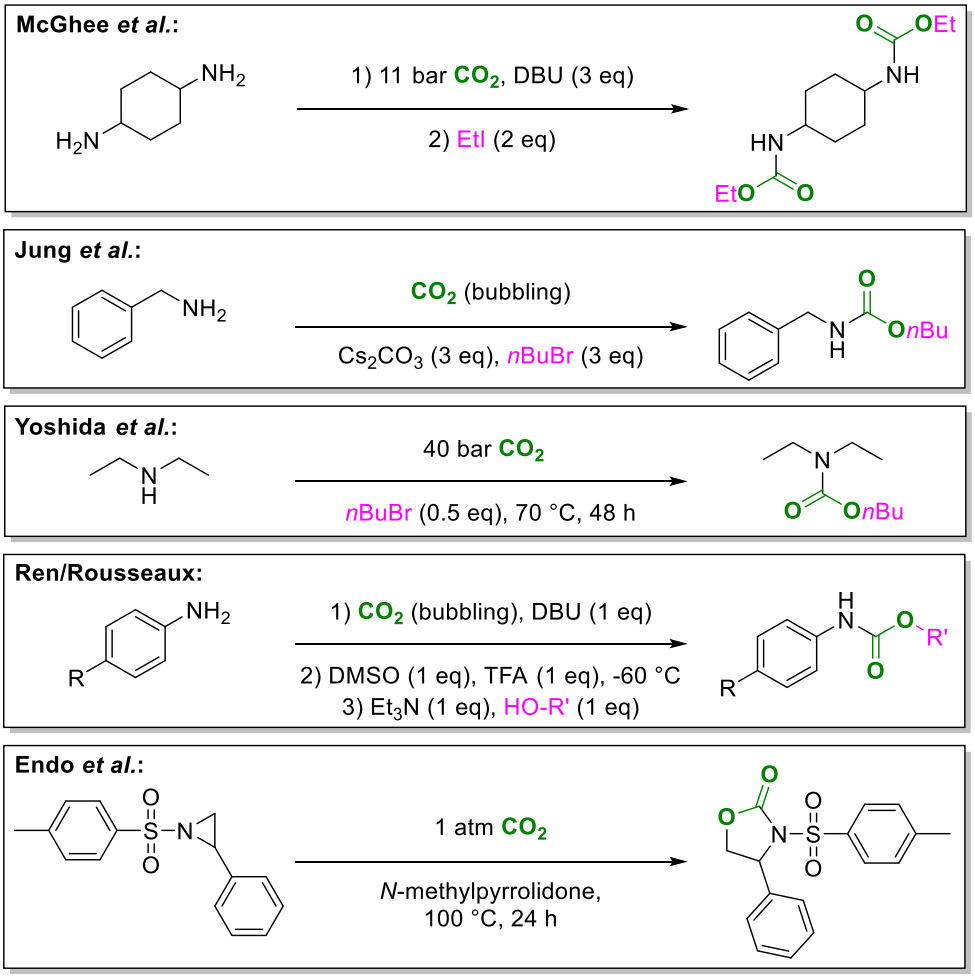

Scheme 4: Literature examples for the metal-free reaction of amines with CO_2 to carbamates.

Selected examples of those transition metal-free catalytic systems for the synthesis of carbamates are mentioned here (see **Scheme 4**): In a work from 1995 published by McGhee *et al.*, diamines could be used to generate dicarbamates with CO_2, base and alkyl chlorides. The drawbacks are the exclusive use of diamines and overpressure up to 11 bar.[41e] Jung *et al.* presented a study, where CO_2 was bubbled through the mixture (at ambient pressure but still with a loss of most of the CO_2 gas) containing 3 eq of each alkyl halide and Cs_2CO_3 as base.[41f] Yoshida *et al.* used high substrate amounts (0.25 mol amine) in an autoclave at 40 bar over 2 days but without any additional reagent. The use of only 0.5 eq of the halide and the resulting maximum yield of 50% was not further justified though. Interestingly, in their case bromides provided the best yields compared to chlorides and iodides.[42] Later, they elaborated this methodology by testing different other halides and amines again at high temperatures up to 120 °C and reaction times up to 96 h. Once more, the yields did not significantly exceed 50%.[43] In fact, alcohols can be used instead of halides too, but yields are dropping significantly due to the high activation barrier of the used alcohols.[44] This was

demonstrated in 2018 when Ren and Rousseaux developed a system using alcohols instead of halides thus making a less harmful environmental impact. However, for generating the active key intermediate it was necessary to use dimethylsulfoxide (DMSO), the relatively weak base triethylamine (Et_3N), the known superbase DBU and a strong acid (namely trifluoroacetic acid, TFA) at the same time in equimolar amounts decreasing the impact of the green aspect of this reaction. Additionally, the reaction sequence consists of three independent steps.[45]

Aziridines are another class of possible substrates – although comparably more difficult to synthesize – as demonstrated by Endo *et al.* with tosylated aziridines as substrates leading to a cyclic carbamate, also known as 2-oxazolidinone. The drawback besides the difficult synthesis of the starting materials is the high reaction time and temperature and the use of an irritant and mutagenic solvent.[46]

In summary, all of these methodologies include either notably harsh reaction conditions, such as high reaction temperatures and/or pressures or the use of additional reagents and exhibit poor functional group tolerance. This drove us to the development of a new, effective, and chemoselective methodology, which works at room temperature and atmospheric pressure using CO_2 as the carbon source.

1.6 Alcohol Oxidation Methods

An additional CO_2 utilization approach besides its fixation onto molecules (*e.g.* as carbamate products) is the employment of CO_2 as a soft oxidant or promoter for redox reactions. To date, utilizing CO_2 in this way has only been governed by heterogeneous catalysts for oxidative dehydrogenation, oxidative coupling and oxidation of alkanes.[18,47] Besides that, homogeneous catalysts have rarely been exploited to utilize CO_2 as soft oxidant and promoter, respectively.[48] Therefore, the development of other protocols using homogeneous catalysts, especially transition metal-free ones, would be adjuvant for this type of reactions due to their non-toxicity, cheaper price and ready accessibility.

The oxidation of primary and secondary alcohols to their corresponding aldehydes and ketones, respectively, is one of the most important transformations in organic chemistry. Consequently, it has been studied for more than 50 years resulting in many scientific review articles and even textbooks.[49] To attain selective oxidation methods as a

key for establishing green and sustainable chemical processes new methodologies are required, especially for the chemical industry.[50] Hence, several new reaction strategies have been explored using transition metal-based catalysts in order to avoid equimolar oxidizing reagents using greener alternatives like H_2O_2 or O_2 instead.[51] Since there is a plethora of these reactions nowadays, only some examples of such new (transition metal-catalyzed) oxidation reactions of alcohols is presented in **Scheme 5**.

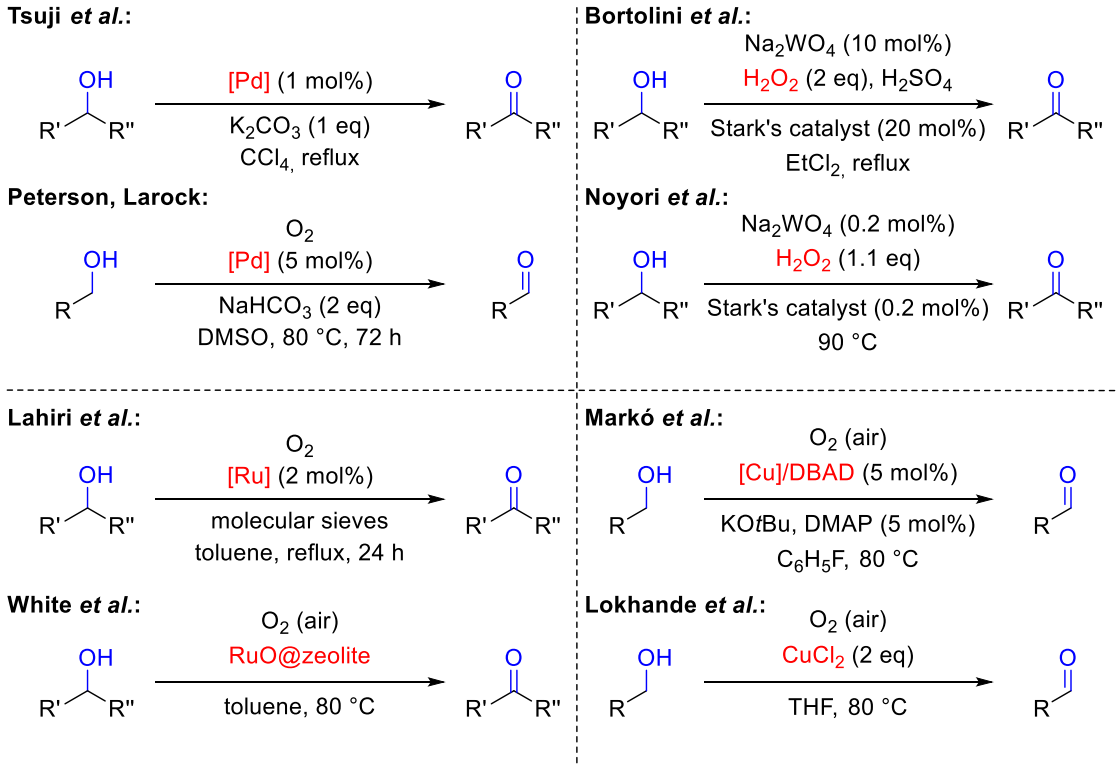

Scheme 5: Different alcohol oxidation methods sorted by their used catalyst or oxidant (Pd, Ru, H_2O_2, Cu), respectively.

An early example was published by Tsuji *et al.* in 1985. They employed the known redox reaction of Pd(II) salts in alcoholic media toward Pd(0) while oxidizing the alcohol to the corresponding carbonyl compound. Previously used Cu salts or aryl halides as sacrificial oxidants for recovery of the Pd(II) catalyst were replaced by CCl_4 in the presence of K_2CO_3 as additive.[52] Another example using a Pd catalyst published in 1997 by Peterson and Larock already employs O_2 as oxidant and DMSO as solvent. The proposed mechanism, which was clarified in 2002 by Stahl *et al.*, is similar.[53] Another approach for the use of a greener oxidant is H_2O_2. The consequential difficulty is based on aqueous reaction media, which hardly dissolve the metal catalysts. Thus, Stark's catalyst as phase transfer catalyst is necessary – while making it less attractive again – as Bortolini *et al.* demonstrated in 1985 and Noyori *et al.* 12 years later. The latter

procedure does not require a further solvent apart from the alcohol itself thus lowering the tungsten and Stark's catalyst amount and, consequently, the environmental impact.[54] However, nowadays oxygen gas is considered an important and green oxidant since it is cheap and ubiquitous. Hence, numerous approaches try to employ O_2 for reactions, either by transition metal catalysts, TEMPO ((2,2,6,6-tetramethylpiperidin-1-yl)oxyl) or even photocatalysis. For instance, in 2015 Samanta and Biswas explored the utilization of 3,6-di(pyridin-2-yl)-1,2,4,5-tetrazine as homogeneous organophotocatalyst for the oxidation of almost exclusively aromatic alcohols.[55] A broader scope of substrates was reached by Das *et al.* in 2018, albeit using simple and cheap fluorenone as catalyst.[56] And since a few years, even heterogeneous metal-free catalysts such as covalent triazine networks can be utilized.[57]

However, selected examples of non-photocatalytic methods are shown and discussed here as well (**Scheme 5**). Lahiri *et al.* presented a simple methodology yet employing a ruthenium catalyst driving the chemical equilibrium to the product side by using molecular sieves but no other additive.[58] An example for heterogeneous catalysts – but still employing Ru – was published by White *et al.*, who used immobilized RuO_2 nanoclusters on zeolite. The reaction itself is rather simple, even employing O_2 from air as oxidant. However, synthesis of this special catalyst is difficult and requires longer reaction times over several steps.[59] More recently, cheaper copper catalysts gained attention within the scientific community. For instance, in 2004 Markó *et al.* developed a Cu(I)-catalyzed alcohol oxidation method. The catalyst is a complex of CuCl, 1,10-phenanthroline (phen) and di-*tert*-butyl azodicarboxylate (DBAD). Additionally, catalytic amounts of KO*t*Bu and an additional base as additives play the major role.[60] Another yet more simple copper-based methodology was presented by Lokhande *et al.* in 2012. Albeit $CuCl_2$ is cheap, 2 equivalents had to be used to accomplish high yields. Besides, almost all substrates were aromatically activated.[61]

As already mentioned, TEMPO is a greener way to activate O_2 as oxidant since it is a non-toxic and air-stable stabilized radical, thus easy to handle, with a high affinity to O_2 molecules. For this reason, it is not surprising that TEMPO has been employed – yet mostly along with transition metal catalysts or toxic nitrites – for oxidation reactions since several decades so just some selected examples are shown here (**Scheme 6**). In 2000, Knochel *et al.* published the use of CuBr with a perfluoroalkylated bipy ligand in perfluorated alkane solvents.[62] This type of Cu(I)/TEMPO-catalyzed reaction was further developed by Stahl and coworkers, who also explored the mechanism later

on.[63] After that, a less complex tetradentate ligand for the copper center and toluene as solvent were employed by Punniyamurthy *et al.*[64] However, an approach bearing lower operational complexity is the use of simple metal salts as published by Misci *et al.* in 2001: Co-catalysis of manganese and cobalt nitrates along with TEMPO converted alcohols to their corresponding carbonyl compounds almost quantitatively.[65] In contrast to these methodologies, in 2004 Hu *et al.* reported the use of elemental bromine and sodium nitrite. Albeit no transition metal was used, two toxic compounds were necessary for the reaction to occur, thus ruling out this reaction procedure for a green chemistry approach, too.[66] Other studies of the same group followed replacing Br_2 with the toxic 1,3-dibromo-5,5-dimethylhydantoin.[67] One year later, the group of Liang replaced Br_2 by another transition metal introducing $FeCl_3$ in this type of reaction[68] and later again replaced Br_2 by HCl as a metal-free way.[69] After that, Hu group again published their progress as *tert*-butyl nitrite was sufficient along with TEMPO.[70]

Since TEMPO is an expensive chemical that is scarcely used in industry, Karimi *et al.* immobilized it through linking with silica gel on a copolymer consisting of ethylene oxide and propylene oxide.[71a]

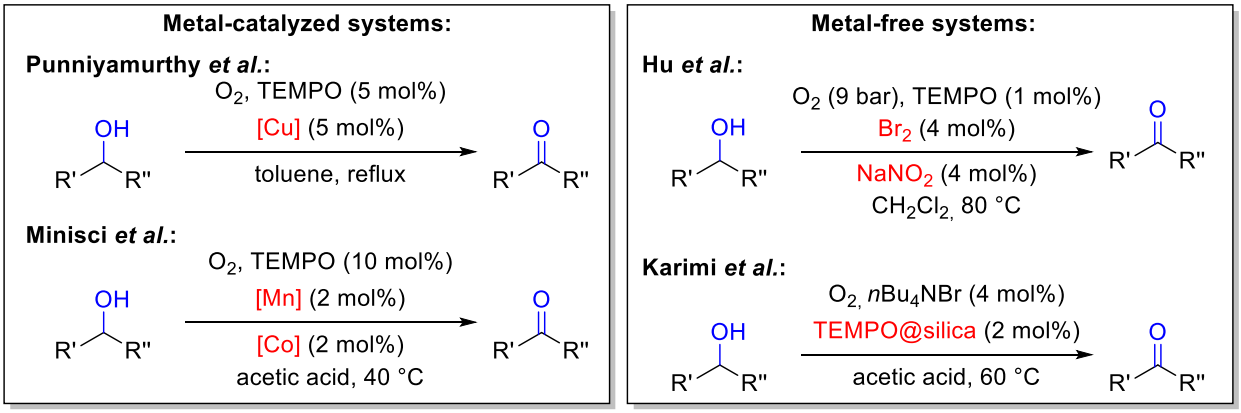

Scheme 6: Different alcohol oxidation methods utilizing TEMPO.

Most of the listed oxidation reactions are transition metal-catalyzed, which implies severe drawbacks or the strict requirement of special reaction conditions, low catalyst loadings and the use of expensive metal catalysts and ligands. Moreover, tedious removal of trace amounts of transition metal residues of the catalyst from the product mixture can be expensive and challenging yet crucial, especially for pharmaceutical molecules. Compared to transition metal-catalyzed oxidation systems, transition metal-free systems are highly appealing due to their cheaper price, their non-toxicity and the possibility of easy separation from reaction mixtures.[71] This drives chemists to develop new methodologies.

Regardless of the progress that has been made in the field of catalyzed oxidation reactions, a publication by Pfizer's medicinal chemists from 2008 showed that the three most popular oxidation methods for alcohols to the corresponding carbonyls used at Pfizer are the Dess-Martin oxidation using periodinane or its precursor 2-iodoxybenzoic acid as oxidants, the Swern oxidation and the TPAP/NMO system.[72] Moreover, there are a few other methods similar to the Swern oxidation known in organic chemistry, in which DMSO acts as the oxidant, mainly the Pfitzner-Moffatt oxidation, the Parikh-Doering oxidation and the Albright-Goldman oxidation, which are shown in **Scheme 7**.[73] The reduced byproduct in all of these oxidations is dimethyl sulfide (DMS), a valuable product *e.g.* acting as sulfidation agent in olefin production, for presulfiding of catalysts, as an ingredient in odorants or as fuel additive.[74] Albeit these methodologies are widely established for the production of pharmaceuticals, they exhibit poor atom efficiency being reflected in a huge excess of promoters and bases, the involvement of toxic reagents (*e.g.* oxalyl chloride) and significant scale-up difficulties. Therefore, the oxidation of alcohols to carbonyl compounds is still circumenvented by the pharmaceutical industry, although being a fundamentally important reaction.[72a]

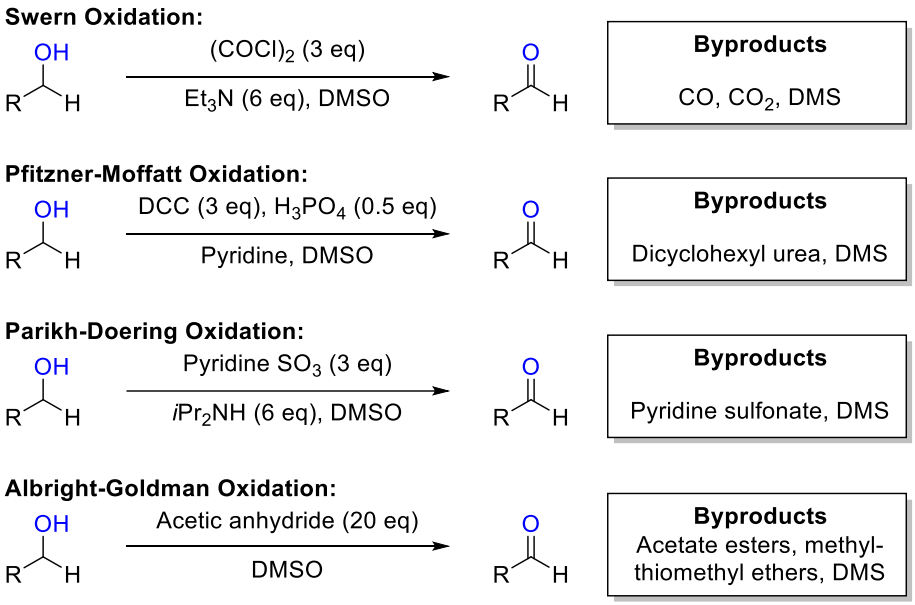

Scheme 7: Transitional metal-free oxidation reactions.

In conclusion, using green and non-toxic reagents and minimizing the amount of released byproducts should be the main aim for a greener and more sustainable approach.[75] For this purpose, CO_2 as an abundant and non-toxic promoter for oxidation reactions has gained tremendous interest, *e.g.* for the oxidative coupling of methane, the oxidative dehydrogenation of alkanes and alkyl aromatics, the oxidative coupling and oxidation of alkanes etc.[18,46] The drawback is its high thermodynamic stability and

kinetic stability, which encumbers its wider application.[7k–l,7m,13a,c,g,15e–f,16a–f,h,31e] Moreover, so far homogeneous catalysts rarely have been explored for the use of CO_2 as a soft promoter in oxidation reactions.[49a,76] In order to overcome these limitations, a transition metal-free oxidation methodology with CO_2 as promoter for the chemoselective transformation of alcohols to their corresponding carbonyl derivatives was developed.

1.7 Generation of *α*-Diketones

The procedure of CO_2-catalyzed alcohol oxidation reactions described in **chapter 1.6** and **3.2.1** was extended utilizing CO_2 as an oxidation promoter for the synthesis of *α*-diketones directly from aldehydes. These *α*-diketones serve as important backbones and intermediates and are often used as building blocks for the synthesis of fine chemicals and pharmaceutically active molecules.[77] Traditional common syntheses rely on the oxidation of either alkenes, alkynes, acyloins or comparable 1,2-dihydroxy compounds as shown in **Scheme 8**. These methods are usually catalyzed by gold, selenium, ruthenium, palladium or copper catalysts also utilizing O_2 or DMSO as actual oxidants (especially when using the more expensive noble metals like Pd).[58,78] Selected examples are shortly discussed here.

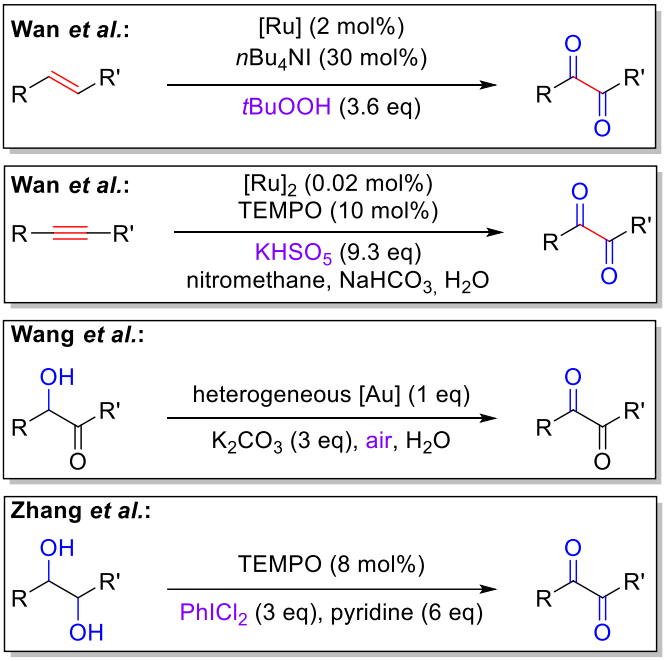

Scheme 8: Traditional oxidation methods for the synthesis of *α*-diketones.

In 2011, a study from Wan *et al.* described the oxidation of alkenes with a simple yet well-defined ruthenium catalyst and an additional ammonium salt as co-catalyst, but also the use of large amounts of the actual oxidant, *tert*-butylhydroperoxide (*t*BuOOH), which is a known carcinogenic and highly flammable, toxic and corrosive compound. In fact, the scope of substrates was limited almost exclusively to aromatically activated alkenes and no fully aliphatic substrates were reported.[78c]

Two years later, the same working group applied the same ruthenium catalyst with TEMPO as co-catalyst on the oxidation of alkynes instead of alkenes substituting *t*BuOOH by the less toxic but still harmful and corrosive potassium peroxysulfate in almost 10 eq as oxidant. The unusual reaction medium mainly consisted of the carcinogenic and mutagenic nitromethane together with sodium bicarbonate and water. The scope of substrates was comparable to the previous reports.[78d]

An even more complex approach was published in 2015 by Wang *et al.* presenting a manganese-catalyzed aerobic oxidative decarboxylative reaction of arylpropynoic acids with arylboronic acids leading toward diaryl-1,2-diketones.[78f]

Four years ago, Zhang *et al.* published a work describing heterogeneous gold nanoclusters as catalyst for the oxidation of benzoin to benzil. This catalyst is reusable too and the reaction proceeds under air and in water. The catalyst is used in equimolar amounts compared to the substrate and 2 eq of K_2CO_3 as adjuvant are used as well.[78o]

A similar work only differing in using gold nanoparticles as catalytic heterogeneous material was published by Samanta *et al.*[80q] A homogeneous version was presented by Nemoto *et al*., although using toxic and corrosive vanadium oxytrichloride.[78s]

Direct oxidation of the diaryl diol is reported with even higher amounts of adjuvants. According to Zhang *et al*., TEMPO acted as a catalyst and was recovered by the actual oxidant iodobenze dichloride. Pyridine was used as a base intercepting with the HCl produced in the process. Nevertheless, almost 10 equivalents of reactants and additives had to be used to quantitively double oxidize hydrobenzoin to benzil.[78v] Moreover, the oxidative cleavage of 1,3-diketones, *α,β*-epoxy ketones and *α,β*-unsaturated ketones is reported starting from even more complex structures, too.[79]

Unfortunately, all mentioned methodologies have severe drawbacks hindering their wide applicability, such as harsh reaction conditions, expensive or tediously synthesized well-defined catalysts, use of over-stoichiometric oxidant amounts, low yields, poor scopes of substrates or major scale-up issues. The synthesis of non-symmetric *α*-diketones *via* the above-mentioned methodologies requires corresponding non-symmetric starting materials as well. Hence, further reaction steps and tedious purifications need to be taken into consideration. In contrast to the introduced methods, especially the synthesis of non-symmetric *α*-diketones directly from aldehydes *via* benzoin condensation and subsequent oxidation is an appealing alternative due to the omitted isolation of benzoin intermediate, less (toxic) byproducts and access to a variety of differnet *α*-diketones only depending on commercially available cheap aldehydes.

This benzoin condensation was described by Wöhler and Liebig in 1832 already and its mechanism was firstly postulated to be cyanide-catalyzed in 1904.[80] Breslow further developed this method by utilizing NHC catalysts such as thiazolium salts.[81] It is thus not astonishing that numerous studies addressed this reaction. Hence, selected examples are mentioned here as well (**Scheme 9**).[82]

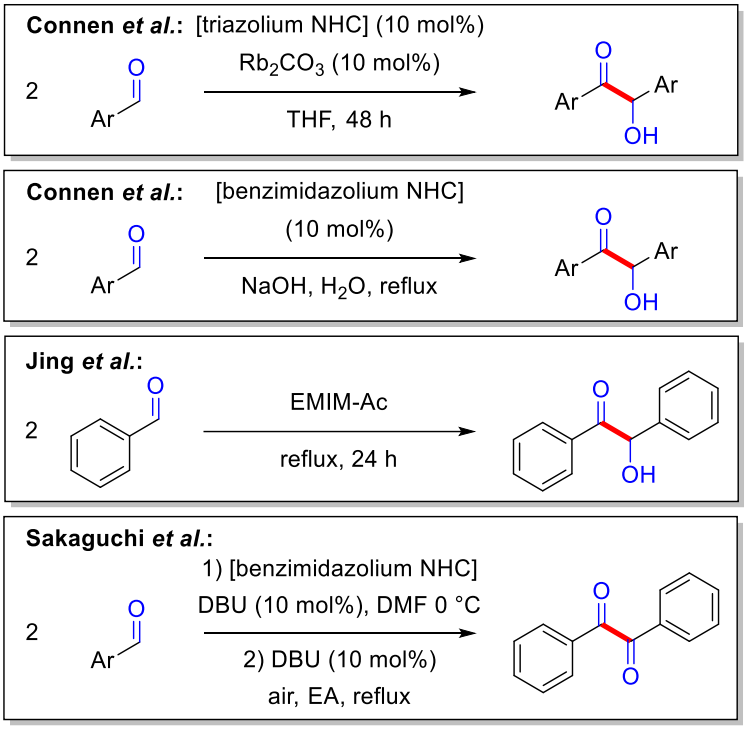

Scheme 9: Traditional oxidation methods for the synthesis of *α*-diketones.

In 2009, Connen *et al.* published about the benzoin condensation with costly triazolium salts as catalyst (*e.g.* namely 4-((1*R*,2*R*)-2-benzamidocyclohexyl)-1-phenyl-1*H*-1,2,4-triazol-4-ium perchlorate) and expensive rubidium carbonate as base.[83] Later, the

same group published a work with the same catalyst type. Broadening the scope of substrates was achieved by applying a huge variety of different triazolium salts. That approach resulted in the optimization of several substrates with different certain catalysts, although only aryl aldehydes were prone to this reaction.[84] Compared to these NHCs, cheaper benzimidazolium salts as catalysts and NaOH as base were used by Jing and coworkers, albeit only applied to aryl aldehydes.[85] Only a single substrate was shown when an ionic liquid consisting of imidazolium salts (EMIM-Ac) was used as NHC surrogate and solvent simultaneously.[86] A two-step reaction cascade was reported by Sakaguchi and his group, who utilized a benzimidazolium catalyst for the benzoin condensation step followed by changing the reaction medium (solvent, base and reaction atmosphere) aiding the final aerobic oxidation step under reflux conditions.[87] However, this reaction sequence hinders wider application due to its complexity in comparison with an *in situ* oxidation step.

So inspired by their catalytic effect in benzoin condensation reactions, NHCs were investigated for this work as well.[82] Because of previous experience with CO_2 being able to softly promote oxidation reactions, CO_2 was chosen as a soft promoter again for the envisioned *in situ* oxidation step. CO_2 is also not expected to interfere as reaction atmosphere with the prior benzoin condensation step (because of the usually short lifetime of NHC–CO_2 adducts, *cf.* also **Figure 2**) while further strengthening the sustainable aspect of this approach.

1.8 Generation of Imines

Imines are valuable intermediates in organic chemistry (*e.g.* for the synthesis of natural products, see **Scheme 55**) and important moieties in drug molecules and agrochemistry as well.[88] For instance, biologically active *β*-lactams can be synthesized *via* [2+2] cycloaddition of imines and ketenes, which represent an important class of antibiotics, such as penicilline and cephalosporine derivatives (**Scheme 10**).[89]

Moreover, the simple base-assisted and CuI-catalyzed reaction of imines, alkynes and carboxylic acid chlorides leads to the class of propargylamides, an important structural moiety within herbicides and fungicides, among others.[90]

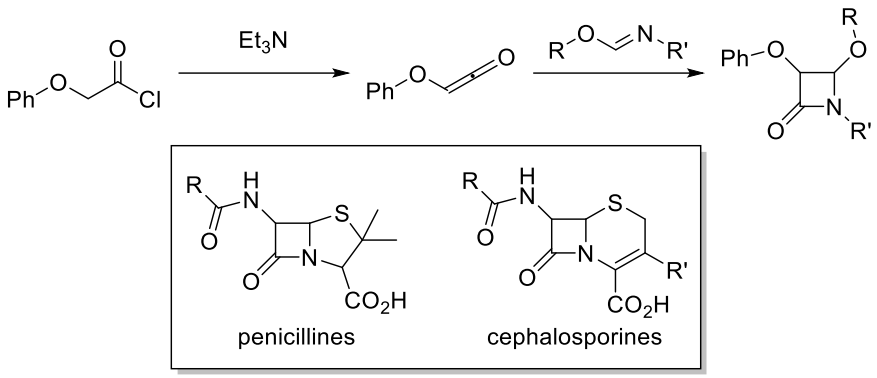

Scheme 10: Synthesis of *β*-lactams from imines and ketenes and clinically relevant *β*-lactam antibiotics.

Acyclic imines are usually synthesized by simple condensation of amines and aldehydes under acid catalysis at an ideal pH value of 4 – 6 in order to hamper side reactions. Dehydrating additives like molecular sieves can be used to additionally shift the equilibrium to the product side. Since imines are prone to the back reaction (*i.e.* hydrolysis), substrates with aromatic moieties stabilizing the product through their beneficial mesomeric effect are usually used.[89,91]

Because the scope of substrates of this traditional method is limited, recent research rather focuses on the oxidation of amines to imines. To date, mostly metal-catalyzed reactions are known employing stoichiometric oxidants like DDQ (2,3-dichloro-5,6-dicyano-1,4-benzoquinone), sulfur or peroxides, high temperatures and expensive transition metal catalysts like gold and palladium. Current research focuses on greener alternatives such as O_2 gas as an alternative oxidant.[3b,92] Selected examples of those methods are discussed here and shown in **Scheme 11**.

In 2006, Guo *et al.* published the oxidation of aromatic acyclic amines using a palladium complex, molecular sieves and sodium acetate as (basic) additives and oxygen as the oxidant. Altogether, 5 mol% of expensive palladium, 1 eq of additive and a large quantity of molecular sieves render this procedure less applicable.[93] Three years later, Che *et al.* presented the oxidation of mainly acyclic amines in the presence of gold nanoparticles supported on graphite as heterogeneous catalyst and O_2 as the oxidant. Unfortunately, the reaction required high temperatures (refluxing toluene) and an expensive gold catalyst, whose purification is deleterious due to the use of cyanides.[94] A similar work was disclosed by Bäckvall *et al.* in 2005 already. With a di-ruthenium complex as catalyst and a DDQ derivative as actual oxidant in overstoichiometric amounts the catalytic system did not meet the demands of a green chemistry setting.[95] Also ruthenium, here immobilized on polymers, was developed as a catalyst for an

application on a similar scope of substrates by Kamal *et al.* Unfortunately, they had to use large amounts of this heterogeneous catalyst, additional molecular sieves and *N*-methylmorpholine *N*-oxide (NMO) as overstoichiometric oxidant.[96] A simpler procedure yet still employing an overstoichiometric oxidant (2 eq of the carcinogenic and toxic *t*BuOOH) and thus not covering green chemistry standards either, was presented by Choi and Doyle utilizing a di-rhodium catalyst.[92e] Kanai *et al.* reported the oxidation of amines to imines with oxygen as oxidant. The drawback is the use of an additional base and a Cu(I) catalyst with ligand along with ketoABNO (9-azabicyclo[3,3,1]nonan-3-one-9-oxyl), a stabilized radical similar to TEMPO.[97]

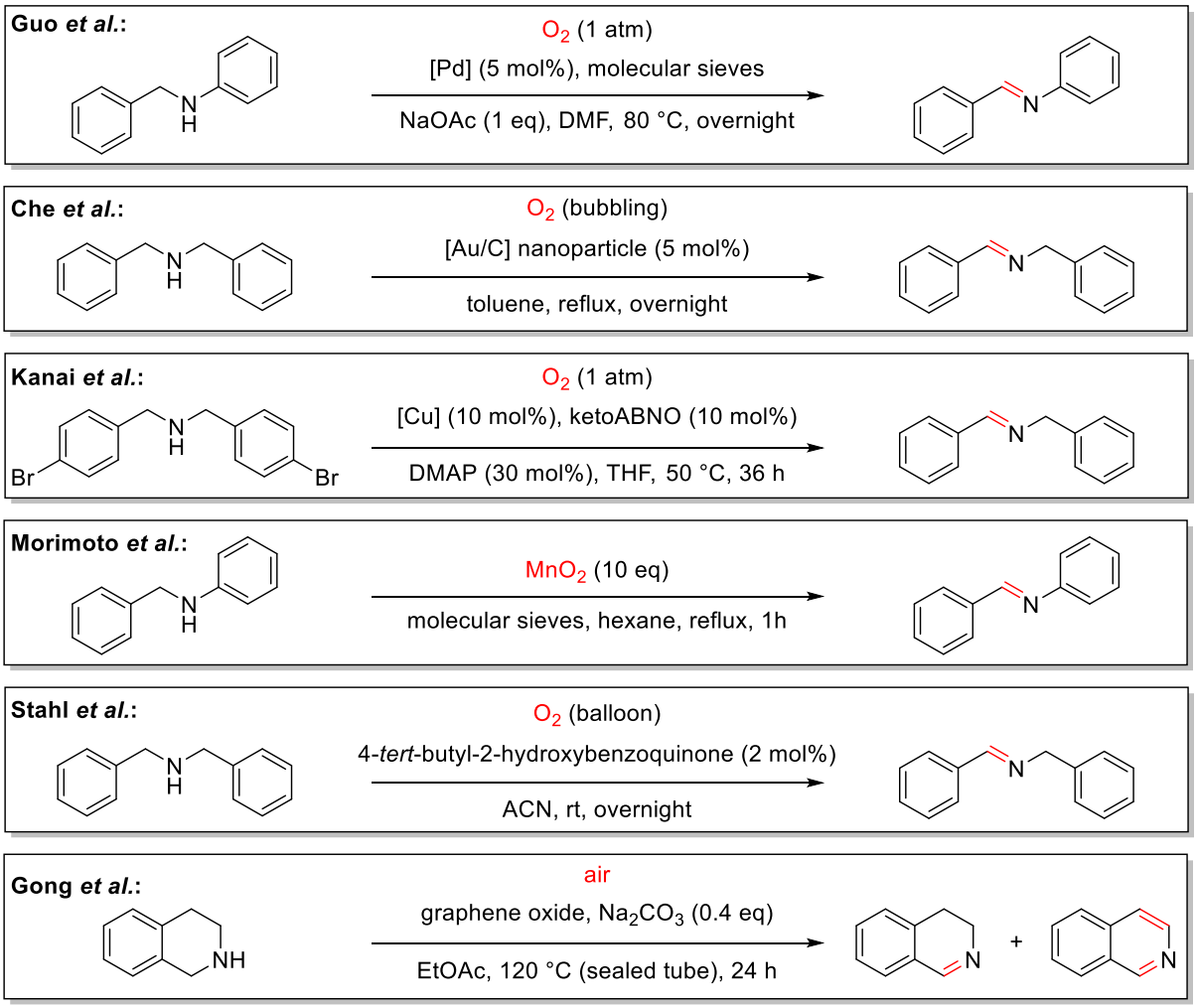

Scheme 11: Oxidation of amines to imines according to literature-known procedures.

Compared to the discussed catalytic oxidation systems, the use of manganese dioxide is much cheaper and easier to conduct. The only drawback is its very low selectivity since MnO_2 is capable of oxidizing several different functional groups. This can also occur *e.g.* when (even phenolic) primary and secondary hydroxyl groups, N–N bonds

(*e.g.* in hydrazine derivatives) or C–N bonds are present in one molecule simultaneously.[98] Another approach is the aerobic oxidative dimerization of primary amines with O_2, either using an iron catalyst like $FeBr_2$ in refluxing chlorobenzene as shown by Gopalaiah and Saini[99] or a benzoquinone derivative as organocatalyst as shown by Wendlandt and Stahl.[100] However, the scope of products is very limited since only symmetric dimers of benzylamine derivatives can be obtained.

In contrast to the oxidation of acyclic amines, the oxidation of cyclic amines like 1,2,3,4-tetrahydroisoquinoline is more difficult, especially if over-oxidation to the fully aromatic isoquinoline is undesired. Thus, it is not surprising that these reactions possess inherent selectivity issues as demonstrated by Gong *et al.* Albeit cheap graphene oxide was used as heterogeneous catalyst, high temperatures, long reaction times and semi-stoichiometric base amounts were necessary. Still serious issues regarding the general yields (27 – 99%) and especially the selectivity between single and double oxidation occurred (usually about a 4:1 ratio).[101] Besides, common non-catalytic yet more selective oxidation procedures rely on overstoichiometric amounts of the harmful and corrosive reactants *N*-chloro- and *N*-bromosuccinimide.[102]

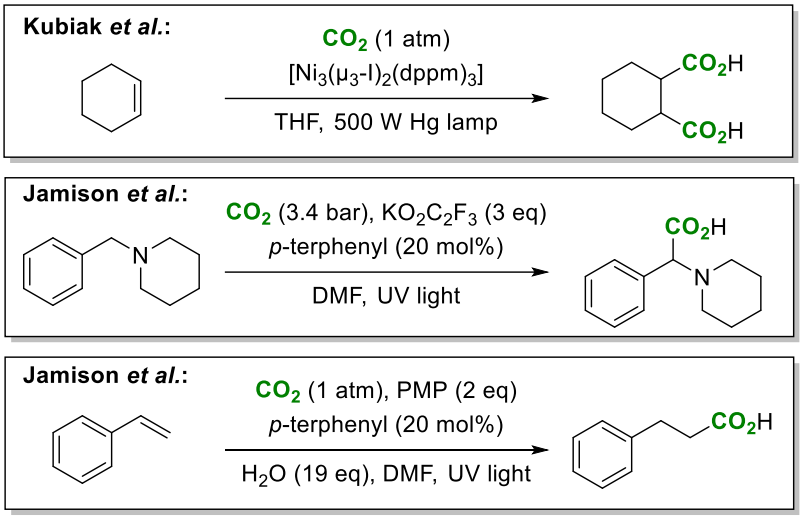

Scheme 12: Carbon dioxide radical anion in organic synthesis.

The mentioned disadvantages and harsh reaction conditions of those published works (especially occurring during thermal reaction procedures) currently drive chemists to develop new methodologies. As already mentioned for the alcohol oxidation in **chapter 1.6**, the focus is mainly laid on photochemistry nowadays. For CO_2 being able to serve as substrate in photochemistry, the generation of its radical anion species is highly interesting and has showed the formation of important platform chemicals like methanol, formic acid and CO. Since radicals are thermally unstable, this radical anion

could be only generated during photo- and electrochemical processes so far.[103] Besides, some examples already exist showing its synthetic applicability during carboxylation reactions (**Scheme 12**).[104]

The first description of the synthetic use of a CO_2 radical was presented by Kubiak *et al.* in 1993. Therein, the double carboxylation of cyclohexene has been shown under nickel catalysis but with a light source exhibiting a high energy demand.[105] In contrast, Murakami's group found the carboxylation in allylic position with a copper-based catalyst and a ketone co-catalyst under UV light irradiation in 2016, although not stating that a CO_2 radical might be involved.[106] However, the CO_2 radical anion can be directly fixed onto a variety of tertiary amines (mainly piperidine derivatives) yielding *α*-amino acids as shown by Jamison *et al.* in 2017. For this procedure, simple *p*-terphenyl was employed as organocatalyst, along with 3 eq potassium trifluoroacetate though, in a continuous photo flow setup exhibiting high yields and regioselectivity.[15i] In the same year the same group published an additional study about the *β*-selective hydrocarboxylation of styrenes utilizing the continuous photo flow reaction setup again. For this reaction 1,2,2,6,6-pentamethylpiperidine (PMP) was necessary as sacrificial electron donor in overstoichiometric amounts and water as cheap proton source.[107] While this work exclusively yielded *β*-carboxylation products, König *et al.* were able to switch the selectivity by choice of the ligand in their nickel-catalyzed reaction. They did als not finally declare a CO_2 radical being involved though.[108]

Additionally, nucleophilic addition of a CO_2 radical anion onto thymine, redox reactions with quinones, alkyl halides, nitrobenzenes and benzaldehydes etc. and the transformation of functional groups in a CO_2-catalyzed way are also reported.[18,20a–d,47,109]

2 Objectives

The utilization of one of the most threatening greenhouse gases regarding the climate change could help changing its reputation from a harmful waste toward a green alternative feedstock. For the afore-mentioned reason, it would be thus highly interesting to generate valuable fine chemicals and pharmaceutically active drug molecules or their respective intermediates *via* mild reaction pathways regarding energy consumption and safe reaction procedures and through replacing toxic and harmful reactants by CO_2.

Thus, four main reactions were envisioned for this thesis as depicted in **Scheme 13** – **16** with the aim laid on mild reaction conditions. Hence, atmospheric CO_2 pressure is one of the key elements for the use of simpler reaction setups and lower operational complexity.

A first step towards the fixation of CO_2 would be the reaction of amines with CO_2 toward carbamates (**Scheme 13**; *cf.* **chapter 1.5**). This reaction should take place with the aid of a base in order to deprotonate the amine and its reaction with CO_2. The alkyl moiety could be provided *e.g.* by an alkyl halide or an alcohol (*cf.* **Scheme 4**).

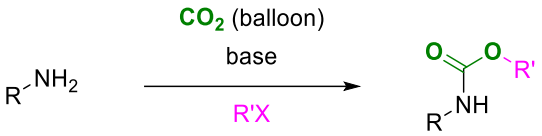

Scheme 13: General reaction scheme for the formation of carbamates from amines and CO_2.

Moreover, the utilization of CO_2 as a soft oxidation promoter was envisioned for the oxidation of primary or secondary alcohol substrates to their respective carbonyl compounds (**Scheme 14**; *cf.* **chapter 1.6**). Since it might be necessary to overcome certain oxidation potentials or activation barriers, the use of a catalyst or additive might be mandatory. Alternatively, a catalyst-free approach similar to the Swern oxidation might be suitable as well (*cf.* **chapter 1.3**).

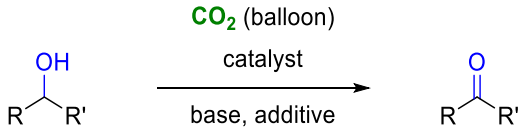

Scheme 14: General reaction scheme for the CO_2-promoted oxidation of alcohols to carbonyl compounds.

When primary alcohols could also be successfully converted to aldehydes, the benzoin condensation and further oxidation into *α*,*β*-diketones should be an interesting target as well like shown in **Scheme 15** (*cf.* **chapter 1.7**). In the ideal case, both benzoin condensation and oxidation reaction should be combined in a one-pot manner. Regarding health issues, no cyanide salts should be used as catalysts but rather NHC catalysts instead.

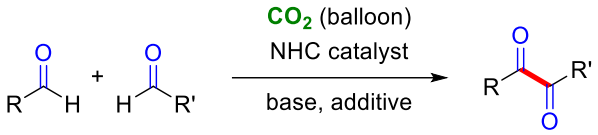

Scheme 15: General reaction scheme for the benzoin condensation of aldehyde substrates and *in situ* CO_2-promoted oxidation toward diketo compounds.

If those CO_2-promoted oxidation reactions of C–O bonds into C=O are successful, broadening the scope of substrates of this reaction oxidation protocol would be at hand as well. Especially the selectivity change from carboxylation reactions as described in **Scheme 13** toward oxidation of C–N bonds could be an interesting target. Thus, the oxidation of amines to imines was also envisioned as depicted in **Scheme 16** (*cf.* **chapter 1.8**).

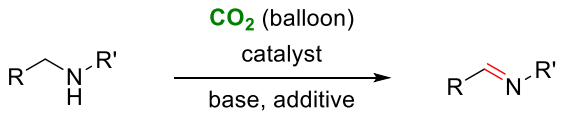

Scheme 16: General reaction scheme for the CO_2-promoted oxidation of amines to imines.

3 Results and Discussion

3.1 CO_2 Fixation: Synthesis of Carbamates From CO_2

3.1.1 Optimization Studies

In the beginning of the optimization studies, several NHC salts were tested driven by the fact that they are known to activate CO_2 easily at atmospheric pressure:[13c] Most prominent reactions are the NHC-catalyzed formation of cyclic carbonates from epoxides[110] and alkynes[111]. Furthermore, NHCs can catalyze the addition of CO_2 to alkynes in order to form alkyne carboxylic acids[112] or even the formylation of secondary amines.[113] In addition, relatively stable adducts of NHCs and CO_2 are known, even when polymer-supported NHCs are used as shown in **Figure 2**.

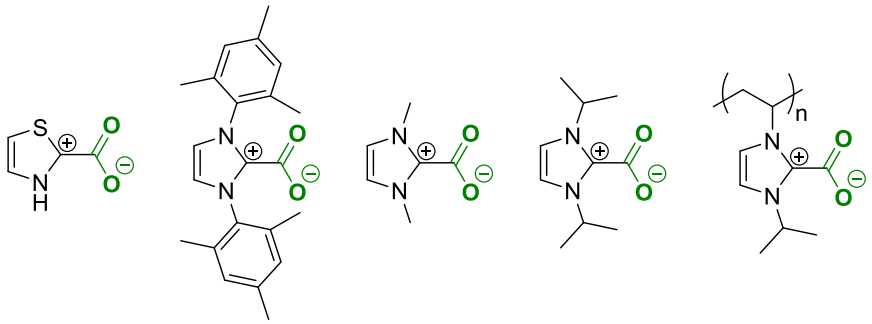

Figure 2: Different literature-known realtively stable NHC–**CO_2** adducts.[114]

Furthermore, a diaryl imidazolium–CO_2 adduct was calculated by means of densitiy functional theory methods (DFT) to transfer the carboxylate to a non-activated imine in order to form the respective carbamate salt in a base-free way.[115]

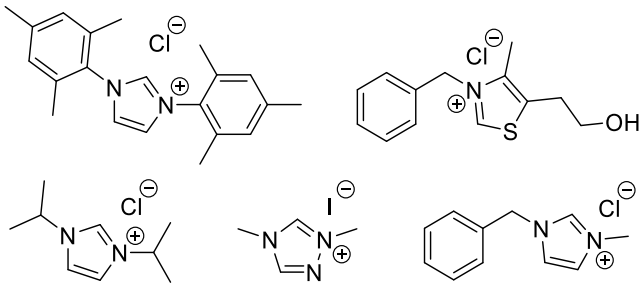

Figure 3: Different NHC salts used for initial screening reactions.

Based on this information, several NHC salts shown in **Figure 3** were examined under different reaction conditions such as different bases for the *in situ* generation of the actual diradical NHC species (or even pre-formation of this active species), different base amounts, reaction temperatures and the generation of the activated NHC prior to

the reaction. However, after conducting control experiments, it was clear that the addition of a base to the reaction mixture was crucial whereas the addition of NHC salts was not. Thus, a rather simple reaction mechanism was anticipated (see **Scheme 25**) and the screening for optimized reaction conditions was limited to different bases, base amounts, solvents, reaction temperatures and times.

Different kinds of organic and inorganic bases have previously shown their potential for the CO_2 fixation onto organic molecules.[16h,116] Moreover, they have clear benefits compared to complex metal catalysts, such as their commercial availability, low costs and low toxicity. These benefits are particularly interesting when it comes to the production of pharmaceuticals or their intermediates. Especially their low toxicity was inspiring toward the development of a mild and chemoselective transition metal-free system for the transformation of amines to carbamates using CO_2 as C1 synthon and *p*-anisidine (**1a**) as model substrate. Several organic and inorganic bases were examined for the reaction of **1a** with CO_2 under atmospheric pressure (maintained with a simple balloon) and room temperature (rt) with ethyl iodide (EtI) employed as the alkylating agent in this model system (**Table 1**). Dimethylsulfoxide (DMSO) was chosen as solvent since its polar aprotic nature makes it a reasonable solvent for dissolving gases like SO_2 and CO_2[117] and thus delivering it to the actual liquid reaction medium.

Delightfully, the first result under these conditions yielded the corresponding product ethyl (4-methoxyphenyl)carbamate (**1b**) in 62% within 16 h in the presence of 1 eq of Cs_2CO_3 at rt (**Table 1**). During the screening of different bases, it turned out that only amidine-type bases such as 1,8-diazabicyclo[5.4.0]undec-7-ene (DBU) and 1,5-diazabicyclo[4.3.0]non-5-ene (DBN) demonstrated comparable higher yields whereas other organic bases like Et_3N and inorganic bases like KOH gave significantly lower yields. When other carbonate salts were tested, only K_2CO_3 showed similar results as Cs_2CO_3. After increasing the Cs_2CO_3 amount to 1.5 eq, the yield could be increased to 91% (isolated yield). Lower amounts of Cs_2CO_3 decreased the yield dramatically indicating that at least equimolar amounts of the base are necessary. Notably, carbonate salts can be also directly obtained from CO_2 while further strengthening the sustainable approach.

Table 1: Optimization of reaction conditions using 4-methoxyaniline as model substrate.

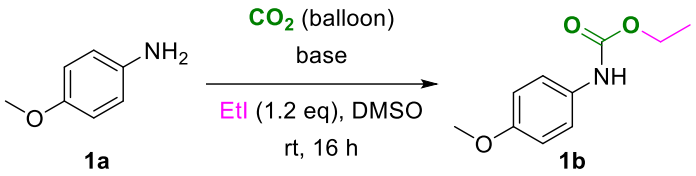

Entry	Base (eq)	Solvent	Yield / %
1	Cs_2CO_3 (1.0)	DMSO	62
2	KOH (1.0)	DMSO	1
3	DBU (1.0)	DMSO	59
4	DBN (1.0)	DMSO	54
5	DMAP (1.0)	DMSO	1
6	Et_3N (1.0)	DMSO	0
7	KO*t*Bu (1.0)	DMSO	10
8	pyridine (1.0)	DMSO	1
9	pyrimidine (1.0)	DMSO	0
10	piperidine (1.0)	DMSO	0
11	K_2CO_3 (1.0)	DMSO	57
12	Na_2CO_3 (1.0)	DMSO	22
13	$NaHCO_3$ (1.0)	DMSO	1
14	$CsHCO_3$ (1.0)	DMSO	13
15	Cs_2CO_3 (1.5)	DMSO	92/91*
16	DBU (1.5)	DMSO	87
17	DBN (1.5)	DMSO	63
18	K_2CO_3 (1.5)	DMSO	84
19	Cs_2CO_3 (0.5)	DMSO	34
20	Cs_2CO_3 (0.75)	DMSO	56
21	Cs2CO3 (1.5)	DMF	69
22	Cs_2CO_3 (1.5)	THF	0
23	Cs_2CO_3 (1.5)	DMA	68
24	Cs_2CO_3 (1.5)	toluene	0
25	Cs_2CO_3 (1.5)	*i*PrOH	0
26	Cs_2CO_3 (1.5)	acetonitrile	0
27	Cs_2CO_3 (1.5)	DMSO	95**

Reaction conditions: 4-methoxyaniline (**1a**, 0.5 mmol), base, dry solvent (2.5 mL), EtI (1.2 eq), CO_2 (balloon), rt, 16 h; *isolated yield; **reaction at 50 °C; yields determined by GC using *n*-dodecane as internal standard.

Screening of other solvents revealed that the reaction in other polar aprotic solvents like *N*,*N*-dimethylacetamide (DMA) and DMF resulted in slightly lower yields than using DMSO. Common organic solvents like tetrahydrofuran (THF) or toluene were not suitable. This hints toward other effects besides the sole solubility of CO_2 in the respective solvent since the solubility of CO_2 in DMF is calculated to be higher than in DMSO.[118]

This effect occurring with the use of different solvents can be explained by the fact that nucleophilicity and basicity of amines are controlled by solvation and polarization in different solvents.[119] The competing effect of a usually higher reaction rate but simultaneously lower solubility of gases in liquids at elevated temperatures resulted in a negligible increase up to 95% (**Table 1**, entry 27).

Since yields of more than 90% (with 1.5 eq Cs_2CO_3) were obtained after overnight reaction, the effect of different reaction times was examined (with 1.0 eq Cs_2CO_3). It revealed a sharp increase during the first 6 h reaching a plateau of up to 16 h followed by a slow decrease with further advancing reaction time (**Figure 4**). A reasonable interpretation of this decrease could be the faster deprotonation and carboxylation rate of the amine substrate whereas decarboxylation of the intermediate carboxylate anion takes place with a slower reaction rate in this equilibrium.

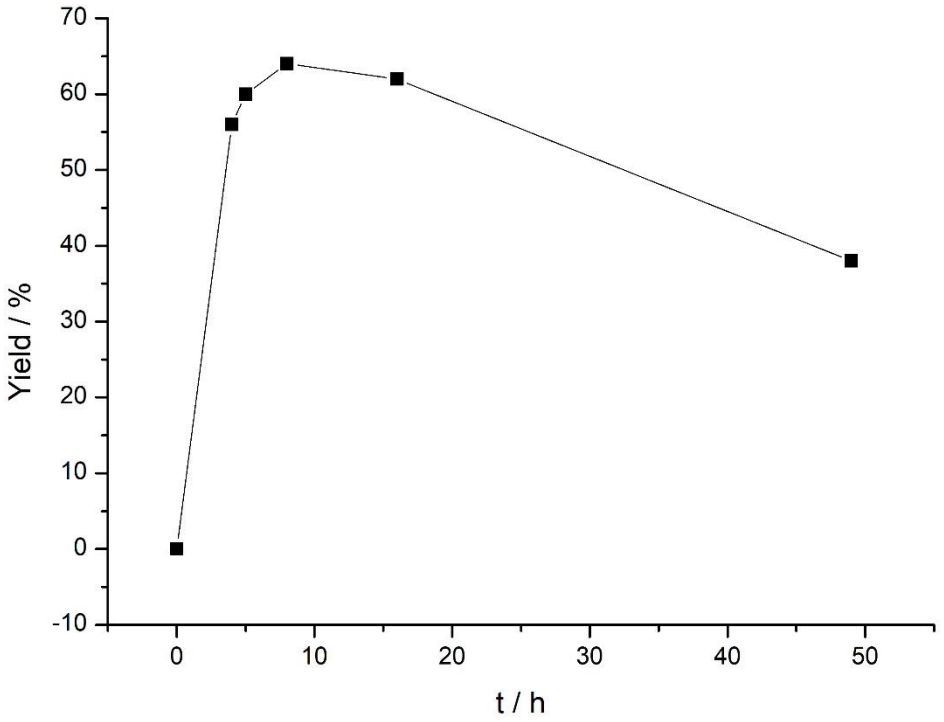

Figure 4: Time course; reaction conditions: 4-methoxyaniline (0.5 mmol), 1.0 eq Cs_2CO_3, dry DMSO (2.5 mL), EtI (1.2 eq, additional 2 h each), CO_2 (balloon), rt; all are isolated yields.

When scaling up the reaction system to a 1.8 g scale without any special precaution 91% of isolated product **1b** were fortunately obtained. However, the drawback of this reaction system is the formation of a salt from EtI and the used base (*i.e.* CsI) in equimolar amounts as byproduct. The formation of H_2CO_3 as second byproduct can lead to a second equilibrium though where CO_2 is generated and participates in the equilibrium of the gas phase and the liquid reaction medium.

3.1.2 Scope of Substrates

After identifying the optimized conditions, the scope of substrates of this carbamate synthesis protocol was explored (**Scheme 17**). Several primary and secondary amines including differently substituted aromatic, heteroaromatic, alicyclic and aliphatic ones were converted to their respective carbamate derivatives with yields up to 90%. Both electron-donating and electron-withdrawing *para* substituents at the aromatic ring reacted well (also *cf.* **Scheme 18**).

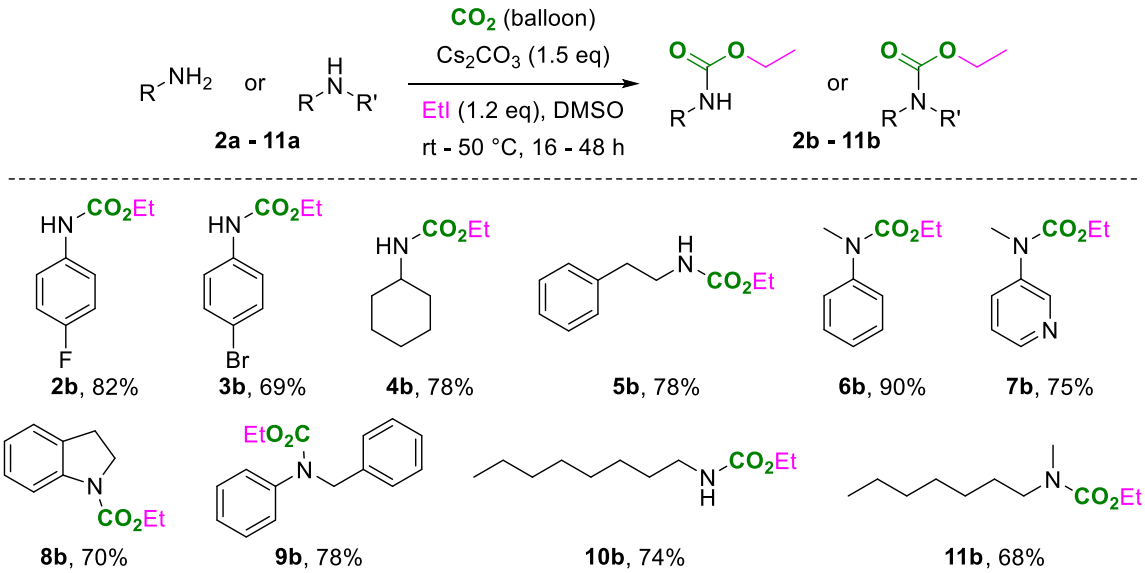

Scheme 17: Synthesis of carbamates using CO_2 as the carbon source; reaction conditions: Substrates (0.5 mmol), Cs_2CO_3 (1.5 eq), DMSO (2.5 mL), EtI (1.2 eq), CO_2 (balloon), rt – 50 °C, 16 – 48 h; all are isolated yields; some reactions were performed by Pradipbhai Hirapara.

The tolerance of reaction systems against different functional groups is highly important for its later application particularly for the synthesis of natural products and pharmaceuticals.[15] Thus, the chemoselectivity was investigated in the presence of different possibly reducible functional groups (**Scheme 18**). Fortunately, under optimized reaction conditions different challenging nitrile, nitro, amide, ester and carbonyl functional groups were well tolerated as well as alkene and alkyne moieties. Thereby, the corresponding carbamate products could be obtained in good to excellent yields. Notably, for none of the examined substrates additional reduction, oxidation or carboxylation of the different functional groups was observed, which demonstrates the excellent chemoselectivity of this reaction system. To date, there is no other example of this type of selectivity for carbamate synthesis.

However, a few substrates such as **2a** demanded longer reaction times and/or higher reaction temperatures. Substrates with fluoro, nitro, nitrile and methyl ester substitution at *para* position (**2a**, **12a**, **13a**, **16a**) required these reaction conditions in order to achieve higher yields. A general forecast for the necessary reaction conditions regarding time and temperature is difficult since *e.g.* fluoro and bromo substituents required different conditions (**2a**: 48 h, 50 °C, **3a**: 16 h, rt). But in general, substrates bearing electron-withdrawing groups seem to require longer reaction times and higher temperatures although it should be easier to deprotonate amines bearing substituents with a –I effect thus weakening the N–H bond of the amine moiety.

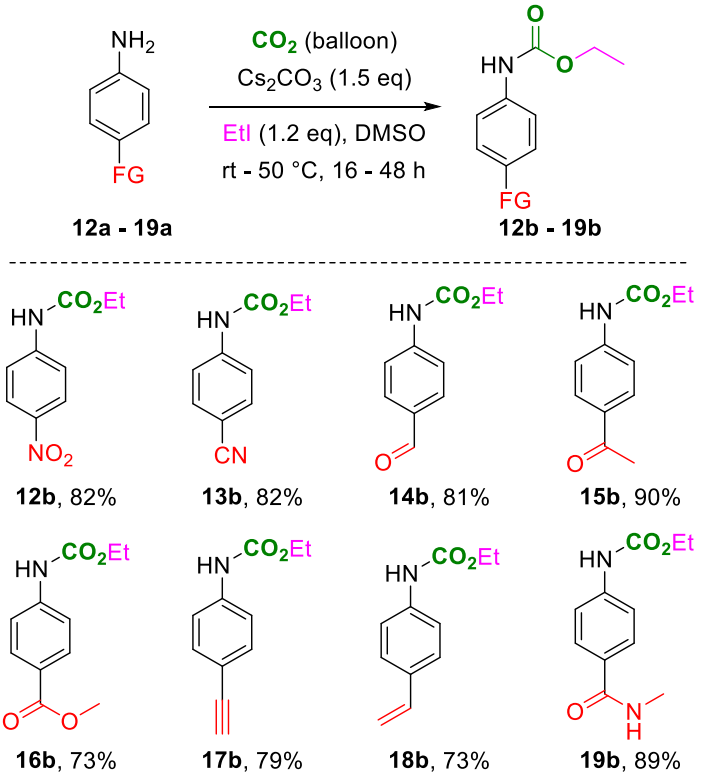

Scheme 18: Functional group (FG) tolerance for the carbamate synthesis using CO_2 as the carbon source; reaction conditions: substrates (0.5 mmol), Cs_2CO_3 (1.5 eq), DMSO (2.5 mL), EtI (1.2 eq), CO_2 (balloon), rt–50 °C, 16–48 h; all are isolated yields; some reactions were performed by Pradipbhai Hirapara.

Nevertheless, *para*-substituted amines with halogen (**2a** – **3a**) or pseudo-halogen (**13a**) groups as well as other electron-withdrawing and -donating groups (**12a**, **14a** – **19a**) and non-symmetric amines (**6a** – **9a**) generally reacted well. In addition, in none of the cases any reduced or dehalogenated product could be observed. Interestingly, heterocyclic amines represented by a pyridine derivative and indoline (**7a** – **8a**) as well as non-aromatic (and thus electronically non-activated) substrates (**4a** – **5a**, **10a** – **11a**) reacted excellently. The difference between the reaction rates of primary

and secondary amines was found to be low, thus no changed reaction conditions had to be applied.

Despite the excellent functional group tolerance and chemoselectivity of this reaction protocol, different types of molecules were not accessible as substrates, summarized in **Scheme 19**. Mostly sterically hindered primary amines and highly polar nucleobases and amino acids only yielded low or no amounts of the desired carbamate product.

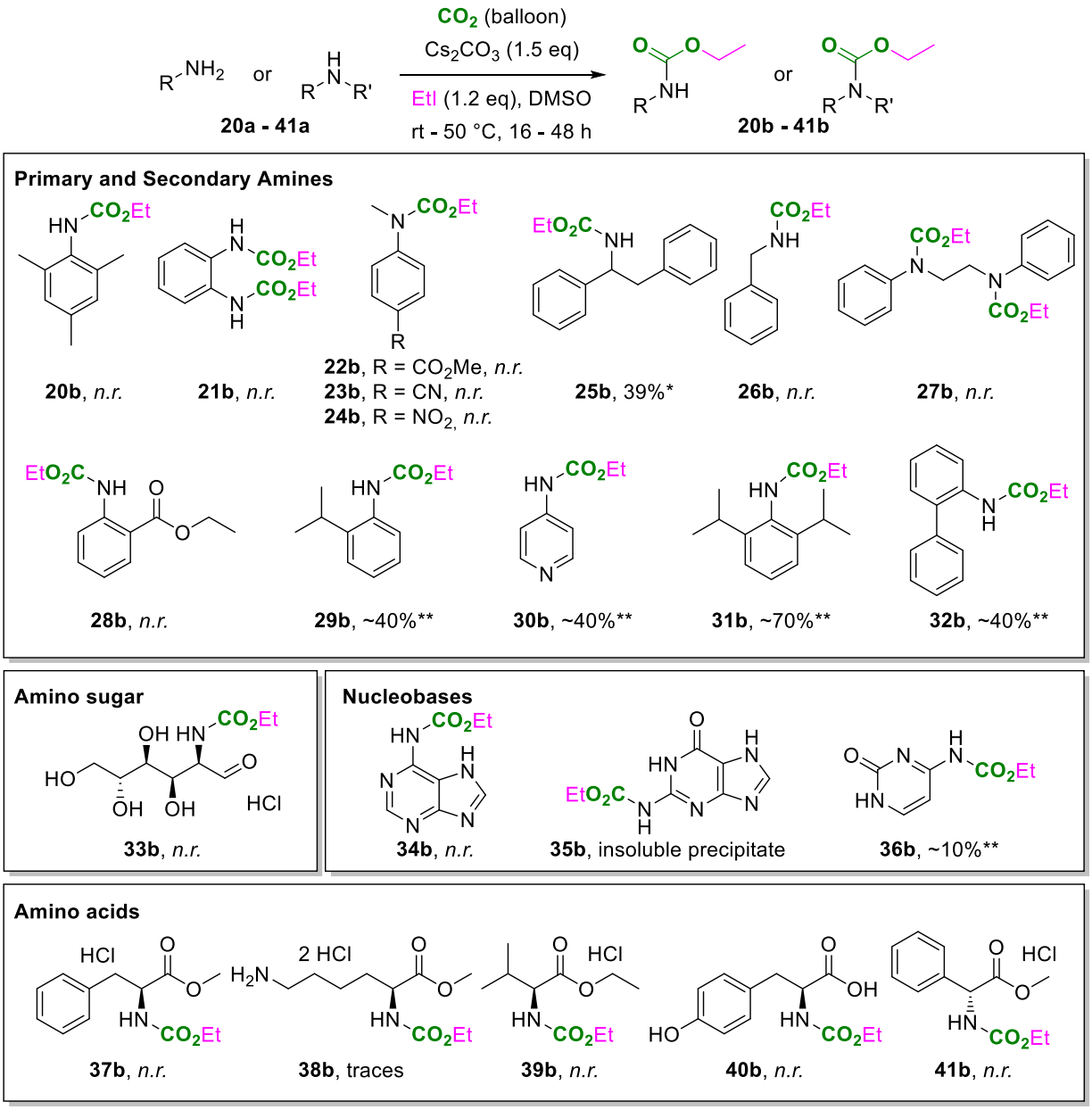

Scheme 19: Different unsuccessful substrates tried for the synthesis of carbamates; reaction conditions: substrates (0.5 mmol), Cs_2CO_3 (1.5 eq), DMSO (2.5 mL), EtI (1.2 eq), CO_2 (balloon), rt – 50 °C, 16 – 48 h; reaction progress monitored by gas chromatography-coupled mass spectrometry (GC-MS); *yield determined by ^{1}H NMR spectroscopy using iodoform as internal standard; **yield estimated by GC-MS.

Sterical hindrance can account for **20a** (as well as the lower yield of **32a**) since it is the only examined example of *ortho*-substitution within the scope of substrates. The steric demand of these methyl groups should be even higher than the one in case of secondary amines (*cf.* **Scheme 17**). In comparison to **29a** and **31a**, steric demand cannot be the only explanation, especially since **31a** successfully reacted well with benzylbromide (BnBr) using longer reaction time and higher temperature (*cf.* **Scheme 4**). Substrates with two possible active sites like **21a** and **27a** did not show any activity at all, not even with higher base amounts (2.5 eq Cs_2CO_3) to factor in the possible double deprotonation. Solely aliphatic amines such as **10a** and **11a** and the aliphatic substrate **5a** with a phenyl group reacted well. In contrast, it is surprising that **25a** only gave a low yield of 39% and could not be isolated and **26a** did not show any activity at all. Heteroaromatic compound **30a** was less active compared to substrate **7a** leading to the suggestion that the position of the heteroatom within the aromatic ring is crucial for electron distribution. However, in case of substrates **25a** and **29a** – **32a** purification issues prohibited obtaining pure product compounds after the reaction.

The examined amino sugar *D*-glucosamine (**33a**) was not accessible as substrate neither in its free form nor as hydrochloride. A possible explanation is the varying accessibility of the competing functional groups for possible deprotonation (OH *vs.* NH_2). Additionally, due to the amount of strongly polar functional groups in that molecule traditional analysis was difficult to undertake. Correspondingly, the same reason applies to the probed nucleobases adenine (**34a**), guanine (**35a**) and cytosine (**36a**). However, in case of **35a** a precipitate was observed after the reaction, which was not soluble in common polar and non-polar solvents and was consequently not further examined. The tested amino acids *L*-phenylalanine methyl ester hydrochloride (**37a**), *L*-lysine methyl ester hydrochloride (**38a**), *L*-valine ethyl ester hydrochloride (**39a**), *L*-tyrosine (**40a**) and *(R)*-2-phenylglycine methyl ester hydrochloride (**41a**) exhibited no or very low activity. An explanation might be that hydrochlorides are not active as substrates (except for **50a**) compared to free amino acids. Especially the free amino acid tyrosine has 3 possible positions for a deprotonation followed by alkylation, thus, opening up uncontrolled reactivity at different unwanted positions.

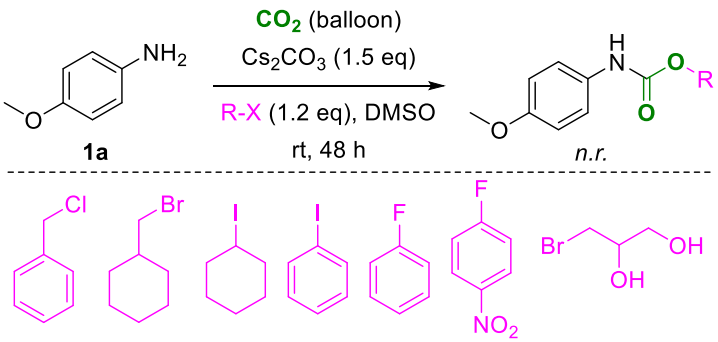

Scheme 20: Different unsuccessful halides tried for the synthesis of carbamates; reaction conditions: 4-methoxyaniline (**1a**, 0.5 mmol), Cs_2CO_3 (1.5 eq), DMSO (2.5 mL), R–X (1.2 eq), CO_2 (balloon), rt, 48 h; reaction progress monitored by GC-MS; some reactions were performed by Pradipbhai Hirapara.

Moreover, a number of halogenated compounds including aromatic and alicyclic examples and a glycerol derivative were not able to react with the carboxylated amine anion, even after a prolonged reaction time of 48 h. The reaction temperature was not increased though due to the naturally high volatility of many halides (**Scheme 20**).

Compared to the successfully used EtI, other iodides are sterically more hindered. Moreover, the electronic situation within a halogenated aromatic compounds completely differs from an alkyl halide. Nonetheless, the non-reactivity of cyclohexyl iodide was surprising and its reactivity could have opened up the direct access to URB-602 from biphenyl amine **46a**. C–Cl and C–F bonds are shorter and stronger than C–Br and C–I bonds and thus harder to break, which could explain the non-reactivity of those halides. In addition, the electronic situation at cyclohexyl bromomethane and the brominated glycerol derivative are different compared to BnBr.

3.1.3 Application of the Carbamate Synthetic Protocol

Organic carbamates play a pivotal role for drug discovery and medicinal chemistry likewise due to their structural similarity with amide-ester hybrid features and they exhibit both excellent chemical and proteolytic stability. Moreover, the formation of hydrogen bonds between the carboxyl moiety and the amine residue enhances biological and pharmacokinetic properties.[34,120] In order to demonstrate the utility of the developed procedure, nortriptyline (an amphiphilic antidepressant[121]) and cinacalcet (used for the treatment of chronic kidney diseases;[122] **Scheme 21**) were chosen as model drug molecules to be modified under optimized reaction conditions.

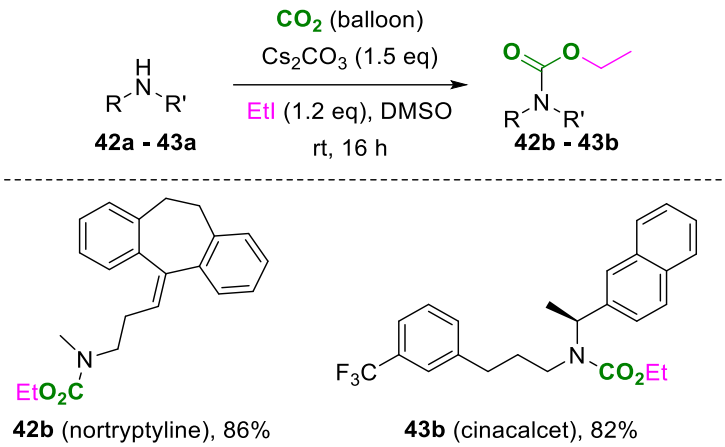

Scheme 21: Pharmaceuticals that underwent carbamate derivatization using CO_2 as a carbon source; reaction conditions: substrates (0.5 mmol), Cs_2CO_3 (1.5 eq), DMSO (2.5 mL), EtI (1.2 eq), CO_2 (balloon), rt, 16 h; all are isolated yields.

In fact, both substrates reacted excellently with up to 86% yield. Again, the selective transformation occurred in the presence of the double bond (**42a**) without further carboxylation (also *cf.* **Scheme 18**, **18a**). Additionally, simple column chromatography without special precaution was successful for the purification of the respective products.

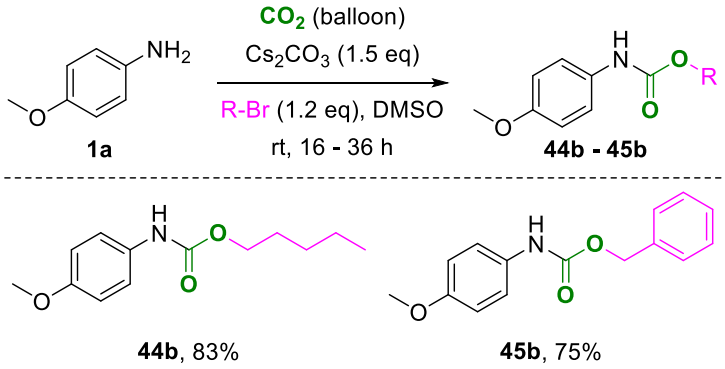

Scheme 22: Different alkyl bromides used for the synthesis of carbamates; reaction conditions: 4-methoxyaniline (**1a**, 0.5 mmol), Cs_2CO_3 (1.5 eq), DMSO (2.5 mL), R–Br (1.2 eq), CO_2 (balloon), rt, 16 – 36 h; all are isolated yields.

The modification of organic carbamate structures is widely used in pharmaceutical research.[123] Variation of the carbamate moiety provides a broader scope for testing of possible new bioactive compounds with a higher efficiency. For this purpose, both positions at the nitrogen and oxygen atom can be varied. Therefore, parallel to the screening of the scope of different amine substrates, alkyl halides other than EtI have been varied to show the possibility of generating a compound library based on this carbamate structure (**Scheme 22**). Notably, not only the already tested alkyl iodide but also alkyl bromides can be applied under similar reaction conditions. *n*-Pentyl bromide and benzyl bromide were investigated as alkylating agents along with model substrate

1a yielding the respective products **44b** and **45b** with a considerable yield of up to 83%. Notably, stirring time with *n*-pentyl bromide was increased from 2 h to 4 h.

Triggered by these findings, the idea of showing the possibility to create a compound library of URB-602 derivatives arose. URB-602 is known as a selective inhibitor of the enzyme monoacylglycerol lipase involved in the hydrolysis of 2-arachidonylglycerol in the brain.[124] This selective enzyme inhibition avoids direct activation of specific receptors leading to less psychoactive side effects. However, while its selectivity remains *in vivo* it changes *in vitro*.[125] Hence, changes in the structure of URB-602 could lead to a powerful inhibitor without or at least less side effects. This modification can be realized either by isosteric replacement, different substituents at the aromatic moiety or other alkyl residues at the carbamate moiety. Compared to these proposed approaches using the presented direct synthesis protocol, it was possible to synthesize a URB-602 derivative directly from biphenyl-3-amine (**46a**) in 69% yield (**Scheme 23**).

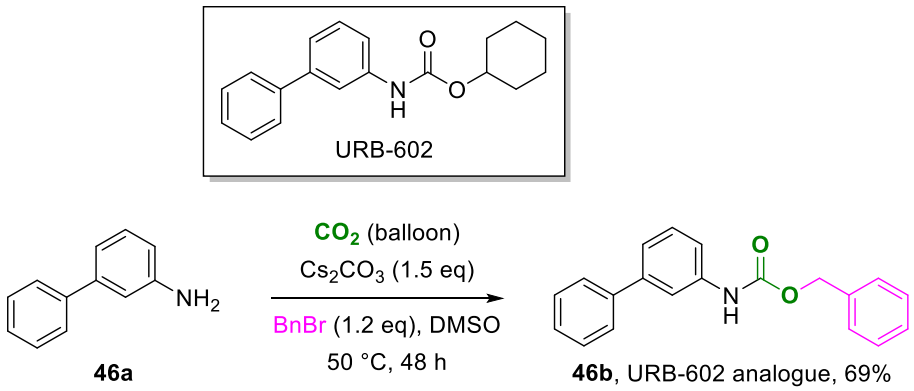

Scheme 23: Synthesis of URB-602 derivative using CO_2 as a carbon source; reaction conditions: 3-phenylaniline (**46a**, 0.5 mmol), Cs_2CO_3 (1.5 eq), DMSO (2.5 mL), BnBr (1.2 eq), CO_2 (balloon), 50 °C, 48 h; isolated yield.

In traditional synthetic organic chemistry as well as in biochemistry protecting groups play a vital role for preventing reactions at undesired sites of the respective substrates.[126] For instance, introduction of a protecting group at the *α*-position of amino acids and peptides is important to prevent unwanted polymerization during the formation of desired peptide bonds. Especially in this case, the introduced protecting groups should prevent epimerization during peptide bond coupling and the deprotection procedure after the actual reaction should be easy and fast. Thus, the most commonly used protecting groups for these substrates are Cbz (carboxybenzyl), Fmoc (9-fluorenylmethoxycarbonyl) and Boc (*tert*-butyloxycarbonyl) with Cbz being the most often used one for peptide syntheses. All mentioned protecting groups share the for-

mation of a carbamate moiety after the reaction of a protecting agent (toxic and corrosive benzylchloroformate in case of Cbz) with the *α*-amino position of amino acids and peptides, respectively. Thus, by using the reaction procedure presented herein, CO_2 can be used as an alternative and green protecting reagent for the amine moieties in organic syntheses or peptide chemistry (**Scheme 24**).

Four different amino acid methyl esters, namely phenylalanine (**47a**), tryptophane (**48a**), methionine (**49a**) and glycine (**50a**), reacted well in good to high yields. The latter one could even be used directly as hydrochloride salt with additional Cs_2CO_3 (2.5 eq in total) for *in situ* removal of hydrochloride. The other amino acids had to be freed of hydrochloride and hydrobromide, respectively, prior to the actual reaction.

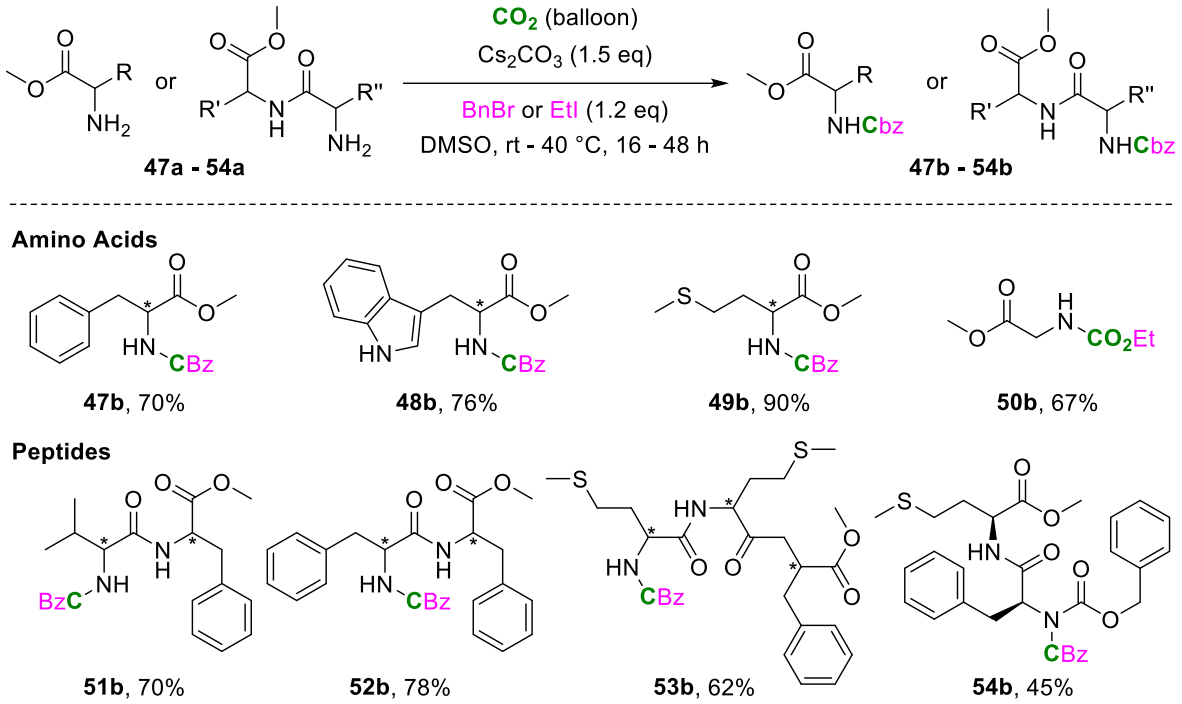

Scheme 24: Protection of amino group in amino acids and peptides using CO_2 as a carbon source; reaction conditions: substrates (0.5 mmol), Cs_2CO_3 (1.5 eq), DMSO (2.5 mL), alkyl halide (1.2 eq), CO_2 (balloon), rt – 40 °C, 16 – 48 h; all are isolated yields; some reactions were performed by Pradipbhai Hirapara.

Additionally, it was possible to extend the scope of substrates using CO_2 as protecting reagent to four different peptides, which were synthesized by combining corresponding amino acid precursors (**Scheme 24**). The so-examined peptides consisted of valine and phenylalanine (**51a**), twice phenylalanine (**52a**), twice methionine with phenylalanine (**53a**) and *L*-phenylalanine with *L*-methionine (**54a**), respectively. All examined peptides reacted well and up to 78% of Cbz protected peptides have been achieved. In none of the cases any other byproducts could be observed besides the already

mentioned equimolar formation of CsI and CsBr, respectively, and only single carbamate formation occurred at the primary amine functionality. All products from amino acids and peptides were recovered after extraction of the reaction mixture with dichloromethane followed by purification *via* column chromatography. After successful demonstration of Cbz protection of molecules comprising of one, two and even three amino acids, it can be assumed that this protection procedure can also be easily applied to higher peptide sequences. Thus, it could open up new alternatives for peptide chemistry.

3.1.5 Proposed Mechanism

The proposed reaction mechanism consists of a three-step reaction: First, a simple deprotonation of the amine occurs, followed by nucleophilic attack of the anion to the electropohilic carbon atom of the CO_2 molecule. Subsequently, quenching by alkylation of the so-formed carboxylate with an alkyl halide leads to the desired carbamate structure (**Scheme 25**).

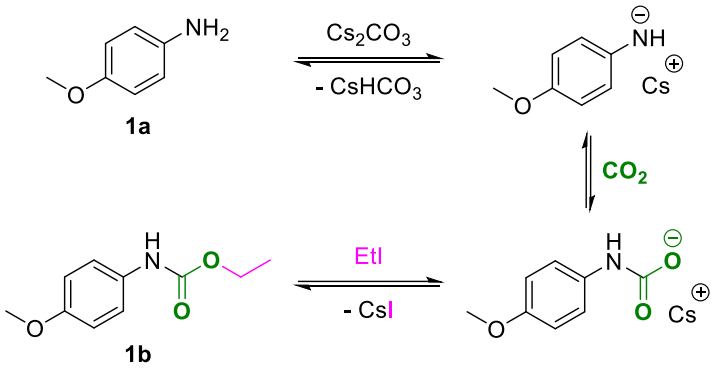

Scheme 25: Proposed reaction mechanism for the synthesis of carbamates.

3.2 CO_2 as Promoter for Oxidations and Dehydrogenations

3.2.1 CO_2-Catalyzed Oxidation of Benzylic and Allylic Alcohols

Similar to replacing C1 synthons like phosgene by CO_2, utilizing CO_2 as oxidant or oxidation promoter is an interesting approach for green and sustainable chemistry, too. The fact that alcohols are ubiquitous triggered the idea of the application of CO_2 as promoter in oxidation reactions of these substrates. As described in **chapter 1.6**, common oxidation methods employ great amounts of toxic or corrosive reactants. Thus, replacing these chemicals and especially toxic oxalyl chloride as used for the Swern oxidation by CO_2 would be an additional green chemistry approach.

Again, as described in **chapter 3.1**, some NHC catalysts were tried as catalysts for an easier CO_2 activation in the beginning of the optimization reactions.[127] However, control experiments demonstrated simple base addition to be sufficient for attaining high reactivity. Later the use of NHCs turned out to be an interesting approach for the utilization of this methodology (*cf.* **chapter 3.2.2**). The following screening for optimized reaction conditions was thus extended to screening of different bases, base amounts, solvents, reaction temperature and reaction time.

3.2.1.1 Optimization Studies

The first screening approach was undertaken with benzyl alcohol as model substrate. Even after extensive screening and careful evaluation of different reaction conditions (different bases such as alcoholates, hydroxydes, amidine-type bases and carbonates, up to 14 bar pressure in an autoclave, extension of reaction time to 64 h or the use of additives like Lewis acids) maximum yields of no more than 65% were reached.

However, extension of the π system from the phenyl ring in the form of cinnamyl alcohol (**55a**) enhanced the reactivity hence it was taken as model substrate. At the outset, a variety of inorganic and organic bases was applied in order to obtain optimized reaction conditions for the synthesis of cinnamaldehyde (**55b**) directly from cinnamyl alcohol under CO_2 atmosphere (**Table 2**).

Organic bases like DMAP and DBU as well as inorganic hydroxides and even strongly basic alcoholates like KO*t*Bu resulted in only 11% product formation in DMSO at 90 °C. Changing the base to a bicarbonate slightly increased the yield to 13% and changing to a carbonate increased it to 44%. When K_3PO_4 was used 90% cinnamaldehyde could

be obtained. Efforts to lower the reaction temperature did not lead to better activity whereas at higher temperature (100 °C) the yield remained unchanged On the one hand, decreasing the base loading from 20 mol% to 10 mol% resulted in a significantly lower yield, but on the other hand higher base amounts did not further increase it either. Control experiments without any base or under N_2, O_2 or air atmosphere showed no or negligible product formation. Reports about the solvent sensitivity of similar simple (only use of a base; yet aerobic) oxidation methodologies showed that common solvents (especially DMSO) hampered the reaction so that ionic liquids had to be taken.[128] In contrast to that, in the herein presented case other solvents than DMSO did not show any activity because of a mechanism similar to Swern oxidation as will be described later. It should be mentioned that no over-oxidation in terms of formation of the corresponding cinnamic acid was observed, which demonstrated the good selectivity in case of primary alcohols.

Table 2: Optimization for alcohol oxidation.

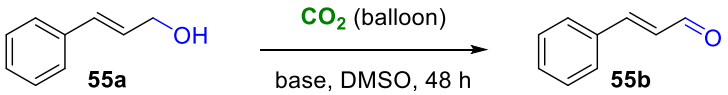

Temp / °C	Base	Base equivalents / mol%	Atmosphere	Yield / %
90	-	-	CO_2	**0**
90	$NaHCO_3$	20	CO_2	**13**
90	DBU	20	CO_2	**7**
90	aniline	20	CO_2	**1**
90	LiOH	20	CO_2	**7**
90	KOH	20	CO_2	**10**
90	KO*t*Bu	20	CO_2	**11**
90	DMAP	20	CO_2	**1**
90	K_2CO_3	20	CO_2	**44**
80	K_3PO_4	20	CO_2	**68**
90	K_3PO_4	20	CO_2	**90/89***
100	K_3PO_4	20	CO_2	**90**
90	K_3PO_4	10	CO_2	**56**
90	K_3PO_4	50	CO_2	**91**
90	K_3PO_4	100	CO_2	**92**
90	K_3PO_4	20	N_2	**0**
90	K_3PO_4	20	O_2	**5**
90	K_3PO_4	20	air	**2**

Reaction conditions: cinnamyl alcohol (**55a**, 0.25 mmol), DMSO (2.5 mL), gas atmosphere *via* balloon, 48 h; yields determined by GC using *n*-dodecane as internal standard; *****yield for 5 mmol scale reaction.

Scaling up the reaction was easily possible giving 89% isolated yield in case of a 5 mmol scale reaction without any special precaution. The reaction still worked using only 1 eq or even 20 mol% of CO_2 instead of a CO_2 ballon. However, a slightly decreased yield was observed (**Table 3**). This proves that CO_2 is not consumed but rather has a catalytic or promoting effect in the reaction mechanism.

Table 3: Different amounts of CO_2.

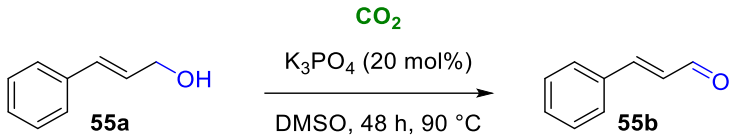

Yield / %	Equivalents CO_2
90	excess (balloon ≈ 500 eq)
84	1.0
80	0.2

Reaction conditions: cinnamyl alcohol (**55a**, 0.25 mmol), DMSO (2.5 mL), 48 h; yields determined by GC using *n*-dodecane as internal standard; *****yield for 5 mmol scale reaction.

Different amounts of CO_2 were tested as follows: The reaction flask containing a nitrogen atmosphere after three vacuum/N_2 cycles was charged with the volumetric amount of 1.0 and 0.2 equivalents of CO_2, respectively, *via* a syringe through a septum. The syringe was purged with CO_2 gas thrice prior to use. The necessary amount was calculated according to the ideal gas law:

$$pV = nRT$$

The temperature in the laboratory was measured to be 20 °C and the pressure was estimated to be 1 atm = 101325 Pa. This is an example calculation for the case of 1.0 equivalent of CO_2 with the scale of the reaction being 0.2325 mmol:

$$V = \frac{nRT}{p} = \frac{0.2325 * 10^{-3}\ mol * 8.314\ kg\ m^2 * 293.15\ K\ m\ s^2}{101325\ s^2\ mol\ K\ kg}$$

$$= 5.6 * 10^{-6}\ m^3 = 5.6\ mL$$

3.2.1.2 Scope of Substrates

With the optimized reaction conditions at hand, a wide variety of primary alcohols was converted to the corresponding aldehydes (**Scheme 26**). A number of different aromatic alcohols in benzylic position or with a prolonged π electron system (*i.e.* cinnamyl

alcohol derivatives) have shown good to excellent reactivity. Among them, substrates with *meta*- and *para*-functionalization bearing electron-donating functional groups (methoxy, benzyloxy and *tert*-butyl groups, **58a** – **62a**, **65a**, **67a**, **69a**) reacted well and also one electron-withdrawing example was found to give 72% yield (**57a**), whereas a nitro group in *meta* position only resulted in 41% (**68a**).

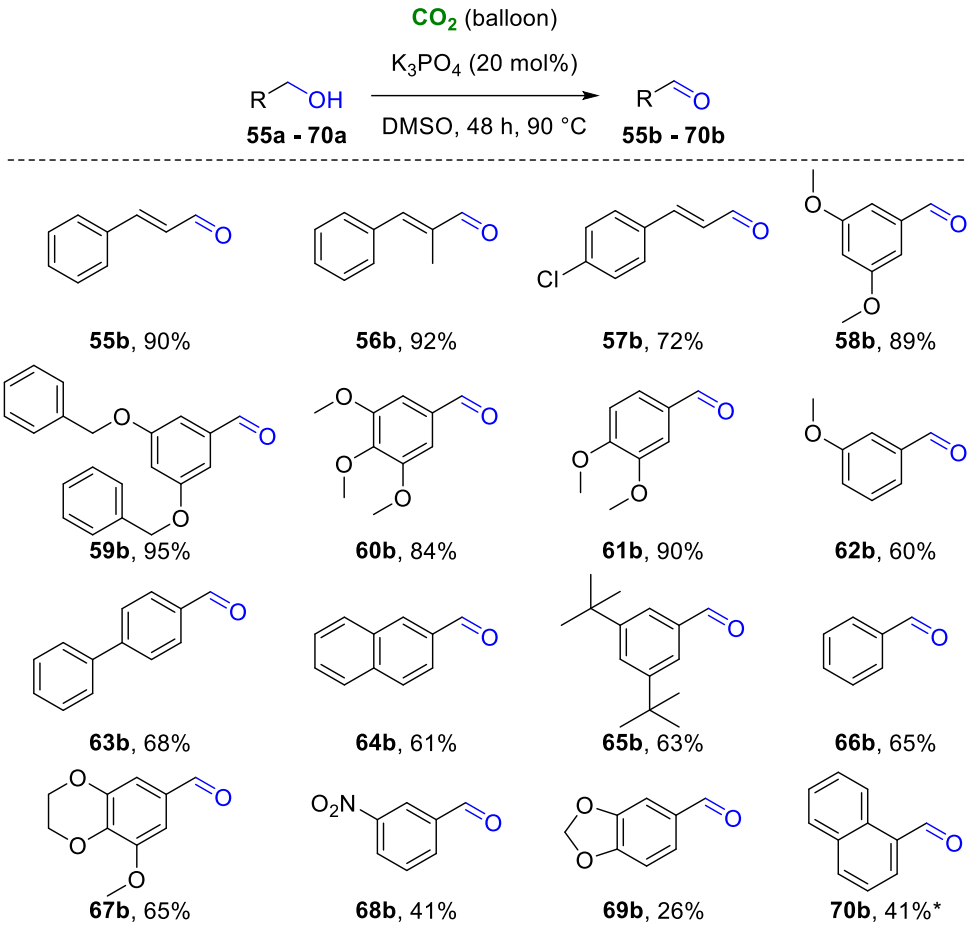

Scheme 26: General scope of substrates for CO_2-assisted oxidation of primary alcohols; reaction conditions: substrates (0.25 mmol), K_3PO_4 (20 mol%), DMSO (2.5 mL), CO_2 (balloon), 90 °C, 48 h; except for **70a** all are isolated yields; *yield determined by ^{1}H NMR spectroscopy using iodoform as internal standard; 1 eq K_3PO_4 was used in case of **57a** and **68a**.

Condensed ring systems (naphthalene derivatives **64a** and **70a**) somehow slightly hampered the reaction yielding only 61% and 41%, respectively. Steric crowding can only account for that to some extent when **64a** and **70a** are compared directly with each other so that electronic effects should play the major role. In contrast, another example is the sterically slightly more crowded cinnamyl alcohol derivative **56a**, which reacted in a similar fashion compared to the non-substituted cinnamyl alcohol **55a**. Again, for none of the tested substrates any over-oxidized products in the form of carboxylic acids could be observed.

Notably, veratraldehyde (**61b**) is an important intermediate during the synthesis of a variety of drug molecules (**Scheme 27**). Among them, one can find verazide, a potential anticancer and antimicrobial agent,[129] amiquinsin for hypotensive treatment,[130] toborinone for the treatment of heart failure and other diseases, such as cancer, allergies, anoxia etc.,[131] the bronchodilators hoquizil and piquizil,[132] a hallucinogenic amphetamine, the vasodilator vetrabutine,[133] prazosin used for the treatment of sleep disorders[134] and the Ca^{2+} channel blocker dimeditiapramine.[135] Even in 5 mmol scale, **61b** was obtained in the same yield of 90% compared to smaller scale without further precaution opening up the possibility for a plethora of follow-up reactions in a greener way.

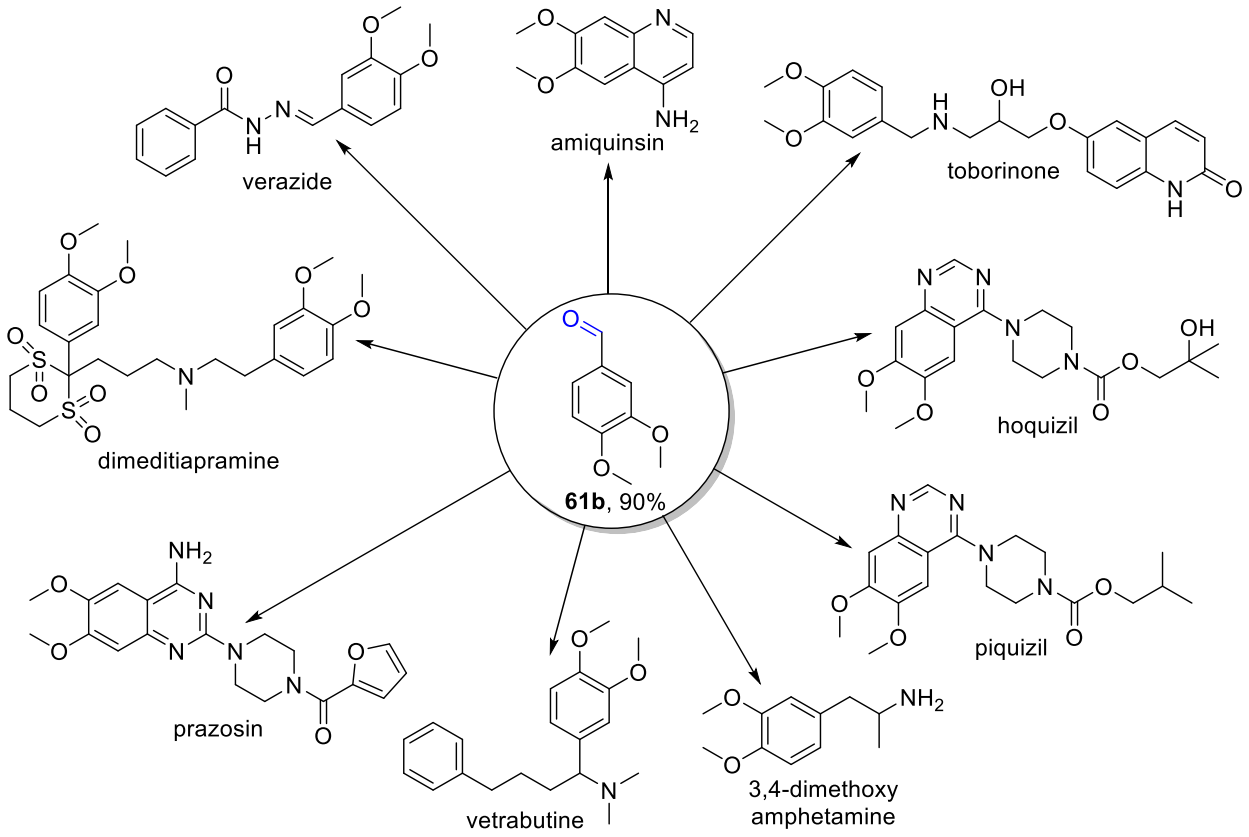

Scheme 27: Key importance of veratraldehyde (**61b**) as pharmaceutical intermediate.

In case of secondary alcohols, shown in **Scheme 28**, a number of symmetrically and non-symmetrically substituted diphenyl methanol derivatives (**73a** – **78a**, **84a** – **86a**) reacted well to their corresponding ketones: Again, *meta*- and *para*-substitution are well tolerated regarding electron-withdrawing (**74a** – **76a**) and electron-donating groups (**77a** – **78a**). Even o*rtho*-substitution, which was not tolerated in case of primary alcohols, with a +I substitutent (**77a**) reacted in 70% yield. Not surprisingly, four examples of secondary cinnamyl alcohol derivatives gave good yields (**71a** – **72a**, **88a** – **89a**). Additionally, different cyclic secondary alcohols in benzylic position with

different ring sizes ranging from 5- to 7-membered rings were converted to their corresponding ketones (**79a** – **83a**). Heteroaromatic compounds with N, O and S as heteroatoms gave nearly quantitative yields (**84a** – **87a**).

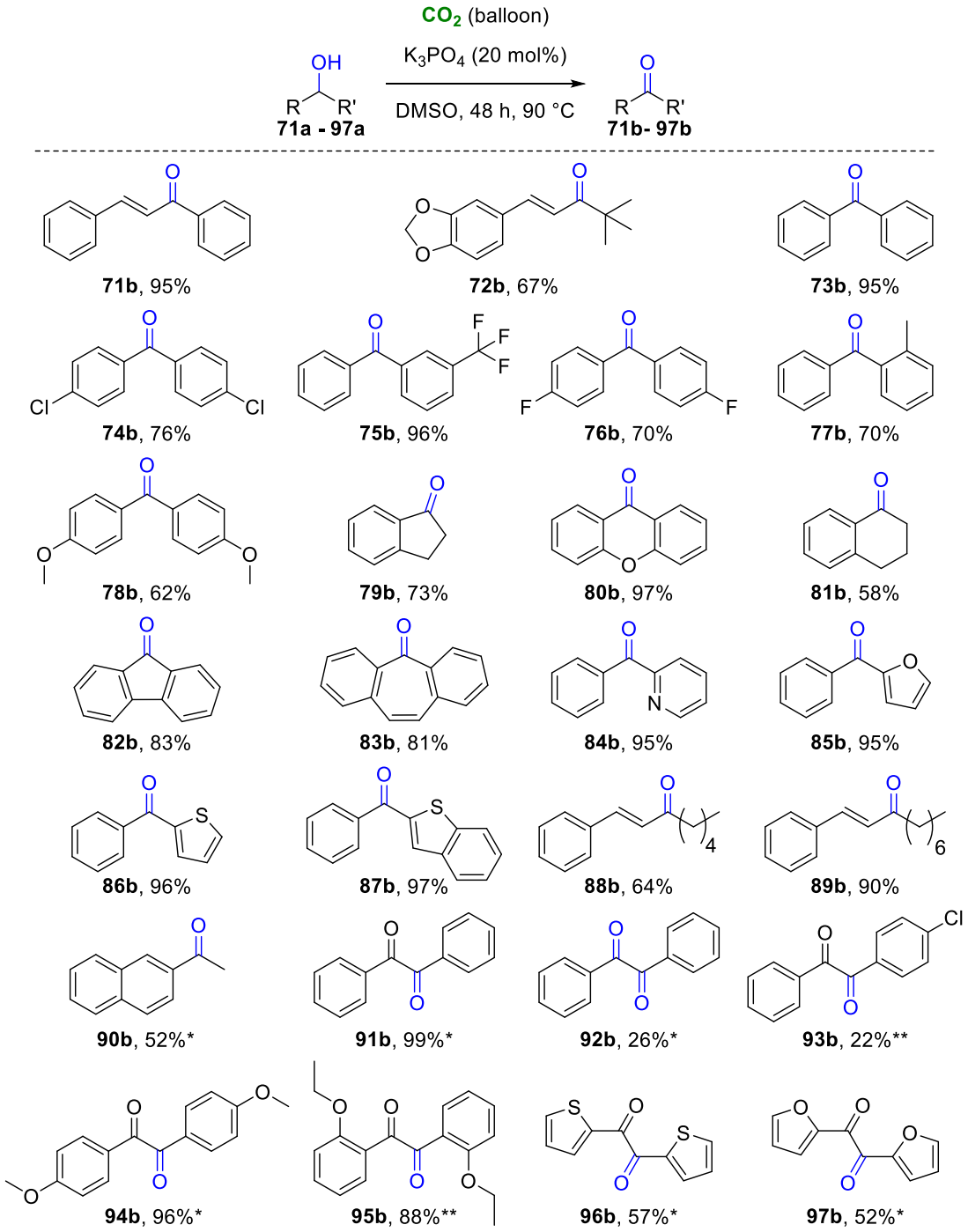

Scheme 28: General scope of substrates for CO_2-assisted oxidation of secondary alcohols; reaction conditions: substrates (0.25 mmol), K_3PO_4 (20 mol%), DMSO (2.5 mL), CO_2 (balloon), 90 °C, 48 h; except for **90a** – **97a** all are isolated yields; *yield determined by GC using *n*-dodecane as internal standard; **yield determined by ^{1}H NMR spectroscopy using iodoform as internal standard; 1 eq K_3PO_4 was used in case of entries **85a** and **87a**.

Four examples of secondary alcohols with only simple aliphatic residues at one side are also included (**72a**, **88a** – **90a**) bearing either branched or alkyl chain groups. Compared to primary alcohol **64a** the similar secondary counterpart **90a** gives a 9% lower yield probably due to higher steric hindrance. Diaromatic ketols gave mostly quantitative yields when no or electron-donating substituents at the aromatic ring were present (**91a**, **94a**, and the sterically more crowded substrate **95a**) whereas an electron-donating substituent (**93a**) strongly diminished the obtained yield.

Diol **92a** was difficult to oxidize, even when the amount of K_3PO_4 was doubled. In contrast to the heteroaromatic substrates with one simple alcohol functional group, which are discussed above (**84a** – **87a**), the heteroaromatic ketol substrates **96a** – **97a** only gave moderate yields. Probably, the electron-donating ability of those heteroaromatic rings is lower due to the keto groups and the electron-withdrawing ability of the heteroatoms O and S, thus reducing the overall electron density at the hydroxyl group and slowing down their reaction.

Notably, ketene products like **71b** – **72b** and **88b** – **89b** can be used for further reactions toward interesting scaffolds. It is known that catalytic amounts of NHCs and equimolar amounts of organic bases are sufficient for the reaction of such ketenes with benzyl bromides forming tertiary enols.[136] Moreover, excess amounts of *N*-hydroxy-4-toluenesulfonamide can react with ketenes under presence of excess amounts of simple bases (*e.g.* K_2CO_3) to isoxaline derivatives, which are an important intermediate for the synthesis versatile heterocyclic scaffolds like isoxazoles, *γ*-amino alcohols and *β*-lactams (*cf.* **Scheme 10**).[137]

Furthermore, potentially oxidizable functional groups such as thiomethyl and aldehyde substituents were grafted onto the aromatic ring of the corresponding alcohol substrates because gaining a high selectivity especially for oxidation reactions plays an important role within the (sustainable) synthesis of natural products or pharmaceuticals (**Scheme 29**).[48a,63–64,138] Delightfully, these functional groups were well tolerated under optimized reaction conditions (**98a** and **103a**). Moreover, different other functional groups, namely ester (**102a**), nitrile (**99a**), nitro (**101a**), alkyne (**100a**) and alkene groups (**101a**) grafted onto the aromatic ring of the corresponding alcohol substrates reacted in good to excellent yields. It is noteworthy to say that in none of the cases any over-oxidized or carboxylated byproducts could be observed. These combined experimental findings clearly demonstrated the strong synthetic potential of this oxidation system.

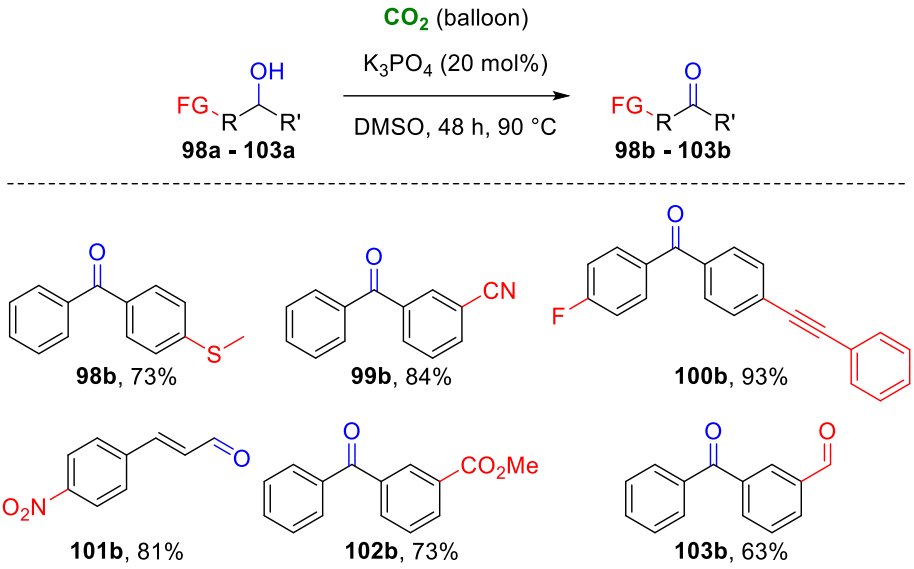

Scheme 29: Functional group selectivity during oxidation reactions; reaction conditions: substrates (0.25 mmol), K_3PO_4 (20 mol%), DMSO (2.5 mL), CO_2 (balloon), 90 °C, 48 h; all are isolated yields; 1 eq K_3PO_4 was used in case of **101a**.

In general, only aromatic alcohols or such with an aromatically extended π electron system (such as cinnamyl alcohol derivatives) were reactive under these reaction conditions. Compounds with only aliphatic chemical surrounding at the hydroxyl group did not show any activity (**Scheme 31**). Unfortunately, not all tested aromatically activated alcohols exhibited reactivity as shown in the following section. **Scheme 30** and **31** display substrates that have at least one primary alcohol functionality, whereas **Scheme 32** shows exclusively secondary alcohols.

Scheme 30 is roughly divided into substrates with functional groups causing a –I (**104a** – **119a**) or +I effect (**127a** – **133a**), condensed ring systems (**135a** – **137a**) and heteroaromatics (**138a** – **142a**). When different aromatically activated alcohols were tested, nitrile groups seem to completely prohibit the reaction (**104a** – **105a**) unless a second activating aromatic ring is present as in case of substrate **99a**. In contrast to the already successfully tested chloro-substituted secondary alcohol substrates **57a** and **74a**, bromo and fluoro substitution precludes any reaction (**106a** – **111a**) as well as chloro substitution at primary alcohol substrates (**115a** – **117a**). Only when a single fluoro atom was present at *para* position, poor product formation could be observed (**112a**). Unfortunately, poly-brominated and poly-fluorinated substrates **107a** – **108a** did not exhibit any activity either, thus blocking the way toward a possible application on PTFE-related polymers. In contrast to trifluoromethylated secondary alcohol **75a**, primary alcohols with that functional group exhibited poor to no reactivity (**113a** – **114a**): Around 30% of **114b** were observed (according to GC-MS estimation)

but only after prolonged reaction time of 88 h. Compared to *para*-nitro cinnamyl alcohol (**101a**), its benzyl alcohol analog **118a** did not exhibit any reactivity. Double aromatically activated **77a** endures *ortho* substitution with a loss in yield (*cf*. **73a**) whereas *ortho* substitution at primary aromatic alcohols inhibits the reaction (**115a** – **116a**, **122a**, **124a**, **126a** – **127a**, **132a**).

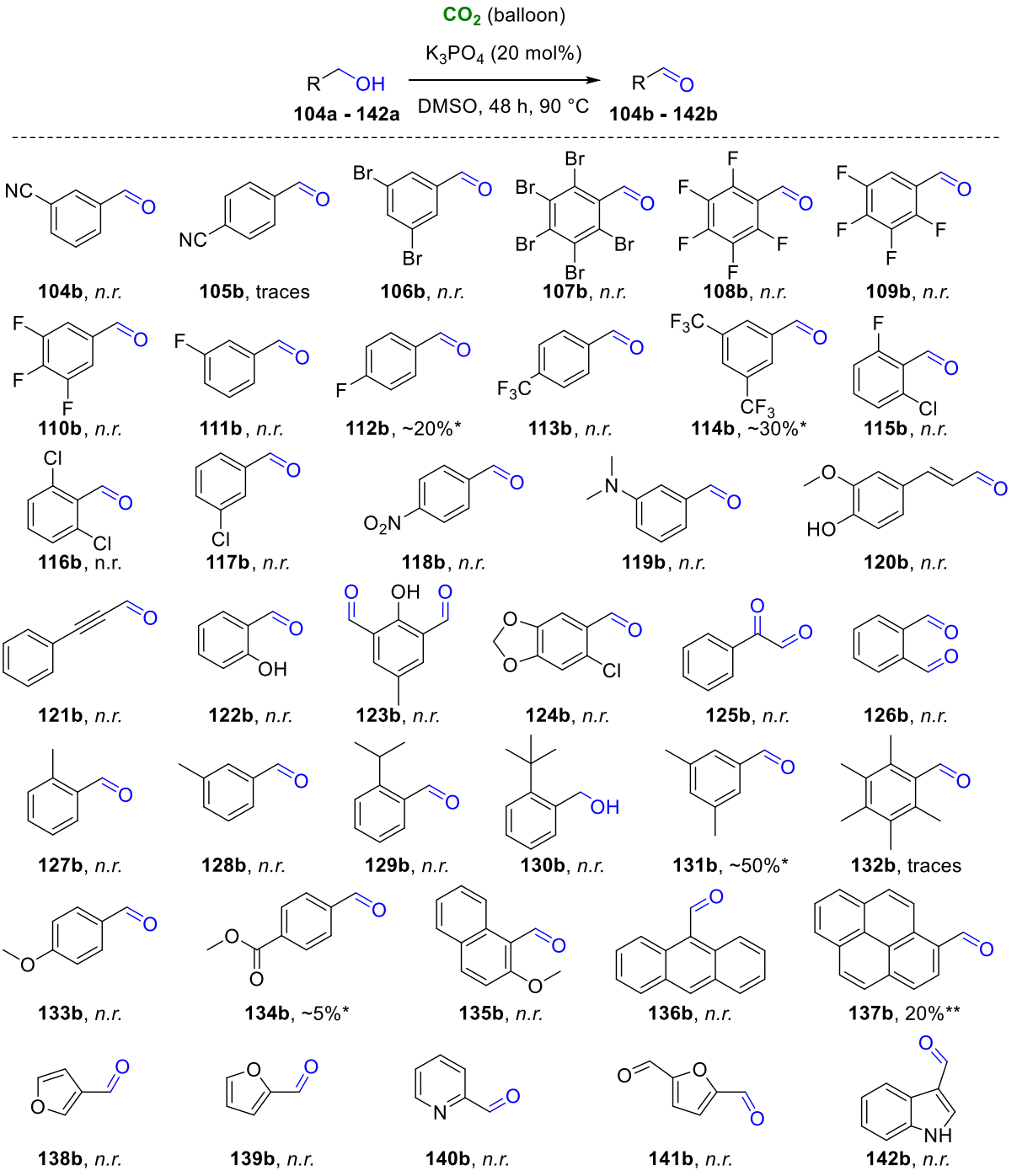

Scheme 30: Scope of unsuccessful aromatically activated primary alcohol substrates; reaction conditions: substrates (0.25 mmol), K_3PO_4 (20 mol%), DMSO (2.5 mL), CO_2 (balloon), 90 °C, 48 h; reaction progress monitored by GC-MS; *yield estimated by GC-MS; **yield determined by ^{1}H NMR spectroscopy using iodoform as internal standard.

When hydroxyl groups were present directly at the aromatic ring, the reaction was completely suppressed as can be seen for **120a** and **122a** – **123a**. Unfortunately, the electronic situation within the π system of a double and triple bond is too different so that the latter one did not provide a sufficient electron density at the hydroxyl group (**121a**). Substrates with two oxidizable hydroxyl groups did neither show oxidation products of one nor two of these groups (**123a**, **125a** – **126a**).

In contrast to sufficiently converted substrates bearing electron-donating methoxy (excluding **133a**) or benzyloxy groups, electron-donating alkyl groups hampered the reaction (**127a** – **132a**). A possible reason is the additional beneficial +M effect having its seeds in the lone pair of the oxygen atom of alkoxy groups, which is not present in case of alkyl moieties. Only double *meta* alkyl substitution (**131a**, *cf*. also double *tert*-butyl-substituted benzyl alcohol **65a**) gave a reasonable amount of product. Unfortunately, the purification if **131b** was not successful since the expected product aldehyde was lost due to its low boiling point (64 °C at 2 mbar). While single, double and triple substitution with a methoxy group at *meta* or *meta* and *para* position resulted in good to excellenct yields (*cf*. with **58a** and **60a** – **62a**), substitution only at *para* position did not show any reactivity (**133a**). The same scheme of the inhibiting effect of a *para* substitution applied to carbonic acid esters as well (*cf*. **102a** and **134a**).

Only two examples of condensed aromatic ring systems showed reactivity, namely 1- and 2-naphthyl methanol (**64a** and **70a**, respectively). When a methoxy group was grafted onto the naphthalene ring in *ortho* position (**135a**) or higher order condensed ring systems such as anthracene (**136a**) and pyrene (**137a**) were used though, the reaction rate was quite low. In contrast to heteroaromatic secondary alcohol substrates including furyl, thiophenyl and benzothiophenyl examples (**85a** – **87a**, **96a** – **97a**), primary heteroaromatic alcohols (including furyl, pyridyl and 1*H*-indolyl) were not converted to the corresponding aldehydes (**138a** – **142a**).

Scheme 31 shows substrates with at least one aliphatic oxidizable hydroxyl group. In case of **143a** – **145a**, phenyl rings are separated from the hydroxyl group by an additional CH/CH_2 group and a keto group, respectively. Furthermore, cyclohexyl (**146a**) as well as simple linear (**147a** – **152a**, **154a** – **155a**) or branched (**153a**) alkyl alcohols did not show any reactivity at all, not even when an ether or nitro group was present (**153a** – **154a**) or when the hydroxyl group was in conjugation with a π electron pair for a possible activation (**152a**). Additionally, the possible products **145b**, **147b** and **154b** – **155b** could not be detected due to limitations of the used GC-MS system (either

too high polarity or too low boiling points). Especially **155a** (*D*-sorbitol) would have been an interesting target since it is a commonly used sweetener but also a natural product appearing in fruits like apples and peaches or can be also produced from cellulose and lignocellulose.[139] **156a** can be seen as model substrate for greater lignin polymers and would have opened up another avenue toward natural product manipulation.[140] Unfortunately, only traces of a single oxidized product were found, presumably the ketone product since the secondary alcohol is activated by the dimethoxy phenyl group (*cf.* **61a**), whereas the primary alcohol group is located in an alkyl surrounding (*cf.* **144a**).

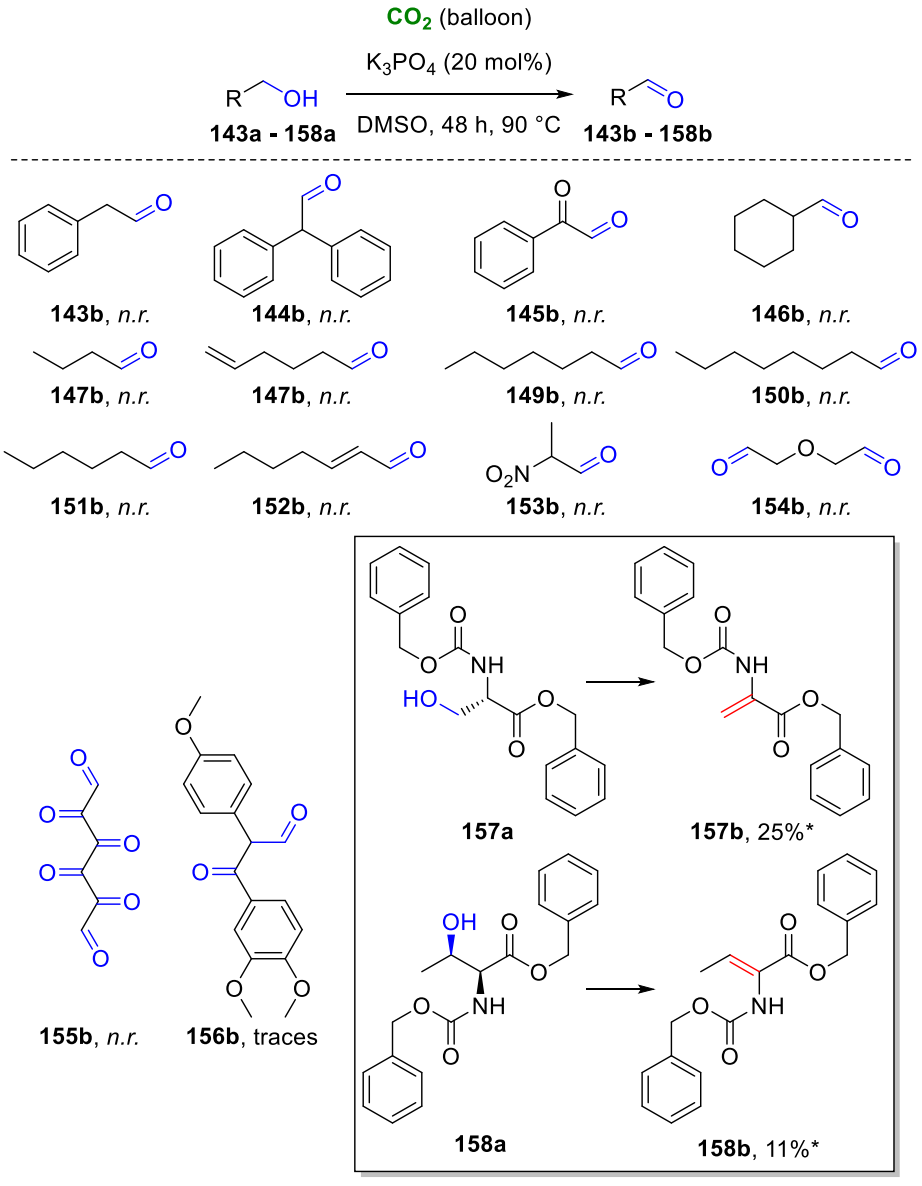

Scheme 31: Scope of unsuccessful aliphatic primary alcohol substrates; reaction conditions: substrates (0.25 mmol), K_3PO_4 (20 mol%), DMSO (2.5 mL), CO_2 (balloon), 90 °C, 48 h; reaction progress monitored by GC-MS; *yield determined by ^{1}H NMR spectroscopy using iodoform as internal standard.

An interesting outcome was seen after careful evaluation of the reaction mixtures of **157a** – **158a**, two aromatic CBz-protected derivatives of serine and threonine, which are essential proteinogenic *α*-amino acids. After purification of the compound and comparison with ESI mass spectra, it was reasonable that a dehydration reaction has occurred. Through the elimination of a water molecule a terminal and internal C=C double bond were formed, respectively. On the one hand, this type of reaction is known at room temperature with bases like DBU and DMAP and *para*-toluenesulfonyl chloride, which reacts with the hydroxyl group to a tosylate, which then has to be deprotected again.[141] On the other hand, at elevated temperature it is also known in polar solvents like DMF with DMAP as base (*e.g.* with 2 eq K_2CO_3 in DMF at 65 °C 84% yield could be obtained after 1 h[142]). Thus, in case of serine derivative **157a** different bases were tried under otherwise optimized reaction conditions (DMSO, 90 °C, 16 h). Among (bi)carbonates, hydroxides, alcoholates and organic bases like DBU and 1,4-diazabicyclo[2.2.2]octane (DABCO), 1 eq LiOH resulted in the highest obtained yield of 15%. Higher base equivalents did not increase the yield significantly. When molecular sieves were added for capturing the byproduct water, the yield could be slightly increased to 19%. Since a base was used, the aqueous workup of the reaction mixture was conducted with 1M HCl instead of distilled water thus further increasing the obtained yield to 27%. Because the reaction also worked under N_2 atmosphere (but only up to 15% yield) and traditional screening approaches did not culminate in a satisfying yield this excursus was cancelled though. In addition, initial screening with threonine derivative **158a** only gave a maximum of 11% yield after prolonged reaction time and elevated temperature (100 °C, 48 h) with otherwise optimized conditions.

In **Scheme 32** exclusively secondary alcohols are summarized. Completely aliphatic alcohols (**159a** – **164a**) did not show any reactivity under optimized reaction conditions as expected from previously examined primary alcohols.

When only one side of the secondary alcohol functional group was aromatically activated, minor reactivity could be observed solely in case of a short alkyl chain. For instance, product formation could be seen for methyl substitution (**165a**) but with a less strong aromaticity compared to **90a** and thus lower reactivity. In contrast, trifluoromethyl substitution (**172a**) hampered the reaction completely. Longer alkyl chains or alicyclic moieties were not tolerated (**166a**, **173a**), not even when methoxy groups as substituents with +M and +I effect (**167a** – **168a**, **174a**) or additional non-aromatic π electrons on the other side (**171a**) were present. The possible product **169b** cannot be

detected by GC-MS. However, no trace of that product could be observed by ^{1}H and ^{13}C nuclear magnetic resonance (NMR) spectroscopy either.

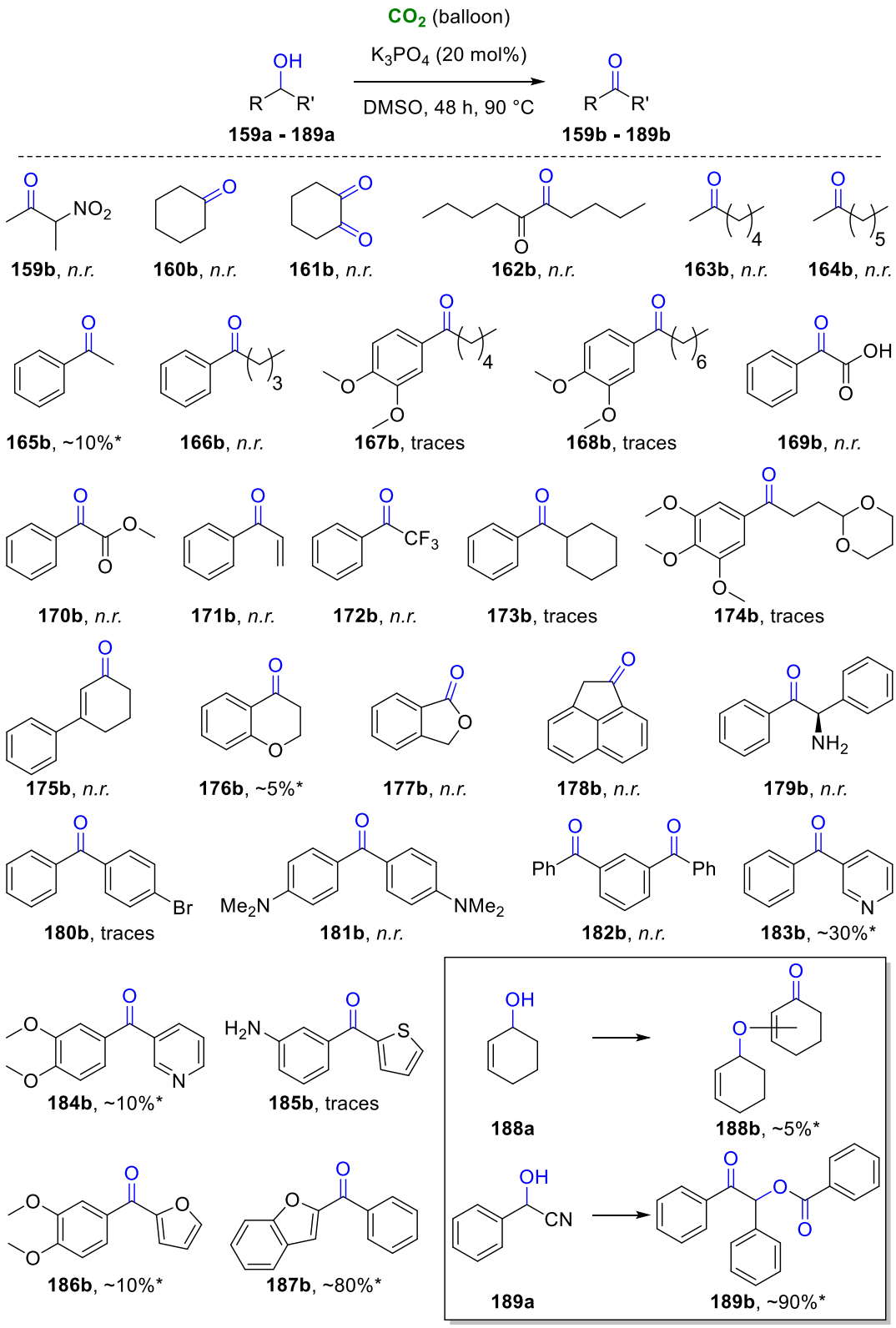

Scheme 32: Scope of unsuccessful secondary alcohol substrates; reaction conditions: substrates (0.25 mmol), K_3PO_4 (20 mol%), DMSO (2.5 mL), CO_2 (balloon), 90 °C, 48 h; reaction progress monitored by GC-MS; *yield estimated by GC-MS.

Additionally, methyl ester derivative **170a** was not reactive, too. Surprisingly, **175a** as alicyclic-substituted cinnamyl alcohol derivative was not reactive at all. Different ring sizes of fused ring systems exhibited poor to no reactivity (**176a** – **178a**).

Albeit some diphenyl methanol and benzoin derivatives showed good to excellent yields previously (**73a** – **78a**, **84a** – **87a**, **91a** – **100a**, **102a** – **103a**), other substitution patterns hampered the reactivity: In case of substrates **179a** and **185a**, a possible competing side reaction could be the carbamate formation at the amino function in the presence of base and CO_2, forming a carbamate anion *in situ* and thus deactivating the hydroxyl group for further oxidation reaction. In contrast to *bis-meta* chloro- and fluoro-substituted **74a** and **76a**, respectively, only traces of ketone product were observed from single bromo-substituted substrate **180a**. *Bis-meta* trimethylamino-substituted **181a** was not reactive under optimized conditions. Unfortunately, when substrate **182a** was used neither single nor double oxidation products could be detected. When 3-pyridyl compound **183a** was used instead of 2-pyridyl substrate **84a**, reactivity was low and surprisingly dropped further when methoxy groups were introduced (**184a**). The same effect applied to substrate **186a** compared to **85a**. A purification issue prohibited obtaining the pure product **187b**. Although the GC-MS spectrum was promising (analog to benzothiophene derivative **87a**), obtaining the keto product was not possible even after a second column chromatography.

An interesting observation was made when simple 1-cyclohexen-2-ol (**188a**) was used: GC-MS and high resolution mass spectrometry (HRMS) implied that there was a keto dimer formed instead of simple oxidation to cyclohexanone, which was not present in the commercial starting material. Unfortunately, the reaction occurred only to a small extent prohibiting further analysis. However, there are no reactions known (according to SciFinder) leading to a dimer regardless of the ether's substitution position at the 1-cyclohexen-2-one ring.

Another product, that was unexpected at first glance, was found when 2-hydroxy-2-phenylacetonitrile (**189a**) was subjected to the reaction system. Most of the starting material was trimerized and doubly oxidized into product **189b**, which was verified by HRMS: *m/z* calcd. for $C_{21}H_{16}O_3$ [M+H$^+$]: 317.1172, found: 317.1171; *m/z* calcd. for $C_{21}H_{16}O_3$ [M+Na$^+$]: 339.0992, found: 339.0995; *m/z* calcd. for $C_{21}H_{16}O_3$ [M+K$^+$]: 355.0731, found: 355.0723. Besides, benzoin (**91a**) and benzil (**91b**) as well as **189b II** were observed in trace amounts as byproducts. The most likely underlying mechanisms should be rather simple though and are depicted in **Scheme 33**. **Path a** of

Scheme 33 describes the well-known Schotten-Baumann reaction, which occurs under elevated pH values as present in the actual reaction system:[143] First, **189a** is oxidized to benzoyl cyanide (**189b I**) as intermediate under optimized oxidation reaction conditions. This reacts with another substrate **189a** to the benzoic acid ester derivative **189b II**, which was found as byproduct in trace amounts. The cyanide functional group is known to behave as pseudohalide and thus the reactivity of 2-hydroxy-2-phenylacetonitrile is expected to be similar to benzoyl chloride. **Path b** describes another well-known reaction, the benzoin condensation in which two equivalents of **189a** decompose spontaneously[143] in the presence of a base to benzaldehyde (**66b**) and KCN. Cyanide salts are known to catalyze benzoin condensation reactions yielding benzoin (**91a**). This can either be further oxidized under optimized reaction conditions to benzil (**91b**, *cf.* **Scheme 28**) or being deprotonated by a base and react with intermediate **189b I** while the nitrile group in the presence of a base again acts as pseudohalide finally releasing trimer product **189b**. Alternatively, catalytic amounts of base are sufficient to deprotonate DMSO, which could attack **91b** forming a reactive anionic epoxide intermediate, which then reacts with aldehyde **66b** to **189b**, too. This latter reaction was published by Bortolini *et al.* in 2013.[144]

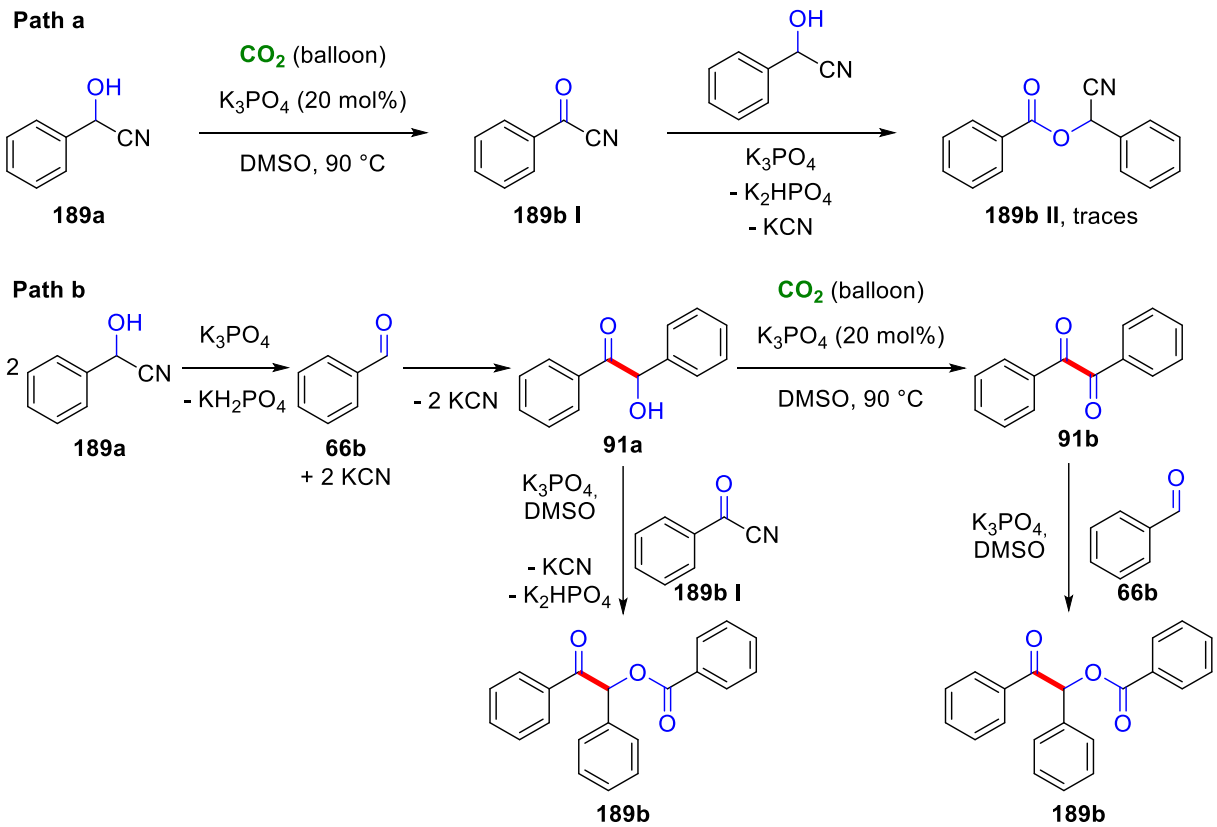

Scheme 33: Reaction details and possible pathways for the reaction of substrate **189a**.

When the reaction was repeated with different temperatures and bases and under N_2 atmosphere, respectively, the amount of benzoin and benzil in the product mixture could be increased in some cases. However, **189b II** was only observed in trace amounts regardless. Notably, benzaldehyde (**66b**) was detected as intermediate *via* GC-MS but not ketone **189b I**, since it is known to decompose in contact with water (during aqueous workup or within the reaction mixture with water formed as byproduct) to phenylglyoxylic acid, which is water-soluble and cannot be detected using GC-MS either. However, the oxidative trimerization of benzaldehydes is known in literature: For instance, Cheon *et al.* published the trimerization of aldehydes with equimolar amounts of NaCN as additive in polar solvents (especially DMSO) and under water-free conditions (molecular sieves). They found that **91a** readily reacts quantitively with **189b I** to **189b** without addition of cyanide salts. A possible application of this trimer was shown as the reaction with thiourea to the heteroaromatic scaffold compound 2,4,5-triphenyl-1,3-oxazole.[145]

3.2.1.3 Application of the Synthetic Alcohol Oxidation Protocol

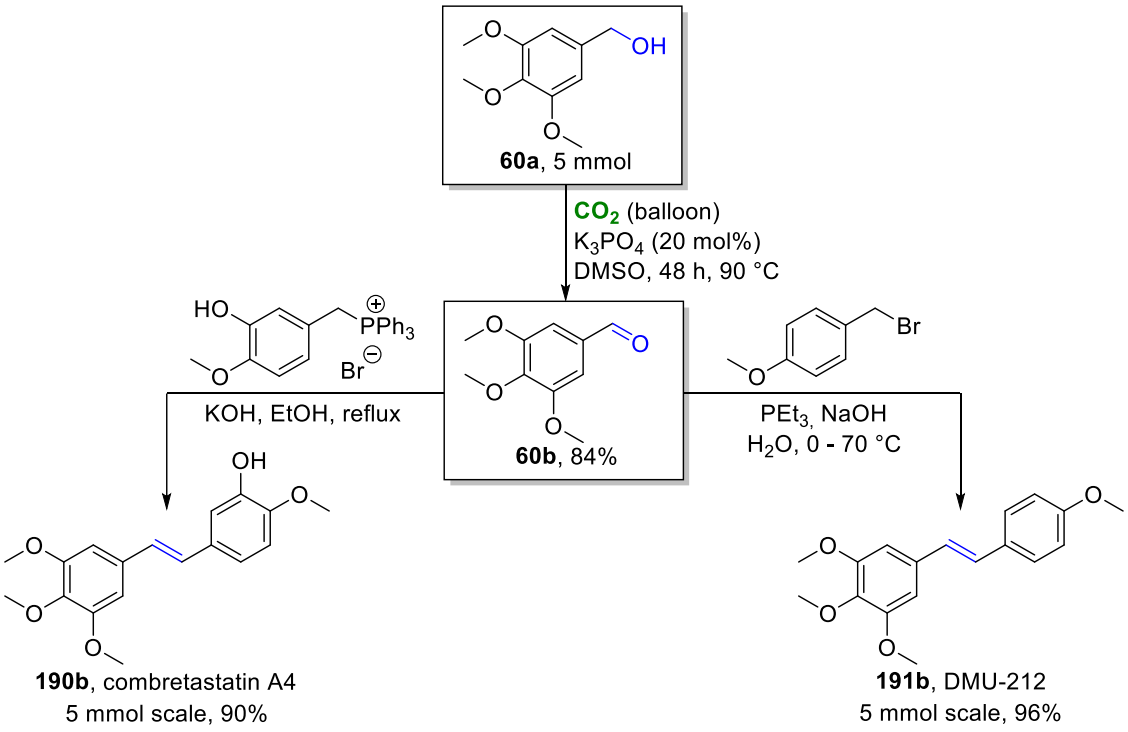

Scheme 34: Transition metal-free synthesis of combretastatin A4 and DMU-212 based on the oxidation of **60a** on large scale.

With this selective oxidation protocol at hand, the next step was to develop a transition metal-free synthesis of pharmaceutically active drug molecules. For that purpose, combretastatin A4, a potent microtubule-targeting and vascular damaging agent, which has been used for cancer chemotherapy,[146] and DMU-212, a pharmaceutical drug used for breast cancer treatment,[147] were chosen as examples. Both drug molecules were successfully synthesized using literature-known procedures after achieving the intermediate 3,4,5-trimethoxybenzaldehyde (**60b**) in 5 mmol scale starting from 3,4,5-trimethoxybenzyl alcohol (**60a**) with the developed reaction protocol (**Scheme 34**). After the oxidation of the alcohol susbtrate succeeded, both drug compounds were synthesized in nearly quantitative yields *via* Wittig reaction.[148]

Moreover, another interesting reaction is the transition metal-free homologation of *α,β*-unsaturated aldehydes (**Scheme 35**). The corresponding homologated products possess structural similarities with a huge number of different natural products such as navenone B, 11-*cis*-retinal or the promising antioxidant and aromatic dicarboxylate carotenoid synechoxanthin, which was just isolated from a cyanobacterium in 2008, etc.[149] Hence, commercialization interests are obvious, too.[150] In order to point toward these conjugated and unsaturated long-chain structures utilizing the developed oxidation method, the homologation sequence started from cinnamyl alcohol (**55a**), which was oxidized to cinnamaldehyde (**55b**). It then underwent addition of vinyl magnesium bromide followed by hot water rearrangement (according to literature procedure[151]). This rearrangement is shortly discussed here (**Scheme 36**).[152]

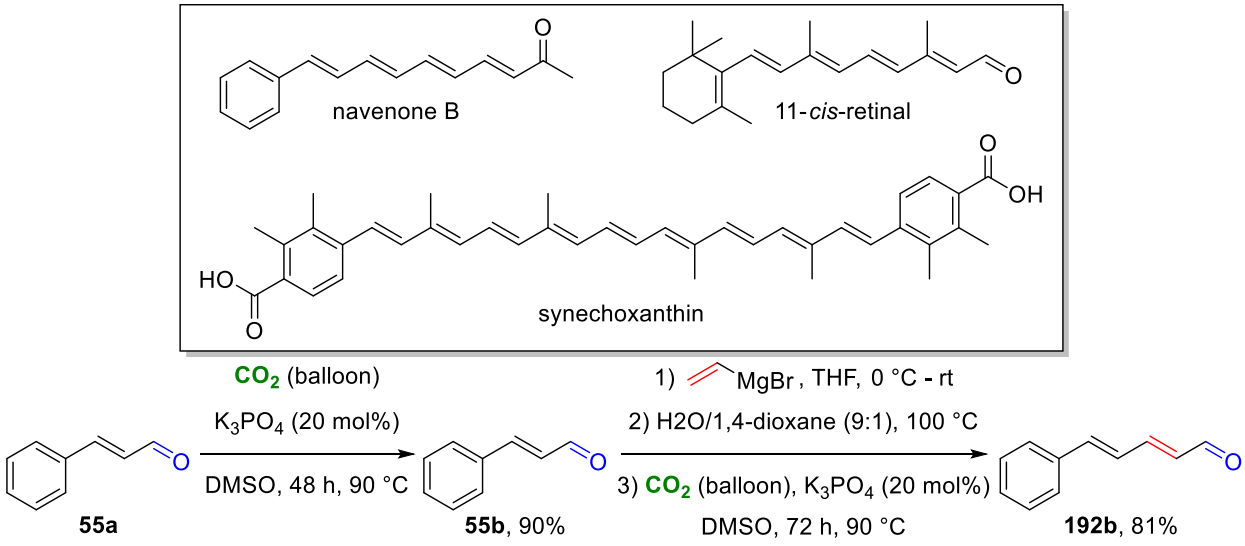

Scheme 35: Transition metal-free homologation of *α,β*-unsaturated aldehydes; all are isolated yields.

55b reacts with the nucleophile Grignard reagent and after an aqueous workup the secondary alcohol **192b I** is obtained in 95% yield. This secondary alcohol undergoes a so-called hot water rearrangement in boiling water, which gives the primary alcohol **192b II** *via* a carbocation in 90% yield. Both **192b I** and **192b II** were isolated and NMR spectra were measured (see appendix). Finally, **192b II** was oxidized again using CO_2 as promoter leading to the corresponding homologated *α,β*-unsaturated aldehyde **192b** with 95% yield. The overall yield is thus 81% (over 3 isolated steps) and still 73% including the prior oxidation step. This serves as a proof of concept for the future strategy of synthesizing aromatic polyenes from commercially available and cheap starting materials and reagents in a sustainable transition metal-free reaction pathway. Similar iterative synthesis strategies including alkene chain extension and subsequent rearrangement steps yielding polyenes are known in literature as well. An example for that is the natural product synthesis of the already mentioned retinal (see **Scheme 35**) by Burke *et al.*, who synthesized retinal from a boronic acid *via* double cross-coupling utilizing a well-defined Pd catalyst and rearrangement reaction, respectively.[153]

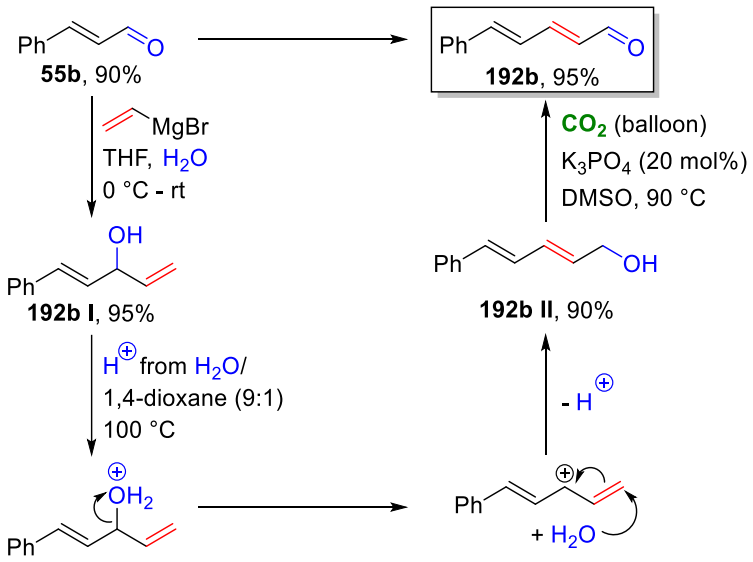

Scheme 36: Detailled mechanism of the reaction from cinnamaldehyde to *α,β*-unsaturated aldehyde **106b**; all are isolated yields.

3.2.1.4 Mechanistic Studies

After this extensive exploration of the scope of substrates and revealing examples of possible applications of this CO_2-promoted alcohol oxidation protocol, the examination of the actual role of CO_2 within this reaction system was the obvious next target. A

summary of the conducted control and labeling reactions is shown in **Scheme 37** with cinnamyl alcohol as model substrate.

The important role of CO_2 was revealed when N_2 and O_2 atmospheres were applied, since no or negligible oxidation products could be observed, respectively (**Scheme 37**, **(A – B)**). In the literature it is reported that CO_2 involved in oxidation reactions can be consumed while being reduced, *e.g.* to methanol.[154] However, in the herein presented case only CO_2 was observed in the headspace of the reaction atmosphere but no other reduction products of CO_2 (*e.g.* CO, formic acid/formate) neither *via in situ* gas phase GC nor by NMR spectroscopy (see **Figure 14** in the appendix).

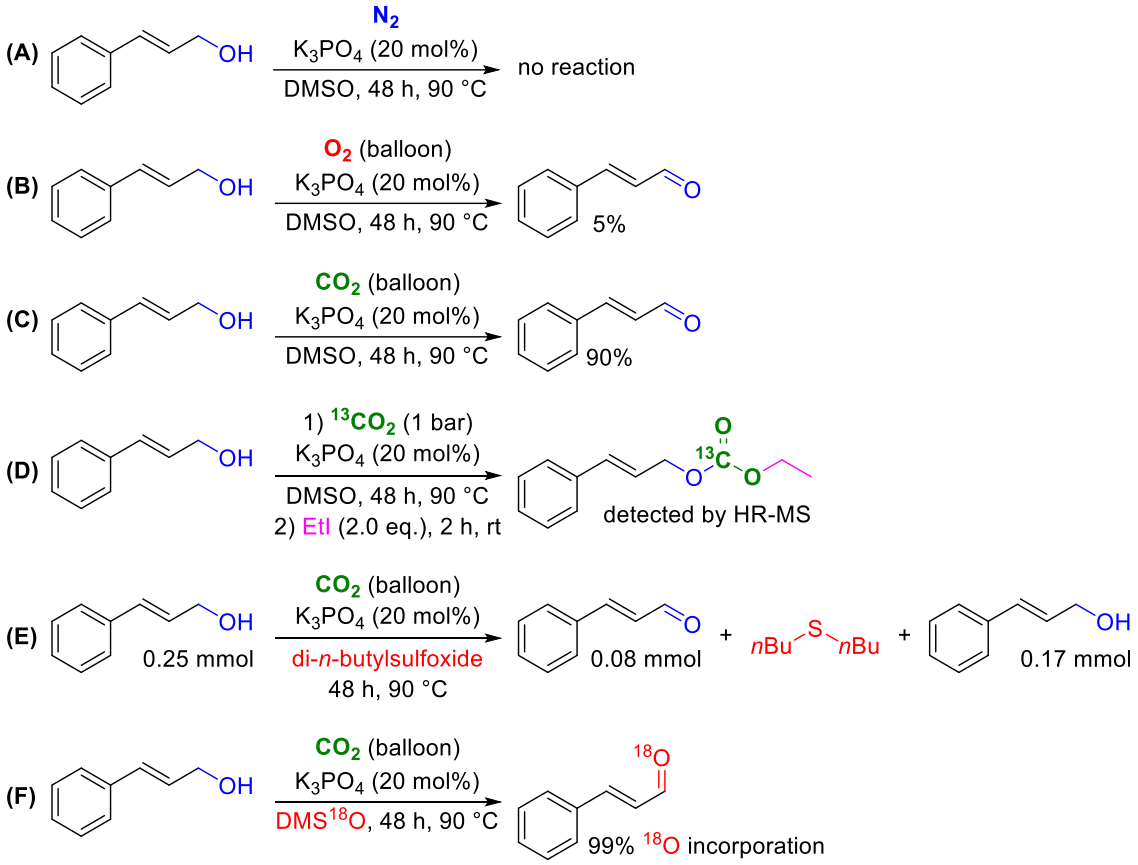

Scheme 37: Control and labeling experiments for the CO_2-promoted oxidation of cinnamyl alcohol; reaction under N_2 atmosphere **(A)**, reaction under O_2 atmosphere **(B)**, optimized reaction conditions for comparison **(C)**, trapping of the carboxylate intermediate **(D)**, reaction with di-*n*-butylsulfoxide as actual oxidant **(E)**, ^{18}O labeling with DMSO^{18}O **(F)**.

It is well known that CO_2 can bind to hydroxyl moieties forming the corresponding *O*-carboxylated intermediate. Unfortunately, observation of an *O*-carboxylated intermediate anion was not possible under $^{13}CO_2$ atmosphere due to its instability within the reaction system.[20e,21] However, addition of EtI after the reaction successfully trapped the corresponding ^{13}C-labeled cinnamyl ethyl carbonate (**Scheme 37**, **(D)**), which was

evidenced by liquid chromatography-coupled electrospray ionization high resolution mass spectrometry (**LC-ESI-HRMS**) in good agreement with calculated masses for the respective adduct cations: *m/z* calcd. for $C_{11}{}^{13}CH_{14}O_3$ [M+H$^+$]: 208.1049, found: 208.1046; *m/z* calcd. for $C_{11}{}^{13}CH_{14}O_3$ [M+Na$^+$]: 230.0869, found: 230.0870.

In order to furnish proof about the actual oxidant, DMSO was replaced by di-*n*-butyl-sulfoxide, which was reduced to di-*n*-butylsulfide in equimolar ratio regarding cinnamaldehyde (**Scheme 37**, **(E)**). Besides, it should be noted that DMS can be found, too (when DMSO was used), but because of the low boiling point of DMS (31 °C) and its associated volatility in the reaction mixture (90 °C), quantification of this byproduct was not possible.[155] Finally, substitution of DMSO by DMS^{18}O incorporated 99% ^{18}O demonstrating that the oxygen atom within the aldehyde product originated from the solvent as actual oxidant (**Scheme 37**, **(F)**).

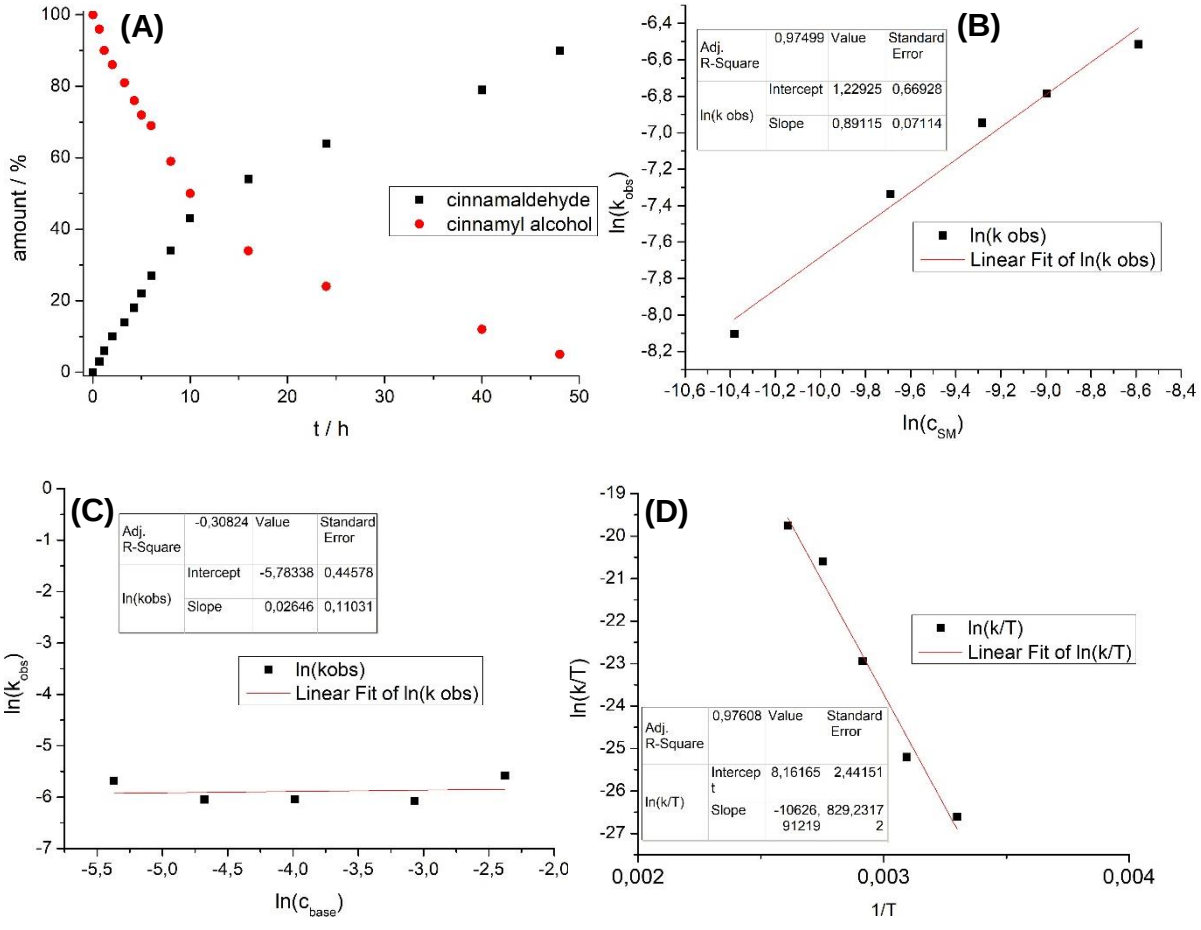

Figure 5: Reaction monitoring under optimized reaction conditions **(A)**, plots for determination of reaction order in respect to cinnamyl alcohol **(B)** and K_3PO_4 **(C)** and Arrhenius-Eyring plot **(D)**.

Monitoring the reaction process under optimized reaction conditions showed a nearly linear increase up to 10 h followed by a less steep increase reaching its maximum at

48 h reaction time (**Figure 5**, **(A)**). For evaluation of the rate-determining step, the reaction progress was monitored under different reaction conditions (different ratios of substrate and base und different temperatures). A 1st order reaction rate with respect to the starting material **(B)** but a reaction rate of 0th order regarding K_3PO_4 **(C)** were observed suggesting that the base is not involved in the rate-limiting step. An Arrhenius-Eyring plot was generated by observing the reaction process at different temperatures between 30 °C and 110 °C, which allows calculation of the activation enthalpy as $\Delta H^{\neq}$ = 21.1 kcal mol^{-1} (88.4 kJ mol^{-1}) and the activation entropy as $\Delta S^{\neq}$ = –30.9 cal mol^{-1} K^{-1} (–129.7 J mol^{-1} K^{-1}) **(D)**. The negative calculated entropy value suggested an associative process involved in the rate-limiting step.

The reaction was further clarified by means of DFT calculations. The first step of the mechanism is most likely proposed to be the formation of the carbonic acid hemiester **B** from alcohol **A** and CO_2 (**Scheme 38**).

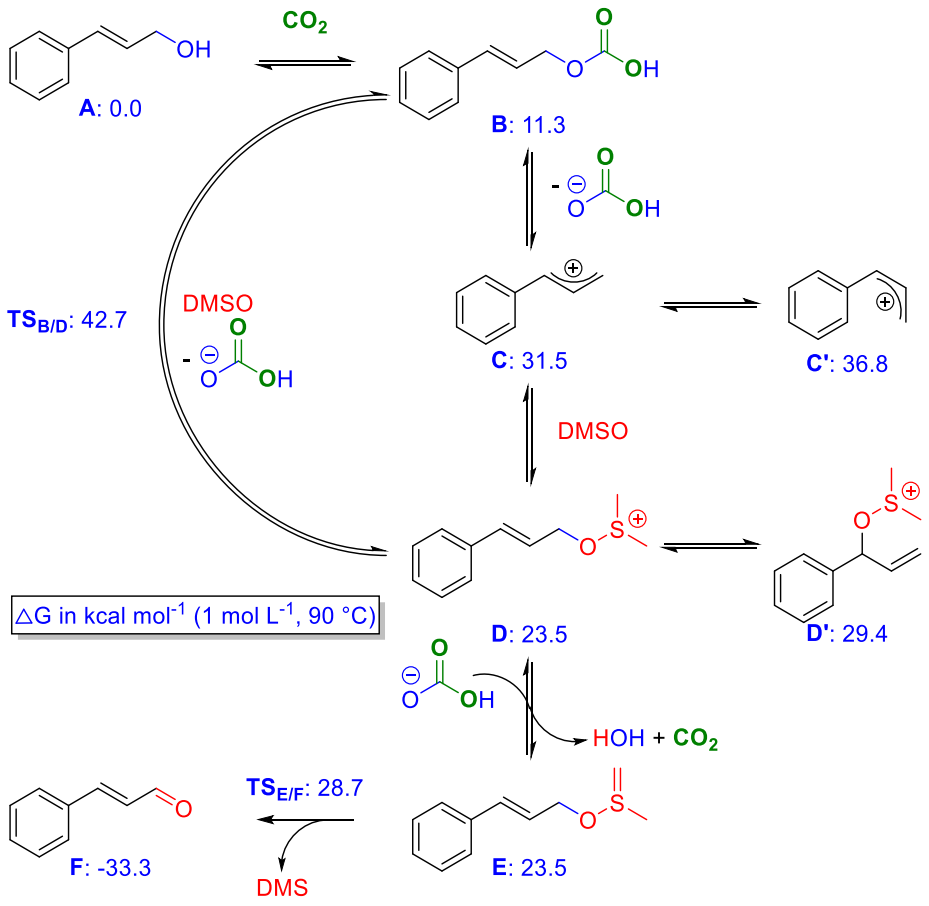

Scheme 38: DFT-calculated pathway of CO_2-promoted oxidation of cinnamyl alcohol; D3(BJ)-B3LYP/def2-TZVPP, COSMO (DMSO) corrected single point energies relative to cinnamyl alcohol **A** in kcal mol^{-1}; calculations were carried out by Markus Finger.

On the one hand, this pre-equilibrium is computed with 11.3 kcal mol^{-1} uphill, but it is necessary to convert the hydroxyl group to a better leaving group as proven earlier by

Tunge, Jessop and List independently.[20d–e,21] On the other hand, the calculated transition state **TS$_{B/D}$** of a direct substitution by DMSO represents a rather high barrier of 42.7 kcal mol^{-1} relative to the starting compound reflecting the low nucleophilicity of DMSO and therefore making it less feasible. Instead, **B** dissociates into a bicarbonate anion and an allyl cation **C**, which is computed at 31.5 kcal mol^{-1} and thus much lower than **TS$_{B/D}$**. Transition states of the dissociation of HCO_3^- and consecutive attack of DMSO at **C** could not be calculated though due to flat energy profiles of the necessary single steps. However, an important difference of energy values comparing linear **C** and bent **C'** explains the significance of π conjugation for stabilizing intermediate cation **C** more than **C'**. Anyhow, this also raises the question of selectivity since DMSO could theoretically attack on any of those involved C atoms. However, both diastereomer **C'** and internal isomer **D'** are at least 5.3 kcal mol^{-1} less stable than **C** and **D**, respectively. This would correspond to a 1:1000 ratio, which is below the experimental detection limit. When intermediate **D** is formed, deprotonation to **E** with the aid of bicarbonate anion releases the catalyst CO_2 and H_2O as byproduct in analogy to the Swern oxidation mechanism. An internal proton shift *via* **TS$_{E/F}$** results in irreversible product formation of aldehyde **F**. The relatively small calculated barrier of this step of 5.2 kcal mol^{-1} in respect to **E** suggests a fast reaction after attack of DMSO onto allylic cation **C** toward **F**. But the actual rate-determining step stays still ambiguous because **C** and **TS$_{E/F}$** both have comparable energy values in relation to the starting compound (see also **Figure 21** in the appendix). Tentatively, product formation is triggered by allyl cation **C**, which is surrounded by stabilizing DMSO molecules in solution until deprotonation.

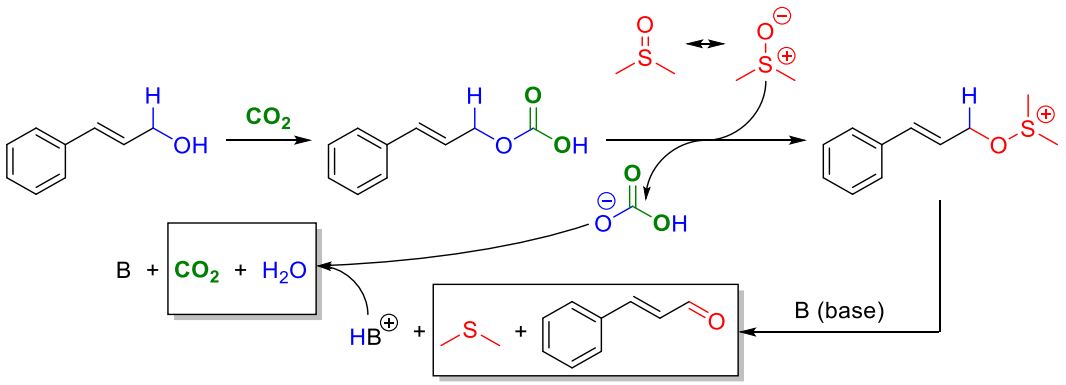

Scheme 39: Plausible mechanism for the CO_2-promoted oxidation of cinnamyl alcohol.

Combination of experimental evidence and computational calculation suggests a reaction mechanism, in which CO_2 played a pivotal role for the transformation of the hydroxyl into a good leaving group (**Scheme 39**). Based on the inability of observing the

intermediate carbonic acid hemiester without the help of a trapping agent and the calculated energy differences of **A** and **B**, the first step should not be rate-determining but a pre-equilibrium. These calculated unfavorable thermodynamics explain on the one hand why the hemiester could not be isolated and the calculated negative activation entropy (*cf.* the already discussed Arrhenius-Eyring plot) on the other hand. The next step, a nucleophilic attack by DMSO, was clearly demonstrated by the ^{18}O labeling experiment, which showed that the oxygen atom of the alcohol substrate is quantitatively replaced by the one from DMSO. The following actual oxidation step (*i.e.* deprotonation of cationic dimethylsulfide group, followed by proton shift) is well known for oxidation reactions with DMSO as actual oxidant. However, in this case the activation of the alcohol substrate is accomplished very mildly by CO_2 in contrast to these known procedures.

3.2.2 CO_2-Assisted Synthesis of *α*-Diketones Directly From Aldehydes

3.2.2.1 Optimization Studies

Since benzoin-type substrates (**91a** – **97a**) reached high yields for their corresponding *α*-diketo compounds combined with the interesting outcome of substrate **189a** regarding its trimerization product, for which the *in situ* benzoin condensation played an important role, the extension of the presented CO_2-promoted alcohol oxidation toward other reaction systems and substrates was at hand.[156] The benzoin condensation reaction rate can be enhanced by DMSO (although it is not completely understood yet[157]), which fits quite well to the developed alcohol oxidation methodology so that a one-pot combination of benzoin condensation and *in situ* oxidation into the *α*-diketone derivative was the focused aim.

Since not only above-mentioned cyanide salts are known to catalyze the benzoin condensation but also *N*-heterocyclic carbenes, a variety of those NHC catalysts (10 mol%) was added to a reaxtion mixture of aldehyde and DMSO together with different bases at the outset of the screening for optimal reaction conditions under CO_2 atmosphere (**Table 4**). As model substrate, heteroaromatic furfural (**193a**) was chosen yielding furil (**193b**).

Table 4: Optimization for the direct synthesis of furil from furfural.

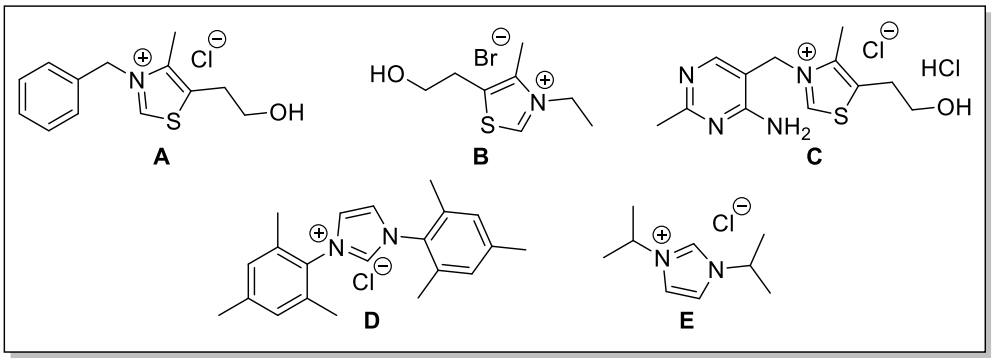

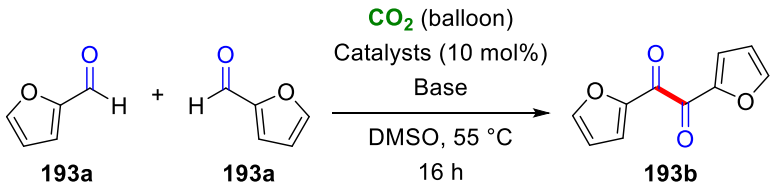

Entry	Catalyst	Base (eq)	Yield / %
1	A	K_2CO_3 (1.5)	49
2	B	K_2CO_3 (1.5)	86/80*
3	C	K_2CO_3 (1.5)	0
4	D	K_2CO_3 (1.5)	20
5	E	K_2CO_3 (1.5)	1
6	B	Cs_2CO_3 (1.5)	50
7	B	KOH (1.5)	43
8	B	LiOH (1.5)	18
9	B	DBU (1.5)	0
10	B	DBN (1.5)	15
11	B	KO*t*Bu (1.5)	26
12	B	DMAP (1.5)	0
13	B	Et_3N (1.5)	1
14	B	NaH (1.5)	7
15	B	aniline (1.5)	0
16	B	pyrimidine (1.5)	0
17	B	K_2CO_3 (1.0)	57
18	B	K_2CO_3 (0.5)	45
19	B	-	0
20	-	K_2CO_3 (1.5)	0
21	B	K_2CO_3 (1.5)	0**
22	B	K_2CO_3 (1.5)	0***

General reaction conditions: furfural (**193a**, 0.25 mmol), base, catalyst, DMSO (2.5 mL), CO_2 (balloon), 55 °C, 16 h; yields determined by GC using *n*-dodecane as internal standard; *5 g scale reaction; **N_2 atmosphere; ***O_2 atmosphere; *reproduced by permission of The Royal Society of Chemistry*.[156]

Delightfully, NHC catalyst **A** (3-benzyl-5-(2-hydroxyethyl)-4-methylthiazolium chloride; 10 mol%) yielded 49% of furil in the presence of 1.5 eq of K_2CO_3 in DMSO at 55 °C

overnight already. When the catalyst was changed to the cheaper 3-ethyl-5-(2-hydroxyethyl)-4-methylthiazolium bromide **B** the yield increased to 86%. Three other NHC catalysts showed minor to no activity for the oxidation step albeit catalyzing the benzoin condensation to some extent but only yielding marginal amounts of *α*-diketone product. Notably, no scale-up issues were identified under otherwise similar conditions leading to 80% furil even in a 5 g scale without any further precautions. Other tested bases like Cs_2CO_3, inorganic hydroxides, NaH, KO*t*Bu and organic bases like DBU, DMAP and pyrimidine showed less activity. A decrease of base loading to 0.5 eq resulted in significantly lower amounts of furil. No product formation was observed in absence of base or catalyst or under N_2 and O_2 atmosphere proving the essential role of CO_2 in this reaction. As expected, the use of solvents other than DMSO did not lead to furil formation (not shown here).

3.2.2.2 Scope of Substrates

With these optimized conditions at hand, the scope of this reaction methodology was investigated (**Scheme 40**). A variety of (hetero)aromatic aldehydes was directly converted to their corresponding *α*-diketones. Electron-donating (**199b** – **200b**, **203b**, **207b**) and -withdrawing groups (**196b**, **198b**) on the rings were well tolerated and led to yields of up to 83%. Substrates with a –I effect gave slightly better yields. Even an *α*-diketone with fused heteroaromatic benzofuran ring systems (**206b**) was obtained in 79%. Notably, the reaction proceeded smoothly for both 1- and 2-substitution patterns on the furan and the thiophene ring, respectively (**193b**, **195b**, **201b** – **202b**).

Several of the used aldehydes, namely furfural (**193a**), HMF (**205a**) and 5-methylfurfural (**207a**) are reported to be obtained from naturally occurring carbohydrates (*i.e.* biomass, one of the most abundant renewable resources) in large scale by many well-known methods. Especially a recently published one reports the dehydrogenation of glucose *via* CO_2 catalysis as mentioned above.[20d,158] These aldehydes attained high priority for the production of fuels and fine chemicals nowadays.[159] With the herein described methodology these aldehydes can be converted into the corresponding *α*-diketones without any purification issue.

Along with homocoupled aldehydes, heterocoupling of two different aldehydes was investigated, too, resulting in non-symmetric *α*-diketones. It is literature-known though

that heterocoupling of two different aldehydes *via* benzoin condensation is more challenging due to its reaction mechanism: The Breslow intermediate, which is formed when an NHC attacks an aldehyde substrate, is generated faster from electrophilic aldehydes along with speeding up the C–C formation step with another more electrophilic aldehyde substrate. Thus, when two aldehydes with different electrophilicity are used, commonly homocoupled products are derived.[160] Early approaches to solve this selectivity issue were undertaken by Ide *et al.* for the cyanide-catalyzed benzoin condensation and Stetter *et al.* for the NHC-catalyzed version.[161] Especially the latter investigation (along with Breslow earlier[81]) showed that thiazolium salts are superior catalysts for the cross-benzoin condensation. Selectivity was found to be highly substrate-dependent, which did not allow general statements. Even though this reaction is well studied, recent literature still states that efficient methods for a selective aldehyde heterocoupling *via* benzoin condensation is still out of reach yet.[160,162]

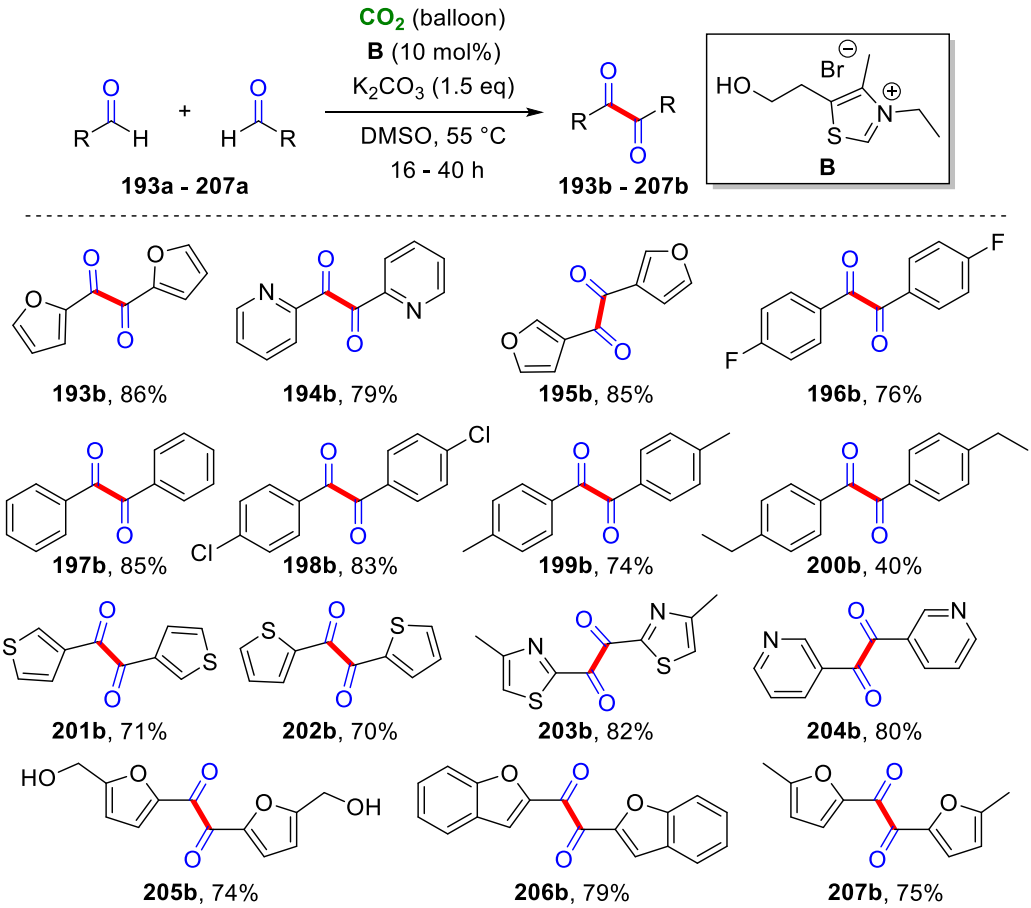

Scheme 40: Synthesis of symmetric *α*-diketones directly from aldehydes; reaction conditions: substrates (0.25 mmol), K_2CO_3 (1.5 eq), catalyst **B** (10 mol%), DMSO (2.5 mL), CO_2 (balloon), 55 °C, 16 – 40 h; all are isolated yields; some reactions were performed by Pradipbhai Hirapara; *reproduced by permission of The Royal Society of Chemistry*.[156]

Notably, modification of the reaction procedure had to be applied in order to suppress the favored homocoupling. For this purpose, a 1:1 ratio of two different aldehydes was applied firstly, but the obtained product mixtures exhibited only poor product selectivity. A subsequent change of this ratio to 1:1.5 increased the product selectivity as was previously stated by Stetter and Dämbkes.[161b] The results of this reaction procedure are shown in **Scheme 41**. Moreover, the first attack of the more electrophilic aldehyde changes the steric and/or electronic conditions of the so-formed Breslow intermediate. The less electrophilic aldehyde is then more attracted to the Breslow intermediate because of the difference between the thiazolium NHC, which was used for the herein reported methodology, and the triazolium NHCs used for the majority of comparable reported methodologies, in which selectivity was a major issue. Notably, in every case homocoupling (and further oxidation to symmetric *α*-diketones) was also observed besides the desired product formation.

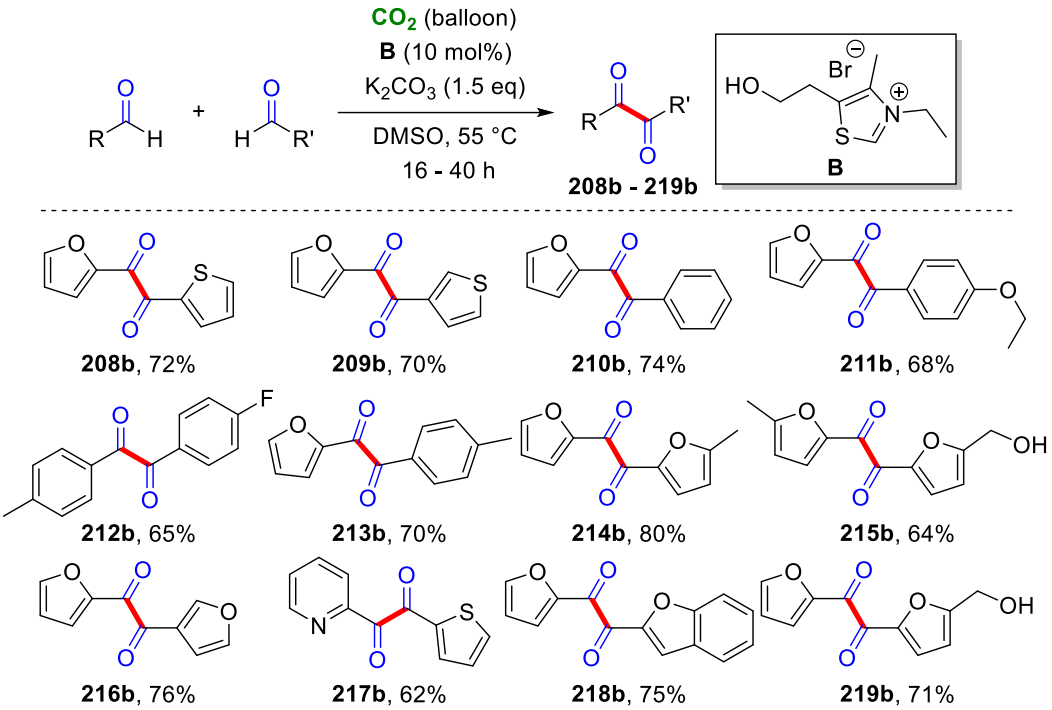

Scheme 41: Synthesis of non-symmetric *α*-diketones directly from two different aldehydes; reaction conditions: substrates (0.25 mmol for R–COH and 0.375 mmol for R'–COH, respectively), K_2CO_3 (1.5 eq), catalyst **B** (10 mol%), DMSO (2.5 mL), CO_2 (balloon), 55 °C, 36 – 48 h; all are isolated yields; some reactions were performed by Pradipbhai Hirapara; *reproduced by permission of The Royal Society of Chemistry*.[156]

With the described change of the starting material's ratio, it is possible to obtain several *α*-diketones with different heteroaromatics (**208b** – **209b**, **214b** – **219b**), products with electron-withdrawing and -donating functional groups (**211b** – **215b**) and *α*-diketones having aromatic and heteroaromatic moieties at once (**210b** – **211b**, **213b**) in high

yields up to 80%. This opens up a new way for the synthesis of asymmetric *α*-diketones since none of them is commercially available and comparable traditional syntheses rely on two or three consecutive synthesis steps. As mentioned for symmetric *α*-diketones also non-symmetric ones can be completely synthesized from potentially biomass-derived aldehydes (**214b** – **215b**, **219b**).

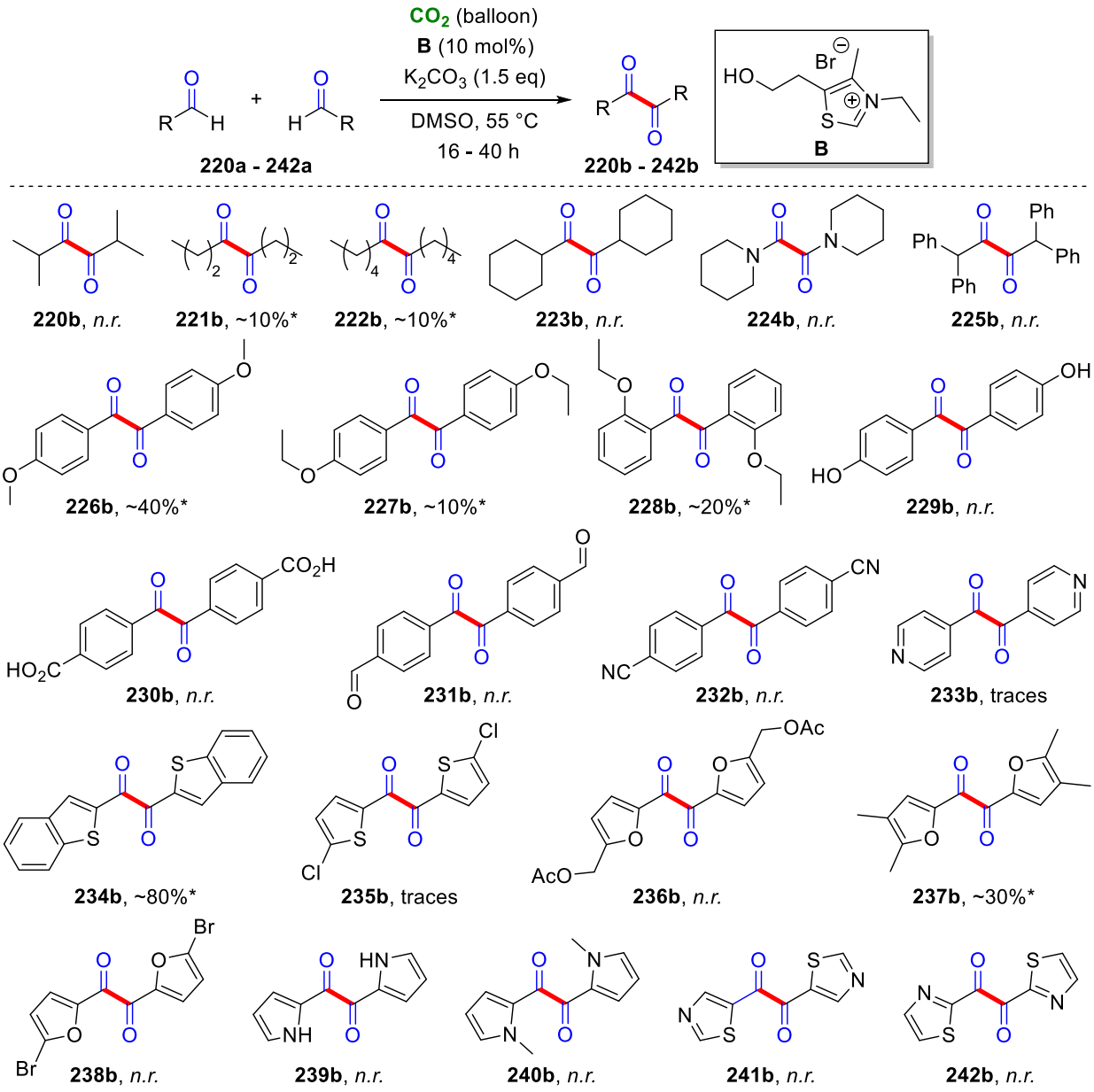

Scheme 42: Unsuccessful syntheses of symmetric *α*-diketones from aldehydes; reaction conditions: substrates (0.25 mmol), K_2CO_3 (1.5 eq), catalyst **B** (10 mol%), DMSO (2.5 mL), CO_2 (balloon), 55 °C, 16 – 40 h; *yield estimated by GC-MS; *n.r.* = no reaction by means of desired symmetric *α*-diketones.

As discussed in **chapter 3.1.2** and **3.2.1.2**, there are several substrates disclosing the limitations of this methodology as well. **Scheme 42** shows an overview over several aldehyde substrates, which underwent optimized reaction conditions with the purpose

of obtaining homocoupled symmetric *α*-diketones, thus only the substrates instead of the products are shown by means of clarity. Correspondingly, **Scheme 43** displays unsuccessful attempts to yield heterocoupled non-symmetric *α*-diketones.

Unfortunately, aliphatic aldehydes were not suitable under these reaction conditions in general. Neither branched (**220a**, **225a**) or linear aliphatic aldehydes (**221a** – **222a**) nor alicyclic aldehydes such as cyclohexyl and 1-piperidinyl aldehyde (**223a** – **224a**) gave the corresponding *α*-diketone in considerable amounts, not even when potentially aromatically activating phenyl groups were present within the direct chemical surrounding (**225a**). The electron density is probably not high enough to form a sufficiently stable Breslow intermediate. The missing +M effect might hinder the stabilization of that intermediate as well. Previous studies also mentioned lower yields or no reactivity at all for aliphatic aldehydes during benzoin condensation reactions.[160,161b]

Albeit benzaldehyde derivatives with alkyl moieties reacted well (**199b** – **200b**) alkoxy or hydroxyl groups seemed to hamper an efficient oxidation reaction regardless of the substitution position (**226a** – **229a**). The potential product of benzoic acid substrate **230a** was not detectable *via* GC-MS, but since the carboxylic acid ester **236a** did not react as well, benzoic acid ester were not further investigated. Dialdehyde **231a** did not react to the corresponding *α*-diketone “dimer” or “trimer” but GC-MS spectra suggested that the starting material was still present in the reaction mixture. Hence, either no reaction happened or oligomerization/polymerization occurred, although no insoluble precipitate was observed. In contrast to *para*-substituted fluoro- and bromobenzaldehyde (**196a**, **198a**), product formation was not observed in the presence of the chemically similar pseudohalide nitrile moiety (**232a**). 5-membered heteroaromatic ring systems reacted well regardless of the position of the heteroatom within the ring (*cf.* 2- and 3-substituted furyl and thiphenyl aldehydes **193a**, **195a** and **201a** – **202a**). However, pyridine derivatives were more sensitive regarding the substitution pattern since 2- and 3-substitution (**194a**, **204a**) gave similar product yields whereas 4-substituted pyridine only yielded traces of the corresponding *α*-diketone (**233a**). A similar case regarding benzofuran and benzothiophene (*cf.* **87b** and **187b**) explained in **chapter 3.2.1.2** was observed here as well: Benzofuran derivative **206b** was obtained purely in high yield whereas benzothiophene derivative **234b** could not be purified despite a promising similar yield estimated by GC-MS for the latter substrate. In contrast to non-substituted thiophene derivatives (**201b** – **202b**) the 5-chloro-substituted **235a** only gave traces of the corresponding *α*-diketone. Apart from furfural derivatives substituted

with one methyl group (**207a**) or a hydroxymethyl group (**205a**), 4,5-dimethyl- and 5-bromo-substitution showed low to no product formation, respectively (**237a** – **238a**). A 1*H*-pyrrole derivative was not active under oxidation conditions even when the nitrogen atom was blocked by a methyl group avoiding deprotonation by the base (**239a** – **240a**). Also both thiazole compounds **241a** – **242a** did not yield the desired product regardless of structural similarity to the used NHC catalyst, which was expected to induce positive intermolecular substrate-catalyst interactions. Benzoin-type intermediates were found in all cases in higher amounts except for aliphatic aldehydes and **229a** – **231a** though, suggesting only a low acceptance of these substrates and substitution patterns during the oxidation step.

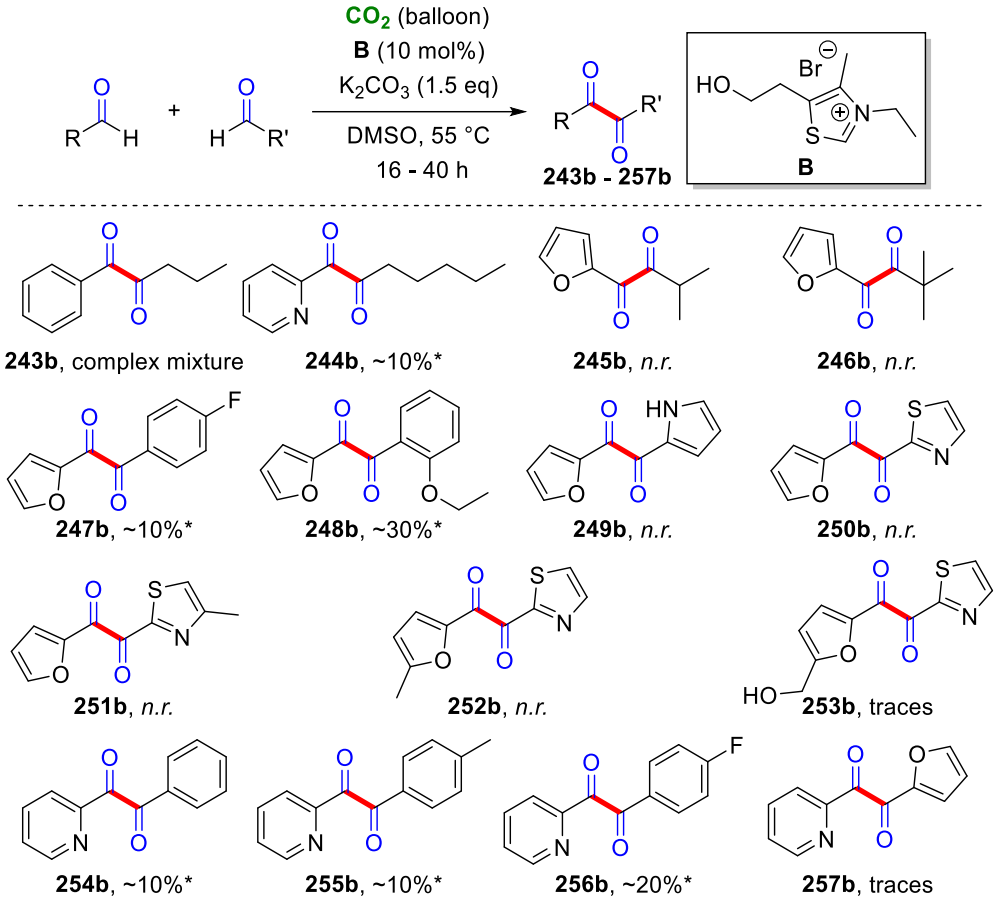

Scheme 43: Unsuccessful syntheses of non-symmetric *α*-diketones from aldehydes; reaction conditions: substrates (0.25 mmol for R–COH and 0.375 mmol for R'–COH, respectively), K_2CO_3 (1.5 eq), catalyst **B** (10 mol%), DMSO (2.5 mL), CO_2 (balloon), 55 °C, 16 – 40 h; *yield estimated by GC-MS; *n.r.* = no reaction by means of desired non-symmetric *α*-diketones.

As expected, the synthesis of non-symmetric *α*-diketones was even more challenging due to the tendency of symmetric product formation (**Scheme 43**). When aromatic and aliphatic aldehydes were used simultaneously, almost exclusively homocoupled *α*-

diketones obtained from the aromatic aldehyde were observed (**243b** – **246b**). Besides, **243b** was accompanied by a complex (statistical) product mixture, which can be expected from published reports.[160] When furfural and pyridine derivatives on the one hand and benzaldehyde derivates on the other hand were used together, they still tended to release mostly homocoupled products (**247b** – **257b**). Only three exceptions were observed previously (**210b** – **211b**, **213b**). This pattern indicates that homocoupling is hindered when furfural and 4-fluorobenzaldehyde or 2-ethoxy-benzaldehyde (**247b** – **248b**) or when 2-pyridyl aldehyde and non-substituted, 4-methyl- or 4-fluorobenzaldehyde or furfural are used together (**254b** – **257b**), respectively. Moreover, furfural seems to be prone to react neither with pyrrole nor thiazol regardless of the substitution pattern (**249b** – **253b**).

3.2.2.3 Application of the *α*-Diketone Synthetic Protocol

After exploration of the possible scope of substrates, possibilities for an application of the synthesized symmetric *α*-diketones were examined. Especially 4,4'-dichlorobenzil (**198b**) was found to be used for the synthesis of a variety of commercially interesting compounds with varying applications. For instance, **198b** serves as intermediate in the synthesis of the neuroprotective agent **258b**, as important precursor for graphene nanoribbons like **259b**, which help improving properties of organic electronic materials in polymer blends, and the known antimalarial agent **260b**, all depicted in **Scheme 44**.[163]

Notably, intermediate **198b** was successfully synthesized in a 5 g scale from cheap reactants and catalyst obtaining 80% yield without further precaution, is commercially available but highly expensive, *e.g.* from Sigma Aldrich (119 €, 10 mg), AK Scientific (717 €, 5 g), Fluorochem (430 €, 5 g) or TCI (319 €, 5 g).

As mentioned above, 5 g furil (**193b**) were synthesized directly from furfural (**193a**) without any purification issue in 80% yield, too. This *α*-diketone can be further transformed into a number of different valuable molecules (**Scheme 45**) such as 2,3-di(furan-2-yl)quinoxaline (**261b**), which was found to slow down the corrosion rate of mild steel in H_2SO_4.[164] Quinoxaline residues are also utilized within polymers resulting in polymeric structures known for their use in the production of LEDs.[165] Moreover, the pyrazine derivative **262b**, occurring in flavors, numerous biologically active substances and agrochemicals, was synthesized from furil in one step with 77% yield.[166] Oxazole

derivative **263b** was obtained *via* Cu(I) catalysis and air-promoted oxidative cyclization, which is an important scaffold for pharmaceuticals and functional materials.[167]

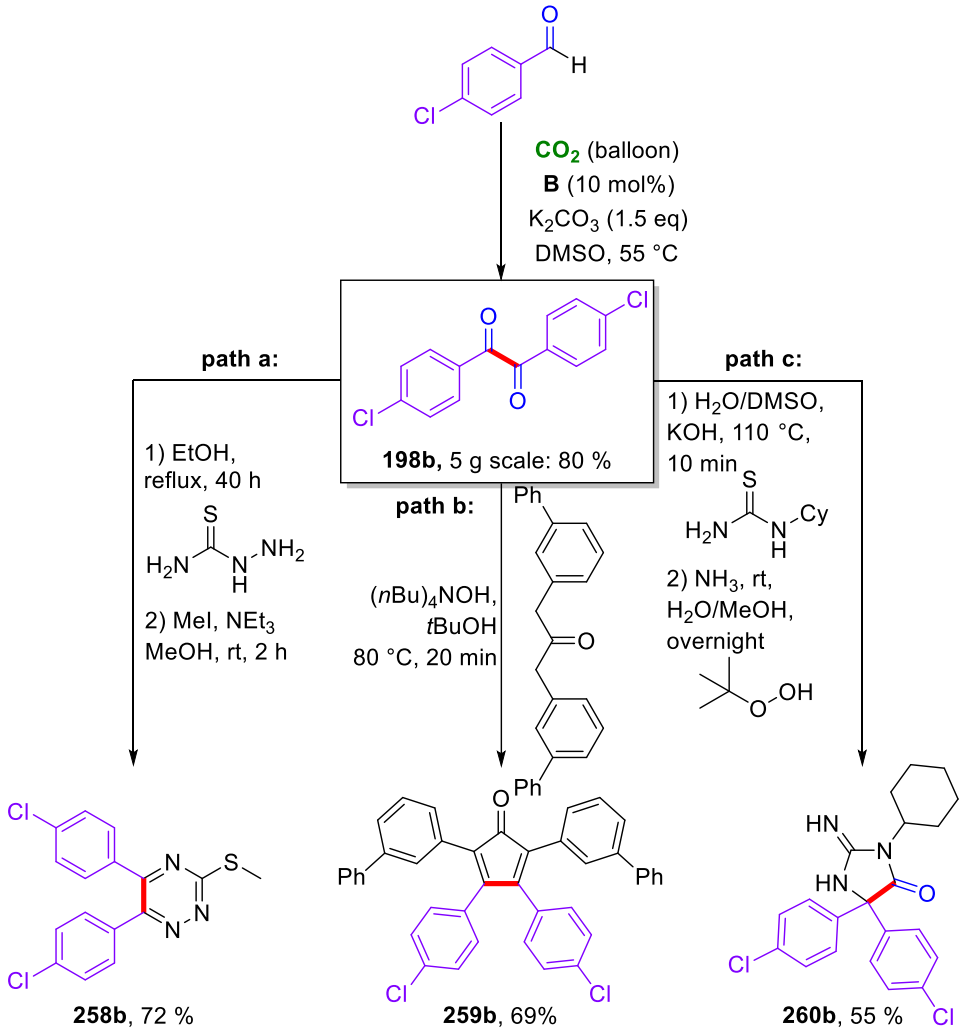

Scheme 44: Synthesis of drug molecules and precursor for graphene nanoribbons from 4,4'-dichlorobenzil **198b**; reaction conditions: **path a: 1) 198b** (0.5 mmol), thiosemicarbazide (1.0 mmol), EtOH, reflux, 40 h; **2)** MeI (1.2 eq), Et_3N (7.2 eq), MeOH, rt 2 h; **path b: 198b** (0.22 mmol), (nBu)$_4$NOH (0.22 mmol), tBuOH, 80 °C, 20 min; **path c: 1)** cyclohexylthiourea (0.58 mmol), **198b** (0.52 mmol), KOH (0.8 mmol), H_2O/DMSO, 110 °C, 10 min; **2)** NH_3, tBuOOH, H_2O/MeOH, rt, overnight; all are isolated yields; *reproduced by permission of The Royal Society of Chemistry*.[156]

Moreover, furil was converted to the known antitumor-active compound **264b** (*via* isolated intermediate **264b'** after the first step) in 58% overall yield (3 steps), which was found to have a high activity against a panel of cancer cell lines.[168] On the one hand, this synthesis relies on an expensive transition metal, but on the other hand, palladium on charcoal is a widely applied catalyst for hydrogenation reactions and can be easily separated from the reaction mixture due to its heterogeneous nature. Moreover, the used hydrogen gas was applied at atmospheric pressure through a simple balloon as used for the application of CO_2 gas. Finally, depending on the used aldehyde (*e.g.*

benzaldehyde in this case) a variety of imidazoles like **265b** can be synthesized from furil as well in high yields, opening up the possibility for a huge number of imidazole backbones when different other commercially cheap available aldehydes are used. These imidazoles are generally important building blocks for the synthesis of a variety of antitumor, antibiotic, antifungal, antiinflammatory and antiallergic drug molecules.[169] To date, there is no report about the direct conversion of biomass-derived furfural into widely utilizable chemicals and pharmaceutical molecules.

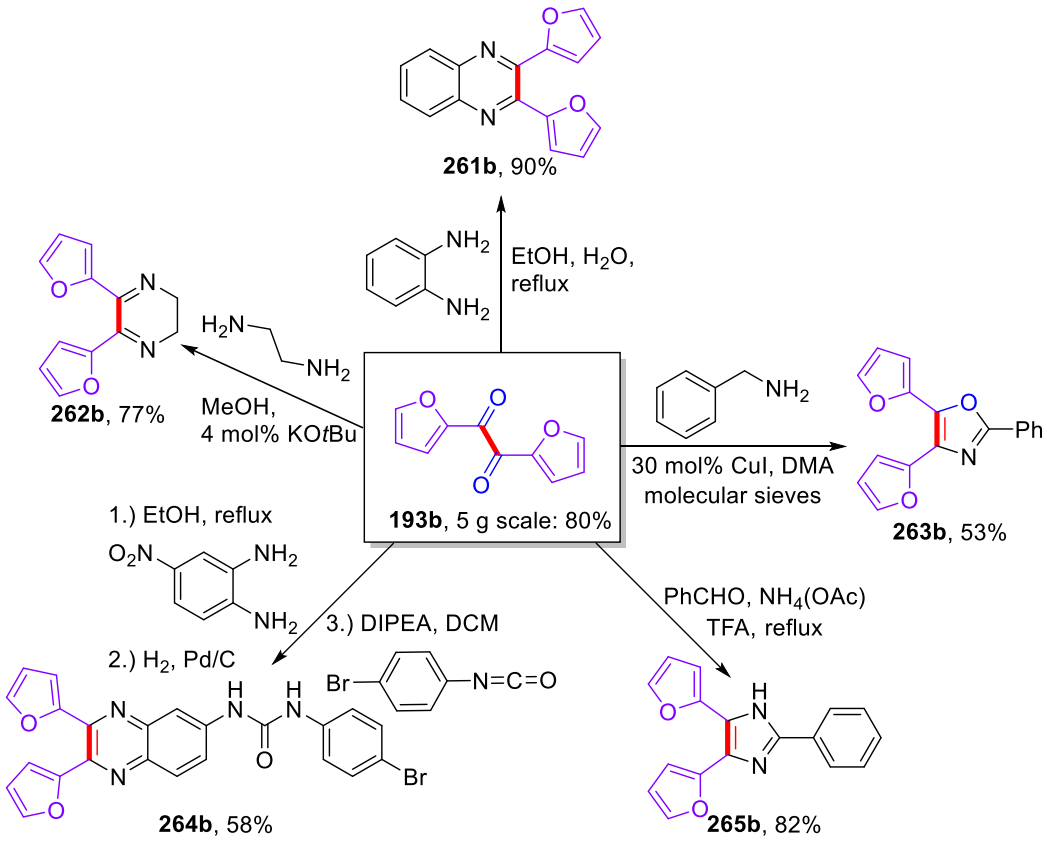

Scheme 45: Conversion of biomass-derived furil to valuable chemicals; *reproduced by permission of The Royal Society of Chemistry*.[156]

3.2.2.4 Mechanistic Studies

After investigating the scope of substrates and the application of synthesized products, it was obvious to investigate the reaction mechanism, too. The main function of the used base K_2CO_3 is the *in situ* generation of a free carbene diradical, which can then act as catalyst for the benzoin condensation *via* a literature-known pathway.[89] Indeed, when the conversion of furfural was monitored over time to a maximum of 24 h under optimized reaction conditions, it revealed that most of the furfural was firstly converted to furoin (**193b'**) within the first 1 h. This furoin intermediate was then slowly oxidized

under CO_2 atmosphere to the corresponding *α*-diketone furil (**Figure 6**). Furthermore, mechanistic experiments were undertaken to provide background information about the role of CO_2, the actual oxidant and possible intermediates (**Scheme 46**).

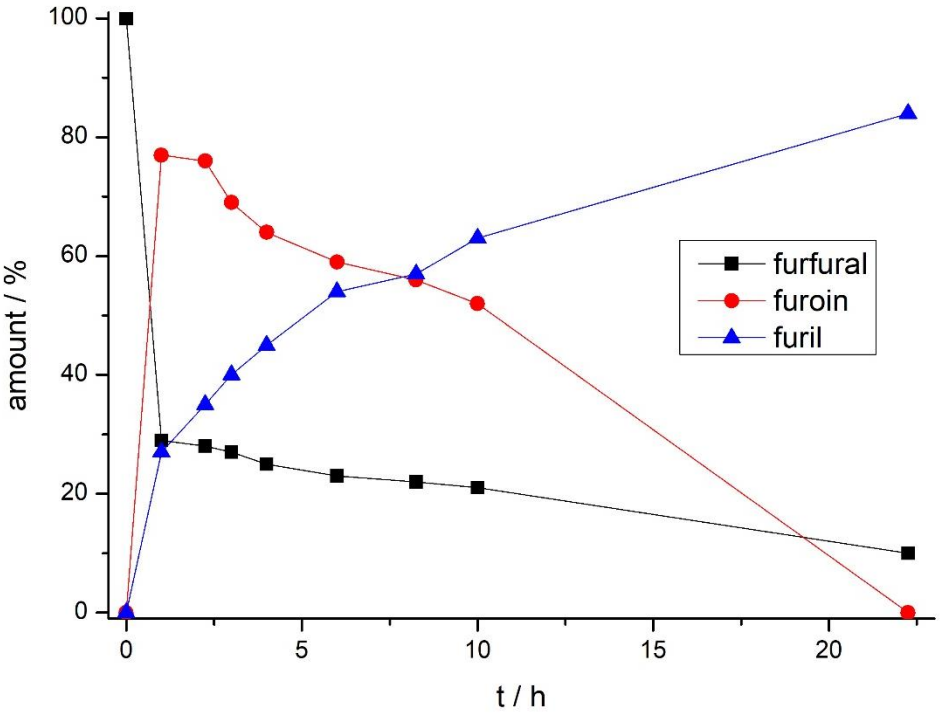

Figure 6: Conversion of furfural **193a** to furoin **193b'** and furil **193b** under optimized reaction conditions; *reproduced by permission of The Royal Society of Chemistry*.[156]

Under inert gas atmosphere (N_2) only intermediate furoin **193b'** was found **(A)**. When furoin was submitted to optimized reaction conditions with CO_2 atmosphere in a separate second step, it quantitatively reacted to furil **(B)**. 3,5-Di-*tert*-butyl-4-hydroxytoluene (BHT) as a known radical scavenger was then added to the reaction mixture to exclude a possible radical pathway and in fact, the overall reaction was not hindered giving almost the same yield of furil as without BHT, ruling out an involvement of radicals in the mechanism **(C)**. As known from **chapter 3.2.1**, CO_2 was not expected to be the actual oxidant but rather the solvent. A hint for that fact was the non-reactivity in reaction media other than DMSO. Again, *in situ* gas phase GC of the headspace of the reaction and NMR spectroscopy of the reaction mixture were utilized for the determination of possible reduction products from CO_2 such as CO, formic acid or its respective salt. Nonetheless, only CO_2 was detected *via in situ* gas phase GC, thus excluding the presence of O_2 as the exogeneous oxidant in the gas phase during the reaction. Moreover, it was again possible to detect the *O*-carboxylated alcohol intermediate. This intermediate was trapped with the aid of EtI as the carbonic acid ethyl ester with both

CO_2 and ^{13}C-labeled CO_2 by an HRMS method in good agreement with calculated masses for the respective adduct cations **(D)**.

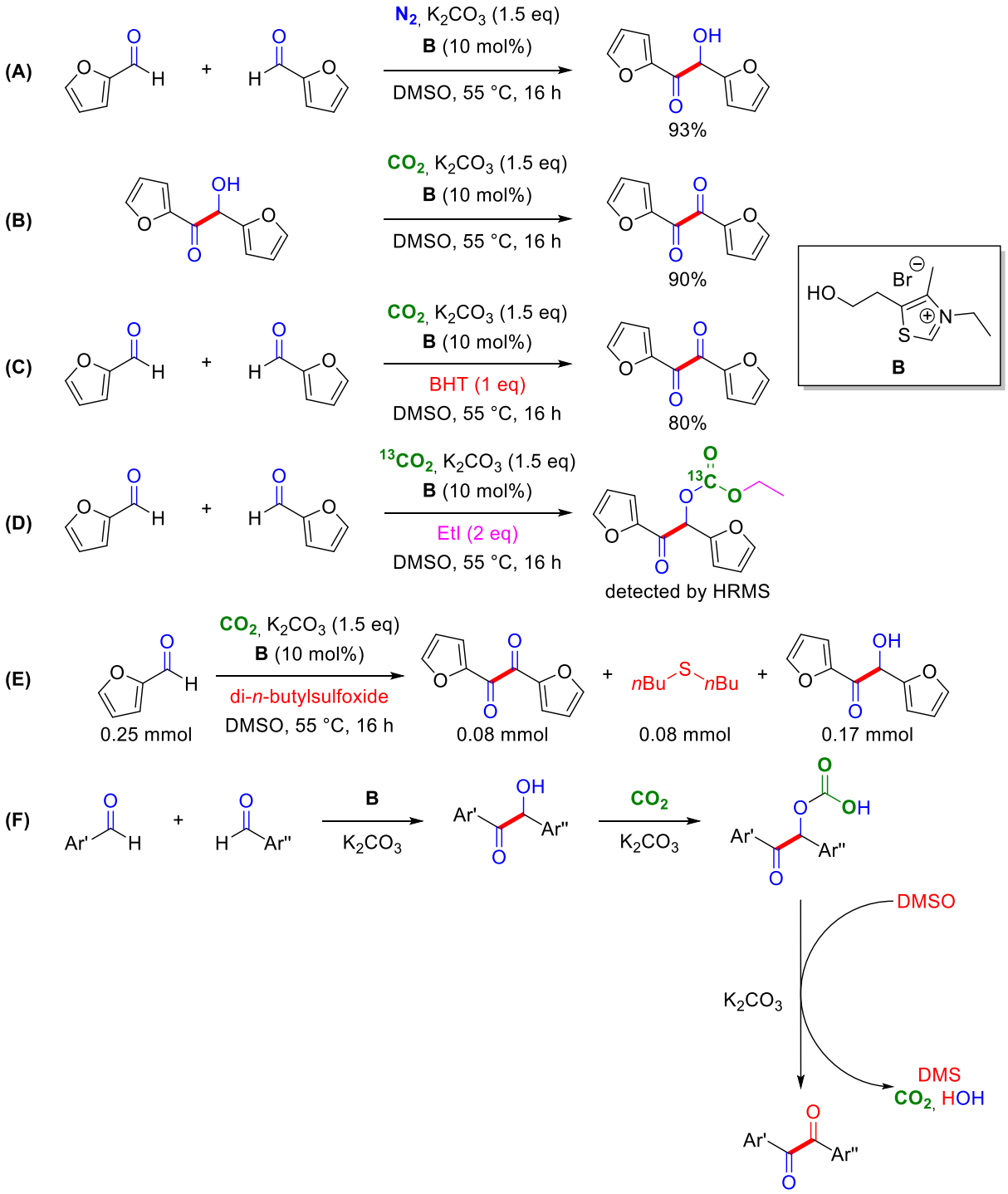

Scheme 46: Experimental evidence for the crucial role of CO_2 (applied *via* a balloon) in the oxidation step; reaction under N_2 atmosphere **(A)**, reaction of furoin to furil **(B)**, reaction with BHT as quencher **(C)**, trapping of the carboxylate intermediate **(D)**, reaction with di-*n*-butylsulfoxide as actual oxidant **(E)**, proposed reaction mechanism **(F)**; *reproduced by permission of The Royal Society of Chemistry*.[156]

For **$^{12}CO_2$** HRMS was measured as follows:
LC-ESI-HRMS: *m/z* calcd. for $C_{13}H_{12}O_6$ [M+H$^+$]: 265.0707, found: 265.0704; *m/z* calcd. for $C_{13}H_{12}O_6$ [M+Na$^+$]: 287.0526, found: 287.0545.

For **$^{13}CO_2$** HRMS was measured as follows:
LC-ESI-HRMS: *m/z* calcd. for $C_{12}{}^{13}C_1H_{12}O_6$ [M+H$^+$]: 266.0740, found: 266.0737; *m/z* calcd. for $C_{12}{}^{13}C_1H_{12}O_6$ [M+Na$^+$]: 288.0559, found: 288.0555.

Since DMSO was expected to act as actual oxidant, the corresponding reduced by-product had to be dimethyl sulfide. Unfortunately, quantification was impossible due to its low boiling point (31 °C).[155] But when DMSO was substituted by di-*n*-butylsulfoxide, the reduced byproduct di-*n*-butylsulfide (boiling point: 189°C) could be quantified in an equimolar ratio compared to furil **(E)**. By summarizing these mechanistic experiments and the reaction progress monitoring a plausible mechanism was postulated with two independent steps **(F)**: First, the NHC-catalyzed benzoin condensation occurs between the aldehyde molecules (regardless of the gas present in the headspace of the reaction) followed by a considerably slower yet selective addition of the CO_2 molecule to the hydroxyl group enabling a Swern-type oxidation step with DMSO as oxidant.

Since the benzoin condensation occurring as first step is literature-known, it shall be only shortly discussed here: In brief, the NHC salt is activated by means of a free carbene *in situ* by the base (K_2CO_3). To this diradical species, the aldehyde can bind *via* formation of a Breslow intermediate. This intermediate, however, is not stable enough to be isolated, not even when MeI is taken for stabilization as reported by Breslow.[81] A second aldehyde molecule is attacking and forms the ketol while the free carbene leaves the intermediate complex. The free carbene is then able to contribute in another catalytic reaction. The role of CO_2 during the second oxidation step was further clarified with the aid of DFT calculations. Since the benzoin condensation is well known, it was not calculated here. Additional alternative pathways were also calculated (see **Figure 24 – 25** in the appendix).

However, the most realistic pathway is depicted in **Scheme 47** and includes the already mentioned *O*-carboxylated intermediate **B**, which transforms the hydroxyl group into a good leaving group. This carbonic acid hemiester is prone to a nucleophilic attack by DMSO[155] but its prior formation is energetically uphill with 13.9 kcal mol^{-1} explaining also its instability and the resulting inability to detect it experimentally. The following rate-determining step can either proceed stepwise following an S_N1 mechanism over

intermediate cation **C** or in a concerted manner as S_N2 directly from **B** to **D**. Considering that both the energy of the charged intermediate's separated ion pair (**C**; according to S_N1) and the (gas phase) free energy of the transition state ($\mathbf{TS_{B/D}}$, according to S_N2) are usually methodically overestimated, it can be assumed that the calculated value of 29.4 kcal mol^{-1} provides an upper limit. However, as a rough estimation that value aligns well with the experimental time frame of 16 h. Once the intermediate sulfonium cation **D** has formed, deprotonation (**E**) and fast proton transfer with formation of dimethyl sulfide as byproduct ($\mathbf{TS_{E/F}}$) leads to the *α*-diketone **F**. Usually, when DMSO is used as the oxidant, it needs to be activated by a strong electrophile like oxalyl chloride (Swern-type), dicyclohexylcarbodiimide (Pfitzner-Moffatt oxidation) or others.[72–73] In contrast to that, it is shown here that CO_2 can act as a very mild and sustainable activating agent for the alcohol substrate and thus replace those cumbersome reagents.

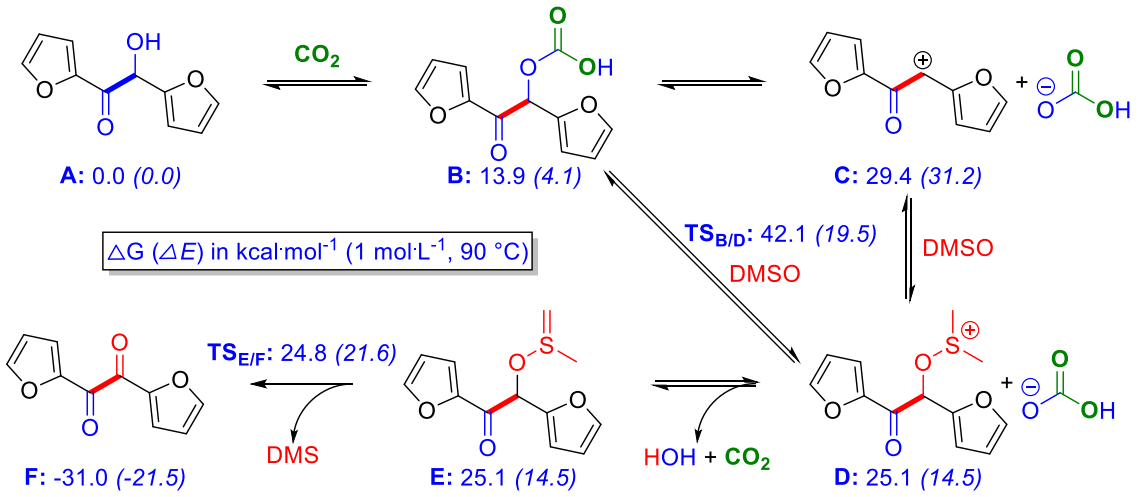

Scheme 47: Calculated pathway of the CO_2-promoted oxidation step; B3LYP/def2-TZVPP, COSMO(DMSO) corrected single point energies relative to furoin **A** (**193b'**) in kcal mol^{-1}; calculations were carried out by Markus Finger; *reproduced by permission of The Royal Society of Chemistry*.[156]

A less likely alternative to the calculated mechanism shown in **Scheme 47** shall be shortly discussed here as well. There are two more possibilities for the reaction step from **A** to **B**: Either CO_2 directly binds in a reversible way to the ketolate anion instead of the ketol since a base is already present within the reaction mixture (for calculation see appendix),[21] thus slightly changing the calculated energy values. Or the free NHC binds to a CO_2 molecule to transfer the carboxylate to the hydroxyl group of the ketol (or ketolate, respectively). This last step was not calculated because of its complexity though. The only observed byproducts were DMS and water while CO_2 remained unchanged. In the end, both NHC and CO_2 were able to participate as catalysts in another reaction cycle. Thus, by combining experimental evidence and DFT calculations it is

justified calling this process “CO_2-catalyzed” since CO_2 exactly acts as catalyst lowering the activation energy by forming an active intermediate (*i.e.* hydroxyl moiety as better leaving group).

3.2.3 Development of an LED Photo Reaction Setup

In this section, the self-constructed LED reaction setup (**Figure 7**) used for the photocatalytic reactions of this thesis shall be shortly introduced. In contrast to the more complex setups already described in recent publications,[15i,30] this setup is made by easily commercially available components and with costs of roughly 50 € per setup.

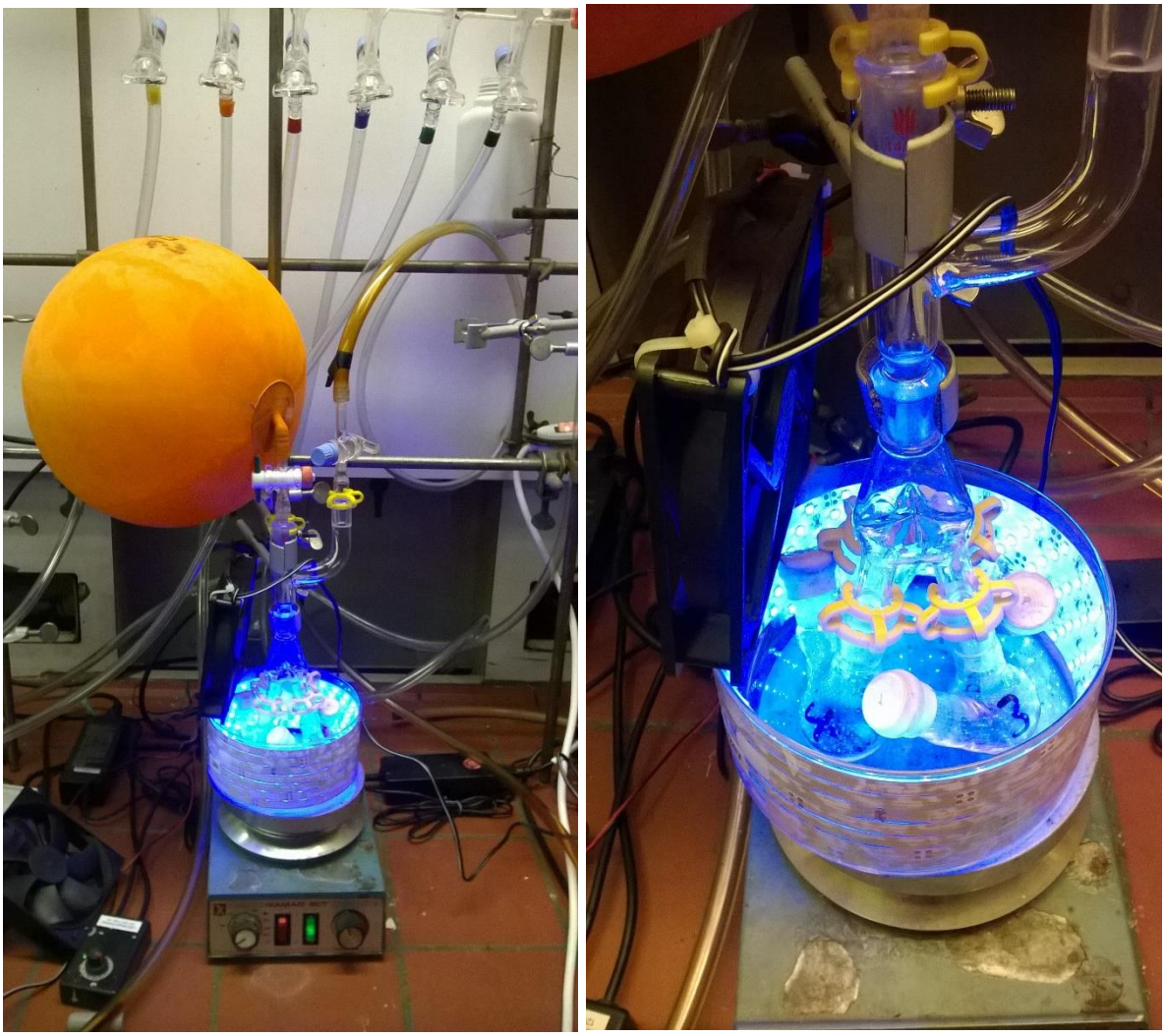

Figure 7: Self-constructed LED reaction setup.

The reaction setup consists of a self-constructed LED light source assembly composed of a 140 mm crystallizing dish with a commercially available 5 m blue LED strip glued to its inside. This LED strip consists of separable LED elements and 3 m of it were used per crystallizing dish in total. This leads to a maximum power of 24 W per LED

setup. The light intensity and the corresponding actual current power of the light source can be adjusted *via* a self-constructed dimmer. The setup is further cooled down by a commercially available 120 mm computer fan directed toward the inside of the crystallizing dish in order to ensure constant room temperature. Furthermore, the dimmer was always set to 50% (equates to 12 W) since higher power would lead to a slight increase of the reaction temperature and in no case further improvement was observed with higher irradiation intensity. During the first experiments, the temperature was monitored in proximity to the actual reaction flasks within the crystallizing dish and did not exceed room temperature by more than 5 °C in any case. Thus, ambient temperature can be assumed as actual reaction temperature when this setup was used.

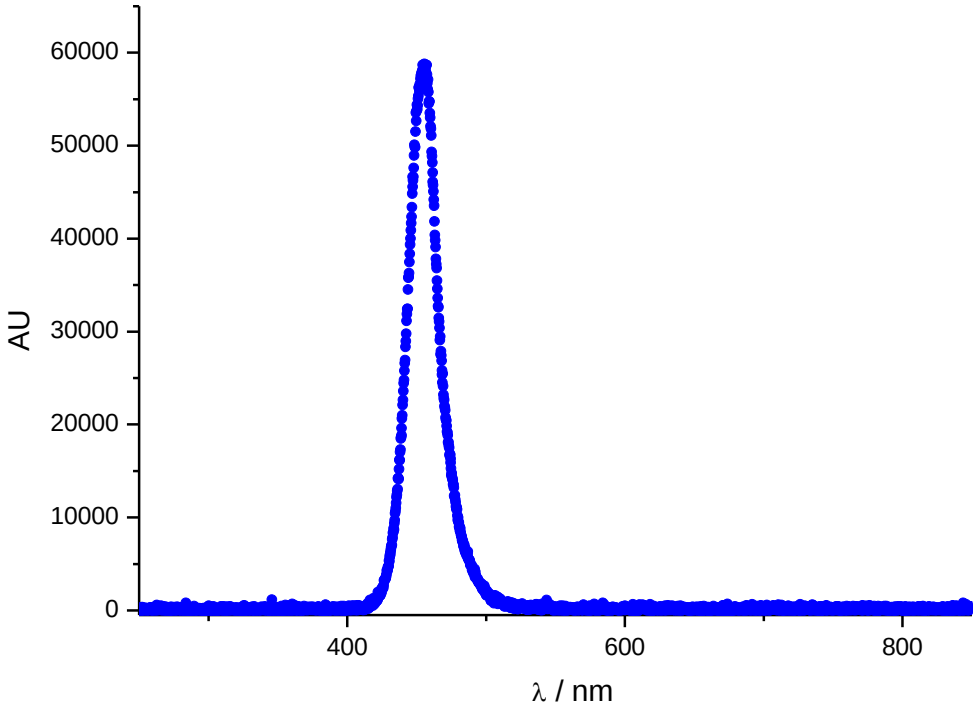

Figure 8: Emission spectrum of the self-constructed blue LED setup; the spectrum was measured by Waldemar Schilling.

Moreover, an emission spectrum was obtained from this LED setup, depicted in **Figure 8**. The maximum emitted wavelength was measured at λ_{max} = 456 nm and the total range of emitted irradiation was measured from 404 nm to 553 nm.

3.2.4 CO_2-Catalyzed Dehydrogenation of Amines to Imines

3.2.4.1 Optimization Studies

After the application of CO_2-catalyzed oxidation methods onto primary and secondary alcohol as well as ketol substrates, broadening the scope of substrates to other oxidizable groups was an interesting further target. Primary experiments suggested that C–C bond oxidation was out of reach for the mild CO_2-catalyzed oxidation due to the absent difference in electronegativity. Thus, substrates similar to hydroxyl compounds were investigated and indeed, closely related simple aromatically activated amines were prone to be oxidized (*i.e.* dehydrogenated) to the corresponding imine derivatives.[170] However, initial experiments under similar (thermal) reaction conditions compared to the previously presented oxidation methods (*cf.* **chapters 3.2.1** and **3.2.2**) using *N*-benzylaniline as model substrate only reached up to about 60% yield. Even after extensive screening of the reaction conditions (not shown here) including different reaction temperatures ranging from 50 – 100 °C, reaction times up to 48 h, a huge variety of different organic and inorganic bases and the respective base amounts, different other solvents and solvent amounts and several additives in different ratios such as boron-, lithium- and aluminum-based Lewis acids and so on, the yield could not be sufficiently increased.

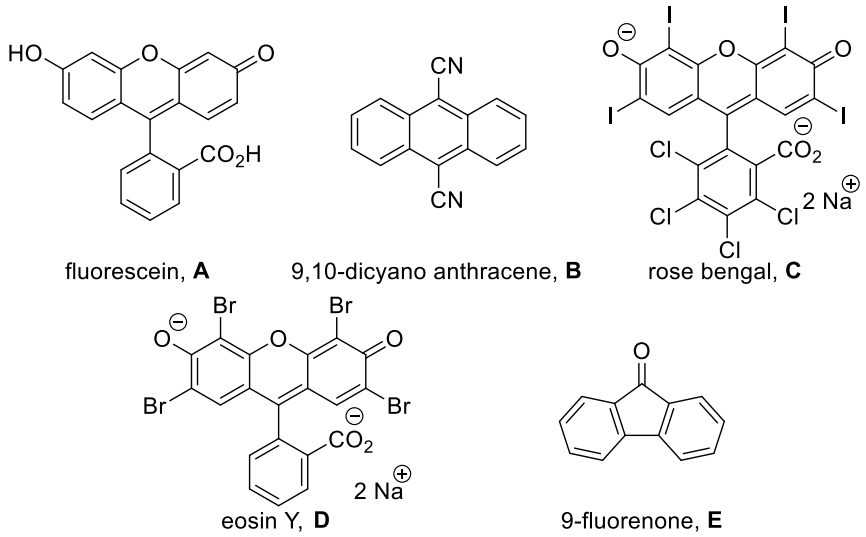

Figure 9: Photocatalysts used for the optimization of amine oxidation reactions.

After this mediocre optimization results, a novel pathway for the activation of CO_2 as soft oxidation promoter was envisioned. Indeed, a more suitable reaction setup was found by application of a self-developed LED photochemistry reaction setup, described in **chapter 3.2.3**. With the aid of this LED setup, CO_2 can undergo an SET forming a

radical species under operationally simple photocatalytic conditions, *e.g.* the already mentioned CO_2 radical anion or hydroxyformyl species, in order to improve its reactivity as known from literature examples (see **chapter 1.3**). Notably, the generation of CO_2 radicals usually needs special equipment or strict reaction conditions. However, it is also reported that small organic molecules like pyridine are able to trap these CO_2 radicals under relatively mild electro- and photochemical reaction conditions.[105,107,120c,126g,171]

According to the green and sustainable chemistry approach the herein disclosed research is devoted to, exclusively transition metal-free photocatalysts, depicted in **Figure 9**, were examined (**Table 5**). All of the tested catalysts are cheap, commercially available and usually used as stains or dyes. Additionally, none of them exhibits harmful or even toxic properties.

Again, the dehydrogenation of *N*-benzylaniline (**266a**) to *N*-benzylideneaniline (**266b**) was chosen as model reaction. The examined reaction conditions also aligned with the sustainable approach by applying only atmospheric CO_2 pressure *via* a balloon and ambient room temperature with irradiation of blue light LEDs consuming only 12 W total. Inorganic bases gave generally lower yields, probably due to partial insolubility within the reaction medium. Hence, liquid and solvent-miscible organic bases like DBU – also being suspected to stabilize CO_2 radicals as described above – were chosen as bases. DMSO was retained as solvent since the mechanism was expected to be a Swern-type mechanism, too. In fact, other solvents led to negligible yields.

First, during the screening of photocatalysts (PC) eosin Y (**D**) was found to give the highest yield so far with 45%. The efficiency of **D** used for this oxidation procedure can be explained based on the measured emission spectrum of the constructed LED reaction setup (**Figure 8**): **D** absorbs incident light at a rather broad range from about 450 – 550 nm,[29d] which overlaps well with the observed emission spectrum of the self-constructed LED setup exhibiting an emission range from 404 nm to 553 nm with the maximum at 456 nm.

Second, other organic bases such as the amidine-type TBD and DBN (1,5-diazabicyclo[4.3.0]non-5-ene) were examined along with simpler ones like pyridine. DBN was found to give 70% of the desired product but by decreasing the DBN amount the yield also dropped. Increasing to 1.2 eq yielded 81% *N*-benzylideneaniline whereas further increase to 1.5 eq only resulted in a slightly higher yield of 83%. Thus, by means of

atom economy 1.2 eq were taken for further investigations. Similar to the base amount, increasing the amount of **D** from 3 mol% in 1% steps did not improve the yield. Yet, decreasing the catalyst loading to 2 mol% or even 1 mol% also decreases the yield significantly. Finally, increasing the reaction time from 16 h to 24 h or even 48 h increased the yield to 86% and 96%, respectively. Moreover, since water was expected to be a byproduct similar to the reported alcohol oxidation, specially dried DBN (stored in dry glassware and over activated molecular sieves) was increasing the yield from comparable 86% to 95%.

Table 5: Optimization table for the oxidation of *N*-benzylaniline to benzylideneaniline.

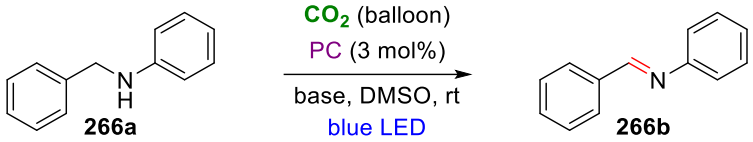

266a **266b**

PC	PC amount / mol%	Base	Base amount / eq	Yield / %
A	3	DBU	1	**16**
B	3	DBU	1	**8**
C	3	DBU	1	**38**
D	3	DBU	1	**45**
E	3	DBU	1	**36**
D	3	TBD	1	**25**
D	3	pyridine	1	**25**
D	3	2,6-lutidine	1	**34**
D	3	quinuclidine	1	**52**
D	3	DBN	0.5	**56**
D	3	DBN	1	**70**
D	3	DBN	1.2	**81**
D	3	DBN	1.5	**83**
D	1	DBN	1.2	**23**
D	2	DBN	1.2	**43**
D	4	DBN	1.2	**82**
D	5	DBN	1.2	**84**
D	3	DBN	1.2	**86***
D	3	DBN	1.2	**96****
D	3	dry DBN	0.5	**88***
D	3	dry DBN	1.2	**95***

Reaction conditions: **266a** (0.134 mmol), PC (3 mol%), base, DMSO (2.5 mL), CO_2 (balloon), 12 W blue LED, rt, 16 h; yields were determined by GC using *n*-dodecane as internal standard; *24 h reaction time; **48 h reaction time.

3.2.4.2 Scope of Substrates

Albeit specially dried DBN gave slightly higher yields, simple commercially available DBN was used for the further exploration of the scope of substrates without prior purification or drying by means of operational simplicity. 48 h reaction time were chosen as tradeoff except for acyclic amines and Hantsch ester-type substrates.

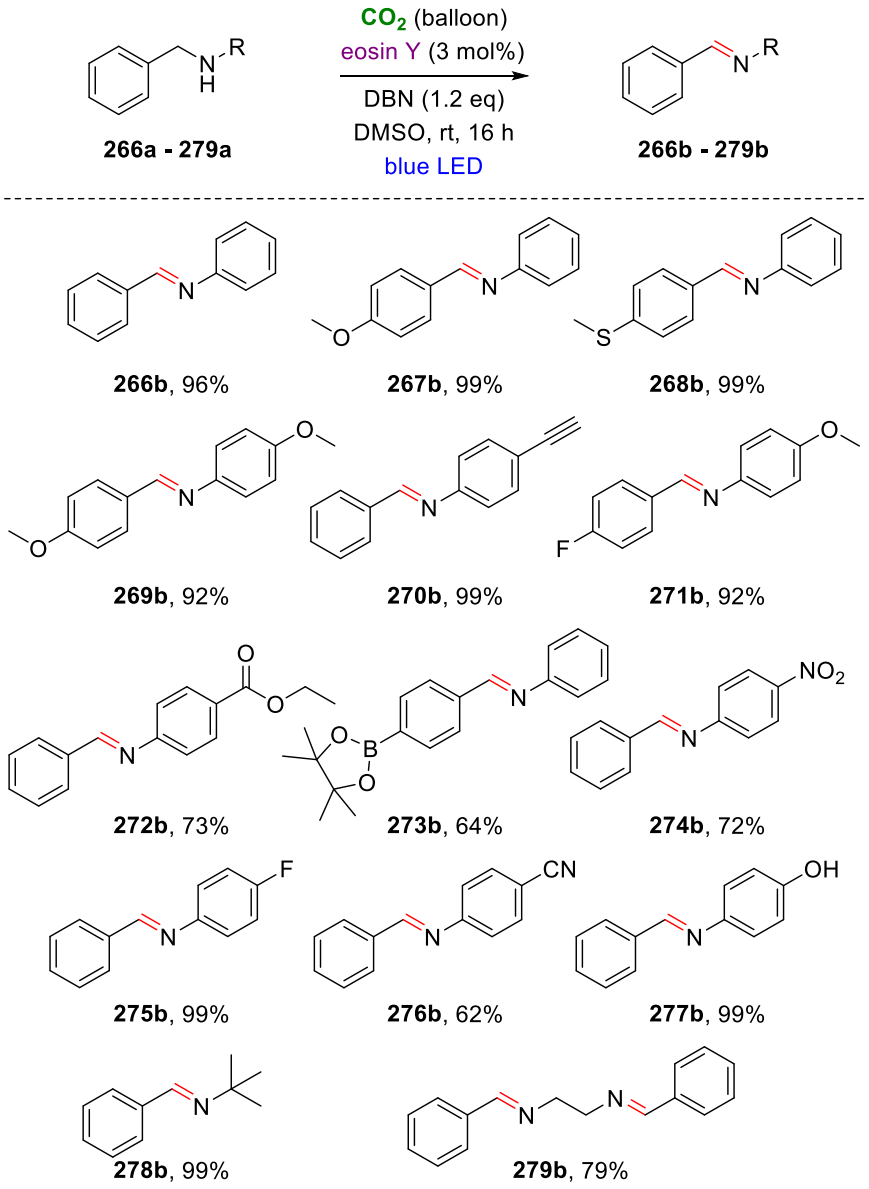

Scheme 48: Scope of substrates of acyclic amines; reaction conditions: substrates (0.134 mmol), eosin Y (3 mol%), DBN (1.2 eq; for **279a** 2.4 eq), DMSO (2.5 mL), CO_2 (balloon), 12 W blue LED, rt, 16 h; all are isolated yields.

With these optimized reaction conditions at hand, several substrates with amine moieties in benzylic position each divided by their backbone compounds related to simple acyclic benzylic amines (**Scheme 48**), 1,2,3,4-tetrahydroisoquinoline derivatives

(**Scheme 49**), indoline derivatives (**Scheme 52**) and substrates of Hantzsch ester-type molecules (**Scheme 53**) were examined.

First of all, a variety of acyclic amines, (mainly *N*-benzylaniline derivatives as varieties of the model substrate; **Scheme 48**) underwent the reaction procedure. Notably, the respective *N*-benzylidene products are known to be simply obtained by stirring of the respective derivatives of *N*-benzylamine and benzaldehyde with molecular sieves overnight.[5] Nevertheless, high yields of the corresponding imines could be obtained with CO_2 as oxidation promoter for a diverse spectrum of different functional groups in almost quantitative yields in most of the cases.

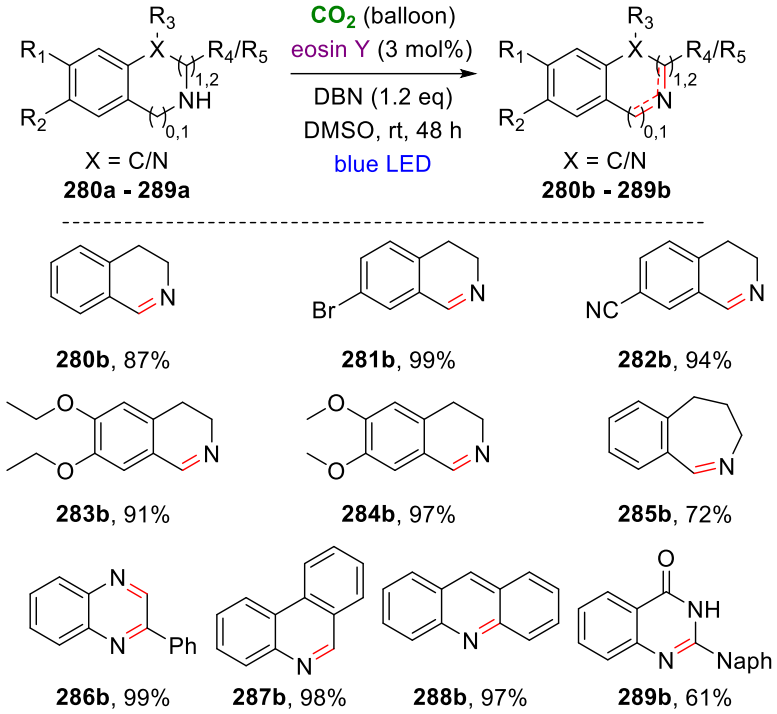

Scheme 49: Scope of substrates related to 1,2,3,4-tetrahydroisoquinoline; reaction conditions: substrates (0.134 mmol), eosin Y (3 mol%), DBN (1.2 eq), DMSO (2.5 mL), CO_2 (balloon), 12 W blue LED, rt, 48 h; all are isolated yields; Naph = 2-naphthyl.

Besides non-substituted model substrate **266a**, differently substituted acyclic amines gave excellent yields, such as *N*-benzylaniline with mesomerically inducing and electron-donating ether and thioether moieties or an alkyne group in *para* position (**267b** – **270b**). Moreover, electron-withdrawing groups like nitro, fluoro, cyano or hydroxyl (**274b** – **277b**) were well tolerated. Even when both electron-withdrawing and -donating groups were present at the same substrate, the yield was almost quantitative (**271b**). Additionally, carboxylic and boronic acid esters gave good yields of their respective imine products (**272b** – **273b**). When the one-side aliphatic *tert*-butylbenzylamine **278a**

was subjected to the reaction setup, 99% yield of the corresponding imine were obtained, thus proving a not necessarily present aromatic activation from both sides of the amine moiety. Also substrate **279a** could count as one-side aliphatic since both imine groups in product **279b** are separated by an ethyl moiety. Because double dehydrogenation was intended, 2.4 eq of DBN were used for substrate **279a**.

After exploring the scope of substrates regarding acyclic imines, cyclic imines were an interesting target because they cannot be synthesized as easily compared to acyclic imines as described above. Thus, selective generation of dihydroisoquinolines is more challenging without obtaining over-dehydrogenated or over-hydrogenated products (depending on the substrate and reaction type; **Scheme 49**).

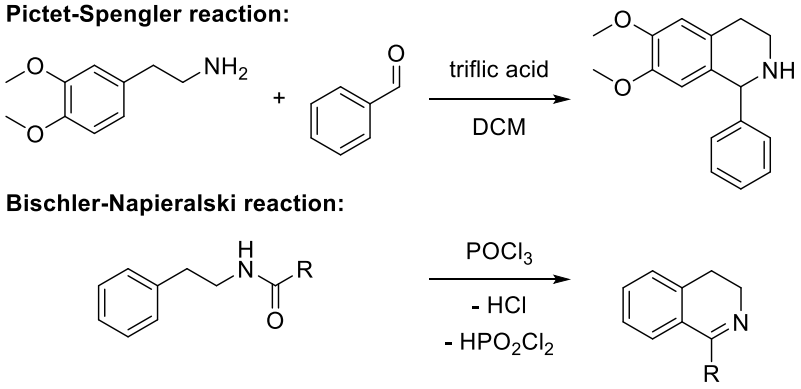

Scheme 50: Pictet-Spengler and Bischler-Napieralski reaction.

Indeed, the developed methodology was able to selectively convert 1,2,3,4-tetrahydroisoquinoline derivatives exclusively at their benzylic position between aromatic ring and nitrogen heteroatom. This reaction delivered their 3,4-dihydroisoquinoline derivatives without obtaining any fully aromatic byproduct as could be expected otherwise. Apart from non-substituted 1,2,3,4-tetrahydroisoquinoline **280a**, substrates with electron-withdrawing bromo and cyano groups as well as electron-donating methoxy and ethoxy groups gave excellent yields throughout (**281b** – **284b**). Even when the ring size of the alicyclic side was enlarged to a 7-membered ring, a high yield was reached (**285b**). Condensed ring systems reacted well (**287b** – **288b**) and the comparably lower yield of substrate **289a** could be explained by steric crowding. In case of 2-phenyl-2,3-dihydroquinoxaline derivative **286a**, the doubly dehydrogenated product **286b** was formed exclusively in quantitative yield. However, the dehydrogenated non-substituted CH_2 group was not in benzylic position and the base loading was not increased either. This phenomenon can be explained by the aromatization as the driving force of this reaction toward a conjugated π system of the so-formed product. This aromatization is

easier for substrates with two heteroatoms rather than one because of their electron lone pairs interfering with the transient intermediate species *via* inducing especially mesomeric effects.

The substrates (*e.g.* a derivative of **283a**) for this reaction can be synthesized by the Pictet-Spengler-type reaction (developed in 1911 and further developed since then[172]) *via* simple addition of an aldehyde to a *β*-phenethylamine (**Scheme 50**). Notably, with this CO_2-catalyzed oxidation method it was possible to selectively obtain several dehydrogenated 3,4-dihydroisoquinolines without over-oxidation to the fully aromatic isoquinoline derivatives in comparison to other less selective reports.[92d,100–101,173] These 3,4-dihydroisoquinolines are traditionally synthesized by the Bischler-Napieralski reaction (**Scheme 50**; already published in 1893[174]). The drawback of this synthesis is the use of overstoichiometric amounts of highly toxic phosphoryl chloride. This could be overcome by using simple and green CO_2 as promoter for the oxidation of 1,2,3,4-tetrahydroisoquinolines as an environmentally friendly and less toxic pathway toward 3,4-dihydroisoquinoline derivatives. Even more, the so-obtained products are more valuable, *e.g.* simple non-substituted 3,4-dihydroisoquinoline **280b** is about 60 times more expensive compared to its respective substrate **280a** (prices based on Sigma Aldrich).

Scheme 51: Dehydrogenation in non-benzylic position of substrate **290a**, related to 1,2,3,4-tetrahydroisoquinoline; reaction conditions: **290a** (0.134 mmol), eosin Y (3 mol%), DBN (1.2 eq), DMSO (2.5 mL), CO_2 (balloon), 12 W blue LED, rt, 48 h; isolated yield.

As an additional and more complex substrate 1,2,3,6,7,11*b*-hexahydro-4*H*-pyrazino[2,1-*a*]isoquinolin-4-one **290a** was tested, and dehydrogenation occurred solely at the C–N bond between 1- and 2-position, which was also proven by NMR spectroscopy (**Scheme 51**).

Since indole derivatives are a common structural motif of natural products (*e.g.* tryptophan and tryptamine alkaloids) and drug molecules (*e.g.* indometacin), it was an interesting target to synthesize those derivatives by oxidizing indoline derivatives to their corresponding indoles (**Scheme 52**).[175]

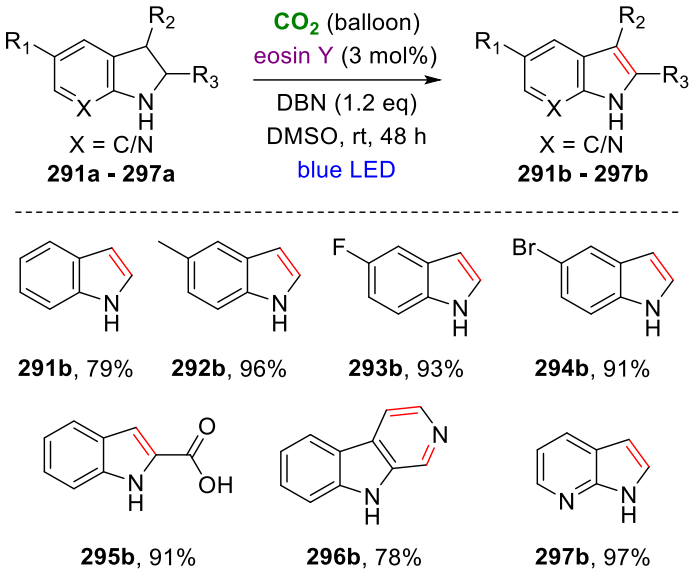

Scheme 52: Scope of substrates of indoline derivatives; reaction conditions: substrates (0.134 mmol), eosin Y (3 mol%), DBN (1.2 eq), DMSO (2.5 mL), CO_2 (balloon), 12 W blue LED, rt, 48 h; all are isolated yields.

Albeit the C–N bond within the indole backbone is not in benzylic position, the driving force for the aimed reactivity was already observed in case of substrate **286a** when fully aromatized **286b** was obtained. Thus, it can be expected that aromatization would happen in case of indoline derivatives although the necessary oxidation would happen between 2- and 3-position, *i.e.* dehydrogenation of a C–C bond to a C=C bond. Indeed, under optimized reaction conditions non-substituted indoline (**291a**) already gave indole in good yield (79%). When substituted indoline derivatives were used, the yield was even higher. Regardless of the electron-donating (**292b**) or -withdrawing nature (**293b** – **294b**) of the substituents, yields were almost quantitative throughout. Moreover, it was possible to obtain a free indole carboxylic acid (**295b**) and the heterocyclic 7-azaindole (**297b**) in excellent yields. Similarly to **286a**, **296a** was doubly dehydrogenated as well and thus fully aromatized 9*H*-pyrido[3,4-*b*]indole **296b** was obtained in good yield. Besides, no singly oxidized product was detected, even though the base loading was not increased either. Moreover, no byproducts, especially no carboxylation of the unprotected nitrogen atoms, were identified in case of indole substrates at all. As completion of the scope of substrates, the aromatization of Hantzsch ester derivatives was aimed at. This dehydrogenation reaction is usually known to proceed quickly but under influence of stoichiometric oxidants (*e.g.* $Fe(NO_3)_3$[176] and $FeCl_3$[177]). Unsaturated Hantzsch ester-type molecules are usually synthesized *via* condensation of a β-diketone, an aldehyde and ammonia or a primary or secondary amine.[178] Further dehydrogenation of these 1,4-unsaturated compounds leads to pyridine derivatives.

As it turned out, this aromatization was also easily achieved *via* CO_2-promoted oxidation (**Scheme 53**). Both the common ethyl and *tert*-butyl Hantzsch ester-type molecules (**298b** – **299b**, **301b**) and even the diketo analog **300b** smoothly underwent the reaction procedure. Presence of a substituent in 4-position did not interfere with the reactivity, thus methyl and phenyl groups were well tolerated. Quantitative conversion was achieved in every case even when the reaction time was shortened to overnight reaction (16 h) without formation of any byproduct at all.

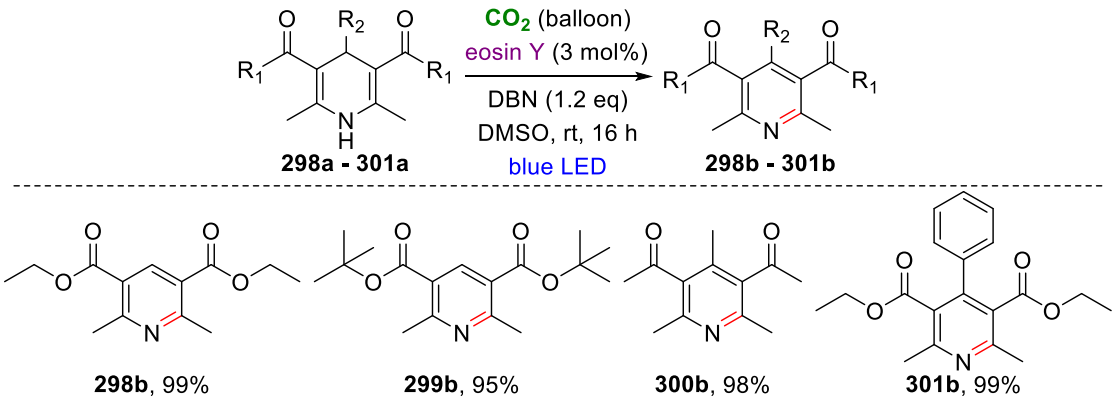

Scheme 53: Scope of substrates of Hantzsch ester-type substrates; reaction conditions: substrates (0.134 mmol), eosin Y (3 mol%), DBN (1.2 eq), DMSO (2.5 mL), CO_2 (balloon), 12 W blue LED, rt, 16 h; all are isolated yields.

Unfortunately, not all of the examined substrates worked as expected (**Scheme 54**). Acyclic amines with a linear aliphatic residue only yielded traces regardless of the chain length (**302a** – **305a**) or other substitution at the alkyl chain such as keto or carboxylic acid groups (**306a** – **307a**). In contrast to the successfully converted *tert*-butylbenzylamine **278a**, these results indicate that the branched alkyl moiety is more capable of stabilizing possible carbocationic intermediates due to the 2 methyl residues both contributing to a +I effect. The only heterocyclic example of an *N*-benzylaniline derivative (**308a**) gave only low yield, hence pointing toward electronic issues when heteroatoms are present in this kind of substrates. Double dehydrogenation within the same molecule (**309a**) was also out of reach even after doubling the base amount. When the C–N bond was not in benzylic position as within *N*-benzylamine but rather in an aniline-type molecule, the reaction did not occur at all (**310a**). Interestingly, albeit based on a different (thermal, metal-catalyzed) mechanism, similar problems with substrates like **302a**, **304a** and **306a** have been described earlier. Yet, the respective authors commented only shortly on electronic and steric effects in general.[93] Also Kamal *et al.* describe the substrate *tert*-butylbenzylamine **278b** as their only one-side aliphatic example in their work from 2006.[96]

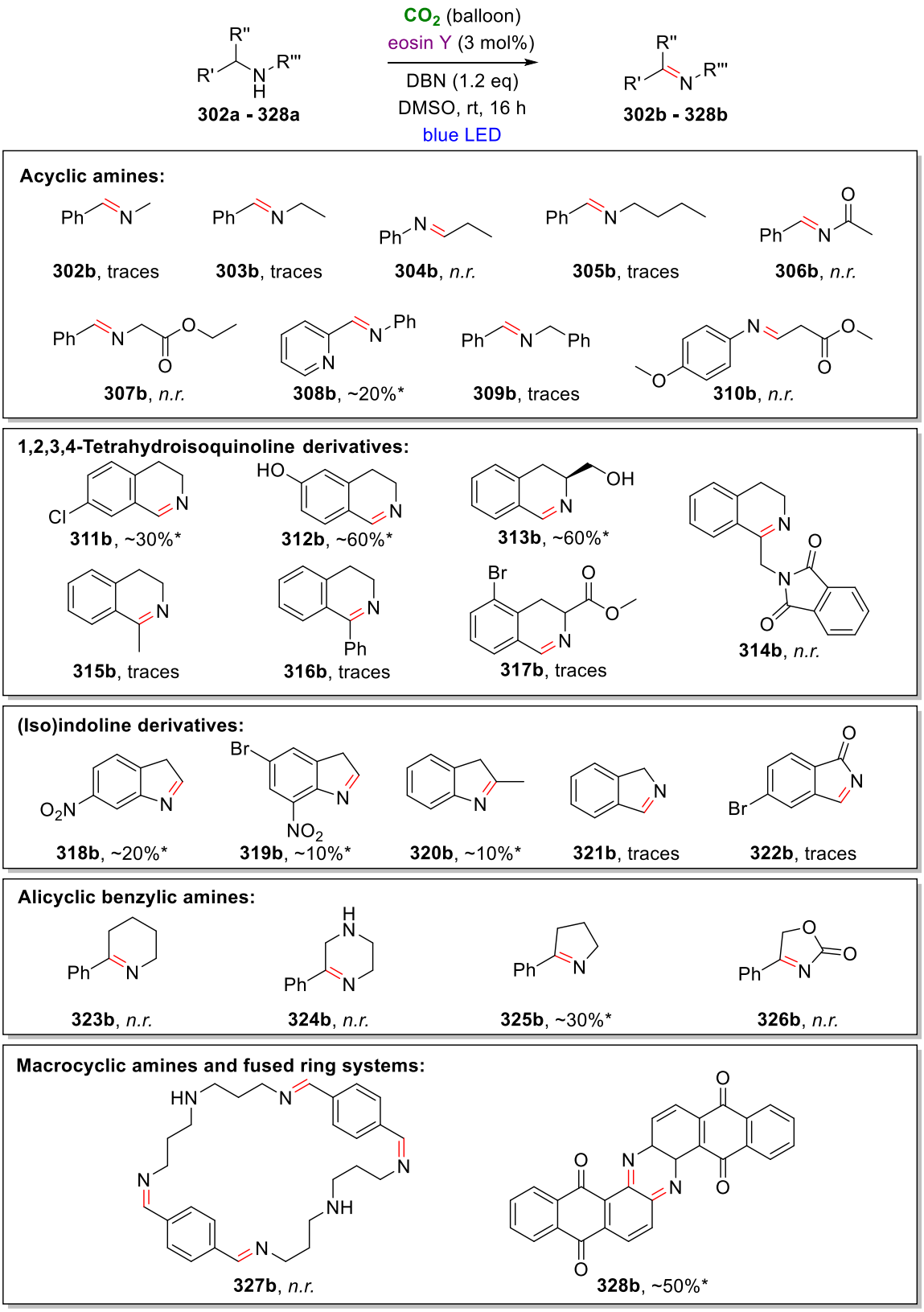

Scheme 54: Unsuccessful substrates for the oxidation of amines to imines; reaction conditions: substrates (0.134 mmol), eosin Y (3 mol%), DBN (1.2 eq), DMSO (2.5 mL), CO_2 (balloon), 12 W blue LED, rt, 16 h; *yield estimated by GC-MS.

In case of 1,2,3,4-tetrahydroisoquinoline derivatives chloro-substitution, even at the same position as nitrile and bromo examined beforehand (*cf.* **281b** – **282b**), was barely

accessible by the optimized reaction conditions (**311a**). Hydroxyl-substituted **312a** could not be isolated due to purification issues despite good yield. Substitution at 3-position with a hydroxymethyl group was actually tolerated (just in contrast to 3-substitution with a carboxylic ester moiety as in case of **317a**) but several purification issues hindered obtaining the pure corresponding product of **313b**.

1-Substitution hampered the reactivity either due to steric or electronic effects at the actually active site (**314a** – **316a**). In case of indoline derivatives, only nitro substituents and 2-substitution seem not to be proceeded by the reaction system (**318a** – **320a**). Since the driving force of the C–C bond dehydrogenation of indoline derivatives was the aromatization of the heterocyclic 5-membered ring, isoindoline derivatives are consequently not reactive at all (**321a** – **322a**).

Alicyclic amines (**323a** – **326a**) were not part of the investigated scope of substrates since most of the examined derivatives were not reactive. Only **325a** showed rather poor activity, but purification issues prohibited further investigations. When macrocyclic substrate **327a** was investigated, no product formation was observed *via* ESI-MS or ^{1}H and ^{13}C NMR spectroscopy, even after increasing the base loading to the sixfold amount according to the number of potentially oxidizable C–N bonds. Analog to other substrates where aromatization played a role as driving force (*cf.* **286b** – **288b**, **296b**), the large fused ring system of **328a** underwent oxidation in semiquantitative amounts. Yet, purification attempts did not yield the expected product.

3.2.4.3 Application of the Amine Dehydrogenation Synthetic Protocol

In respect to the scope of substrates of acyclic amines (*cf.* **Scheme 48**), it can be rationalized that this developed dehydrogenation method could be also applied as a reaction step within more complex reaction sequences. Those reaction sequences, which are commonly used *e.g.* for natural product syntheses, usually require water and/or acids. Especially because imine groups are prone to hydrolysis, the developed CO_2-catalyzed method could be useful for a late-stage modification of more complex amine structures to imines in a water- and acid-free pathway. Moreover, both imine products **269b** and **271b** are known as useful intermediates during the synthesis of pyrrolidinone and piperidinone derivatives, respectively. These are valuable com-

pounds in medicine, *e.g.* for urokinase receptor binding studies.[179] Furthermore, acyclic imines like the ones shown in **Scheme 48** are also used for the synthesis of artificial amino acids.[180]

The partially dehydrogenated 3,4-dihydroisoquinoline derivatives depicted in **Scheme 49** are known to be used for the synthesis of isoquinoline alkaloids. For instance, the synthesized dimethoxy-substituted derivative **284b** was successfully used in the literature for the three-step natural product synthesis of the potential antitumor agent crispine A and the one-step synthesis of the isoquinoline alkaloid natural product berine (**Scheme 55**).[181]

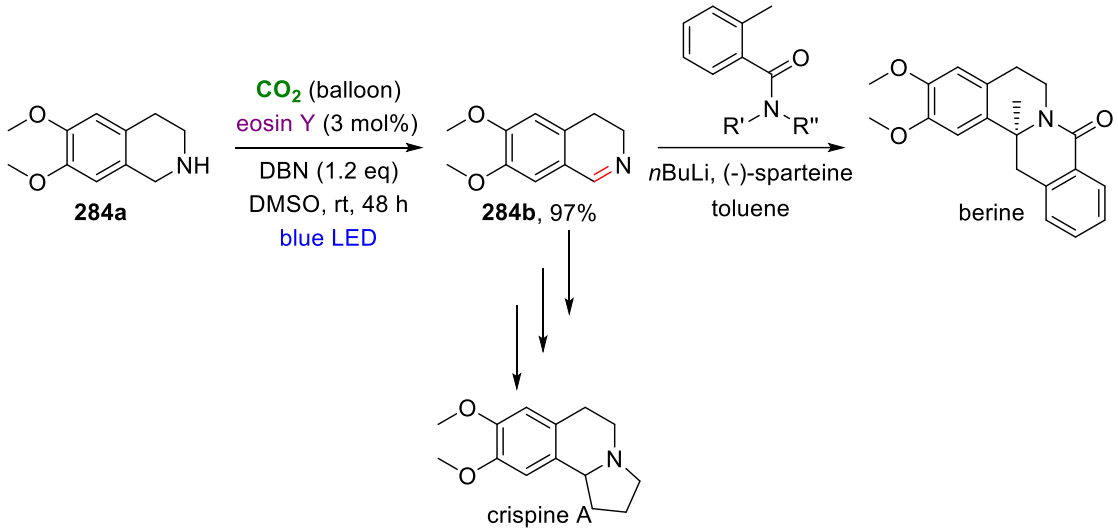

Scheme 55: Potential literature-known synthesis of crispine A and berine from product **284b**.

For demonstrating the applicability of the developed mild CO_2-catalyzed oxidation method, a one-pot reaction was implemented consisting of the condensation of an aromatic diamine with an aromatic aldehyde under optimized reaction conditions. This was followed up by an *in situ* aromatization of the so-formed 5- and 6-membered ring, respectively (**329b** – **331b**; **Scheme 56**). The condensation step is literature-known to proceed at rt, usually within 24 – 60 h.[182] Under optimized photocatalytic reaction conditions, this step did not only proceeded in shorter time but both steps yielded high amounts of desired heteroaromatic compounds within 16 h of total reaction time. Three different aldehydes were chosen representing substituted benzaldehyde (**329b**) and aldehydes with 5- as well as 6-membered heteroaromatic backbones derived from furane and pyridine (**330b** – **331b**).

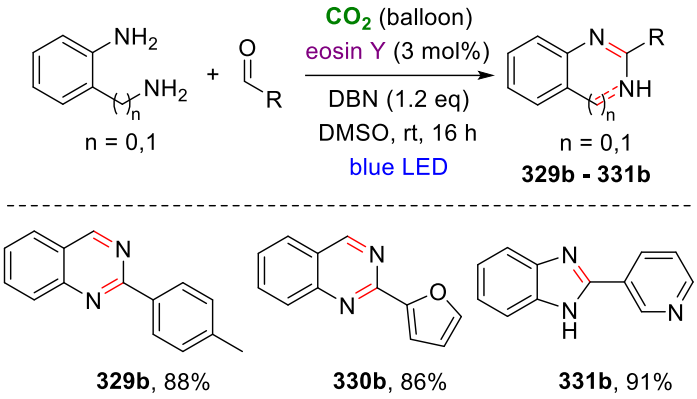

Scheme 56: Condensation of diamine and aldehyde and *in situ* oxidation to the heteroaromatic derivative; reaction conditions: substrates (0.134 mmol), **D** (3 mol%), DBN (1.2 eq), DMSO (2.5 mL), CO_2 (balloon), 12 W blue LED, rt, 16 h; all are isolated yields.

As a final application, the potential of the developed methodology was tested as the transition metal-free synthesis and oxidation of pharmaceutically active molecules (**Scheme 57**). For that purpose the psychoactive indole alkaloid harmaline[183] (**332a**) and the calcium channel blocker nifedipine (**333a**), used for the treatment of angina pectoris and hypertension,[184] were oxidized/aromatized within 16 h in good yields.

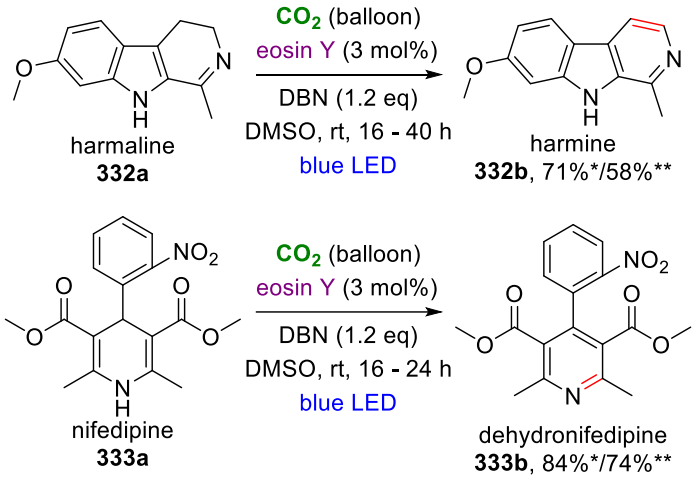

Scheme 57: reaction conditions: substrates (0.134 mmol), eosin Y (3 mol%), DBN (1.2 eq), DMSO (2.5 mL), CO_2 (balloon), 12 W blue LED, rt, 16 – 40 h; all are isolated yields; *CO_2 balloon, **20 mol% CO_2.

The product harmine **332b** is a well-known monoamine inhibitor possessing anti-HIV and anti-tumor characteristics[183,185] but is also used as an important intermediate in drug molecule syntheses as shown in patented processes.[186] The second product dehydronifedipine (**333b**) is the active metabolite of **333a** (metabolized *in vivo* by the cytochrome P450 isomers CYP3A4 and CYP3A5) and its actual active agent within the organism.[187] Moreover, for specific studies of the metabolistic mechanisms it is important to have a mild synthetic pathway for the aromatization and isolation of these

Hantzsch ester-type drug molecules.[188] Additionally, these two interesting applications of drug molecules were chosen to testify whether catalytic amounts of CO_2 were sufficient for an effective transformation. Indeed, both products were obtained in good to high yields both with excess (balloon) and catalytic amounts (20 mol%) of CO_2. Only about 10% difference in yield was observed thus both proving the catalytic nature of CO_2 within the reaction mechanism and the sustainability of the developed oxidation reaction approach.

3.2.4.4 Mechanistic Studies

Table 6: Mechanistic experiments: different CO_2 amounts and control experiments.

Entry	Changed reaction parameter	Yield / %
1	0.2 eq CO_2	**70**
2	1.0 eq CO_2	**84**
3	CO_2 balloon (≈ 500 eq)	**96**
4	O_2 balloon	**5**
5	N_2 atmosphere	**1**
6	no light	**0**
7	no catalyst	**0**
8	no base	**0**
9	0.2 eq BHT	**12**
10	1.0 eq BHT	**0**
11	0.2 eq TEMPO	**0**
12	1.0 eq TEMPO	**0**
13	benzoquinone	**2**

Reaction conditions: **266a** (0.134 mmol), **D** (3 mol%), DBN (1.2 eq), DMSO (2.5 mL), CO_2 (balloon), 12 W blue LED, rt, 48 h; yields were determined by GC using *n*-dodecane as internal standard.

After the development of the scope of substrates and highlighting possible applications for the synthesized imine products, further investigation of the reaction mechanism was of greater interest. The photocatalytic reaction mechanism was expected to exhibit several differences compared to the previously reported mechanisms of the CO_2-catalyzed alcohol and ketol oxidation, respectively. For this purpose, several experiments, listed in **Table 6**, were conducted to elucidate the role of different reaction parameters. First, the role of CO_2 had to be clarified. Thus, experiments with different volumetrically

measured CO_2 amounts (entries 1 – 3; *cf.* **Table 3**) were undertaken and it was found that catalytic amounts were sufficient while only slightly decreasing the yield.

Therefore, CO_2 is not consumed during the reaction ruling out the possibility of CO_2 being the actual oxidant. Consequently, no reduced products from CO_2 like CO, formic acid or formate salts were detected either by NMR spectroscopy or *in situ* gas phase GC analysis of the headspace of the reaction. Besides, the latter one also excluded the presence of O_2 as exogeneous oxidant in the gas phase during the reaction (see **Figure 27** – **28** in the appendix). Instead, a hint for DMS as a byproduct was found in ^1H NMR spectra suggesting an analogy to the above-described mechanisms and the well-known Swern oxidation mechanism.

Under oxygen and nitrogen atmosphere or under omission of catalyst, base and irradiation with blue LEDs only low or no product formation was observed, respectively (**Table 6**, entries 4 – 8). This emphasizes both the important role of CO_2 and the irradiation with light, hence pointing toward a photochemistry approach rather than thermal reaction conditions. Moreover, an experiment under O_2 atmosphere again ruled out the possibility of traces of oxygen gas being the actual oxidant present in the reaction atmosphere. When BHT and TEMPO were applied as radical quenchers, low to no activity was observed depending on the added amount of the specific quencher, which demonstrates the radical nature of important intermediates (entries 9 – 12). Finally, benzoquinone was used as a literature-known reactant intercepting CO_2 radical anions.[24] Especially this latter result triggered the idea of trapping the supposed CO_2 radical anion with DMPO as trapping reagent and subjecting this adduct to electron paramagnetic resonance (EPR) spectroscopy (**Figure 10**).

The background measurements of DMPO in DMSO **(a)**, optimized reaction conditions yet under N_2 atmosphere **(b)** or under CO_2 atmosphere but without light irradiation **(c)** with DMPO being present in both cases as well did not show signals within the envisioned magnetic field range. This proves that no background signal from DMPO or possible contaminating compounds was obtained and neither radicals were formed within the reaction system itself under inert gas nor without light irradiation.

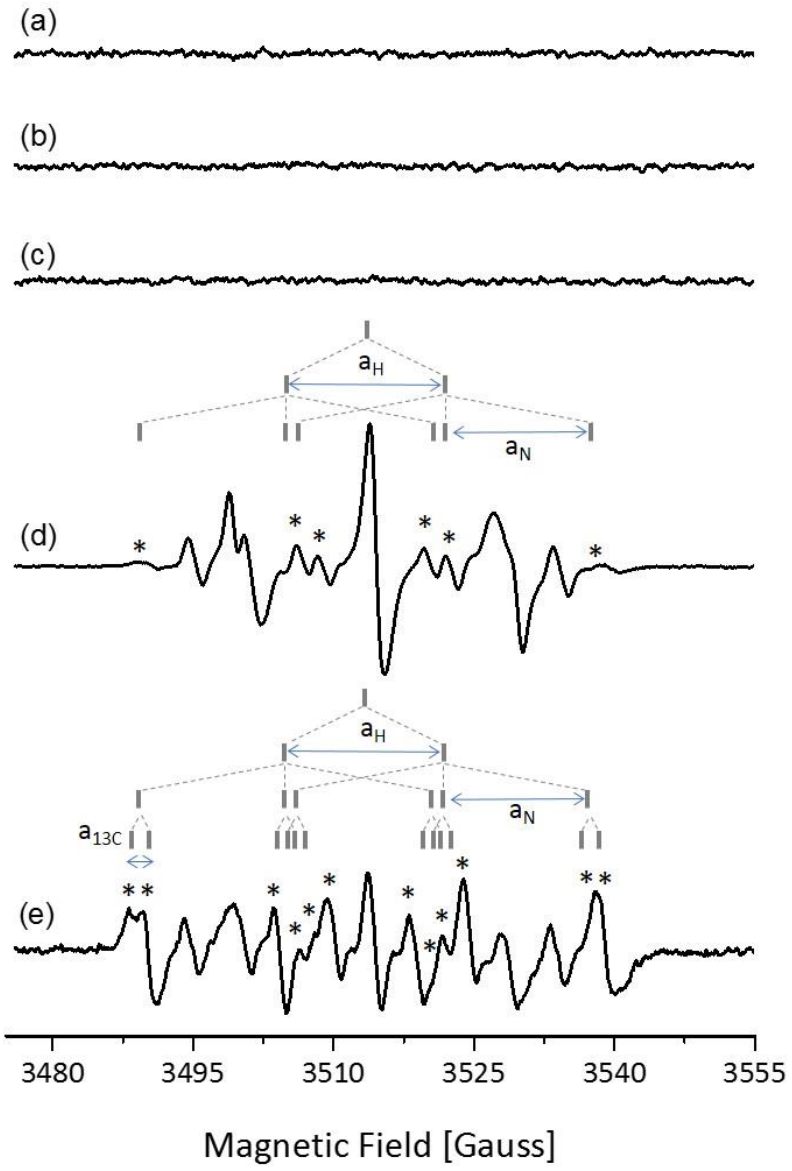

Figure 10: X-band EPR and background spectra of DMPO+CO_2 adducts measured under different conditions using DMPO as a trapping agent: **(a)** N_2 atmosphere, DMPO/DMSO (54 mM), without light irradiation; **(b)** N_2 atmosphere, DMPO/DMSO (54 mM), **D** (3 mol%), DBN (1.2 eq), **266a** (0.134 mmol), blue LED light (18 h); **(c)** $^{12}CO_2$ atmosphere (balloon), DMPO/DMSO (54 mM), **D** (3 mol%), DBN (1.2 eq), **266a** (0.134 mmol), without light irradiation; **(d)** $^{12}CO_2$ atmosphere (balloon), DMPO/DMSO (5 mM), **D** (3 mol%), **266a** (0.134 mmol), DBN (1.2 eq), blue LED light for 18 h; **(e)** $^{13}CO_2$ atmosphere, DMPO/DMSO (54 mM), **D** (3 mol%), **266a** (0.134 mmol), DBN (1.2 eq), blue LED light for 18 h; *distinctive *hf* lines of $^{12}CO_2$- and $^{13}CO_2$-centered sub-spectra in **(d)** and **(e)**, respectively; experimental conditions: Bruker ElexSys E500 CW/Transient X-band EPR spectrometer equipped with the Bruker SHQ (ER4122 SHQE-W1) resonator, microwave frequency 9.87 GHz, microwave power 20 mW, field modulation 1 G, receiver gain 60 dB; conversion time 5.18 ms, 400 and 81 averaged scans for **(a)** – **(c)** and **(d)** – **(e)**, respectively; measurements and discussion of EPR experiments were done with the help of Igor Tkach.

In fact, after blue light irradiation under optimized reaction conditions with CO_2 being present, several DMPO adducts were formed and could be observed by EPR spectroscopy. The spectral lines of those several adducts overlap and assemble the observed EPR spectra. Notably, those radical spectra were only detected when all optimized reaction conditions were fulfilled along with addition of DMPO. All species exhibited partially resolved hyperfine (*hf*) patterns mainly due to an internal interaction of the electron spin with the ^{14}N (I = 1) and *β*-^{1}H (I = ½) magnetic nuclei, which is a typical observation when DMPO is used as spin trap agent.[189] However, the decay times associated with the contributing spectra were different, therefore preventing systematic follow-up studies.

Moreover, due to the relatively high viscosity of the reaction mixture (emerging from DMSO), correlation times of the observed adducts were prolonged. Hence, anisotropic contributions were visible and led to a deviation from isotropic-limit values. This further complicates analysis of the contributing subspectra. Thus, exact assignment of possible adducts is still ambiguous and cannot be resolved without further special studies. However, initial examination of the observed spectra revealed that the *hf* structure of one of the subspectra (**Figure 10**, **(d)**, marked by stars) is in close agreement with the previously reported data for DMPO–CO_2 radical adducts.[190]

When the reaction was performed under $^{13}CO_2$ atmosphere, additional *hf* line splitting occured (**Figure 10**, **(e)**, marked by stars) as expected by an internal *hf* interaction with the magnetic ^{13}C isotope (I = ½). This observed effect further supports the assumption that CO_2 species contributed to the observed subspectrum as part of the measured overall EPR signal.

As already mentioned above, DMSO was suspected to be the actual oxidant since a hint for DMS was found. Based on this finding, an experiment using di-*n*-butylsulfoxide as solvent instead of DMSO was conducted (**Scheme 58**) since the so-formed byproduct di-*n*-butylsulfide was easier to quantify due to its higher boiling point compared to DMS (188 °C compared to 37 °C, respectively). Analysis of the reaction mixture *via* GC and GC-MS showed evidence of the solvent being the actual oxidant forming the corresponding di-*n*-butylsulfide. Di-*n*-butylsulfide was quantified in similar amounts as the main product **266b**, which proved the respective sulfoxide being the actual oxidant.

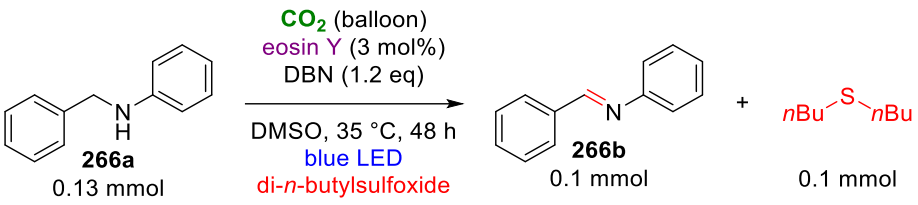

Scheme 58: Reaction of **266a** in di-*n*-butylsulfoxide as solvent; reaction conditions: **266a** (0.134 mmol), **D** (3 mol%), DBN (1.2 eq), DMSO (2.5 mL), CO_2 (balloon), 12 W blue LED, rt, 48 h; yield of **266b** was determined by GC using *n*-dodecane as internal standard; amount of $(n\text{-Bu})_2S$ was determined *via* GC-MS.

Furthermore, the progress of the model reaction was monitored over a total timespan of 48 h (**Figure 11**, **(A)**). This revealed that more than 80% of the conversion occurs within 24 h in an almost linear way with a short induction period during the first 1 – 2 h, which is typical for photocatalytic reactions. When the reaction was carried out with different concentrations of DBN **(B)**, starting material **(C)** and catalyst **(D)**, the chosen concentrations were plotted against the observed rate constants in a logarithmic way.

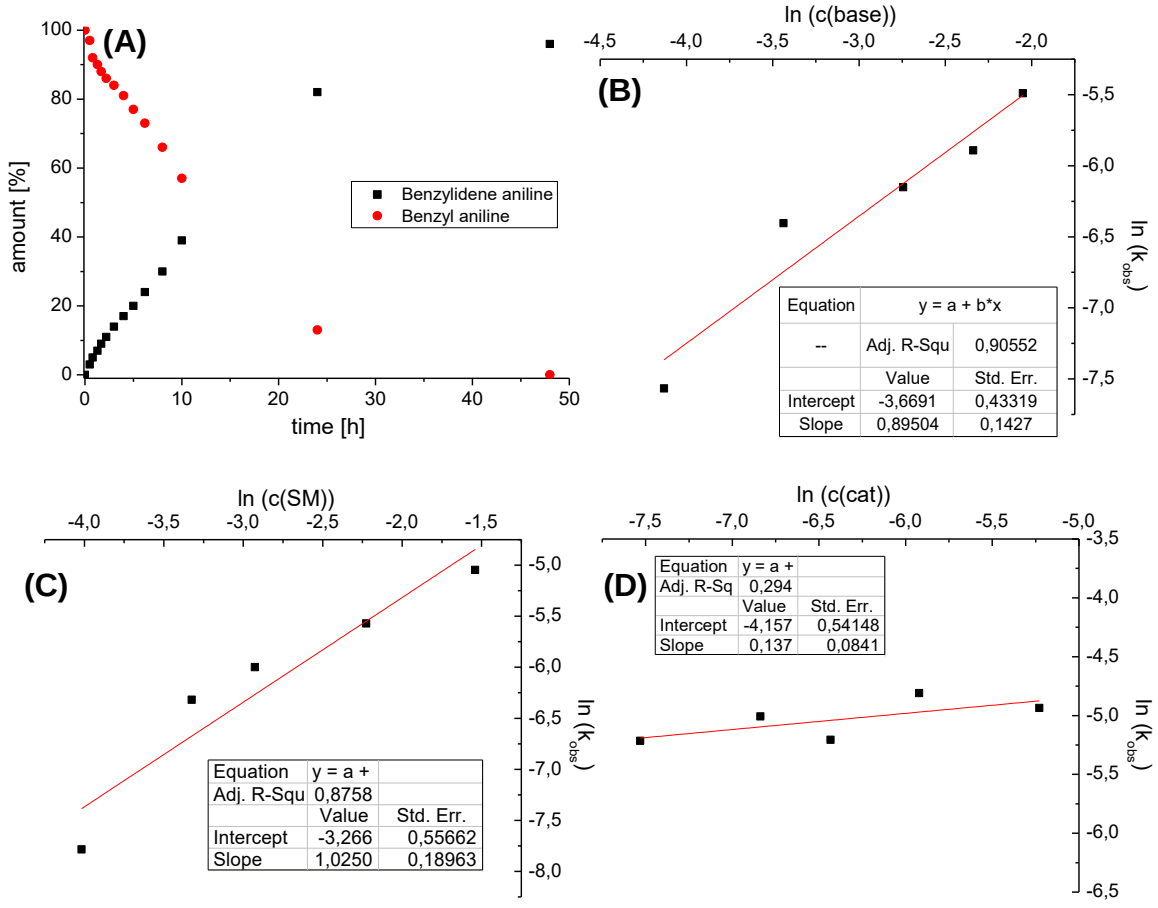

Figure 11: Reaction of **266a** under optimized reaction conditions: Reaction monitoring over 48 h **(A)**, plots for determination of reaction order in respect to DBN **(B)**, **266a (C)** and eosin Y **(D)**.

This enabled the determination of the reaction orders revealing 1st reaction order in respect to both DBN and *N*-benzylaniline and a 0th reaction order for the catalyst. A

nearly linear increase with base and starting material concentration was observed so the respective 1st reaction orders for both cases were not surprising. The calculated 0th reaction order regarding the catalyst is also reasonable, since photocatalytic reactions are more complex by means of other intermediates being involved in the reaction mechanism besides of a simple substrate-catalyst adduct.

Moreover, a Stern-Volmer plot was generated from results of recording excitation/emission spectra of eosin Y at its excitation and emission maxima (533 nm and 550 nm, respectively) with different amounts of quenchers of the excited state of the photocatalyst from the reaction mixture (*i.e.* substrate **266a** and CO_2; **Figure 12**). The fluorescence intensity decreased dramatically with increasing amine concentration, but no change was observed in case of saturation with CO_2. This showed that the catalyst firstly reacted with the starting material after its excitation but not with CO_2.

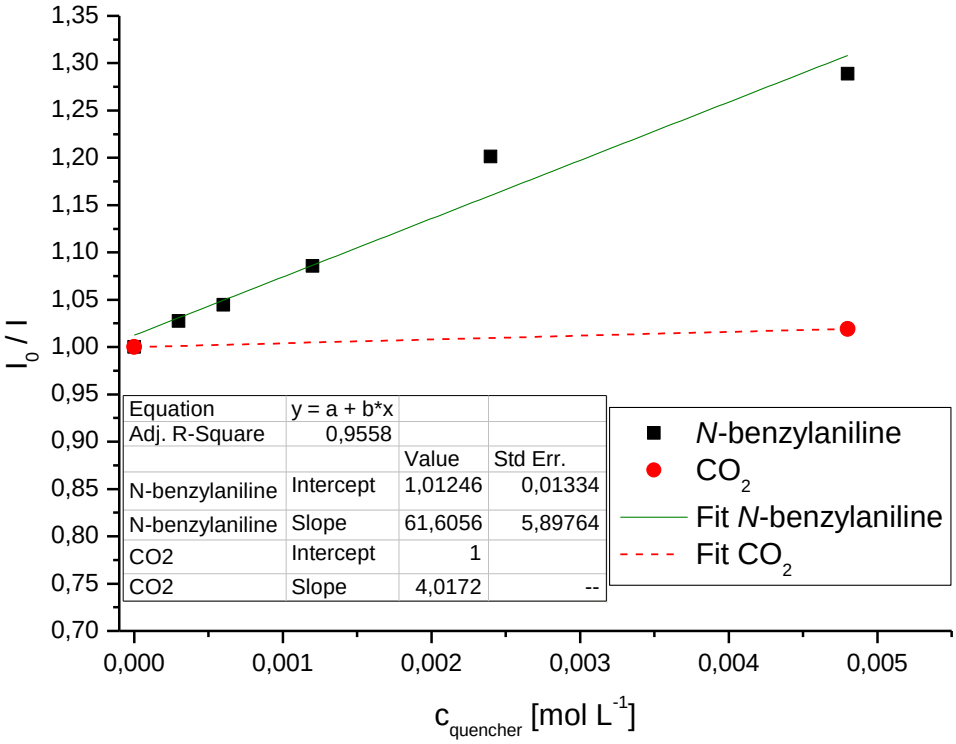

Equation	y = a + b*x		
Adj. R-Square	0,9558		
		Value	Std Err.
N-benzylaniline	Intercept	1,01246	0,01334
N-benzylaniline	Slope	61,6056	5,89764
CO2	Intercept	1	
CO2	Slope	4,0172	--

Figure 12: Stern-Volmer plot for **D** with **266a** and CO_2 as potential quenchers.

Next, KIE experiments were carried out in order to identify or eliminate the C–H bond cleavage as possible rate-determining step as a result of three independent runs each (**Scheme 59**). Using mono- and di-deuterated **280a** resulted in a calculated average KIE of 1.3 excluding the C–H bond cleavage of the starting material to be the rate-determining step. Additionally, a hint for D_2O as byproduct was found in a ^2H NMR spectrum recorded from the reaction mixture of **280a-*d*$_2$** in non-deuterated DMSO (see **Figure 29** in the appendix).

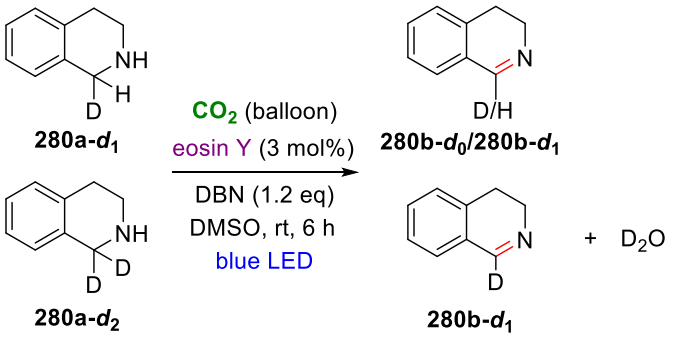

Scheme 59: KIE experiment with mono- and di-deuterated substrate **280a**; reaction conditions: substrate (0.134 mmol), eosin Y (3 mol%), DBN (1.2 eq), DMSO (2.5 mL), CO_2 (balloon), 12 W blue LED, rt, 6 h.

Considering all experimental data mentioned above, DFT and *ab initio* calculations were performed for the dehydrogenation of **280a** as model reaction (for computational details, see **chapter 5.3.3**).

Since the presence of CO_2 is essential for the reaction to occur, the primary focus was laid on the reductive role of CO_2 in the mechanism. Thus, by identifying the energetically most favorable species to be reduced the overall reaction mechanism should be revealed. For the calculations, the COSMO-RS solvent model for DMSO was chosen to calculate the standard redox potential of five different possible species (**Figure 13**).

The reduction of sole CO_2 to its radical anion exhibits a substantial calculated redox potential of –2.79 V, which is in reasonable agreement with the literature data of –2.21 V for its necessary reduction potential.[15i] Since eosin Y has been shown in literature to overcome only an approximated redox potential of –1.06 V, the relevant reaction cannot be interpreted with the involvement of a free CO_2 radical anion.[29d,191]

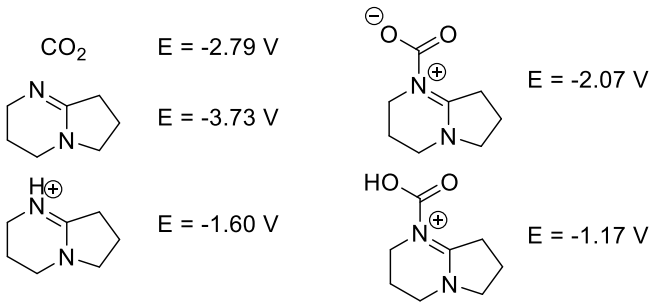

Figure 13: Calculated redox potentials of the DBN-related species that may occur in the reaction mixture; values are given for single electron reduction; calculations were carried out by Oldamur Hollóczki.

The base DBN was found to have an even higher redox potential of –3.73 V making its reduction unlikely as well. However, DBN as a so-called superbase can be protonated in solution, thus decreasing the redox potential significantly. In light of the above-

mentioned overestimation of the redox potential of CO_2, it is possible, although unlikely, that the protonated base could be reduced by eosin Y. However, since CO_2 is also known to act as Lewis acid, it is prone to react with bases in general. The reaction of CO_2 and DBN to a zwitterionic compound is accompanied by a reaction Gibbs free energy of $\Delta G = -0.5$ kcal mol^{-1}. For the resulting adduct, a slightly less negative potential of –2.07 V was found compared with a free CO_2 molecule and notably more negative compared to protonated DBN. Just like DBN, the DBN–CO_2 adduct is also prone to undergo protonation, which is once again accompanied with a lower redox potential of –1.17 V. The difference between this calculated value and the literature data for eosin Y is within the expected error range of the applied computational methods. Because of that it can be assumed that the CO_2 reduction to its radical anion is apparently aided by DBN. This is also in good agreement with the experimental proof for the base being substantial for the reaction to proceed (see **Table 6**, entry 8). However, since DBN is a stronger base than the DBN–CO_2 adduct, it is reasonable to question the accessibility of DBN–CO_2H in the presence of excess DBN. The Gibbs free energy difference for a proton transfer from DBNH$^+$ to DBN–CO_2 was found to be only $\Delta G = 8.2$ kcal mol^{-1}, which is an energy demand that is possible to overcome at room temperature. This energy demand is easily compensated within the reduction process with $\Delta G = -9.9$ kcal mol^{-1}, which results in the more stable intermediate DBN–CO_2H compared to DBNH$^+$.

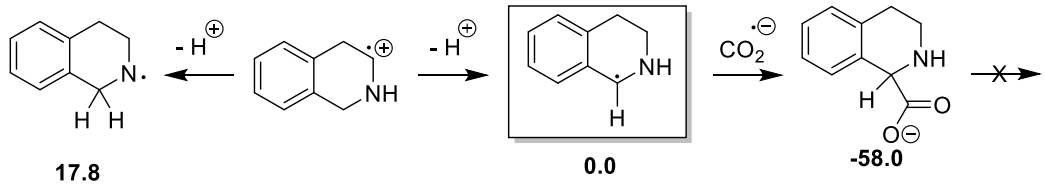

Scheme 60: Possible reactions of the amine radical cation with the base and the carbon dioxide radical anion; the numbers below the structures are relative Gibbs free energies with respect to the amine radical and the free carbon dioxide radical anion; calculations were carried out by Oldamur Hollóczki.

Starting from the amine radical cation, two possible amine radicals can be formed through deprotonation by DBN (**Scheme 60**). However, deprotonation at the nitrogen atom is less favorable with a Gibbs free energy of $\Delta G = 17.8$ kcal mol^{-1} compared to deprotonation at the carbon center between the aromatic ring and the nitrogen atom. This might be explained by stabilizing mesomeric conjugation of the nitrogen's lone electron pair and the aromatic ring. Since a CO_2 radical anion species is present in the system, the first assumption was a recombination of the sole CO_2 radical anion with

the neutral amine radical as first reaction step. This would result in a carboxylate anion with a Gibbs free energy of $\Delta G = -58.0$ kcal mol^{-1} indeed exhibiting a high affinity of those two radicals to recombine. However, there seems to be no feasible reaction path for this carboxylate anion to further react in a way leading to the desired imine product and dimethylsulfide. Consequently, no reasonable intermediates or transition states corresponding to a reaction of this anion and DMSO could be calculated. This is in distinct agreement with the lack of any evidence for such carboxylate intermediates, thus ruling out this anionic adduct of starting material and CO_2.

To summarize all mechanistic experiments and calculations a reasonable reaction mechanism was postulated, inspired by the Swern oxidation (**Scheme 61**): First, CO_2 forms a zwitterionic intermediate with the base (DBN), which is protonated *in situ*. The proton source might be either a previously successful reaction (see deprotonation step of the substrate radical cation) or present water. This protonated cationic intermediate can undergo reduction by a photocatalyst radical cation as calculated previously. Simultaneously, the catalyst eosin Y is energetically elevated to an excited state *via* visible blue light irradiation. This excited state can undergo SET with the amine substrate **A** forming a substrate radical cation and a photocatalyst radical anion. This photocatalyst radical anion reacts back to its ground state while reducing the protonated CO_2–DBN adduct to a neutral radical species.

Meanwhile, the cationic radical amine substrate is deprotonated with the aid of DBN to neutral radical amine intermediate **B**. Then, **B** reacts with DMSO to (1,2,3,4-tetrahydroisquinoline-1-yl)oxyl (**C**) while directly releasing byproduct DMS in agreement with the observed reduction of the S=O bond with di-*n*-butylsulfoxide (*cf.* **Scheme 58**). The evaporation of DMS from the reaction mixture further shifts the energetics of this step in a manner that it becomes more likely. During the next step, **C** reacts with the neutral radical CO_2–DBN adduct to the non-radical carbonic acid hemiester intermediate **D**, which is energetically highly favorable. **D** can then decompose to CO_2, water and the product in a thermodynamically favored step ($\Delta G = -6.1$ kcal mol^{-1}). Both CO_2 and byproduct water were experimentally detected by ^{2}H NMR and *in situ* gas phase GC measurements, respectively. From a thermodynamic point of view, it should be noted, that the formation of intermediates **B** and **C** is slightly energetically uphill (in comparison to **A**). However, this energetic input can be probably delivered at room temperature while the strongly lower energetic level of **D** and **E** make up for this energy input. Along with the increase in entropy when the slightly energetically higher **E** is formed from **D**,

both water as the second byproduct and CO_2 as catalyst are released. Moreover, when amine radical **B** is formed, it is infolded by DMSO molecules while the DBN–CO_2 radical adduct has to diffuse through the solvent for recombination with **C**. Despite the high affinity of amine radical **B** to a CO_2 radical species, it is possible that **B** immediately reacts with DMSO.

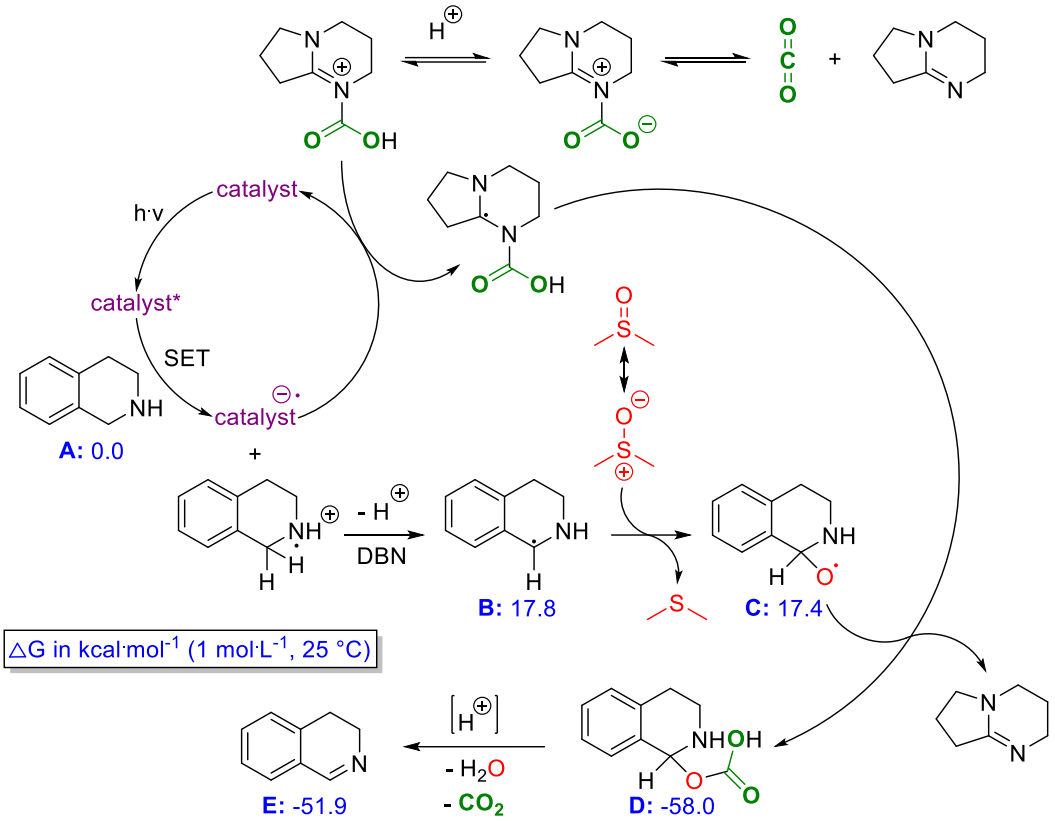

Scheme 61: Proposed reaction mechanism; DLPNO-CCSD(T)/def2-TZVPP, COSMO-RS (DMSO) corrected single point energies relative to **A** in kcal mol^{-1}; calculations were carried out by Oldamur Hollóczki.

4 Summary and Outlook

In summary, finding mild reaction procedures for the fixation and other valorization of the greenhouse gas CO_2 was highly successful regarding the initial aim. This utilization was also covered by finding suitable applications such as the formation of drug molecules and valuable intermediates for potential further syntheses.

At first, carbamates were generated by an unprecedented and simple method using cheaper carbonate bases and an alkyl halide in high yields with high selectivity and an excellent functional group tolerance. This method was also suitable for the simple and metal-free derivatization of drug molecules and the highly chemoselective protection of amino acids and peptides. For this, the well-established CBz protecting group was formed from CO_2 and benzylbromide, thus replacing the toxic benzylchloroformate as commonly used protecting agent. Even though this is a great step toward greener syntheses, the limitations of this method were also discussed. Moreover, the major drawback is the use of harmful alkyl halides and the formation of equimolar amounts of alkali metal halides byproducts. The use of alcohols instead, as published by De Vos *et al.*,[41b] or other greener reactants could solve this issue. However, initial attempts using different alcohols did not succeed under optimized reaction conditions so far making further research necessary to resolve this drawback.

Second, CO_2 was successfully employed as oxidation promoter during the oxidation of general primary and secondary alcohols to their corresponding carbonyl compounds. Furthermore, the oxidation of ketols to diketone products and the oxidation of amines to imines was accessible. Albeit the reaction pathway was changed from electron pair chemistry to radical chemistry in case of amine oxidation, all three are based on the renowned Swern oxidation using DMSO as actual oxidant yet replacing the toxic oxalyl chloride with CO_2. Regarding the general oxidation of primary and secondary alcohols, a vast number of aromatically activated substrates was successfully converted in mostly high yields exhibiting a good functional group tolerance. Especially the high yields obtained from large scale reactions were delightfully observed. Those reactions yielded veratraldehyde (**61b**) as key intermediate for a number of drug molecule syntheses. Additionally, the actual synthesis of two drug molecules was enabled starting from 3,4,5-trimethoxybenzaldehyde (**60b**). Along with that, the metal-free homologation of *α*,*β*-unsaturated aldehydes was demonstrated as a proof of concept. Moreover,

the detailed mechanistic studies provided insight in the suspected role of CO_2. Nevertheless, for in-depth information about the general scope of substrates, more research should be done.

Especially the different ambiguous effects of substitution pattern and the inductive and mesomeric effects of the substituents grafted onto the aromatic moiety could be a trigger for further studies. For instance, some improvement could be sustained when sinapyl alcohol (**Scheme 62**) would be used instead of coniferyl alcohol **120a**. Sinapyl alcohol has higher inductive effects owing to two methoxy groups in 3- and 5-position (*cf.* **58a**, **60a** – **62a**). In addition, sinapyl alcohol can be obtained from biomass as a precursor of lignin, thus strengthening the sustainable approach of this method. Since cinnamyl alcohol substrates are well tolerated by this procedure, it would be interesting to subject vinyl alcohols to the optimized reaction conditions.

In case of successful oxidation reactions, the products could be further used *e.g.* for conducting a Baylis-Hillman reaction. This Baylis-Hillman reaction could employ a simple base in catalytic amounts such as DABCO, DBU or DMAP[192] with a second carbonyl substrate (generated by this method) yielding an *α*-hydroxyvinylcarbonyl. This resulting product exhibits a tertiary alcohol functional group, which is not prone to further oxidation as displayed in **Scheme 62**. However, the aza-Baylis-Hillman reaction with amines instead of alcohols should not work under these conditions since the amine substrate would be carboxylated *in situ*. This chapter was completed with mechanistic studies about the presented novel CO_2-catalyzed oxidation process.

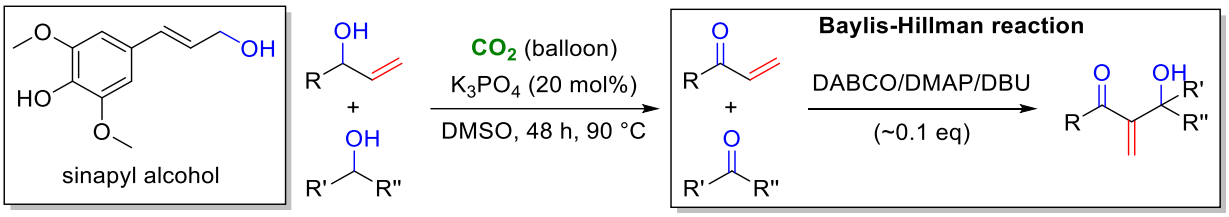

Scheme 62: Sinapyl alcohol as alternative substrate for alcohol oxidation and possible application of vinyl alcohol substrates for the Baylis-Hillman reaction.

After also successfully oxidizing ketol substrates under optimized conditions, it was nearby to test, whether those substrates could be generated *in situ via* benzoin condensation and further oxidized to the corresponding diketones. Delightfully, the chosen cheap NHC catalyst was well tolerated under similar reaction conditions. After slight modifications of the reaction conditions, a suitable catalytic system was found that was

able to provide *α*-diketones directly from simple and cheap aromatic aldehydes. Notably, attempts to first oxidize primary alcohols to their respective aldehydes, which then undergo benzoin condensation and further oxidation (as a three-step one-pot reaction) failed. The reason might be the different reaction conditions compared to the previous oxidation method. Thus, the first oxidation step did not occur already. Changing the reaction conditions after the first step might achieve this envisioned three-step reaction but with the prize of a rather uncomely three-step two-pot reaction. Further optimization as a goal of follow-up research in that regard might offer another solution though. Regarding the scope of substrates, homocoupled products were obtained in high yields and with good functional group tolerance. In contrast to that, heterocoupling was more difficult and generated more byproducts since one substrate had to be added in 1.5 equivalents. Consequently, the excess of one substrate facilitated the homocoupling of this respective aldehyde. Besides, homocoupled byproducts were observed in any of those cases as byproduct also from the aldehyde employed in lower amounts. However, application of particularly expensive obtained products showed a sustainable metal-free way for the synthesis of relevant drug molecules and heterocyclic scaffold intermediates for further syntheses. Detailed mechanistic investigations completed those studies.

Finally, after changing attention from the oxidation of C–O to C–N bonds, the different nature of the substrates forced the application of a new reaction setup, which has its roots in photochemistry for the above-mentioned reasons. With this new reactivity applied to the CO_2-catalyzed Swern-type oxidation reactions, it was possible to oxidize a vast number of simple acyclic benzylic amines. Among them, 1,2,3,4-tetrahydroisoquinoline and indoline derivatives as well as Hantzsch ester-type substrates with a large spectrum of different functional groups were successfully oxidized. Double oxidation or C–C bond dehydrogenation were observed in some cases due to full aromatization of the final product. However, one-side aliphatic substrates were not well tolerated in general as in case of alcohol oxidation despite the new reaction mechanism. Further screening of photocatalysts (*i.e.* different redox potentials) and light sources could possibly overcome this. Applications were shown in terms of the condensation of diamines and aldehydes with *in situ* aromatization to heteroaromatic scaffolds and the modification of drug molecules. Detailed mechanistic studies showed evidence for a CO_2 radical species. Besides, further EPR studies, *e.g.* with different other (isotope-

labeled) spin traps or other measurement parameters, would be needed to make unambiguous statements about the radical species involved.

Regarding the noble aims postulated in the beginning it can be legitimately said that the herein presented research results may indeed help for the utilization of CO_2 in both ways, either as its utilization on the way or as its direct fixation. Of course, it would be reasonable to first utilize it as a catalyst and then fixate it afterwards. This strategy would accomplish a double benefit of CO_2 besides the fact of reducing its emissions into the atmosphere. Especially the disclosed CO_2-catalyzed reactions are rather a proof of concept yet, so further research should be undertaken in order to translate those developed methodologies into valuable synthetic strategies for the future.

5 Appendix

5.1 Materials and Methods

Unless otherwise stated, commercial reagents were used without purification and reactions were run under CO_2 atmosphere with exclusion of moisture from reagents and solvents using standard techniques for manipulating air-sensitive compounds.

^{1}H NMR spectra (300, 400 and 500 MHz) and ^{13}C NMR spectra (75.58, 100.62 and 125.71 MHz) were recorded using Bruker spectrometers AVANCE III 300, AVANCE III HD 400, AVANCE III 400, AVANCE III HD 500 and Varian spectrometers Mercury VX 300, VNMRS 300 and Inova 500 with $CDCl_3$ and DMSO-d_6 as solvents. NMR spectra were calibrated using solvent residual signals ($CDCl_3$: δ ^{1}H = 7.26, δ ^{13}C = 77.16; DMSO-d_6: δ ^{1}H = 2.50, δ ^{13}C = 39.52).

ESI mass spectra were recorded on Bruker Daltonic spectrometers maXis (ESI-QTOF-MS) and micrOTOF (ESI-TOF-MS). GC-MS mass spectra were recorded on Thermo Finnigan spectrometers TRACE (Varian GC Capillary Column; wcot fused silica coated CP-SIL 8CB for amines; 30 m x 0.25 mm x 0.25 µm) and DSQ (Varian FactorFour Capillary Column; VF-5ms 30 m x 0.25 mm x 0.25 µm). Citations at measured GC-MS data throughout **chapter 5.4** refer to the mention of theses compounds in the literature (checked by SciFinder). Gas chromatography was performed on an Agilent Technologies chromatograph 7890A GC System (Supelcowax 10 Fused Silica Capillary Column; 30 m x 0.32 mm x 0.25 µm). GC calibrations were carried out with authentic samples and *n*-dodecane as an internal standard. *In situ* gas phase GC measurements of the headspace of the reactions were conducted by a Shimadzu GC-2014 equipped with a TCD detector and a ShinCarbon ST 80/100 Silco column.

Absorption-emission spectra were recorded on a Jasco FP-8500 Spectrofluorometer and UV/Vis spectra were recorded on a Jasco V-770 Spectrophotometer. The emission spectrum of the self-constructed LED reaction setup was recorded by an Ocean Optics Flame-T equipped with a P200-5-UV-Vis probe.

pH values were obtained from a SCHOTT pH-Meter CG818 equipped with a Mettler Toledo InLab Routine glass electrode stored in 3 M KCl solution (Mettler Toledo) and calibrated with buffer solutions of pH 4 (citrate/HCl, Grüssing GmbH) and pH 7 (KH_2PO_4/Na_2HPO_4, Grüssing GmbH).

5.2 Reaction Procedures

5.2.1 Reaction Procedures Regarding the Synthesis of Carbamates From CO_2

A 10 mL two-necked flask containing a stirring bar was charged with 0.5 mmol substrate and 0.75 mmol of base. After purging the flask thrice with vacuum and two times with nitrogen, the CO_2 atmosphere was incorporated through a CO_2-filled balloon. Afterwards, dry DMSO (2.5 mL) was added. In case of a liquid substrate, this was added after the purging. The resulting mixture was stirred for 16 – 48 h at rt – 50 °C. Subsequently, 0.6 mmol of alkyl halide were added under inert gas conditions and the mixture was stirred for additional 2 – 4 h at rt. Then, the resulting mixture underwent an aqueous workup and was extracted thrice with excess of DCM or EA and the combined organic layers were dried over anhydrous Na_2SO_4, filtered and concentrated *in vacuo*. In general, products were purified by using silica gel chromatography with EA and *n*-hexane as solvents and, if needed, 1 V% Et_3N.

Synthesis of Peptides:

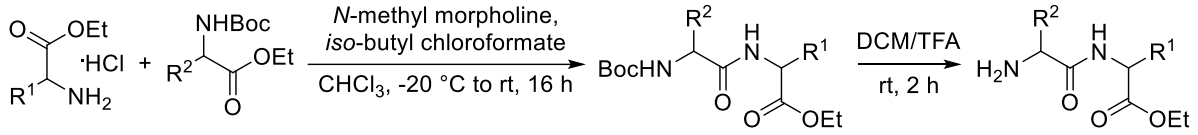

Scheme 63: General synthesis of peptides.

4 mmol of *N*-boc-phenylalanine were dissolved in 10 mL chloroform in a 25 mL round bottom flask and cooled to –20 °C (**Scheme 63**). 4 mmol of *N*-methylmorpholine and 4.3 mmol of *iso*-butyl chloroformate were added and the resulting mixture was stirred for 10 min at –20 °C. After then, 4 mmol of amino acid ester hydrochloride were added into the round bottom flask, followed by quick addition of 4 mmol of *N*-methylmorpholine. The reaction mixture was kept at –20 °C for 1 h and then stirred at rt overnight (16 h). After finishing the reaction, the reaction mixture was washed with 2M HCl solution and 1 mol% $NaHCO_3$ solution in a separatory funnel. The organic layer was dried over anhydrous Na_2SO_4 and then concentrated *in vacuo*. Afterwards, purification was done by silica gel column chromatography with EA, *n*-hexane and 1 V% Et_3N.

Removal of the Boc Protecting Group:

Directly to the reaction mixture (1 g) in 10 mL DCM, 10 mL of TFA were added. The resulting mixture was then stirred at rt for 2 h, after which it was concentrated *in vacuo*: The crude mixture was partitioned between saturated aqueous $NaHCO_3$ and EA and the combined organic layers were dried over Na_2SO_4 and concentrated *in vacuo*. Afterwards, purification was done by silica gel column chromatography with EA, *n*-hexane and 1 V% Et_3N.

5.2.2 Reaction Procedures Regarding the CO_2-Catalyzed Oxidation of Benzylic and Allylic Alcohols

A 10 mL two-necked flask containing a stirring bar was charged with 0.25 mmol substrate and 0.05 mmol of anhydrous K_3PO_4 (20 mol%; stored in glove box). After purging the flask thrice with vacuum and two times with nitrogen the CO_2 atmosphere was incorporated through a CO_2-filled balloon. Afterwards, dry DMSO (2.5 mL) was added. The resulting mixture was stirred for 48 h at 90 °C (the progress can be monitored *via* GC-MS or TLC). Then, the resulting mixture underwent an aqueous workup (using distilled water; or brine in case of slurry phase separation) and was extracted thrice with EA. The combined organic layers were dried over anhydrous Na_2SO_4, filtered and concentrated *in vacuo*. Products were purified *via* silica gel chromatography with EA and *n*-hexane as solvents (typically 20:80 EA:*n*-hexane).

Procedure for the Synthesis of Combretastatin A4 (**190b**):

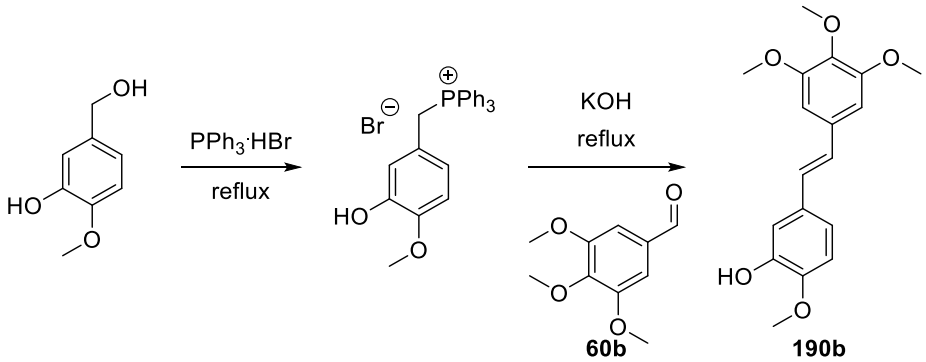

Scheme 64: Synthesis of combretastatin A4 (**190b**).

The synthesis of product **190b** was done according to the literature (**Scheme 64**).[148b] 13.83 mmol (2.14 g) of 3-hydroxy-4-methoxy benzyl alcohol and 13.52 mmol (4.64 g)

of triphenylphosphine hydrobromide were refluxed under a nitrogen atmosphere in dry ACN (40 mL) for 6 h. After cooling to rt, the solvent was removed *in vacuo* to gain the phosphonium salt, which was taken for the next step without further purification.

After that 5 mmol 3,4,5-trimethoxy benzaldehyde (984.1 mg, 0.6 eq, to phosphonium salt) and 8.4 mmol KOH (468.3 mg, 1.0 eq) were added to the phosphonium salt (8.4 mmol, 4 g), dissolved in ethanol (100 mL) and refluxed for 10 h. After cooling to rt distilled water was added to the reaction mixture and the crude product was extracted with EA. To remove remaining impurities purification was done *via* column chromatography (50:50 EA:*n*-hexane).

Procedure for the Synthesis of DMU-212 (**191b**):

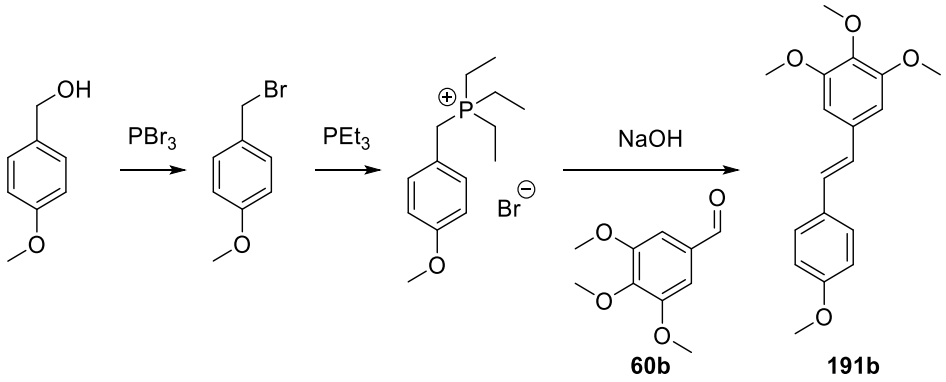

Scheme 65: Synthesis of DMU-212 (**191b**).

The first step of the synthesis of product **191b** was done according to the literature (**Scheme 65**).[194] To a solution of 5 mmol (0.63 mL) of 4-methoxy benzyl alcohol in 20 mL diethylether 6 mmol (0.57 mL) of phosphorus tribromide were added dropwise at 0 °C and stirred for 30 min. The solvent was removed *in vacuo* and the crude 4-methoxy benzyl bromide was taken for the next step without further purification.

The second and third step were done according to another literature-known reaction.[148a] 5 mmol (1005.3 mg) of the crude 4-methoxy benzyl bromide were dissolved in dry dichloromethane under a nitrogen atmosphere. 5 mmol triethylphosphane (0.74 mL) were added at 0 °C and the resulting mixture was stirred at rt for 1 h. The solvent was removed *in vacuo* to yield the crude phosphonium salt, which was taken for the next step without further purification.

5 mmol 4-methoxybenzyl-triethylphosphonium bromide (1190.5 mg) were stirred with 2 mL distilled water for 15 min at rt. After that 20 mmol NaOH (797.6 mg) and after 2

more minutes 4.8 mmol of 3,4,5-trimethoxy benzaldehyde (934.5 mg) were added. After vigorous stirring for 3 h at 70 °C and cooling to rt water was added to the mixture and stirred for additional 10 min. The pure solid product was obtained through suction filtration and washing with distilled water until the product became a white solid.

Procedure for the Synthesis of Homologated Aldehyde Product **192b** *via* **192b I** and **192b II**:

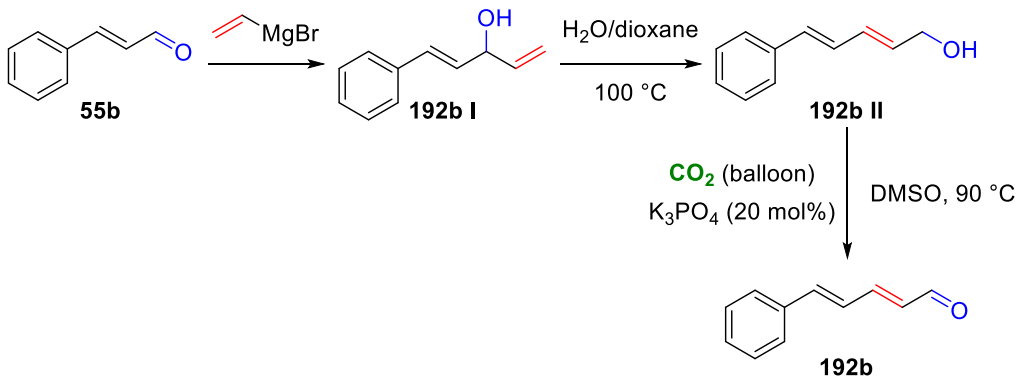

Scheme 66: Synthesis of homologated aldehyde **192b** *via* **192b I** and **192b II**.

The first and second step were done according to the literature (**Scheme 66**).[151] 5 mmol cinnamaldehyde (0.63 mL) were dissolved in 16 mL dry THF under a nitrogen atmosphere. At 0 °C, 6 mL of a 1M solution of vinyl magnesium bromide in THF were added dropwise and stirred for 30 min. After that, the mixture was allowed to warm to rt and stirred for 2 h. The reaction was quenched with saturated NH_4Cl solution and extracted with EA (4x75 mL). The organic layers were combined, dried over anhydrous Na_2SO_4 and the solvent was removed *in vacuo*. The crude product was purified *via* column chromatography using EA:*n*-hexane (20:80) as solvents to yield 95% of 1-phenylpenta-1,4-dien-3-ol (**192b I**).

4.75 mmol 1-phenylpenta-1,4-dien-3-ol (761.1 mg) were dissolved in 10.5 mL of dry 1,4-dioxane under a nitrogen atmosphere. 94 mL of degassed Milli-Q water were added and the resulting mixture was stirred vigorously at 100 °C for 1 h. After cooling to rt, brine was added and the crude product was extracted with EA (3x100 mL). The organic layers were combined and dried over anhydrous Na_2SO_4 and the solvent was removed *in vacuo*. The crude product was purified *via* column chromatography using EA:*n*-hexane (50:50) as solvents to yield 90% of 5-phenylpenta-2,4-dien-1-ol (**192b II**).

The third step followed our own oxidation protocol: 4.2 mmol 5-phenylpenta-2,4-dien-1-ol (672.9 mg) and 0.84 mmol anhydrous K_3PO_4 (178.3 mg, 20 mol%; stored in glove

box) were stirred at 90 °C under a CO_2 atmosphere in 42 mL dry DMSO for 72 h. Distilled water was added to quench the reaction and the crude product was extracted thrice with EA. The organic layers were combined and dried over anhydrous Na_2SO_4 and the solvent was removed *in vacuo*. The crude product was purified *via* column chromatography using EA:*n*-hexane (20:80) as solvents to yield 95% of 5-phenylpenta-2,4-dienal (**192b**).

5.2.3 Reaction Procedures Regarding the CO_2-Assisted Synthesis of *α*-Diketones From Aldehydes

General procedure for the synthesis of symmetric *α*-diketones:

A 10 mL two-necked flask containing a stirring bar was charged with 0.5 mmol substrate, 10 mol% of 3-ethyl-5-(2-hydroxyethyl)-4-methylthiazolium bromide and 0.75 mmol of K_2CO_3. After purging the flask thrice with vacuum and two times with nitrogen the CO_2 atmosphere was incorporated through a CO_2-filled balloon. Afterwards, dry DMSO (2.5 mL) was added. The resulting mixture was stirred for 16–48 h at 55 °C. Then, the resulting mixture underwent an aqueous workup and was extracted thrice with excess of EA, after which the combined organic layers were dried over anhydrous Na_2SO_4, filtered and concentrated *in vacuo*. In general, products were purified by using silica gel chromatography with EA and *n*-hexane as solvents and, if needed, 1 V% Et_3N.

General procedure for the synthesis of non-symmetric *α*-diketones:

A 10 mL two-necked flask containing a stirring bar was charged with 0.25 mmol of one substrate and 0.375 mmol of the other substrate: In case of compound **208b** – **211b**, **213b** – **214b**, **216b** and **218b** – **219b**, 0.25 mmol of 2-furfuraldehyde (**193a**) was taken; for compound **212b**, 4-methyl benzaldehyde, for compound **215b**, 5-methyl furfuraldehyde and for compound **217b** 2-pyridine carboxaldehyde were taken in 0.25 mmol amounts. Additionally, 10 mol% 3-ethyl-5-(2-hydroxyethyl)-4-methylthiazolium bromide and 0.75 mmol of K_2CO_3 were loaded into the flask. After purging the flask thrice with vacuum and two times with nitrogen, the CO_2 atmosphere was incorporated through a CO_2-filled balloon. Afterwards, dry DMSO (2.5 mL) was added. The resulting mixture was stirred for 36–48 h at 55 °C. Then, the resulting mixture underwent an

aqueous workup and was extracted thrice with excess of EA and the combined organic layers were dried over anhydrous Na_2SO_4, filtered and concentrated *in vacuo*. In general, products were purified by using silica gel chromatography with EA and *n*-hexane as solvents and, if needed, 1 V% Et_3N.

Procedures for the Application of 4,4'-Dichlorobenzil (**198b**):

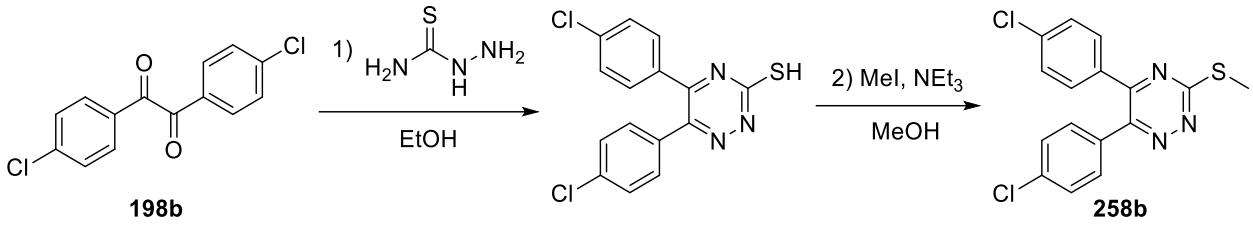

Scheme 67: Synthesis of **258b** from **198b**.

This synthesis was conducted according to the literature-known procedure (**Scheme 67**):[163a]

1) 4,4'-Dichlorobenzil (0.5 mmol, **198b**) was mixed with thiosemicarbazide (1 mmol) in 7 mL ethanol. The mixture was refluxed for 40 h. The solvent was removed under vacuum and the product was dissolved in dichloromethane, then the organic layer was washed with water and dried with Na_2SO_4, filtered and the solvent was removed *in vacuo* to yield the crude product, which was purified by column chromatography to give 48% of 5,6-bis(4-chlorophenyl)-1,2,4-triazine-3-thiol.

2) To a stirring solution of 5,6-bis(4-chlorophenyl)-1,2,4-triazine-3-thiol (0.09 mmol) in methanol (5 mL), methyl iodide (0.108 mmol), and Et_3N (0.65 mmol) were added and the mixture was stirred for 2 h at rt. The solvent was removed under reduced pressure. Water and DCM were added to the mixture. The organic phase was separated, dried over Na_2SO_4, filtered and evaporated under reduced pressure and the residue was crystallized from methanol to yield 72% (2 steps) of 5,6-bis(4-chlorophenyl)-3-(methylthio)-1,2,4-triazine **258b**.

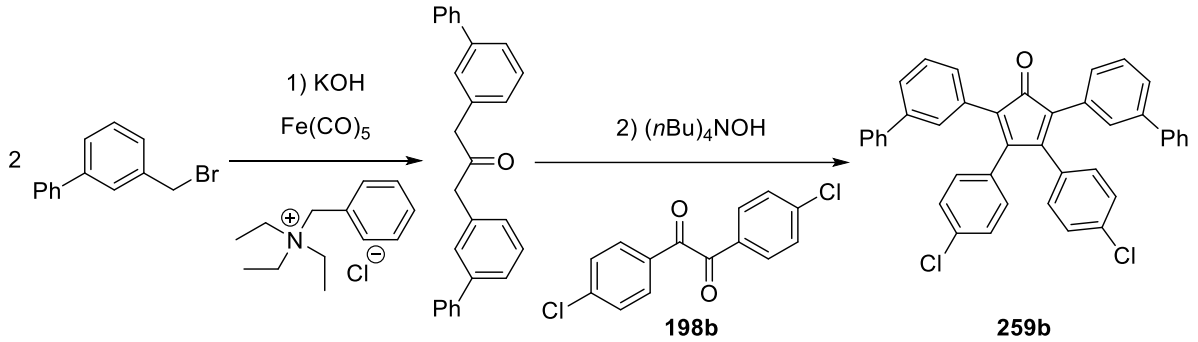

Scheme 68: Synthesis of **259b** from **198b**.

This synthesis was conducted according to the literature-known procedure (**Scheme 68**):[163c]

1) To a solution of 3-(bromomethyl)-biphenyl (7,12 mmol), $Fe(CO)_5$ (3,73 mmol) and benzyltriethylammonium chloride (0,237 mmol) in 17 mL DCM a solution of KOH (30,8 mmol) in 1 mL water was added and the mixture was refluxed overnight. After cooling to rt, the mixture was quenched with 1M HCl and the organic phase was concentrated *in vacuo*. The crude product was first purified by column chromatography and then dissolved in DCM and reprecipitated by addition of methanol to give 38% of 1,3-di(biphenyl-3-yl)propan-2-on.

2) To a degassed solution of 4,4'-dichlorobenzil (0,22 mmol, **198b**) and 1,3-di(biphenyl-3-yl)propan-2-on (0,22 mmol) in *tert*-butanol (2,3 mL) at 80 °C a methanol solution of tetrabutylammonium hydroxide (1.0 M, 0.22 mmol) was added. After stirring at 80 °C for 20 min, the reaction was quenched with water and the reaction mixture was extracted thrice with DCM. The combined organic layers were washed with brine, dried over Na_2SO_4, filtered and evaporated to give a purple crude product. Purification by column chromatography gave 69% of 2,5-di([1,1'-biphenyl]-3-yl)-3,4-bis(4-chlorophenyl)cyclopenta-2,4-dien-1-one **259b**.

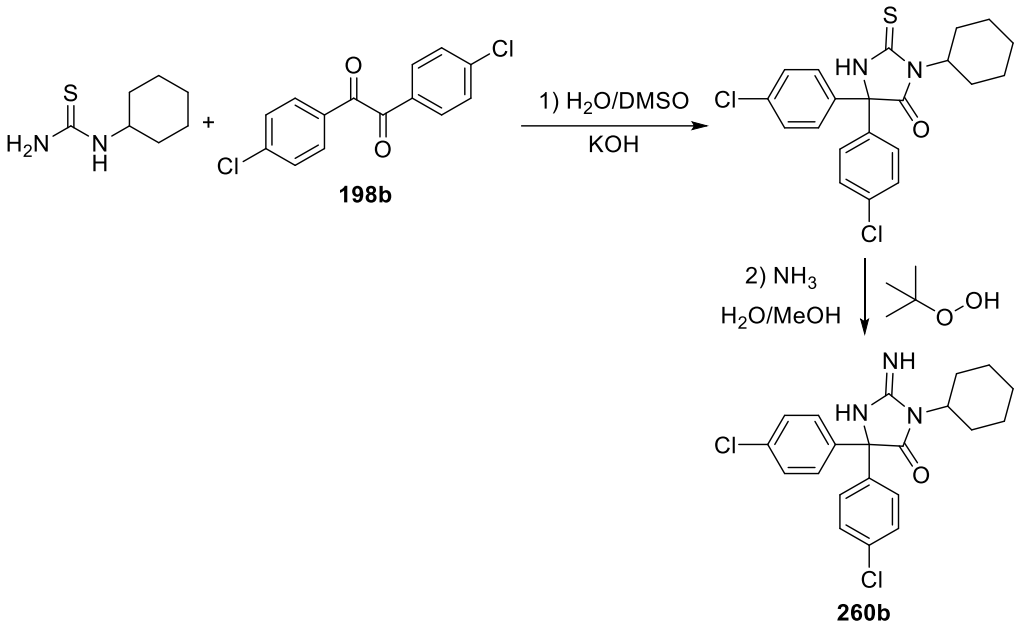

Scheme 69: Synthesis of **260b** from **198b**.

This synthesis was conducted according to the literature-known procedure (**Scheme 69**).[163b]

1) Cyclohexylthiourea (0,58 mmol) and 4,4'-dichlorobenzil (0,52 mmol, **198b**) were heated up to 110 °C in 3 mL DMSO. Then, a solution of KOH (0,8 mmol) in 1.6 mL water was added dropwise and the mixture was stirred for 10 min. After cooling to rt, the product was extracted with DCM. The organic phase was washed with water and dried over anhydrous Na_2SO_4. The solvent was removed under reduced pressure and the resulting crude product was used for the next reaction step without further purification.

2) To a solution of 5,5-bis(4-chlorophenyl)-2-thioxoimidazolidin-4-one (0,5 mmol), 2.8 mL NH_3 (40% solution in water) and 0.7 mL hydroperoxide (70% solution in water) were added. The reaction mixture was stirred at rt overnight. The crude product was extracted with DCM and the solvent was removed under reduced pressure. After column chromatography, the product was obtained in 55% yield (after two steps).

Procedures for the Application of Furil (**193b**):

This synthesis was conducted according to the literature-known procedure (**Scheme 70**).[195]

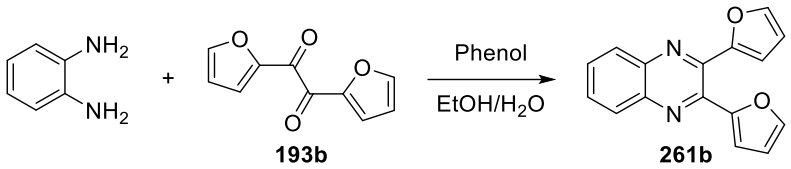

Scheme 70: Synthesis of **223b** from **198b**.

A solution of *o*-phenylenediamine (0.25 mmol) and furil (0.25 mmol, **193b**) in ethanol:water (7:3, 2.5 mL) was stirred at rt in the presence of catalytic amount of phenol (20 mol%, 0.05 mmol). The progress of the reaction was monitored by TLC (EA: *n*-hexane 5:95). After completion of the reaction, water (5 mL) was added to the mixture and was allowed to stand at rt for 30 min. During this time, crystals of the pure product were formed which were collected by filtration and dried. For further purification, the product was recrystallized from hot ethanol to yield 90% of 2,3-di(furan-2-yl)quinoxaline **261b**.

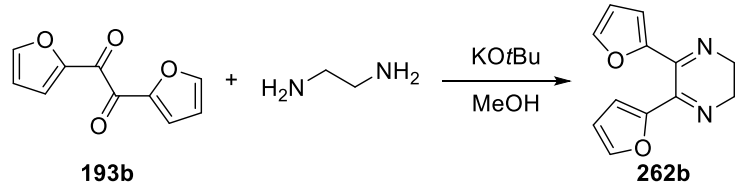

Scheme 71: Synthesis of **262b** from **193b**.

This synthesis was conducted according to the literature-known procedure (**Scheme 71**).[166]

0.53 mmol of furil (**193b**) was dissolved in 1 mL of methanol and was made homogeneous by stirring with a magnetic spinning bar. To this 0.53 mmol of ethylene diamine and 0.0212 mmol *t*BuOK were added. Stirring was continued until the reaction is completed (checked by TLC, 15 h). Methanol was evaporated under reduced pressure, and the crude product was purified by column chromatography yielding 77% of 5,6-di(furan-2-yl)-2,3-dihydropyrazine **262b**.

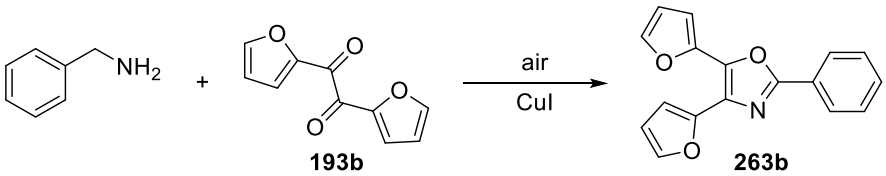

Scheme 72: Synthesis of **263b** from **193b**.

This synthesis was conducted according to the literature-known procedure (**Scheme 72**):[167]

To a solution of furil (0.275 mmol, **193b**) in 1.5 mL dry DMA, CuI (0.0826 mmol) and 4 Å molecular sieves (140 mg) were added after it. Finally, benzylamine (0.826 mmol) was added in two portions and stirring was continued for 21 h. After that, the reaction mixture was extracted with EA, dried with anhydrous Na_2SO_4 and filtered. Then, the solvent was removed under reduced pressure and the product was purified by silica gel column chromatography to afford 53% of 4,5-di(furan-2-yl)-2-phenyloxazole **263b**.

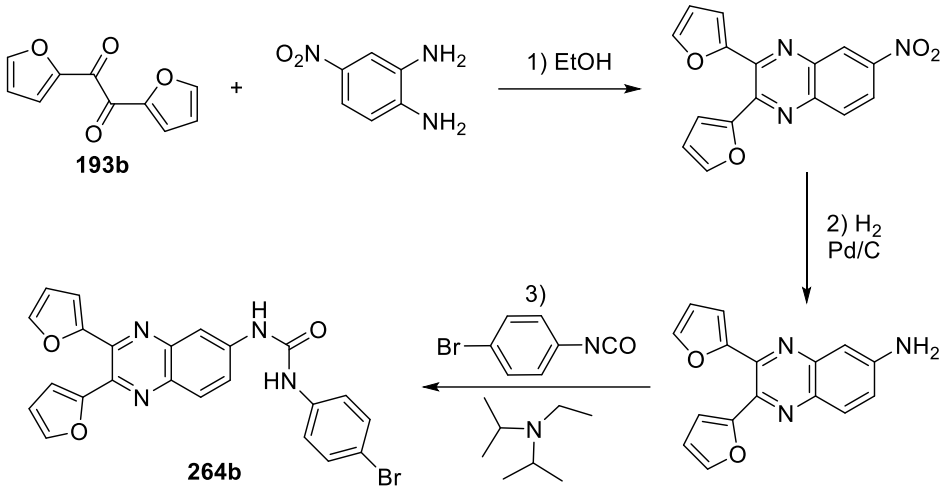

Scheme 73: Synthesis of **264b** from **193b**.

This synthesis was conducted according to the literature-known procedure (**Scheme 73**):[168]

1) 1 mmol of furil (**193b**) and 1 mmol of 4-nitrobenzene-1,2-diamine were dissolved in 10 mL ethanol and refluxed for 63 h. The solvent was removed under reduced pressure and recrystallization gave 2,3-di(furan-2-yl)-6-nitroquinoxaline in 60% yield.

2) 0.592 mmol of 2,3-di(furan-2-yl)-6-nitroquinoxaline and 12 mg of Pd/C (5%) were loaded into a two-necked flask. After purging the flask thrice with vacuum and twice with nitrogen, the flask was filled with an H_2 atmosphere *via* a balloon (1 atm pressure) and 3.5 mL ethanol were loaded. The reaction mixture was stirred at rt for 16 h. After that, the reaction mixture was dissolved in DCM and filtered through a plug of cotton. The solvents were removed under reduced pressure to yield 92% of pure 2,3-di(furan-2-yl)quinoxalin-6-amine.

3) 0.527 mmol of 2,3-di(furan-2-yl)quinoxalin-6-amine, 0.79 mmol of 1-bromo-4-isocyanatobenzene and 1.58 mmol of *N*-ethyl-*N*-isopropylpropan-2-amine were dissolved in 15 mL DCM and stirred for 48 h at rt. The resulting mixture was treated with water. The

aqueous phase was extracted thrice with dichloromethane. The combined organic layers were dried with anhydrous Na_2SO_4, filtered and the solvent removed under reduced pressure. The product **264b** was purified by column chromatography in 58% yield.

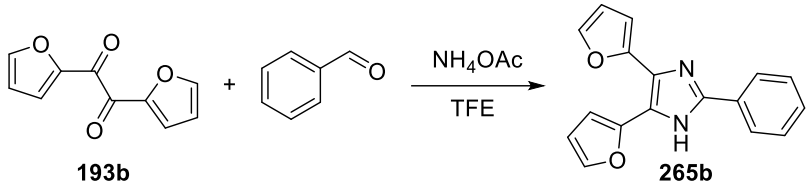

Scheme 74: Synthesis of **265b** from **193b**.

This synthesis was conducted according to the literature-known procedure (**Scheme 74**).[196]

Furil (0.254 mmol), benzaldehyde (0.254 mmol), and ammonium acetate (0.588 mmol) were dissolved in 2 mL 2,2,2-trifluoroethanol and refluxed for 8 h. During that time, a precipitation of light-yellow crystals occurred gradually. The mixture was cooled to rt and the precipitate was filtered. The crude product was purified by column chromatography (EA, *n*-hexane) to yield 4,5-di(furan-2-yl)-2-phenyl-1*H*-imidazole **265b** in 82% yield.

5.2.4 General Reaction Procedure Regarding the CO_2-Catalyzed Dehydrogenation of Amines to Imines

A 10 mL two-necked flask containing a stirring bar was charged with 0.134 mmol substrate. After purging the flask thrice with vacuum and two times with nitrogen the CO_2 atmosphere was incorporated through a CO_2-filled balloon. Afterwards dry DMSO (2.5 mL) and DBN (1.2 eq, 0.16 mL of a 1 M solution in dry DMSO) were added. The resulting mixture was stirred for 48 h at irradiation of visible blue light. The progress can be monitored *via* GC-MS or TLC. Then, the resulting mixture underwent an aqueous workup (using distilled water; or brine in case of slurry phase separation) and was extracted thrice with EA. The combined organic layers were dried over anhydrous Na_2SO_4, filtered and concentrated *in vacuo*. Products were purified *via* silica gel chromatography with EA and *n*-hexane and 1 V% Et_3N as solvents (typically 20:80 EA:*n*-hexane).

5.3 Mechanistic Details

5.3.1 Mechanistic Details Regarding the CO_2-Catalyzed Oxidation of Benzylic and Allylic Alcohols

In situ Gas Phase GC:

An *in situ* gas GC measurement of the headspace of a reaction from cinnamyl alcohol to cinnamaldehyde was carried out after 48 h reaction time (**Figure 14**). The curve is indicating that there is no other gas than CO_2. The source of N_2 gas is the front part of the needle of the used gas-tight syringe; **7.5 min: N_2, 29.5 min: CO_2.**

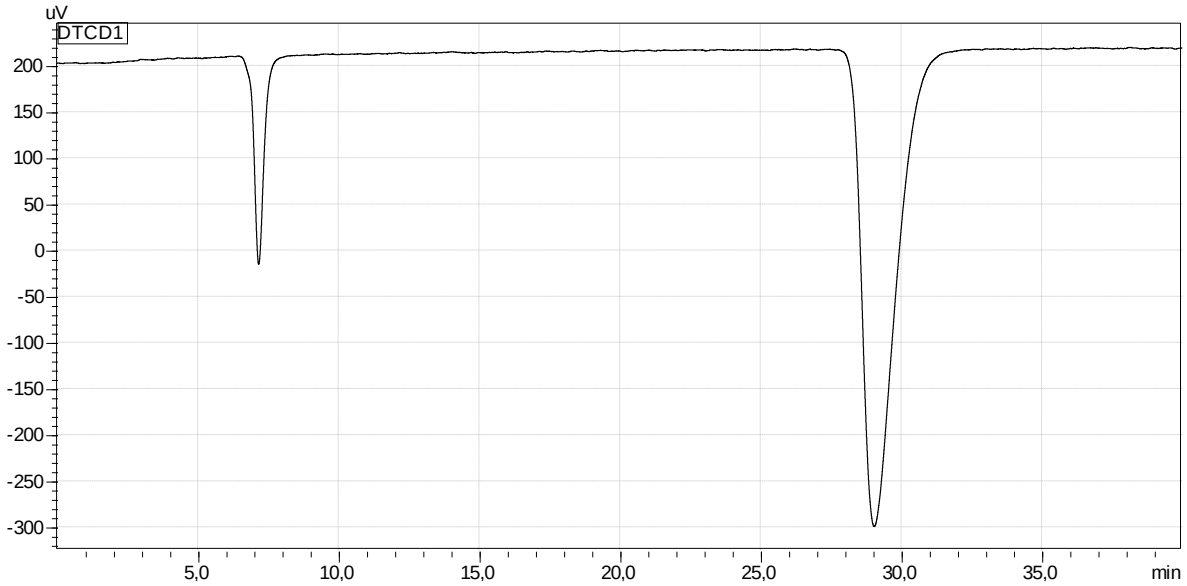

Figure 14: *In situ* gas phase GC measurement; measured by the working group of Prof. Inke Siewert.

Oxidation of Cinnamyl Alcohol with ^{18}O-Labeled DMSO:

Synthesis of ^{18}O-labeled DMSO was done according to literature procedures (**Scheme 75**):[197]

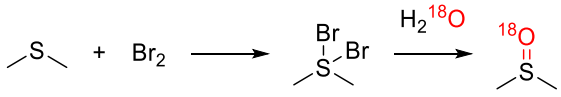

Scheme 75: Synthesis of ^{18}O-labeled DMSO.

1) First, dimethylsulfur dibromide was prepared by dropwise addition (ca. 30 min) of 7.2 mL Br_2 (132 mmol) to a stirred solution of 9.7 mL dimethyl sulfide (132 mmol) in 120 mL CCl_4 at 0 °C. The resulting mixture was stirred for additional 2 h at rt. The

yellow-orange product was collected by filtration and washed with cold CCl_4 to give 26 g yellow product after drying *in vacuo*.

2) 6.25 g Me_2SBr_2 (28.1 mmol) were added in 2 portions (10 min interval) to a stirred solution of 7.9 mL Et_3N (56.3 mmol) and 0.25 mL ^{18}O-labeled water (13.8 mmol; 97% ^{18}O) in 19 mL dry THF at 0 °C. The precipitate was removed by filtration and washed thrice with diethylether. The solvents of the organic solution were removed by distillation and the dark brown residue was dried *in vacuo* to give 0.5 g $DMS^{18}O$.

MS (GC-MS): *m/z* calcd. for $C_2H_6{}^{18}O$ [M^+]: 80.13, found: 80.16.

The reaction of cinnamyl alcohol and ^{18}O-labeled DMSO was conducted according to the general reaction procedure described in **chapter 5.2.2** (**Scheme 76**).

MS (ESI): *m/z* calcd. for $C_9H_8{}^{18}O$ [$M+H^+$]: 135.0690, found: 135.0688.

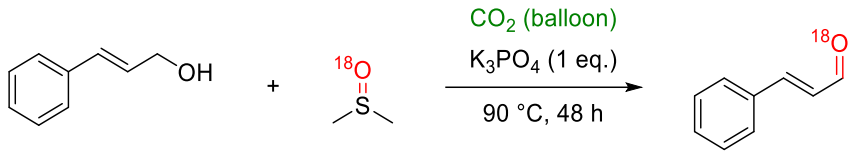

Scheme 76: Synthesis of ^{18}O-labeled DMSO.

Kinetic Studies:

In general, the kinetic experiments were done according to the general reaction procedure described in **chapter 5.2.2** but with varying concentrations of cinnamyl alcohol or K_3PO_4 or different temperatures as depicted in **Table 7 – 9**. Samples (as whole reaction mixtures, no aliquots) were taken after the indicated timespan and analyzed *via* GC with *n*-dodecane as internal standard. The obtained values were plotted as product concentration against the time at different concentrations of starting material and base or different temperatures, respectively (**Figure 15 – 17**).

Table 7: Different concentrations of cinnamyl alcohol

c(SM_0) / M	c(P) / M	t / h
0.031	0.001	2.0
0.031	0.002	4.0
0.031	0.002	6.3
0.031	0.003	8.0
0.031	0.004	9.8
0.062	0.011	2.0
0.062	0.011	4.0
0.062	0.013	6.3
0.062	0.014	8.0
0.062	0.016	9.8
0.093	0.021	2.0
0.093	0.023	4.3
0.093	0.025	6.0
0.093	0.026	8.0
0.093	0.029	10.0
0.186	0.035	2.0
0.186	0.038	4.0
0.186	0.042	6.3
0.186	0.045	8.0
0.186	0.046	9.8
0.124	0.031	2.0
0.124	0.033	4.0
0.124	0.036	6.3
0.124	0.038	8.0
0.124	0.040	9.8

Table 8: Different concentrations of K_3PO_4

c(K_3PO_4) / mM	c(P) / M	t / h
4.7	0.0086	2.0
4.7	0.0145	4.1
4.7	0.0260	6.4
4.7	0.0287	8.3
9.3	0.0162	2.0
9.3	0.0222	4.1
9.3	0.0287	6.4
9.3	0.0308	8.3
18.6	0.0193	2.0
18.6	0.0231	4.3
18.6	0.0264	6.0
18.6	0.0307	8.0
18.6	0.0390	10.0
46.5	0.0155	2.0
46.5	0.0250	4.1
46.5	0.0280	6.4
46.5	0.0309	8.3
93.0	0.0088	2.0
93.0	0.0207	4.1
93.0	0.0242	6.4
93.0	0.0345	8.3

Table 9: Different temperatures

T / °C	t / s	c(P) / mM
30	7200	0.000
30	15000	0.004
30	22200	0.009
30	30000	0.020
50	7200	0.580
50	15000	0.599
50	22200	0.619
50	30000	0.666
70	7200	1.245
70	15000	1.428
70	22200	1.706
70	30000	2.089
90	7200	19.302
90	15300	22.742
90	21600	25.119
90	28800	28.429
90	36000	31.056
110	7200	27.866
110	15000	33.998
110	22200	44.091
110	30000	50.048

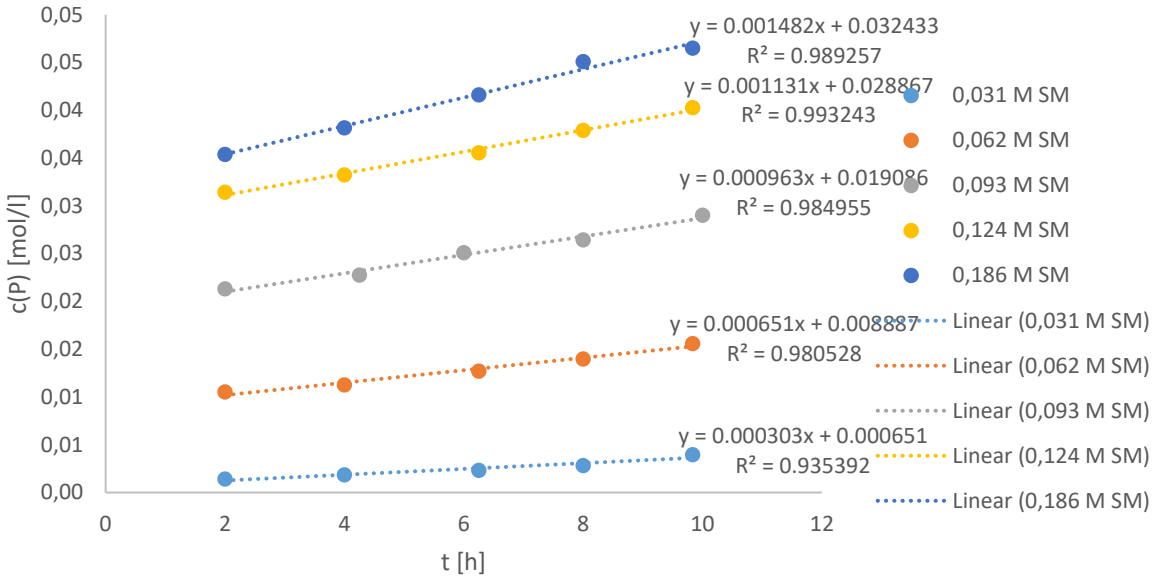

Figure 15: Product concentration plotted against reaction time at different cinnamyl alcohol concentrations; for each data point a separate reaction was conducted using different concentrations of cinnamyl alcohol (0.031 mol L^{-1}, 0.062 mol L^{-1}, 0.093 mol L^{-1} 0.124 mol L^{-1}, 0.186 mol L^{-1}) with constant concentrations of K_3PO_4 (18.6 mmol L^{-1}) in 2.5 mL DMSO at 90 °C under a CO_2 atmosphere (balloon) and submitted to GC analysis with *n*-dodecane as internal standard after the indicated timespan.

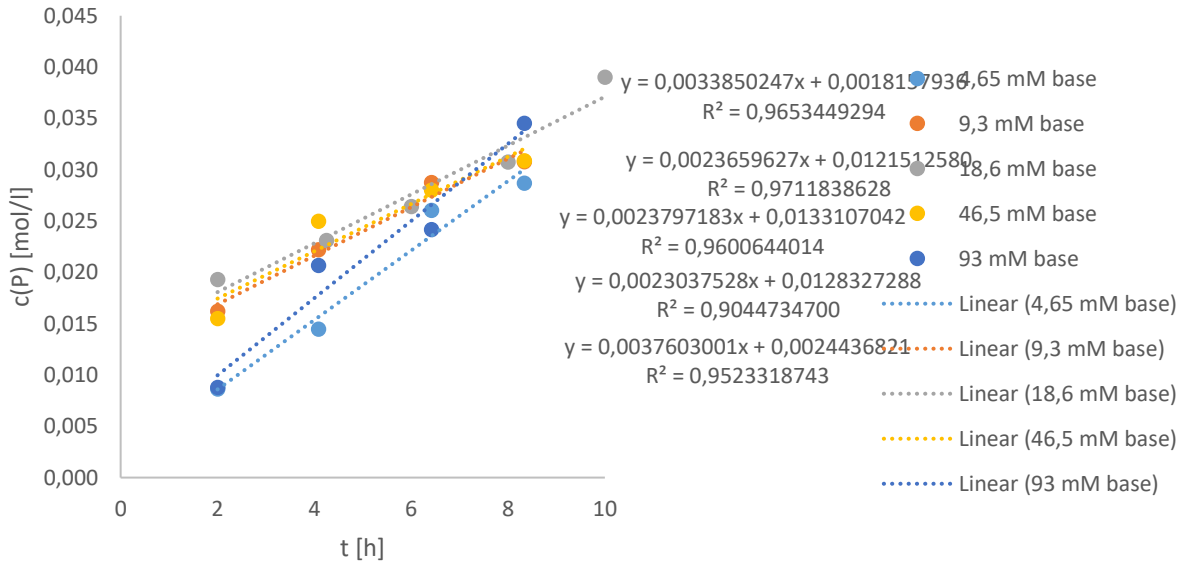

Figure 16: Product concentration plotted against reaction time at different K_3PO_4 concentrations; for each data point a separate reaction was conducted using different concentrations of K_3PO_4 (4.65 mmol L^{-1}, 9.3 mmol L^{-1}, 18.6 mmol L^{-1}, 46.5 mmol L^{-1}, 93.0 mmol L^{-1}) with constant concentration of cinnamyl alcohol (0.0931 mol L^{-1}) in 2.5 mL DMSO at 90 °C under a CO_2 atmosphere (balloon) and submitted to GC analysis with *n*-dodecane as internal standard after the indicated timespan.

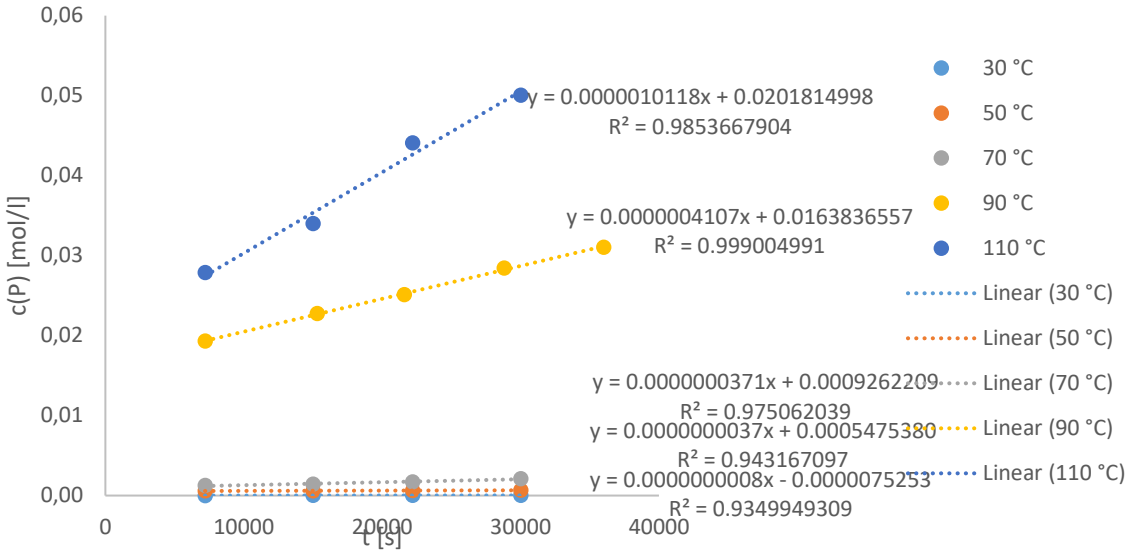

Figure 17: Product concentration plotted against reaction time at different temperatures; for each data point a separate reaction was conducted using a constant concentration of K_3PO_4 (18.6 mmol L^{-1}) with constant concentration of cinnamyl alcohol (0.0931 mol L^{-1}) in 2.5 mL DMSO at different temperatures (30 °C, 50 °C, 70 °C, 90 °C, 110 °C) under a CO_2 atmosphere (balloon) and submitted to GC analysis with *n*-dodecane as internal standard after the indicated timespan.

With the slopes of these curves we were now able to plot the logarithmic concentration of starting material and base, respectively, against the logarithmic observed rate constant k_{obs} (**Figure 18 – 20**).

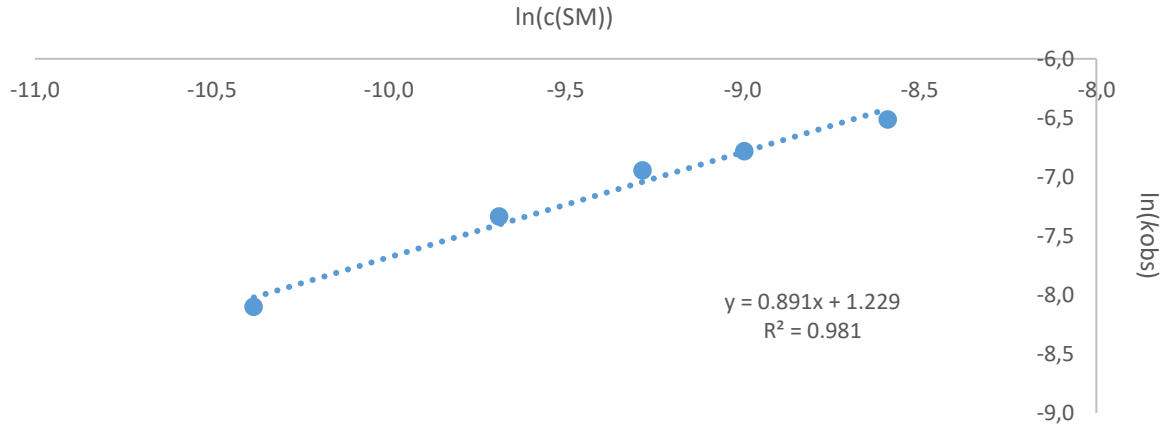

Figure 18: ln(k_{obs}) against ln(c_{SM}); standard error: 0.09754.

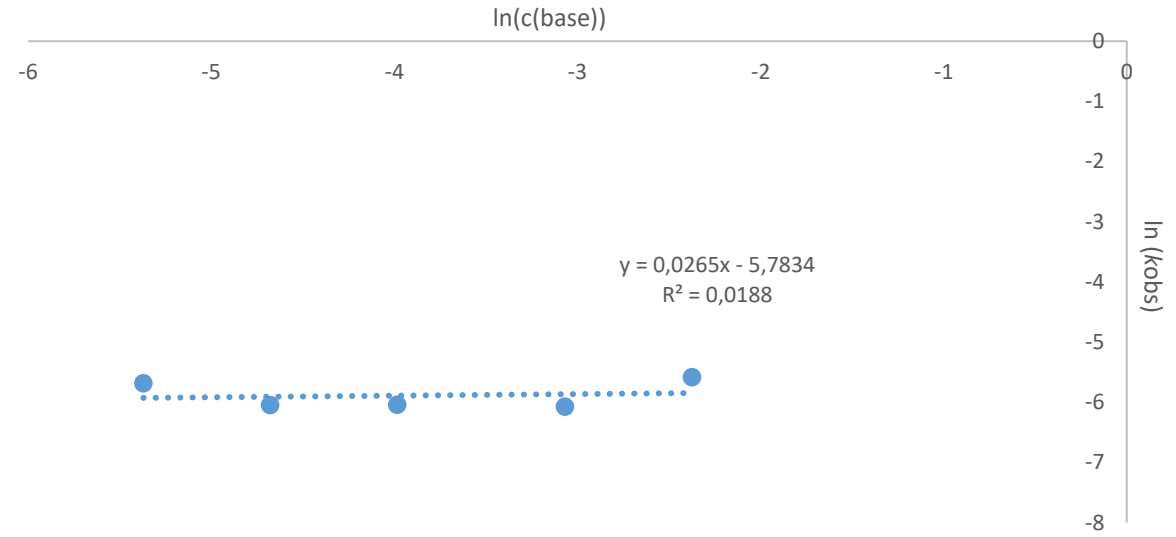

Figure 19: ln(k_{obs}) against ln(c_{base}); standard error: 0.2654763.

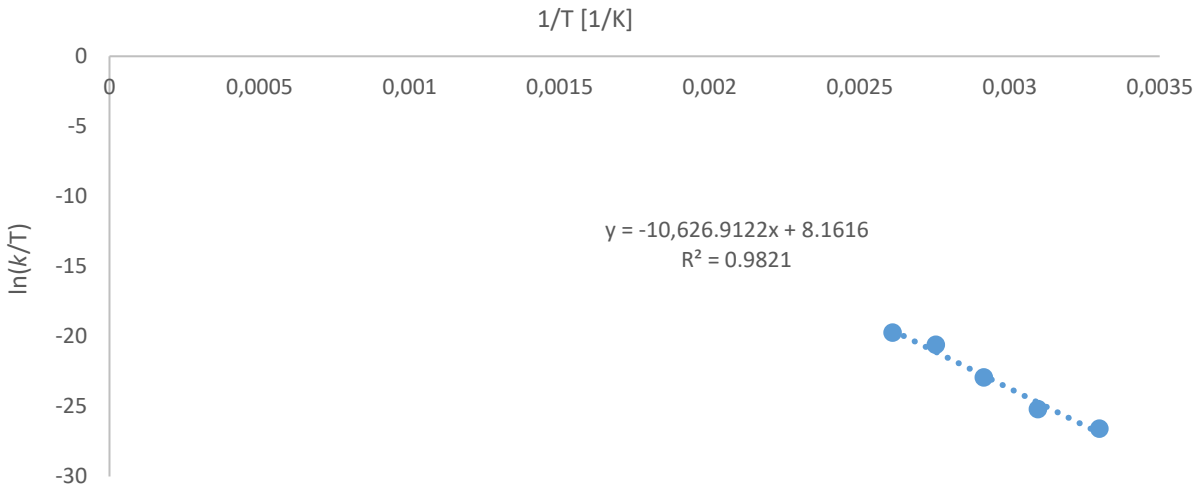

Figure 20: Arrhenius-Eyring plot; ln(k/T) against 1/T; standard error: 0.4516807.

From the slope and the intercept of the Arrhenius-Eyring plot the activation enthalpy $\Delta H^{\neq}$ and the activation entropy $\Delta S^{\neq}$ can be calculated using the following equation

$$\boldsymbol{ln\left(\frac{k}{T}\right) = \frac{-\Delta H^{\neq}}{RT} + ln\left(\frac{k_B}{h}\right) + \frac{\Delta S^{\neq}}{R}}$$

$$\boldsymbol{\Delta H^{\neq} = 10626.9 * R = 88.4\ \frac{kJ}{mol} = 21.1 \frac{kcal}{mol}}$$

$$\boldsymbol{\Delta S^{\neq} = \left(8.1616 - ln\left(\frac{k_B}{h}\right)\right) * R = -129.7\ \frac{J}{mol * K} = -30.9 \frac{cal}{mol * K}}$$

with R being the universal gas constant, k_B the Boltzmann constant and h Planck's constant.

Details Regarding DFT Calculations:

All DFT calculations were performed within the Turbomole 7.0[198] program package. The molecular structures were optimized using the B3LYP[199] functional combined with Grimme's dispersion correction with Becke-Johnson damping (D3(BJ))[200], applying increased convergence criteria (10^{-8} H in total energy and 10^{-4} au in in the maximum norm of the Cartesian gradient) and a fine integration grid (m4 in Turbomole convention). Ahlrich's revised all electron basis sets were utilized throughout.[201] No symmetry restrains were imposed and the optimized structures were defined as minima (no negative eigenvalue) or transition states (one negative eigenvalue) by vibrational analyses at the D3(BJ)-B3LYP/def2-TZVP level of theory. Additionally, the nature of the located transition states was confirmed by displacement of the structures along the vibration mode that represents the reaction coordinate followed by full structure optimizations. Conformers of the different structures have been fully evaluated and the ones with the lowest single point energies chosen.

To account for solvent energies, the (free) energies have been evaluated by single point calculations in the optimized structures applying the same method (D3(BJ)-B3LYP) but a slightly larger basis set (def2-TZVPP) and the conductor-like screening model (COSMO)[202] (ε = 47 for DMSO). Implicit solute-solvent interactions by hydrogen bonds were evaluated by structure optimizations with an additional DMSO molecule attached to the acidic proton. However, in most cases the entropic loss was larger than the energy gain. Only for the ester intermediate **A**, the molecule was stabilized by 0.7 kcal mol^{-1} (11.3 vs. 12.0 kcal mol^{-1}; **Figure 21**).

The free energies have been obtained by ideal gas statistical mechanics (100 kPa, 363.15 K) and corrected to standard solution conditions (1 mol L^{-1}, 363.15 K) by:

$$G_{sol} = G_{gas} + RTln\frac{RT}{p}$$

$$G_{sol} = G_{gas} + RTln(30.19)$$

$$G_{sol} = G_{gas} + 2.46 \text{ kcal/mol}$$

The *G* value of the DMSO molecule has been further corrected by applying the actual concentration in the pure solvent which is (ρ = 1.095 g mL^{-1} (25 °C), c = 14.02 mol L^{-1}):

$$G'_{sol} = G_{sol} + RTlnc$$

$$G'_{sol} = G_{solv} + 1.91 \text{ kcal/mol}$$

The actual density of DMSO will be lower at 90 °C. However, the error is small (< 0.2 kcal mol^{-1}). That gives an overall correction factor of 4.37 kcal·mol^{-1} for DMSO.

The final energies were calculated by adding the single point energy and the corrected free energy (G) from the vibrational analyses at the D3(BJ)-B3LYP/def2-TZVP level, containing the zero point energy, thermal and entropic corrections (**Figure 38**).

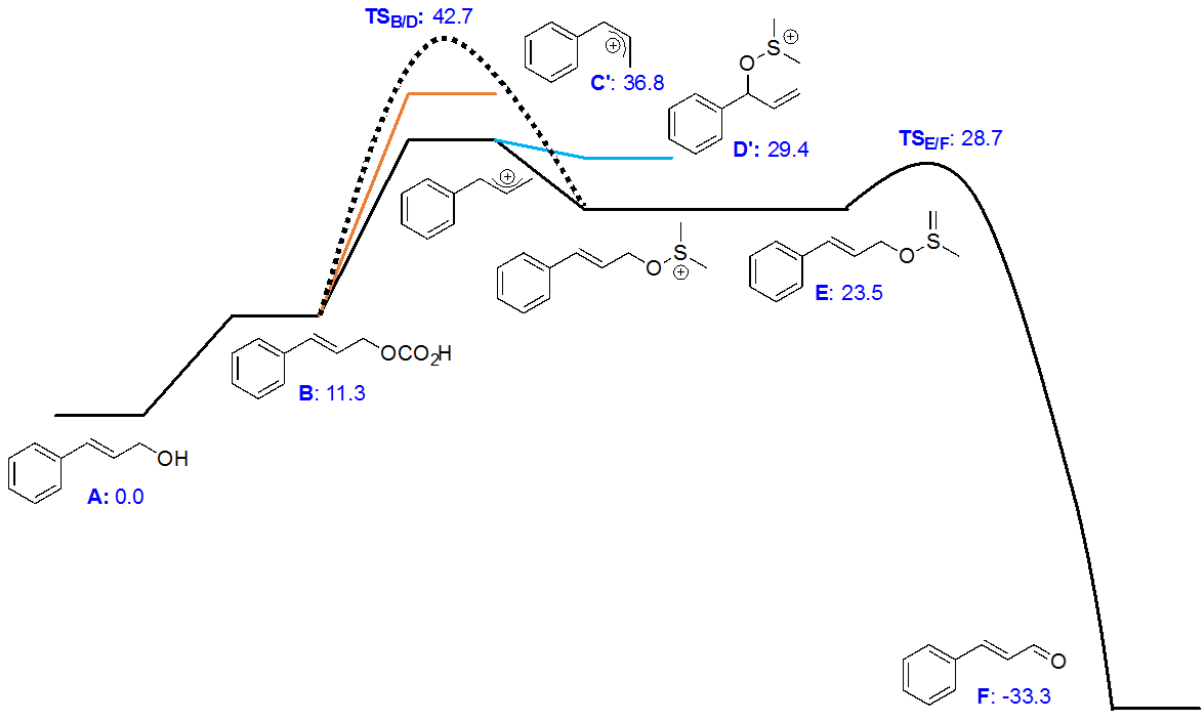

Figure 21: Calculated energy profile including alternative pathways.

Table 10: Structures of calculated compounds **A – F**.

A	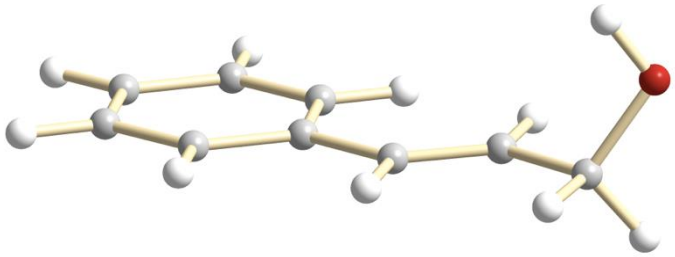
B	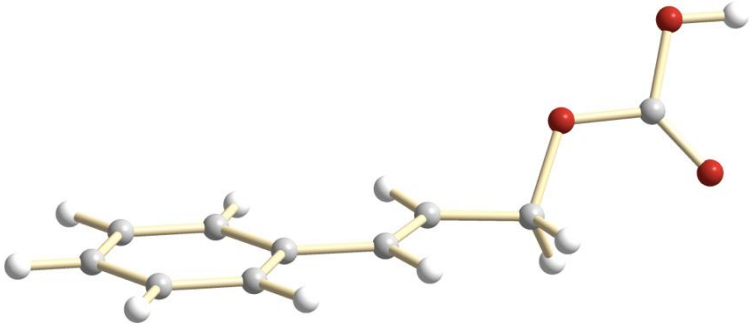
B·DMSO	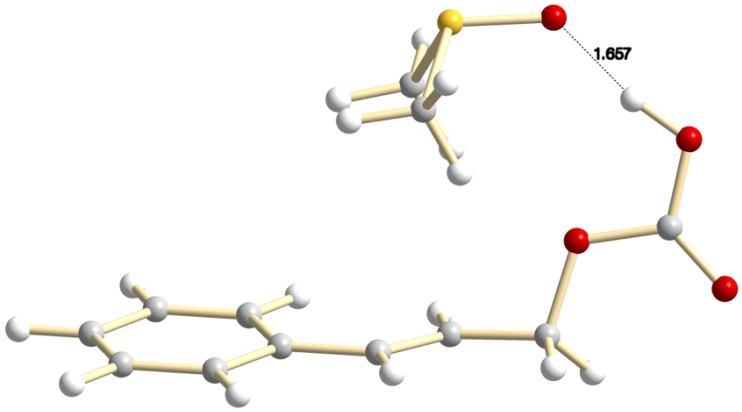
C	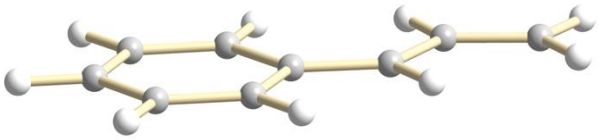
C'	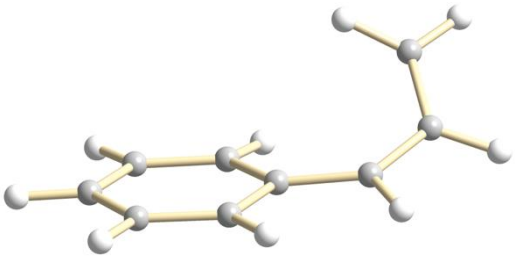

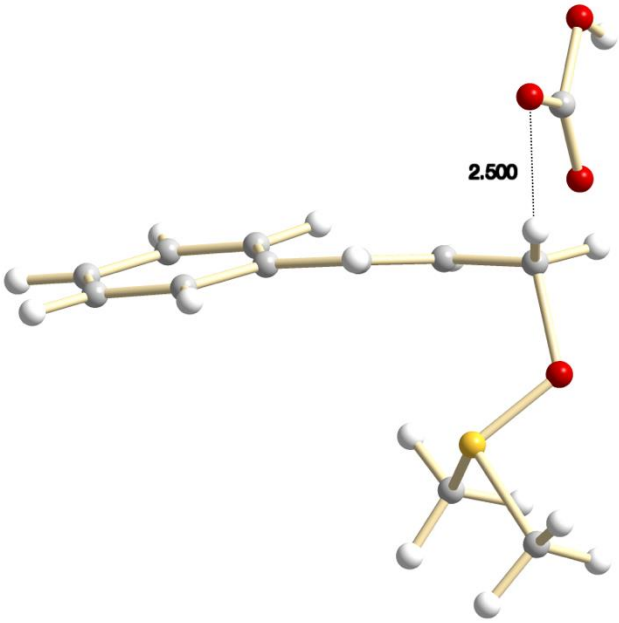

$TS_{B/D}$

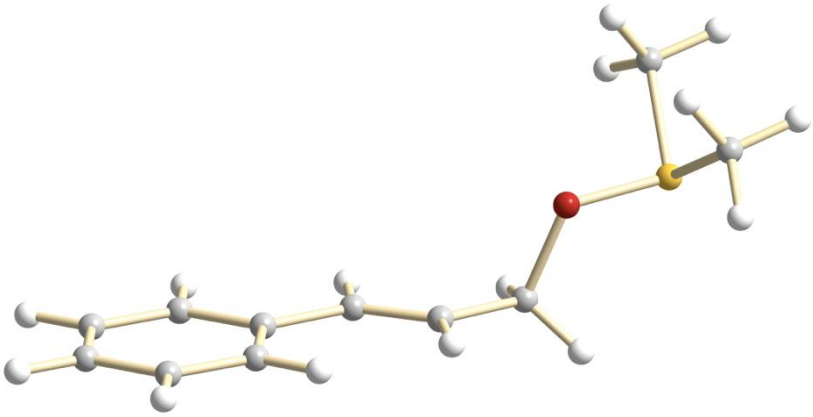

D

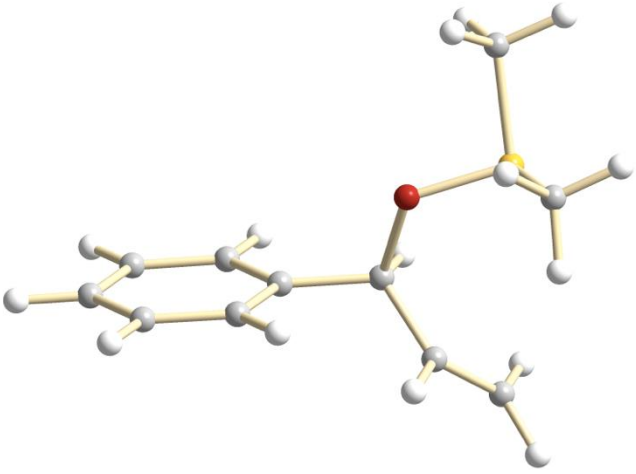

D’

E

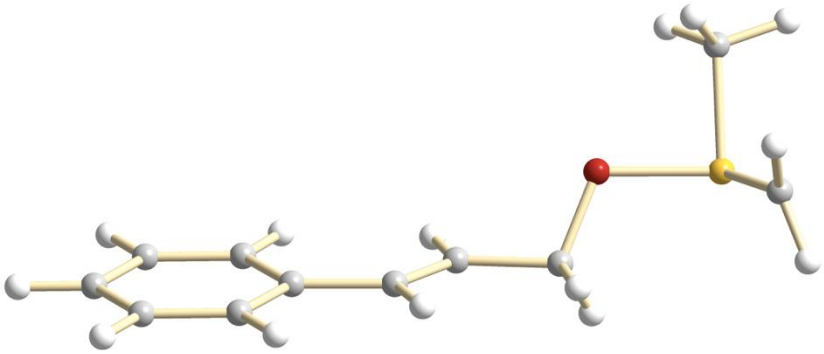

$TS_{E/F}$

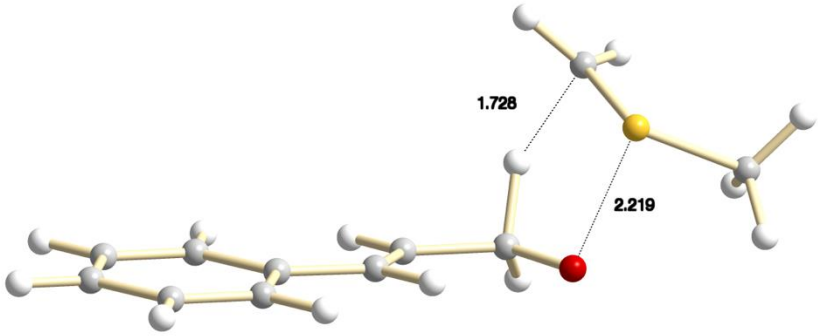

F

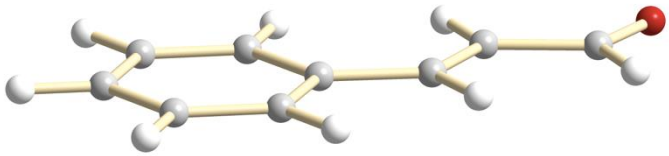

Table 11: xyz coordinates of the calculated structures.

CO_2
3
Energy = -188.5873351766
C 0.0263438 0.0000000 -0.0000019
O -1.1336183 -0.0000000 0.0000010
O 1.1862745 -0.0000000 0.0000010

DMSO
10
Energy = -553.1643118688
S -2.4490823 0.8662338 0.7785258

C	-4.0711733	0.8491649	-0.0413156
H	-4.5684120	-0.1046256	0.1385877
H	-4.6509970	1.6592503	0.3980458
H	-3.9315131	1.0270240	-1.1078957
C	-1.7127882	-0.4680965	-0.2120012
H	-0.6774732	-0.5619199	0.1116910
H	-2.2455428	-1.4022814	-0.0308038
H	-1.7500047	-0.1898030	-1.2654936
O	-1.7749958	2.1273696	0.3638801

H_2O

3

Energy = -76.42649010690

O	-0.0123480	0.0000000	0.0000000
H	0.5724125	-0.7651042	0.0000000
H	0.5724124	0.7651043	0.0000000

HCO_3^-

5

Energy = -264.4578056723

C	-1.7856041	1.1151180	-0.0000032
O	-1.0866106	2.1302468	0.0000026
O	-1.0293467	-0.1224951	-0.0000027
H	-1.7319142	-0.7838111	0.0000194
O	-3.0219248	0.9394914	0.0000012

DMS

9

Energy = -477.9618981180

S	-2.4458118	0.8794646	0.7211457
C	-4.0915630	0.8692625	-0.0363943
H	-4.5919425	-0.0864035	0.1258530
H	-4.6711673	1.6567829	0.4439215
H	-4.0325182	1.0764765	-1.1057791

C	-1.6847998	-0.4753365	-0.2104033
H	-0.6640110	-0.5825795	0.1547148
H	-2.2187426	-1.4123503	-0.0462765
H	-1.6564305	-0.2503700	-1.2774413

A

20

Energy = -424.1129256105

C	-4.1359144	1.7346637	-0.1465728
C	-2.7482233	1.7836281	-0.1605508
C	-2.0637455	2.9984506	-0.0430740
C	-2.8209937	4.1707306	0.0840252
C	-4.2053678	4.1236961	0.0986673
C	-4.8711212	2.9055772	-0.0158489
H	-4.6421238	0.7819577	-0.2383515
H	-2.1790458	0.8670633	-0.2627295
H	-2.3232975	5.1277075	0.1682373
H	-4.7714599	5.0414778	0.1974035
H	-5.9530418	2.8731698	-0.0053823
C	-0.5988470	2.9885793	-0.0561450
H	-0.1526363	2.0081423	-0.2078154
C	0.2259401	4.0277690	0.0923776
H	-0.1594361	5.0283197	0.2626443
C	1.7147068	3.9084251	0.0757978
H	2.0089444	2.8736738	-0.1388164
H	2.1462381	4.5450602	-0.7004496
O	2.3045308	4.3681361	1.2949218
H	1.8880068	3.8897563	2.0212872

B

23

Energy = -612.6993213762

C	-4.1820534	1.8194585	-0.3500521
C	-2.7950233	1.8156111	-0.4138443

C	-2.0516338	2.9553041	-0.0884493
C	-2.7471522	4.1081691	0.2991240
C	-4.1307246	4.1134379	0.3639582
C	-4.8559584	2.9691980	0.0403064
H	-4.7354758	0.9246597	-0.6053467
H	-2.2731485	0.9158223	-0.7176361
H	-2.2029278	5.0095598	0.5478679
H	-4.6495678	5.0147220	0.6653292
H	-5.9371986	2.9779015	0.0904915
C	-0.5908011	2.8889079	-0.1640099
H	-0.1968945	1.9453544	-0.5335164
C	0.2831175	3.8405243	0.1660343
H	-0.0474625	4.7961610	0.5580377
C	1.7510889	3.6818537	0.0012392
H	2.0162633	2.6858928	-0.3546777
H	2.1666098	4.4146537	-0.6943764
O	2.3703439	3.9015471	1.2980151
C	3.6994549	3.8935460	1.2981232
O	4.1274147	4.1167469	2.5538523
H	5.0940449	4.1003178	2.5188991
O	4.4179605	3.7171948	0.3474481

B·DMSO

33

Energy = -1165.887210638

C	-3.2964336	2.5512087	2.0161118
C	-2.0581382	2.2735001	1.4524798
C	-1.2137358	3.3005515	1.0167409
C	-1.6517138	4.6234116	1.1680170
C	-2.8864756	4.9019919	1.7308717
C	-3.7156830	3.8675153	2.1580598
H	-3.9335346	1.7393841	2.3433026
H	-1.7351151	1.2449452	1.3429730
H	-1.0234358	5.4416152	0.8416752
H	-3.2074278	5.9305959	1.8371351

H	-4.6801613	4.0890472	2.5964157
C	0.0909096	2.9505658	0.4521414
H	0.3225776	1.8882178	0.4608276
C	1.0104897	3.7828864	-0.0372969
H	0.8276477	4.8516673	-0.0716346
C	2.3528555	3.3402109	-0.5051300
H	2.4111375	2.2545177	-0.6008828
H	2.6311222	3.7833769	-1.4615582
O	3.3015070	3.7766192	0.4987821
C	4.6209249	3.7179287	0.1374083
O	5.4017243	4.0840264	1.1310128
H	4.9012106	4.2985778	1.9685368
O	4.9957253	3.3739157	-0.9496237
S	2.9667485	4.5400231	4.0991808
C	1.8682054	5.5567329	3.0831011
H	0.8355597	5.3918407	3.3910856
H	2.1512053	6.5933472	3.2574132
H	2.0166367	5.2865100	2.0406043
C	2.3094741	2.9241356	3.6186967
H	2.9172821	2.1777057	4.1273923
H	1.2727659	2.8503267	3.9477296
H	2.3887763	2.8178006	2.5394907
O	4.3361850	4.6502061	3.4863890

$TS_{B/D}$

33

Energy = -1165.806004892

C	-4.3693581	-0.7563266	-0.2825551
C	-3.0613604	-1.2000469	-0.4199851
C	-1.9964976	-0.5036609	0.1647239
C	-2.2865817	0.6451314	0.9159299
C	-3.5929536	1.0853840	1.0541704
C	-4.6400920	0.3915577	0.4523397
H	-5.1781041	-1.3107947	-0.7419427
H	-2.8544045	-2.1010391	-0.9861226

H	-1.4870248	1.1751632	1.4164341
H	-3.7994361	1.9673609	1.6472851
H	-5.6594779	0.7365779	0.5687982
C	-0.6318826	-0.9840906	-0.0316306
H	-0.5426395	-1.9951483	-0.4207165
C	0.4830269	-0.2848280	0.2255435
H	0.4607479	0.7169001	0.6348923
C	1.8315924	-0.7706476	-0.0864168
H	1.9795267	-1.8420381	-0.0404302
H	2.6210051	-0.1852124	0.3552764
O	1.7415506	-0.7805328	2.4120152
C	2.0417989	0.3876777	2.7452417
O	2.2571063	0.5629439	4.1078841
H	2.4825413	1.4980789	4.1977009
O	2.1674347	1.4017106	2.0231347
S	0.9149388	-0.3614927	-2.6264136
C	0.3926308	1.3615023	-2.6041337
H	-0.2103700	1.5394303	-3.4950399
H	-0.2045544	1.5051369	-1.7079203
H	1.2784664	1.9945171	-2.5876579
C	1.8303814	-0.3702491	-4.1728193
H	2.2872709	-1.3532666	-4.2644776
H	1.1226999	-0.2082496	-4.9854385
H	2.5934870	0.4055004	-4.1504963
O	2.1439382	-0.4410445	-1.6530511

C

18

Energy = -348.0168387884

C	-4.1336695	1.7204870	-0.1534489
C	-2.7596304	1.7328741	-0.2113013
C	-2.0426632	2.9552878	-0.0776506
C	-2.7690504	4.1643135	0.1156708
C	-4.1406702	4.1390396	0.1714683
C	-4.8219868	2.9214498	0.0377435

H	-4.6792787	0.7926018	-0.2543529
H	-2.2075296	0.8132891	-0.3586116
H	-2.2451892	5.1036538	0.2190589
H	-4.6981495	5.0537796	0.3182973
H	-5.9038141	2.9125643	0.0837151
C	-0.6464602	2.9095276	-0.1417445
H	-0.2027779	1.9290529	-0.2927439
C	0.2609607	3.9878817	-0.0323903
H	-0.1046235	4.9948848	0.1190085
C	1.5909501	3.7618584	-0.1159324
H	1.9849708	2.7634328	-0.2669754
H	2.3091256	4.5677688	-0.0349955

C’

18

Energy = -348.0081372317

C	-4.1089497	1.6893742	0.1073493
C	-2.7510883	1.7493641	-0.0980639
C	-2.0997487	3.0089919	-0.2408346
C	-2.8880020	4.1957150	-0.2553764
C	-4.2462845	4.1197339	-0.0636772
C	-4.8539178	2.8726327	0.1295598
H	-4.6017683	0.7362075	0.2402024
H	-2.1568228	0.8446842	-0.1184682
H	-2.4229437	5.1441298	-0.4817359
H	-4.8523269	5.0148608	-0.0906466
H	-5.9264687	2.8222307	0.2698989
C	-0.7074817	3.0132138	-0.3608775
H	-0.2462313	2.0534932	-0.5812497
C	0.1900222	4.1081316	-0.2348718
H	1.1459786	4.0056895	-0.7382477
C	-0.0071678	5.1663577	0.5787064
H	-0.8730233	5.2428541	1.2230625
H	0.7442904	5.9400527	0.6703332

D

28

Energy = -901.2186970242

C	-4.3143351	2.0043733	0.3907144
C	-2.9851256	1.9949293	0.7856286
C	-2.0939422	2.9776604	0.3347179
C	-2.5741392	3.9759311	-0.5263390
C	-3.8998868	3.9842840	-0.9200826
C	-4.7739493	2.9991584	-0.4630863
H	-4.9903585	1.2392895	0.7486329
H	-2.6268945	1.2203649	1.4531009
H	-1.9104102	4.7497977	-0.8884007
H	-4.2596991	4.7594729	-1.5836951
H	-5.8107140	3.0112896	-0.7729079
C	-0.7126592	2.9142853	0.7810382
H	-0.4878132	2.0800025	1.4416076
C	0.2898259	3.7597114	0.4907483
H	0.1401057	4.6168739	-0.1536245
C	1.6311288	3.5759725	1.0484410
H	2.1062779	4.5000186	1.3770832
H	1.6681888	2.8211310	1.8312163
O	2.5189640	3.0477809	-0.0980925
S	4.0885848	3.0104074	0.1714617
C	4.4886185	1.3019358	-0.1874602
H	5.5750286	1.2062379	-0.1770889
H	4.0567265	0.6974012	0.6081385
H	4.0741302	1.0289654	-1.1564867
C	4.7281269	3.8356691	-1.2831770
H	4.4631302	4.8879306	-1.1970780
H	5.8130483	3.7242833	-1.2782244
H	4.2864629	3.3913404	-2.1737165

D’

28

Energy = -901.2164171700

C	-0.6648848	-0.9546812	3.4913025

C	-0.2997183	-1.2308129	2.1806558
C	0.1661524	-0.2115842	1.3514090
C	0.2520927	1.0929444	1.8430999
C	-0.1251739	1.3694333	3.1477716
C	-0.5794595	0.3454900	3.9740809
H	-1.0161098	-1.7515345	4.1331310
H	-0.3660021	-2.2443968	1.8037653
H	0.6019657	1.8962674	1.2075754
H	-0.0604382	2.3814047	3.5248269
H	-0.8652750	0.5628258	4.9948078
C	0.5680742	-0.5382342	-0.0444142
H	0.4654212	-1.6050385	-0.2375795
C	1.8967986	-0.0415482	-0.4899955
H	2.1396325	0.9868120	-0.2473769
C	2.7753746	-0.8152354	-1.1189418
H	2.5616974	-1.8547032	-1.3408519
H	3.7509849	-0.4462252	-1.4073224
S	-0.4623503	-0.1986368	-2.4776514
C	-2.2130926	-0.2629645	-2.8437944
H	-2.3213213	-0.3432338	-3.9258150
H	-2.6071027	-1.1555787	-2.3617052
H	-2.6970486	0.6338865	-2.4609993
C	-0.0048084	1.3651756	-3.2241768
H	1.0422819	1.5364658	-2.9839845
H	-0.1277226	1.2648946	-4.3033102
H	-0.6378727	2.1555466	-2.8242959
O	-0.5222516	0.1352254	-0.9215612

E

27

Energy = -900.8099755487

C	-4.3095885	2.4227104	0.8630399
C	-2.9353670	2.4418583	1.0613349
C	-2.0721494	3.0012490	0.1126193
C	-2.6370678	3.5451015	-1.0488730

C	-4.0077642	3.5282003	-1.2478795
C	-4.8526247	2.9664965	-0.2935961
H	-4.9556871	1.9833918	1.6127342
H	-2.5168919	2.0170291	1.9662199
H	-1.9988274	3.9870932	-1.8024904
H	-4.4229388	3.9552917	-2.1522804
H	-5.9232458	2.9546909	-0.4529762
C	-0.6315120	2.9961195	0.3775908
H	-0.3452628	2.5574878	1.3302950
C	0.3404085	3.4598199	-0.4092133
H	0.1150615	3.9215718	-1.3647068
C	1.7873258	3.3963344	-0.0581404
H	1.9254262	2.9188280	0.9187572
H	2.3325953	2.7954182	-0.8024189
O	2.3024390	4.7242185	-0.0449162
S	4.0769337	4.7529936	0.0511525
C	3.9864402	6.5484856	0.1500659
H	5.0015517	6.9300552	0.0769183
H	3.3702238	6.9080697	-0.6691886
H	3.5369221	6.8215674	1.1029506
C	4.7435072	4.2966574	1.4522215
H	5.1469884	3.2956175	1.4773159
H	4.5536732	4.8202062	2.3799343

$TS_{E/F}$

27

Energy = -900.7966385411

C	-4.0731829	-1.4063922	-0.0655082
C	-2.7192263	-1.2616166	-0.3376773
C	-2.0724476	-0.0290083	-0.1846425
C	-2.8389546	1.0588176	0.2575711
C	-4.1900326	0.9169224	0.5288392
C	-4.8168019	-0.3167431	0.3691350
H	-4.5474726	-2.3715366	-0.1936884
H	-2.1442544	-2.1146478	-0.6783235

H	-2.3720652	2.0258047	0.3925311
H	-4.7607892	1.7724117	0.8687538
H	-5.8725973	-0.4242899	0.5827981
C	-0.6440527	0.0617791	-0.4890856
H	-0.1635651	-0.8640680	-0.7897658
C	0.1264535	1.1511079	-0.4538594
H	-0.2780996	2.1204866	-0.1756893
C	1.5956438	1.1287764	-0.7447471
H	1.9263280	2.0210972	-1.3052914
H	2.0900880	1.3731281	0.3334346
O	2.1237862	-0.0070195	-1.1650554
S	3.2437685	-0.7604315	0.5958077
C	4.7417345	-0.5250215	-0.3784724
H	5.6067055	-0.8711250	0.1852698
H	4.6136413	-1.1078158	-1.2873378
H	4.8344692	0.5259979	-0.6397063
C	3.1115431	0.6076075	1.4986395
H	2.4472473	0.5632409	2.3494681
H	3.8710238	1.3753696	1.4729239

F (product)

18

Energy = -422.9144610987

C	-4.0519476	1.7071043	0.0016229
C	-2.6672690	1.7946302	0.0012910
C	-2.0223976	3.0379008	-0.0007510
C	-2.8115651	4.1973036	-0.0029374
C	-4.1929553	4.1100910	-0.0028269
C	-4.8191905	2.8653293	-0.0004492
H	-4.5315945	0.7367868	0.0033571
H	-2.0693765	0.8910655	0.0028014
H	-2.3399572	5.1707494	-0.0051463
H	-4.7880416	5.0143268	-0.0047039
H	-5.8997785	2.8019987	-0.0003638
C	-0.5666853	3.0736321	-0.0006850

H	-0.0834044	2.0989332	-0.0035753
C	0.2341994	4.1510931	0.0029406
H	-0.1419550	5.1671725	0.0067346
C	1.6855784	3.9972351	0.0024861
H	2.0404049	2.9438484	-0.0017685
O	2.4755541	4.9157163	0.0064203

5.3.2 Mechanistic Details Regarding the CO_2-Assisted Synthesis of *α*-Diketones From Aldehydes

In situ Gas Phase GC:

Gas phase GC measurements of the headspace of a reaction from furfurladehyde to furil were conducted. In the middle of the reaction time (8 h; **Figure 22**) and in the end (16 h; **Figure 23**) the curves are same. The source of N_2 gas is the front part of the needle of the used gas-tight syringe. The signal at 7.5 minutes can be assigned to N_2 gas and the one at 29.5 minutes to CO_2.

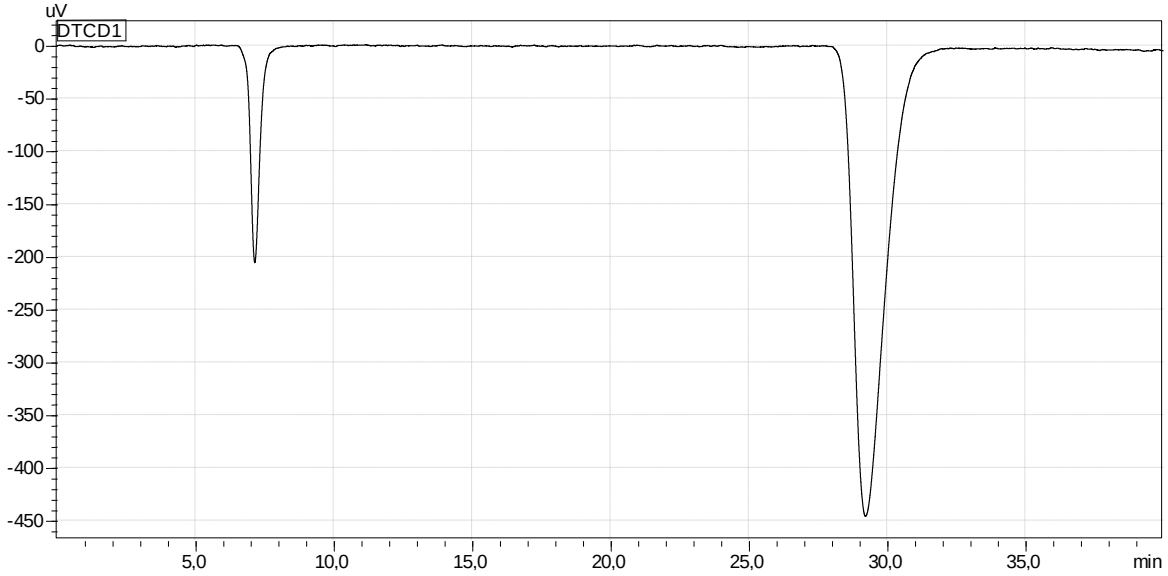

Figure 22: *In situ* gas phase GC measurements after 8 h reaction time; measured by the working group of Prof. Inke Siewert.

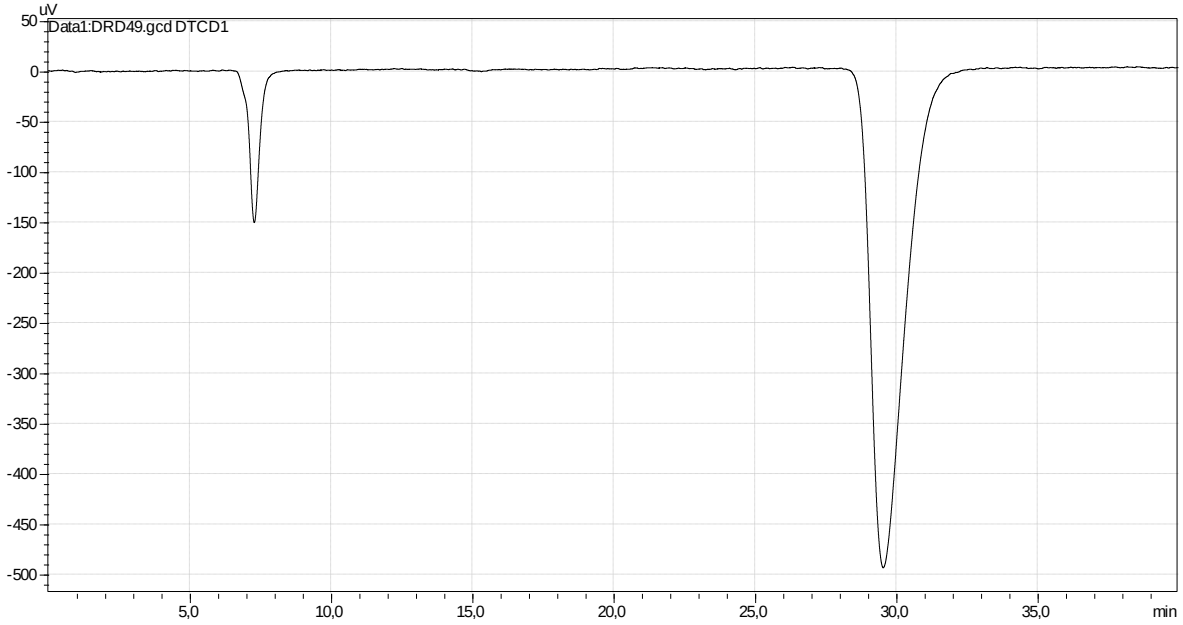

Figure 23: *In situ* gas phase GC measurements after 16 h reaction time; measured by the working group of Prof. Inke Siewert.

Details Regarding DFT Calculations:

All DFT calculations were performed within the Turbomole 7.0[198] program package. The molecular structures were optimized using the B3LYP[199] functional combined with Grimme's dispersion correction with Becke-Johnson damping (D3(BJ))[200], applying increased convergence criteria (10^{-8} H in total energy and 10^{-4} au in in the maximum norm of the Cartesian gradient) and a fine integration grid (m4 in Turbomole convention). Ahlrich's revised all electron basis sets were utilized throughout.[201] No symmetry restrains were imposed and the optimized structures were defined as minima (no negative eigenvalue) or transition states (one negative eigenvalue) by vibrational analyses at the D3(BJ)-B3LYP/def2-TZVP level of theory. Additionally, the nature of the located transition states was confirmed by displacement of the structures along the vibration mode that represents the reaction coordinate followed by full structure optimizations.

To account for solvent energies, the (free) energies have been evaluated by single point calculations in the optimized structures applying the same method (D3(BJ)-B3LYP) but a slightly larger basis set (def2-TZVPP) and the conductor-like screening model (COSMO)[202] (ε = 47 for DMSO). We find that the energy loss in the formation of charged species is largely compensated by the COSMO correction. The final energies were calculated by adding the single point energies with the zero-point vibrational energy (ZPVE) or the free energy (G) that were obtained from the vibrational analyses at the D3(BJ)-B3LYP/def2-TZVP level. Conformers of the different structures have been fully evaluated and the ones with the lowest single point energies chosen.

Two alternative pathways were identified as described below:

a) Activation of DMSO by CO_2

Nucleophilic attack of DMSO at CO_2 does not occur if not accompanied by a proton shift from one methyl group of DMSO to CO_2. The transitions state for this reaction has been located but is rather high in energy (50.2 kcal/mol) compared to the energies of the path presented in the text. Scans of the possible reaction of DMSO with the CO_2–NHC adduct using a simplified model of the NHC catalyst were not productive (see **Figure 24**).

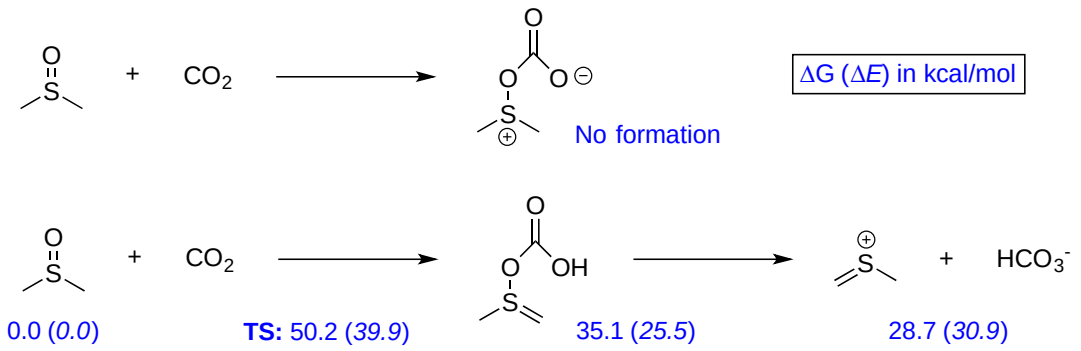

Figure 24: Evaluated pathways for the reaction between DMSO and CO_2.

b) DMSO as hydride acceptor

Frequently, DMSO has been suggested to act as a hydride acceptor. To evaluate this possibility, we have calculated the thermodynamic hydricities (ΔG_{H^-}) for the theoretical reaction:

$$AH \rightarrow A^+ + H^-$$

as: $$\Delta G_{H^-}(AH) = G(A^+) + G(H^-) - G(AH)$$

The energy of the hydride ion was obtained from its SCF energy using $H = E_{SCF} + {}^5/_2 \cdot RT$ (1.48 kcal·mol^{-1} at 298.15 K) while the free energies for the rest were calculated as described above. This approach is rather crude but should be valid for a comparative study.

According to the results shown in **Figure 25**, hydride transfer to DMSO is uphill and therefore not expected to take place. On the other hand, for entropic reasons (release of CO_2), the carboxylate ester is indeed a better hydride donor than the hydroxyl compound (lines 1 and 2), possibly explaining the mediating effect of CO_2. However, the best hydride donor would be the deprotonated hydroxyl compound (line 3). All in all, even when we neglect that DMSO should not act as hydride acceptor, the calculated energies do poorly explain while oxidation only takes place in presence of CO_2.

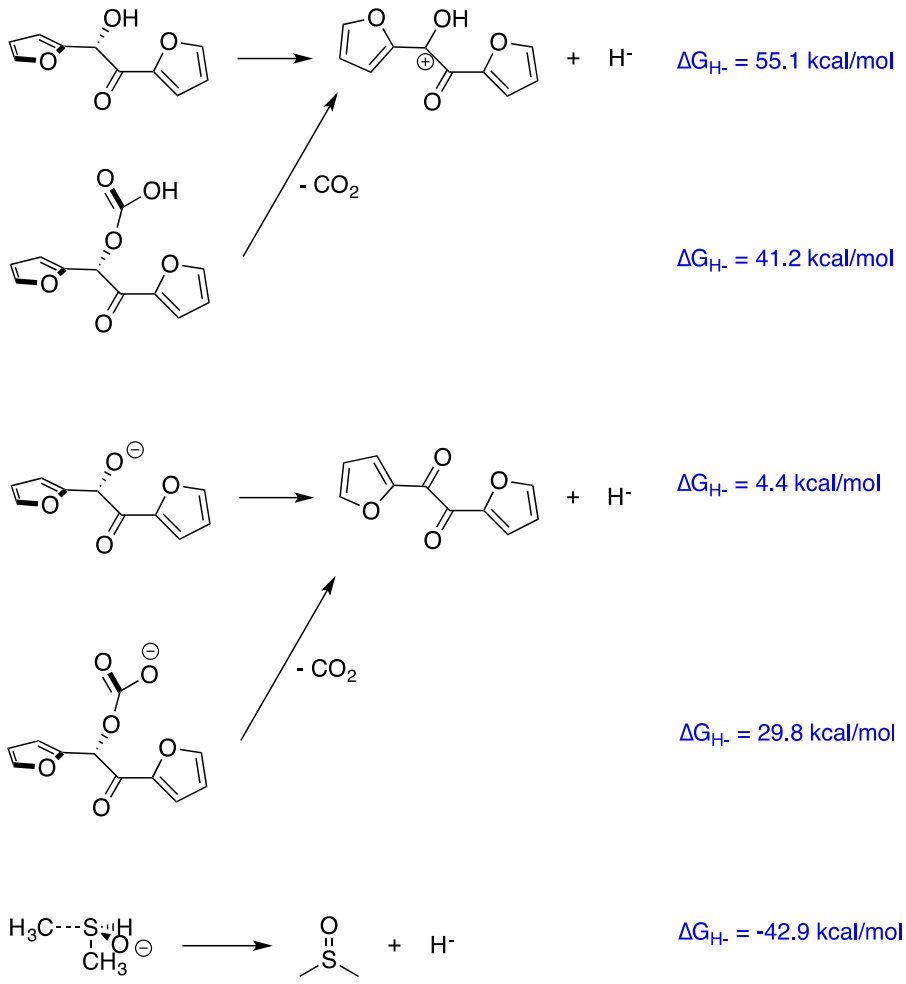

Figure 25: Calculated thermodynamic hydricities of possible intermediates in the oxidation step.

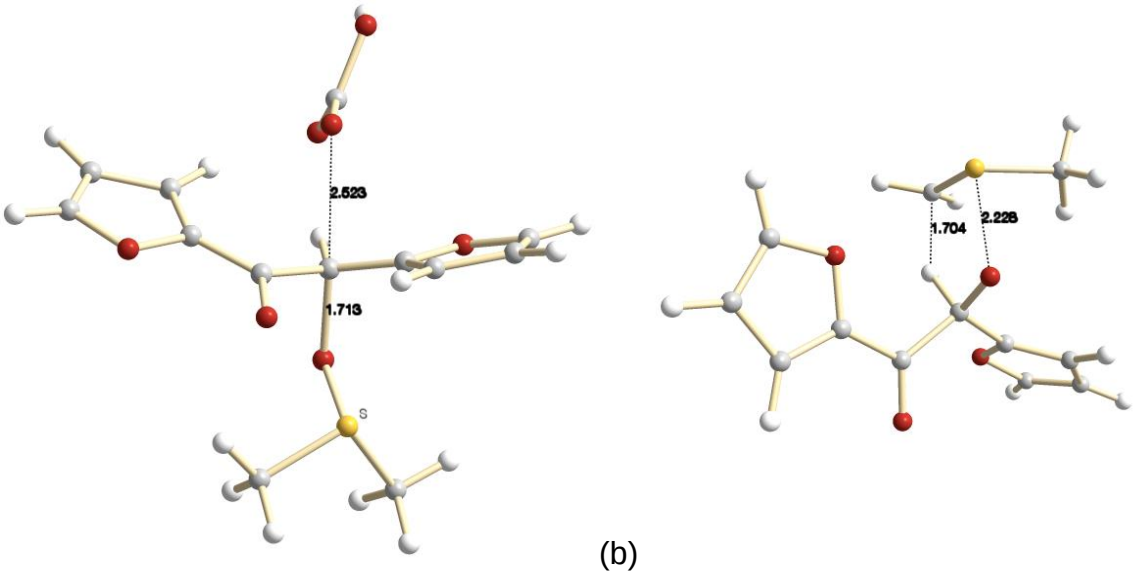

(a) (b)

Figure 26: Structures of the transition states of (a) the direct subtitution of HCO_3^- by DMSO and (b) the proton shift to the sulfonium ylide.

Table 12: xyz coordinates of the calculated structures.

CO_2

3

Energy = -188.5873351766

C	0.0263438	0.0000000	-0.0000019
O	-1.1336183	-0.0000000	0.0000010
O	1.1862745	-0.0000000	0.0000010

DMSO

10

Energy = -553.1643118688

S	-2.4490823	0.8662338	0.7785258
C	-4.0711733	0.8491649	-0.0413156
H	-4.5684120	-0.1046256	0.1385877
H	-4.6509970	1.6592503	0.3980458
H	-3.9315131	1.0270240	-1.1078957
C	-1.7127882	-0.4680965	-0.2120012
H	-0.6774732	-0.5619199	0.1116910
H	-2.2455428	-1.4022814	-0.0308038
H	-1.7500047	-0.1898030	-1.2654936
O	-1.7749958	2.1273696	0.3638801

H_2O

3

Energy = -76.42649010690

O	-0.0123480	0.0000000	0.0000000
H	0.5724125	-0.7651042	0.0000000
H	0.5724124	0.7651043	0.0000000

HCO_3^-

5

Energy = -264.4578056723

C	-1.7856041	1.1151180	-0.0000032
O	-1.0866106	2.1302468	0.0000026

O	-1.0293467	-0.1224951	-0.0000027
H	-1.7319142	-0.7838111	0.0000194
O	-3.0219248	0.9394914	0.0000012

DMS

9

Energy = -477.9618981180

S	-2.4458118	0.8794646	0.7211457
C	-4.0915630	0.8692625	-0.0363943
H	-4.5919425	-0.0864035	0.1258530
H	-4.6711673	1.6567829	0.4439215
H	-4.0325182	1.0764765	-1.1057791
C	-1.6847998	-0.4753365	-0.2104033
H	-0.6640110	-0.5825795	0.1547148
H	-2.2187426	-1.4123503	-0.0462765
H	-1.6564305	-0.2503700	-1.2774413

$C_5H_3O–CHOH–CO–C_5H_3O$

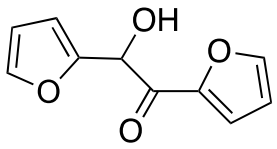

22

Energy = -686.6472290993

C	-3.5627286	1.4418544	0.0846460
C	-2.3303366	1.6779968	0.6041957
C	-1.9787988	3.0125146	0.2294400
C	-3.0224789	3.4920387	-0.4914487
O	-3.9972178	2.5520470	-0.5933501
H	-1.7443205	0.9780212	1.1711225
H	-1.0678443	3.5370115	0.4640894
H	-3.2170870	4.4294059	-0.9821674
C	-4.5338766	0.3251008	0.1321351
H	-5.1123468	0.3455763	-0.7985103
C	-3.8919758	-1.0673861	0.2666069

C	-4.8176034	-2.2010200	0.1766515
C	-4.6125426	-3.5454167	0.2860313
O	-6.1485171	-1.9641562	-0.0835770
C	-5.8735492	-4.1717038	0.0860097
H	-3.6629137	-4.0120833	0.4838894
C	-6.7661607	-3.1688635	-0.1327366
H	-6.0907304	-5.2262986	0.1002239
H	-7.8237312	-3.1515500	-0.3312922
O	-2.7117145	-1.2634642	0.4598144
O	-5.4201529	0.5121666	1.2507841
H	-6.2212278	0.0010812	1.0823372

$C_5H_3O–CHOCO_2H–CO–C_5H_3O$

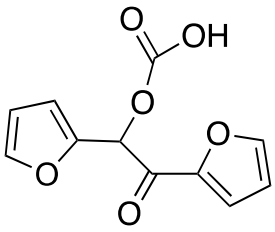

25

Energy = -875.2325822909

C	-3.7646459	1.5567458	0.1894496
C	-3.8998356	2.6050503	1.0380098
C	-2.7081161	3.3870625	0.8977008
C	-1.9404192	2.7502075	-0.0192377
O	-2.5746537	1.6300841	-0.4680145
H	-4.7392212	2.7939574	1.6846394
H	-2.4626168	4.2991925	1.4149297
H	-0.9741590	2.9473109	-0.4479545
C	-4.6118833	0.3816054	-0.1280993
H	-4.5476729	0.1574850	-1.1953161
C	-4.2283392	-0.8851761	0.6693456
C	-4.9666478	-2.1005883	0.3485190
C	-4.9266625	-3.3543366	0.8912482
O	-5.8777542	-2.0758805	-0.6771399
C	-5.8602562	-4.1411667	0.1658915

H	-4.2967478	-3.6560332	1.7104344
C	-6.4040577	-3.3153012	-0.7716097
H	-6.0975719	-5.1807473	0.3155399
H	-7.1407345	-3.4590838	-1.5428944
O	-3.3508392	-0.8757818	1.5028991
O	-5.9798695	0.6637982	0.2159701
C	-6.7843830	1.0156469	-0.7937895
O	-8.0013861	1.2542201	-0.2816925
H	-8.5663203	1.5123335	-1.0235829
O	-6.4890887	1.1032454	-1.9542838

$C_5H_3O–CH–CO–C_5H_3O$ (cation)

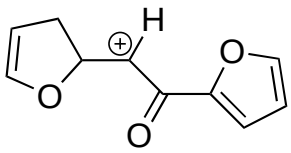

20

Energy = -610.5530923279

C	-3.5777722	1.3602478	-0.1066753
C	-2.2516178	1.5431222	0.3808411
C	-1.9062948	2.8544977	0.1400058
C	-3.0149119	3.4366465	-0.4814903
O	-4.0038711	2.5870007	-0.6374956
H	-1.6764341	0.7580150	0.8438136
H	-0.9801024	3.3533469	0.3722629
H	-3.1812778	4.4418432	-0.8420070
C	-4.4281272	0.3143304	-0.1494409
H	-5.4014624	0.4764878	-0.5941544
C	-4.0571280	-1.0284822	0.3928608
C	-5.0862476	-2.0284488	0.2549006
C	-6.3672495	-2.0236071	-0.2781399
O	-4.8060082	-3.2742573	0.7300755
C	-6.8774453	-3.3238571	-0.1153228
H	-6.8801469	-1.1917384	-0.7306012
C	-5.8847983	-4.0406040	0.5032522

H	-7.8447848	-3.6927809	-0.4104171
H	-5.8155939	-5.0657231	0.8275217
O	-2.9660116	-1.2201759	0.9004654

Transition state: $C_5H_3O–CHOCO_2H–CO–C_5H_3O$ + DMSO (direct path)

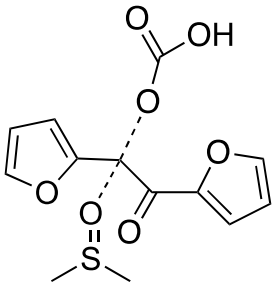

35

Energy = -1428.357579410

C	-0.3081428	-1.1121805	1.1560740
C	-1.5795172	-1.5386227	1.4167308
C	-1.5182136	-2.2744295	2.6332307
C	-0.2144711	-2.2545751	3.0218971
O	0.5364922	-1.5652895	2.1341174
H	-2.4449904	-1.3190010	0.8179672
H	-2.3354124	-2.7398985	3.1575855
H	0.3100487	-2.6594661	3.8696321
C	0.2972494	-0.3136068	0.1180327
H	1.2211865	0.1833528	0.4023081
C	-0.6271195	0.4008210	-0.8476709
C	-0.2549546	1.7120349	-1.3011982
C	0.7759168	2.5634945	-0.9914691
O	-1.0352360	2.2687488	-2.2892960
C	0.6208813	3.6964745	-1.8271772
H	1.5166219	2.3889253	-0.2210569
C	-0.4907031	3.4632542	-2.5841956
H	1.2410666	4.5763576	-1.8547206
H	-0.9950768	4.0371640	-3.3431008
O	-1.5792819	-0.2201462	-1.3134630
O	-0.1537882	1.5080918	1.8043190
C	0.9977417	1.7825272	2.1958302

O	1.0695933	2.3920353	3.4387124
H	2.0132024	2.5394821	3.5847445
O	2.0892597	1.5786823	1.6084418
S	0.0474646	-2.5536732	-1.4859563
C	-0.1490329	-2.2135733	-3.2385859
H	-0.6532220	-3.0672727	-3.6923114
H	-0.7779669	-1.3286221	-3.3038243
H	0.8280575	-2.0449447	-3.6881718
C	1.2050192	-3.9261115	-1.5592826
H	1.4665511	-4.1657749	-0.5303943
H	0.7027519	-4.7739100	-2.0254560
H	2.0903900	-3.6320442	-2.1203411
O	0.9982408	-1.4142629	-0.9915672

$C_5H_3O–CHOS(CH_3)_2–CO–C_5H_3O$ (cation)

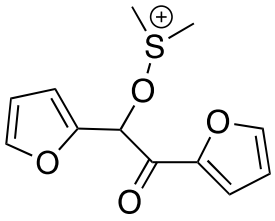

30

Energy = -1163.774049383

C	0.4765297	-1.1596670	0.2234005
C	-0.8093322	-1.4746190	0.5520373
C	-0.7361077	-2.3618565	1.6658390
C	0.5860408	-2.5210363	1.9359672
O	1.3404783	-1.7994390	1.0682122
H	-1.6991929	-1.1098556	0.0659945
H	-1.5574430	-2.8100801	2.1983431
H	1.1271415	-3.0804478	2.6792383
C	1.0725539	-0.3299380	-0.8332080
H	2.0091603	0.1121704	-0.4995553
C	0.0919074	0.7346700	-1.3402062
C	-0.0427383	1.9325590	-0.5684347
C	-0.8620174	3.0280030	-0.6894017

O	0.7665628	2.0851665	0.5326477
C	-0.5429341	3.8898185	0.3841526
H	-1.5983200	3.1772428	-1.4612137
C	0.4487825	3.2685899	1.0904136
H	-0.9831544	4.8460841	0.6098269
H	1.0023232	3.5413775	1.9727963
O	-0.5451692	0.5024450	-2.3583327
S	0.3955503	-1.9946869	-2.7578039
C	0.5863879	-1.4376909	-4.4476154
H	0.0288754	-2.1334995	-5.0758116
H	0.1509809	-0.4440465	-4.4987368
H	1.6426812	-1.4329924	-4.7101819
C	1.2528331	-3.5679672	-2.8247498
H	1.2768061	-3.9592647	-1.8093462
H	0.6712181	-4.2325531	-3.4645963
H	2.2602862	-3.4293091	-3.2129682
O	1.5242139	-1.1332693	-1.9978640

$C_5H_3O–CHOSC_2H_5–CO–C_5H_3O$

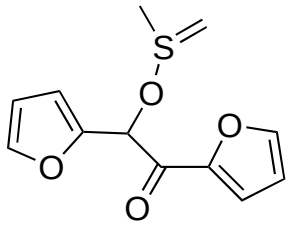

29

Energy = -1163.350717425

C	-3.8419755	1.5920023	0.1259946
C	-4.0492241	2.7864124	0.7330911
C	-2.8152480	3.5084553	0.6341317
C	-1.9524125	2.6974805	-0.0244566
O	-2.5648700	1.5230296	-0.3487438
H	-4.9661575	3.1035019	1.1980936
H	-2.6046309	4.4966631	1.0074055
H	-0.9258950	2.7941051	-0.3303145
C	-4.7098829	0.4057574	-0.1073578

H	-4.5511755	0.0549462	-1.1445705
C	-4.3902146	-0.7747585	0.8257611
C	-5.0436003	-2.0503646	0.5168554
C	-5.0479843	-3.2350197	1.1951985
O	-5.7747527	-2.1839213	-0.6373907
C	-5.8229352	-4.1459033	0.4255300
H	-4.5472263	-3.4132567	2.1312073
C	-6.2339076	-3.4566622	-0.6733333
H	-6.0429008	-5.1752623	0.6529089
H	-6.8241935	-3.7241878	-1.5326869
O	-3.6578968	-0.6751703	1.7850428
O	-6.0631582	0.6909818	0.1079180
S	-6.9159631	1.2901590	-1.4300001
C	-6.3831223	0.6178916	-2.7969452
H	-6.5056486	-0.4337226	-3.0135469
H	-5.7053668	1.2141985	-3.3884605
C	-8.3451541	0.3094636	-0.9472454
H	-8.5671127	0.5363291	0.0919932
H	-9.1742499	0.5876482	-1.5941750
H	-8.0946511	-0.7434633	-1.0526266

Transition state: $C_5H_3O–CHOSC_2H_5–CO–C_5H_3O$

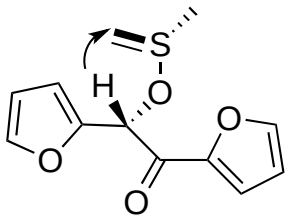

29

Energy = -1163.341237827

C	0.9169516	1.6934720	0.0482809
C	1.0129424	2.7481824	0.8975257
C	1.7096063	3.7800517	0.1889107
C	1.9836053	3.2770650	-1.0400099
O	1.5001105	2.0074828	-1.1466638
H	0.6440262	2.7709989	1.9082973

H	1.9762756	4.7583938	0.5524920
H	2.4882147	3.6653534	-1.9069545
C	0.2901135	0.3443538	0.1778475
H	-0.2856453	0.2061966	-0.8743819
C	1.2968554	-0.8165417	0.1914411
C	0.7555880	-2.1768259	0.1061639
C	1.3719944	-3.3858078	0.2560592
O	-0.5676376	-2.3762010	-0.1962344
C	0.3794895	-4.3821083	0.0430560
H	2.4132923	-3.5235705	0.4913784
C	-0.7735921	-3.7126472	-0.2290786
H	0.5025826	-5.4510312	0.0868314
H	-1.7762432	-4.0323175	-0.4545464
O	2.4905488	-0.6360986	0.3037305
O	-0.6088533	0.2319914	1.1438576
S	-2.5434424	0.2346782	0.0384649
C	-1.8806793	0.3092170	-1.4646289
H	-1.9078424	-0.5968044	-2.0513297
H	-1.7259782	1.2536261	-1.9657994
C	-2.7675713	1.9604370	0.5184631
H	-1.9379664	2.5492742	0.1364448
H	-3.7227871	2.3232157	0.1423128
H	-2.7491606	1.9819047	1.6053582

$C_5H_3O–CO–CO–C_5H_3O$

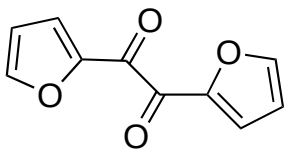

20

Energy = -685.4509262878

C	-3.7180294	-0.7257678	-0.1985809
C	-2.3898780	-0.7842034	0.1436874
C	-1.9675661	0.5512833	0.3655576
C	-3.0631418	1.3322656	0.1434718

O	-4.1280759	0.5829932	-0.1958401
H	-1.8026093	-1.6824468	0.2052912
H	-0.9850659	0.8899494	0.6473505
H	-3.2280838	2.3952703	0.1872927
C	-4.7309278	-1.7188036	-0.5151174
C	-4.2666769	-3.1910991	-0.5156883
C	-5.2791751	-4.1841592	-0.1979931
C	-6.6074777	-4.1257213	0.1436438
O	-4.8691348	-5.4929447	-0.1950771
C	-7.0299513	-5.4611904	0.3651832
H	-7.1947641	-3.2274902	0.2047811
C	-5.9342716	-6.2421931	0.1437244
H	-8.0126489	-5.7998200	0.6462986
H	-5.7693401	-7.3051879	0.1878246
O	-5.8815936	-1.4289744	-0.7822435
O	-3.1164793	-3.4808052	-0.7850502

5.3.3 Mechanistic Details Regarding the Dehydrogenation of Amines

In situ Gas Phase GC:

An *in situ* gas GC measurement of the headspace of a reaction from *N*-benzylaniline to *N*-benzylideneaniline was carried out after 16 h reaction time (**Figure 27 – 28**). The curve is indicating that there is no other gas than CO_2. The source of N_2 gas is the front part of the needle of the used gas-tight syringe; **7.5 min: N_2, 29.5 min: CO_2.**

Figure 27: *In situ* gas phase GC measurement; measured by the working group of Prof. Inke Siewert.

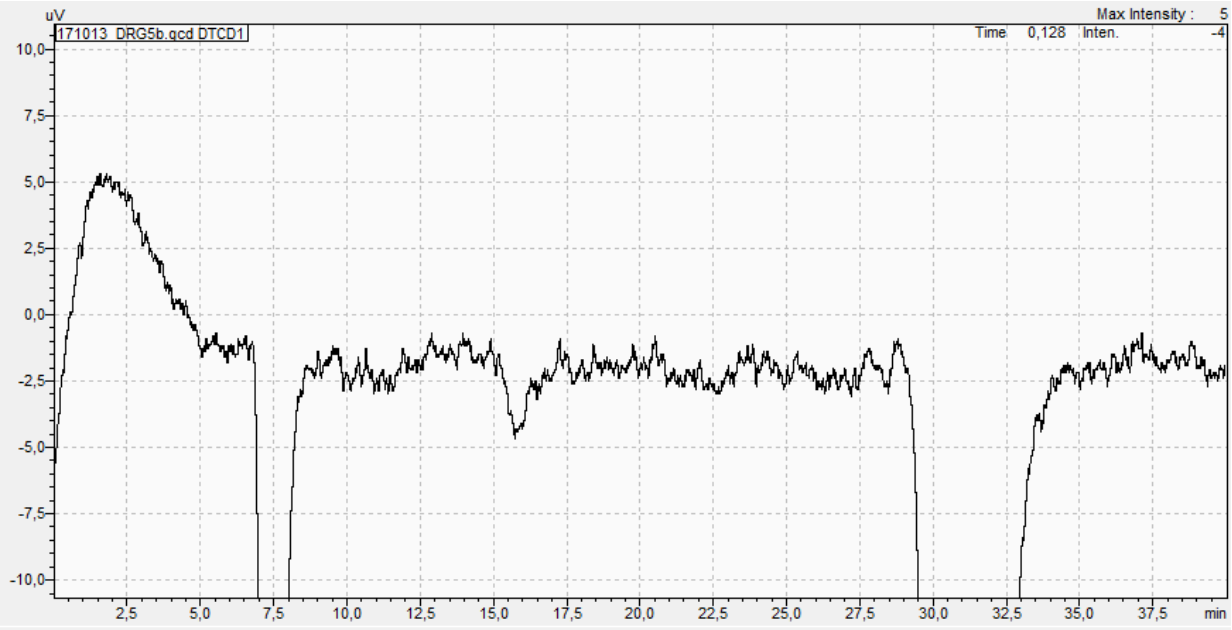

Figure 28: Zoom-in of the *in situ* gas phase GC measurement; measured by the working group of Prof. Inke Siewert.

Different amounts of CO_2:

The reaction flask (see **chapter 5.2.4**) containing a nitrogen atmosphere after three vacuum/N_2 cycles was charged with the volumetric amount of 1.0 and 0.2 equivalents of CO_2, respectively, through a septum *via* syringe. The syringe was purged with CO_2 gas thrice prior to use. The necessary amount was calculated according to the ideal gas law:

$$pV = nRT$$

The temperature in the laboratory was measured to be 20 °C, the pressure was estimated to be 1 atm = 101325 Pa. This is an example calculation for the case of 1.0 equivalent of CO_2 with the scale of the reaction being 0.134 mmol:

$$V = \frac{nRT}{p} = \frac{0.134 * 10^{-3}\ mol * 8.314\ kg\ m^2 * 293.15\ K\ m\ s^2}{101325\ s^2\ mol\ K\ kg} = 3.2 * 10^{-6}\ m^3 = 3.2\ ml$$

KIE experiments:

Mono- and di-deuterated starting materials **280a-*d*$_1$** and **280a-*d*$_2$** were synthesized according to literature procedure (**Scheme 77 – 78**)[203]:

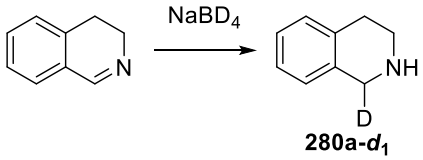

280a-*d*$_1$

Scheme 77: Deuteration of 3,4-dihydroisoquinoline to **280a-*d*$_1$**.

280a-*d*$_1$: 6.5 mL ethanol were added to 3.1 mmol $NaBD_4$ (127.9 mg) followed by slow addition of 0.35 mL 3,4-dihydroisoquinoline (2.962 mmol). The mixture was stirred at rt for 1 h, cooled to 0 °C and quenched with 1 M HCl. Afterwards, solid NaOH was added until the solution became basic (controlled by pH indicator paper). The solution was dried with Na_2SO_4 and concentrated in vacuo to give **280a-*d*$_1$**, which was used without further purification (quantitative conversion; > 95% deuteration).

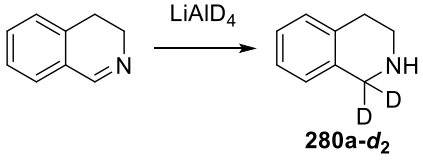

280a-*d*$_2$

Scheme 78: Deuteration of 3,4-dihydroisoquinoline to **280a-*d*$_2$**.

280a-*d*$_1$: 15 mL dry THF were added to 6.6 mmol $LiAlD_4$ (277.1 mg) followed by addition of 0.35 mL 3,4-dihydroisoquinoline (2.962 mmol) under nitrogen atmosphere. The mixture was refluxed for 40 h, cooled to 0 °C and quenched with 1 M HCl. After extraction with EA the solution was dried with Na_2SO_4 and concentrated in vacuo to give **280a-*d*$_1$** which was used without further purification (quantitative conversion; > 95% deuteration).

The so-synthesized starting materials **280a-*d*$_1$** and **280a-*d*$_2$**, respectively, were dehydrogenated (see **Scheme 59**) according to the general reaction procedure (see **chapter 5.2.4**). After 7 h the resulting products were analyzed by GC using *n*-dodecane as internal standard and in case of **280a-*d*$_2$** compared with a non-deuterated sample under the same reaction conditions. The calculated KIE is a result of the average of three independent runs for each starting material:

$$\frac{k_H}{k_D} \sim \frac{n(P_H)}{n(P_D)} = 0.13$$

Both starting materials give the same KIE so that we can assume that there is no effect of the orientation of the deuterium atom in **280a-*d*$_1$** neither an effect of the double deuteration of **280a-*d*$_1$.**

Deuterium NMR:

A ^{2}H NMR spectrum was recorded in order to detect possible deuterated byproducts from the reaction of deuterated starting material **280a-*d*$_2$** in non-deuterated DMSO. We found a hint for D_2O as byproduct at 3.30 ppm in ^{2}H NMR. The signal at 8.88 ppm could be assigned to **280b-*d*$_1$** and at 4.97 to **280a-*d*$_2$**.

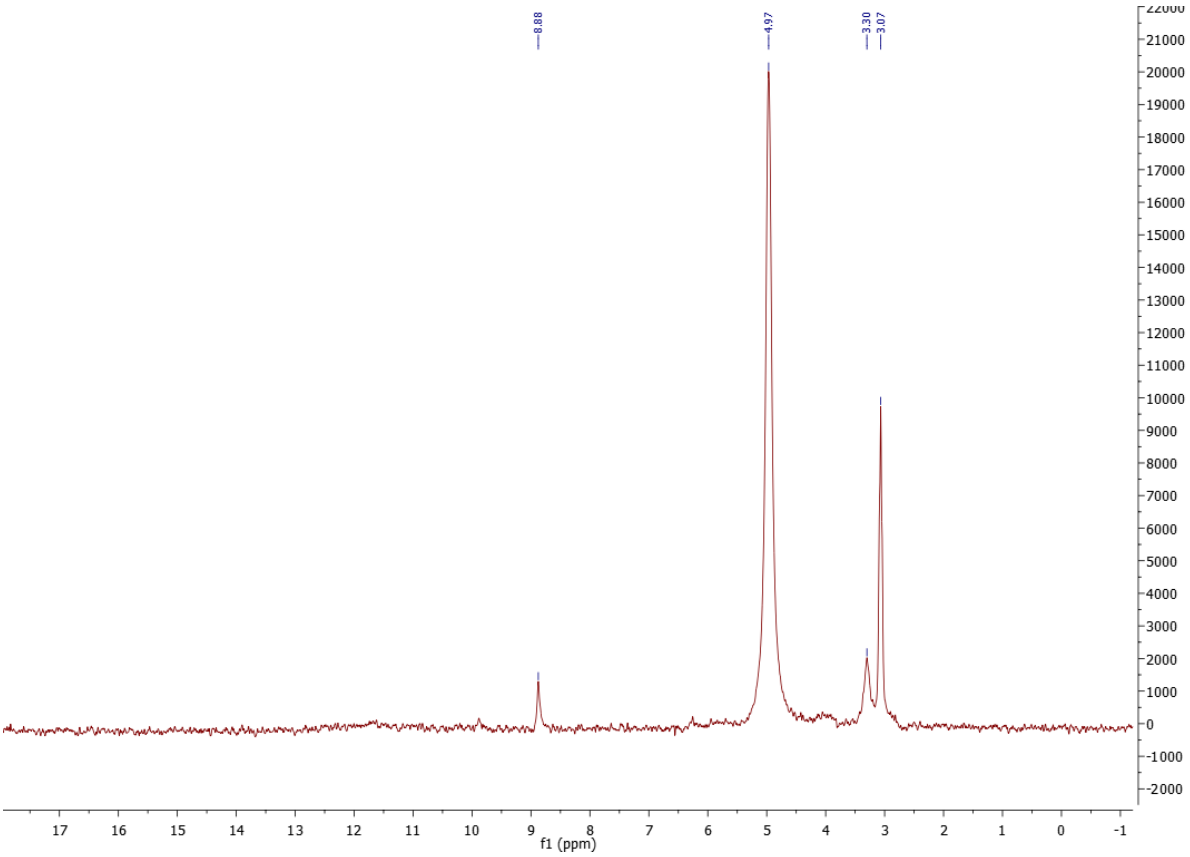

Figure 29: ^{2}H NMR in non-deuterated DMSO.

Carbamate as possible intermediate/byproduct from *N*-benzylaniline:

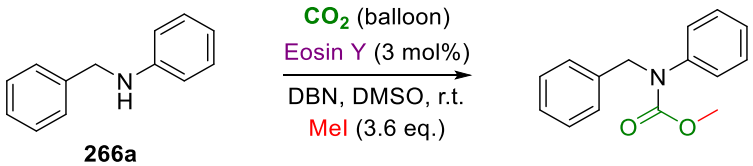

Scheme 79: Reaction of **266a** to the respective methyl carbamate.

A 10 mL two-necked flask containing a stirring bar was charged with 0.134 mmol *N*-benzylaniline (24.3 mg). After purging the flask thrice with vacuum and two times with argon the CO_2 atmosphere was incorporated through a CO_2-filled balloon. Afterwards

dry DMSO (2.5 mL), DBN (1.2 eq, 0.16 mL of a 1 M solution in dry DMSO) and de-gassed methyl iodide (0.03 mL; 0.48 mmol. 3.6 eq) were added. The resulting mixture was stirred for 24 h at rt (**Scheme 79**).

ESI-HRMS: *m/z* calcd. for $C_{15}H_{15}NO_2$ [M+H$^+$]: 242.1176, found: 242.1174; *m/z* calcd. for $C_{15}H_{15}NO_2$ [M+Na$^+$]: 264.0995, found: 264.0996.

<u>Bicarbonate salt as possible intermediate/byproduct from non-dried DBN:</u>

CO_2 was bubbled through commercial DBN for about 3 minutes. The formed white precipitate was collected and submitted to ^{1}H and ^{13}C NMR in D_2O as solvent, thus confirming the formation of a DBNH$^+$ bicarbonate salt (**Figure 30 – 31**).

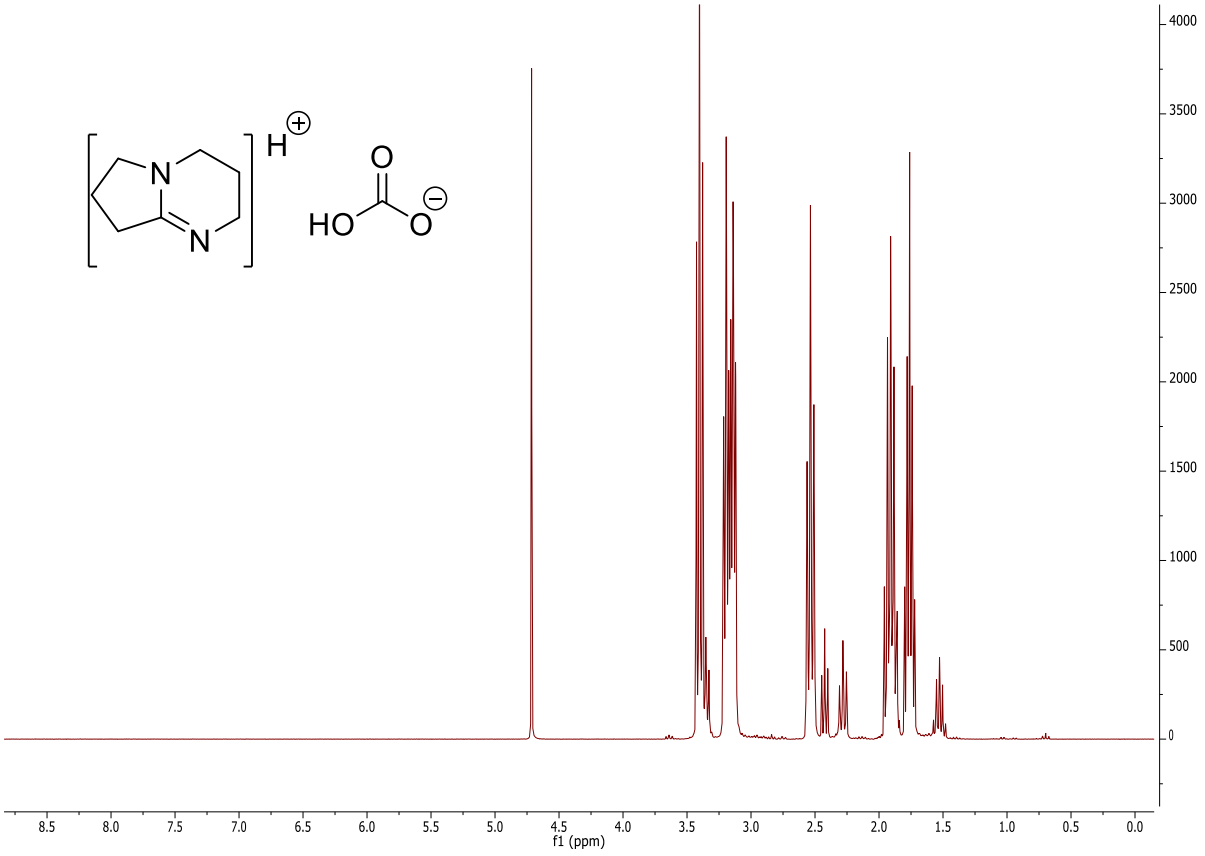

Figure 30: ^{1}H NMR in D_2O.

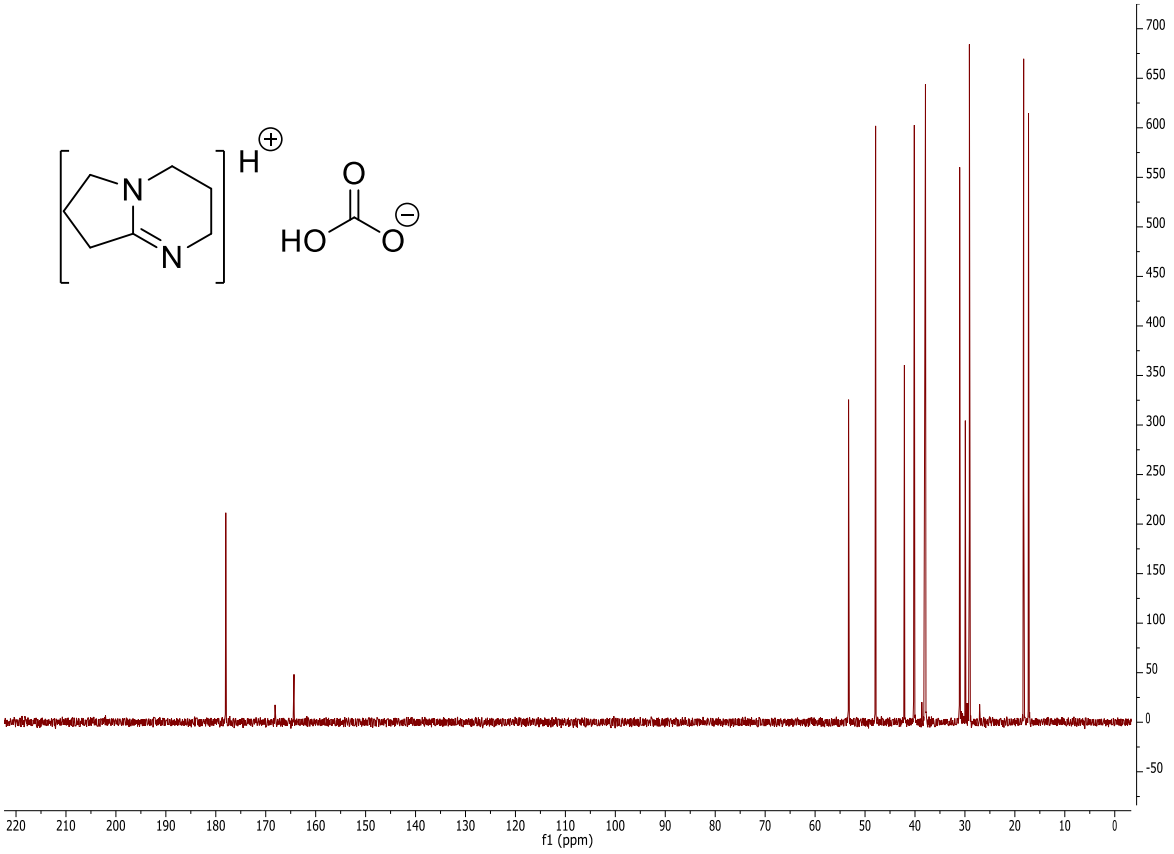

Figure 31: ^{13}C NMR in D_2O.

Stern-Volmer Plot:

To determine the reactive species in the beginning of the photocatalytic reaction absorption-emission spectra for a Stern-Volmer plot were acquired. At first, a 3D spectrum for excitation and emission of eosin Y was recorded in order to detect the maxima of absorption and emission. The resulting spectrum is depicted in **Figure 32** with 3 absorption bands.

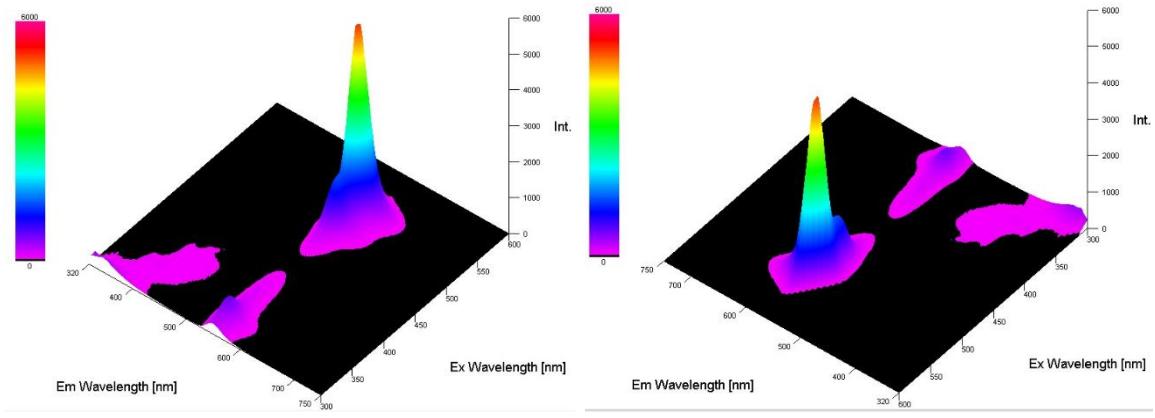

Figure 32: 3D absorption-emission spectrum of eosin Y in DMSO.

Figure 33 shows a comparison spectrum of DBN. The excitation maximum was measured at 533 nm and the emission maximum at 550 nm. These wavelengths were used for further measurements.

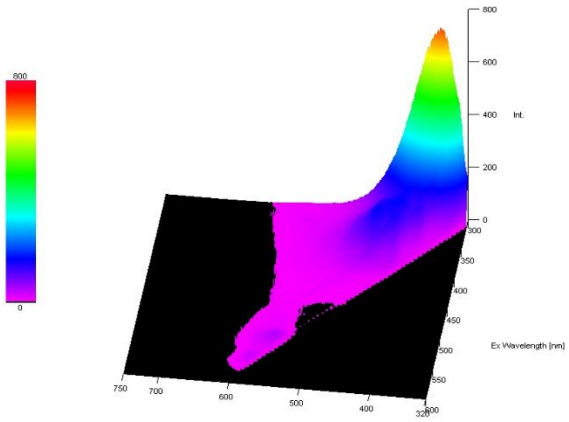

Figure 33: 3D absorption-emission spectrum of DBN in DMSO.

EPR studies:

Room temperature X-band CW EPR experiments were performed on a Bruker ElexSys E500 CW/Transient EPR spectrometer equipped with the SHQ Bruker microwave resonator (ER4122 SHQE-W1). The short-living radical intermediates were trapped with a DMPO spin trap. General instrument settings and the experimental parameters were as follows: 9.87 GHz microwave frequency; 20 mW microwave power; 0.5 G field modulation; 60 dB receiver gain; 5.18 ms conversion time, number of averaged scans: 400.

Spectra simulations were performed using EasySpin MATLAB-based package.[204] Three different adducts making up the total spectrum could be recognized. All species exhibit EPR line splittings due to a typical for DMPO adducts *hf* interaction with ^{14}N and β-proton. Their exact assignment is a matter of further studies. The EPR spectra of the adducts were simulated first in isotropic limit to identify the *hf* interaction patterns and then in a fast-motion regime to optimize the rotational correlation time and g- and *hf*-tensor anisotropies for the observed species. All *hf* interactions were considered as anisotropic, axially symmetric tensors for the best fit with the experimental spectrum.

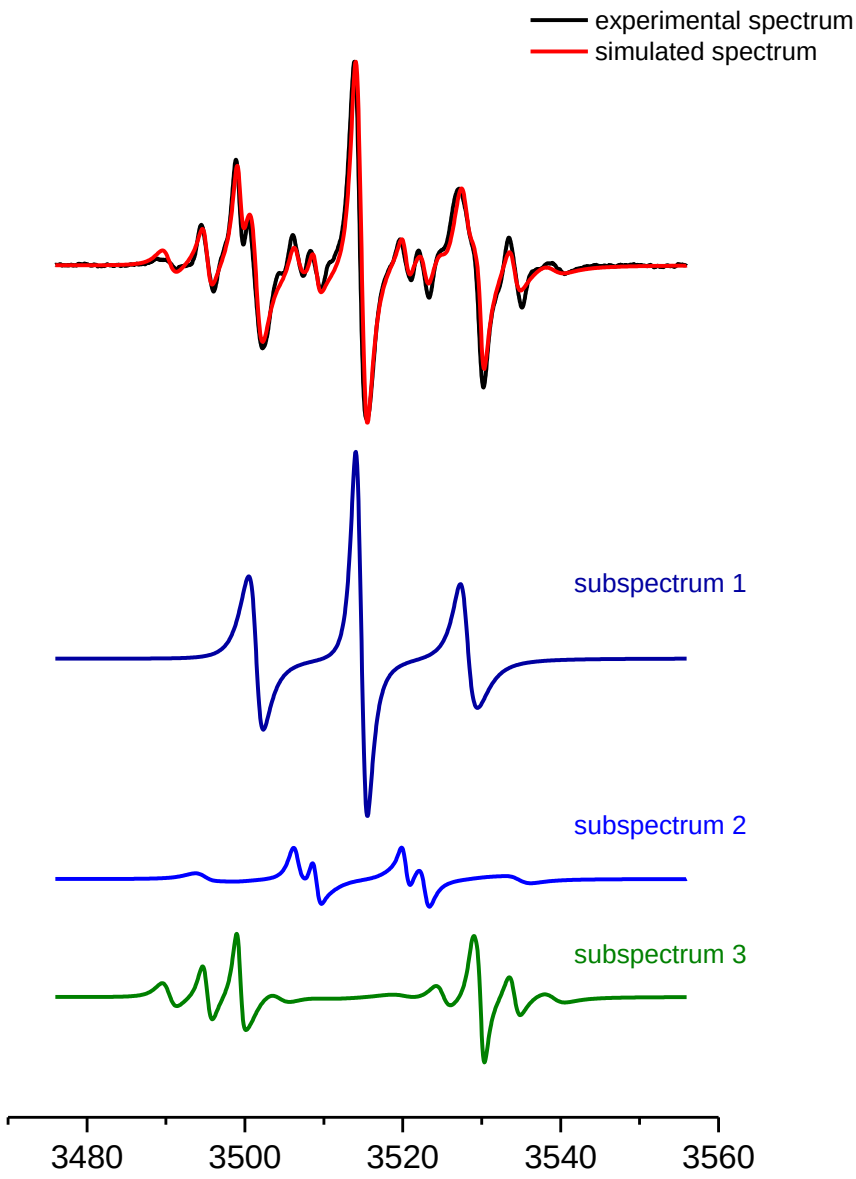

Figure 34: Experimental spectrum of DMPO adducts prepared and measured under reaction conditions in CO_2 atmosphere (black). The simulated spectrum (red) and three radical contributors (subspectrum 1, 2 and 3) are shown for comparison; measurements and discussion of EPR experiments were done with the help of Igor Tkach.

Figure 34 shows the experimental (black) and simulated (red) EPR spectra. The experimental spectrum was measured under reaction conditions (including blue light irradiation) in CO_2 atmosphere. The spectra for all 3 adducts (subspectra 1, 2 and 3) making up the total simulated spectrum are shown for comparison.

The adduct spectra were simulated with the following parameters:

Subspectrum 1:

S = ½, *hf* interaction with ^{14}N(I=1) and ^{1}H (I = ½); Isotropic g-value = 2.0072 (arbitrary value); g-tensor eigenvalue deviations from the isotropic symmetry: $\Delta g_1 = 0.00024$; $\Delta g_2 = -a\ 0.00011$; $\Delta g_3 = -0.00013$.

^{14}N *hf*-tensor eigenvalue components: $\mathrm{A}^{14\mathrm{N}}(\mathrm{iso}) = 46.5\ \mathrm{MHz}$; $\mathrm{A}^{14\mathrm{N}}(\mathrm{axial}) = 22.5\ \mathrm{MHz}$; ^{1}H *hf*-tensor eigenvalue components: $\mathrm{A}^{1\mathrm{H}}(\mathrm{iso}) = -3.9\ \mathrm{MHz}$; $\mathrm{A}^{1\mathrm{H}}(\mathrm{axial}) = 3.0\ \mathrm{MHz}$; Correlation time τ = 10.4 ns; Weight parameter = 0.51.

Subspectrum 2:

S = ½, *hf* interaction with ^{14}N(I=1) and two ^{1}H (I = ½); Isotropic g-value = 2.0072 (arbitrary value); g-tensor eigenvalue deviations from the isotropic symmetry: $\Delta g_1 = 0.0021$; $\Delta g_2 = -0.0019$; $\Delta g_3 = -0.00016$.

^{14}N *hf*-tensor eigenvalue components: $\mathrm{A}^{14\mathrm{N}}(\mathrm{iso}) = 44.2\ \mathrm{MHz}$; $\mathrm{A}^{14\mathrm{N}}(\mathrm{axial}) = 19.5\ \mathrm{MHz}$; ^{1}H *hf*-tensor eigenvalue components: $\mathrm{A}^{1\mathrm{H}}(\mathrm{iso}) = -52.7\ \mathrm{MHz}$; $\mathrm{A}^{1\mathrm{H}}(\mathrm{axial}) = 5.5\ \mathrm{MHz}$; ^{1}H *hf*-tensor eigenvalue components: $\mathrm{A}^{1\mathrm{H}}(\mathrm{iso}) = 0.9\ \mathrm{MHz}$; $\mathrm{A}^{1\mathrm{H}}(\mathrm{axial}) = 18.2\ \mathrm{MHz}$; Correlation time τ = 3.7 ns; Weight parameter = 0.20.

Subspectrum 3:

S = ½, *hf* interaction with ^{14}N(I=1) and two ^{1}H (I = ½); Isotropic g-value = 2.0072 (arbitrary value); g-tensor eigenvalue deviations from the isotropic symmetry: $\Delta g_1 = -0.0026$; $\Delta g_2 = 0.0011$; $\Delta g_3 = 0.0016$.

^{14}N *hf*-tensor eigenvalue components: $\mathrm{A}^{14\mathrm{N}}(\mathrm{iso}) = 4.3\ \mathrm{MHz}$; $\mathrm{A}^{14\mathrm{N}}(\mathrm{axial}) = -49.5\ \mathrm{MHz}$; ^{1}H *hf*-tensor eigenvalue components: $\mathrm{A}^{1\mathrm{H}}(\mathrm{iso}) = 99.0\ \mathrm{MHz}$; $\mathrm{A}^{1\mathrm{H}}(\mathrm{axial}) = 53.6\ \mathrm{MHz}$; ^{1}H *hf*-tensor eigenvalue components: $\mathrm{A}^{1\mathrm{H}}(\mathrm{iso}) = 1.28\ \mathrm{MHz}$; $\mathrm{A}^{1\mathrm{H}}(\mathrm{axial}) = 73.7\ \mathrm{MHz}$; Correlation time τ = 1.4 ns; Weight parameter = 0.29.

Kinetic Studies:

In general, the kinetic experiments were carried out according to the general reaction procedure described in **chapter 5.2.4** but with varying concentrations of *N*-benzylaniline, DBN and eosin Y, respectively, as depicted in **Table 13 – 15**. Samples (as whole reaction mixtures, no aliquots) were taken after the indicated timespan and analyzed *via* GC with *n*-dodecane as internal standard. The obtained values were plotted as product concentration against the time at different concentrations of starting material, base or catalyst, respectively (**Figure 35 – 37**).

Table 13: Different concentrations of *N*-benzylaniline

c(SM) / M	c(P) / M	t / h
0.018	0.001587	2
0.018	0.002433	4
0.018	0.003736	6
0.018	0.003928	8
0.036	0.003046	2
0.036	0.008246	4
0.036	0.012415	6
0.036	0.013664	8
0.0536	0.002441	2
0.0536	0.009151	4
0.0536	0.013523	6
0.0536	0.017532	8
0.108	0.002128	2
0.108	0.005401	4
0.108	0.013822	6
0.108	0.024697	8
0.2144	0.002121	2
0.2144	0.015682	4
0.2144	0.028238	6
0.2144	0.040826	8

Table 14: Different concentrations of DBN

c(base) / M	c(P) / M	t / h
0.01608	0.006332	2
0.01608	0.008924	4
0.01608	0.008748	6
0.01608	0.010432	8
0.03216	0.014200	2
0.03216	0.018053	4
0.03216	0.019290	6
0.03216	0.024817	8
0.06432	0.012441	2
0.06432	0.018151	4
0.06432	0.021523	6
0.06432	0.025532	8
0.09648	0.014121	2
0.09648	0.019443	4
0.09648	0.025681	6
0.09648	0.030455	8
0.12864	0.021188	2
0.12864	0.031779	4
0.12864	0.038768	6
0.12864	0.046392	8

Table 15: Different concentrations of eosin Y

c(PC) / mM	c(P) / M	t / h
0.536	0.00219	2
0.536	0.02417	4
0.536	0.02921	6
0.536	0.03671	8
1.072	0.00712	2
1.072	0.01706	4
1.072	0.03433	6
1.072	0.04596	8
1.608	0.00244	2
1.608	0.00915	4
1.608	0.01352	6
1.608	0.03753	8
2.68	0.00615	2
2.68	0.01169	4
2.68	0.02434	6
2.68	0.05623	8
5.36	0.00400	2
5.36	0.02402	4
5.36	0.04037	6
5.36	0.04647	8

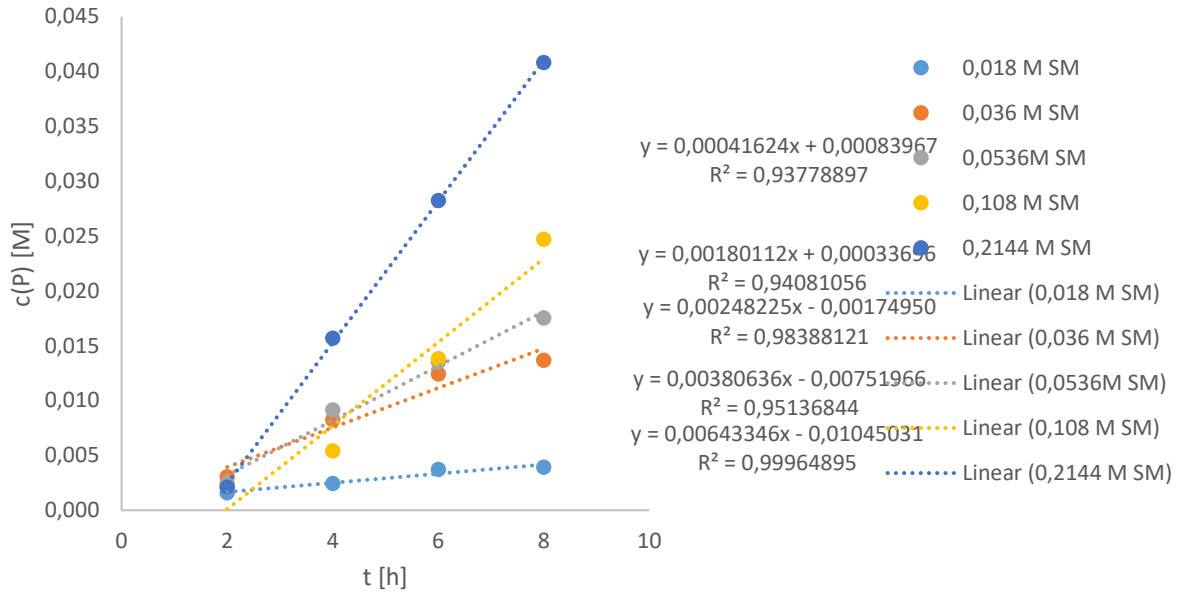

Figure 35: Product concentration plotted against reaction time at different *N*-benzylaniline concentrations; for each data point a separate reaction was conducted using different concentrations of *N*-benzylaniline (18 mmol L^{-1}, 36 mmol L^{-1}, 53.6 mmol L^{-1}, 108 mmol L^{-1}, 214.4 mmol L^{-1}) with constant concentration of DBN (64.3 mmol L^{-1}) and eosin Y (1.61 mmol L^{-1}) in 2.5 mL DMSO at rt under a CO_2 atmosphere (balloon) and blue LED light irradiation and submitted to GC analysis with *n*-dodecane as internal standard after the indicated timespan.

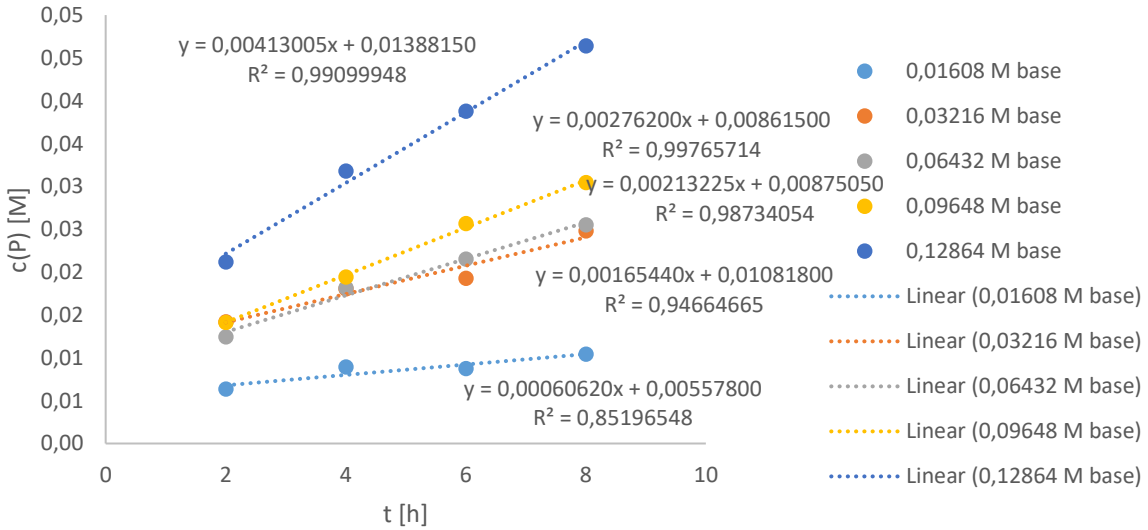

Figure 36: Product concentration plotted against reaction time at different DBN concentrations; for each data point a separate reaction was conducted using different concentrations of DBN (16.1 mmol L^{-1}, 32.2 mmol L^{-1}, 64.3 mmol L^{-1}, 96.5 mmol L^{-1}, 128.6 mmol L^{-1}) with constant concentration of *N*-benzylaniline (0.0536 mol L^{-1}) and eosin Y (1.61 mmol L^{-1}) in 2.5 mL DMSO at rt under a CO_2 atmosphere (balloon) and blue LED light irradiation and submitted to GC analysis with *n*-dodecane as internal standard after the indicated timespan.

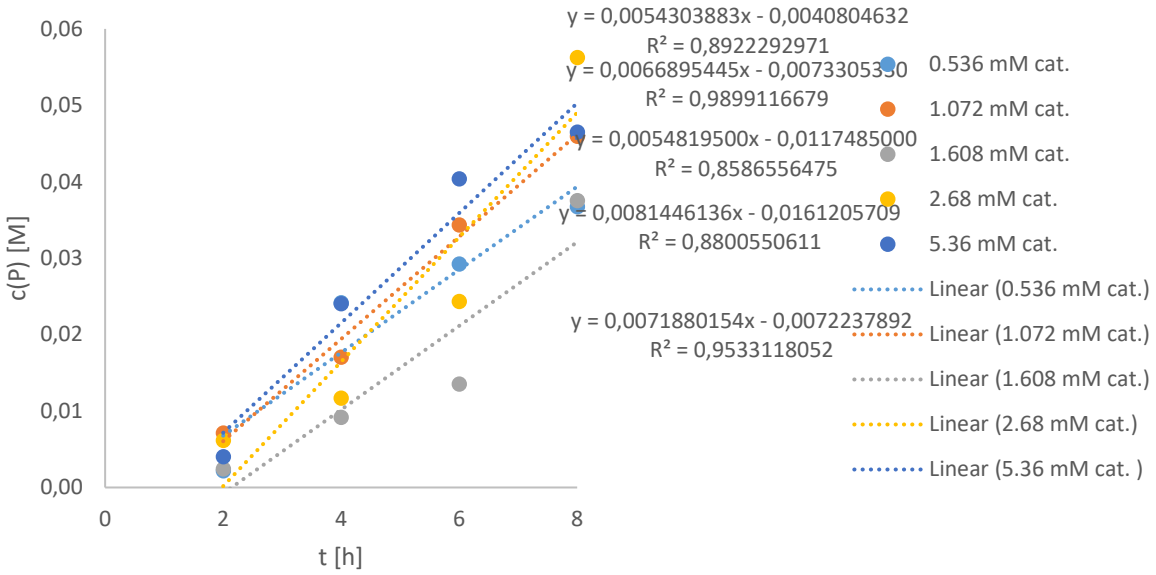

Figure 37: Product concentration plotted against reaction time at different eosin Y concentrations; for each data point a separate reaction was conducted using different concentrations of eosin Y (0.536 mmol L^{-1}, 1.072 mmol L^{-1}, 1.608 mmol L^{-1}, 2.68 mmol L^{-1}, 5.46 mmol L^{-1}) with constant concentration of *N*-benzylaniline (0.0536 mol L^{-1}) and DBN (64.3 mmol L^{-1}) in 2.5 mL DMSO at rt under a CO_2 atmosphere (balloon) and blue LED light irradiation and submitted to GC analysis with *n*-dodecane as internal standard after the indicated timespan.

With the slopes of these curves we were now able to plot the logarithmic concentration of starting material, base and catalyst, respectively, against the logarithmic observed rate constant k_{obs} (**Figure 38 – 40**).

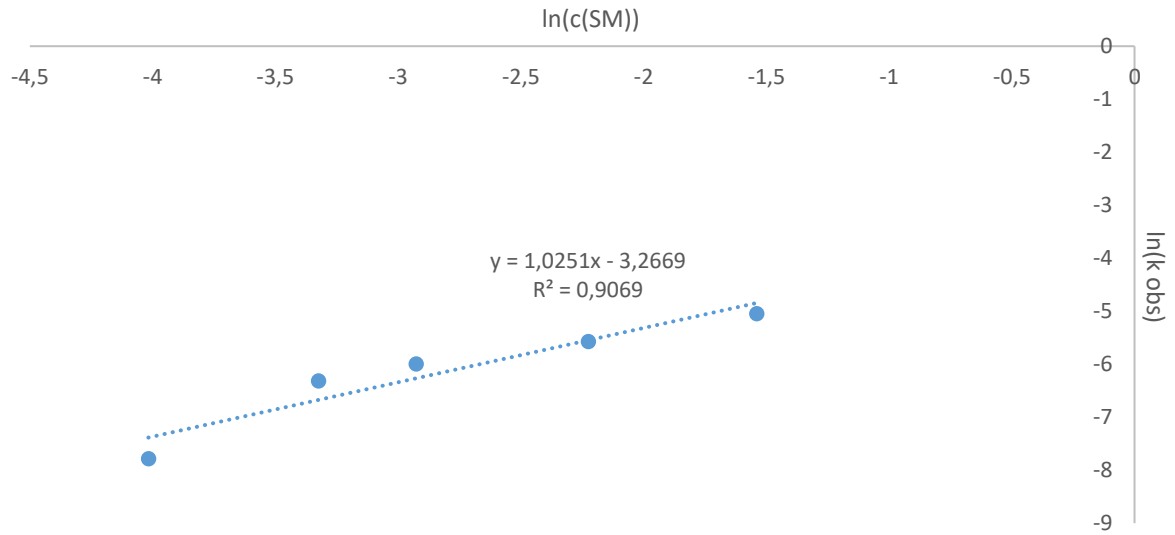

Figure 38: ln(k_{obs}) against ln(c_{SM}); standard error: 0.36529.

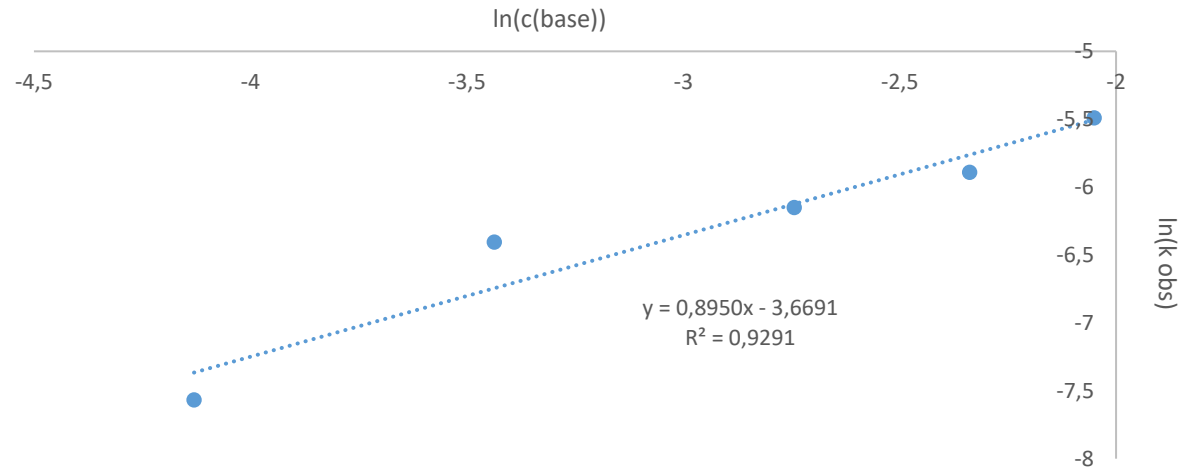

Figure 39: ln(k_{obs}) against ln(c_{base}); standard error: 0.24111.

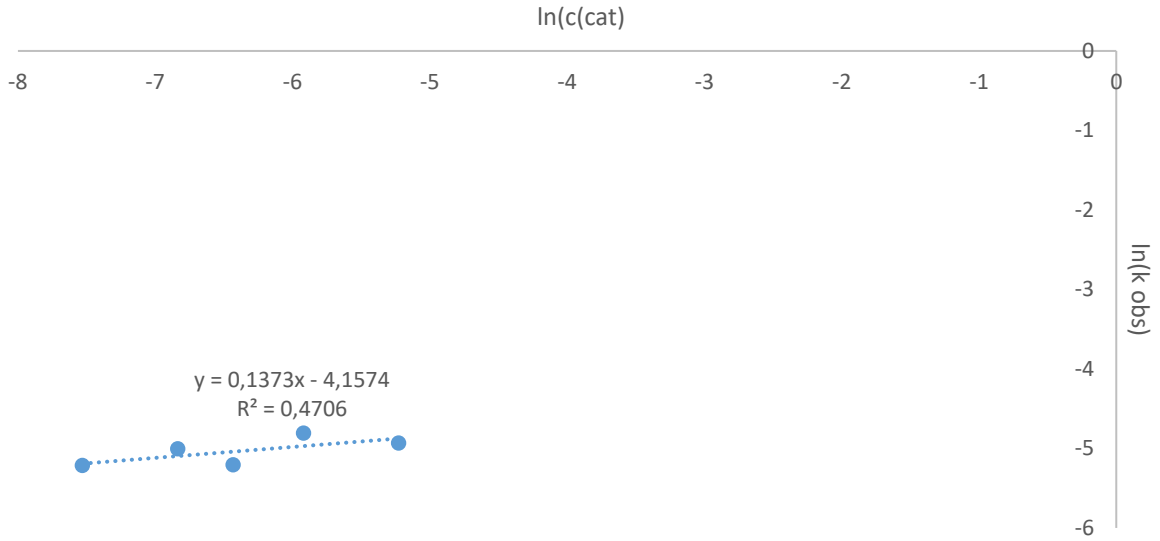

Figure 40: ln(k_{obs}) against ln(c_{cat}); standard error: 0.14743.

<u>Details Regarding DFT Calculations:</u>

All structures were optimized by the ORCA 4.0.1 software package[205] with the M06 functional[206] with a D3 dispersion correction with zero dumping[200a] and a def2-TZVPP basis set.[201a] Influences of the solvent on the structures were introduced by a conductor-like polarizable continuum model (CPCM) for DMSO.[207] The Hessian was calculated to verify the nature of the obtained stationary points.

DLPNO-CCSD(T) single point energies were calculated with a def2-TZVPP and a def2-QZVPP basis set as well as with a def2-TZVPP basis set and tight settings for

the local pairs. The obtained energies were used in the extrapolation scheme developed by Neese and Liakos to the corresponding DLPNO-CCSD(T)/CBS complete basis set energies.[208]

The Gibbs free energies of solvation were estimated by the COSMO-RS method[209] as implemented in the COSMOthermX14 program package.[210] With the aim to achieve the best available accuracy the BP-TZVPD-FINE method was applied, which calculates the correction based on single point calculations performed by Turbomole[211] with the BP86 functional[202a] and a def2-TZVPD basis set.[201a,212]

The redox potential was calculated from the sum of all energy contributions above, based on a scheme originally developed for metal cations.[213] Due to the fact, that redox potentials are generally listed as relative values compared to the standard hydrogen electrode (SHE) the obtained potentials were transformed to analogous representatives by calculating the difference to the total potential of the SHE of 4.44 eV.[214]

5.4 Analytical Data of the Products

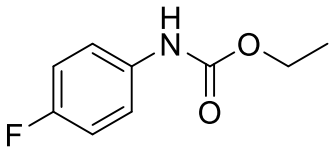

Ethyl (4-fluorophenyl)carbamate (2b): 48 h, 50 °C; **^{1}H NMR** (300.54 MHz, $CDCl_3$): *δ* 7.47 – 7.28 (m, 2H), 7.08 – 6.89 (m, 2H), 6.62 (s, 1H), 4.22 (q, *J* = 7.1 Hz, 2H), 1.30 (t, *J* = 7.1 Hz, 3H); **^{13}C NMR** (75.58 MHz, $CDCl_3$): *δ* 160.69, 153.92, 134.06, 120.60, 115.91, 61.45, 14.68; **MS (GC-MS):** *m/z* 183 $[M^+]$[215]; 82% yield.

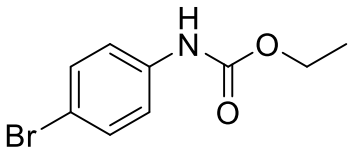

Ethyl (4-bromophenyl)carbamate (3b): 16 h, rt; **^{1}H NMR** (300.14 MHz, $CDCl_3$): *δ* 7.43 – 7.36 (m, 2H), 7.31 – 7.25 (m, 2H), 6.70 (s, 1H), 4.22 (q, *J* = 7.1 Hz, 2H), 1.30 (t, *J* = 7.1 Hz, 3H); **^{13}C NMR** (125.71 MHz, $CDCl_3$): *δ* 153.47, 137.17, 131.98, 120.31, 115.89, 61.57, 14.73; **MS (GC-MS):** *m/z* 244 $[M+H^+]$[216]; 69% yield.

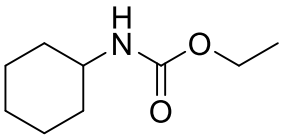

Ethyl cyclohexylcarbamate (4b): 16 h, rt; **^{1}H NMR** (300.14 MHz, $CDCl_3$): *δ* 4.55 (s, 1H), 4.08 (q, *J* = 7.3 Hz, 2H), 3.44 (s, 1H), 2.55 – 1.26 (m, 7H), 1.22 (t, *J* = 7.1 Hz, 3H), 1.18 – 0.65 (m, 3H); **^{13}C** NMR (125.71 MHz, $CDCl_3$): *δ* 155.84, 60.58, 49.85, 33.66, 25.72, 25.00, 14.87; **MS (GC-MS):** 171 $[M^+]$[217]; 78% yield.

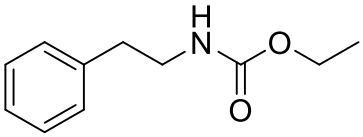

Ethyl phenethylcarbamate (5b): 16 h, rt; **^{1}H NMR** (300.14 MHz, $CDCl_3$): *δ* 7.39 – 7.08 (m, 5H), 4.70 (s, 1H), 4.11 (q, *J* = 7.1 Hz, 2H), 3.44 (q, *J* = 6.7 Hz, 2H), 2.81 (q, *J* = 7.0 Hz, 2H), 1.23 (t, *J* = 7.1 Hz, 3H); **^{13}C NMR** (125.71 MHz, $CDCl_3$): *δ* 156.57, 138.86, 128.81, 128.64, 126.51, 60.85, 42.27, 36.37, 14.85; **MS (GC-MS):** *m/z* 193 $[M^+]$[218]; 78% yield.

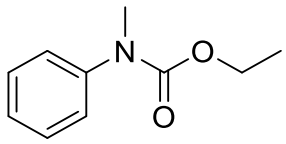

Ethyl methyl(phenyl)carbamate (6b): 40 h, rt; **^{1}H NMR** (300.54 MHz, $CDCl_3$): *δ* 7.37 – 7.14 (m, 5H), 4.15 (q, *J* = 7.1 Hz, 2H), 3.29 (s, 3H), 1.22 (t, *J* = 7.1 Hz, 3H); **^{13}C NMR** (75.58 MHz, $CDCl_3$): *δ* 155.83, 143.52, 128.88, 125.98, 125.78, 61.79, 37.74, 14.73; **MS (GC-MS):** *m/z* 179 $[M^+]$[219]; 90% yield.

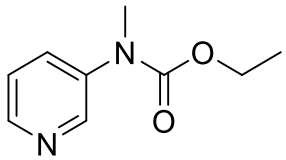

Ethyl methyl(pyridin-3-yl)carbamate (7b): 16 h, rt; **^{1}H NMR** (300.14 MHz, $CDCl_3$): *δ* 8.53 (d, *J* = 2.7 Hz, 1H), 8.40 (dd, *J* = 4.8, 1.5 Hz, 1H), 7.59 (d, *J* = 7.7 Hz, 1H), 7.26 (ddd, *J* = 8.2, 4.8, 0.8 Hz, 1H), 4.17 (q, *J* = 7.1 Hz, 2H), 3.31 (s, 3H), 1.23 (t, *J* = 7.1 Hz, 3H); **^{13}C NMR** (125.71 MHz, $CDCl_3$): *δ* 155.32, 146.88, 146.57, 139.91, 132.56, 123.31, 62.25, 37.41, 14.70; **MS (GC-MS):** *m/z* 180 $[M^+]$[220]; 75% yield.

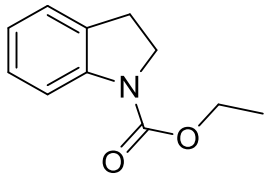

Ethyl indoline-1-carboxylate (8b): 16 h, rt; **^{1}H NMR** (300.54 MHz, $CDCl_3$): *δ* 7.69 (s, 1H), 7.23 – 7.10 (m, 2H), 6.94 (dt, *J* = 7.4, 1H), 4.38 – 4.17 (m, 2H), 4.00 (t, *J* = 8.7 Hz, 2H), 3.10 (t, *J* = 8.7 Hz, 2H), 1.46 – 1.27 (m, 3H); **^{13}C NMR** (75.58 MHz, $CDCl_3$): *δ* 153.38, 142.72, 130.98, 127.48, 124.75, 122.46, 114.79, 61.35, 47.45, 27.47, 14.76; **MS (GC-MS):** *m/z* 191 $[M^+]$[221]; 70% yield.

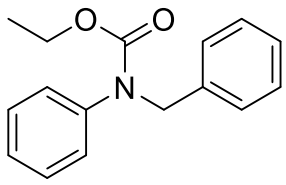

Ethyl benzyl(phenyl)carbamate (9b): 20 h, rt; **^{1}H NMR** (300.14 MHz, $CDCl_3$): *δ* 7.48 – 7.07 (m, 10H), 4.91 (s, 2H), 4.24 (q, *J* = 7.1 Hz, 2H), 1.26 (t, *J* = 7.1 Hz, 3H); **^{13}C NMR** (125.71 MHz, $CDCl_3$): *δ* 155.87, 142.24, 138.12, 128.84, 128.44, 127.86, 127.28, 126.95, 126.41, 61.95, 54.38, 14.78; **MS (GC-MS):** 255 $[M^+]$[218]; 78% yield.

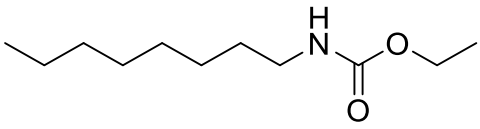

Ethyl octylcarbamate[5] **(10b):** 20 h, rt; **^{1}H NMR** (300.14 MHz, $CDCl_3$): *δ* 4.64 (s, 1H), 4.09 (q, *J* = 7.1 Hz, 2H), 3.14 (q, *J* = 6.7 Hz, 2H), 1.47 (p, *J* = 7.1 Hz, 2H), 1.37 – 1.15 (m, 13H), 0.89 – 0.84 (t, *J* = 7.1 Hz, 3H); **^{13}C NMR** (125.71 MHz, $CDCl_3$): *δ* 156.69, 60.74, 41.18, 31.99, 30.24, 29.45, 29.40, 26.96, 22.84, 14.88, 14.28; **MS (GC-MS):** *m/z* 201 $[M^+]$[222]; 74% yield.

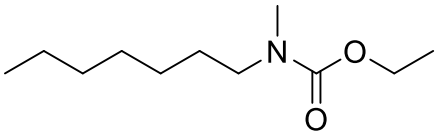

Ethyl heptyl(methyl)carbamate (11b): 16 h, 50 °C; **^{1}H NMR** (300.54 MHz, $CDCl_3$): *δ* 4.11 (q, *J* = 7.1 Hz, 2H), 3.21 (t, *J* = 7.4 Hz, 2H), 2.86 (s, 3H), 1.49 (p, *J* = 7.3 Hz, 2H), 1.32 – 1.18 (m, 11H), 0.87 (t, *J* = 6.7 Hz, 3H); **^{13}C NMR** (75.58 MHz, $CDCl_3$): *δ* 156.72, 61.15, 48.68, 31.91, 29.17, 27.93, 27.71, 26.75, 22.73, 14.88, 14.20; **MS (GC-MS):** *m/z* 201 $[M^+]$; **MS (ESI-HRMS):** *m/z* calcd. for $C_{11}H_{23}NO_2$ $[M+Na^+]$: 202.1802, found: 202.1804; 68% yield.

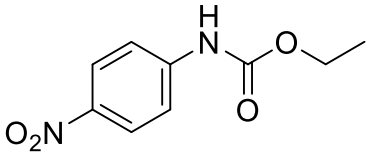

Ethyl (4-nitrophenyl)carbamate (12b): 48 h, rt; **^{1}H NMR** (300.14 MHz, $CDCl_3$): *δ* 8.19 (d, *J* = 9.0 Hz, 2H), 7.55 (d, *J* = 9.2 Hz, 2H), 7.00 (s, 1H), 4.27 (q, *J* = 7.1 Hz, 2H), 1.33 (t, *J* = 7.1 Hz, 3H); **^{13}C NMR** (125.71 MHz, $CDCl_3$): *δ* 152.86, 144.04, 143.05, 125.29, 117.76, 62.18, 14.66; **MS (GC-MS):** *m/z* 210 $[M^+]$[223]; 82% yield.

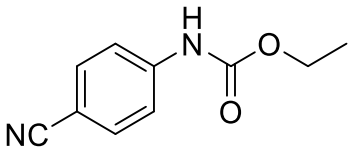

Ethyl (4-cyanophenyl)carbamate (13b): 39 h, 50 °C; **^{1}H NMR** (500 MHz, $CDCl_3$): *δ* 8.19 (d, *J* = 9.0 Hz, 2H), 7.55 (d, *J* = 9.2 Hz, 2H), 7.00 (s, 1H), 4.27 (q, *J* = 7.1 Hz, 2H), 1.33 (t, *J* = 7.1 Hz, 3H); **^{13}C NMR** (125.71 MHz, $CDCl_3$): *δ* 152.86, 144.04, 143.05, 125.29, 117.76, 62.18, 14.66; **MS (GC-MS**): *m/z* 190 $[M^+]$[224]; 82% yield.

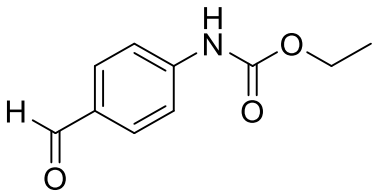

Ethyl (4-formylphenyl)carbamate (14b): 16 h, rt; **^{1}H NMR** (300.54 MHz, $CDCl_3$): *δ* 10.57 (s, 1H), 9.91 (s, 1H), 8.47 (d, *J* = 8.0 Hz, 1H), 7.76 – 7.48 (m, 2H), 7.22 – 7.10 (m, 1H), 4.25 (q, *J* = 7.1 Hz, 2H), 1.34 (t, *J* = 7.1 Hz, 3H); **^{13}C NMR** (75.58 MHz, $CDCl_3$): *δ* 195.21, 153.88, 141.53, 136.18, 121.98, 121.43, 118.44, 61.56, 14.63; **MS (GC-MS):** *m/z* 193 $[M^+]$[225]; 81% yield.

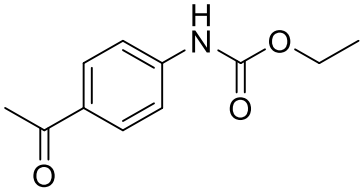

Ethyl (4-acetylphenyl)carbamate (15b): 39 h, 50 °C; **^{1}H NMR** (300.14 MHz, DMSO-d_6): *δ* 9.97 (s, 1H), 7.89 (d, *J* = 8.7 Hz, 2H), 7.59 (d, *J* = 8.6 Hz, 2H), 4.16 (q, *J* = 7.1 Hz, 2H), 2.50 (s, 2H), 1.26 (t, *J* = 7.1 Hz, 2H); **^{13}C NMR** (126 MHz, DMSO-d_6): *δ* 196.31, 153.31, 143.76, 130.96, 129.45, 117.24, 60.50, 26.25, 14.37; **MS (GC-MS)**: *m/z* 207 $[M^+]$[226]; 90% yield.

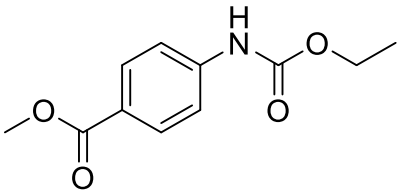

Methyl 4-((ethoxycarbonyl)amino)benzoate (16b): 39 h, 50 °C; **^{1}H NMR** (500 MHz, DMSO-d_6): *δ* 9.99 (s, 1H), 7.92 – 7.84 (m, 2H), 7.64 – 7.56 (m, 2H), 4.15 (q, *J* = 7.1 Hz, 2H), 3.80 (s, 3H), 1.25 (t, *J* = 7.1 Hz, 3H); **^{13}C NMR** (125.71 MHz, DMSO-d_6): *δ* 165.84, 153.31, 143.82, 130.24, 123.08, 117.37, 60.49, 51.69, 14.35; **MS (GC-MS)**: *m/z* 223 $[M^+]$[227]; 73% yield.

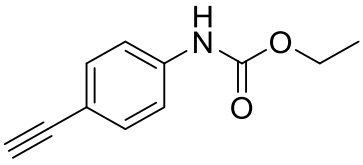

Ethyl (4-ethynylphenyl)carbamate (17b): 16 h, 50 °C; **^{1}H NMR** (300.14 MHz, $CDCl_3$): *δ* 7.45 – 7.38 (m, 2H), 7.39 – 7.31 (m, 2H), 6.84 (s, 1H), 4.22 (q, *J* = 7.1 Hz, 2H), 3.03 (s, 1H), 1.30 (t, *J* = 7.1 Hz, 3H); **^{13}C NMR** (125.71 MHz, $CDCl_3$): *δ* 153.17, 138.38,

134.05, 132.86, 118.05, 116.59, 83.39, 61.41, 14.54; **MS (GC-MS)**: *m/z* 189 [M^+][224]; 79% yield.

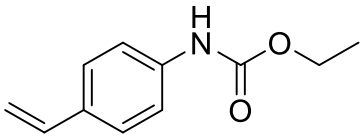

Ethyl (4-vinylphenyl)carbamate (18b): 16 h, rt; **^{1}H NMR** (300.53 MHz, $CDCl_3$): *δ* 7.35 (s, 4H), 6.75 – 6.54 (m, 2H), 5.66 (d, *J* = 17.6, 1H), 5.17 (d, *J* = 10.9, 1H), 4.23 (q, *J* = 7.1 Hz, 2H), 1.31 (t, *J* = 7.1 Hz, 3H); **^{13}C NMR** (75.58 MHz, $CDCl_3$) *δ* 153.61, 137.65, 136.25, 132.98, 127.04, 118.69, 112.75, 61.41, 14.69; **MS (GC-MS)**: *m/z* 191 [M^+][228]; 73% yield.

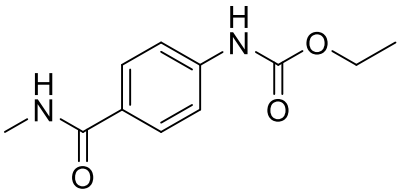

Ethyl (4-(methylcarbamoyl)phenyl)carbamate (19b): 16 h, rt; ^{1}H NMR (300.14 MHz, DMSO-d_6): *δ* 9.80 (s, 1H), 8.21 (d, *J* = 4.7 Hz, 1H), 7.75 (d, *J* = 8.7 Hz, 2H), 7.51 (d, *J* = 8.7 Hz, 2H), 4.14 (q, *J* = 7.1 Hz, 2H), 2.76 (d, *J* = 4.5 Hz, 3H), 1.25 (t, *J* = 7.1 Hz, 3H); **^{13}C NMR** (126 MHz, DMSO-d_6): *δ* 165.87, 153.14, 141.48, 128.07, 127.63, 117.02, 60.21, 26.05, 14.39; **MS (GC-MS)**: *m/z* 222 [M^+]; **MS (ESI-HRMS):** *m/z* calcd. for $C_{11}H_{14}N_2O_3$ [$M+H^+$]: 223.1077, found: 223.1079; 89% yield.

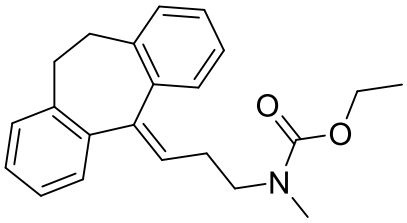

Ethyl(3-(10,11-dihydro-5H-dibenzo[*a,d*][7]annulen-5-ylidene)propyl)(methyl)carbamate (42b): 16 h, rt; **^{1}H NMR** (300.14 MHz, $CDCl_3$): *δ* 7.34 – 6.98 (m, 8H), 5.81 (t, *J* = 7.2 Hz, 1H), 4.21 – 3.93 (m, 2H), 3.39 – 3.22 (m, 4H), 2.77 (d, *J* = 15.6 Hz, 4H), 2.34 (s, 3H), 1.32 – 1.02 (m, 3H); **^{13}C NMR** (100.62 MHz, $CDCl_3$): *δ* 156.56, 141.15, 139.51, 137.12, 130.13, 128.14, 127.60, 127.22, 126.12, 125.83, 61.24, 48.62, 33.86, 32.07, 14.75; **MS (GC-MS):** *m/z* 335 [M^+][229]; 86% yield.

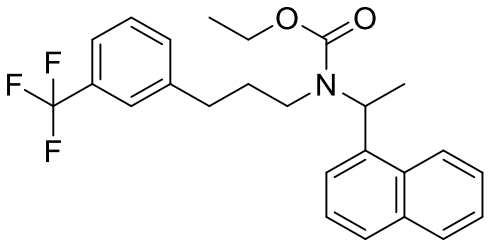

Ethyl (1-(naphthalen-1-yl)ethyl)(3-(3-(trifluoromethyl)phenyl)propyl)carbamate (43b): 16 h, rt; **^{1}H NMR** (400.13 MHz, $CDCl_3$): *δ* 8.15 (s, 1H), 7.91 – 7.78 (m, 2H), 7.58 – 7.47 (m, 2H), 7.47 – 7.32 (m, 3H), 7.23 (t, *J* = 7.7 Hz, 1H), 6.92 (s, 1H), 6.85 (d, *J* = 7.7 Hz, 1H), 6.32 – 6.07 (m, 1H), 4.45 – 4.20 (m, 1H), 3.14 – 3.02 (m, 2H), 2.80 (t, *J* = 11.8 Hz, 2H), 2.16 (t, *J* = 7.4 Hz, 2H), 1.63 (d, *J* = 6.9 Hz, 3H), 1.52 – 1.35 (m, 1H), 1.27 (t, *J* = 7.1 Hz, 3H); **^{13}C NMR** (100.62 MHz, $CDCl_3$): *δ* 156.35, 142.54, 136.25, 133.79, 132.42, 131.57, 128.85, 128.58, 126.79, 126.03, 125.67, 125.03, 124.84, 124.39, 124.02, 122.61, 61.51, 50.15, 41.69, 33.04, 30.68, 21.16, 17.17, 14.89, 14.32; **MS (GC-MS):** *m/z* 429 [M^+]; **HR MS (ESI-HRMS)MS:** *m/z* calcd. for $C_{25}H_{26}F_3NO_2$ [$M+H^+$]: 430.1988, found: 430.1980; 82% yield.

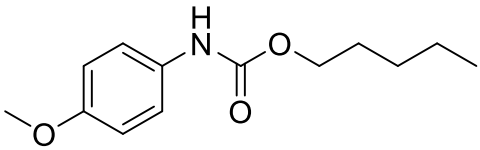

Pentyl (4-methoxyphenyl)carbamate (44b): 16 h, rt; **^{1}H NMR** (400.13 MHz, $CDCl_3$): *δ* 7.28 (d, *J* = 8.3 Hz, 2H), 6.90 – 6.80 (m, 2H), 6.46 (s, 1H), 4.14 (t, *J* = 6.7 Hz, 2H), 3.78 (s, 3H), 1.72 – 1.59 (m, 2H), 1.42 – 1.30 (m, 4H), 0.99 – 0.85 (m, 3H); **^{13}C NMR** (100.62 MHz, $CDCl_3$): *δ* 156.06, 154.23, 131.19, 120.77, 114.39, 65.47, 55.65, 28.81, 28.17, 22.50, 14.13; **MS (GC-MS):** *m/z* 237 [M^+][230]; 83% yield.

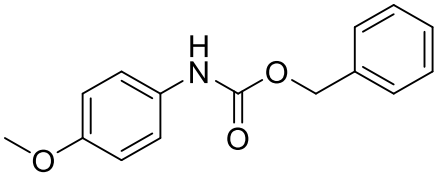

Benzyl (4-methoxyphenyl)carbamate (45b): 16 h, rt; **^{1}H NMR** (400.13 MHz, $CDCl_3$): *δ* 7.43 – 7.33 (m, 5H), 7.29 (d, *J* = 7.8 Hz, 2H), 6.88 – 6.83 (m, 2H), 6.58 (s, 1H), 5.19 (s, 2H), 3.78 (s, 3H); **^{13}C NMR** (100.62 MHz, $CDCl_3$): *δ* 156.19, 153.82, 136.32, 130.95, 128.73, 128.43, 120.77, 114.40, 67.07, 55.64, 29.84; **MS (GC-MS):** *m/z* 257 [M^+][231]; 75% yield.

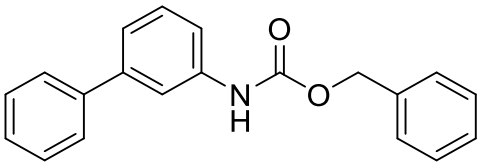

***N*-([1,1'-Biphenyl]-3-yl)-2-phenylacetamide (46b):** 48 h, 50 °C; **^{1}H NMR** (300.54 MHz, $CDCl_3$): *δ* 7.69 – 7.27 (m, 14H), 6.81 (s, 1H), 5.23 (s, 2H); **^{13}C NMR** (75.56 MHz, $CDCl_3$): *δ* 153.49, 142.34, 140.81, 138.32, 136.13, 129.55, 128.86, 128.76, 128.51, 128.45, 127.29, 122.50, 117.66, 67.21; **MS (ESI):** *m/z* 304.1 [M+H$^+$]; **MS (ESI-HRMS):** *m/z* calcd. for $C_{20}H_{17}NO_2$ [M+Na$^+$]: 326.1151, found: 326.1147; 69% yield.

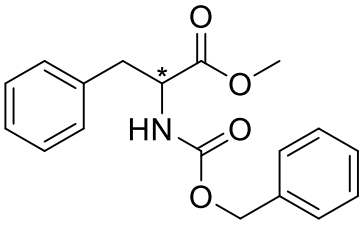

Methyl ((benzyloxy)carbonyl)-phenylalaninate (47b): 48 h, 40 °C; **^{1}H NMR** (300.14 MHz, $CDCl_3$): *δ* 7.42 – 7.15 (m, 10H), 7.01 (d, *J* = 9.4 Hz, 1H), 5.20 – 5.07 (m, 2H), 4.82 – 4.60 (m, 1H), 3.12 (dd, *J* = 5.7, 2.8 Hz, 2H), 2.18 (s, 3H); **^{13}C NMR** (125.71 MHz, $CDCl_3$): *δ* 171.94, 155.63, 136.32, 135.74, 129.32, 128.58, 128.24, 128.14, 127.20, 67.13, 54.99, 52.48, 38.46, 31.12. **MS (ESI):** *m/z* 336.1 [M+Na$^+$]; **MS (ESI-HRMS):** *m/z* calcd. for $C_{18}H_{19}NO_4$ [M+Na$^+$]: 336.1206, found: 336.1210; 70% yield.

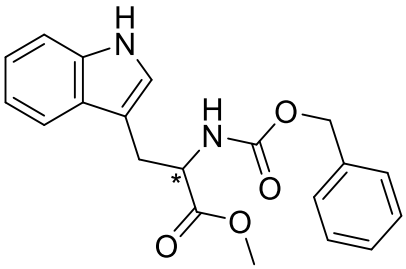

Methyl ((benzyloxy)carbonyl)-tryptophanate (48b): 48 h, 40 °C; **^{1}H NMR** (300.54 MHz, $CDCl_3$): *δ* 8.24 (s, 1H), 7.62 – 7.03 (m, 9H), 6.92 (d, *J* = 2.4 Hz, 1H), 5.39 (d, *J* = 8.2 Hz, 1H), 5.18 – 5.06 (m, 2H), 4.81 – 4.67 (m, 1H), 3.68 (s, 3H), 3.32 (d, *J* = 5.5 Hz, 2H); **^{13}C NMR** (75.58 MHz, $CDCl_3$): *δ* 172.38, 155.75, 136.18, 136.05, 128.42, 128.07, 128.02, 127.41, 122.81, 122.10, 119.54, 118.46, 111.21, 109.61, 66.86, 54.45, 52.28, 27.84; **MS (ESI):** *m/z* 375.1 [M+Na$^+$]; **MS (ESI-HRMS):** *m/z* calcd. for $C_{20}H_{20}N_2O_4$ [M+Na$^+$]: 375.1315, found: 375.1322; 76% yield.

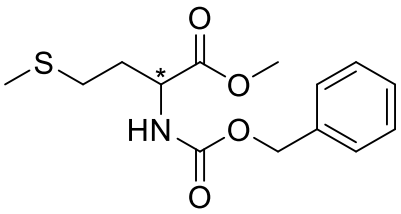

Methyl ((benzyloxy)carbonyl)-methioninate (49b): 16 h, rt; **^{1}H NMR** (300.14 MHz, $CDCl_3$): *δ* 7.46 – 7.22 (m, 5H), 5.48 (d, *J* = 8.2 Hz, 1H), 5.11 (s, 2H), 4.57 – 4.43 (m, 1H), 3.74 (s, 3H), 2.52 (t, *J* = 7.6 Hz, 2H), 2.08 (s, 3H), 2.07 – 1.87 (m, 2H); **^{13}C NMR** (125.71 MHz, $CDCl_3$): *δ* 172.38, 155.85, 136.19, 128.54, 128.22, 128.12, 67.18, 53.28, 52.63, 32.14, 30.05, 15.63; **MS (ESI):** *m/z* 320.1 [M+Na$^+$]; **MS (ESI-HRMS):** *m/z* calcd. for $C_{14}H_{19}NO_4S$ [M+Na$^+$]: 320.0927, found: 336.0928; 90% yield.

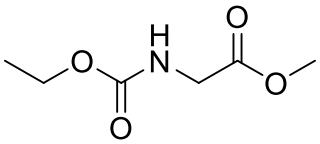

Methyl (ethoxycarbonyl)glycinate (50b): 16 h, rt; **^{1}H NMR** (400.13 MHz, $CDCl_3$): *δ* 5.24 (s, 1H), 4.12 (q, *J* = 7.1 Hz, 2H), 3.95 (d, *J* = 5.9 Hz, 2H), 3.74 (s, 3H), 1.23 (t, *J* = 7.1 Hz, 3H); **^{13}C NMR** (100.62 MHz, $CDCl_3$): *δ* 170.78, 156.68, 61.42, 52.42, 42.67, 14.64; **MS (GC-MS):** *m/z* 161 [M$^+$][232]; 67% yield.

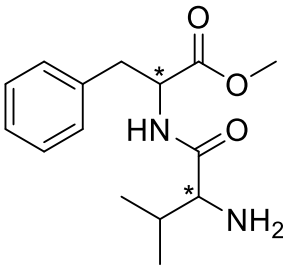

Methyl-valyl-phenylalaninate (51a): **^{1}H NMR** (300.14 MHz, DMSO-d_6): *δ* 8.47 (d, *J* = 7.7 Hz, 1H), 7.34 – 7.08 (m, 5H), 5.10 (s, 2H), 4.62 – 4.39 (m, 1H), 3.60 (s, 3H), 3.26 (d, *J* = 5.0 Hz, 1H), 3.16 – 2.84 (m, 2H), 2.06 – 1.87 (m, 1H), 0.88 (d, *J* = 6.9 Hz, 3H), 0.78 (d, *J* = 6.8 Hz, 3H); **MS (ESI):** *m/z* 279.1 [M+H$^+$]; **MS (ESI-HRMS):** *m/z* calcd. for $C_{15}H_{22}N_2O_3$ [M+H$^+$]: 279.1703, found: 279.1704; 50% yield.

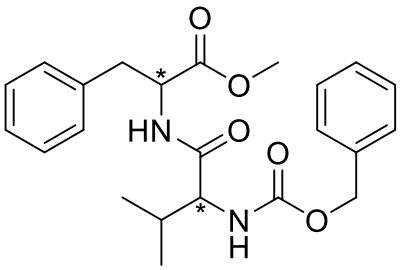

Methyl ((benzyloxy)carbonyl)-valyl-phenylalaninate (51b): 24 h, 40 °C; **^{1}H NMR** (300.14 MHz, $CDCl_3$): *δ* 7.54 – 7.01 (m, 10H), 6.49 (d, *J* = 7.8 Hz, 1H), 5.43 (d, *J* = 9.0 Hz, 1H), 5.12 (d, *J* = 5.8 Hz, 2H), 4.98 – 4.84 (m, 1H), 4.16 – 4.01 (m, 1H), 3.73 (s, 3H), 3.18 – 3.08 (m, 2H), 2.10 (h, *J* = 6.7 Hz, 1H), 0.93 (dd, *J* = 16.6, 6.8 Hz, 6H). **^{13}C NMR** (125.71 MHz, $CDCl_3$): *δ* 171.65, 170.84, 156.29, 136.32, 135.64, 129.25, 128.65, 128.56, 128.19, 128.04, 127.21, 67.15, 60.38, 53.27, 52.45, 38.11, 31.31, 19.28, 17.91; **MS (ESI):** *m/z* 413.2 [M+H$^+$]; **MS (ESI-HRMS):** *m/z* calcd. for $C_{23}H_{28}N_2O_5$ [M+H$^+$]: 413.2071, found: 413:2071; 70% yield.

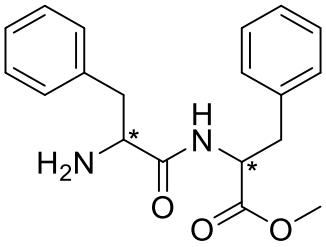

Methyl-phenylalanyl-phenylalaninate (52a): **^{1}H NMR** (300.14 MHz, DMSO-d_6): *δ* 8.35 – 8.19 (m, 1H), 7.42 – 6.94 (m, 10H), 4.67 – 4.44 (m, 1H), 3.60 (s, 3H), 3.54 – 3.40 (m, 1H), 3.28 (s, 2H), 3.03 – 2.91 (m, 2H), 2.66 – 2.53 (m, 2H); **MS (ESI):** *m/z* 327.2 [M+H$^+$]; **MS (ESI-HRMS):** *m/z* calcd. for $C_{19}H_{22}N_2O_3$ [M+H$^+$]: 327.1703, found: 327.1703; 56% yield.

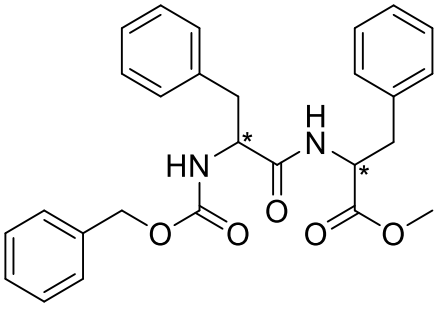

Methyl ((benzyloxy)carbonyl)-phenylalanyl-phenylalaninate (52b): 24 h, 40 °C; **^{1}H NMR** (400.13 MHz, $CDCl_3$): *δ* 7.40 – 6.89 (m, 15H), 6.29 (d, *J* = 6.5 Hz, 1H), 5.30 (d, *J* = 6.2 Hz, 1H), 5.07 (s, 2H), 4.84 – 4.74 (m, 1H), 4.42 (d, *J* = 6.9 Hz, 1H), 3.67 (s, 3H), 3.11 – 2.93 (m, 4H); **^{13}C NMR** (100.62 MHz, $CDCl_3$): *δ* 171.42, 170.47, 155.96, 136.34, 135.67, 129.46, 129.36, 129.30, 128.81, 128.65, 128.31, 128.12, 127.24,

127.16, 67.19, 56.14, 53.43, 52.41, 38.44, 38.02, 29.82; **MS (ESI):** *m/z* 461.2 [M+H$^+$]; **MS (ESI-HRMS):** *m/z* calcd. for $C_{27}H_{28}N_2O_5$ [M+H$^+$]: 461.2071, found: 461:2069; 78% yield.

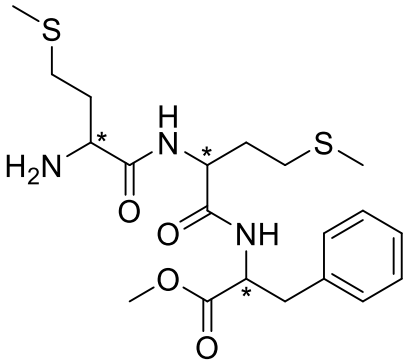

Methyl-methionyl-methionyl-phenylalaninate (53a): ^{1}H NMR (300.14 MHz, DMSO-d_6): δ 8.41 (d, *J* = 7.5 Hz, 1H), 8.17 (s, 1H), 7.31 – 7.14 (m, 5H), 4.56 – 4.34 (m, 2H), 3.91 – 3.71 (m, 2H), 3.59 (s, 3H), 3.47 – 3.31 (m, 1H), 3.12 – 2.88 (m, 2H), 2.49 – 2.45 (m, 1H), 2.44 – 2.33 (m, 2H), 2.02 (s, 3H), 2.01 (s, 3H), 1.90 – 1.60 (m, 2H), 0.94 – 0.61 (m, 1H); **MS (ESI):** *m/z* 442.2 [M+H$^+$]; **MS (ESI-HRMS):** *m/z* calcd. for $C_{20}H_{31}N_3O_4S_2$ [M+H$^+$]: 442.1829, found: 442.1825; 49% yield

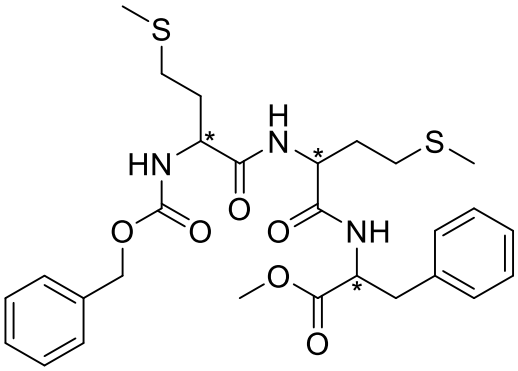

Methyl ((benzyloxy)carbonyl)-methionyl-methionyl-phenylalaninate (53b): 48 h, 40 °C; **^{1}H NMR** (300.14 MHz, $CDCl_3$): δ 7.39 – 7.10 (m, 10H), 7.08 (d, *J* = 1.5 Hz, 1H), 6.95 (d, *J* = 8.1 Hz, 1H), 5.81 (d, *J* = 8.2 Hz, 1H), 5.17 – 4.99 (m, 2H), 4.90 – 4.77 (m, 1H), 4.64 (q, *J* = 6.9 Hz, 1H), 4.40 (q, *J* = 7.3 Hz, 1H), 3.69 (s, 3H), 3.08 (t, *J* = 6.0 Hz, 2H), 2.57 – 2.44 (m, 4H), 2.05 (s, 3H), 2.01 (s, 3H), 1.99 – 1.86 (m, 4H); **^{13}C NMR** (125.71 MHz, $CDCl_3$): δ 171.54, 171.12, 170.41, 156.13, 136.16, 135.69, 129.21, 128.67, 128.56, 128.23, 128.09, 127.22, 67.25, 54.06, 53.50, 52.47, 52.28, 37.94, 31.95, 31.49, 30.25, 30.06, 15.46, 15.19; **MS (ESI):** *m/z* 576.2 [M+H$^+$]; **MS (ESI-HRMS):** *m/z* calcd. for $C_{28}H_{37}N_3O_6S_2$ [M+H$^+$]: 576.2197, found: 576.2191; 62% yield.

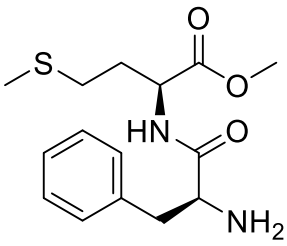

Methyl *L*-phenylalanyl-*L*-methioninate (54a): **^{1}H NMR** (300.14 MHz, DMSO-d_6): δ 8.35 (d, J = 7.8 Hz, 1H), 8.19 – 8.02 (m, 2H), 7.35 – 7.12 (m, 5H), 4.48 – 4.17 (m, 1H), 3.82 – 3.65 (m, 1H), 3.63 (s, 3H), 3.20 – 2.67 (m, 2H), 2.50 – 2.33 (m, 2H), 2.03 (s, 3H), 1.92 – 1.84 (m, 2H); **MS (ESI):** *m/z* 311.1 [M+H$^+$]; **MS (ESI-HRMS):** *m/z* calcd. for $C_{15}H_{22}N_2O_3S$ [M+H$^+$]: 311.1424, found: 311.1425; 52% yield.

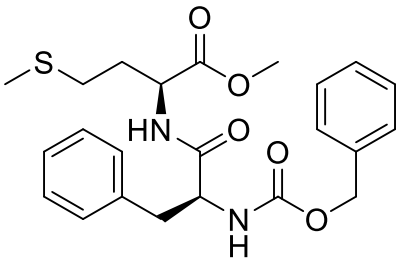

Methyl ((benzyloxy)carbonyl)-*L*-phenylalanyl-*L*-methioninate (54b): 48 h, 40 °C; **^{1}H NMR** (300.14 MHz, $CDCl_3$): δ 7.41 – 7.14 (m, 10H), 6.57 (d, J = 7.7 Hz, 1H), 5.37 (d, J = 8.1 Hz, 1H), 5.08 (s, 2H), 4.70 – 4.57 (m, 1H), 4.46 (q, J = 7.2 Hz, 1H), 3.71 (s, 3H), 3.19 – 2.98 (m, 2H), 2.39 (t, J = 7.7 Hz, 2H), 2.03 (s, 3H), 2.03 – 1.82 (m, 2H); **^{13}C NMR** (125.71 MHz, $CDCl_3$) δ 171.68, 170.67, 155.90, 136.19, 129.36, 128.75, 128.57, 128.25, 128.07, 127.12, 67.27, 56.31, 52.65, 51.78, 38.47, 31.65, 29.94, 15.60, 1.24; **MS (ESI):** *m/z* 467.1 [M+Na$^+$]; **MS (ESI-HRMS):** *m/z* calcd. for $C_{23}H_{28}N_2O_5S$ [M+Na$^+$]: 467.1611, found: 467.1612; 45% yield.

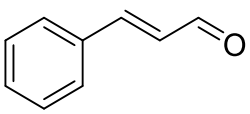

Cinnamaldehyde (55b): **^{1}H NMR** (300 MHz, $CDCl_3$): δ 9.52 (d, J = 7.7 Hz, 1H), 7.44 – 7.35 (m, 2H), 7.31 (s, 1H), 7.28 – 7.24 (m, 3H); 6.53 (dd, J = 16.0, 7.7 Hz, 1H); **^{13}C NMR** (75 MHz, $CDCl_3$): δ 193.56, 152.66, 133.99, 131.22, 129.06, 128.53, 128.46; **MS (GC-MS):** *m/z* 132 [M$^+$][233]; 90% yield.

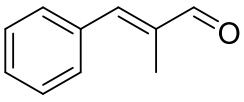

2-Methyl-3-phenylacrylaldehyde (56b): **^{1}H NMR** (300 MHz, $CDCl_3$): δ 9.59 (s, 1H), 7.59 – 7.35 (m, 5H), 7.26 (s, 1H), 2.07 (t, J = 1.6 Hz, 3H); **^{13}C NMR** (75 MHz, $CDCl_3$):

δ 195.62, 149.88, 138.49, 135.26, 130.13, 129.67, 128.82, 11.06; **MS (GC-MS):** *m/z* 146 [M^+][234]; 92% yield.

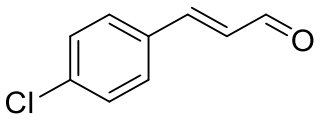

4-Chlorocinnamaldehyde (57b): 1 eq K_3PO_4; **^{1}H NMR** (300 MHz, $CDCl_3$): *δ* 9.71 (d, *J* = 7.6 Hz, 1H), 7.54 – 7.34 (m, 4H), 6.72 (d, *J* = 7.6 Hz, 1H), 6.66 (d, *J* = 7.6 Hz, 1H); **^{13}C NMR** (75 MHz, $CDCl_3$): *δ* 197.11, 139.32, 135.68, 131.47, 128.93; **MS (GC-MS):** *m/z* 166 [M^+][235]; 72% yield.

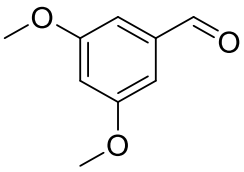

3,5-Dimethoxybenzaldehyde (58b): ^{1}H NMR (300 MHz, $CDCl_3$): *δ* 9.91 (s, 1H), 7.01 (d, *J* = 2.4 Hz, 2H), 6.71 (t, *J* = 2.3 Hz, 1H), 3.85 (s, 6H); **^{13}C NMR** (75 MHz, $CDCl_3$): *δ* 192.05, 161.41, 138.57, 107.34, 107.28, 55.79; **MS (GC-MS):** *m/z* 166 [M^+][236]; 89% yield.

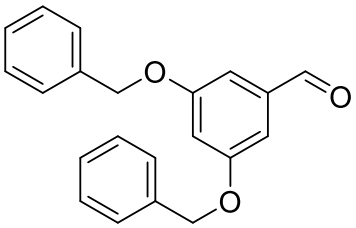

3,5-Bis(benzyloxy)benzaldehyde (59b): ^{1}H NMR (300 MHz, $CDCl_3$): *δ* 9.90 (s, 1H), 7.50 – 7.33 (m, 10H), 7.11 (d, *J* = 2.3 Hz, 2H), 6.87 (s, 1H), 5.10 (s, 4H); **^{13}C NMR** (75 MHz, $CDCl_3$): *δ* 191.94, 160.65, 160.55, 136.38, 128.84, 128.38, 127.71, 108.86, 108.48, 70.56; **MS (GC-MS):** *m/z* 318 [M^+][237]; 95% yield.

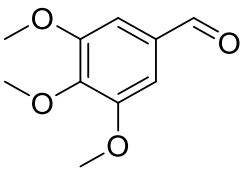

3,4,5-Trimethoxybenzaldehyde (60b): ^{1}H NMR (300 MHz, $CDCl_3$): *δ* 9.85 (s, 1H), 7.11 (s, 2H), 3.92 (s, 3H), 3.91 (s, 6H); **^{13}C NMR** (75 MHz, $CDCl_3$): *δ* 191.12, 153.74, 143.72, 131.81, 106.83, 61.08, 56.37; **MS (GC-MS):** *m/z* 196 [M^+][238]; 84% yield.

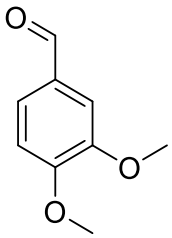

3,4-Dimethoxybenzaldehyde (61b): ^{1}H NMR (300 MHz, $CDCl_3$): *δ* 9.81 (s, 1H), 7.41 (dd, *J* = 8.2, 1.9 Hz, 1H), 7.36 (d, *J* = 1.9 Hz, 1H), 6.94 (d, *J* = 8.2 Hz, 1H), 3.92 (s, 3H), 3.90 (s, 3H); **^{13}C NMR** (75 MHz, $CDCl_3$): *δ* 190.86, 154.50, 149.64, 130.16, 126.83, 110.44, 108.99, 56.18, 56.01; **MS (GC-MS):** *m/z* 166 $[M^+]$[239]; 90% yield.

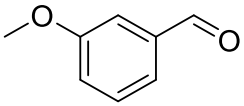

3-Methoxybenzaldehyde (62b): ^{1}H NMR (300 MHz, $CDCl_3$): *δ* 9.97 (s, 1H), 7.53 – 7.34 (m, 3H), 7.25 – 7.08 (m, 1H), 3.86 (s, 3H); **^{13}C NMR** (75 MHz, $CDCl_3$): *δ* 192.21, 160.28, 137.94, 130.14, 123.63, 121.62, 112.19, 55.59; **MS (GC-MS):** *m/z* 136 $[M^+]$[240]; 60% yield.

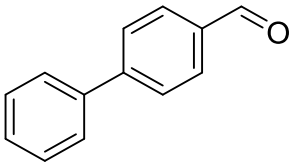

4-Biphenylmethanal (63b): ^{1}H NMR (300 MHz, $CDCl_3$): *δ* 10.07 (s, 1H), 8.00 – 7.91 (m, 2H), 7.80 – 7.74 (m, 2H), 7.68 – 7.62 (m, 2H), 7.54 – 7.40 (m, 3H); **^{13}C NMR** (75 MHz, $CDCl_3$): *δ* 192.06, 147.36, 139.88, 135.36, 130.42, 129.16, 128.62, 127.84, 127.52; **MS (GC-MS):** *m/z* 182 $[M^+]$[241]; 68% yield.

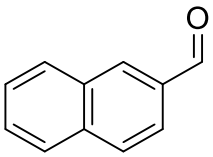

2-Naphthaldehyde (64b): ^{1}H NMR (300 MHz, $CDCl_3$): *δ* 10.16 (s, 1H), 8.34 (d, *J* = 1.1 Hz, 1H), 8.06 – 7.85 (m, 4H), 7.70 – 7.53 (m, 2H); **^{13}C NMR** (75 MHz, $CDCl_3$): *δ* 192.32, 136.59, 134.62, 134.28, 132.79, 129.65, 129.23, 128.21, 127.21, 122.92; **MS (GC-MS):** *m/z* 156 $[M^+]$[242]; 61% yield.

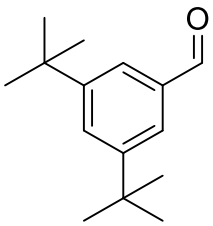

3,5-Di-*tert*-butylbenzaldehyde (65b): ^{1}H NMR (300 MHz, $CDCl_3$): *δ* 10.01 (s, 1H), 7.78 – 7.69 (m, 3H), 1.37 (s, 18H); **^{13}C NMR** (75 MHz, $CDCl_3$): *δ* 193.31, 151.99, 136.37, 129.02, 124.28, 35.12, 31.47; **MS (GC-MS):** *m/z* 218 $[M^+]$[243]; 63% yield.

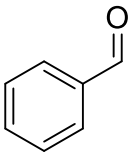

Benzaldehyde (66b): ^{1}H NMR (300 MHz, $CDCl_3$): *δ* 10.00 (s, 1H), 7.91 – 7.83 (m, 2H), 7.67 – 7.59 (m, 1H), 7.55 – 7.46 (m, 2H); **^{13}C NMR** (75 MHz, $CDCl_3$): *δ* 192.46, 136.48, 134.52, 129.79, 129.06; **MS (GC-MS):** *m/z* 106 $[M^+]$[244]; 65% yield.

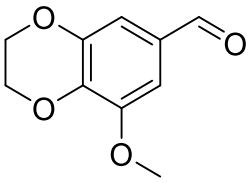

8-Methoxy-2,3-dihydrobenzo[*b*][1,4]dioxine-6-carbaldehyde (67b): ^{1}H NMR (300 MHz, $CDCl_3$): *δ* 9.97 (s, 1H), 7.44 (s, 2H), 4.61 – 4.48 (m, 4H), 4.13 (s, 3H); **^{13}C NMR** (75 MHz, $CDCl_3$): *δ* 190.91, 120.15, 114.69, 103.28, 65.07, 64.13, 56.48, 29.87, 29.87, 29.71; **MS (GC-MS):** *m/z* 194 $[M^+]$[245]; 65% yield.

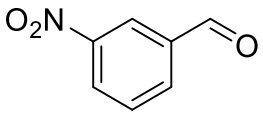

3-Nitrobenzaldehyde (68b): 1 eq K_3PO_4; **^{1}H NMR** (300 MHz, $CDCl_3$): *δ* 10.12 (d, *J* = 0.5 Hz, 1H), 8.71 (ddd, *J* = 2.1, 1.6, 0.5 Hz, 1H), 8.49 (ddd, *J* = 8.2, 2.3, 1.1 Hz, 1H), 8.23 (ddd, *J* = 7.6, 1.2 Hz, 1H), 7.83 – 7.71 (m, 1H); **^{13}C NMR** (75 MHz, $CDCl_3$): *δ* 189.83, 148.93, 137.53, 134.75, 130.51, 128.71, 124.60; **MS (GC-MS):** *m/z* 151 $[M^+]$[246]**;** 41% yield.

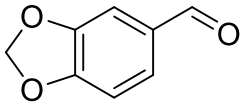

Benzo[*d*][1,3]dioxole-5-carbaldehyde (69b): ^{1}H NMR (300 MHz, Chloroform-d): *δ* 9.81 (s, 1H), 7.41 (dd, *J* = 7.9, 1.6 Hz, 1H), 7.34 (dd, *J* = 1.6, 0.4 Hz, 1H), 6.93 (dd,

J = 7.9, 0.4 Hz, 1H), 6.08 (s, 2H); **^{13}C NMR** (75 MHz, $CDCl_3$): *δ* 190.37, 153.25, 148.87, 132.08, 128.75, 108.50, 107.11, 102.24; **MS (GC-MS):** *m/z* 150 [M^+][247]; 26% yield.

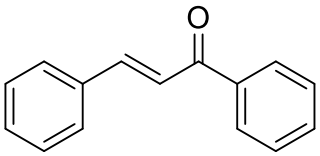

Chalcone (71b): ^{1}H NMR (300 MHz, $CDCl_3$): *δ* 8.00 – 7.92 (m, 2H), 7.74 (d, J = 15.7 Hz, 1H), 7.62 – 7.38 (m, 6H), 7.38 – 7.31 (m, 3H); **^{13}C NMR** (75 MHz, $CDCl_3$): *δ* 190.55, 144.84, 138.23, 134.91, 132.77, 130.54, 128.96, 128.63, 128.51, 128.45, 122.13; **MS (GC-MS):** *m/z* 208 [M^+][248]; 95% yield.

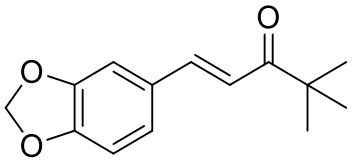

1-(Benzo[*d*][1,3]dioxol-5-yl)-4-methylpent-1-en-3-one (72b): ^{1}H NMR (300 MHz, $CDCl_3$): *δ* 7.64 – 7.54 (m, 1H), 7.12 – 7.03 (m, 2H), 6.96 (d, *J* = 15.5 Hz, 1H), 6.82 (d, *J* = 8.0 Hz, 1H), 6.01 (d, *J* = 0.4 Hz, 2H), 1.56 (s, 1H), 1.22 (d, *J* = 0.4 Hz, 6H); **^{13}C NMR** (75 MHz, $CDCl_3$): *δ* 204.32, 142.84, 129.55, 124.93, 120.14, 118.99, 118.96, 108.74, 106.75, 101.69, 43.33, 26.56; **MS (ESI-HRMS):** *m/z* calcd. for $C_{14}H_{16}O_3$ [$M+H^+$]: 233.1172, found: 233.1170; 67% yield.

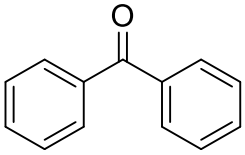

Benzophenone (73b): ^{1}H NMR (300 MHz, $CDCl_3$): *δ* 7.85 – 7.78 (m, 4H), 7.63 – 7.55 (m, 2H), 7.52 – 7.45 (m, 4H); **^{13}C NMR** (75 MHz, $CDCl_3$): *δ* 196.82, 137.75, 132.51, 130.16, 128.39; **MS (GC-MS):** *m/z* 182 [M^+][235]; 95% yield.

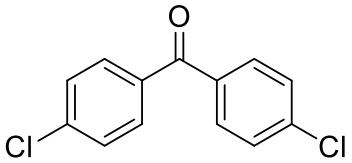

4,4'-Dichlorobenzophenone (74b): ^{1}H NMR (300 MHz, $CDCl_3$): *δ* 7.76 – 7.70 (m, 4H), 7.51 – 7.44 (m, 4H); **^{13}C NMR** (75 MHz, $CDCl_3$): *δ* 194.43, 139.32, 135.68, 131.47, 128.93; **MS (GC-MS):** *m/z* 250 [M^+][249]; 76% yield.

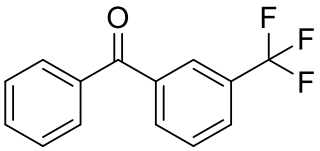

3-(trifluoromethyl)benzophenone (75b): **^{1}H NMR** (300 MHz, $CDCl_3$): δ 8.11 – 8.03 (m, 1H), 8.03 – 7.93 (m, 1H), 7.88 – 7.77 (m, 3H), 7.67 – 7.60 (m, 2H), 7.56 – 7.47 (m, 2H); **^{13}C NMR** (75 MHz, $CDCl_3$): δ 195.18, 138.28, 136.75, 133.10, 133.09, 132.99, 130.01, 128.93, 128.84, 128.55, 126.71; **MS (GC-MS):** *m/z* 250 $[M^+]^{[250]}$; 96% yield.

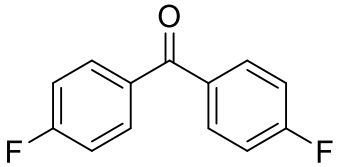

4,4'-Difluorobenzophenone (76b): **^{1}H NMR** (300 MHz, $CDCl_3$): δ 7.90 – 7.70 (m, 4H), 7.23 – 7.10 (m, 4H); **^{13}C NMR** (75 MHz, $CDCl_3$): δ 193.89, 167.21, 163.84, 133.86, 133.82, 132.67, 132.55, 115.83, 115.53; **MS (GC-MS):** *m/z* 218 $[M^+]^{[251]}$; 70% yield.

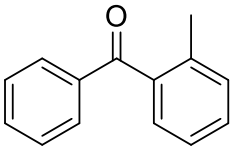

Phenyl(*o*-tolyl)methanone (77b): **^{1}H NMR** (300 MHz, $CDCl_3$): δ 7.80 – 7.71 (m, 2H), 7.58 – 7.49 (m, 1H), 7.49 – 7.14 (m, 6H), 2.29 (q, *J* = 0.5 Hz, 3H); **^{13}C NMR** (75 MHz, $CDCl_3$): δ 198.73, 138.75, 137.87, 136.85, 133.24, 131.11, 130.35, 130.24, 128.62, 128.57, 125.31, 20.10; **MS (GC-MS):** *m/z* 196 $[M^+]^{[252]}$; 70% yield.

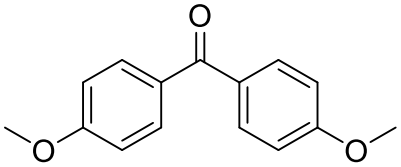

4,4'-Dimethoxybenzophenone (78b): **^{1}H NMR** (300 MHz, $CDCl_3$): δ 7.83 – 7.74 (m, 4H), 6.99 – 6.91 (m, 4H), 3.89 (s, 6H); **^{13}C NMR** (75 MHz, $CDCl_3$): δ 194.42, 162.83, 132.20, 130.78, 113.45, 55.45; **MS (GC-MS):** *m/z* 242 $[M^+]^{[251]}$; 62% yield.

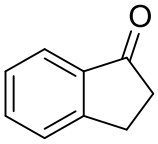

1-Indanone (79b): **^{1}H NMR** (300 MHz, $CDCl_3$): δ 7.81 – 7.70 (m, 1H), 7.64 – 7.57 (m, 1H), 7.53 – 7.42 (m, 1H), 7.43 – 7.33 (m, 1H), 3.29 – 3.07 (m, 2H), 2.78 – 2.62 (m,

2H); **^{13}C NMR** (75 MHz, $CDCl_3$): *δ* 207.16, 155.26, 137.21, 134.70, 127.39, 126.81, 123.83, 36.34, 25.93; **MS (GC-MS):** *m/z* 132 $[M^+]$[253]; 73% yield.

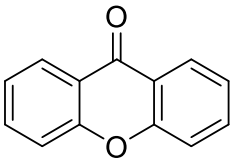

Xanthydrone (80b): ^{1}H NMR (300 MHz, $CDCl_3$): *δ* 8.34 (ddd, *J* = 8.0, 1.8, 0.5 Hz, 2H), 7.76 – 7.67 (m, 2H), 7.48 (ddd, *J* = 8.5, 1.1, 0.5 Hz, 2H), 7.37 (ddd, *J* = 8.1, 7.1, 1.1 Hz, 2H); **^{13}C NMR** (75 MHz, $CDCl_3$): *δ* 177.31, 156.29, 134.92, 126.85, 124.02, 121.98, 118.09; **MS (GC-MS):** *m/z* 196 $[M^+]$[254]; 97% yield.

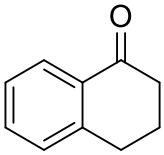

***α*-Tetralone (81b): ^{1}H NMR** (300 MHz, $CDCl_3$): *δ* 8.06 – 7.97 (m, 1H), 7.53 – 7.43 (m, 1H), 7.38 – 7.20 (m, 2H), 2.96 (t, *J* = 6.1 Hz, 2H), 2.71 – 2.59 (m, 2H), 2.21 – 2.08 (m, 2H); **^{13}C NMR** (75 MHz, $CDCl_3$): *δ* 198.40, 144.57, 133.46, 132.74, 128.86, 127.26, 126.71, 39.27, 29.81, 23.40; **MS (GC-MS):** *m/z* 146 $[M^+]$[255]; 58% yield.

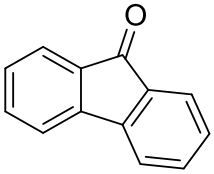

9-Fluorenone (82b): ^{1}H NMR (300 MHz, $CDCl_3$): *δ* 7.68 – 7.62 (m, 2H), 7.53 – 7.43 (m, 4H), 7.28 (ddd, *J* = 7.4, 6.8, 1.7 Hz, 2H); **^{13}C NMR** (75 MHz, $CDCl_3$): *δ* 194.00, 144.55, 134.79, 134.28, 129.19, 124.42, 120.42; **MS (GC-MS):** *m/z* 180 $[M^+]$[256]; 83% yield.

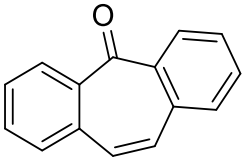

Dibenzosuberenone (83b): ^{1}H NMR (300 MHz, $CDCl_3$): *δ* 8.32 – 8.17 (m, 2H), 7.67 – 7.58 (m, 2H), 7.57 – 7.49 (m, 4H), 7.05 (s, 2H); **^{13}C NMR** (75 MHz, $CDCl_3$): *δ* 193.13, 138.79, 135.03, 132.04, 131.76, 130.86, 130.29, 128.95; **MS (GC-MS):** *m/z* 206 $[M^+]$[257]; 81% yield.

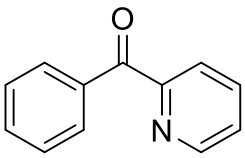

Phenyl(pyridine-2-yl)methanone (84b): **^{1}H NMR** (300 MHz, $CDCl_3$): *δ* 8.74 (ddd, *J* = 4.8, 1.7, 0.9 Hz, 1H), 8.09 – 8.02 (m, 3H), 7.91 (td, *J* = 7.7, 1.7 Hz, 1H), 7.63 – 7.56 (m, 1H), 7.53 – 7.45 (m, 3H); **^{13}C NMR** (75 MHz, $CDCl_3$): *δ* 194.02, 155.27, 148.70, 137.20, 136.43, 133.06, 131.13, 128.31, 126.29, 124.77; **MS (GC-MS):** *m/z* 183 $[M^+]$[258]; 95% yield.

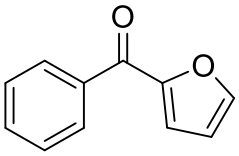

Phenyl(2-furyl)methanone (85b): ^{1}H NMR (300 MHz, $CDCl_3$): *δ* 7.95 – 7.88 (m, 2H), 7.64 (dd, *J* = 1.7, 0.7 Hz, 1H), 7.57 – 7.49 (m, 1H), 7.47 – 7.40 (m, 2H), 7.17 (dd, *J* = 3.6, 0.7 Hz, 1H), 6.53 (dd, *J* = 3.6, 1.7 Hz, 1H); **^{13}C NMR** (75 MHz, $CDCl_3$): *δ* 182.70, 152.50, 147.21, 137.44, 132.71, 129.44, 128.56, 120.65, 112.34; **MS (GC-MS):** *m/z* 172 $[M^+]$[259]; 95% yield.

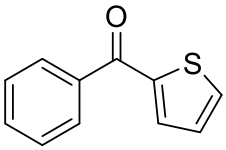

Phenyl(thiophen-2-yl)methanone (86b): **^{1}H NMR** (300 MHz, $CDCl_3$): *δ* 7.89 – 7.84 (m, 2H), 7.71 (dd, *J* = 5.0, 1.1 Hz, 1H), 7.64 (dd, *J* = 3.8, 1.1 Hz, 1H), 7.62 – 7.56 (m, 1H), 7.53 – 7.45 (m, 2H), 7.16 (dd, *J* = 5.0, 3.8 Hz, 1H); **^{13}C NMR** (75 MHz, $CDCl_3$): *δ* 188.29, 143.73, 138.25, 134.93, 134.29, 132.36, 129.25, 128.51, 128.06; **MS (GC-MS):** *m/z* 188 $[M^+]$[260]; 96% yield.

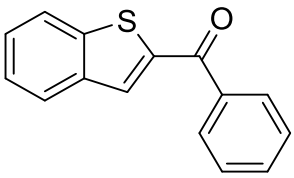

1 eq K_3PO_4; **Benzo[*b*]thiophen-2-yl(phenyl)methanone (87b):** **^{1}H NMR** (300 MHz, $CDCl_3$): *δ* 7.96 – 7.89 (m, 4H), 7.87 (dd, *J* = 2.6, 0.9 Hz, 1H), 7.67 – 7.60 (m, 1H), 7.57 – 7.39 (m, 4H); **^{13}C NMR** (75 MHz, $CDCl_3$): *δ* 189.77, 143.28, 142.88, 139.22, 138.04, 132.61, 132.33, 129.41, 128.67, 127.59, 126.20, 125.19, 123.07; **MS (GC-MS):** *m/z* 238 $[M^+]$[261]; 97% yield.

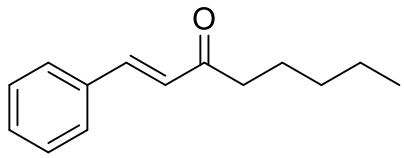

1-Phenyloct-1-en-3-one (88b): **^{1}H NMR** (600 MHz, $CDCl_3$): *δ* 7.59 – 7.53 (m, 3H), 7.42 – 7.37 (m, 3H), 6.74 (d, *J* = 16.2 Hz, 1H), 2.70 – 2.63 (m, 2H), 1.73 – 1.65 (m, 2H), 1.42 – 1.30 (m, 4H), 0.94 – 0.89 (m, 3H); **^{13}C NMR** (126 MHz, $CDCl_3$): *δ* 200.58, 142.30, 134.70, 130.40, 128.98, 128.29, 126.37, 41.14, 31.74, 24.31, 22.73, 14.18; **MS (GC-MS):** *m/z* 202 $[M^+]$[262]; 64% yield.

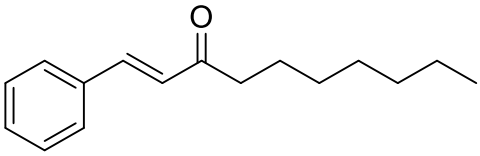

1-Phenyldec-1-en-3-one (89b): **^{1}H NMR** (600 MHz, $CDCl_3$): *δ* 7.64 – 7.51 (m, 3H), 7.40 (d, *J* = 4.2 Hz, 3H), 6.74 (d, *J* = 16.2 Hz, 1H), 2.71 – 2.60 (m, 2H), 1.68 (p, *J* = 7.4 Hz, 2H), 1.40 – 1.23 (m, 8H), 0.89 (d, *J* = 7.0 Hz, 3H); **^{13}C NMR** (126 MHz, $CDCl_3$): *δ* 200.63, 142.32, 134.73, 130.42, 129.00, 128.31, 126.40, 41.21, 31.93, 29.54, 29.34, 24.66, 22.86, 14.32; **MS (GC-MS):** *m/z* 202 $[M^+]$[263]; 90% yield.

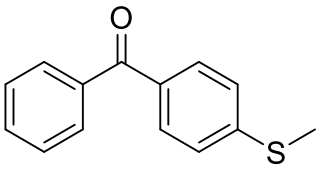

64 h, ***S*-Methyl-4-benzoylthiophenol (98b):** **^{1}H NMR** (300 MHz, $CDCl_3$): *δ* 7.81 – 7.71 (m, 4H), 7.64 – 7.54 (m, 1H), 7.53 – 7.43 (m, 2H), 7.36 – 7.27 (m, 2H), 2.54 (s, 3H); **^{13}C NMR** (75 MHz, $CDCl_3$): *δ* 195.77, 145.26, 137.87, 133.67, 132.16, 130.63, 129.81, 128.25, 124.86, 14.86; **MS (GC-MS):** *m/z* 228 $[M^+]$[264]; 73% yield.

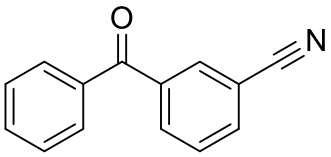

40 h, **3-Cyanobenzophenone (99b):** **^{1}H NMR** (300 MHz, $CDCl_3$): *δ* 8.20 – 8.00 (m, 2H), 7.90 – 7.73 (m, 3H), 7.68 – 7.57 (m, 2H), 7.56 – 7.49 (m, 2H); **^{13}C NMR** (75 MHz, $CDCl_3$): *δ* 194.36, 138.63, 135.32, 133.81, 133.26, 130.06, 129.98, 129.38, 128.66, 128.47, 117.91, 112.86; **MS (GC-MS):** *m/z* 207 $[M^+]$[265]; 84% yield.

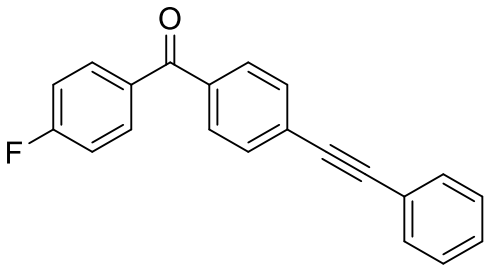

(4-Fluorophenyl)(4-(phenylethynyl)phenyl)methanone (100b): ^{1}H NMR (300 MHz, $CDCl_3$): *δ* 7.88 – 7.81 (m, 2H), 7.80 – 7.74 (m, 2H), 7.67 – 7.61 (m, 2H), 7.60 – 7.54 (m, 2H), 7.41 – 7.36 (m, 3H), 7.23 – 7.14 (m, 2H); **^{13}C NMR** (75 MHz, $CDCl_3$): *δ* 194.58, 167.27, 163.90, 136.79, 132.79, 131.91, 131.63, 130.05, 128.97, 128.60, 127.85, 122.81, 115.85, 92.73, 88.71; **MS (GC-MS):** *m/z* 300 $[M^+]$[266]; 93% yield.

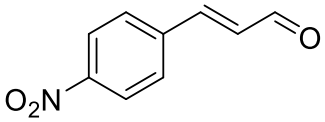

3-(4-Nitrophenyl)acrylaldehyde (101b): ^{1}H NMR (300 MHz, $CDCl_3$): *δ* 9.78 (d, *J* = 7.4 Hz, 1H), 8.33 – 8.23 (m, 2H), 7.77 – 7.68 (m, 2H), 7.53 (d, *J* = 16.1 Hz, 1H), 6.81 (dd, *J* = 16.1, 7.4 Hz, 1H); **^{13}C NMR** (75 MHz, $CDCl_3$): *δ* 192.88, 148.91, 140.07, 131.89, 129.17, 124.48; **MS (GC-MS):** *m/z* 177 $[M^+]$[267]; 81% yield.

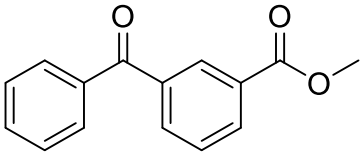

1 eq K_3PO_4; **Methyl 3-benzoylbenzoate (102b): ^{1}H NMR** (300 MHz, $CDCl_3$): *δ* 8.48 – 8.40 (m, 1H), 8.30 – 8.23 (m, 1H), 8.06 – 7.96 (m, 1H), 7.85 – 7.76 (m, 2H), 7.67 – 7.47 (m, 4H), 3.94 (s, 3H); **^{13}C NMR** (75 MHz, $CDCl_3$): *δ* 195.29, 166.45, 138.15, 137.24, 134.21, 133.34, 132.95, 131.13, 130.58, 130.21, 128.76, 128.64, 52.54; **MS (GC-MS):** *m/z* 240 $[M^+]$[268]; 73% yield.

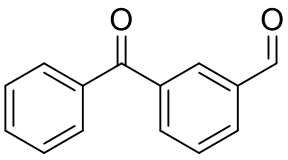

3-Formylbenzophenone (103b): ^{1}H NMR (300 MHz, $CDCl_3$): *δ* 10.09 (s, 1H), 8.30 – 8.24 (m, 1H), 8.16 – 8.05 (m, 2H), 7.84 – 7.78 (m, 2H), 7.73 – 7.59 (m, 2H), 7.56 – 7.47 (m, 2H); **^{13}C NMR** (75 MHz, $CDCl_3$): *δ* 195.60, 191.51, 138.70, 137.01, 136.53, 135.57, 133.13, 132.81, 131.47, 130.16, 129.40, 128.72; **MS (GC-MS):** *m/z* 210 $[M^+]$[269]; 63% yield.

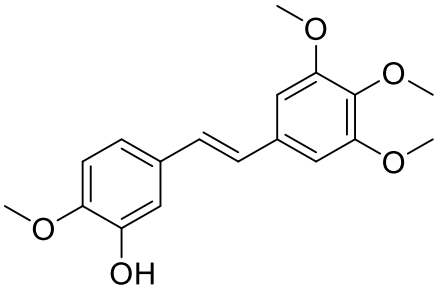

Combretastatin A4 (190b): ^{1}H NMR (300 MHz, $CDCl_3$): *δ* 7.14 (d, *J* = 2.1 Hz, 1H), 7.03 – 6.80 (m, 5H), 6.71 (s, 1H), 3.91 (d, *J* = 0.7 Hz, 9H), 3.86 (s, 3H); **^{13}C NMR** (75 MHz, $CDCl_3$): *δ* 153.54, 146.57, 145.98, 137.94, 133.47, 131.20, 127.97, 127.25, 119.33, 111.91, 110.83, 103.61, 61.10, 56.29, 56.16; **MS (GC-MS):** *m/z* 316 $[M^+]^{[270]}$; 90% yield.

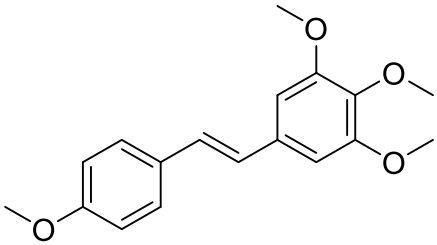

DMU-212 (191b): ^{1}H NMR (300 MHz, $CDCl_3$): *δ* 7.50 – 7.40 (m, 2H), 7.03 – 6.85 (m, 4H), 6.72 (s, 2H), 3.92 (s, 6H), 3.87 (s, 3H), 3.83 (s, 3H); **^{13}C NMR** (75 MHz, $CDCl_3$): *δ* 159.47, 153.56, 133.59, 130.20, 127.92, 127.78, 126.74, 114.33, 103.58, 61.11, 56.30, 55.48; **MS (GC-MS):** *m/z* 300 $[M^+]^{[271]}$; 96% yield.

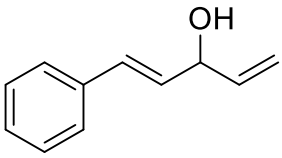

1-Phenylpenta-1,4-dien-3-ol (192b I): ^{1}H NMR (300 MHz, $CDCl_3$): *δ* 7.36 – 7.31 (m, 2H), 7.29 – 7.23 (m, 2H), 7.22 – 7.16 (m, 1H), 6.56 (dd, *J* = 15.9, 1.2 Hz, 1H), 6.18 (dd, *J* = 15.9, 6.4 Hz, 1H), 5.93 (ddd, *J* = 17.2, 10.3, 5.8 Hz, 1H), 5.28 (dt, *J* = 17.2, 1.4 Hz, 1H), 5.14 (dt, *J* = 10.3, 1.3 Hz, 1H), 4.81 – 4.69 (m, 1H), 1.87 (s, 1H); **^{13}C NMR** (75 MHz, $CDCl_3$): *δ* 139.38, 136.69, 130.94, 130.47, 128.70, 127.90, 126.67, 115.53, 73.94; **MS (GC-MS):** *m/z* 160 $[M^+]^{[151]}$; 95% yield.

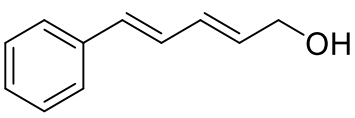

5-Phenylpenta-2,4-dien-1-ol (192b II): ^{1}H NMR (300 MHz, $CDCl_3$): *δ* 7.30 (d, *J* = 7.4 Hz, 2H), 7.22 (t, *J* = 7.4 Hz, 2H), 7.19 – 7.08 (m, 1H), 6.70 (dd, *J* = 15.6, 10.4

Hz, 1H), 6.46 (d, *J* = 15.7 Hz, 1H), 6.32 (dd, *J* = 15.2, 10.4 Hz, 1H), 5.86 (dt, *J* = 15.2, 5.9 Hz, 1H), 4.14 (d, *J* = 5.9 Hz, 2H), 1.82 (s, 1H); **^{13}C NMR** (75 MHz, $CDCl_3$): *δ* 137.22, 132.83, 132.66, 131.65, 128.71, 128.27, 127.70, 126.49, 63.42; **MS (GC-MS):** *m/z* 160 $[M^+]$[151]; 90% yield.

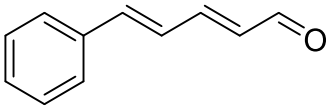

5-Phenylpenta-2,4-dienal (192b): 72 h, **^{1}H NMR** (300 MHz, $CDCl_3$): *δ* 9.62 (d, *J* = 7.9 Hz, 1H), 7.56 – 7.47 (m, 2H), 7.46 – 7.33 (m, 3H), 7.27 (ddd, *J* = 15.2, 6.9, 3.4 Hz, 1H), 7.08 – 6.95 (m, 2H), 6.27 (dd, *J* = 15.2, 7.9 Hz, 1H); **^{13}C NMR** (75 MHz, $CDCl_3$): *δ* 193.64, 152.08, 142.54, 135.74, 131.77, 129.81, 129.07, 127.66, 126.34; **MS (GC-MS):** *m/z* 158 $[M^+]$[151]; 95% yield.

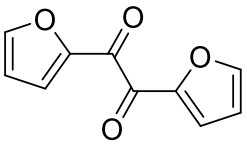

Furil (193b): 16 h; **^{1}H NMR** (300 MHz, $CDCl_3$): *δ* 7.78 (dd, *J* = 1.7, 0.7 Hz, 2H), 7.64 (dd, *J* = 3.7, 0.7 Hz, 2H), 6.63 (dd, *J* = 3.7, 1.7 Hz, 2H); **^{13}C NMR** (75 MHz, $CDCl_3$): *δ* 177.00, 149.60, 149.49, 124.78, 113.19; **MS (ESI-HRMS):** *m/z* calcd. for $C_{10}H_6O_4$ $[M+Na^+]$: 213.0158, found: 213.0159; 86% yield.

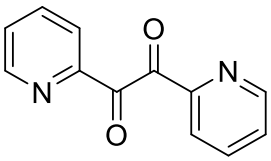

1,2-Di(pyridin-2-yl)ethane-1,2-dione (194b): 25 h; **^{1}H NMR** (300 MHz, $CDCl_3$): *δ* 8.63 – 8.54 (m, 2H), 8.25 – 8.16 (m, 2H), 7.98 – 7.86 (m, 2H), 7.53 – 7.42 (m, 2H); **^{13}C NMR** (75 MHz, $CDCl_3$): *δ* 197.02, 151.94, 149.63, 137.30, 127.98, 122.51; **MS (GC-MS):** *m/z* 212 $[M^+]$[78o]; 79% yield.

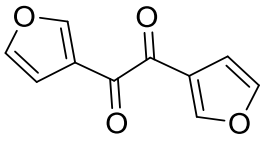

1,2-Di(furan-3-yl)ethane-1,2-dione (195b): 16 h; **^{1}H NMR** (300 MHz, $CDCl_3$): *δ* 8.52 (dd, *J* = 1.4, 0.8 Hz, 2H), 7.49 (dd, *J* = 2.0, 1.4 Hz, 2H), 6.92 (dd, *J* = 1.9, 0.7 Hz, 2H); **^{13}C NMR** (75 MHz, $CDCl_3$): *δ* 184.27, 152.04, 144.13, 123.11, 109.26; **MS (ESI-HRMS):** *m/z* calcd. for $C_{10}H_6O_4$ $[M+Na^+]$: 213.0158, found: 213.0160; 85% yield.

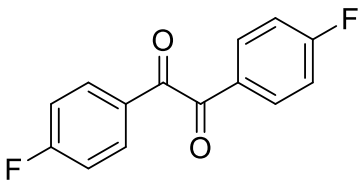

1,2-Bis(4-fluorophenyl)ethane-1,2-dione (196b): 40 h; **^{1}H NMR** (300 MHz, $CDCl_3$): *δ* 8.14 – 8.02 (m, 2H), 7.33 – 7.21 (m, 2H); **^{13}C NMR** (126 MHz, $CDCl_3$): *δ* 192.18, 167.91, 165.86, 132.82, 129.45, 116.45; **MS (GC-MS):** *m/z* 246 $[M^+]$[78o]; 76% yield.

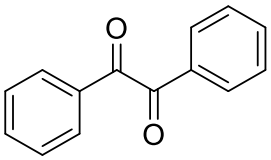

Benzil (197b): 24 h; **^{1}H NMR** (300 MHz, $CDCl_3$): *δ* 8.04 – 7.93 (m, 4H), 7.72 – 7.61 (m, 2H), 7.57 – 7.44 (m, 4H); **^{13}C NMR** (75 MHz, $CDCl_3$): *δ* 194.68, 135.00, 133.16, 130.04, 129.15; **MS (GC-MS):** *m/z* 210 $[M^+]$[272]; 85% yield.

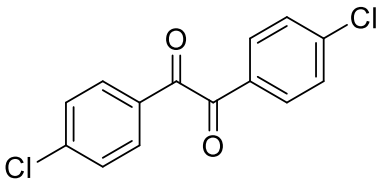

4,4‘-Dichlorobenzil (198b): 20 h; **^{1}H NMR** (300 MHz, Acetone-d_6): *δ* 7.88 (d, *J* = 8.9 Hz, 4H), 7.54 (d, *J* = 8.9 Hz, 4H); **^{13}C NMR** (126 MHz, Acetone-d_6): *δ* 193.35, 141.79, 132.20, 130.28; **MS (GC-MS):** *m/z* 278 $[M^+]$[273]; 83% yield.

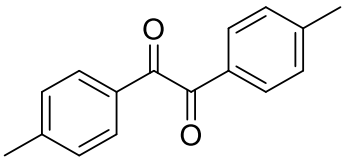

4,4‘-Dimethylbenzil (199b): 40 h; **^{1}H NMR** (300 MHz, $CDCl_3$): *δ* 8.08 – 7.73 (m, 4H), 7.40 – 7.21 (m, 4H), 2.43 (s, 6H); **^{13}C NMR** (126 MHz, $CDCl_3$): *δ* 194.42, 146.07, 130.76, 130.03, 129.73, 22.10; **MS (GC-MS):** *m/z* 238 $[M^+]$[78o]; 74% yield.

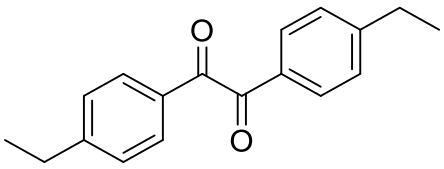

4,4‘-Diethylbenzil (200b): 40 h; **^{1}H NMR** (300 MHz, $CDCl_3$): *δ* 8.03 – 7.82 (m, 4H), 7.35 – 7.30 (m, 4H), 2.72 (q, J = 7.6 Hz, 4H), 1.26 (t, J = 7.6 Hz, 6H); **^{13}C NMR** (126 MHz, $CDCl_3$): *δ* 194.67, 146.32, 131.01, 130.28, 129.98, 28.23, 14.40; **MS (GC-MS):** *m/z* 266 $[M^+]$[274]; 40% yield.

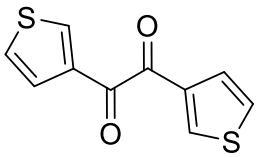

1,2-Di(thiophen-3-yl)ethane-1,2-dione (201b): 16 h; **^{1}H NMR** (300 MHz, $CDCl_3$): *δ* 8.36 (dd, *J* = 2.9, 1.2 Hz, 2H), 7.70 (dd, *J* = 5.1, 1.2 Hz, 2H), 7.39 (dd, *J* = 5.1, 2.9 Hz, 2H); **^{13}C NMR** (75 MHz, $CDCl_3$): *δ* 185.90, 137.80, 137.50, 127.71, 127.01; **MS (GC-MS):** *m/z* 222 $[M^+]$[275]; 71% yield.

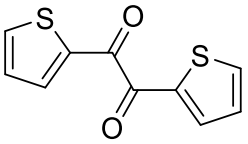

1,2-Di(thiophen-2-yl)ethane-1,2-dione (202b): 24 h; **^{1}H NMR** (300 MHz, $CDCl_3$): *δ* 8.07 (dd, *J* = 3.9, 1.2 Hz, 2H), 7.84 (dd, *J* = 4.9, 1.2 Hz, 2H), 7.21 (dd, *J* = 4.9, 3.9 Hz, 2H); **^{13}C NMR** (75 MHz, $CDCl_3$): *δ* 182.55, 138.77, 137.60, 137.39, 128.80; **MS (ESI-HRMS):** *m/z* calcd. for $C_{10}H_6O_2S_2$ $[M+Na^+]$: 244.9701, found: 244.9703; 70% yield.

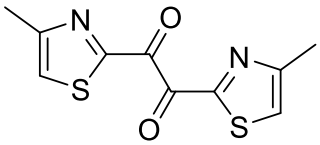

1,2-Bis(4-methylthiazol-2-yl)ethane-1,2-dione (203b): 16 h; **^{1}H NMR** (300 MHz, $CDCl_3$): *δ* 7.41 (d, *J* = 0.9 Hz, 2H), 2.51 (s, 6H); **^{13}C NMR** (75 MHz, $CDCl_3$): *δ* 184.67, 161.83, 157.12, 123.21, 17.26; **MS (ESI-HRMS):** *m/z* calcd. for $C_{10}H_8N_2O_2S_2$ $[M+H^+]$: 253.0100, found: 253.0103; 82% yield.

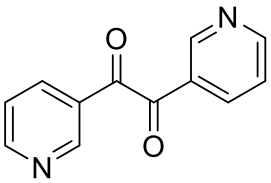

1,2-Di(pyridin-3-yl)ethane-1,2-dione (204b): 24 h; **^{1}H NMR** (300 MHz, $CDCl_3$): *δ* 9.22 (d, *J* = 2.7 Hz, 2H), 8.90 (d, 2H), 8.36 (d, 2H), 7.66 – 7.41 (m, 2H); **^{13}C NMR** (75 MHz, $CDCl_3$): *δ* ^{13}C NMR (75 MHz, $CDCl_3$) *δ* 189.92, 154.08, 150.48, 136.08, 127.31, 122.93; **MS (ESI-HRMS):** *m/z* calcd. for $C_{12}H_8N_2O_2$ $[M+H^+]$: 213.0659, found: 213.0658; 80% yield.

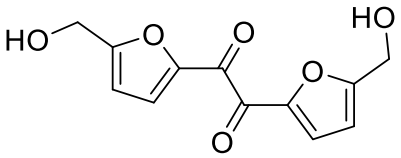

1,2-Bis(5-(hydroxymethyl)furan-2-yl)ethane-1,2-dione (205b): 24 h; **^{1}H NMR** (300 MHz, DMSO-*d*$_6$): *δ* 7.57 (d, *J* = 3.6 Hz, 2H), 6.65 (d, *J* = 3.7 Hz, 2H), 5.61 (t, *J* = 6.0 Hz, 2H), 4.55 (d, *J* = 5.9 Hz, 4H); **^{13}C NMR** (75 MHz, DMSO-*d*$_6$): *δ* 177.63, 164.03, 147.85, 126.02, 110.30, 55.98; **MS (ESI-HRMS):** *m/z* calcd. for $C_{12}H_{10}O_6$ [M+Na$^+$]: 273.0370, found: 273.0363; 74% yield.

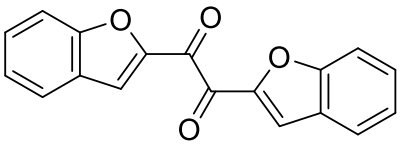

1,2-Di(benzofuran-2-yl)ethane-1,2-dione (206b): 24 h; **^{1}H NMR** (300 MHz, $CDCl_3$): *δ* 8.03 (d, *J* = 1.0 Hz, 2H), 7.81 – 7.76 (m, 2H), 7.70 – 7.61 (m, 2H), 7.61 – 7.53 (m, 2H), 7.43 – 7.31 (m, 2H); **^{13}C NMR** (75 MHz, $CDCl_3$): *δ* 178.79, 156.84, 149.41, 130.15, 127.17, 124.61, 124.41, 121.17, 112.85; **MS (ESI-HRMS):** *m/z* calcd. for $C_{18}H_{10}O_4$ [M+H$^+$]: 291.0652, found: 291.0645; 79% yield.

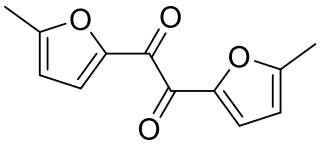

1,2-Bis(5-methylfuran-2-yl)ethane-1,2-dione (207b): 24 h; **^{1}H NMR** (300 MHz, $CDCl_3$):*δ* 7.52 (dd, *J* = 3.6, 0.6 Hz, 2H), 6.25 (dd, *J* = 3.6, 0.9 Hz, 2H), 2.54 – 2.33 (s, 6H); **^{13}C NMR** (75 MHz, $CDCl_3$): *δ* 176.84, 161.37, 148.77, 126.85, 110.28, 14.40; **MS (ESI-HRMS):** *m/z* calcd. for $C_{12}H_{10}O_4$ [M+Na$^+$]: 241.0471, found: 241.0471; 75% yield.

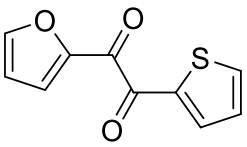

1-(Furan-2-yl)-2-(thiophen-2-yl)ethane-1,2-dione (208b): 40 h; furan-2-carbaldehyde (0.25 mmol), thiophene-2-carbaldehyde (0.375 mmol); **^{1}H NMR** (300 MHz, $CDCl_3$): *δ* 8.07 (dd, *J* = 3.9, 1.2 Hz, 1H), 7.84 (dd, *J* = 4.9, 1.2 Hz, 1H), 7.78 (dd, *J* = 1.7, 0.7 Hz, 1H), 7.63 (dd, *J* = 3.7, 0.7 Hz, 1H), 7.21 (dd, *J* = 4.9, 3.9 Hz, 1H), 6.64 (dd, *J* = 3.7, 1.7 Hz, 1H); **^{13}C NMR** (75 MHz, $CDCl_3$): *δ* 182.11, 177.55, 149.51, 138.92, 137.50, 137.33, 128.85, 124.73, 113.19, 100.15; **MS (GC-MS):** *m/z* 206 [M$^+$][79a]; 72% yield.

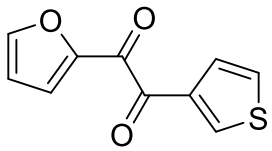

1-(Furan-2-yl)-2-(thiophen-3-yl)ethane-1,2-dione (209b): 40 h; furan-2-carbaldehyde (0.25 mmol), thiophene-3-carbaldehyde (0.375 mmol); **^{1}H NMR** (300 MHz, $CDCl_3$): *δ* 8.46 (dd, *J* = 2.9, 1.2 Hz, 1H), 7.77 (dd, *J* = 1.7, 0.7 Hz, 1H), 7.71 (dd, *J* = 5.2, 1.2 Hz, 1H), 7.53 (dd, *J* = 3.7, 0.7 Hz, 1H), 7.38 (dd, *J* = 5.1, 2.9 Hz, 1H), 6.63 (dd, *J* = 3.7, 1.7 Hz, 1H); **^{13}C NMR** (75 MHz, $CDCl_3$): *δ* 183.96, 178.92, 149.90, 149.37, 137.83, 137.51, 127.81, 126.90, 124.24, 113.11; **MS (ESI-HRMS):** *m/z* calcd. for $C_{10}H_6O_3S$ [M+Na^+]: 228.9930, found: 228.9932; 70% yield.

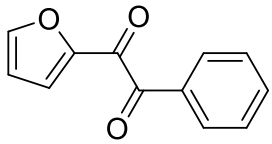

1-(Furan-2-yl)-2-phenylethane-1,2-dione (210b): 48 h; furan-2-carbaldehyde (0.25 mmol), benzaldehyde (0.375 mmol); **^{1}H NMR** (300 MHz, $CDCl_3$): *δ* 8.10 – 7.97 (m, 2H), 7.76 (dd, *J* = 1.7, 0.7 Hz, 1H), 7.72 – 7.60 (m, 1H), 7.57 – 7.47 (m, 2H), 7.39 (dd, *J* = 3.7, 0.7 Hz, 1H), 6.63 (dd, *J* = 3.6, 1.7 Hz, 1H); **^{13}C NMR** (75 MHz, $CDCl_3$): *δ* 191.68, 180.56, 150.17, 149.31, 135.00, 132.81, 130.35, 129.08, 123.39, 113.11 **MS (GC-MS):** *m/z* 200 [M^+][276]; 74% yield.

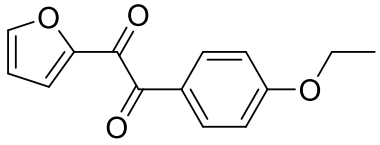

1-(4-Ethoxyphenyl)-2-(furan-2-yl)ethane-1,2-dione (211b): 48 h; furan-2-carbaldehyde (0.25 mmol), 4-ethoxy benzaldehyde (0.375 mmol); **^{1}H NMR** (300 MHz, $CDCl_3$): *δ* 8.08 – 7.95 (m, 2H), 7.74 (dd, *J* = 1.6, 0.7 Hz, 1H), 7.37 (dd, *J* = 3.7, 0.7 Hz, 1H), 7.01 – 6.86 (m, 2H), 6.61 (dd, *J* = 3.7, 1.7 Hz, 1H), 4.13 (q, *J* = 7.0 Hz, 2H), 1.45 (t, *J* = 7.0 Hz, 3H); **^{13}C NMR** (75 MHz, $CDCl_3$): *δ* 190.22, 181.09, 164.63, 150.33, 149.06, 132.86, 125.59, 123.19, 114.86, 112.99, 64.18, 14.74; **MS (ESI-HRMS):** *m/z* calcd. for $C_{14}H_{12}O_4$ [M+H^+]: 245.0808, found: 245.0806; 68% yield.

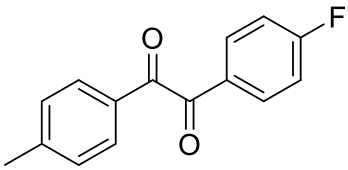

1-(4-Fluorophenyl)-2-(p-tolyl)ethane-1,2-dione (212b): 48 h; 4-methyl benzaldehyde (0.25 mmol), 4-fluoro benzaldehyde (0.375 mmol); purified *via* GPC; **^{1}H NMR** (300 MHz, $CDCl_3$): *δ* 8.08 – 7.95 (m, 2H), 7.91 – 7.82 (m, 2H), 7.37 – 7.23 (m, 2H), 7.23 – 7.12 (m, 2H), 2.44 (s, 3H); **^{13}C NMR** (75 MHz, $CDCl_3$): *δ* 193.94, 168.89, 146.51, 132.93, 132.80, 130.64, 130.22, 129.94, 116.64, 116.35, 22.10; **MS (ESI-HRMS):** *m/z* calcd. for $C_{15}H_{11}FO_2$ [M+H$^+$]: 265.0635, found: 265.0636; 65% yield.

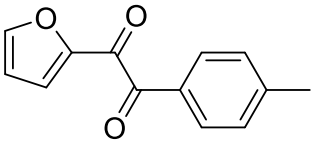

1-(Furan-2-yl)-2-(p-tolyl)ethane-1,2-dione (213b): 36 h; furan-2-carbaldehyde (0.25 mmol), 4-methyl benzaldehyde (0.375 mmol); **^{1}H NMR** (300 MHz, $CDCl_3$): *δ* 7.98 – 7.88 (m, 2H), 7.75 (dd, *J* = 1.7, 0.7 Hz, 1H), 7.37 (dd, *J* = 3.7, 0.7 Hz, 1H), 7.34 – 7.28 (m, 2H), 6.61 (dd, *J* = 3.7, 1.7 Hz, 1H), 2.44 (s, 3H); **^{13}C NMR** (75 MHz, $CDCl_3$): *δ* 191.40, 180.87, 150.23, 149.17, 146.34, 130.46, 130.34, 129.81, 123.23, 113.04, 22.07; **MS (ESI-HRMS):** *m/z* calcd. for $C_{13}H_{10}O_3$ [M+Na$^+$]: 237.0522, found: 237.0525; 70% yield.

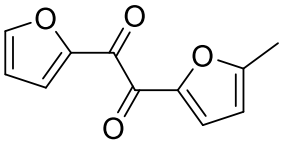

1-(Furan-2-yl)-2-(5-methylfuran-2-yl)ethane-1,2-dione (214b): 36 h; furan-2-carbaldehyde (0.25 mmol), 5-methyl furan-2-carbaldehyde (0.375 mmol); purified *via* GPC; **^{1}H NMR** (300 MHz, $CDCl_3$): *δ* 7.76 (dd, *J* = 1.6, 0.8 Hz, 1H), 7.62 (dd, *J* = 3.7, 0.8 Hz, 1H), 7.55 (dd, *J* = 3.6, 0.8 Hz, 1H), 6.62 (dd, *J* = 3.7, 1.7 Hz, 1H), 6.27 (d, *J* = 2.7 Hz, 1H), 2.46 (s, 3H); **^{13}C NMR** (75 MHz, $CDCl_3$): *δ* 177.56, 161.66, 149.79, 149.28, 148.62, 127.10, 124.58, 113.12, 110.40, 14.43; **MS (ESI-HRMS):** *m/z* calcd. for $C_{11}H_8O_4$ [M+H$^+$]: 205.0501, found: 205.0497; 80% yield.

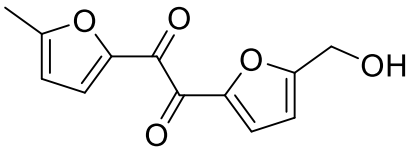

1-(5-(Hydroxymethyl)furan-2-yl)-2-(5-methylfuran-2-yl)ethane-1,2-dione (215b): 48 h; 5-methyl furan-2-carbaldehyde (0.25 mmol), 5-(hydroxymethyl) furan-2-carbaldehyde (0.375 mmol); **^{1}H NMR** (300 MHz, $CDCl_3$): *δ* 7.58 (d, *J* = 3.6 Hz, 1H), 7.54 (dd, *J* = 3.6, 0.6 Hz, 1H), 6.53 (d, *J* = 3.6 Hz, 1H), 6.27 (dd, *J* = 3.6, 0.9 Hz, 1H), 4.75 (s, 2H), 2.46 (s, 3H); **^{13}C NMR** (75 MHz, $CDCl_3$): *δ* 177.39, 176.27, 161.82, 161.69, 149.33, 148.62, 127.14, 125.86, 110.52, 110.42, 57.97, 14.43; **MS (ESI-HRMS):** *m/z* calcd. for $C_{12}H_{10}O_5$ [M+H$^+$]: 235.0601, found: 235.0601; 64% yield.

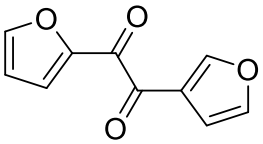

1-(Furan-2-yl)-2-(furan-3-yl)ethane-1,2-dione (216b): 36 h; furan-2-carbaldehyde (0.25 mmol), furan-3-carbaldehyde (0.375 mmol); **^{1}H NMR** (300 MHz, $CDCl_3$): *δ* 8.48 (dd, *J* = 1.4, 0.8 Hz, 1H), 7.82 – 7.73 (m, 1H), 7.72 – 7.64 (m, 1H), 7.49 (dd, *J* = 1.9, 1.4 Hz, 1H), 6.92 (dd, *J* = 2.0, 0.8 Hz, 1H), 6.63 (dd, *J* = 3.7, 1.7 Hz, 1H); **^{13}C NMR:** (75 MHz, $CDCl_3$): *δ* 184.08, 177.03, 152.03, 149.56, 149.45, 144.27, 124.94, 123.39, 113.17, 109.09; **MS (ESI-HRMS):** *m/z* calcd. for $C_{10}H_6O_4$ [M+Na$^+$]: 213.0158, found: 213.0166; 76% yield.

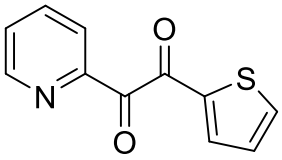

1-(Pyridin-2-yl)-2-(thiophen-2-yl)ethane-1,2-dione (217b): 48 h; picolinaldehyde (0.25 mmol), thiophene-2-carbaldehyde (0.375 mmol); **^{1}H NMR** (300 MHz, $CDCl_3$): *δ* 8.75 – 8.68 (m, 1H), 8.24 – 8.15 (m, 1H), 8.01 – 7.88 (m, 1H), 7.83 (dd, *J* = 4.9, 1.1 Hz, 1H), 7.70 (dd, *J* = 3.9, 1.1 Hz, 1H), 7.57 – 7.50 (m, 1H), 7.18 (dd, *J* = 4.9, 3.9 Hz, 1H); **^{13}C NMR** (75 MHz, $CDCl_3$): *δ* 192.76, 187.31, 151.59, 150.03, 140.25, 137.38, 136.38, 136.23, 128.78, 128.21, 123.93; **MS (ESI-HRMS):** *m/z* calcd. for $C_{11}H_7NO_2S$ [M+H$^+$]: 218.0270, found: 218.0278; 62% yield.

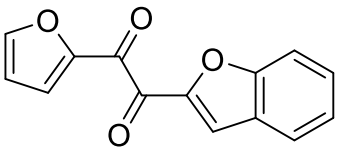

1-(Benzofuran-2-yl)-2-(furan-2-yl)ethane-1,2-dione (218b): 48 h; furan-2-carbaldehyde (0.25 mmol), benzofuran-2-carbaldehyde (0.375 mmol); **^{1}H NMR** (300 MHz, $CDCl_3$): *δ* 7.99 (d, *J* = 1.0 Hz, 1H), 7.81 – 7.74 (m, 2H), 7.71 – 7.59 (m, 2H), 7.59 – 7.49 (m, 1H), 7.41 – 7.27 (m, 1H), 6.66 (dd, *J* = 3.7, 1.7 Hz, 1H); **^{13}C NMR** (75 MHz, $CDCl_3$): *δ* 179.14, 176.87, 156.75, 149.71, 149.57, 149.35, 130.01, 127.17, 125.07, 124.54, 124.34, 120.88, 113.33, 112.81; **MS (ESI-HRMS):** *m/z* calcd. for $C_{14}H_8O_4$ [M+H$^+$]: 241.0495, found: 241.0505; 75% yield.

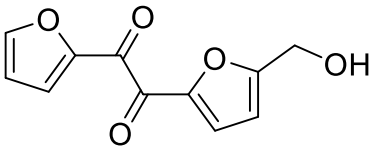

1-(Furan-2-yl)-2-(5-(hydroxymethyl)furan-2-yl)ethane-1,2-dione (219b): 48 h; furan-2-carbaldehyde (0.25 mmol), 5-(hydroxymethyl) furan-2-carbaldehyde (0.375 mmol); **^{1}H NMR** (300 MHz, $CDCl_3$): *δ* 7.78 (dd, *J* = 1.7, 0.8 Hz, 1H), 7.63 (dd, *J* = 3.7, 0.8 Hz, 1H), 7.60 (d, *J* = 3.7 Hz, 1H), 6.63 (dd, *J* = 3.7, 1.7 Hz, 1H), 6.55 (d, *J* = 3.7 Hz, 1H), 4.76 (s, 2H), 2.22 (s, 1H); **^{13}C NMR** (75 MHz, $CDCl_3$): *δ* 177.01, 176.81, 162.09, 149.61, 149.53, 149.15, 126.11, 124.85, 113.22, 110.59, 57.96; **MS (ESI-HRMS):** *m/z* calcd. for $C_{11}H_8O_5$ [M+H$^+$]: 221.0444, found: 221.0445; 71% yield.

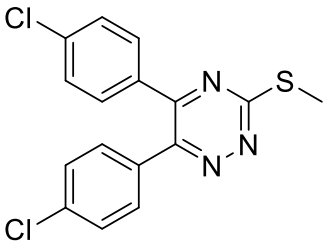

5,6-Bis(4-chlorophenyl)-3-(methylthio)-1,2,4-triazine (258b): ^{1}H NMR (400 MHz, $CDCl_3$): *δ* 7.93 – 7.87 (m, 2H), 7.52 – 7.47 (m, 2H), 7.42 – 7.37 (m, 2H), 7.30 – 7.24 (m, 2H), 3.23 (s, 3H); **^{13}C NMR** (75 MHz, $CDCl_3$): *δ* 158.39, 148.08, 144.01, 138.17, 128.92, 128.07, 127.79, 114.55, 112.33, 43.34; **MS (ESI-HRMS):** *m/z* calcd. for $C_{16}H_{11}Cl_2N_3S$ [M-H$^-$]: 345.9972, found: 345.9963[199a]; 72% yield.

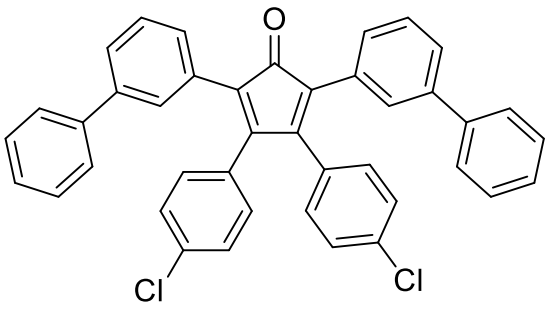

2,5-Di([1,1'-biphenyl]-3-yl)-3,4-bis(4-chlorophenyl)cyclopenta-2,4-dien-1-one (259b): **^{1}H NMR** (300 MHz, $CDCl_3$): *δ* 7.51 – 7.26 (m, 18H), 7.25 – 7.17 (m, 4H), 6.99 – 6.92 (m, 4H); **^{13}C NMR** (75 MHz, $CDCl_3$): *δ* 199.75, 153.10, 141.17, 140.84, 135.11, 131.49, 130.89, 130.72, 129.22, 128.98, 128.87, 128.84, 127.49, 127.19, 126.76, 125.99; **MS (ESI-HRMS):** *m/z* calcd. for $C_{41}H_{26}Cl_2O$ [M+H$^+$]: 605.1433, found: 605.1402[199c]; 69% yield.

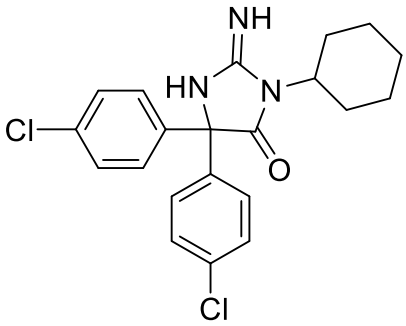

5,5-Bis(4-chlorophenyl)-2-iminoimidazolidin-4-one (260b): **^{1}H NMR** (300 MHz, $CDCl_3$): *δ* 8.01 (s, 1H), 7.35 (d, *J* = 8.7 Hz, 4H), 7.21 (d, *J* = 8.8 Hz, 4H), 4.54 (t, *J* = 12.4 Hz, 1H), 2.41 – 1.13 (m, 10H); **MS (ESI-HRMS):** *m/z* calcd. for $C_{21}H_{21}N_3Cl_2O$ [M+H$^+$]: 402.1134, found: 402.1121[199b]; 55% yield.

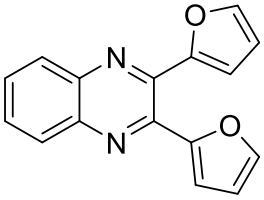

2,3-Di(furan-2-yl)quinoxaline (261b): **^{1}H NMR** (300 MHz, $CDCl_3$): *δ* 8.20 – 8.07 (m, 2H), 7.81 – 7.67 (m, 2H), 7.62 (dd, *J* = 1.8, 0.8 Hz, 2H), 6.66 (dd, *J* = 3.5, 0.8 Hz, 2H), 6.56 (dd, *J* = 3.5, 1.8 Hz, 2H); **^{13}C NMR** (75 MHz, $CDCl_3$): *δ* 150.96, 144.34, 142.79, 140.77, 130.52, 129.26, 113.11, 112.04; **MS (GC-MS):** *m/z* 262 [M$^+$][164]; 90% yield.

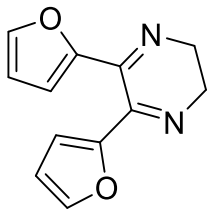

5,6-Di(furan-2-yl)-2,3-dihydropyrazine (262b): **^{1}H NMR** (300 MHz, $CDCl_3$): *δ* 7.45 (dd, *J* = 1.8, 0.8 Hz, 2H), 6.47 (dd, *J* = 3.5, 0.8 Hz, 2H), 6.39 (dd, *J* = 3.5, 1.8 Hz, 2H), 3.60 (s, 4H); **^{13}C NMR** (75 MHz, $CDCl_3$): *δ* 150.42, 149.41, 144.49, 114.15, 111.46, 45.04; **MS (GC-MS):** *m/z* 214 $[M^+]$[166]; 77% yield.

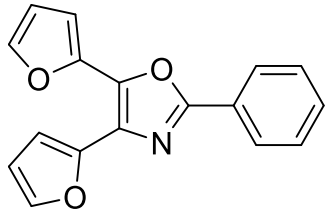

4,5-Di(furan-2-yl)-2-phenyloxazole (263b): **^{1}H NMR** (300 MHz, $CDCl_3$): *δ* 7.33 (dd, *J* = 1.8, 0.8 Hz, 2H), 7.30 – 7.15 (m, 5H), 7.06 (dd, *J* = 3.5, 0.8 Hz, 2H), 6.41 (dd, *J* = 3.5, 1.8 Hz, 2H); **^{13}C NMR** (75 MHz, $CDCl_3$): *δ* 158.39, 148.08, 144.01, 138.17, 128.92, 128.74, 128.42, 128.07, 127.79, 114.55, 112.33; **MS (GC-MS):** *m/z* 277 $[M^+]$[167]; 53% yield.

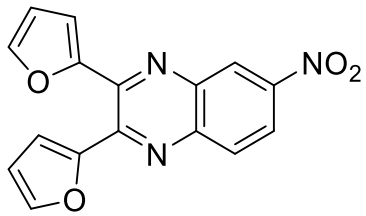

2,3-Di(furan-2-yl)-6-nitroquinoxaline (264b'): **^{1}H NMR** (300 MHz, Chloroform-d) δ 8.99 (dd, *J* = 2.5, 0.5 Hz, 1H), 8.47 (dd, *J* = 9.2, 2.5 Hz, 1H), 8.21 (dd, *J* = 9.2, 0.5 Hz, 1H), 7.67 (dd, *J* = 1.8, 0.8 Hz, 1H), 7.65 (dd, *J* = 1.8, 0.8 Hz, 1H), 6.88 (dd, *J* = 3.5, 0.8 Hz, 1H), 6.83 (dd, *J* = 3.5, 0.8 Hz, 1H), 6.61 (ddd, *J* = 3.5, 1.8 Hz, 2H); **^{13}C NMR** (75 MHz, $CDCl_3$) δ 150.34, 150.28, 148.08, 145.58, 145.10, 144.83, 144.34, 143.13, 139.38, 130.58, 125.47, 123.74, 115.46, 114.61, 112.55, 112.41; **MS (GC-MS):** *m/z* 307 $[M^+]$[168]; 92% yield.

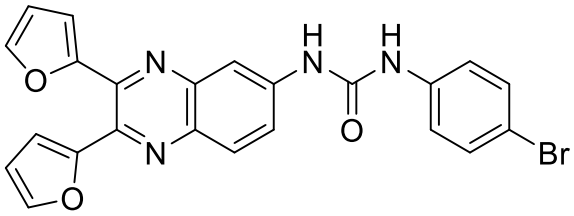

1-(4-Bromophenyl)-3-(2,3-di(furan-2-yl)quinoxalin-6-yl)urea (264b): ^{1}H NMR (300 MHz, C_6D_6): *δ* 9.21 (dd, *J* = 7.5, 1.5 Hz, 1H), 8.14 – 7.95 (m, 2H), 7.90 – 7.78 (m, 2H), 7.58 (s, 1H), 7.39 (s, 1H), 7.30 (d, *J* = 7.5 Hz, 2H), 7.26 – 7.16 (m, 2H), 7.09 (d, *J* = 7.6 Hz, 2H), 6.91 – 6.75 (m, 2H); **^{13}C NMR** (75 MHz, C_6D_6): *δ* 152.97, 149.86, 146.48, 146.39, 146.03, 141.92, 139.19, 138.80, 136.31, 131.15, 128.06, 121.75, 120.30, 118.44, 118.24, 112.58, 112.27; **MS (ESI-HRMS):** *m/z* calcd. for $C_{23}H_{15}BrN_4O_3$ [M+H$^+$]: 475.0400, found: 475.0376[168]; 58% yield.

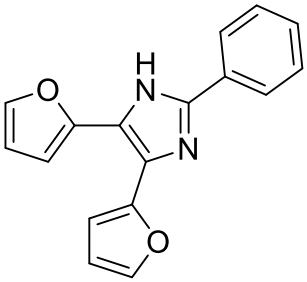

4,5-Di(furan-2-yl)-2-phenyl-1H-imidazole (265b): ^{1}H NMR (300 MHz, $CDCl_3$): *δ* 7.97 – 7.82 (m, 2H), 7.55 – 7.30 (m, 5H), 7.00 (d, *J* = 3.3 Hz, 2H), 6.53 (dd, *J* = 3.4, 1.8 Hz, 2H); **^{13}C NMR** (75 MHz, $CDCl_3$): *δ* 194.50, 172.68, 141.64, 129.45, 129.09, 125.66, 120.16, 111.97, 107.94, 107.87; **MS (GC-MS):** *m/z* 276 [M$^+$][169]; 82% yield.

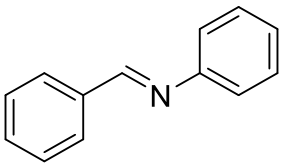

***N*-Benzylideneaniline (266b): ^{1}H NMR** (400 MHz, $CDCl_3$): *δ* 8.50 (s, 1H), 8.01 – 7.89 (m, 2H), 7.56 – 7.50 (m, 3H), 7.49 – 7.41 (m, 2H), 7.32 – 7.21 (m, 3H); **^{13}C NMR** (101 MHz, $CDCl_3$): *δ* 160.46, 152.20, 136.34, 131.47, 129.25, 128.92, 128.87, 126.04, 120.98; **MS (GC-MS):** *m/z* 181 [M$^+$][277]; 96% yield.

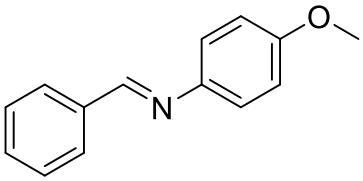

1-(4-Methoxyphenyl)-*N*-phenylmethanimine (267b): ^{1}H NMR (300 MHz, $CDCl_3$): *δ* 8.49 (s, 1H), 7.93 – 7.86 (m, 2H), 7.50 – 7.42 (m, 3H), 7.26 – 7.20 (m, 2H),

6.98 – 6.91 (m, 2H), 3.84 (s, 3H); **^{13}C NMR** (75 MHz, $CDCl_3$): *δ* 158.56, 158.44, 145.10, 136.62, 131.17, 128.87, 128.73, 122.33, 114.55, 55.66; **MS (GC-MS):** *m/z* 211 $[M^+]$[278]; 99% yield.

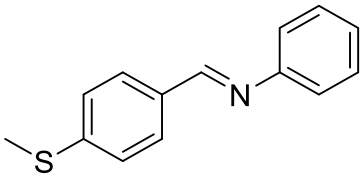

1-(4-(methylthio)phenyl)-N-phenylmethanimine (268b): ^{1}H NMR (300 MHz, $CDCl_3$): *δ* 8.40 (s, 1H), 7.88 – 7.76 (m, 2H), 7.48 – 7.28 (m, 4H), 7.27 – 7.18 (m, 3H), 2.54 (s, 3H); **^{13}C NMR** (75 MHz, $CDCl_3$): *δ* 159.71, 152.26, 143.35, 133.08, 130.12, 129.27, 125.90, 125.38, 121.00, 15.29; **MS (GC-MS):** *m/z* 227 $[M^+]$[279]; 99% yield.

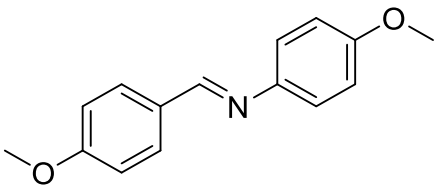

***N*-1-bis(4-methoxyphenyl)methanimine (269b): ^{1}H NMR** (300 MHz, $CDCl_3$): *δ* 9.89 (s, 1H), 7.91 – 7.78 (m, 4H), 7.08 – 6.93 (m, 4H), 3.90 (s, 6H); **^{13}C NMR** (75 MHz, $CDCl_3$): *δ* 190.94, 164.76, 132.14, 130.14, 114.47, 55.74; **MS (GC-MS):** *m/z* 241 $[M^+]$[280]; 92% yield.

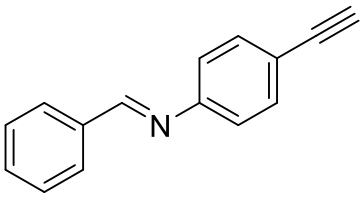

N-(4-ethynylphenyl)-1-phenylmethanimine (270b): ^{1}H NMR (300 MHz, $CDCl_3$): *δ* 7.42 – 7.26 (m, 5H), 7.26 (s, 1H), 6.66 – 6.52 (m, 4H), 2.96 (s, 1H); **^{13}C NMR** (75 MHz, $CDCl_3$): *δ* 160.51, 154.19, 133.62, 131.46, 130.38, 127.33, 127.07, 119.67, 117.13, 112.58, 107.19; **MS (GC-MS):** *m/z* 205 $[M^+]$[279]; 99% yield.

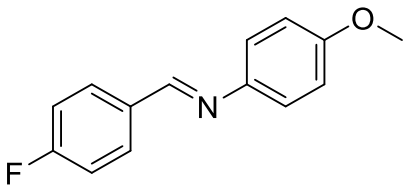

1-(4-fluorophenyl)-*N*-(4-methoxyphenyl)methanimine (271b): ^{1}H NMR (300 MHz, $CDCl_3$): *δ* 8.46 (s, 1H), 7.96 – 7.86 (m, 2H), 7.31 – 7.21 (m, 2H), 7.17 (dd, *J* = 8.9, 8.4 Hz, 2H), 7.01 – 6.78 (m, 2H), 3.85 (s, 3H); **^{13}C NMR** (75 MHz, $CDCl_3$): *δ* 166.32,

158.50, 156.89, 144.86, 130.57, 122.29, 116.14, 115.85, 114.58, 55.64; **MS (GC-MS):** *m/z* 229 [M$^+$][281]; 92% yield.

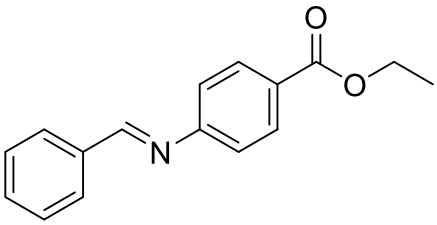

Ethyl 4-(benzyldeneamino)benzoate (272b): ^{1}H NMR (300 MHz, $CDCl_3$): *δ* 8.43 (s, 1H), 8.19 – 8.02 (m, 2H), 7.99 – 7.87 (m, 2H), 7.61 – 7.41 (m, 3H), 7.21 (d, *J* = 8.7 Hz, 2H), 4.39 (q, *J* = 7.1 Hz, 2H), 1.41 (t, *J* = 7.1 Hz, 3H); **^{13}C NMR** (75 MHz, $CDCl_3$): *δ* 166.45, 161.70, 156.26, 135.93, 131.97, 130.92, 129.15, 128.96, 127.85, 120.74, 61.00, 14.49; **MS (GC-MS):** *m/z* 253 [M$^+$][282]; 73% yield.

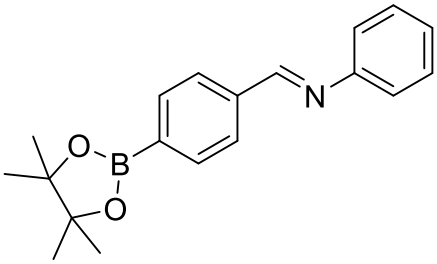

***N*-Phenyl-1-(4(4,4,5,5-tetramethyl-1,3,2-dioxaborolan-2-yl)phenyl)methan-imine (273b): ^{1}H NMR** (300 MHz, $CDCl_3$): *δ* 8.48 (s, 1H), 7.91 – 7.86 (m, 2H), 7.49 – 7.44 (m, 3H), 7.21 – 7.16 (m, 2H), 6.90 – 6.85 (m, 2H), 2.17 (s, 12H); **^{13}C NMR** (126 MHz, $CDCl_3$): *δ* 207.20, 158.46, 154.87, 144.86, 136.56, 131.16, 128.87, 128.71, 122.50, 116.07, 58.86, 31.10; **MS (ESI-HRMS):** *m/z* calcd. for $C_{19}H_{22}BNO_2$ [M+H$^+$]: 308.1816, found: 308.1818; 64% yield.

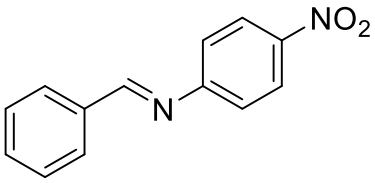

***N*-(4-Nitrophenyl)-1-phenylmethanimine (274b): ^{1}H NMR** (300 MHz, $CDCl_3$): *δ* 8.36 (s, 1H), 8.24 – 8.17 (m, 2H), 7.85 (dt, *J* = 7.7, 1.2 Hz, 2H), 7.52 – 7.40 (m, 3H), 7.23 – 7.12 (m, 2H); **^{13}C NMR** (75 MHz, $CDCl_3$): *δ* 162.79, 132.56, 129.44, 129.13, 125.20, 121.39; **MS (GC-MS):** *m/z* 226 [M$^+$][283]; 72% yield.

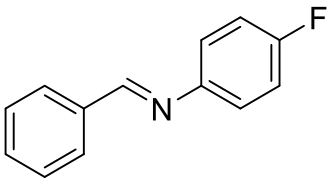

***N*-(4-fluorophenyl)-1-phenylmethanimine (275b): ^{1}H NMR** (300 MHz, $CDCl_3$): *δ* 8.45 (s, 1H), 7.94 – 7.86 (m, 2H), 7.53 – 7.45 (m, 3H), 7.24 – 7.17 (m, 2H), 7.13 – 7.02 (m, 2H); **^{13}C NMR** (75 MHz, $CDCl_3$): *δ* 160.28, 136.28, 131.58, 128.95, 128.93, 122.49, 122.39, 116.16, 115.86; **MS (GC-MS):** *m/z* 199 $[M^+]$[284]; 99% yield.

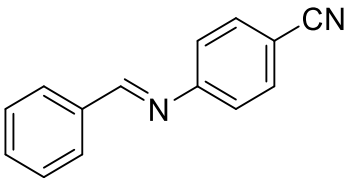

4-(Benzylideneamino)benzonitrile (276b): ^{1}H NMR (300 MHz, $CDCl_3$): *δ* 8.40 (s, 1H), 7.95 – 7.88 (m, 2H), 7.71 – 7.65 (m, 2H), 7.58 – 7.46 (m, 3H), 7.30 – 7.18 (m, 2H); **^{13}C NMR** (75 MHz, $CDCl_3$): *δ* 162.51, 156.19, 135.62, 133.46, 132.38, 129.33, 129.07, 121.67, 119.13, 109.19; **MS (GC-MS):** *m/z* 206 $[M^+]$[285]; 62% yield.

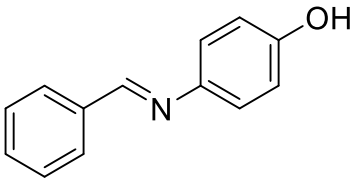

4-(Benzylideneamino)phenol (277b): ^{1}H NMR (300 MHz, $CDCl_3$): *δ* 8.48 (s, 1H), 7.94 – 7.82 (m, 2H), 7.47 (ddd, *J* = 3.4, 2.7, 1.5 Hz, 3H), 7.23 – 7.12 (m, 2H), 6.93 – 6.83 (m, 2H), 4.90 (s, 1H); **^{13}C NMR** (75 MHz, $CDCl_3$): *δ* 158.74, 131.24, 128.90, 128.77, 122.52, 116.06; **MS (GC-MS):** *m/z* 197 $[M^+]$[286]; 99% yield.

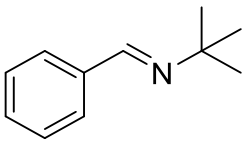

***N-tert*-butyl-1-phenylmethanimine (278b): ^{1}H NMR** (300 MHz, $CDCl_3$): *δ* 8.29 (s, 1H), 7.83 – 7.71 (m, 2H), 7.45 – 7.35 (m, 3H), 1.32 (s, 9H); **^{13}C NMR** (75 MHz, $CDCl_3$): *δ* 155.23, 137.31, 130.25, 128.61, 128.01, 57.34, 29.86; **MS (GC-MS):** *m/z* 161 $[M^+]$[287]; 99% yield.

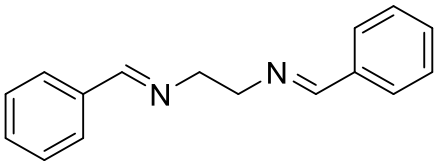

***N*,*N*'-(Ethane-1,2-diyl)bis(1-phenylmethanimine) (279b): ^{1}H NMR** (300 MHz, $CDCl_3$): *δ* 8.52 (d, J = 0.5 Hz, 2H), 7.96 – 7.89 (m, 4H), 7.53 – 7.45 (m, 6H), 7.29 (s, 4H); **13C NMR (75 MHz, $CDCl_3$):** *δ* 159.87, 150.14, 136.44, 131.49, 128.95, 121.97; **MS (GC-MS):** *m/z* 236 (M^+)[288]; 79% yield.

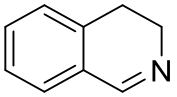

3,4-dihydroisoquinoline (280b): ^{1}H NMR (300 MHz, $CDCl_3$): *δ* 8.32 (t, *J* = 2.0 Hz, 1H), 7.39 – 7.10 (m, 4H), 3.80 – 3.72 (m, 2H), 2.79 – 2.67 (m, 2H); **^{13}C NMR** (75 MHz, $CDCl_3$): *δ* 160.33, 136.37, 131.06, 128.57, 127.45, 127.21, 127.11, 47.45, 25.08; **MS (GC-MS):** *m/z* 131 $[M^+]$[289]; 87% yield.

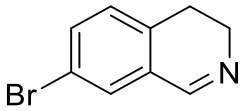

7-Bromo-3,4-dihydroisoquinoline (281b): ^{1}H NMR (300 MHz, $CDCl_3$): *δ* 8.33 – 8.19 (s, 1H), 7.47 (dd, *J* = 8.0, 2.1 Hz, 1H), 7.41 (d, *J* = 2.1 Hz, 1H), 7.05 (d, *J* = 8.0 Hz, 1H), 3.83 – 3.74 (m, 2H), 2.76 – 2.64 (m, 2H); **^{13}C NMR** (75 MHz, $CDCl_3$): *δ* 159.01, 135.21, 133.97, 130.17, 129.26, 120.58, 120.14, 47.43, 24.62; **MS (GC-MS):** *m/z* 209 $[M^+]$[101]; 99% yield.

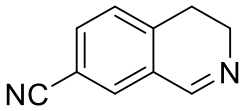

3,4-Dihydroisoquinoline-7-carbonitrile (282b): ^{1}H NMR (300 MHz, $CDCl_3$): *δ* 8.35 (s, 1H), 7.64 (dd, *J* = 7.8, 1.7 Hz, 1H), 7.59 – 7.53 (m, 1H), 7.31 – 7.27 (m, 1H), 3.89 – 3.78 (m, 2H), 2.88 – 2.76 (m, 2H); **^{13}C NMR** (75 MHz, $CDCl_3$): *δ* 158.11, 141.53, 134.31, 130.36, 128.51, 118.15, 111.32, 46.78, 42.68, 25.03; **MS (ESI-HRMS):** *m/z* calcd. for $C_{10}H_8N_2$ $[M+H^+]$: 157.0760, found: 157.0762; 94% yield.

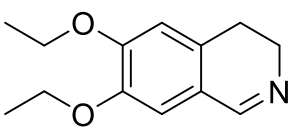

6,7-Diethoxy-3,4-dihydrotetraisoquinoline (283b): ^{1}H NMR (300 MHz, $CDCl_3$): *δ* 8.20 (s, 1H), 6.81 (s, 1H), 6.66 (s, 1H), 4.11 (dq, *J* = 8.4, 7.0 Hz, 4H), 3.72 (ddd,

J = 8.1, 7.0, 2.2 Hz, 2H), 2.69 – 2.62 (m, 2H), 1.46 (td, *J* = 7.0, 4.7 Hz, 6H); **^{13}C NMR** (75 MHz, $CDCl_3$): *δ* 159.91, 151.40, 147.51, 130.13, 121.66, 113.05, 112.19, 65.13, 64.73, 47.44, 42.83, 24.94, 14.98; **MS (ESI-HRMS):** *m/z* calcd. for $C_{13}H_{17}NO_2$ [M+H$^+$]: 220.1332, found: 220.1335; 91% yield.

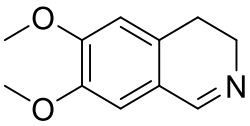

6,7-Dimethoxy-3,4-dihydroisoquinoline (284b): ^{1}H NMR (300 MHz, $CDCl_3$): *δ* 9.05 (s, 1H), 8.39 (d, *J* = 5.8 Hz, 1H), 7.51 (d, *J* = 5.6 Hz, 1H), 7.26 (s, 2H), 7.20 (s, 1H), 7.07 (s, 1H), 4.04 (s, 6H); **^{13}C NMR** (75 MHz, $CDCl_3$): *δ* 150.12, 142.18, 132.70, 119.37, 105.49, 104.73, 56.25, 56.21; **MS (GC-MS):** *m/z* 191 [M$^+$][289]; 97% yield.

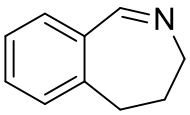

4,5-Dihydro-3H-benzo[c]azepine (285b): ^{1}H NMR (300 MHz, $CDCl_3$): *δ* 8.50 (s, 1H), 7.60 – 7.28 (m, 4H), 3.63 (td, *J* = 6.2, 1.7 Hz, 2H), 2.78 (t, *J* = 6.8 Hz, 2H), 2.35 – 2.17 (m, 2H); **^{13}C NMR** (75 MHz, $CDCl_3$): *δ* 163.90, 130.15, 129.91, 129.11, 126.29, 51.60, 32.71, 32.20; **MS (GC-MS):** *m/z* 145 [M$^+$][290]; 72% yield.

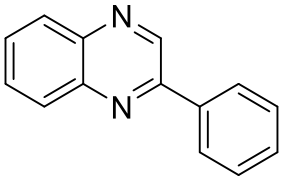

2-Phenylquinoxaline (286b): ^{1}H NMR (300 MHz, $CDCl_3$): *δ* 9.33 (s, 1H), 8.25 – 8.09 (m, 4H), 7.84 – 7.71 (m, 2H), 7.63 – 7.52 (m, 3H); **^{13}C NMR** (75 MHz, $CDCl_3$): *δ* 152.01, 143.50, 142.46, 141.73, 136.94, 130.42, 130.33, 129.77, 129.29, 129.26, 127.70; **MS (GC-MS):** *m/z* 206 [M$^+$][291]; 99% yield.

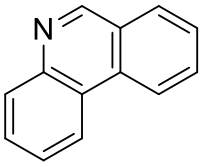

Phenanthridine (287b): ^{1}H NMR (300 MHz, $CDCl_3$): *δ* 7.73 – 7.69 (m, 1H), 7.72 – 7.63 (m, 1H), 7.34 – 7.27 (m, 2H), 7.21 (td, *J* = 7.4, 1.3 Hz, 1H), 7.17 – 7.06 (m, 2H), 6.84 (ddd, *J* = 7.8, 7.3, 1.2 Hz, 1H), 6.67 (ddd, *J* = 7.9, 1.2, 0.5 Hz, 1H); **^{13}C NMR** (75 MHz, $CDCl_3$): *δ* 145.86, 132.89, 128.95, 127.80, 127.27, 126.15, 123.74, 122.57, 120.16, 119.43, 115.26, 46.56; **MS (GC-MS):** *m/z* 179 [M$^+$][292]; 98% yield.

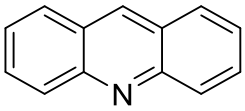

Acridine (288b): **^{1}H NMR** (300 MHz, $CDCl_3$): δ 8.73 (s, 1H), 8.24 (dd, *J* = 8.9, 1.0 Hz, 2H), 8.02 – 7.92 (m, 2H), 7.77 (ddd, *J* = 8.8, 6.6, 1.4 Hz, 2H), 7.52 (ddd, *J* = 8.5, 6.6, 1.1 Hz, 2H); **^{13}C NMR** (75 MHz, $CDCl_3$): δ 149.21, 136.11, 130.38, 129.55, 128.31, 126.70, 125.77; **MS (GC-MS):** *m/z* 179 $[M^+]$[293]; 97% yield.

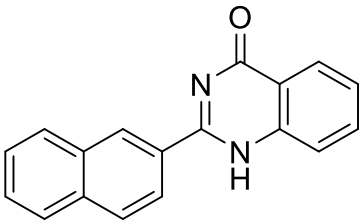

2-(Naphthalen-2-yl)quinazolin-4-one (289b): **^{1}H NMR** (300 MHz, DMSO-d_6): δ 8.38 (s, 1H), 8.10 – 7.89 (m, 4H), 7.68 (ddd, *J* = 15.3, 8.1, 1.7 Hz, 2H), 7.54 (dd, *J* = 6.2, 3.3 Hz, 2H), 7.31 – 7.22 (m, 1H), 6.81 – 6.75 (m, 1H), 6.69 (td, *J* = 7.5, 1.2 Hz, 1H); **^{13}C NMR** (75 MHz, DMSO-d_6): δ 163.59, 147.86, 138.86, 133.33, 132.99, 132.46, 128.10, 127.95, 127.56, 127.37, 126.40, 125.84, 124.82, 117.17, 114.94, 114.41; **MS (ESI-HRMS):** *m/z* calcd. for $C_{18}H_{12}N_2O$ $[M+H^+]$: 273.1022, found: 273.1020; 61% yield.

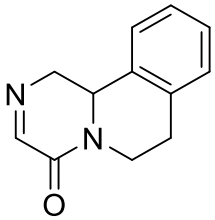

3,6,7,11*b*-Tetrahydro-4*H*-pyrazino[2,1-*a*]isoquinolin-4-one (290b): **^{1}H NMR** (300 MHz, $CDCl_3$): δ 7.91 – 7.84 (m, 1H), 7.24 – 7.15 (m, 4H), 4.74 – 4.04 (m, 2H), 3.50 – 3.00 (m, 2H), 3.00 – 2.80 (m, 2H); **^{13}C NMR** (75 MHz, $CDCl_3$): δ 157.32, 134.50, 132.19, 129.54, 127.57, 127.23, 125.79, 122.49, 56.00, 52.41, 37.38, 29.25; **MS (GC-MS):** *m/z* 200 $[M^+]$[294]; 77% yield.

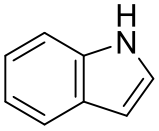

Indole (291b): **^{1}H NMR** (300 MHz, $CDCl_3$): δ 8.10 – 8.04 (m, 1H), 7.81 (ddt, *J* = 7.7, 1.5, 0.8 Hz, 1H), 7.48 (dq, *J* = 8.1, 1.0 Hz, 1H), 7.39 – 7.24 (m, 3H), 6.70 (ddd, *J* = 3.1, 2.0, 1.0 Hz, 1H); **^{13}C NMR** (75 MHz, $CDCl_3$): δ 135.89, 127.97, 124.27, 122.08, 120.84, 119.93, 111.16, 102.67; **MS (GC-MS):** *m/z* 117 $[M^+]$[295]; 79% yield.

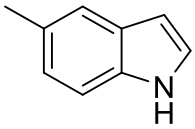

5-Methylindole (292b): ^{1}H NMR (300 MHz, $CDCl_3$): *δ* 7.96 (s, 1H), 7.49 (dd, *J* = 1.7, 0.8 Hz, 1H), 7.30 (d, *J* = 8.3 Hz, 1H), 7.20 – 7.12 (m, 1H), 7.08 (dd, *J* = 8.3, 1.6 Hz, 1H), 6.52 (ddd, *J* = 3.1, 2.1, 1.0 Hz, 1H), 2.51 (s, 3H); **^{13}C NMR** (75 MHz, $CDCl_3$): *δ* 134.22, 129.11, 128.25, 124.35, 123.72, 120.45, 110.78, 102.19, 21.55; **MS (GC-MS):** *m/z* 131 $[M^+]$[296]; 96% yield.

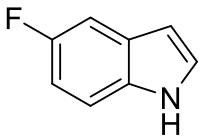

5-Fluoroindole (293b): ^{1}H NMR (300 MHz, $CDCl_3$): *δ* 8.12 (s, 1H), 7.36 – 7.23 (m, 3H), 7.01 – 6.93 (m, 1H), 6.54 (ddd, *J* = 3.1, 2.1, 0.9 Hz, 1H); **^{13}C NMR** (75 MHz, $CDCl_3$): *δ* 159.65, 156.55, 132.45, 128.40, 128.27, 126.02, 111.76, 111.63, 110.71, 110.36, 105.71, 105.40, 102.96, 102.90, **MS (GC-MS):** *m/z* 135 $[M^+]$[101]; 93% yield.

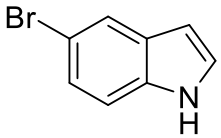

5-Bromoindole (294b): ^{1}H NMR (300 MHz, $CDCl_3$): *δ* 8.14 (s, 1H), 7.81 – 7.76 (m, 1H), 7.34 – 7.18 (m, 3H), 6.51 (ddd, *J* = 3.1, 2.1, 0.8 Hz, 1H); **^{13}C NMR** (75 MHz, $CDCl_3$): *δ* 134.52, 129.76, 125.48, 124.98, 123.34, 113.16, 112.56, 102.45; **MS (GC-MS):** *m/z* 195 $[M^+]$[297]; 91% yield.

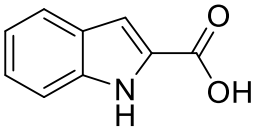

Indole-2-carboxylic acid (295b): ^{1}H NMR (300 MHz, $CDCl_3$): *δ* 8.91 (s, 1H), 7.78 – 7.68 (m, 1H), 7.48 – 7.43 (m, 1H), 7.41 – 7.33 (m, 2H), 7.25 – 7.13 (m, 1H); **^{13}C NMR** (75 MHz, $CDCl_3$): *δ* 166.05, 137.30, 127.48, 126.12, 126.07, 122.90, 121.10, 111.96, 110.87; **MS (GC-MS):** *m/z* 161 $[M^+]$[296]; 91% yield.

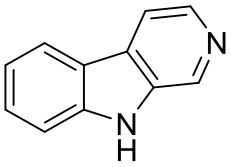

Pyrido[3,4-*b*]indole (296b): ^{1}H NMR (300 MHz, $CDCl_3$): *δ* 8.97 (s, 1H), 8.56 (s, 1H), 8.47 (d, *J* = 5.3 Hz, 1H), 8.15 (d, *J* = 7.9 Hz, 1H), 7.99 (dd, *J* = 5.3, 1.1 Hz, 1H), 7.63 – 7.51 (m, 2H), 7.32 (ddd, *J* = 8.0, 6.3, 1.8 Hz, 1H); **^{13}C NMR** (126 MHz, $CDCl_3$): *δ* 140.85, 138.31, 135.92, 133.21, 129.58, 129.05, 122.03, 121.46, 120.51, 115.02, 111.88; **MS (GC-MS):** *m/z* 168 $[M^+]$[298]; 78% yield.

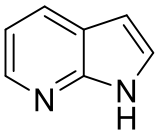

Pyrrolo[2,3-*b*]pyridine (297b): ^{1}H NMR (300 MHz, $CDCl_3$): *δ* 11.86 (s, 1H), 8.38 (dd, *J* = 4.8, 1.6 Hz, 1H), 7.99 (dd, *J* = 7.8, 1.6 Hz, 1H), 7.42 (d, *J* = 3.5 Hz, 1H), 7.11 (dd, *J* = 7.8, 4.8 Hz, 1H), 6.53 (d, *J* = 3.5 Hz, 1H); **^{13}C NMR** (75 MHz, $CDCl_3$): *δ* 149.04, 142.36, 129.16, 125.50, 120.72, 115.81, 100.64; **MS (GC-MS):** *m/z* 118 $[M^+]$[299]; 97% yield.

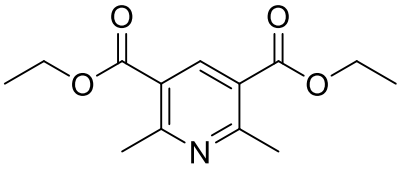

Diethyl 2,6-dimethylpyridine-3,5-dicarboxylate (298b): ^{1}H NMR (300 MHz, $CDCl_3$): *δ* 8.66 (s, 1H), 4.38 (q, *J* = 7.1 Hz, 4H), 2.83 (s, 6H), 1.40 (t, *J* = 7.1 Hz, 6H); **^{13}C NMR** (75 MHz, $CDCl_3$): *δ* 166.09, 162.34, 141.02, 123.20, 61.53, 25.09, 14.41; **MS (GC-MS):** *m/z* 251 $[M^+]$[300]; 99% yield.

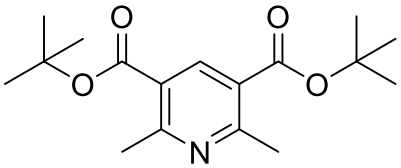

Di-*tert*-butyl-2,6-dimethylpyridine-3,5-dicarboxylate (299b): ^{1}H NMR (300 MHz, $CDCl_3$): *δ* 8.52 (s, 1H), 2.80 (s, 6H), 1.61 (s, 18H); **^{13}C NMR** (75 MHz, $CDCl_3$): *δ* 175.17, 161.28, 140.90, 124.79, 82.25, 28.37, 25.13; **MS (GC-MS):** *m/z* 307 $[M^+]$[301]; 95% yield.

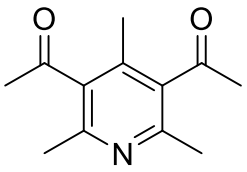

1,1'-(2,4,6-Trimethylpyridine-3,5-diyl)bis(ethan-1-one) (300b): ^{1}H NMR (300 MHz, $CDCl_3$): *δ* 2.49 (s, 6H), 2.43 (s, 6H), 2.11 (s, 3H); **^{13}C NMR** (75 MHz, $CDCl_3$): *δ* 205.91, 152.01, 137.60, 135.69, 32.38, 22.61, 16.10; **MS (GC-MS):** *m/z* 205 $[M^+]$[302]; 98% yield.

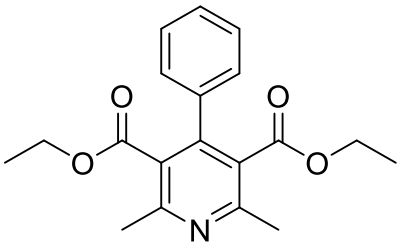

Diethyl-2,6-dimethyl-4-phenylpyridine-3,5-dicarboxylate (301b): ^{1}H NMR (300 MHz, $CDCl_3$): *δ* 7.41 – 7.30 (m, 3H), 7.30 – 7.20 (m, 2H), 3.99 (q, *J* = 7.1 Hz, 4H), 2.60 (s, 6H), 0.89 (t, *J* = 7.1 Hz, 6H); **^{13}C NMR** (75 MHz, $CDCl_3$): *δ* 167.99, 155.54, 146.23, 136.72, 128.52, 128.23, 128.18, 127.05, 61.44, 23.04, 13.67; **MS (GC-MS):** *m/z* 327 $[M^+]$[303]; 99% yield.

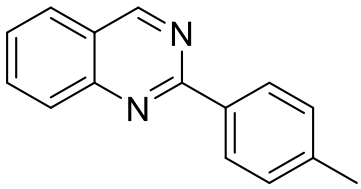

2-*p*-Tolylquinazoline (329b): ^{1}H NMR (300 MHz, $CDCl_3$): *δ* 9.47 (s, 1H), 8.55 – 8.52 (m, 2H), 8.11 – 8.07 (m, 1H), 7.95 – 7.89 (m, 2H), 7.64 – 7.59 (m, 1H), 7.38 – 7.34 (m, 2H), 2.47 (s, 3H); **^{13}C NMR** (75 MHz, $CDCl_3$): *δ* 161.29, 160.55, 150.95, 140.99, 135.47, 134.15, 129.54, 128.70, 128.67, 128.67, 127.24, 127.15, 123.66, 21.65; **MS (GC-MS)**: *m/z* 220 $[M^+]$[304]; 88% yield.

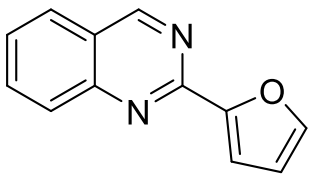

2-(Furan-2-yl)quinazoline (330b): ^{1}H NMR (300 MHz, $CDCl_3$): *δ* 9.41(s, 1H), 8.14 – 8.10 (m, 1H), 7.95 – 7.90 (m, 2H), 7.72 – 7.71 (m, 1H), 7.65 – 7.60 (m, 1H), 7.47 – 7.49 (m, 1H), 6.65 – 6.63 (m, 1H); **^{13}C NMR** (75 MHz, $CDCl_3$): *δ* 160.7, 150.5,

145.3, 134.5, 128.4, 127.3, 123.4, 114.1, 112.3; **MS (GC-MS)**: *m/z* 196 $[M^+]$[304]; 86% yield.

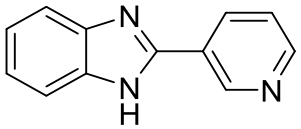

2-(Pyridin-3-yl)benzimidazole (331b): ^{1}H NMR (300 MHz, $CDCl_3$): *δ* 9.07 – 9.06 (m, 1H), 8.72 – 8.69 (m, 1H), 8.31 – 8.28 (m, 1H), 7.45 – 7.40 (m, 1H), 7.15 – 7.10 (m, 2H), 6.83 – 6.76 (m, 2H); **^{13}C NMR** (75 MHz, $CDCl_3$): *δ* 153.99, 151.72, 150.72, 142.73, 136.34, 134.84, 132.18, 128.51, 123.79, 118.47, 117.03, 115.69; **MS (GC-MS)**: *m/z* 195 $[M^+]$[305]; 91% yield.

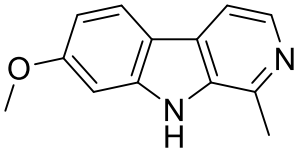

Harmine (332b): ^{1}H NMR (300 MHz, $CDCl_3$): *δ* 8.15 (s, 1H), 7.47 (dd, *J* = 8.6, 0.7 Hz, 2H), 7.01 – 6.72 (m, 3H), 3.86 (s, 3H), 2.35 (s, 3H); **^{13}C NMR** (126 MHz, DMSO-d_6): *δ* 157.12, 156.72, 137.48, 128.51, 120.35, 119.39, 114.53, 110.20, 94.55, 55.14, 47.61, 22.01; **MS (ESI-HRMS):** *m/z* calcd. for $C_{13}H_{12}N_2O$ $[M+H^+]$: 213.1022, found: 213.1024; yield: 71% (CO_2 balloon), 45% (0.2 eq CO_2, 16 h), 54% (0.2 eq CO_2, 24 h), 58% (0.2 eq CO_2, 40 h).

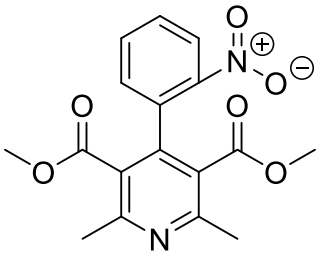

Dehydronifedipine (333b): ^{1}H NMR (300 MHz, $CDCl_3$): *δ* 7.49 – 7.28 (m, 4H), 2.49 (s, 6H), 2.43 (s, 6H); **^{13}C NMR (75 MHz, $CDCl_3$):** *δ* 164.49, 130.74, 130.50, 129.70, 126.88, 52.19, 33.31; **MS (ESI-HRMS):** *m/z* calcd. for $C_{17}H_{16}N_2O_6$ $[M+H^+]$: 345.1081, found: 345.1078; yield: 84% (CO_2 balloon), 72% (0.2 eq CO_2, 16 h), 74% (0.2 eq CO_2, 24 h).

5.5 NMR Spectra of the Products

2b

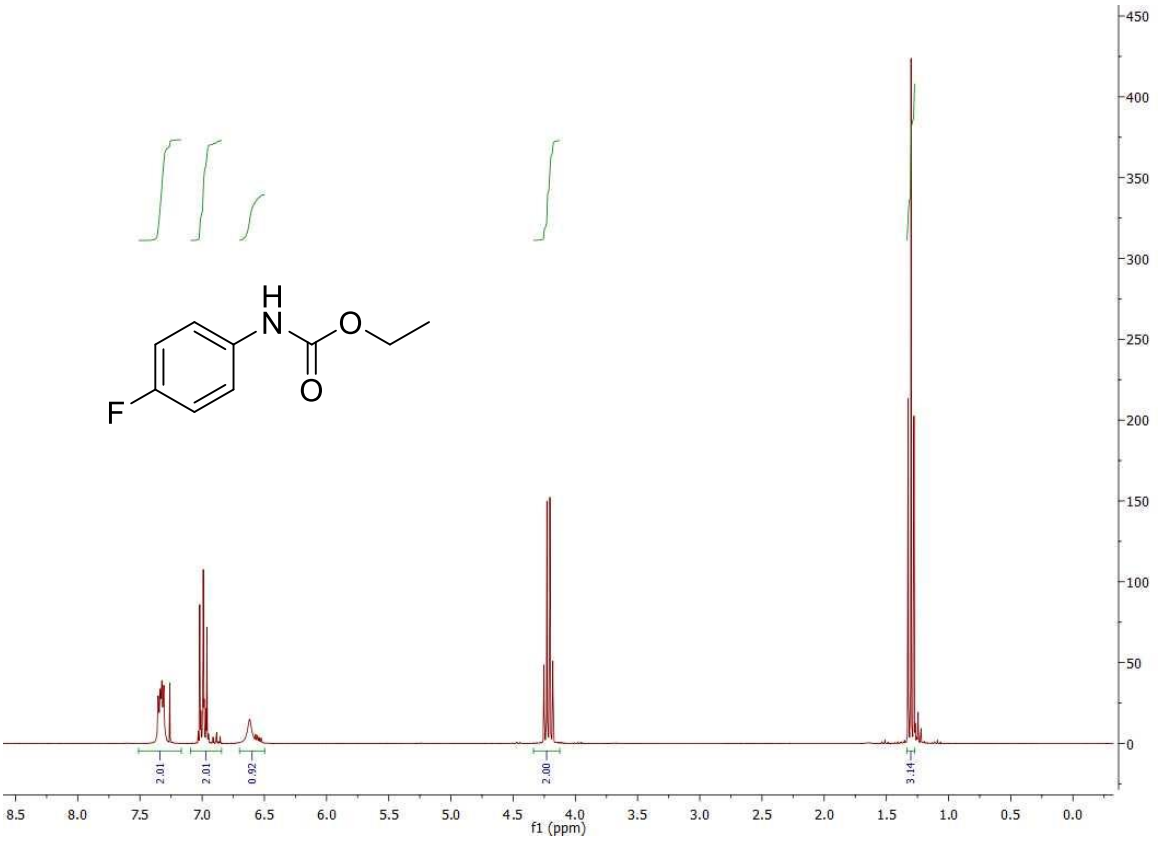

^{1}H NMR spectrum in $CDCl_3$.

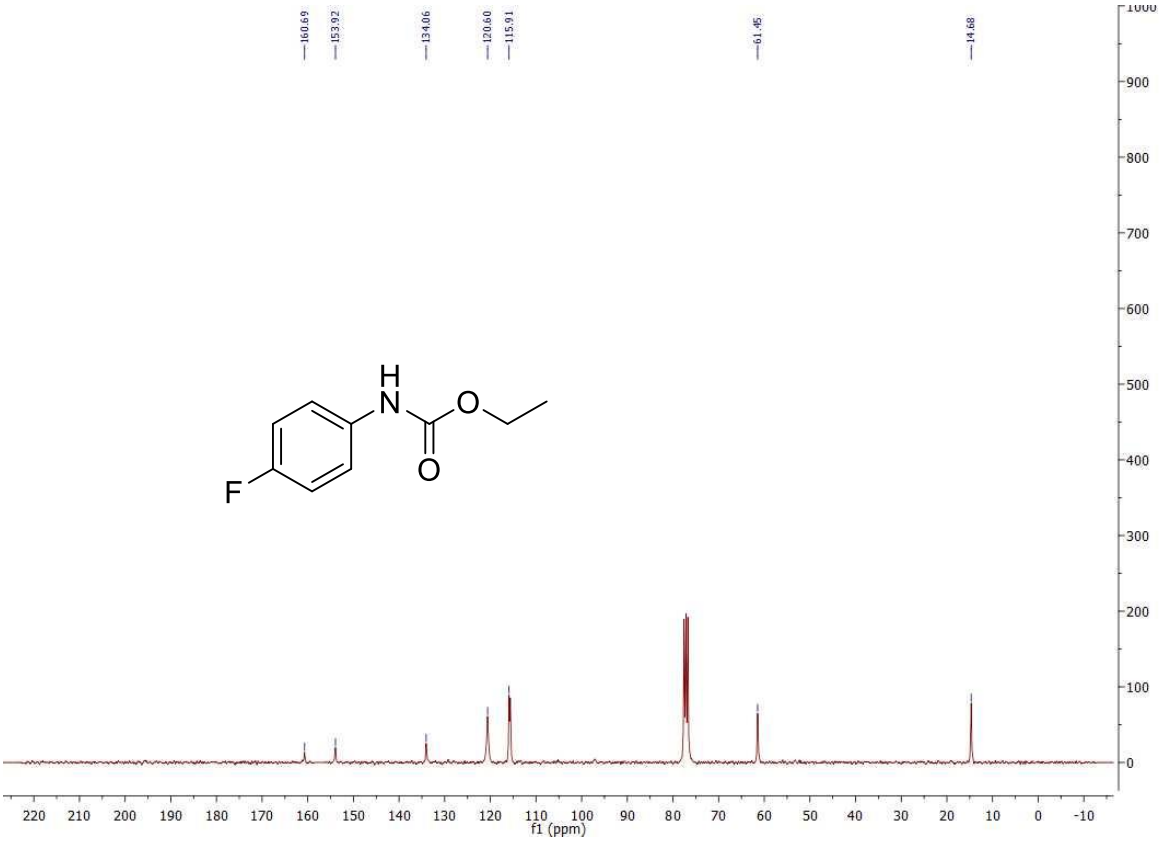

^{13}C NMR spectrum in $CDCl_3$.

3b

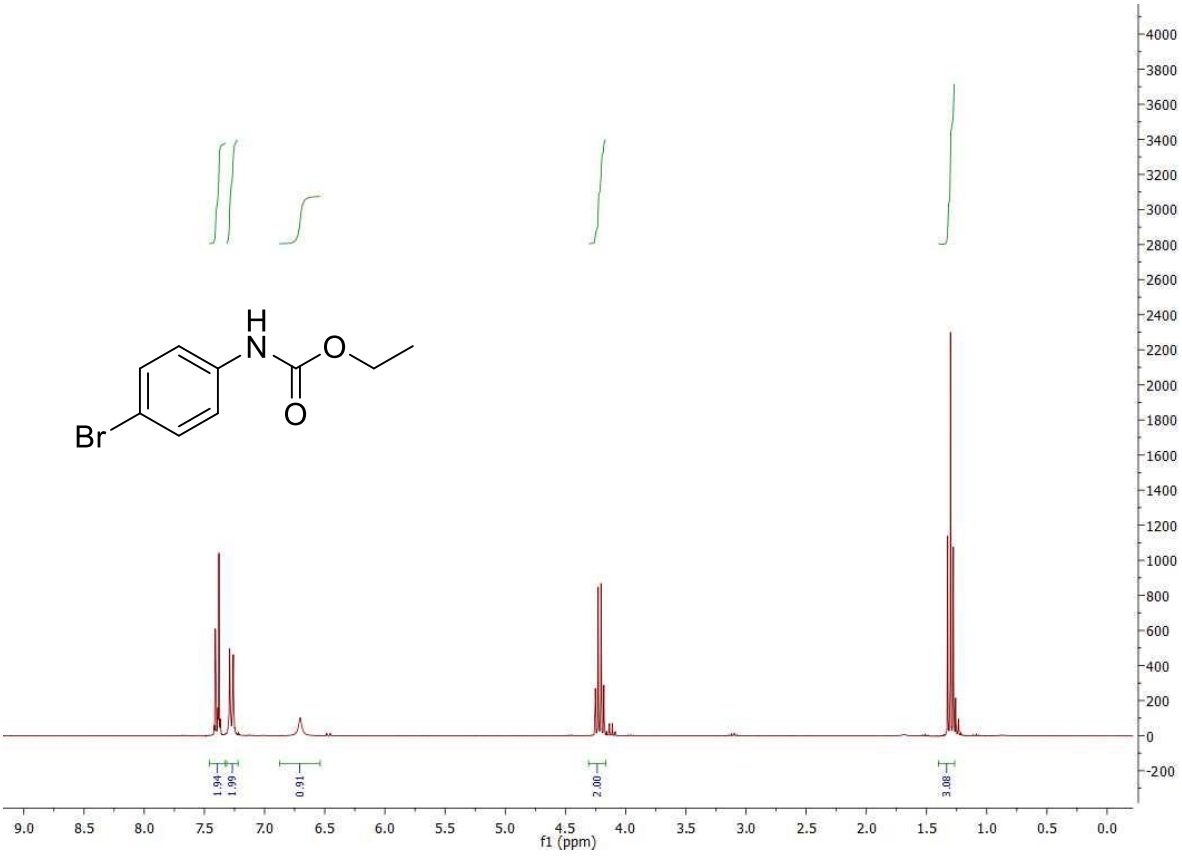

^{1}H NMR spectrum in $CDCl_3$.

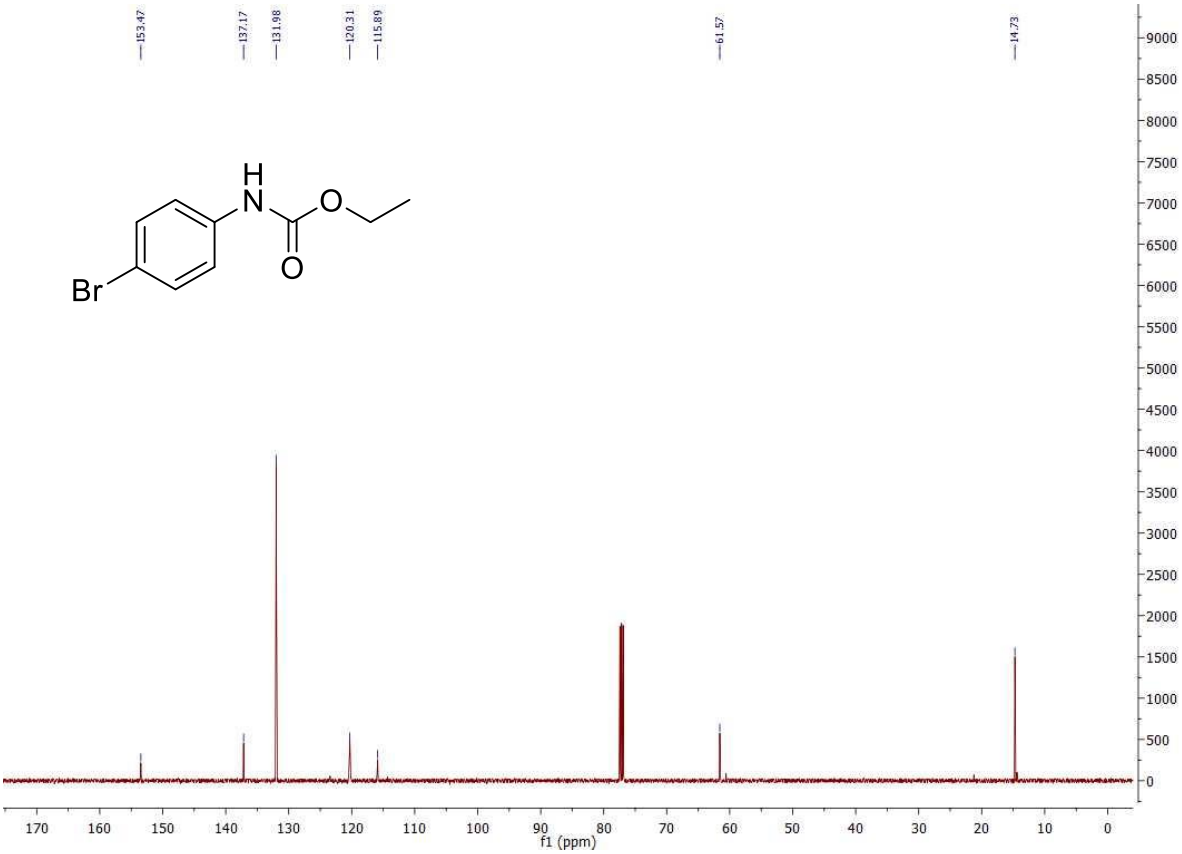

^{13}C NMR spectrum in $CDCl_3$.

4b

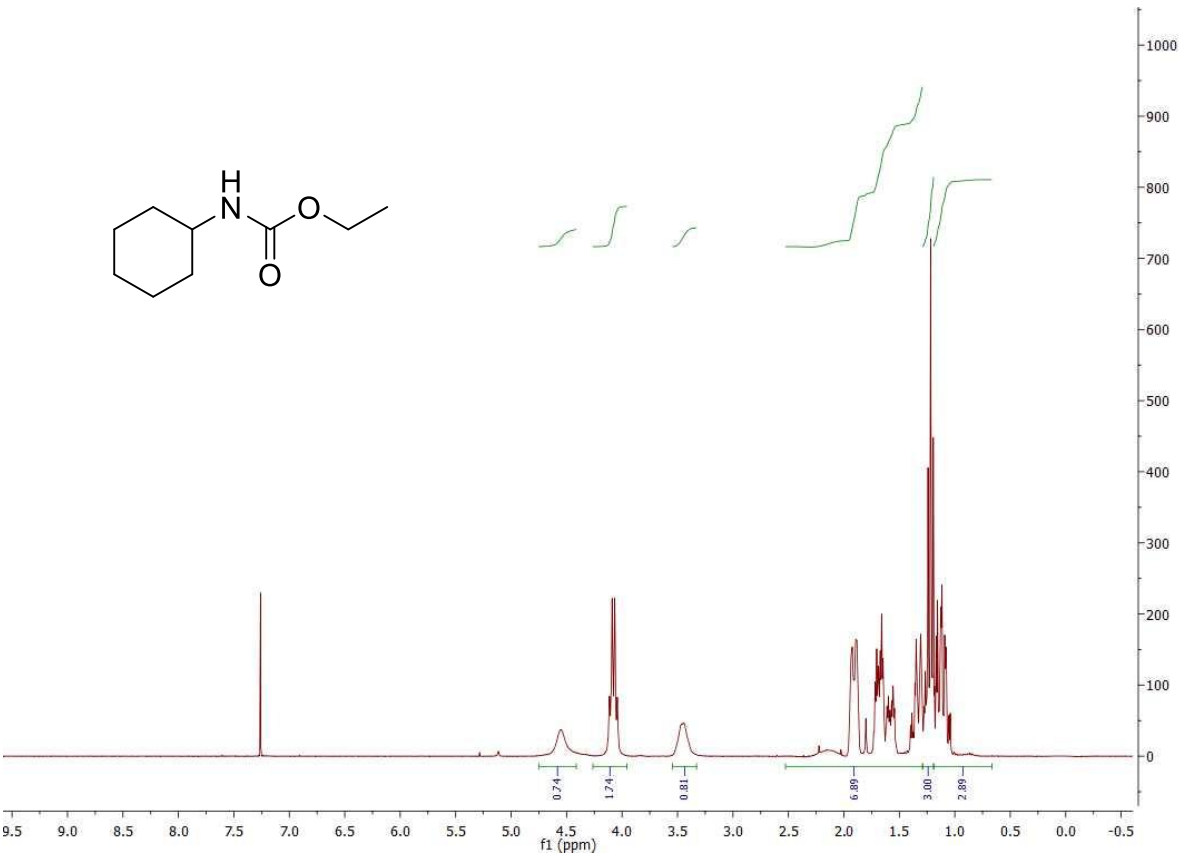

^{1}H NMR spectrum in $CDCl_3$.

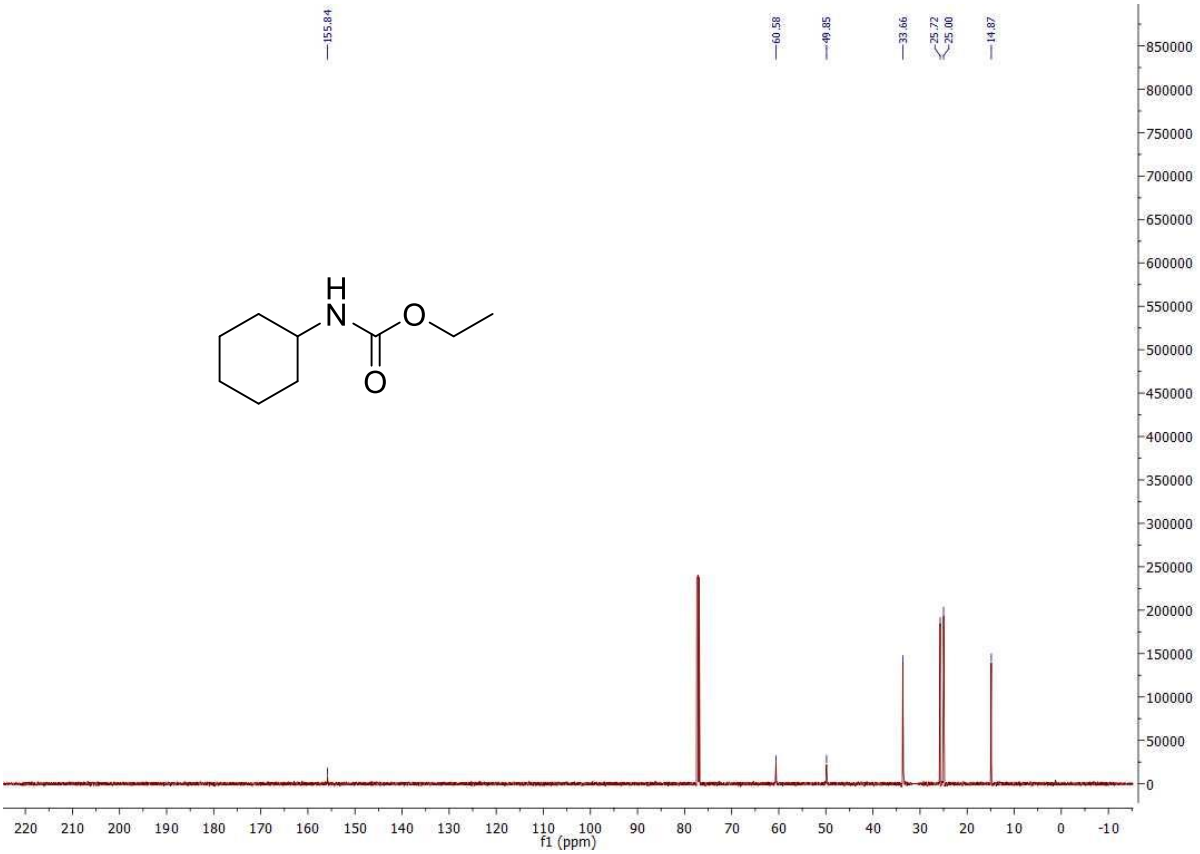

^{13}C NMR spectrum in $CDCl_3$.

5b

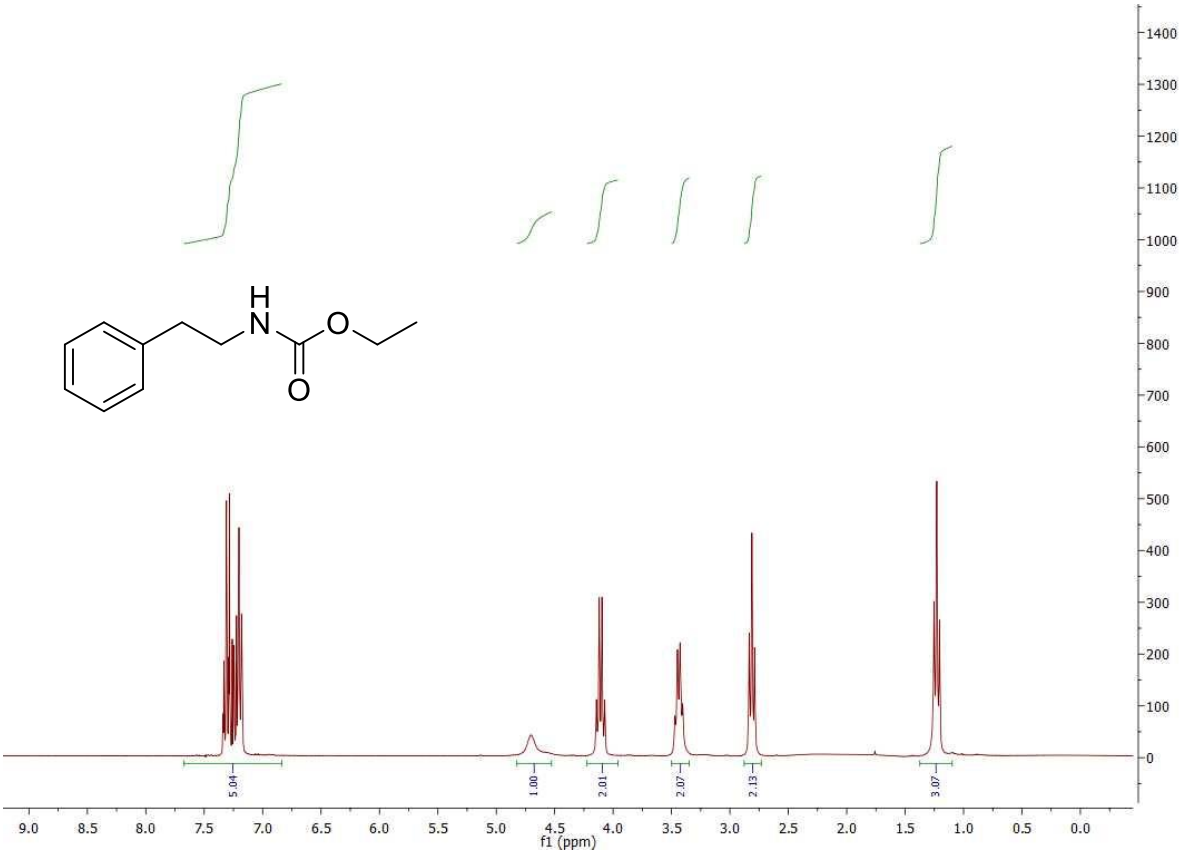

^{1}H NMR spectrum in $CDCl_3$.

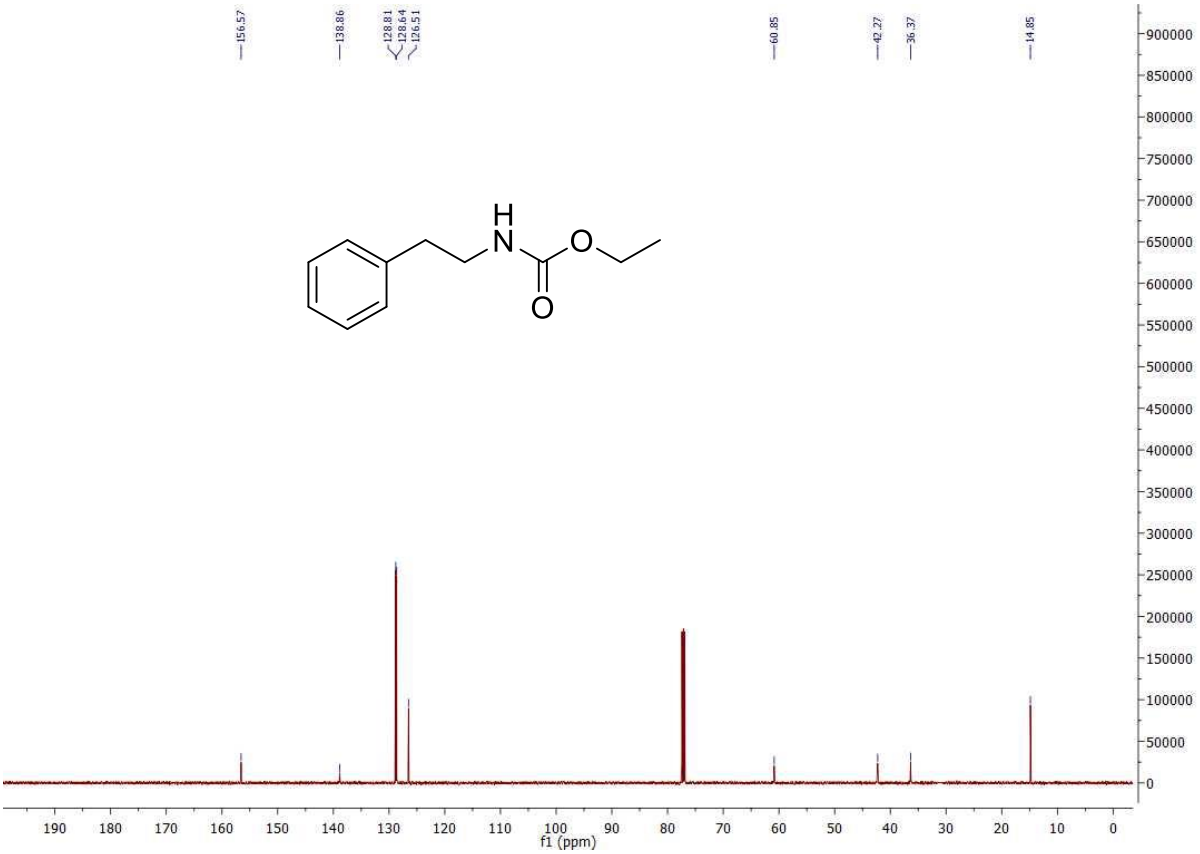

^{13}C NMR spectrum in $CDCl_3$.

6b

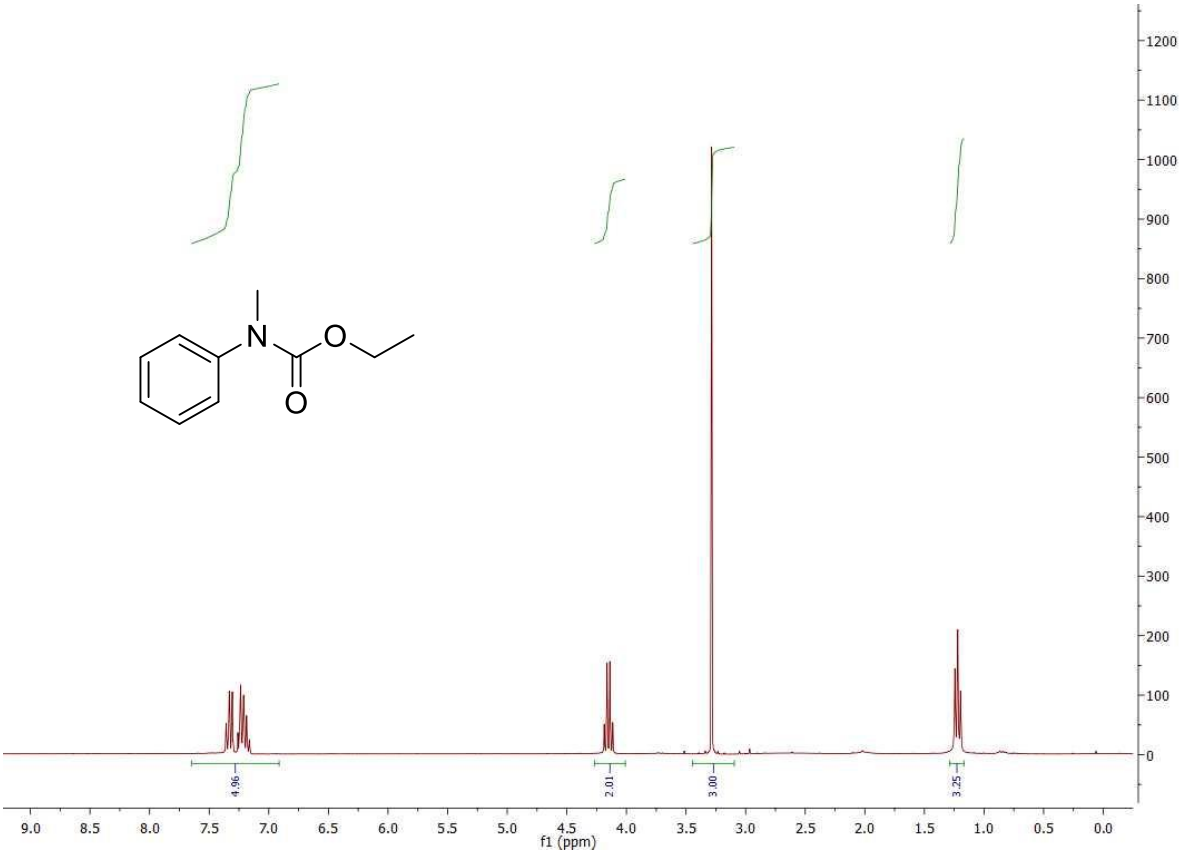

^{1}H NMR spectrum in $CDCl_3$.

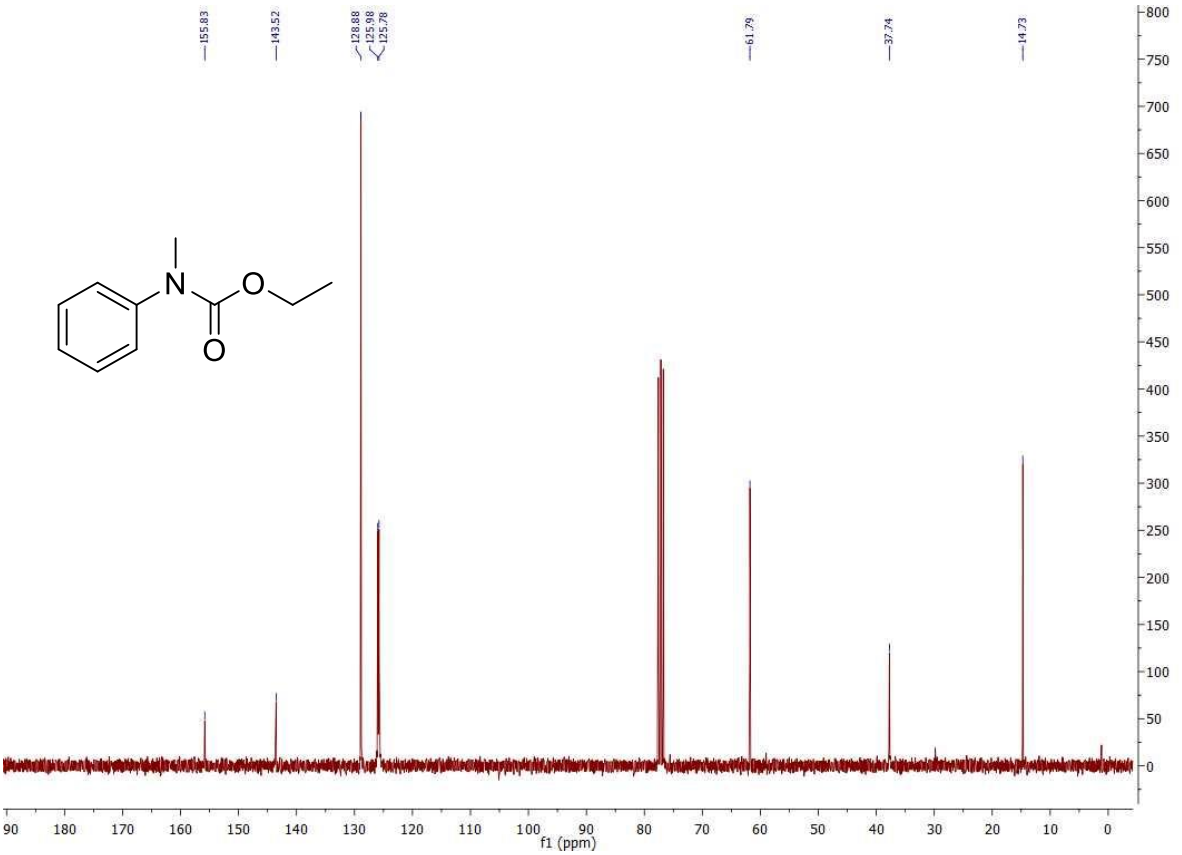

^{13}C NMR spectrum in $CDCl_3$.

7b

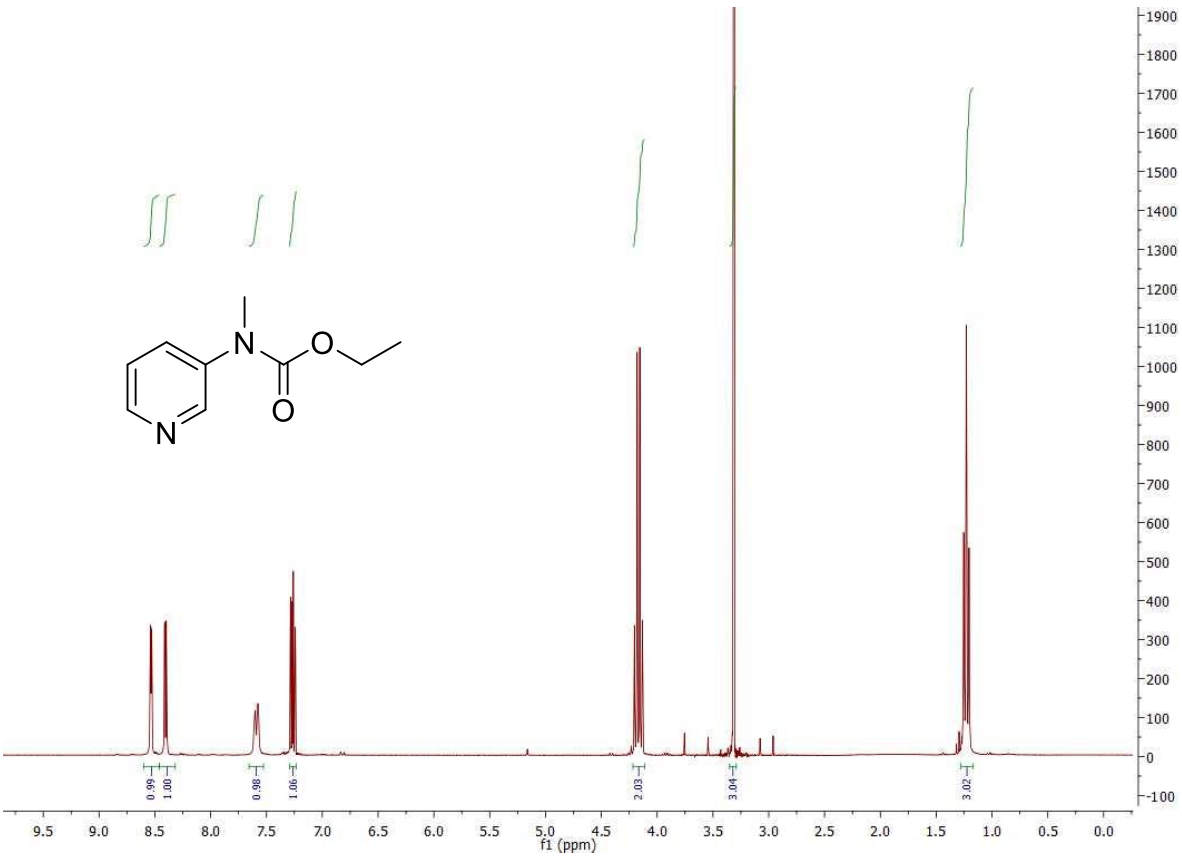

^{1}H NMR spectrum in $CDCl_3$.

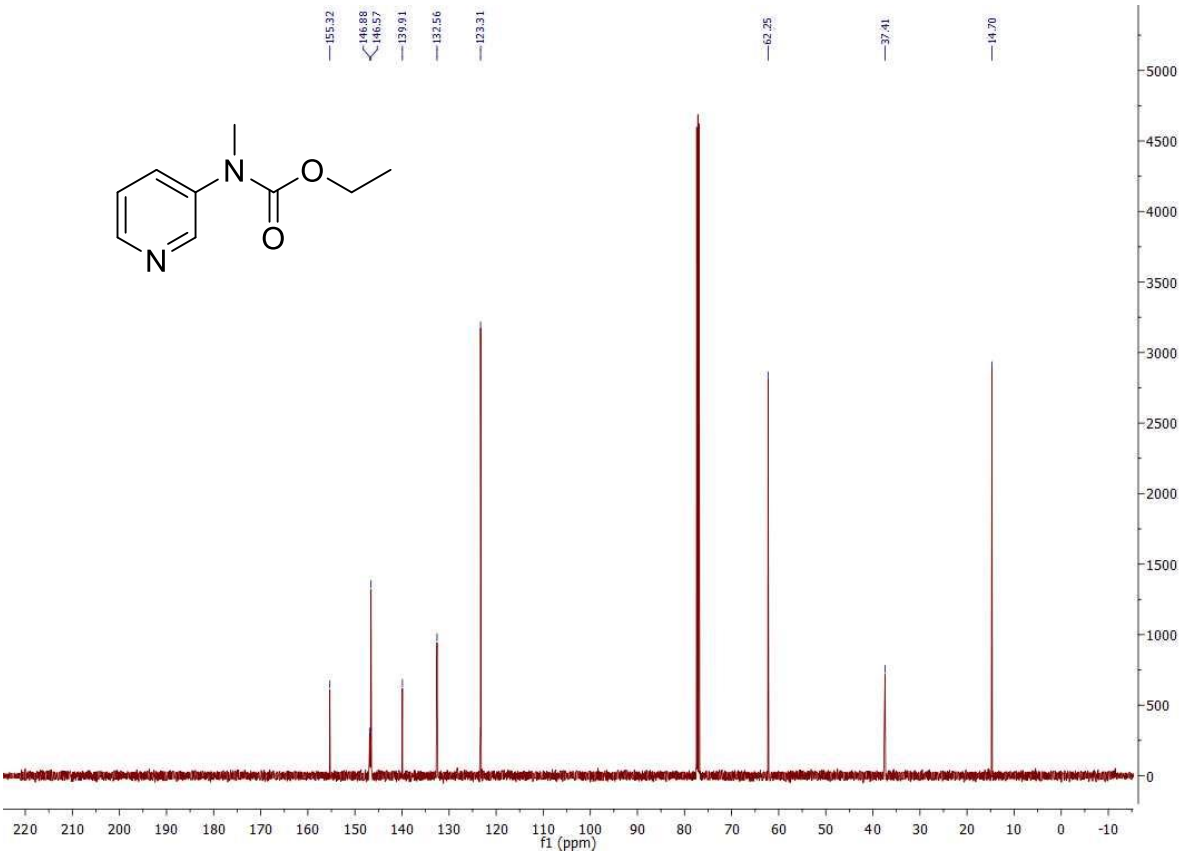

^{13}C NMR spectrum in $CDCl_3$.

8b

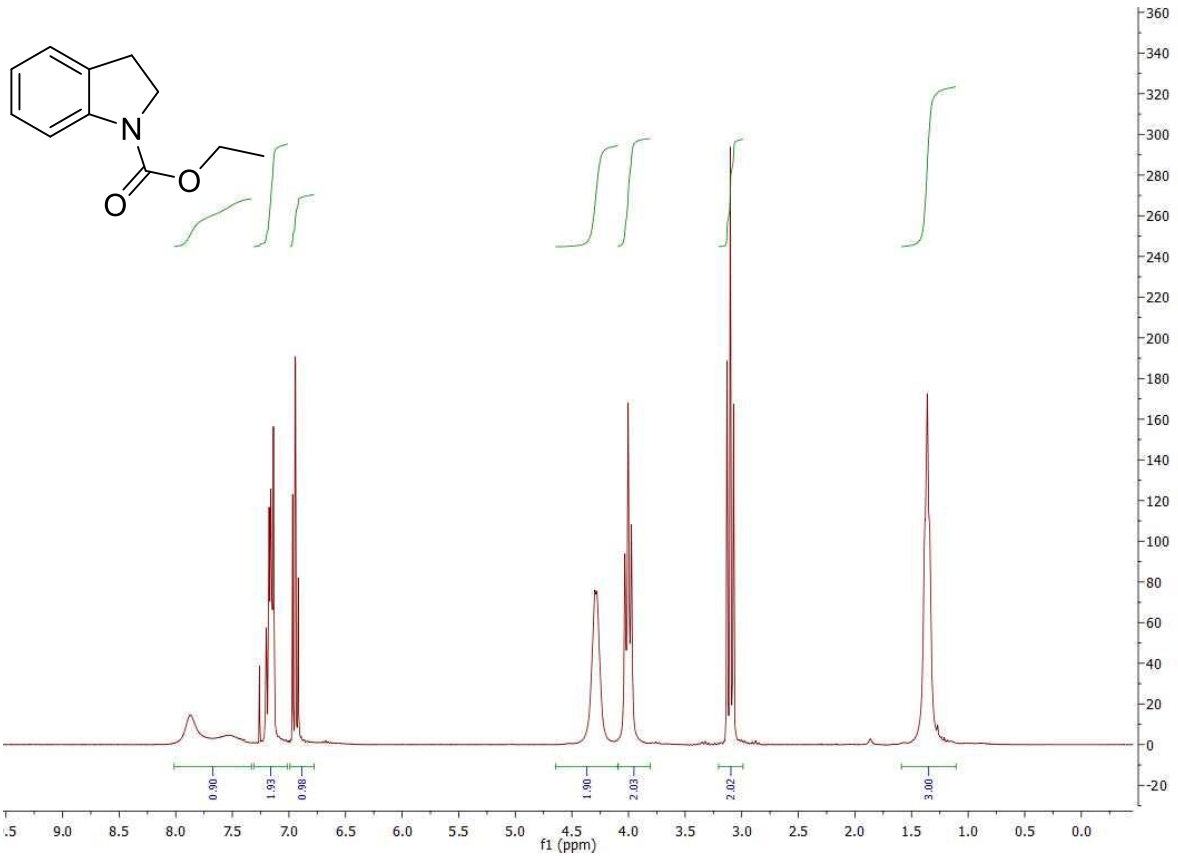

^{1}H NMR spectrum in $CDCl_3$.

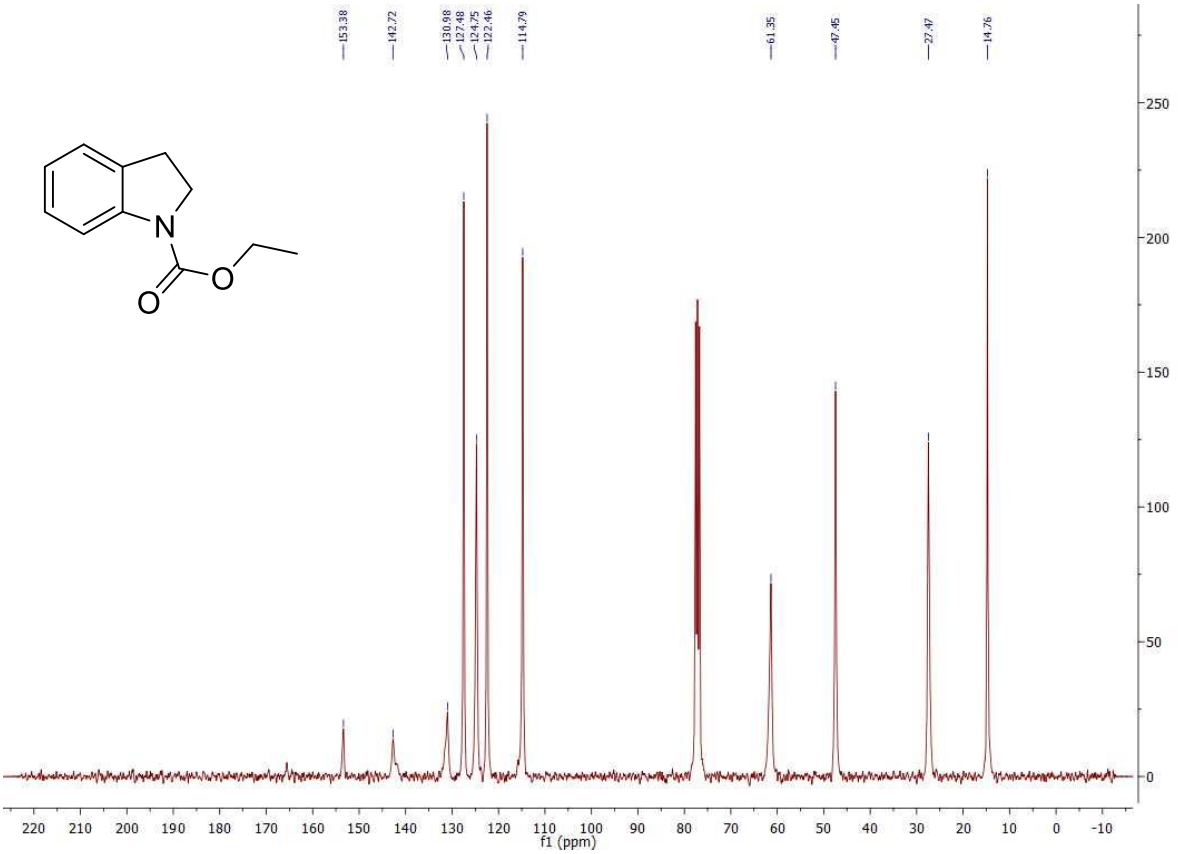

^{13}C NMR spectrum in $CDCl_3$.

9b

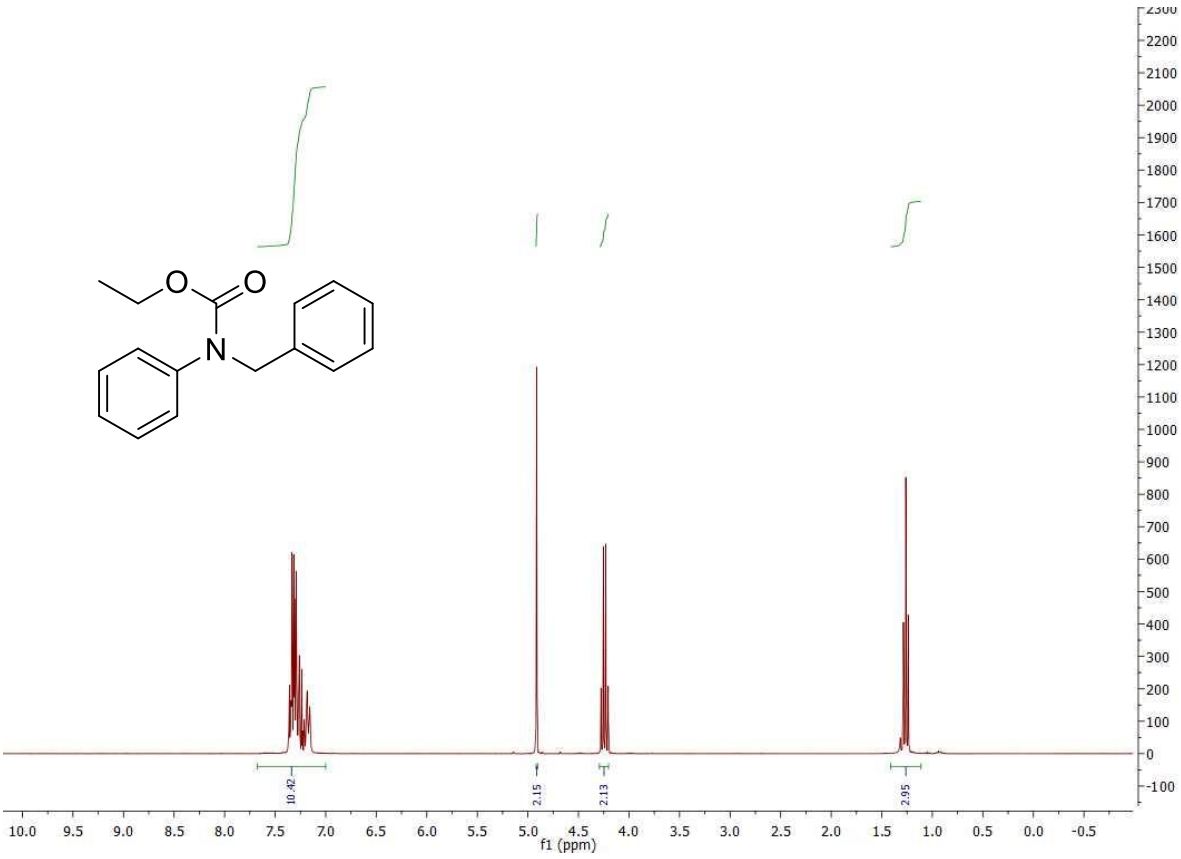

^{1}H NMR spectrum in $CDCl_3$.

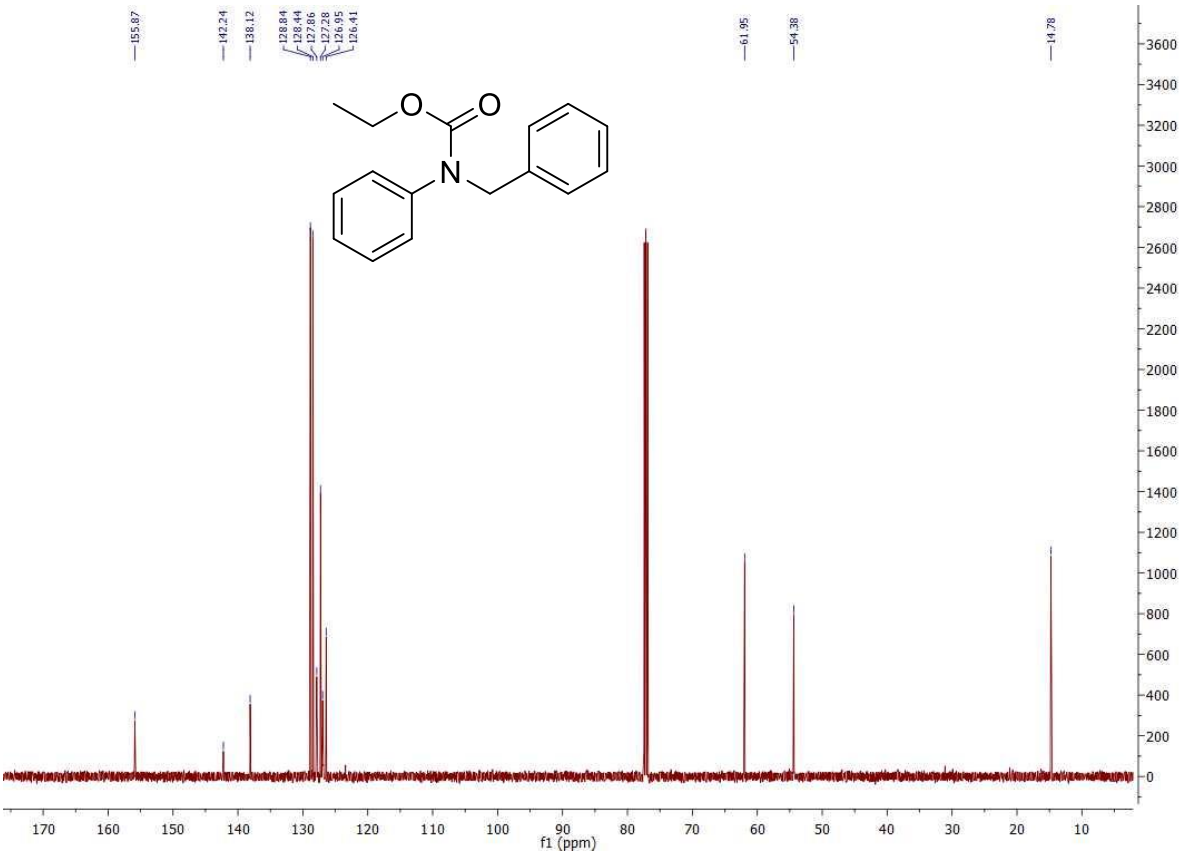

^{13}C NMR spectrum in $CDCl_3$.

10b

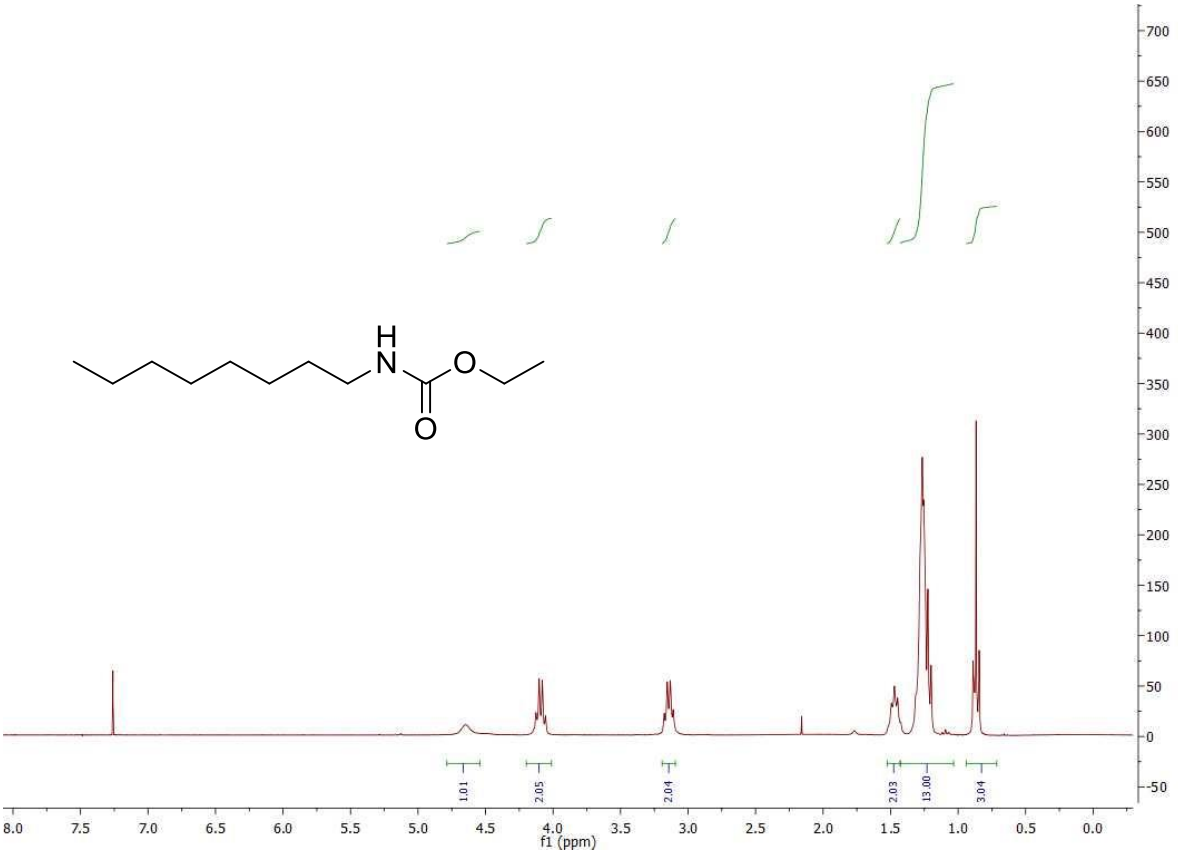

^{1}H NMR spectrum in $CDCl_3$.

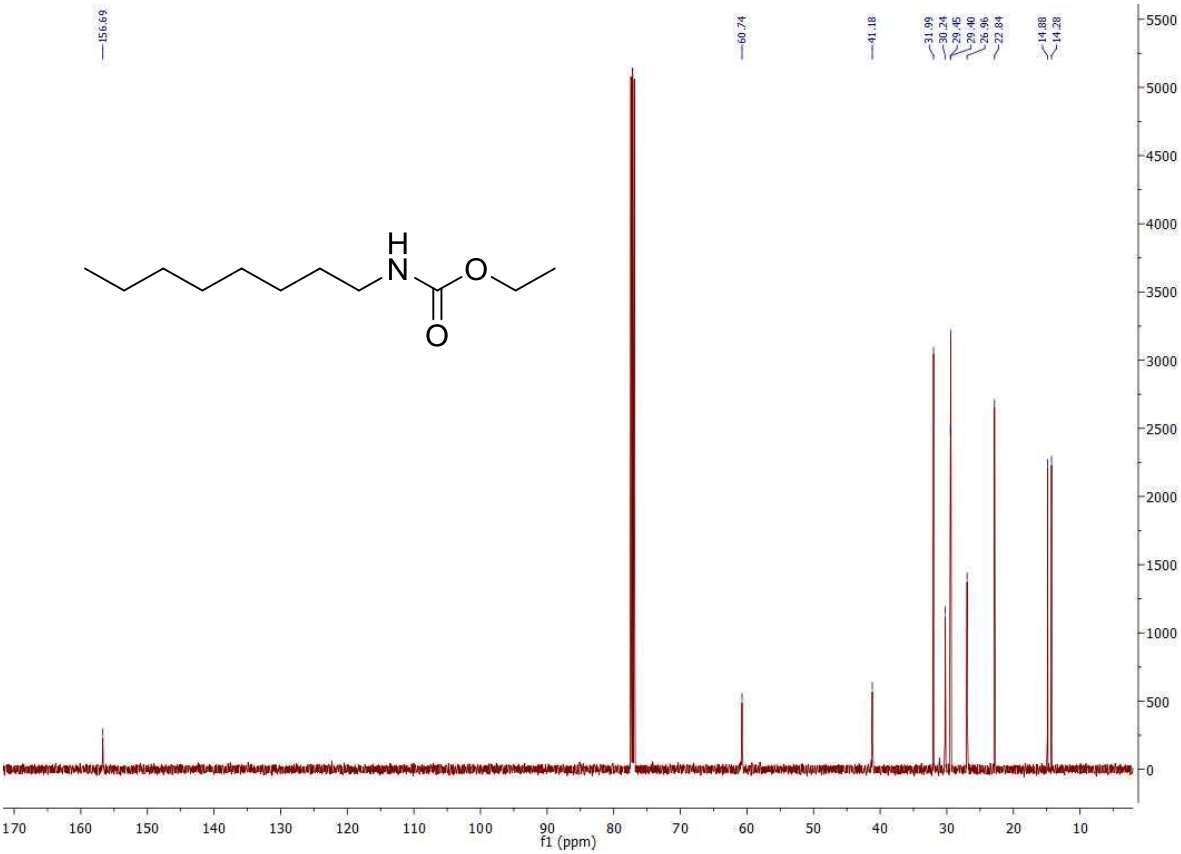

^{13}C NMR spectrum in $CDCl_3$.

11b

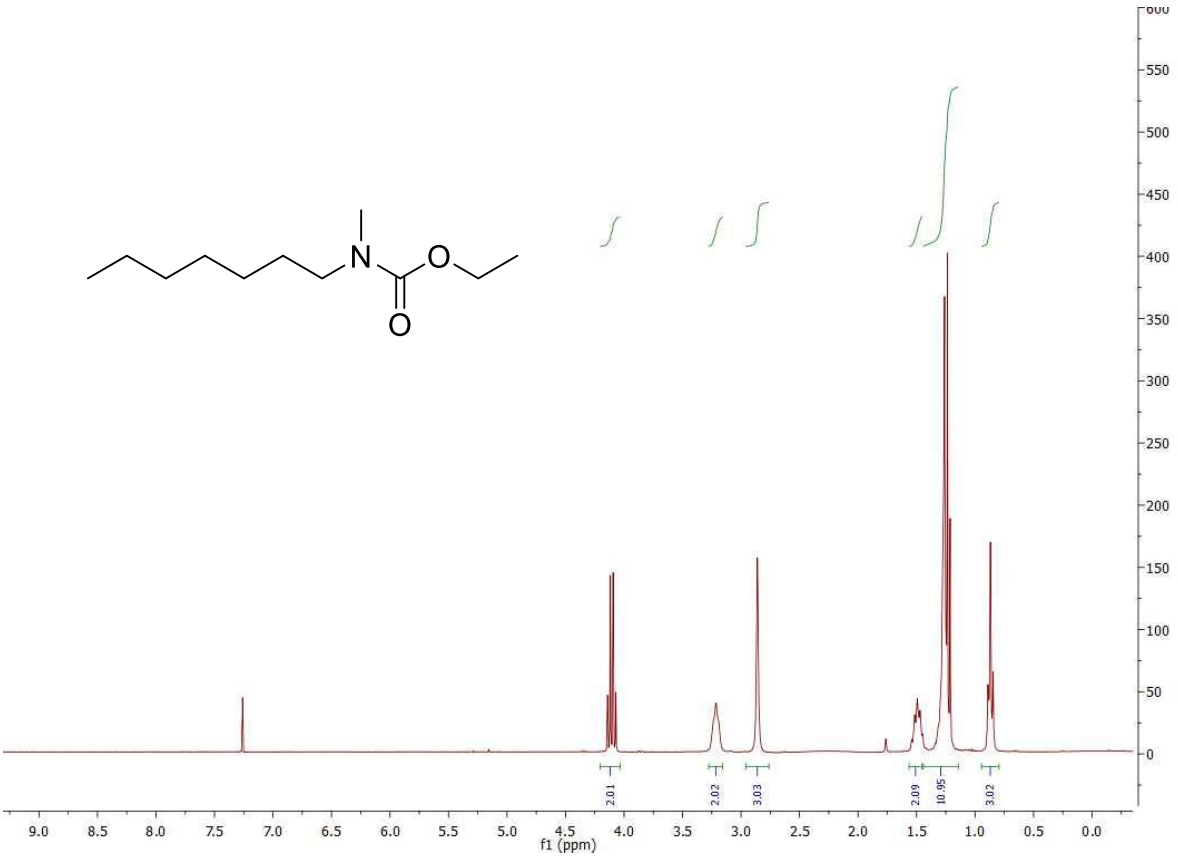

^{1}H NMR spectrum in $CDCl_3$.

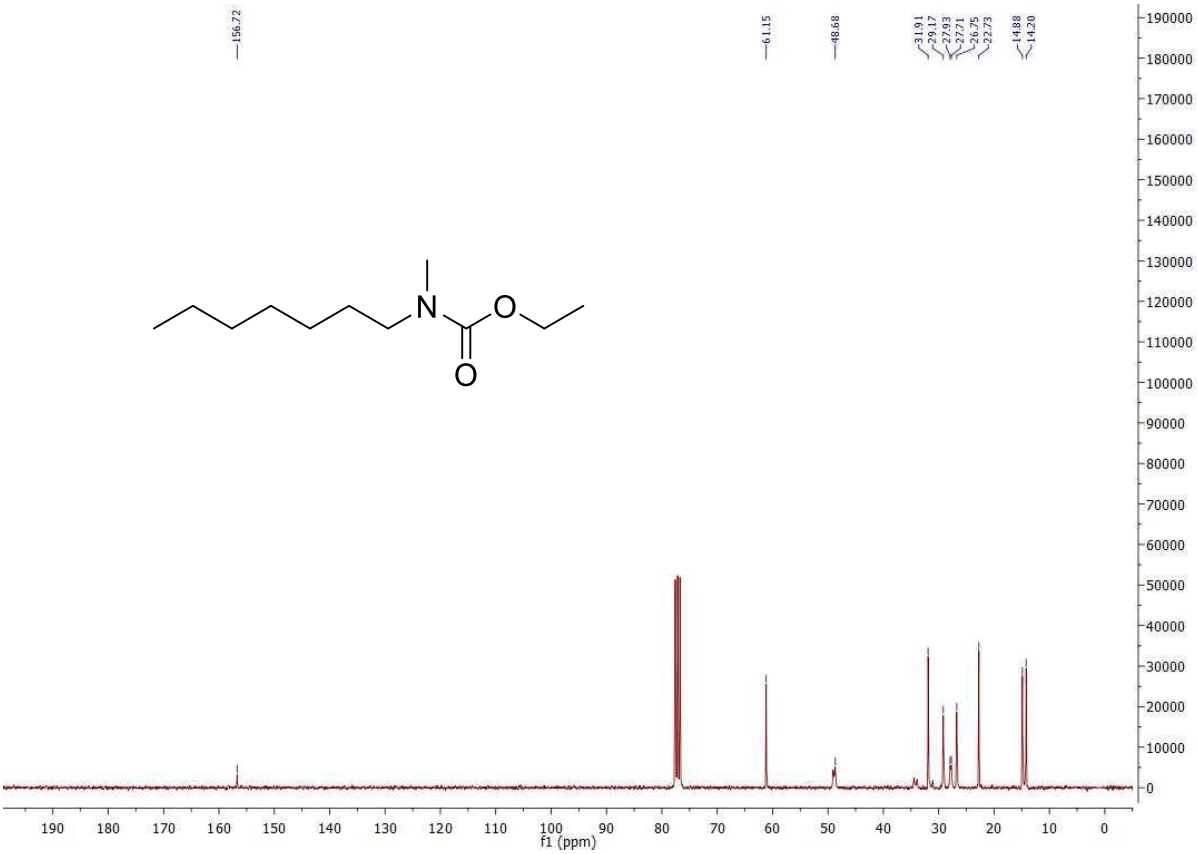

^{13}C NMR spectrum in $CDCl_3$.

12b

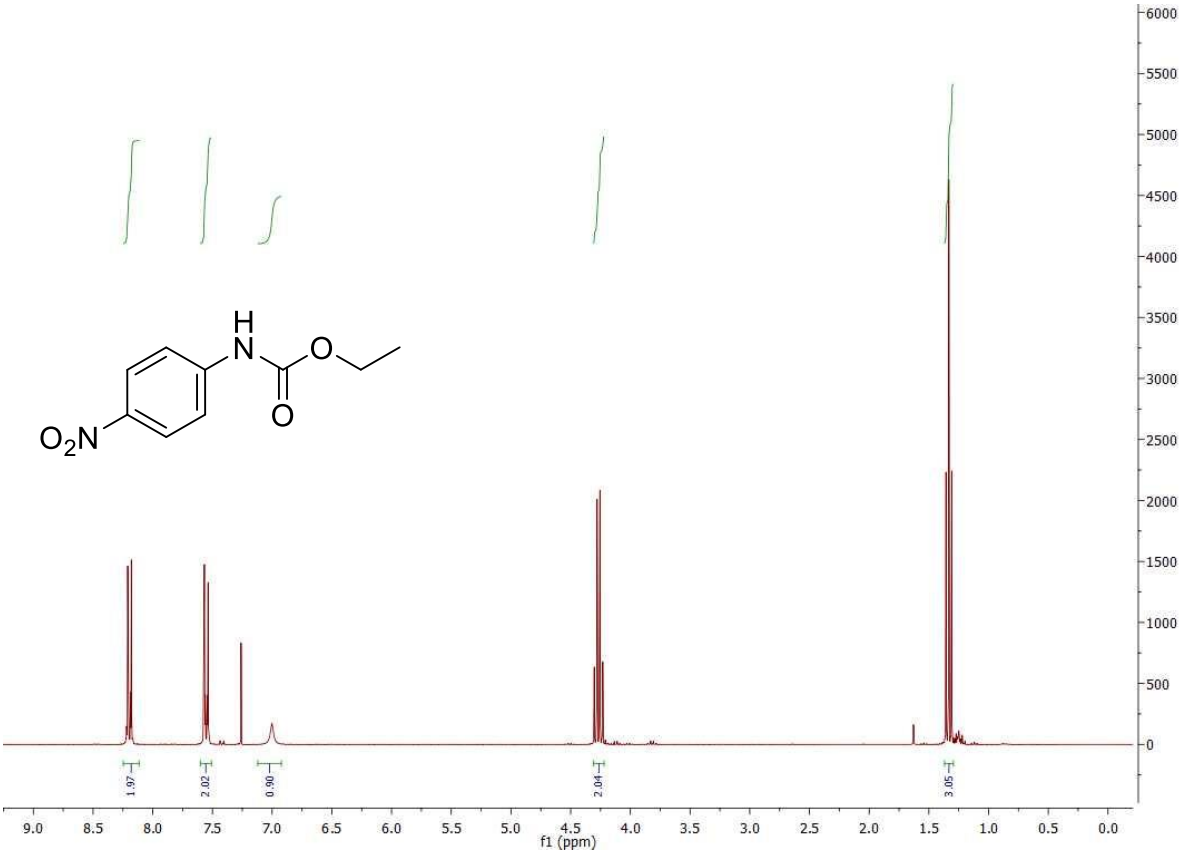

^{1}H NMR spectrum in $CDCl_3$.

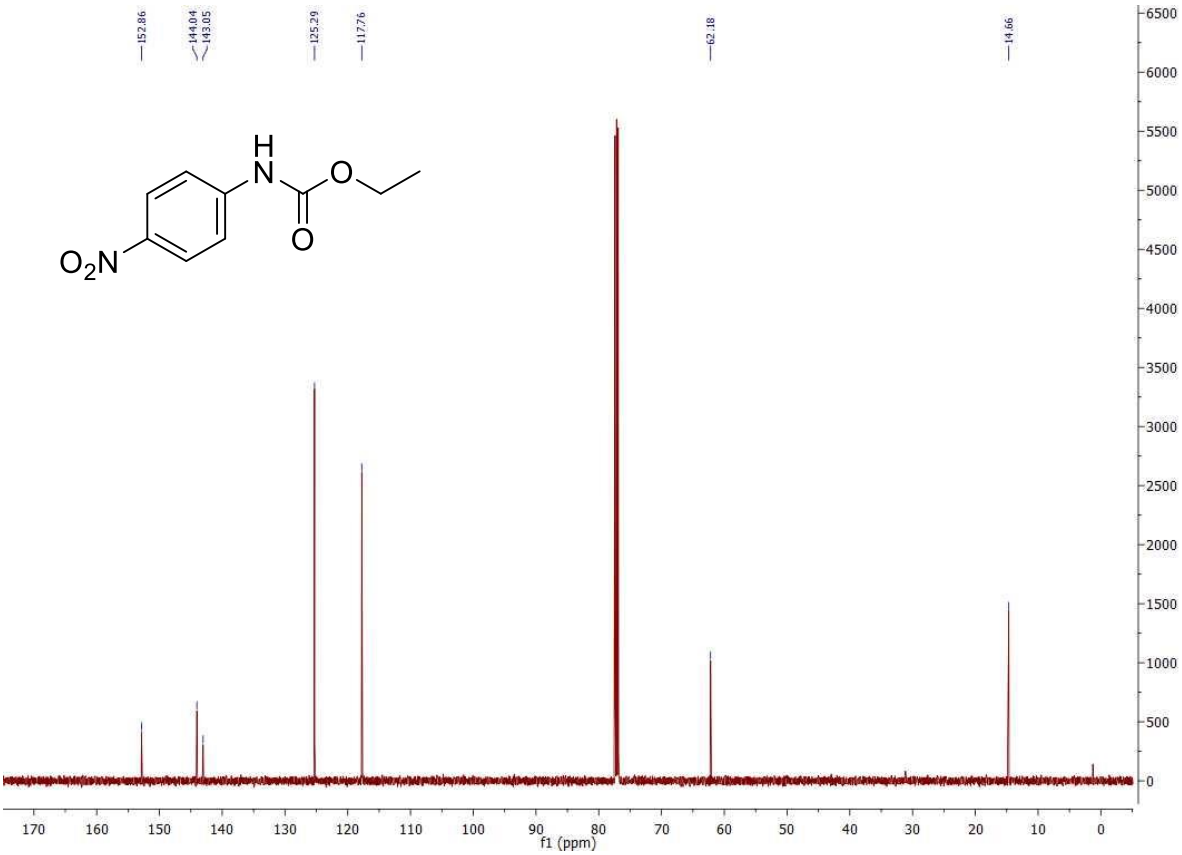

^{13}C NMR spectrum in $CDCl_3$.

13b

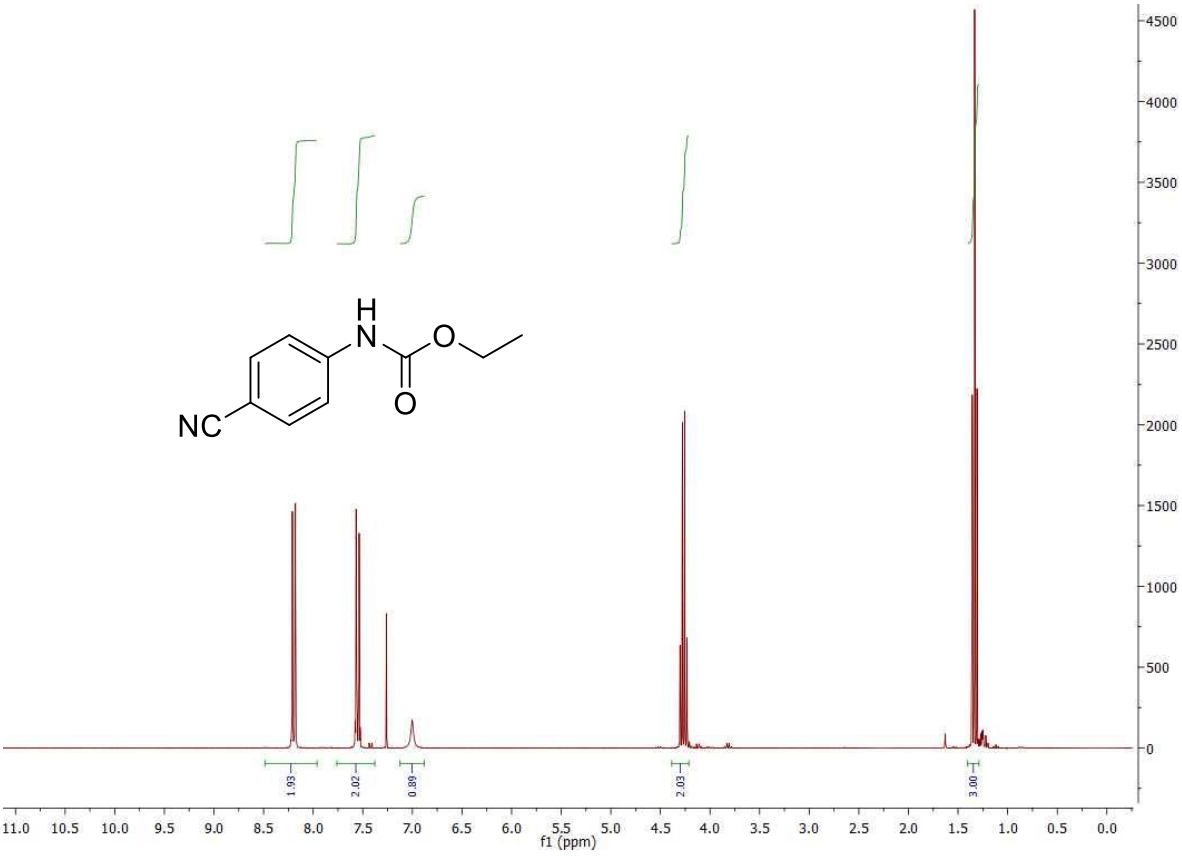

^{1}H NMR spectrum in $CDCl_3$.

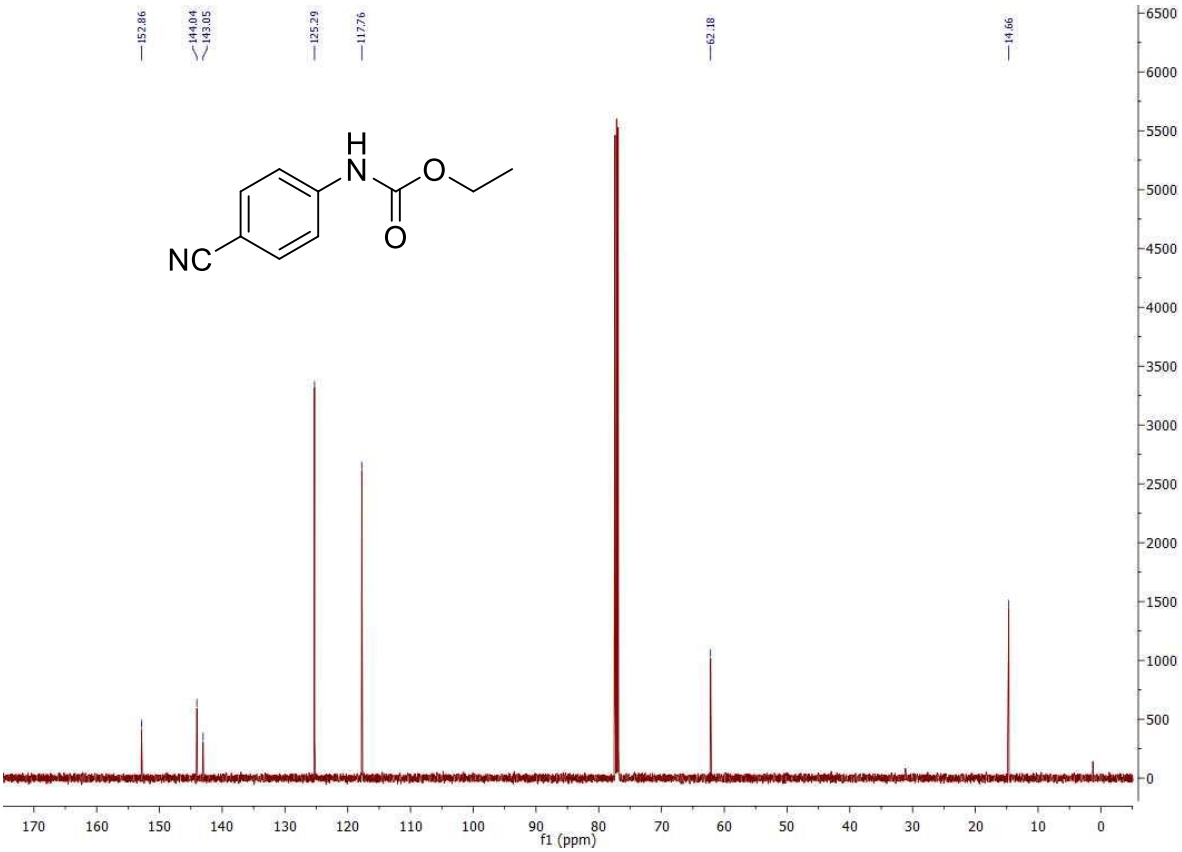

^{13}C NMR spectrum in $CDCl_3$.

14b

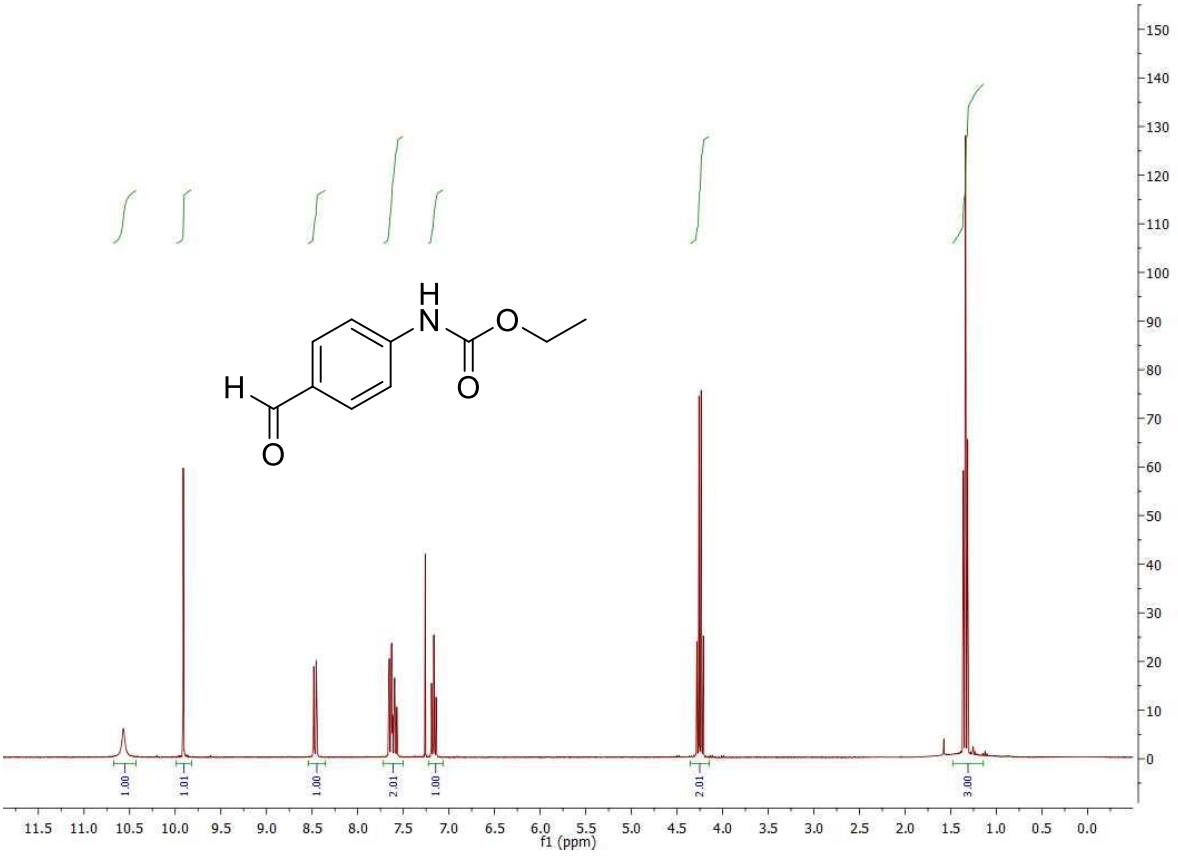

^{1}H NMR spectrum in $CDCl_3$.

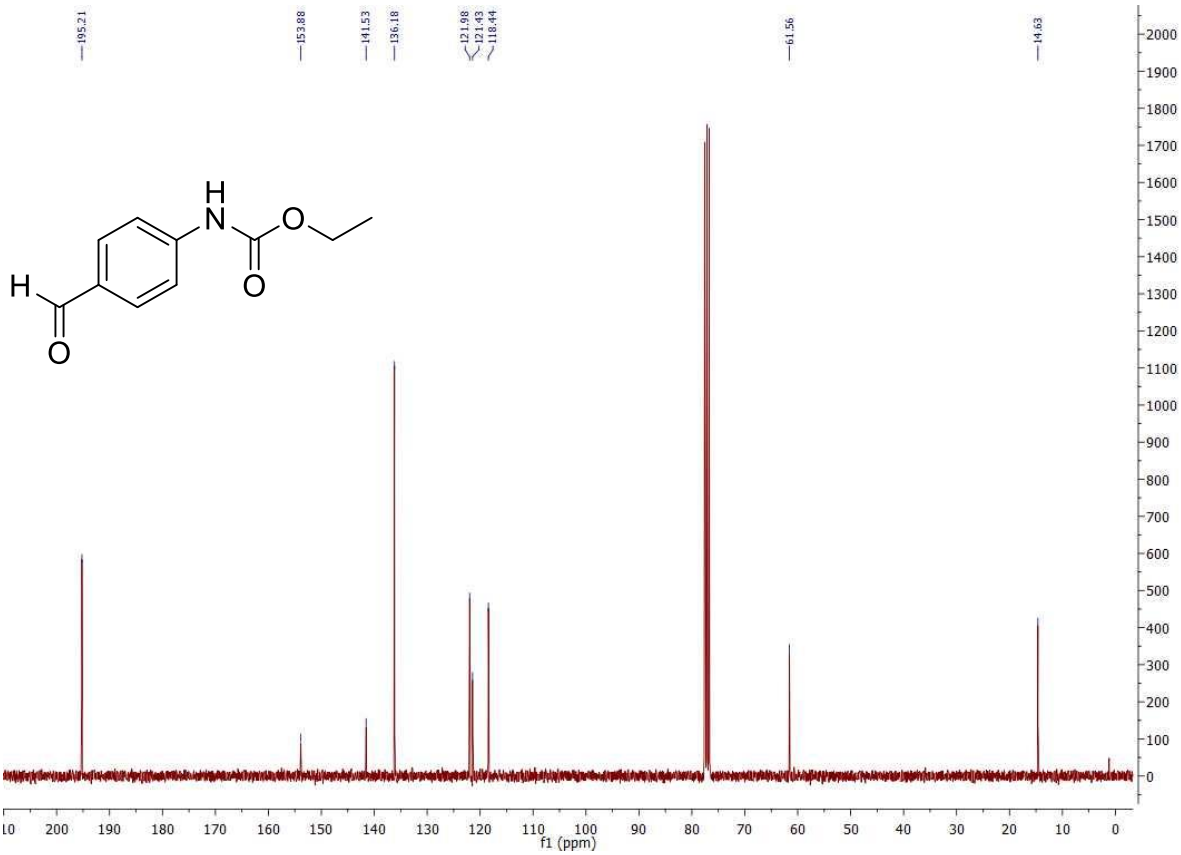

^{13}C NMR spectrum in $CDCl_3$.

15b

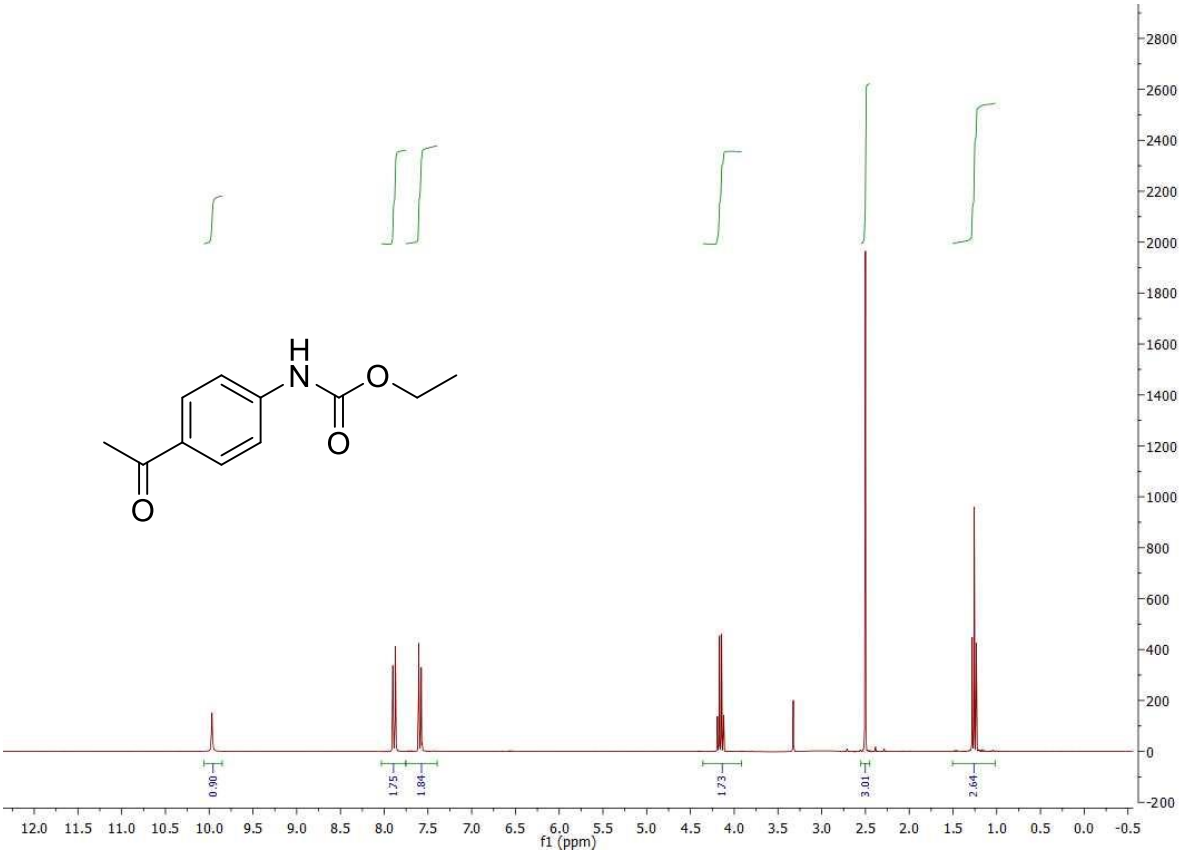

^{1}H NMR spectrum in DMSO-d_6.

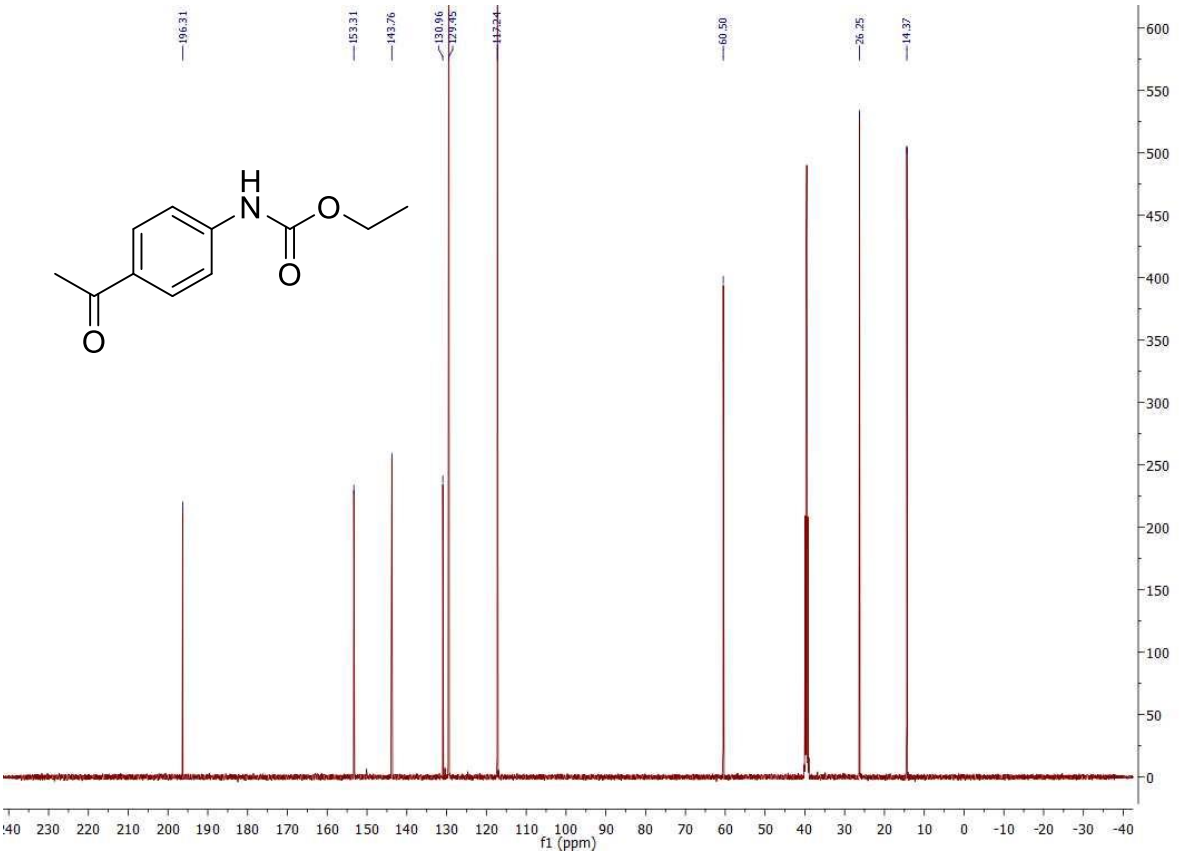

^{13}C NMR spectrum in DMSO-d_6.

16b

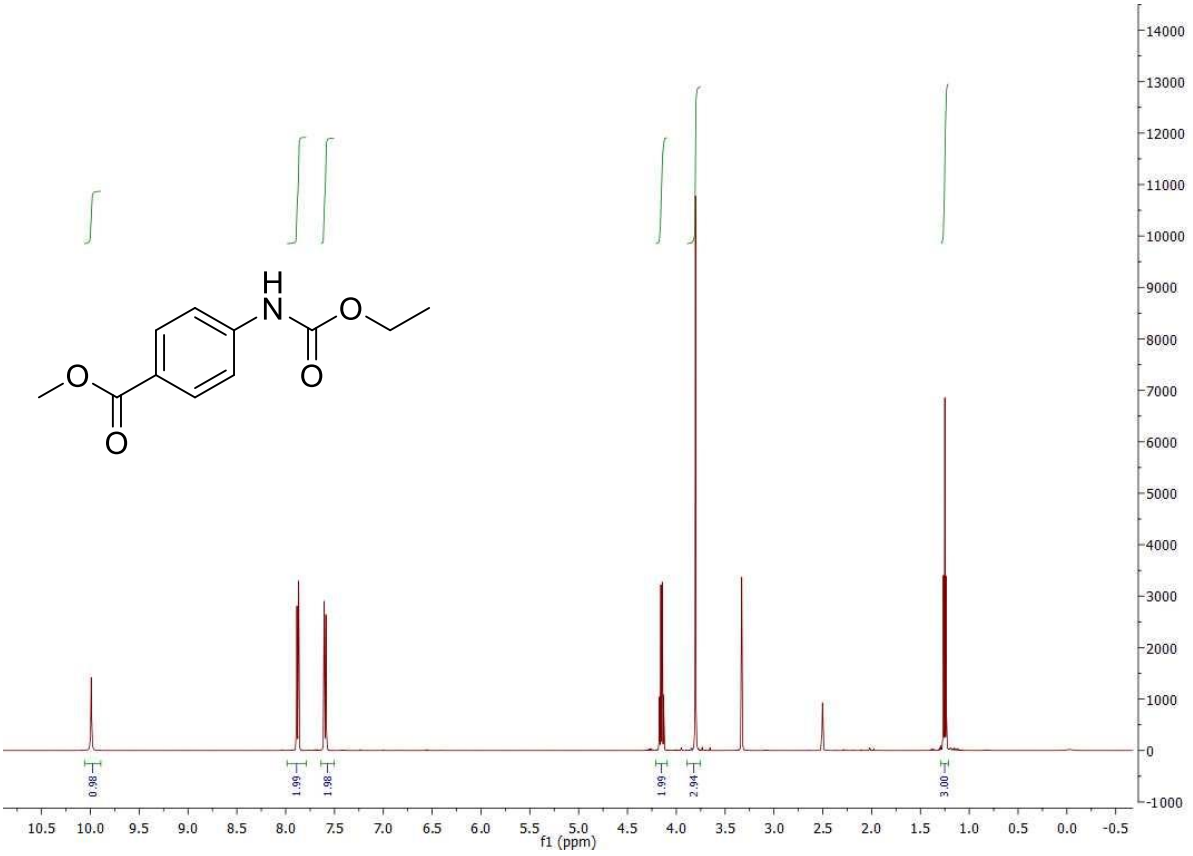

^{1}H NMR spectrum in DMSO-d_6.

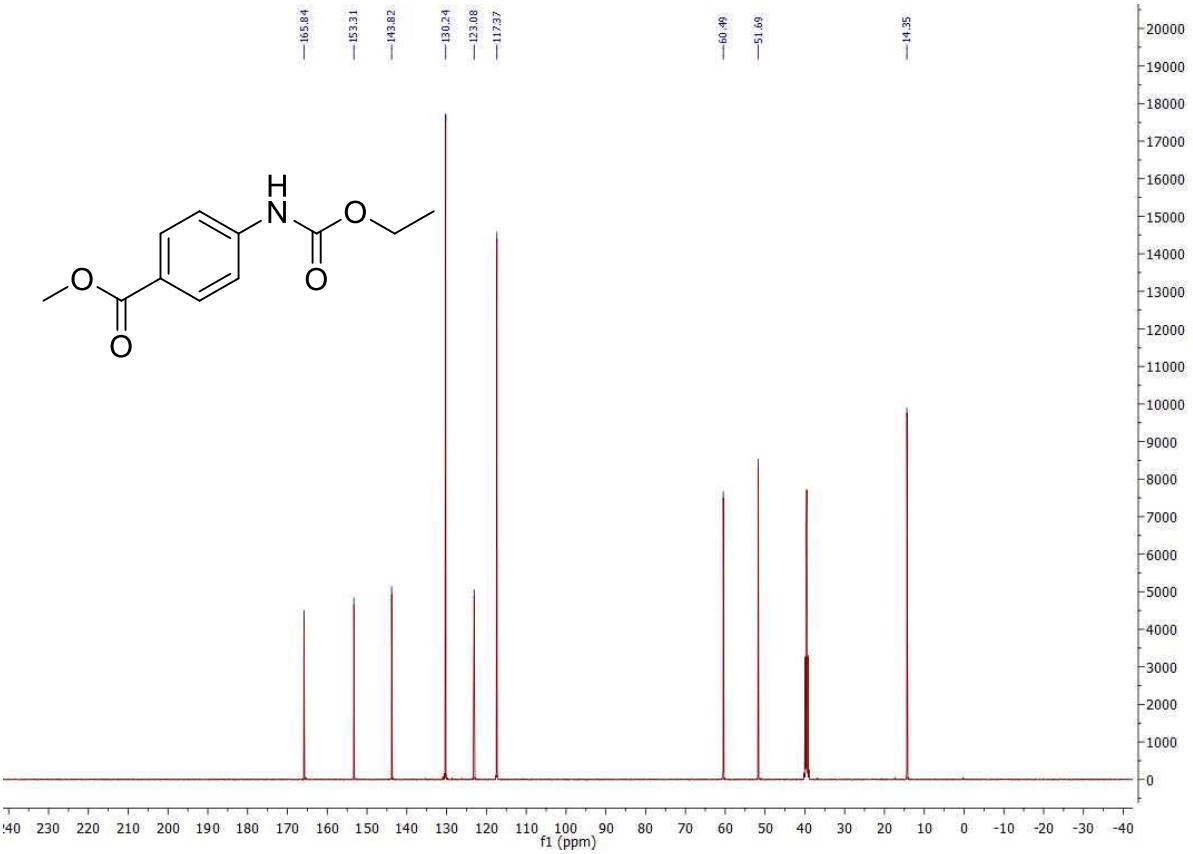

^{13}C NMR spectrum in DMSO-d_6.

17b

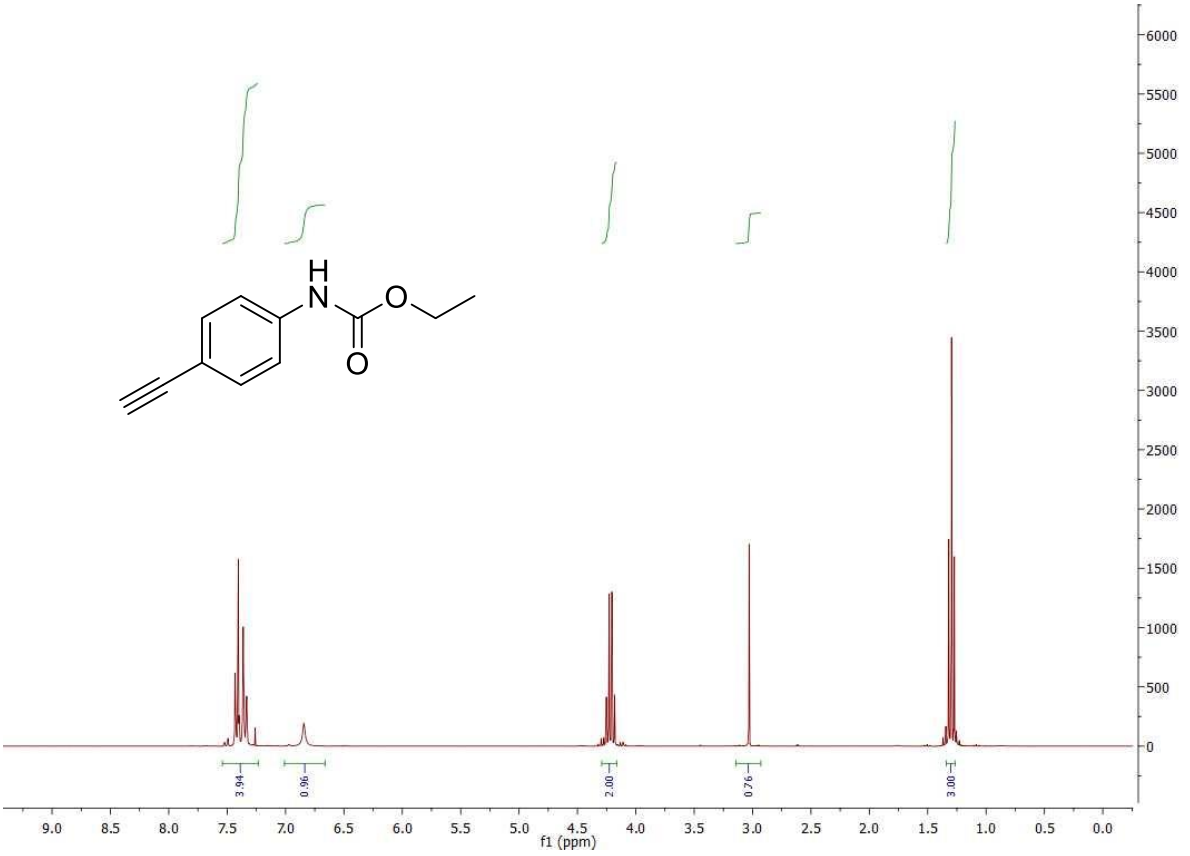

^{1}H NMR spectrum in $CDCl_3$.

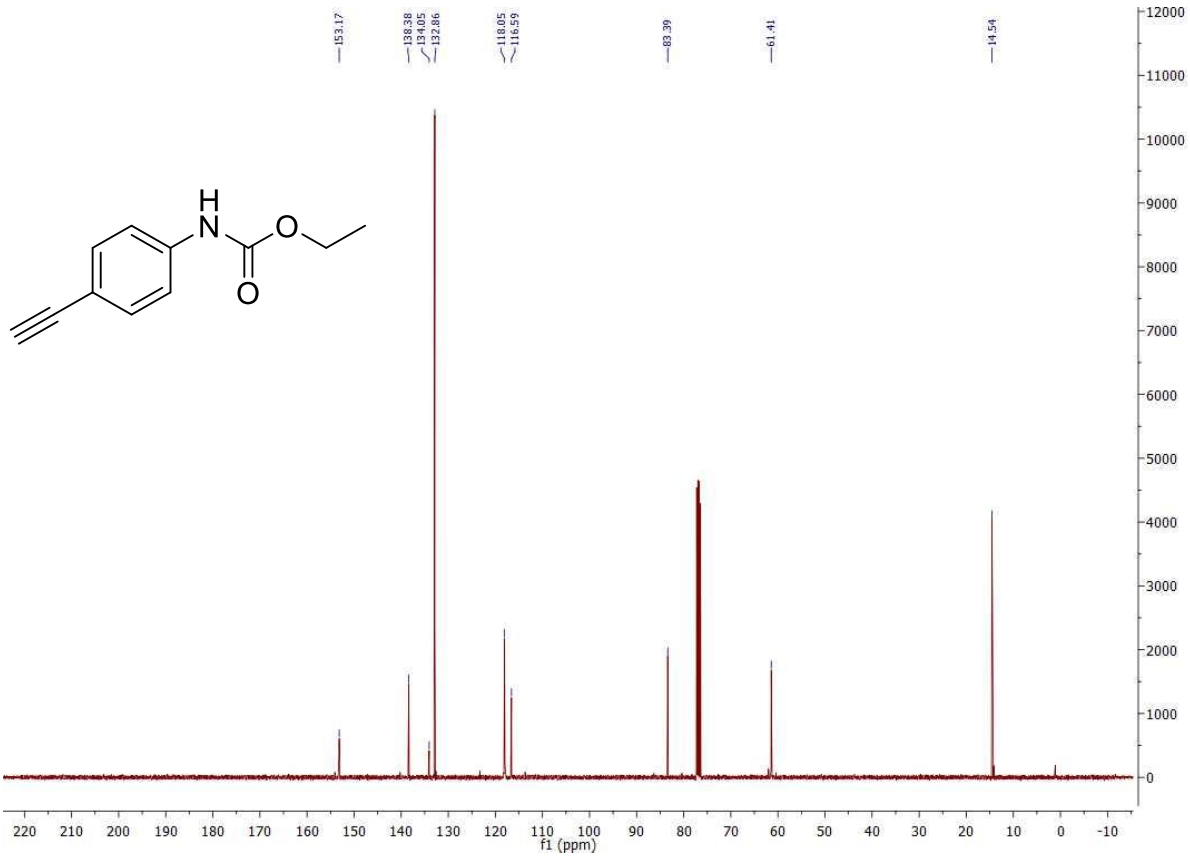

^{13}C NMR spectrum in $CDCl_3$.

18b

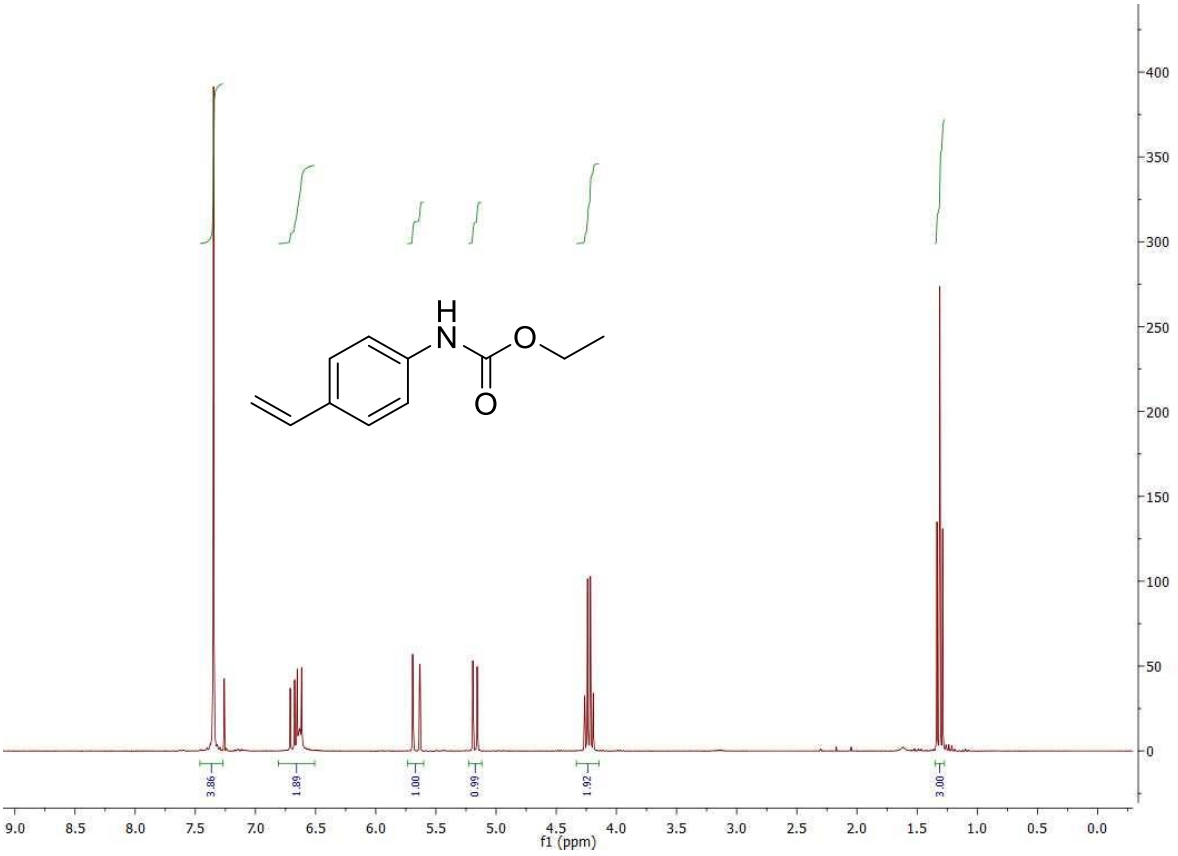

^{1}H NMR spectrum in $CDCl_3$.

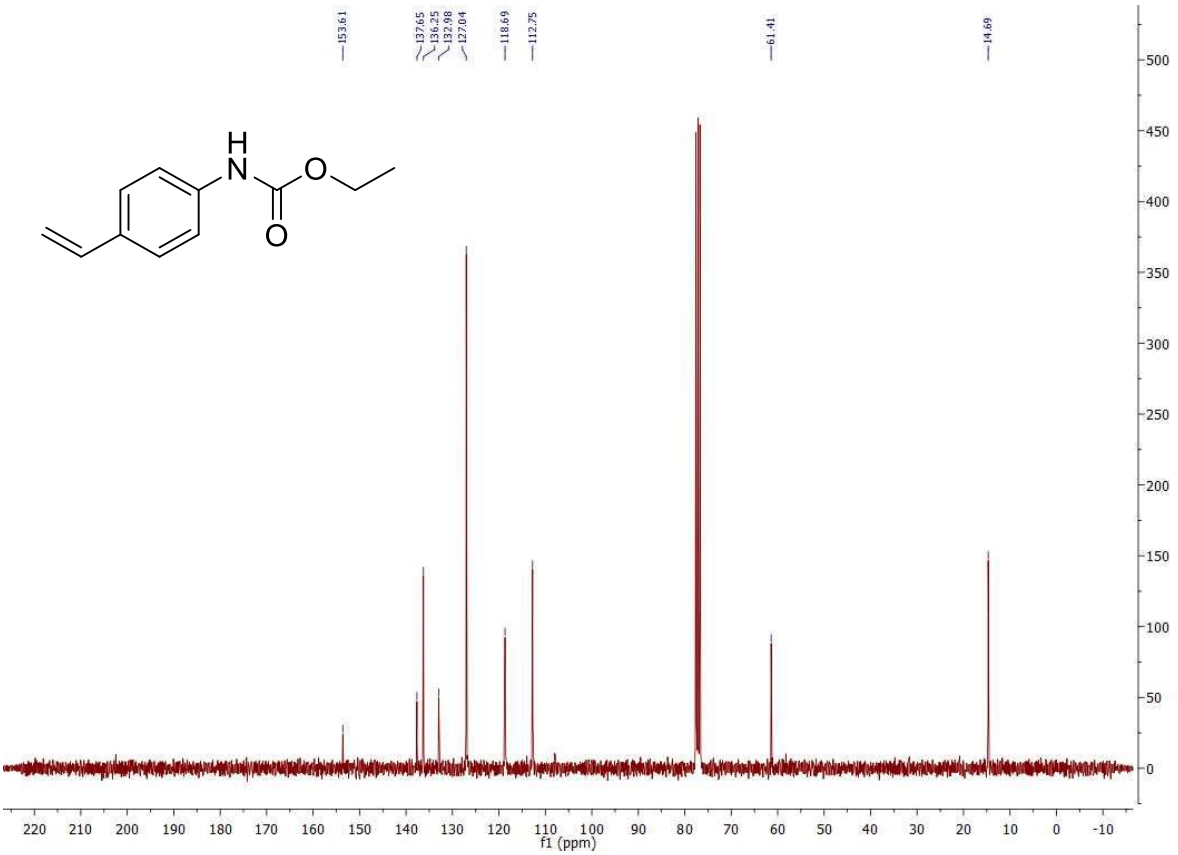

^{13}C NMR spectrum in $CDCl_3$.

19b

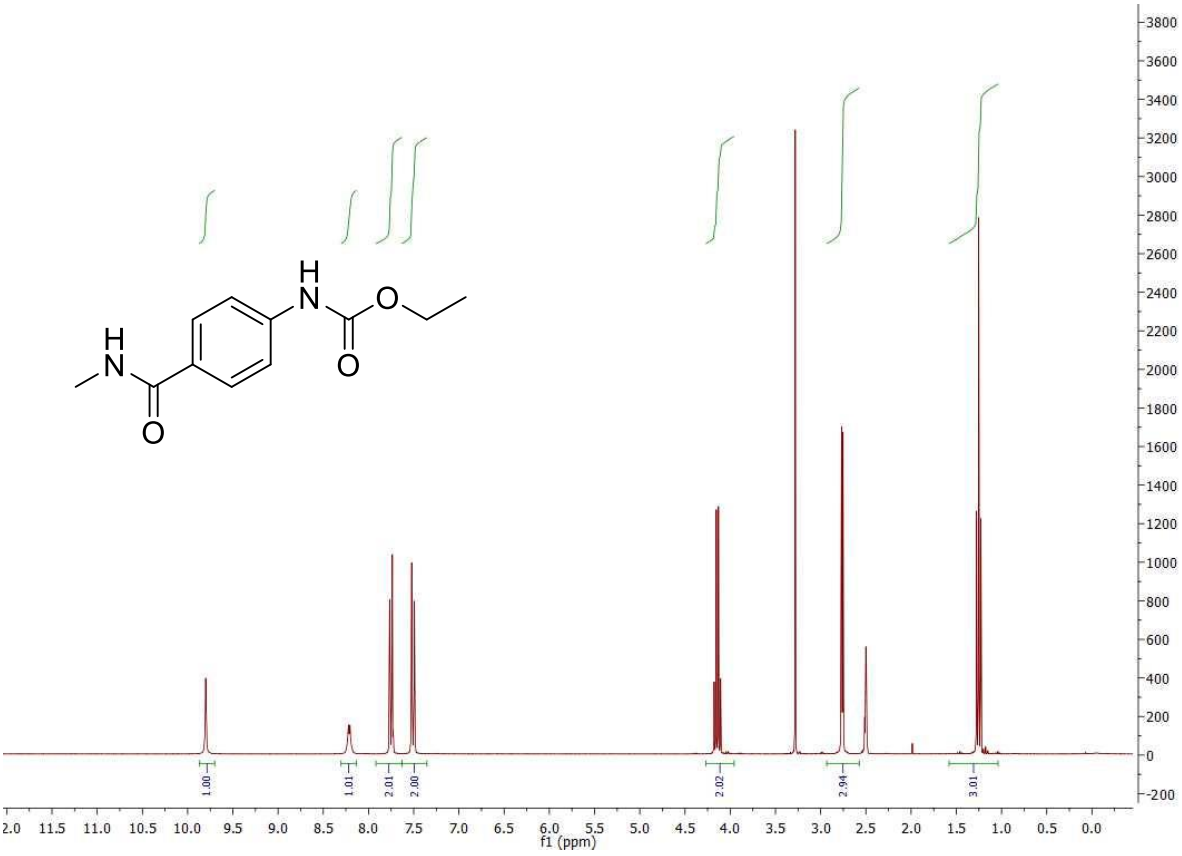

^{1}H NMR spectrum in $CDCl_3$.

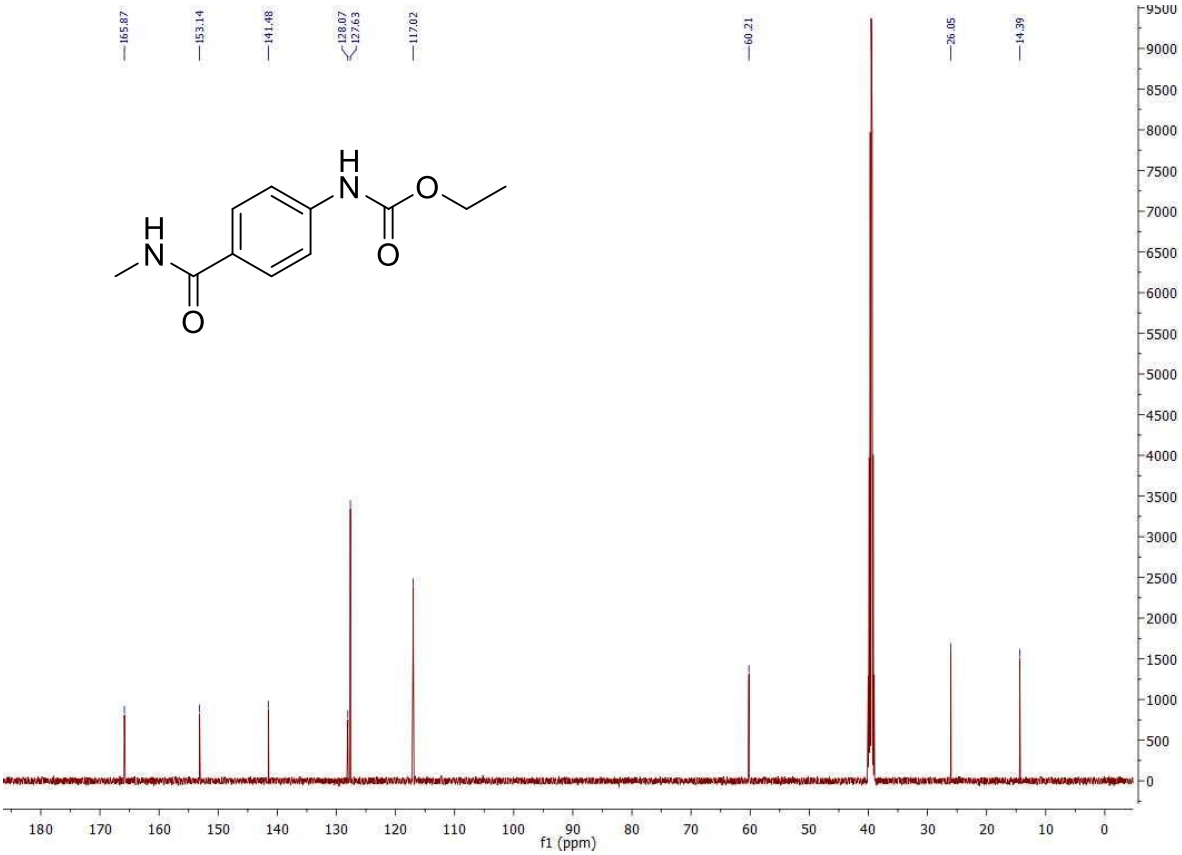

^{13}C NMR spectrum in $CDCl_3$.

42b

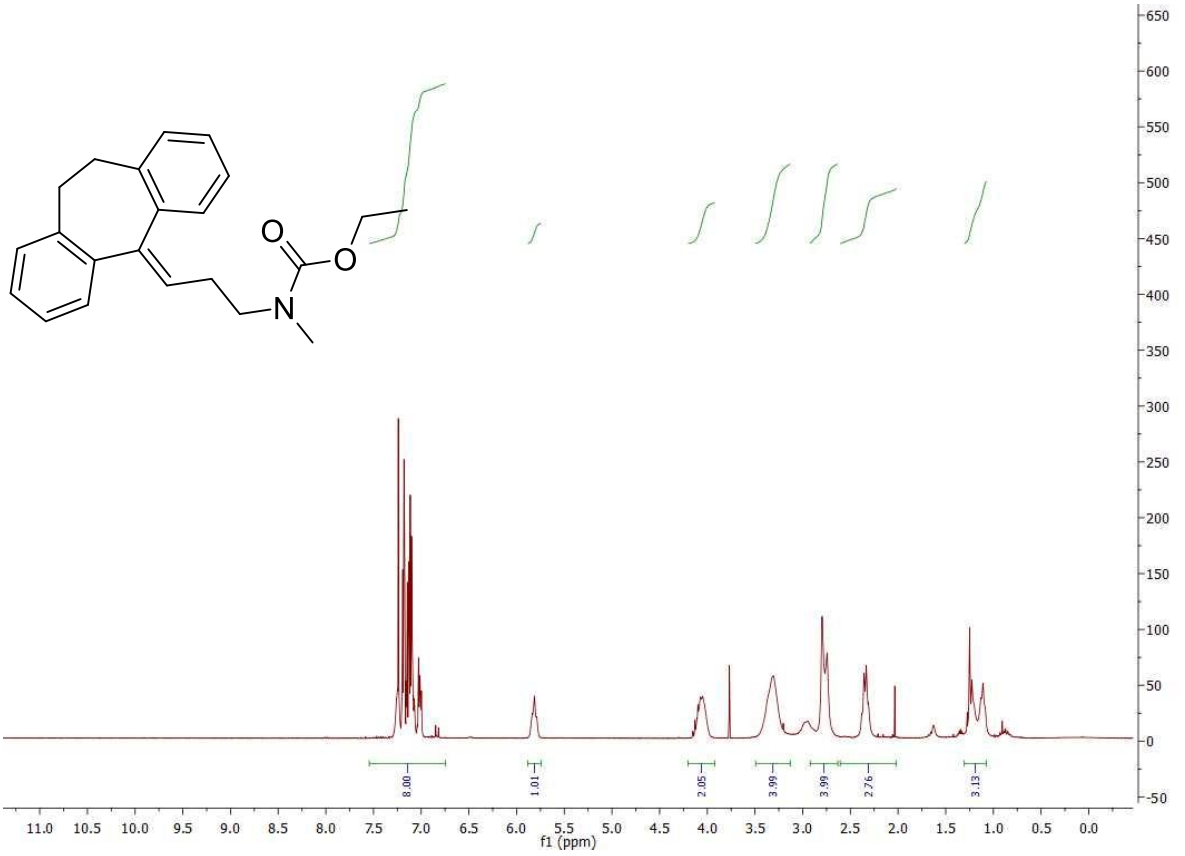

^{1}H NMR spectrum in $CDCl_3$.

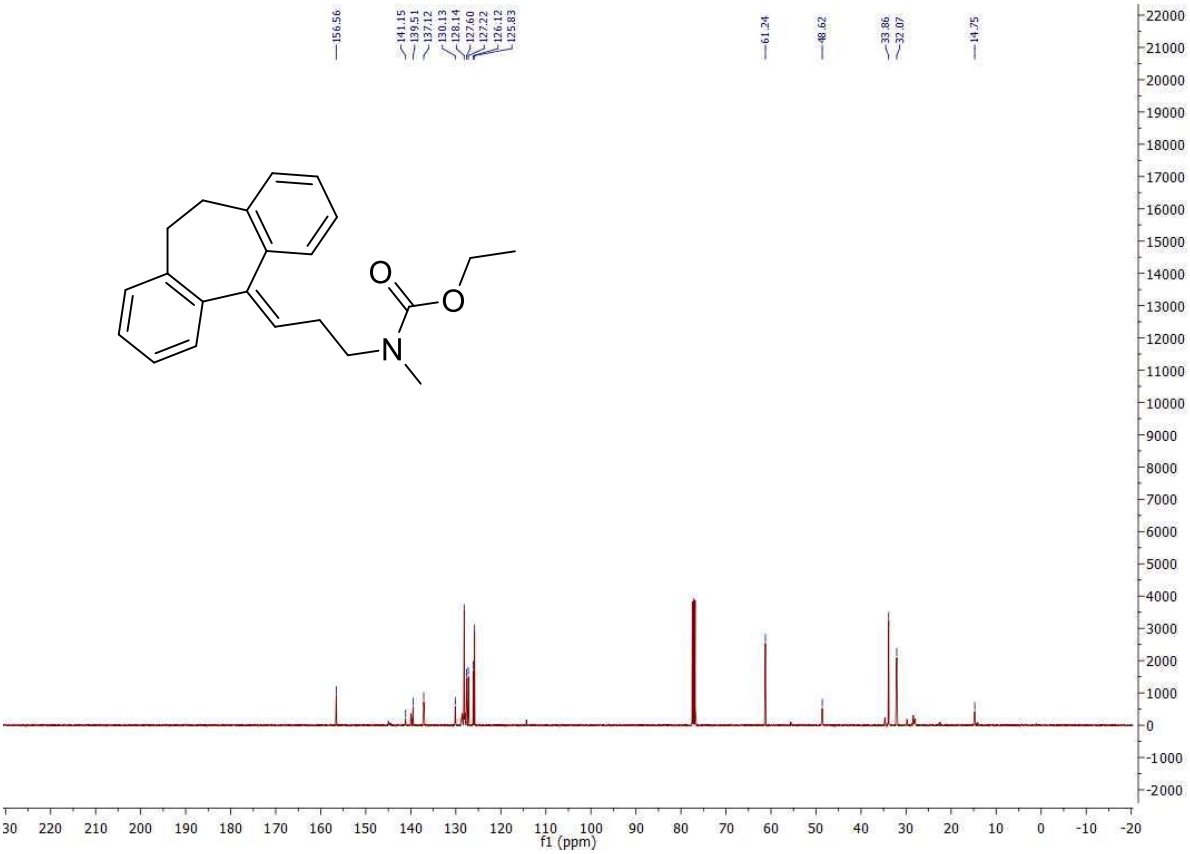

^{13}C NMR spectrum in $CDCl_3$.

43b

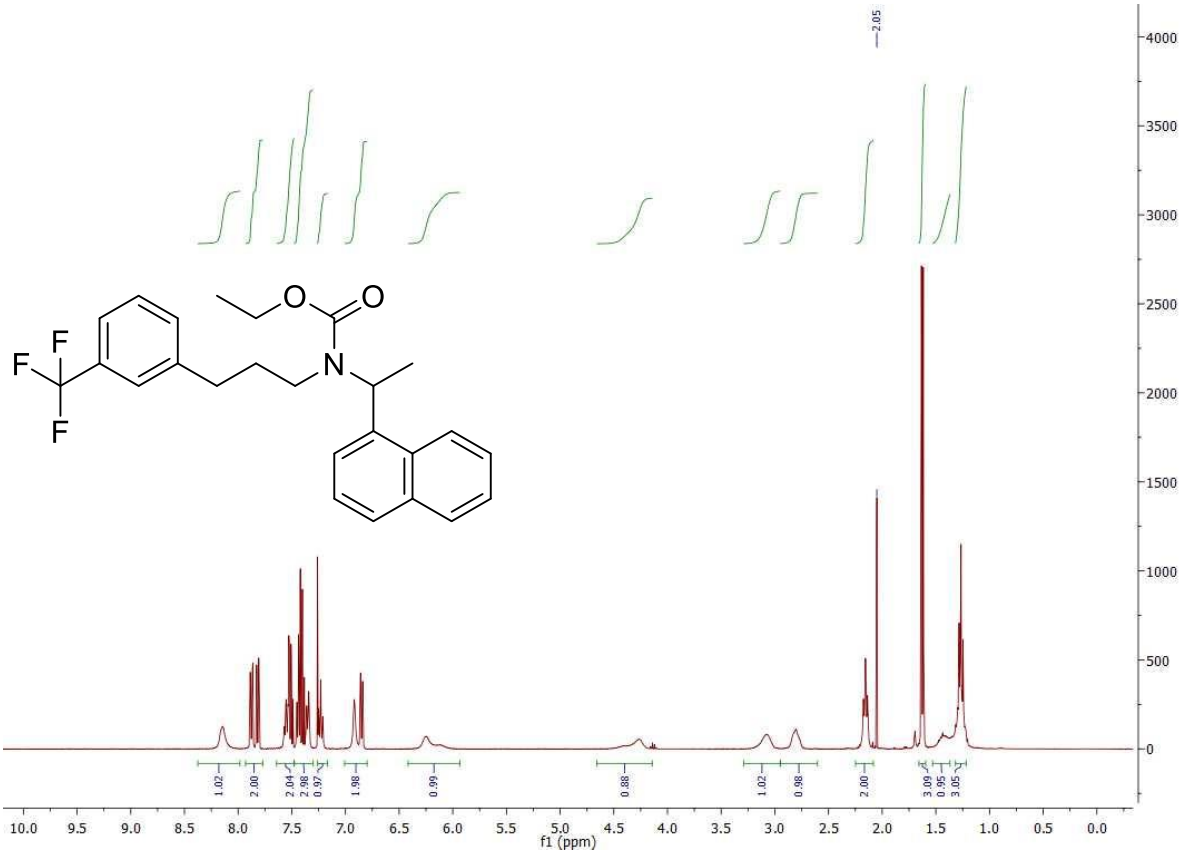

^{1}H NMR spectrum in $CDCl_3$.

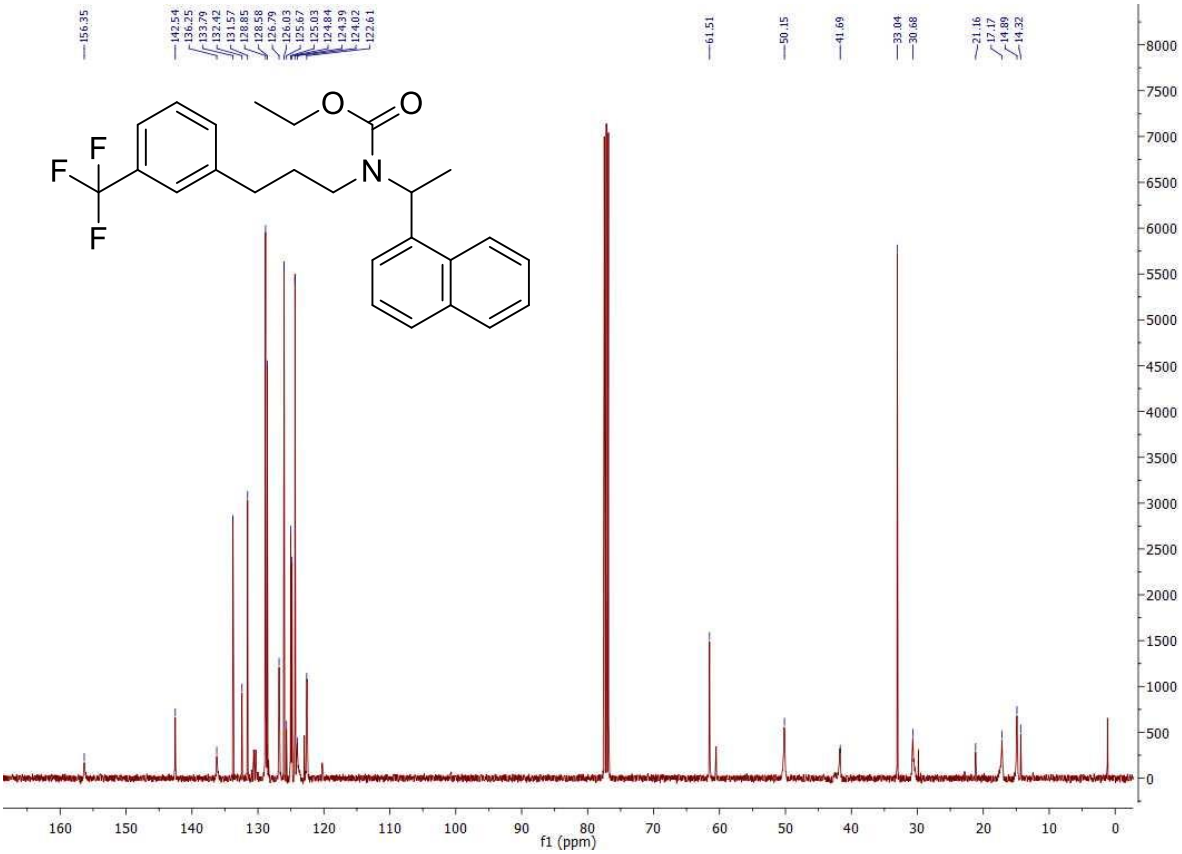

^{13}C NMR spectrum in $CDCl_3$.

44b

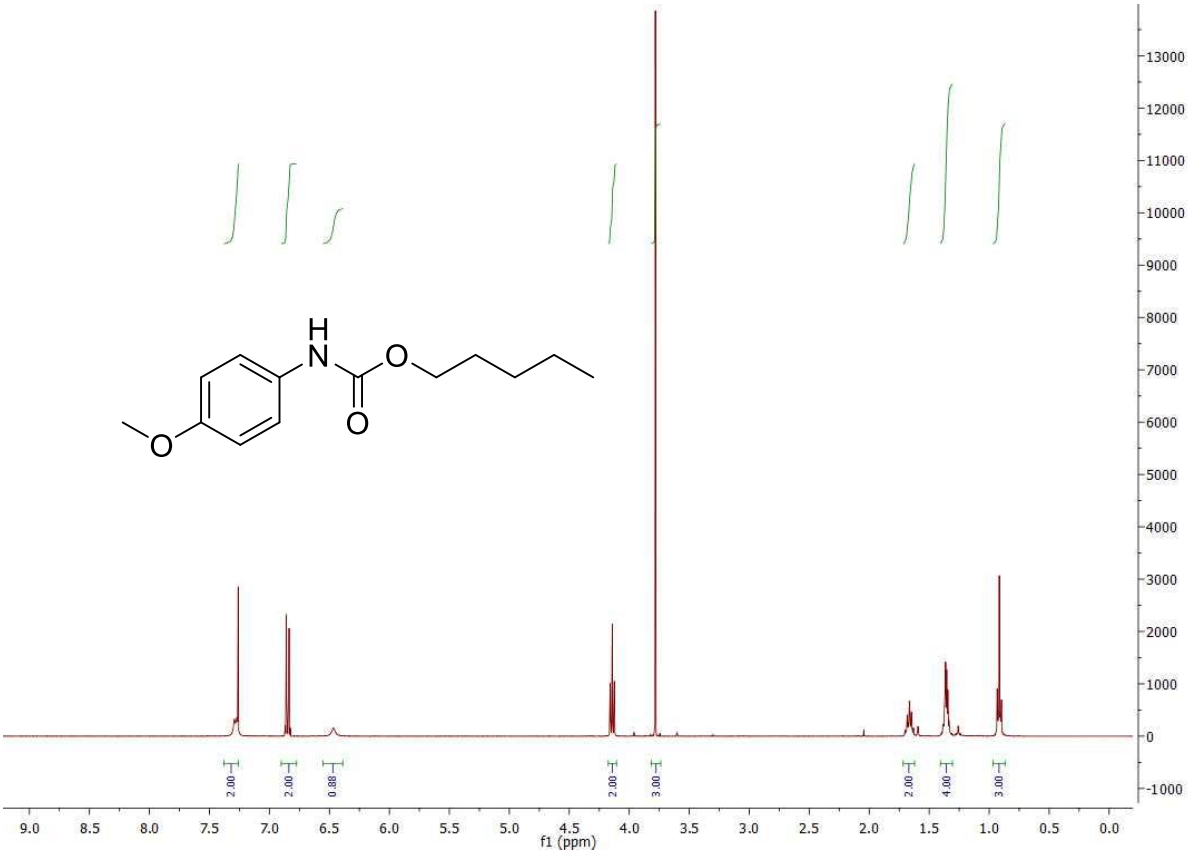

^{1}H NMR spectrum in $CDCl_3$.

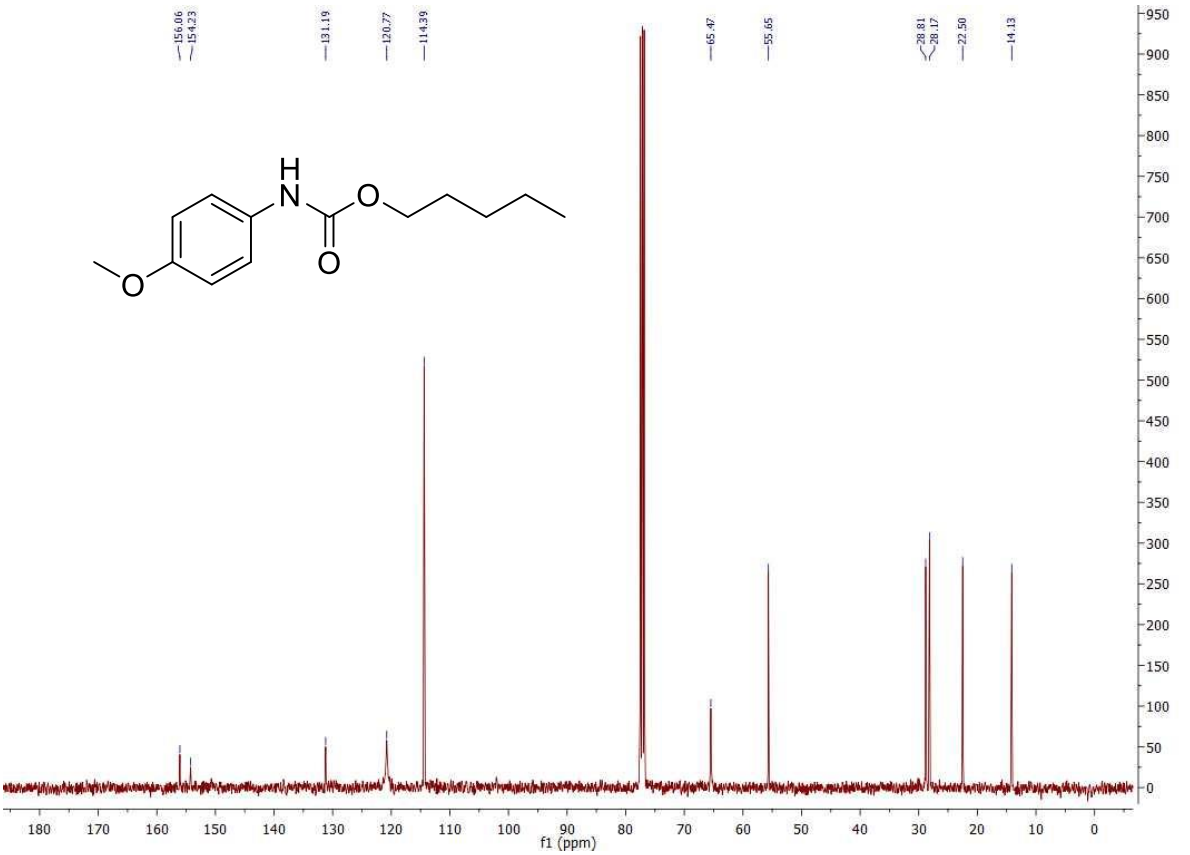

^{13}C NMR spectrum in $CDCl_3$.

45b

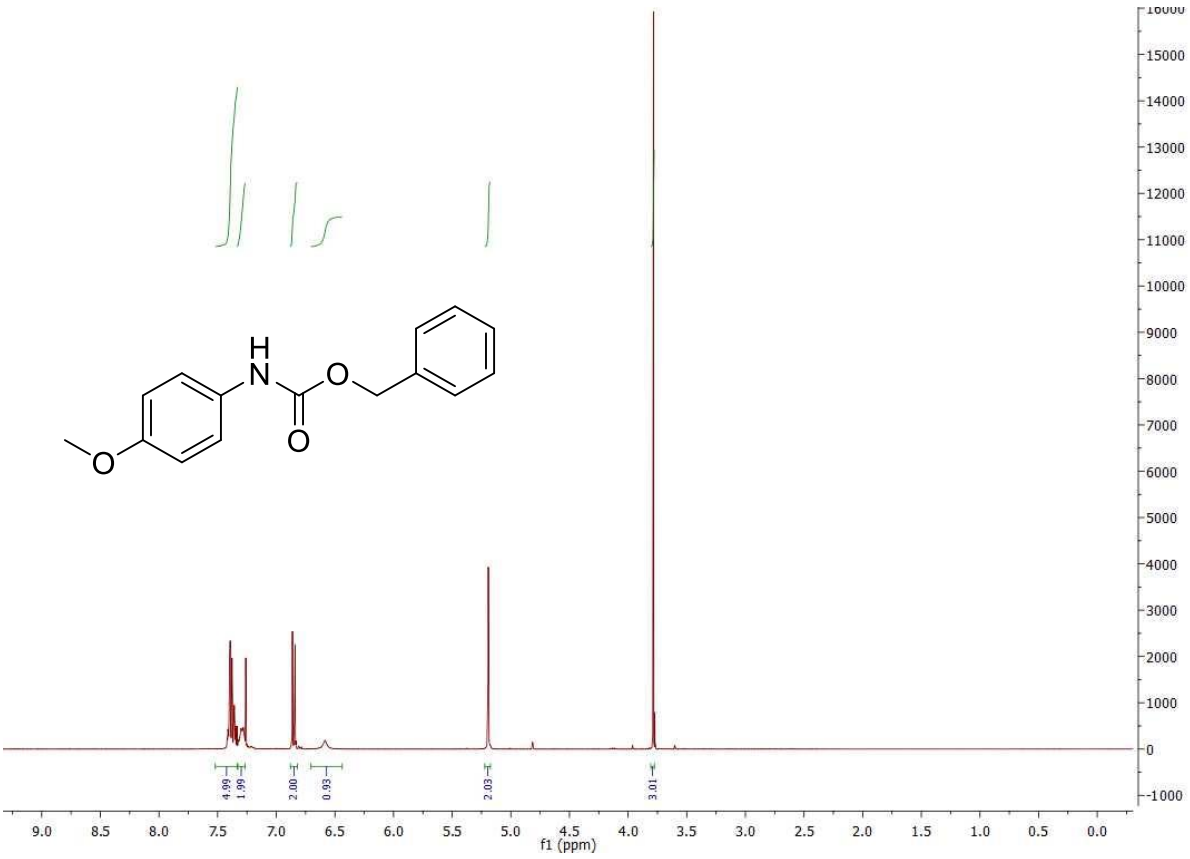

^{1}H NMR spectrum in $CDCl_3$.

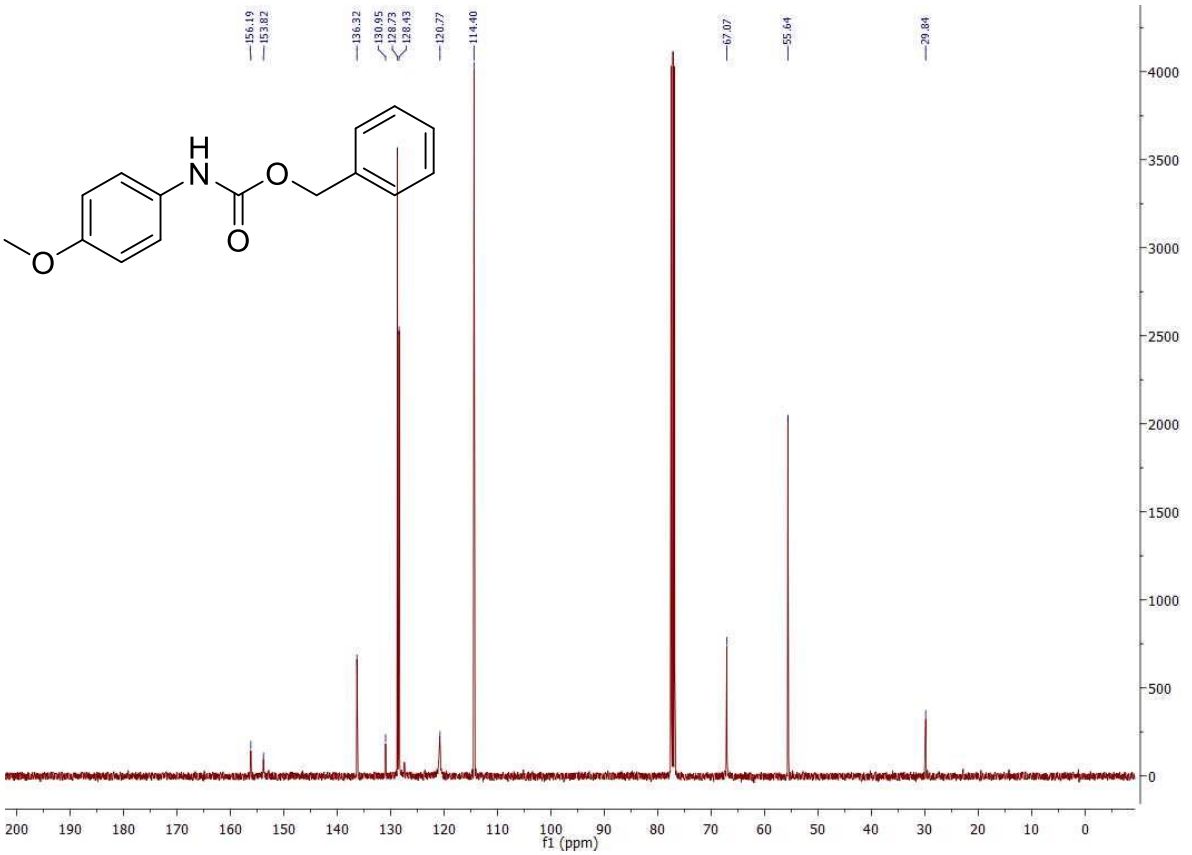

^{13}C NMR spectrum in $CDCl_3$.

46b

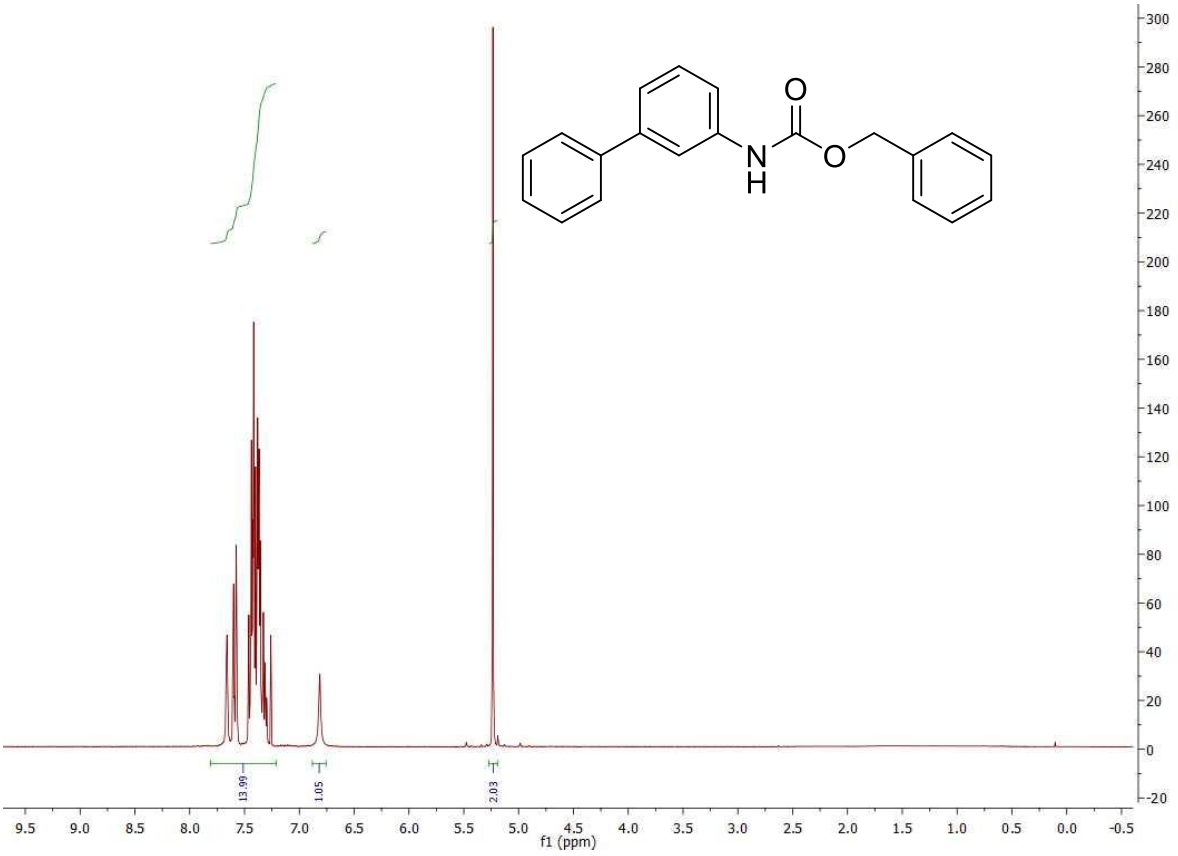

^{1}H NMR spectrum in $CDCl_3$.

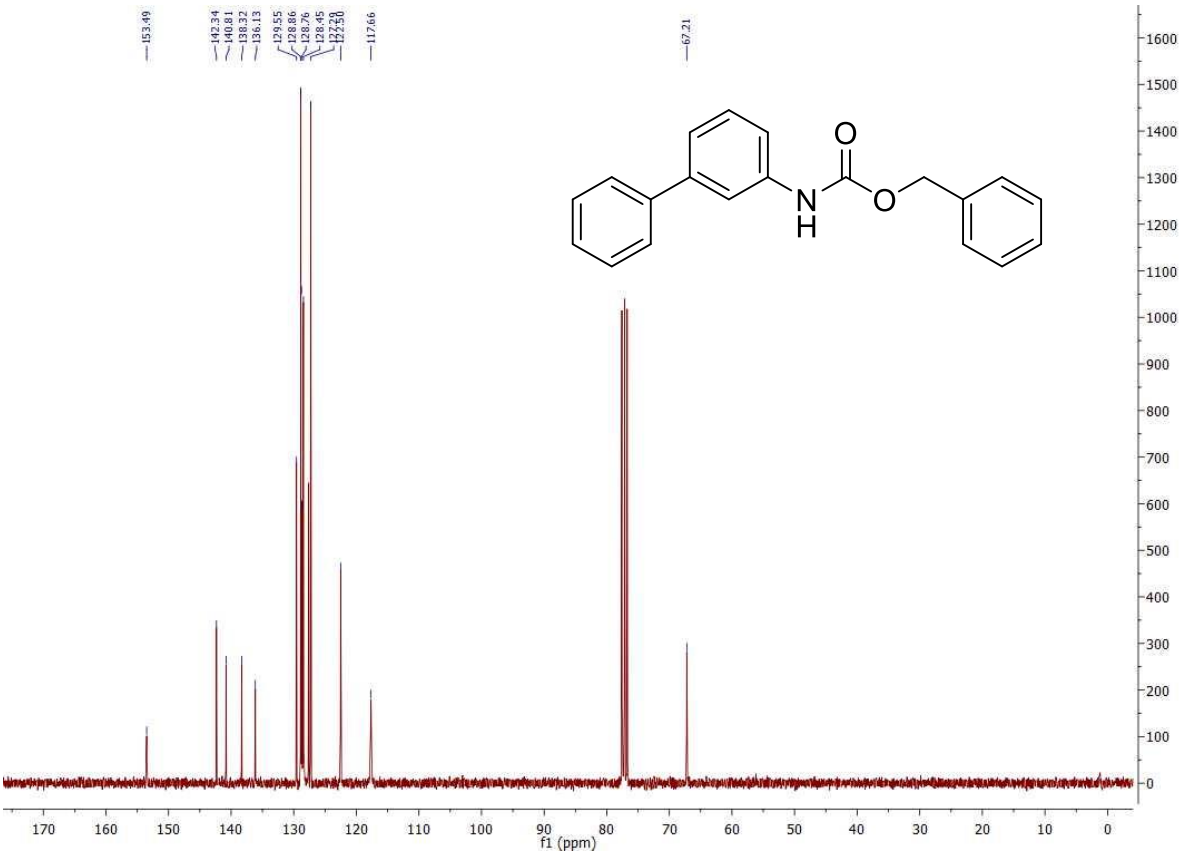

^{13}C NMR spectrum in $CDCl_3$.

47b

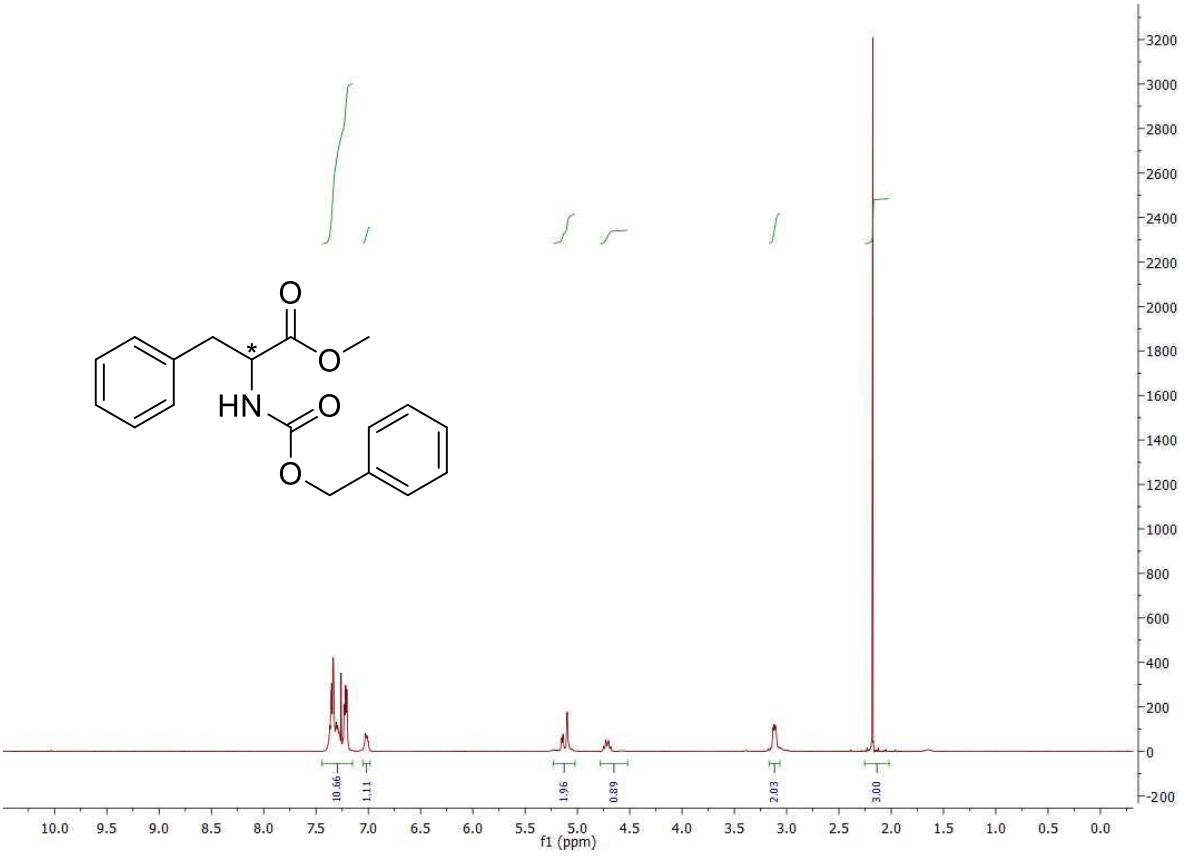

^{1}H NMR spectrum in $CDCl_3$.

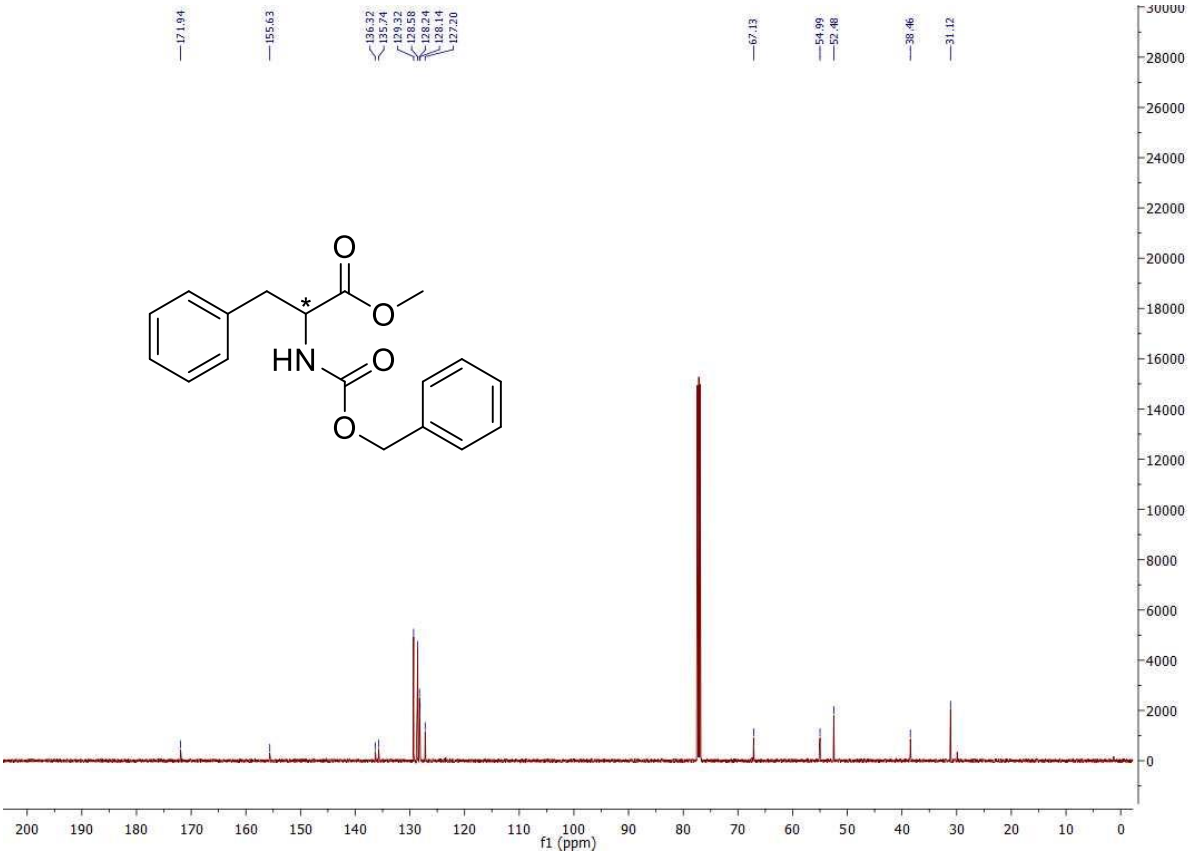

^{13}C NMR spectrum in $CDCl_3$.

48b

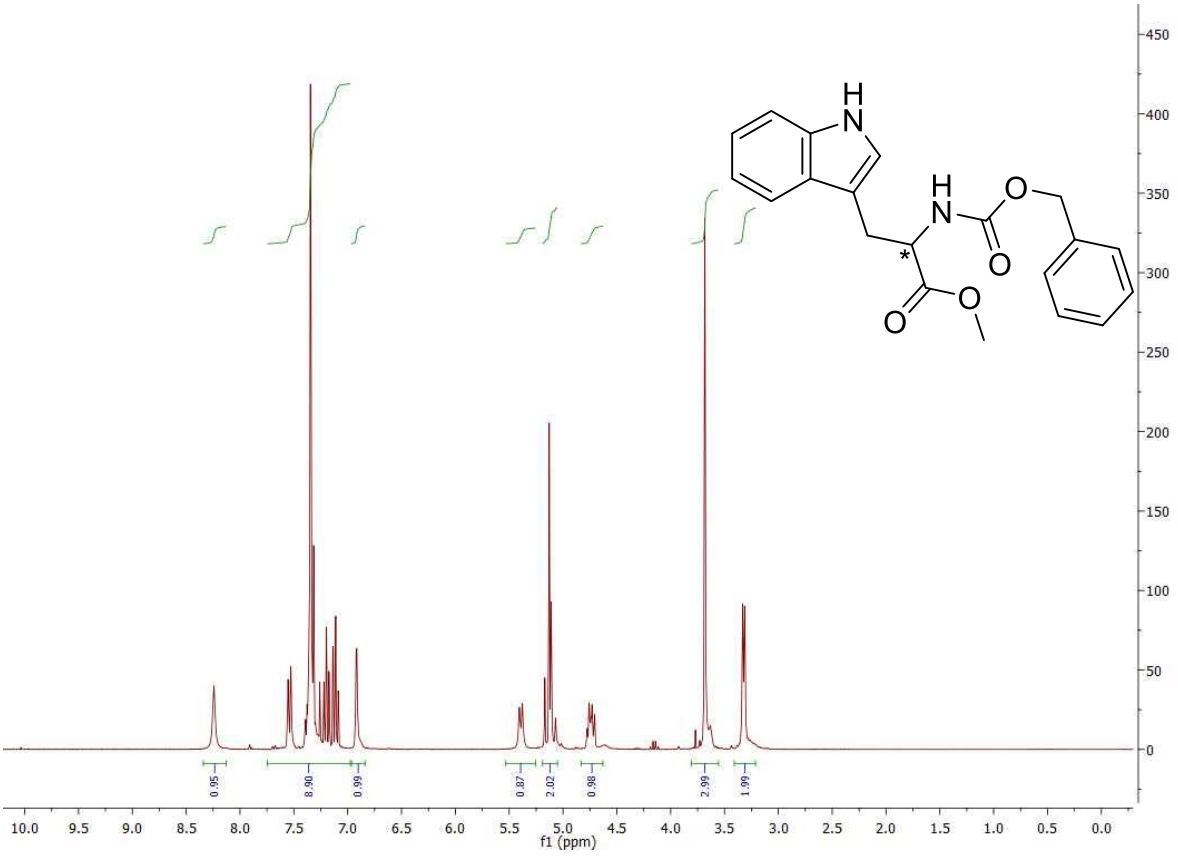

^{1}H NMR spectrum in $CDCl_3$.

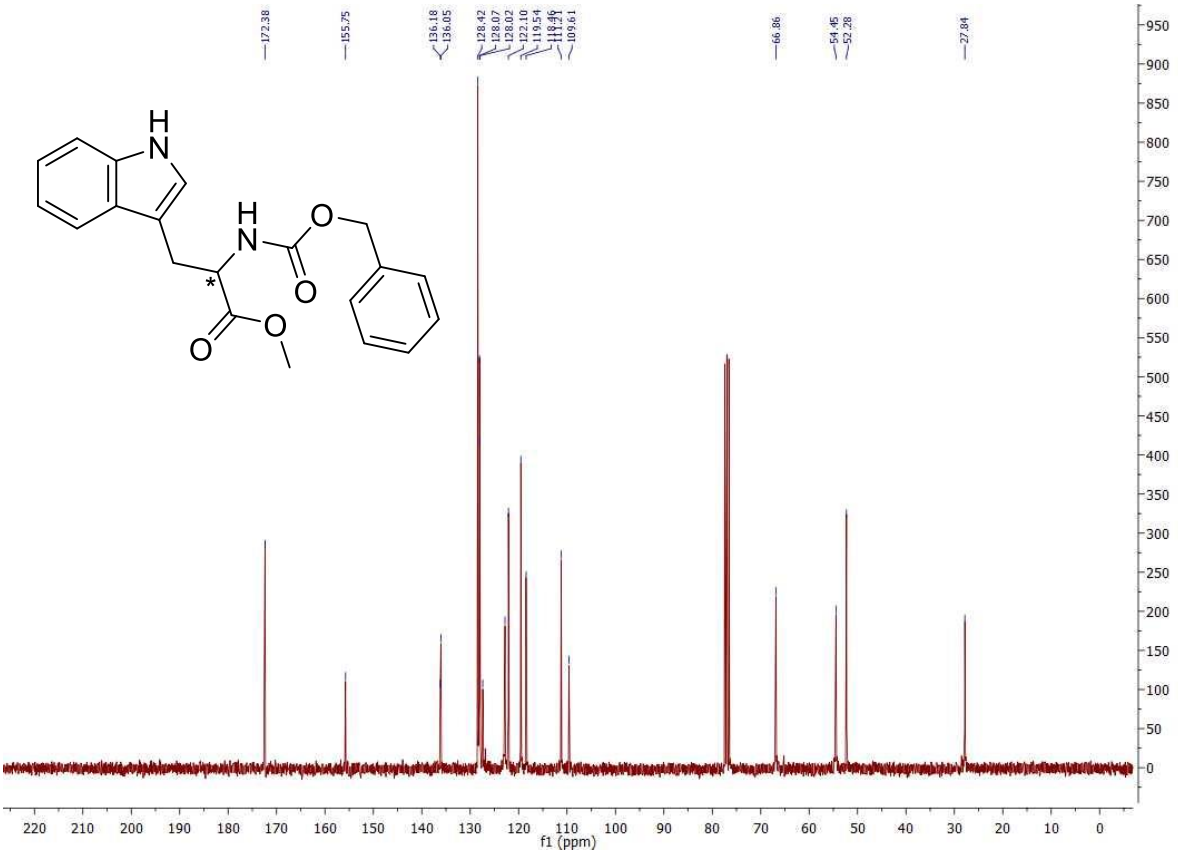

^{13}C NMR spectrum in $CDCl_3$.

49b

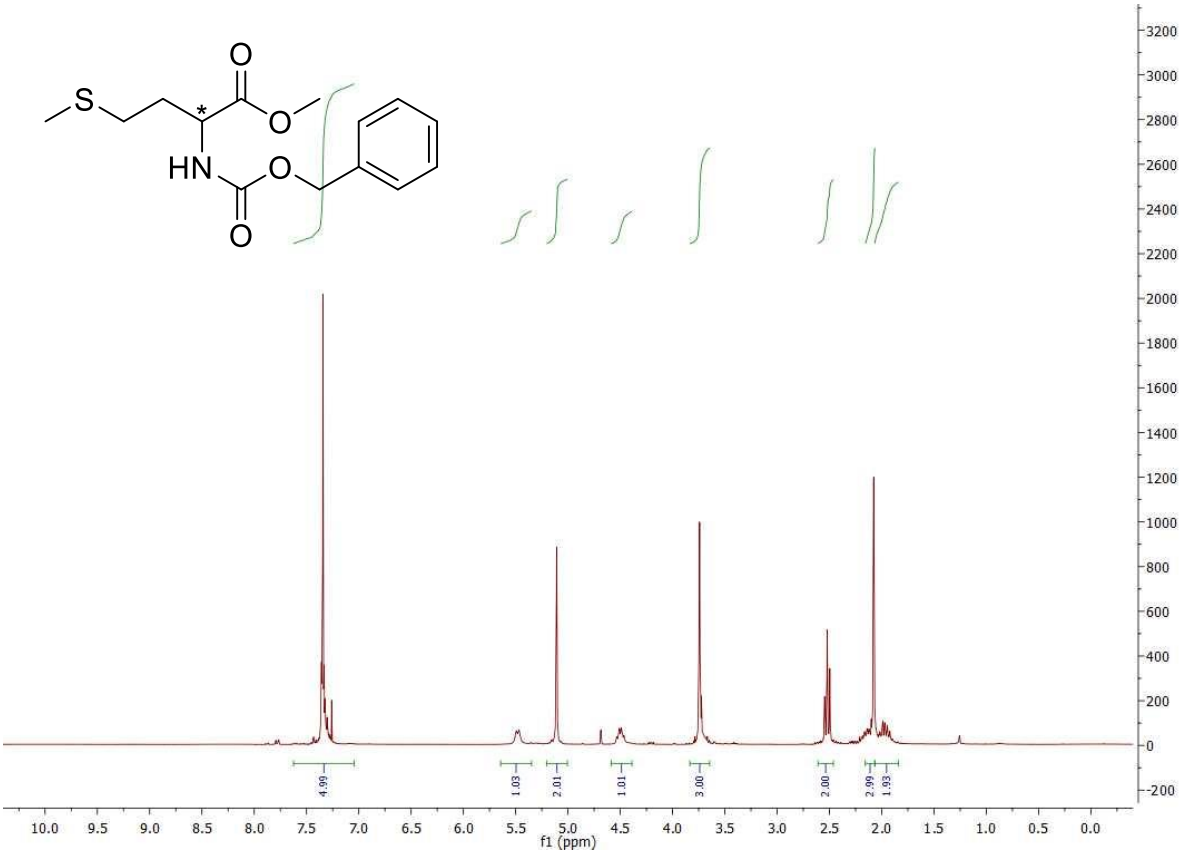

^{1}H NMR spectrum in $CDCl_3$.

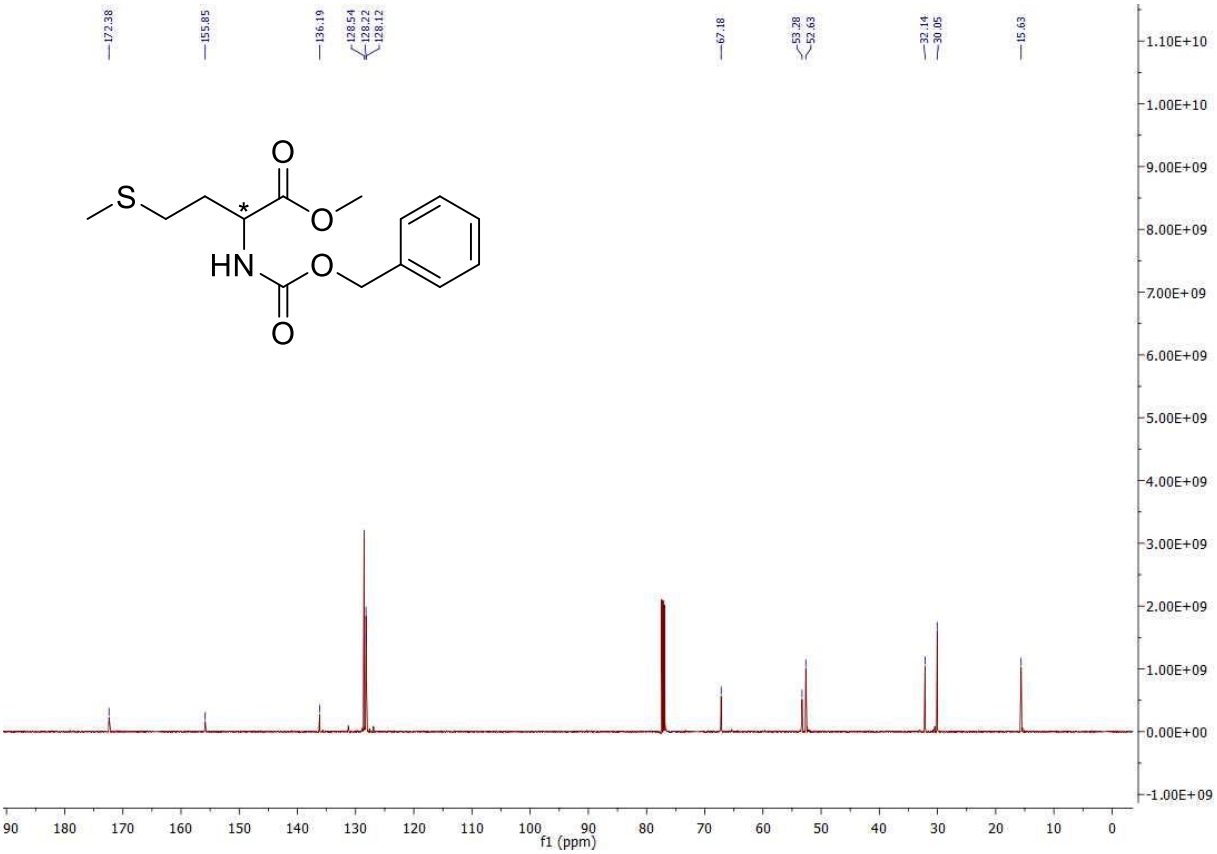

^{13}C NMR spectrum in $CDCl_3$.

50b

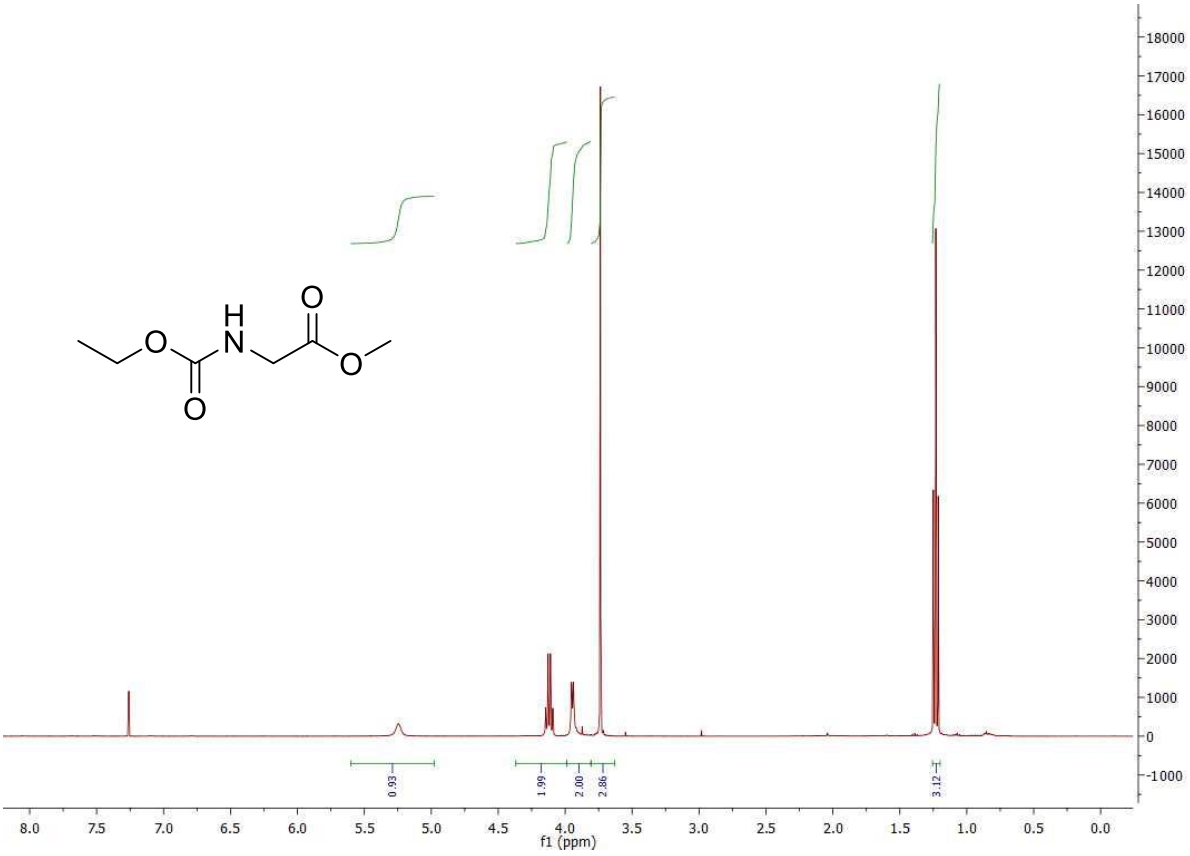

^{1}H NMR spectrum in $CDCl_3$.

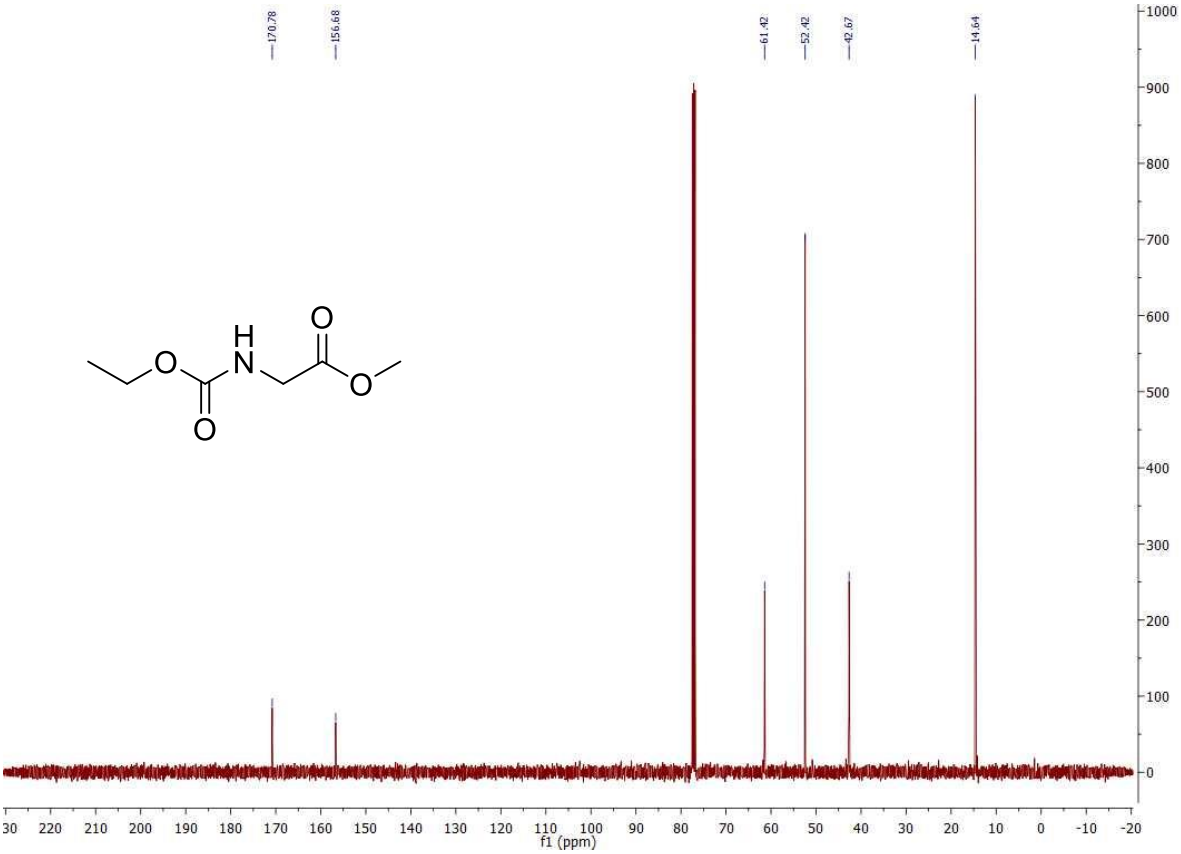

^{13}C NMR spectrum in $CDCl_3$.

51a

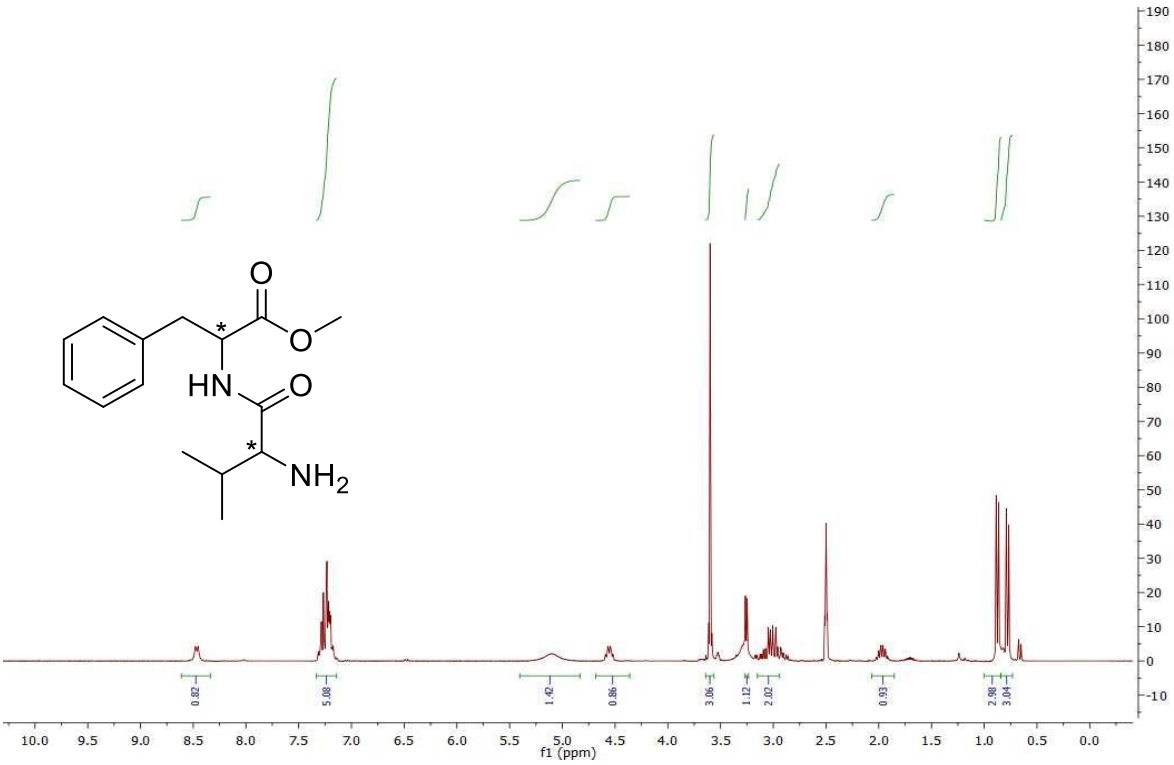

^{1}H NMR spectrum in DMSO-d_6.

51b

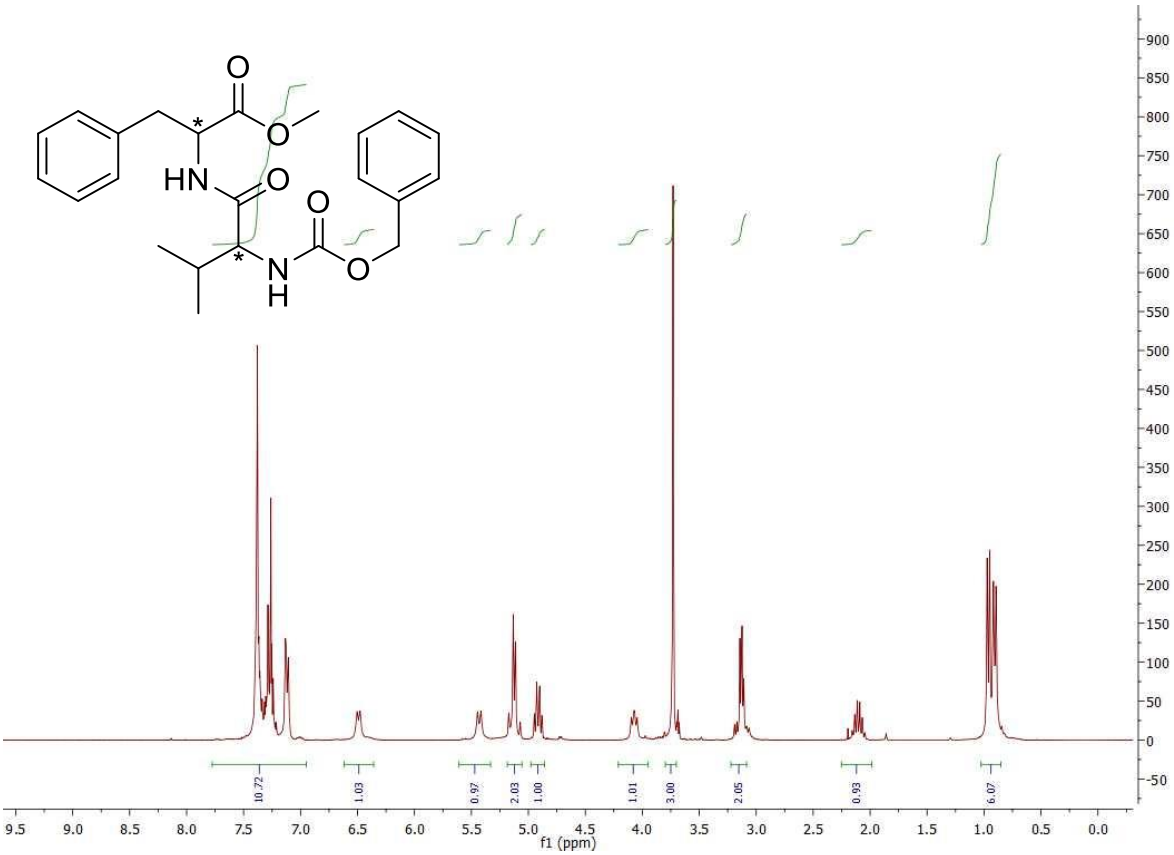

^{1}H NMR spectrum in $CDCl_3$.

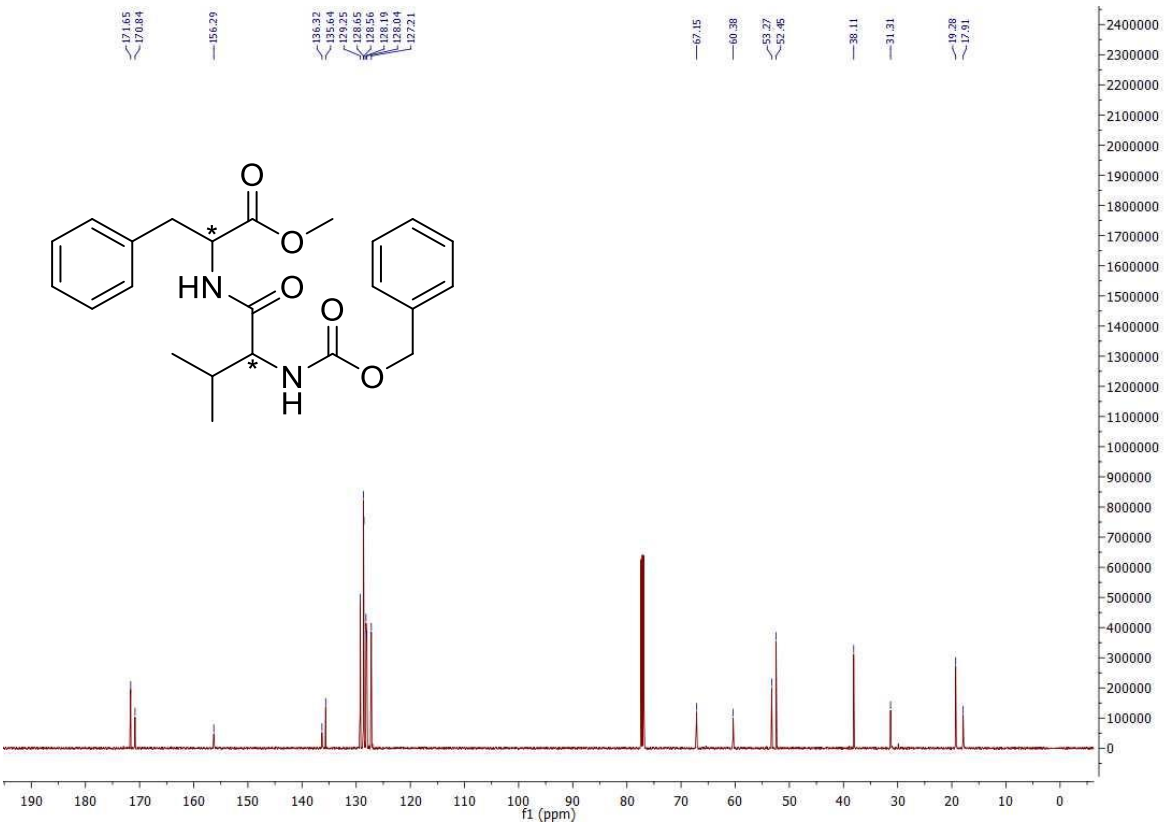

^{13}C NMR spectrum in $CDCl_3$.

52a

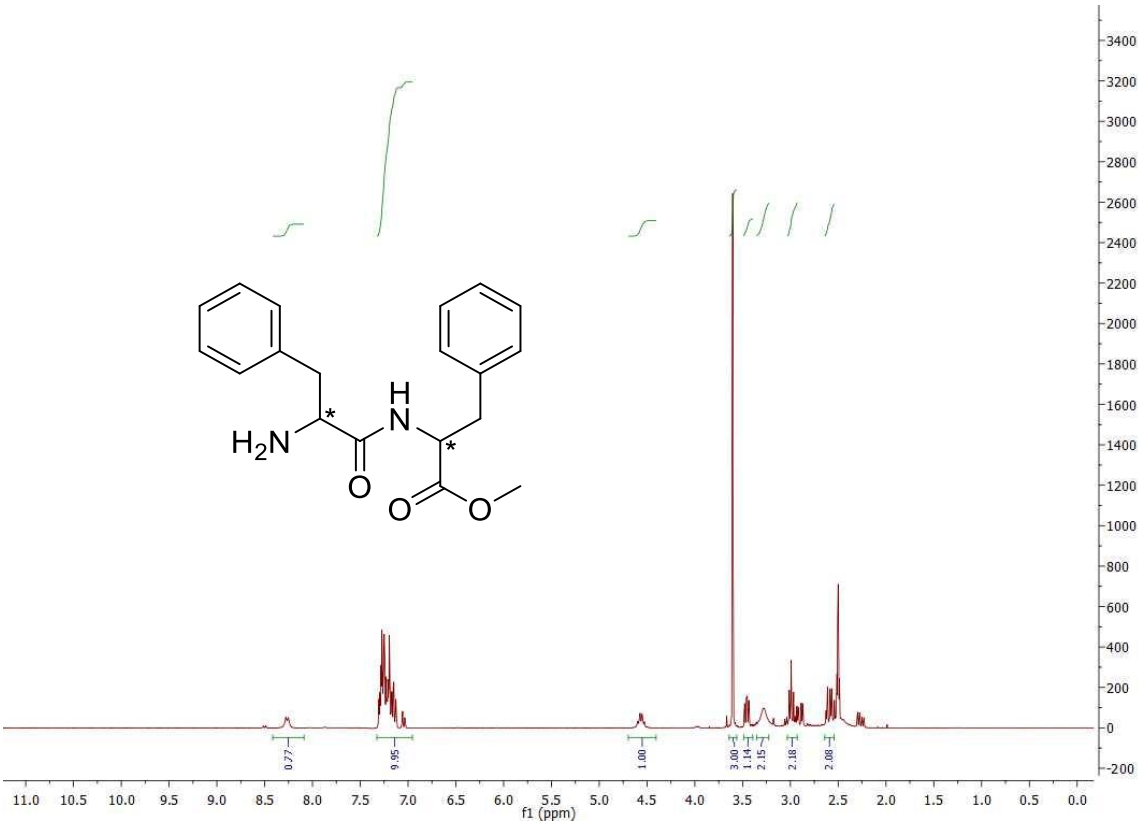

^{1}H NMR spectrum in DMSO-d_6.

52b

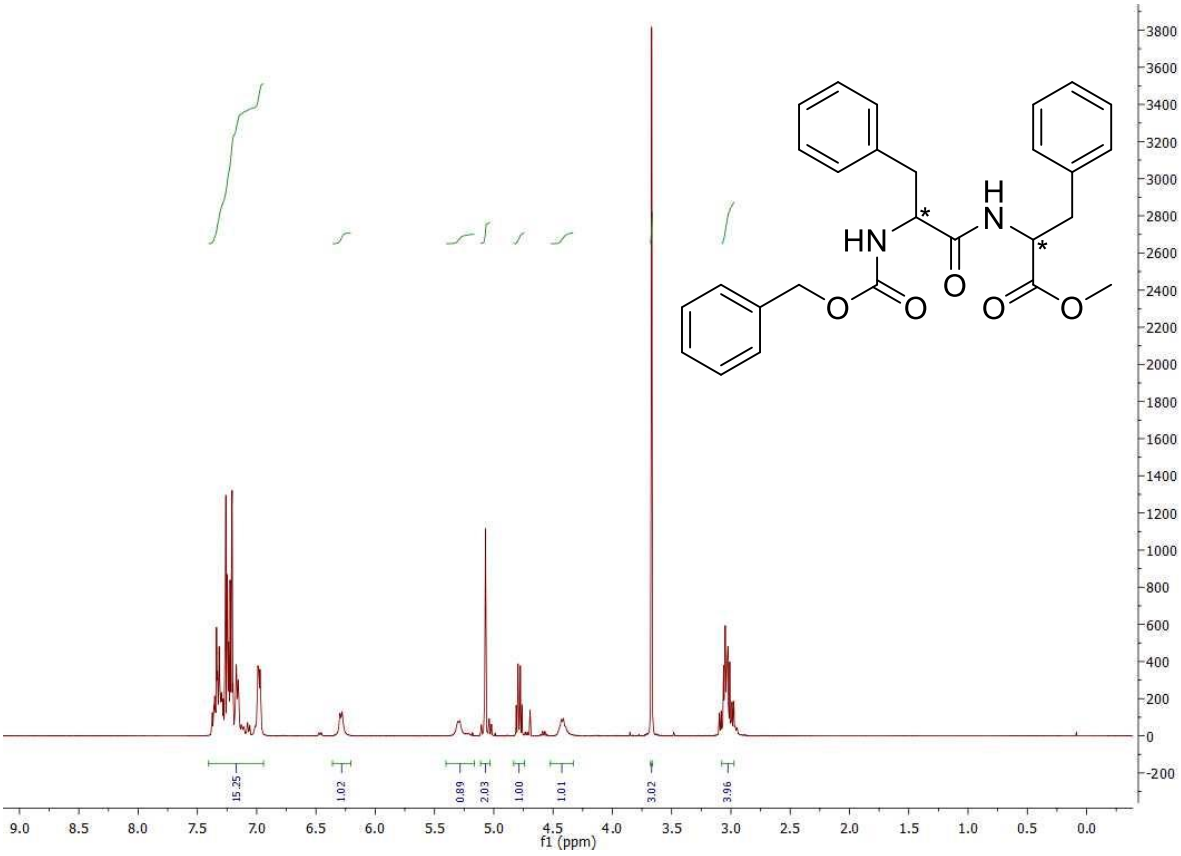

^{1}H NMR spectrum in $CDCl_3$.

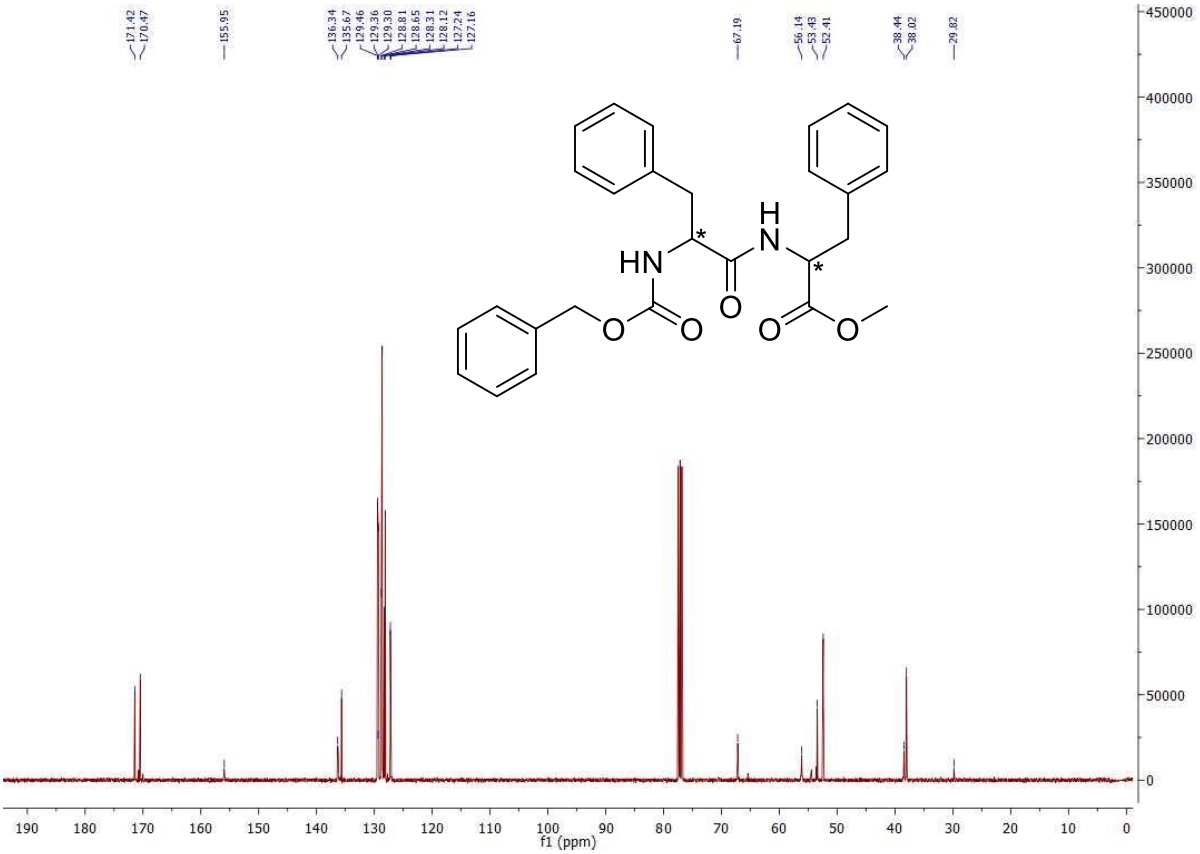

^{13}C NMR spectrum in $CDCl_3$.

53a

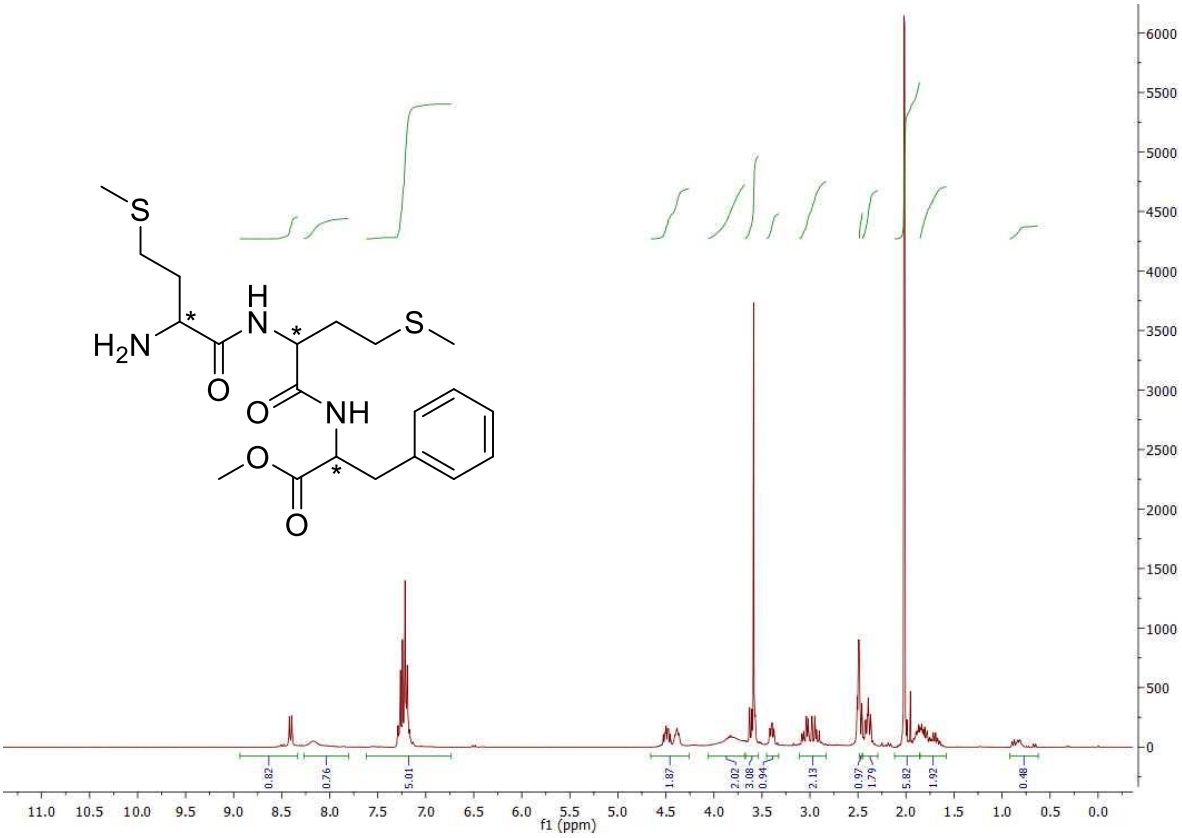

^{1}H NMR spectrum in DMSO-d_6.

53b

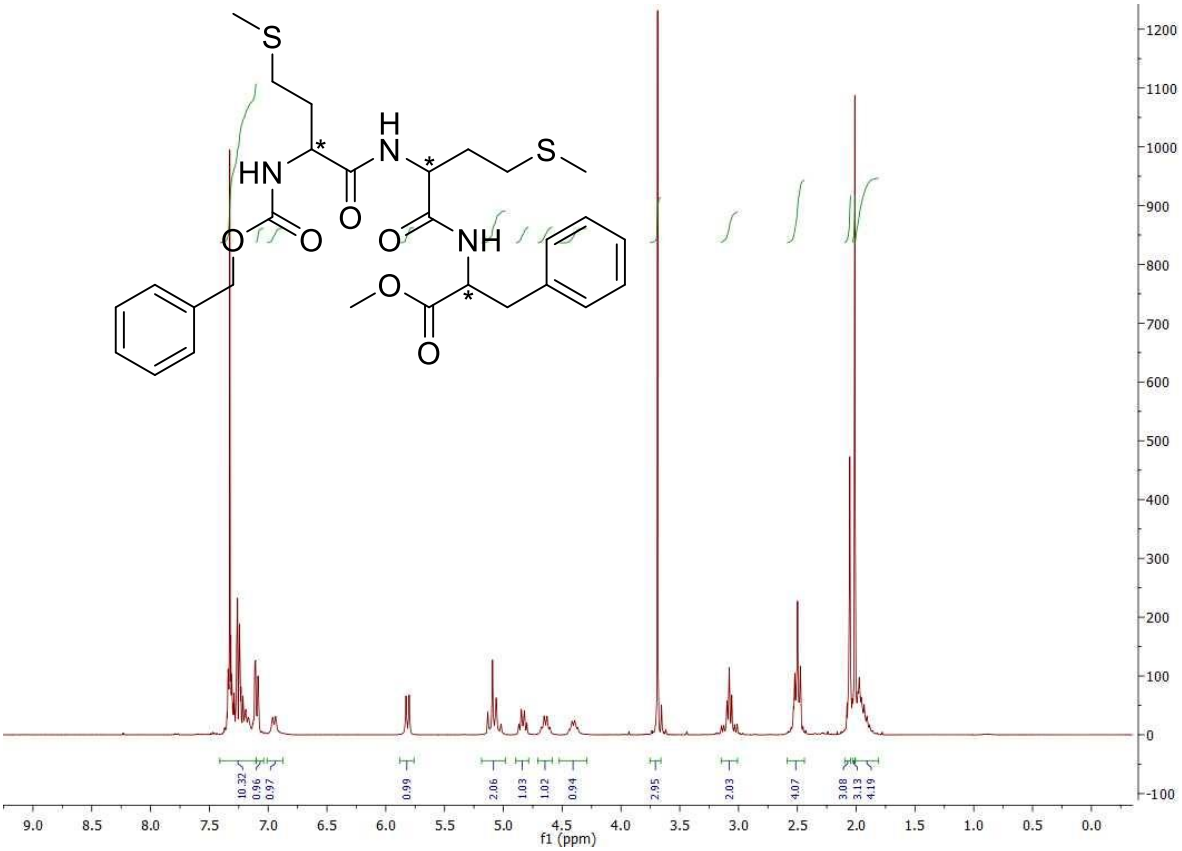

^{1}H NMR spectrum in $CDCl_3$.

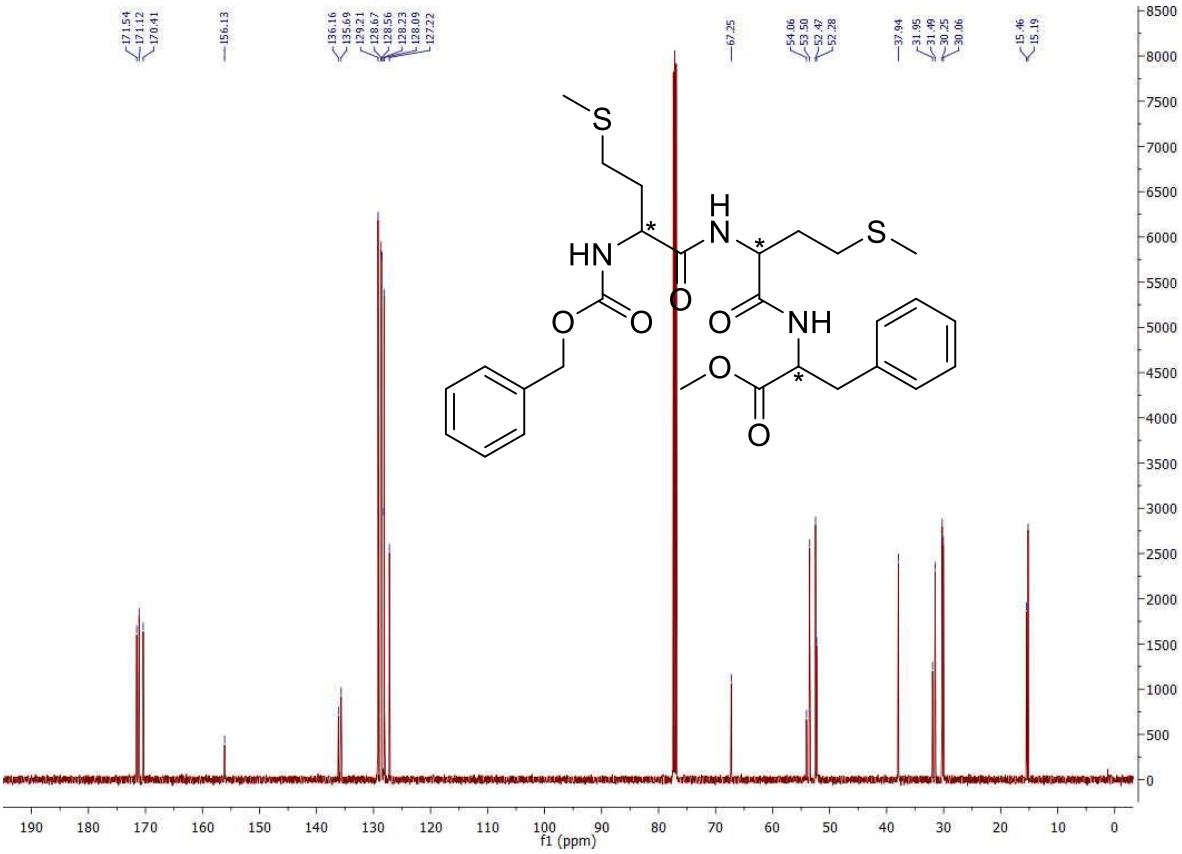

^{13}C NMR spectrum in $CDCl_3$.

54b

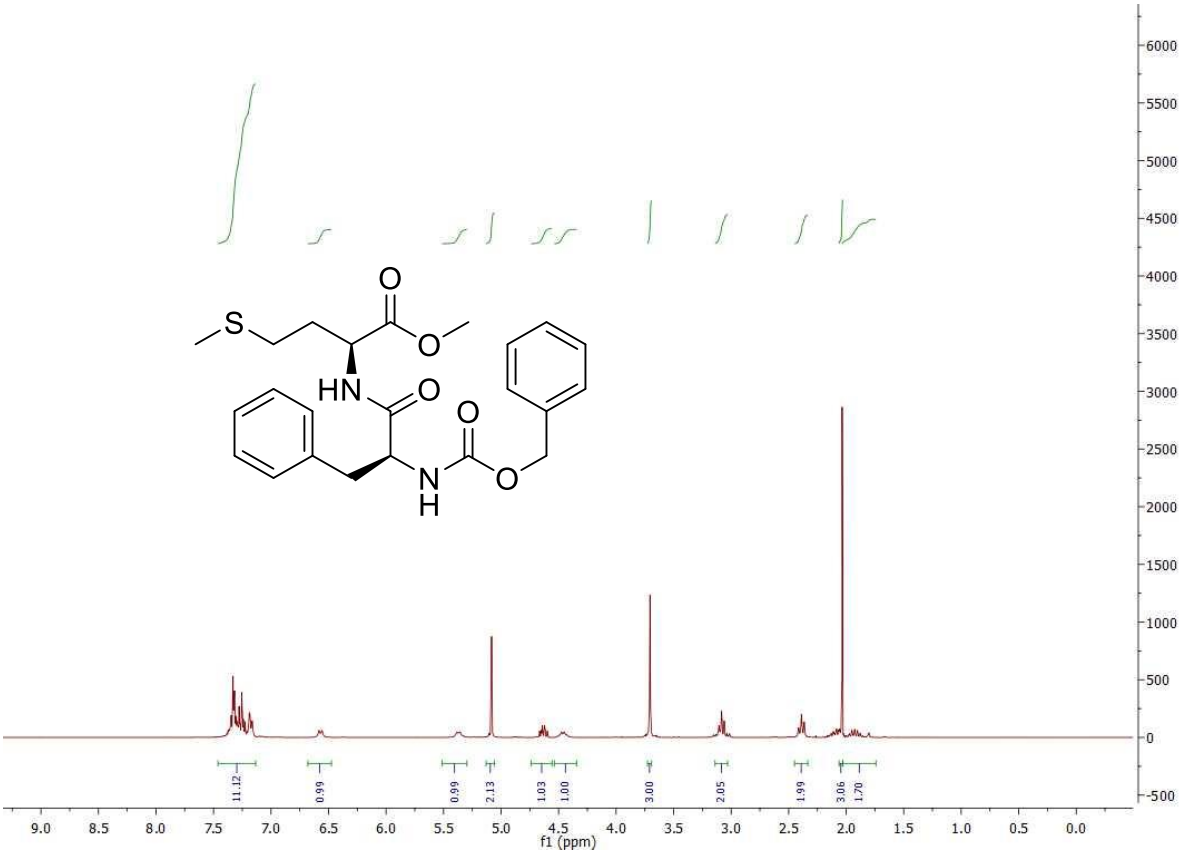

^{1}H NMR spectrum in $CDCl_3$.

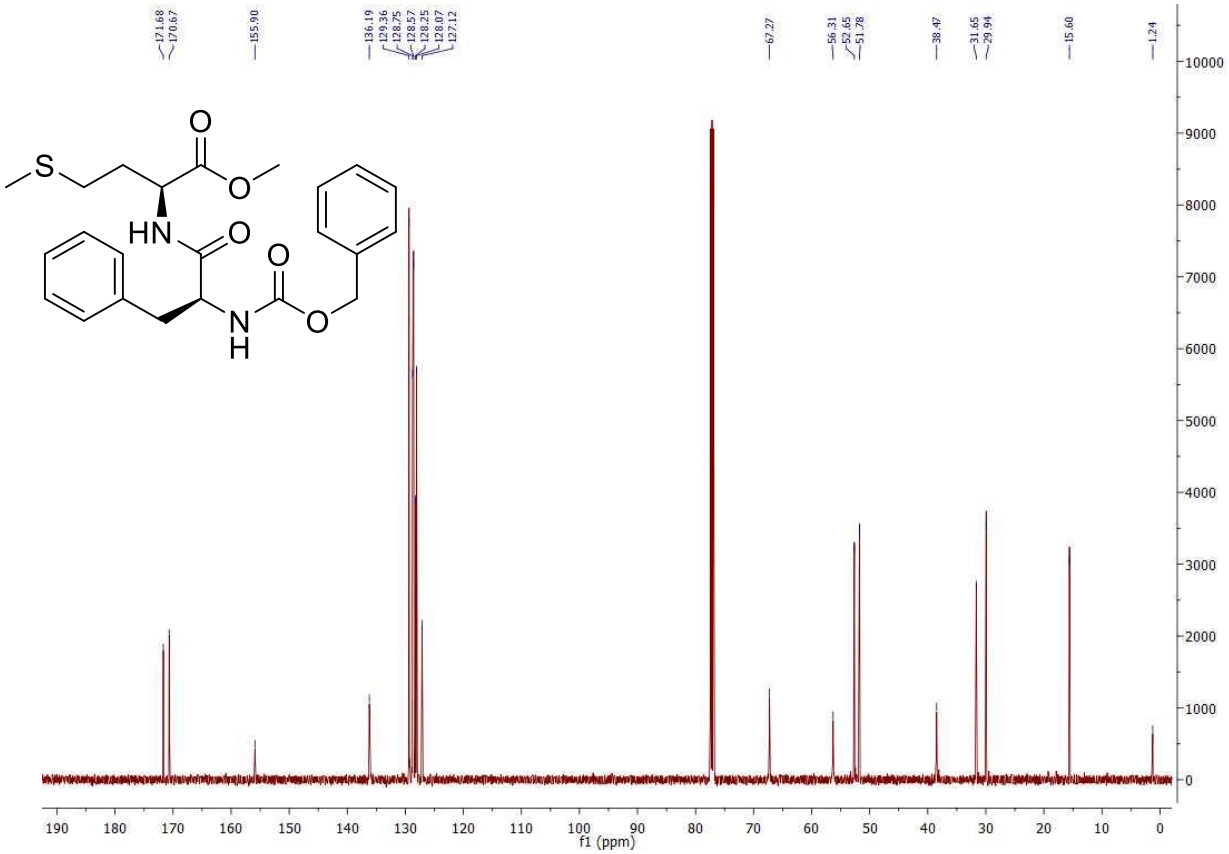

^{13}C NMR spectrum in $CDCl_3$.

55b

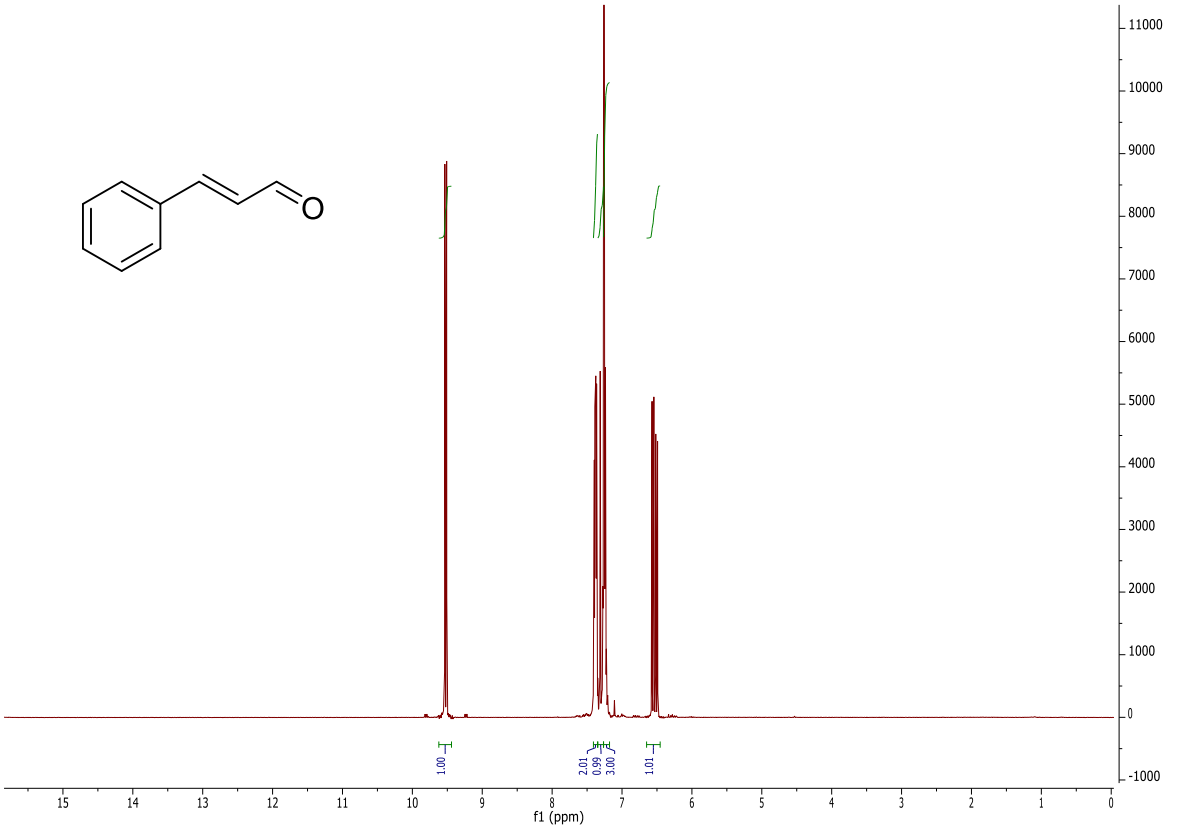

^{1}H NMR spectrum in $CDCl_3$.

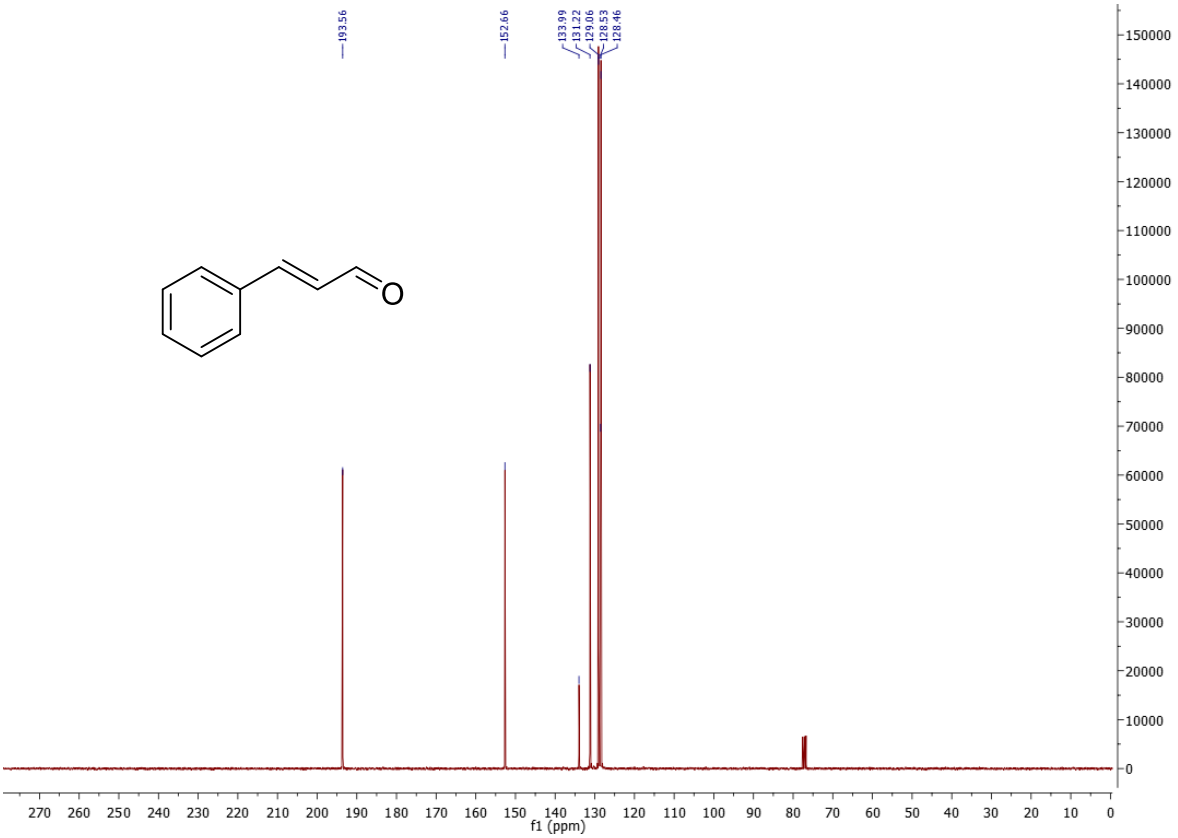

^{13}C NMR spectrum in $CDCl_3$.

56b

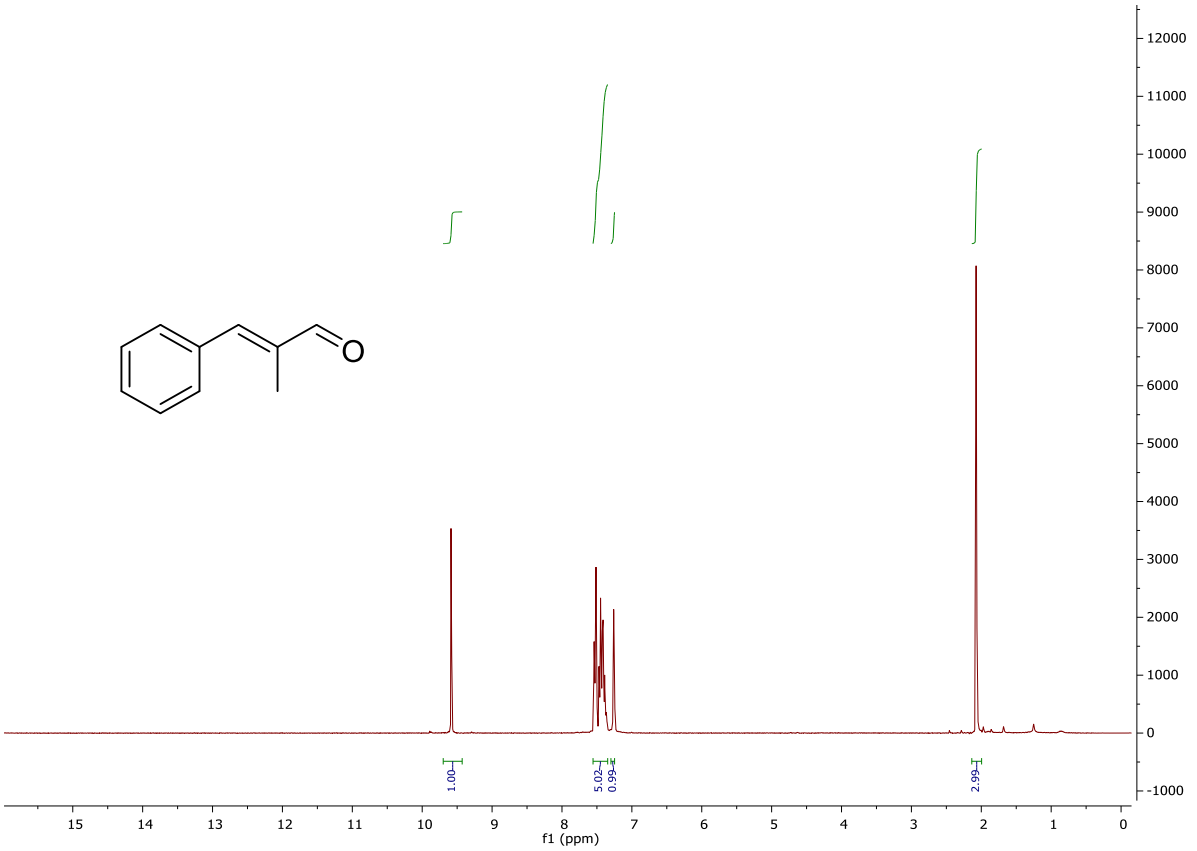

^{1}H NMR spectrum in $CDCl_3$.

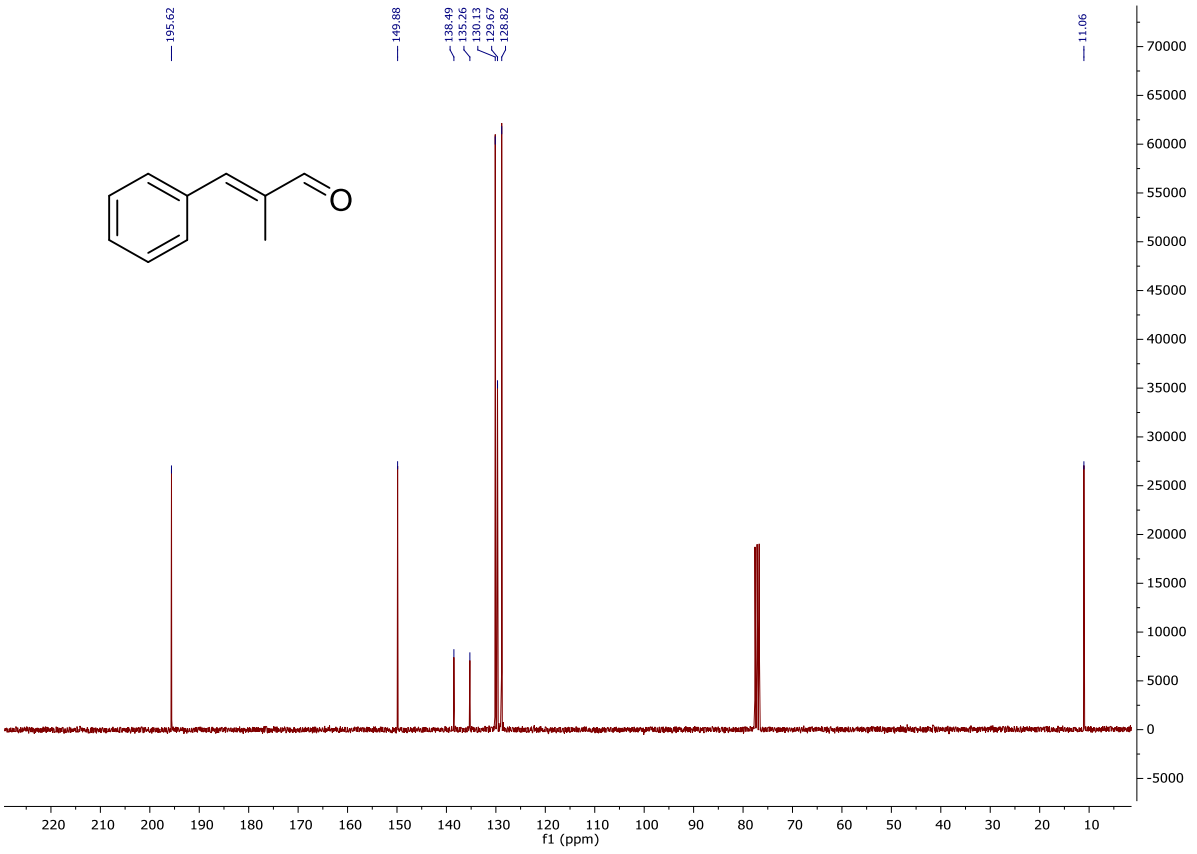

^{13}C NMR spectrum in $CDCl_3$.

57b

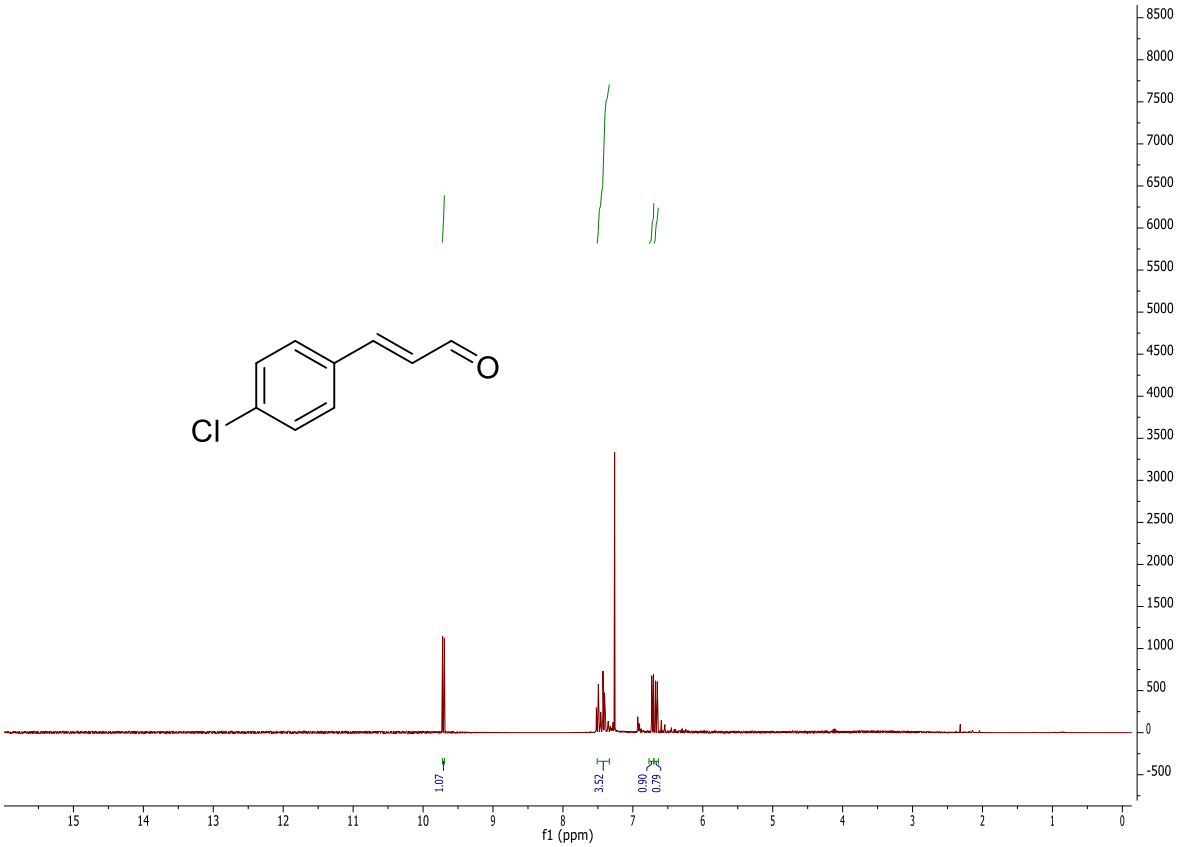

^{1}H NMR spectrum in $CDCl_3$.

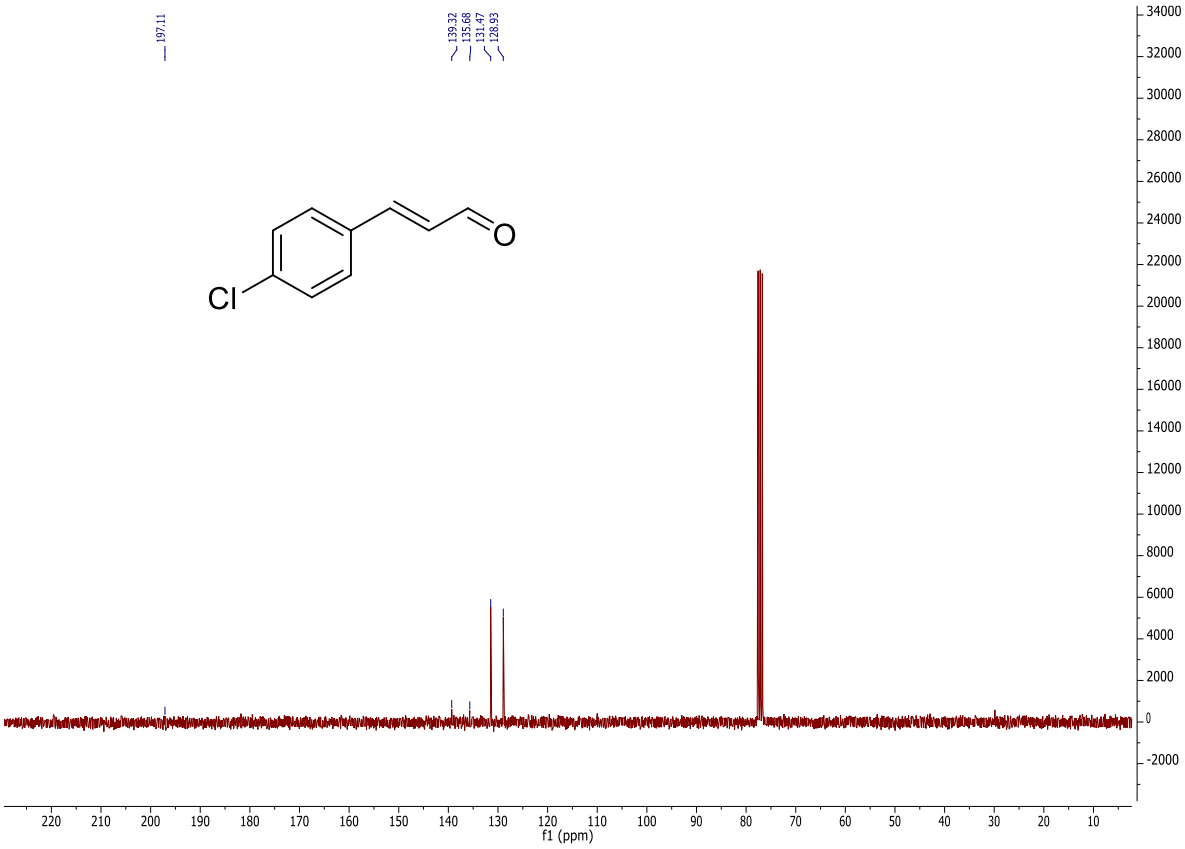

^{13}C NMR spectrum in $CDCl_3$.

58b

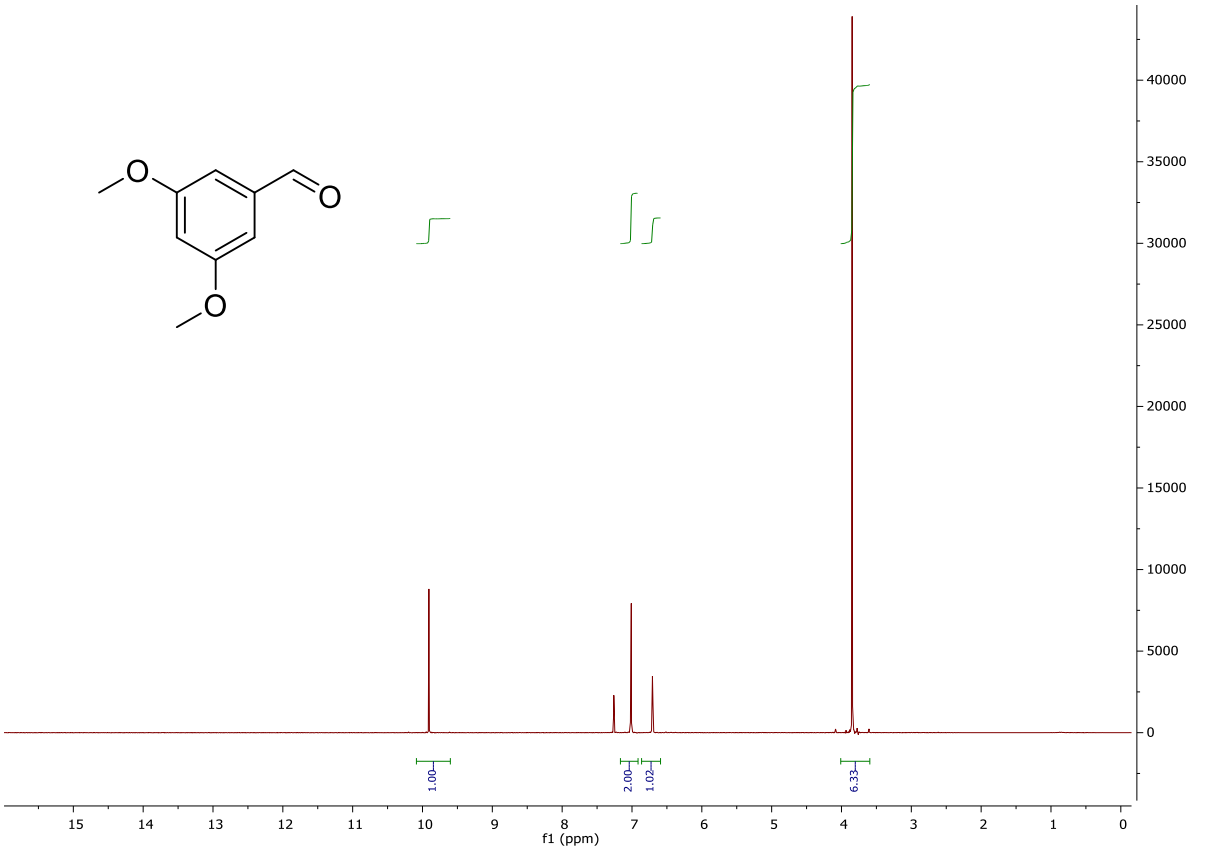

^{1}H NMR spectrum in $CDCl_3$.

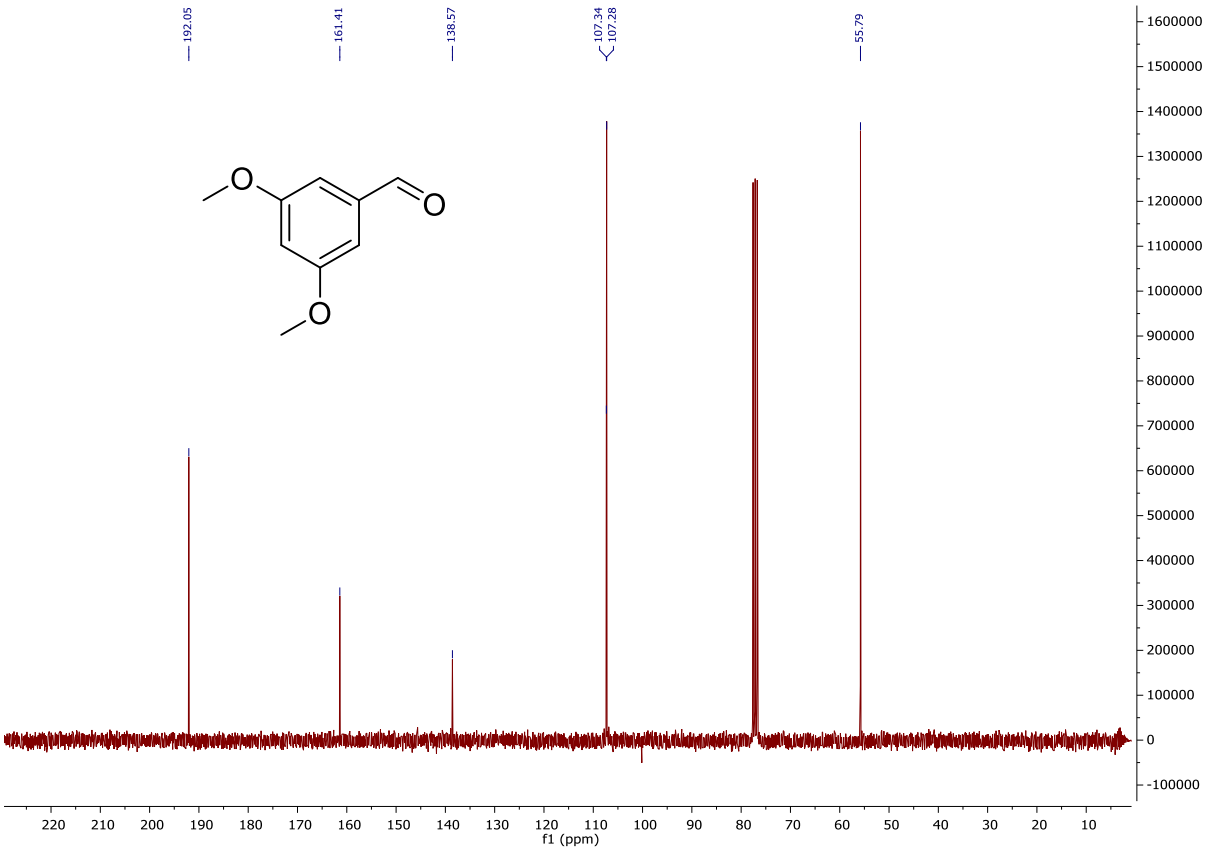

^{13}C NMR spectrum in $CDCl_3$.

59b

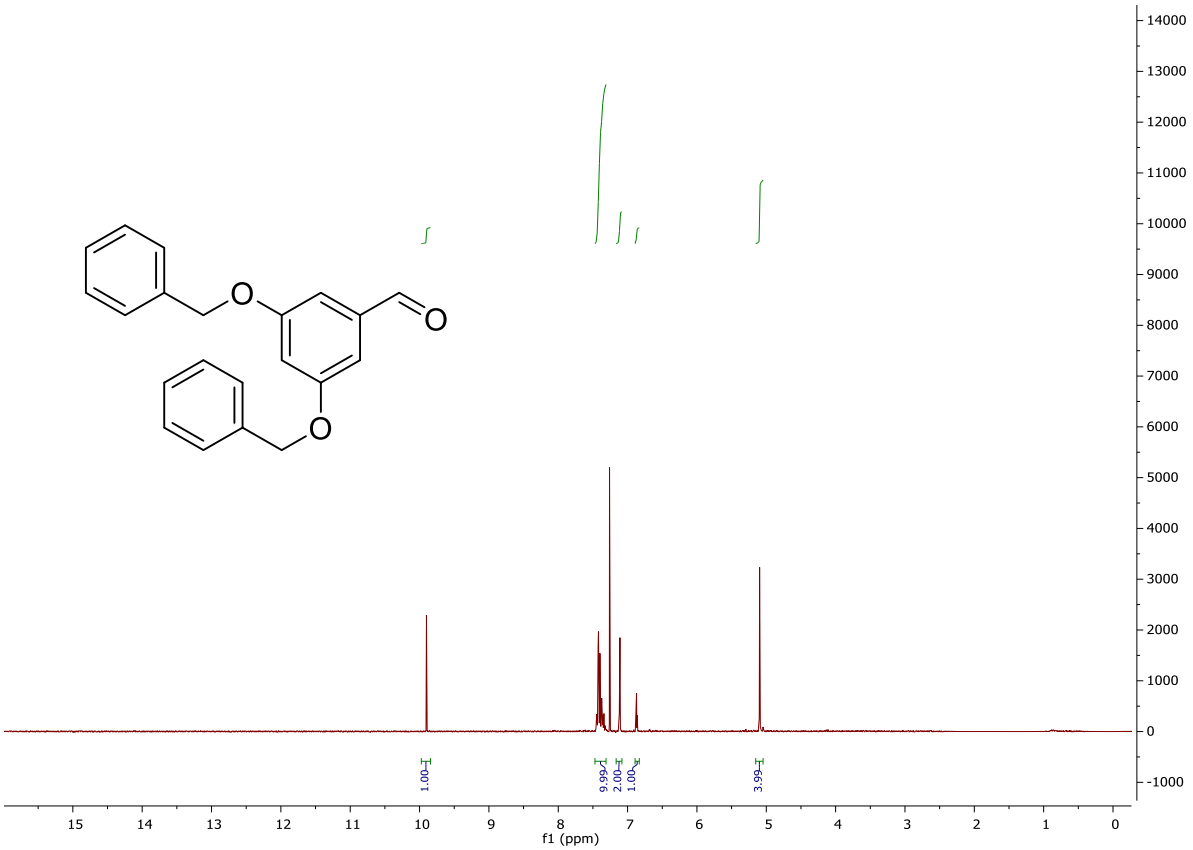

^{1}H NMR spectrum in $CDCl_3$.

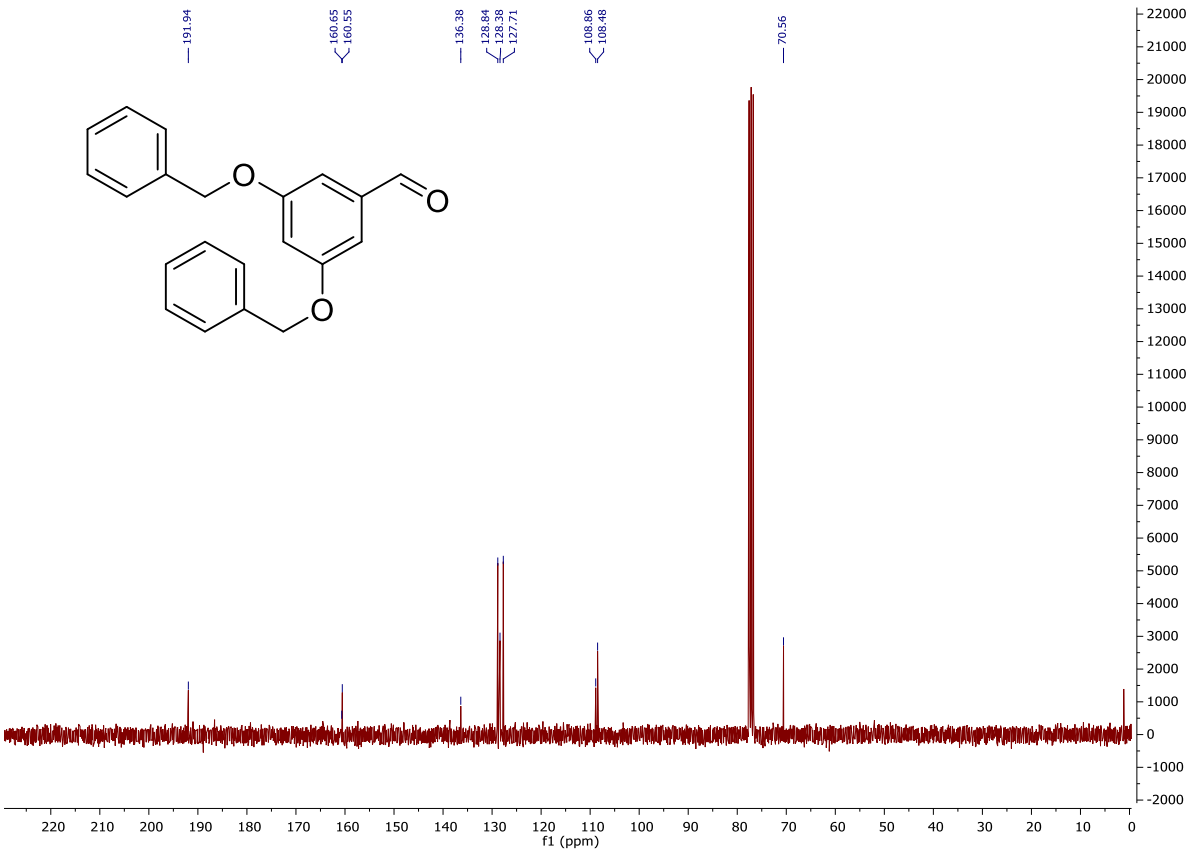

^{13}C NMR spectrum in $CDCl_3$.

60b

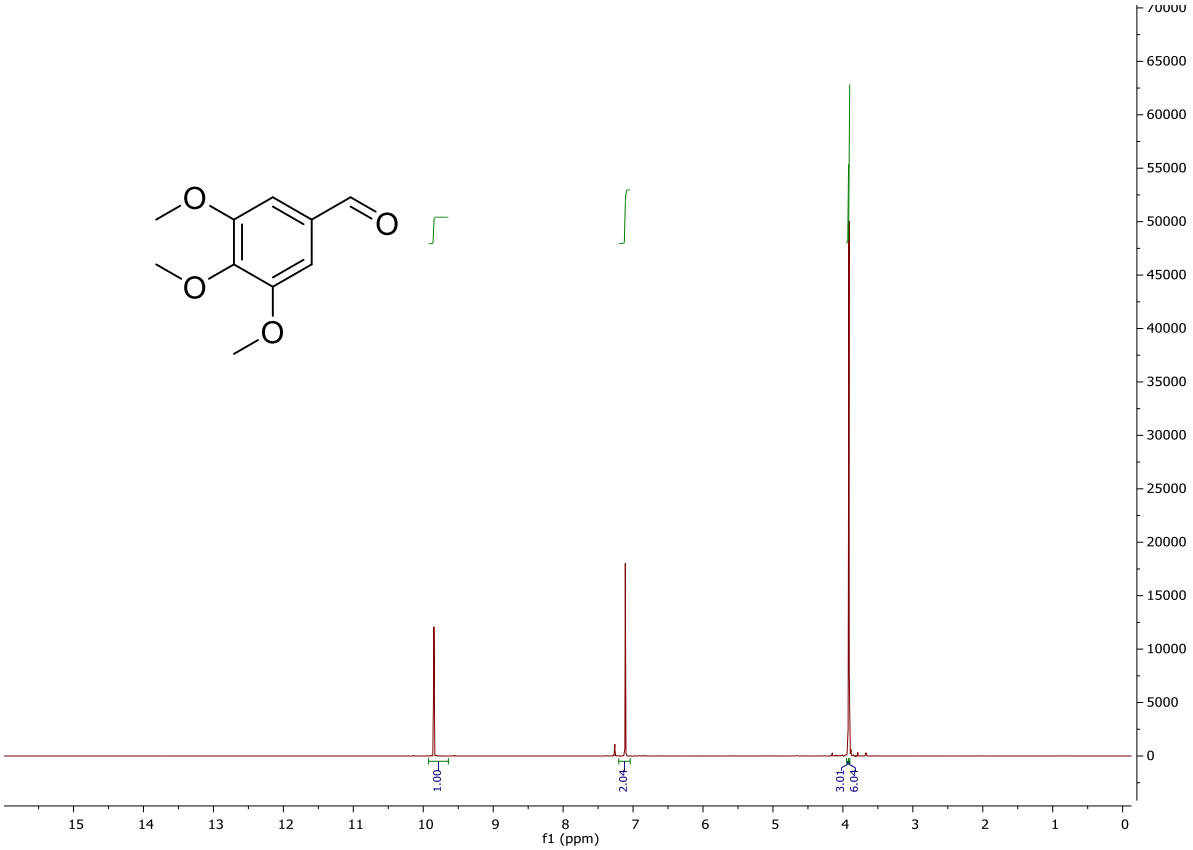

^{1}H NMR spectrum in $CDCl_3$.

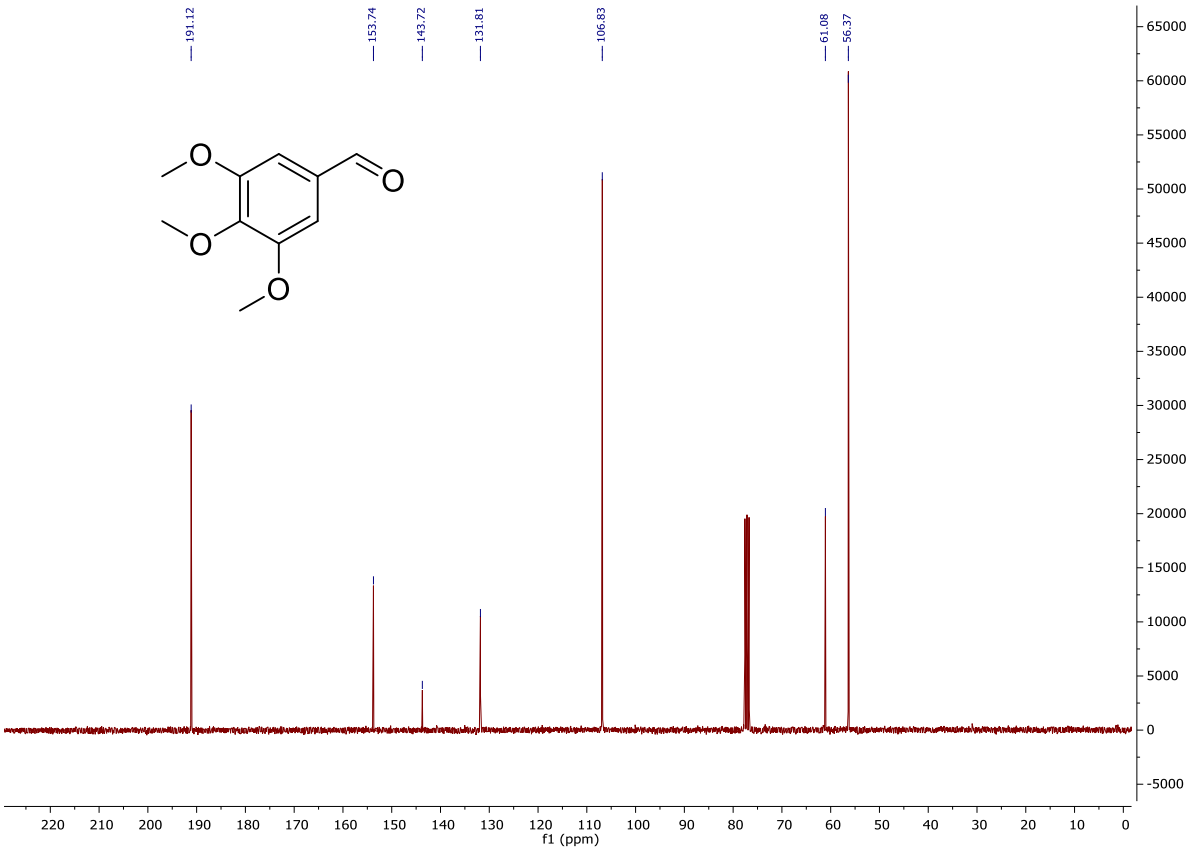

^{13}C NMR spectrum in $CDCl_3$.

61b

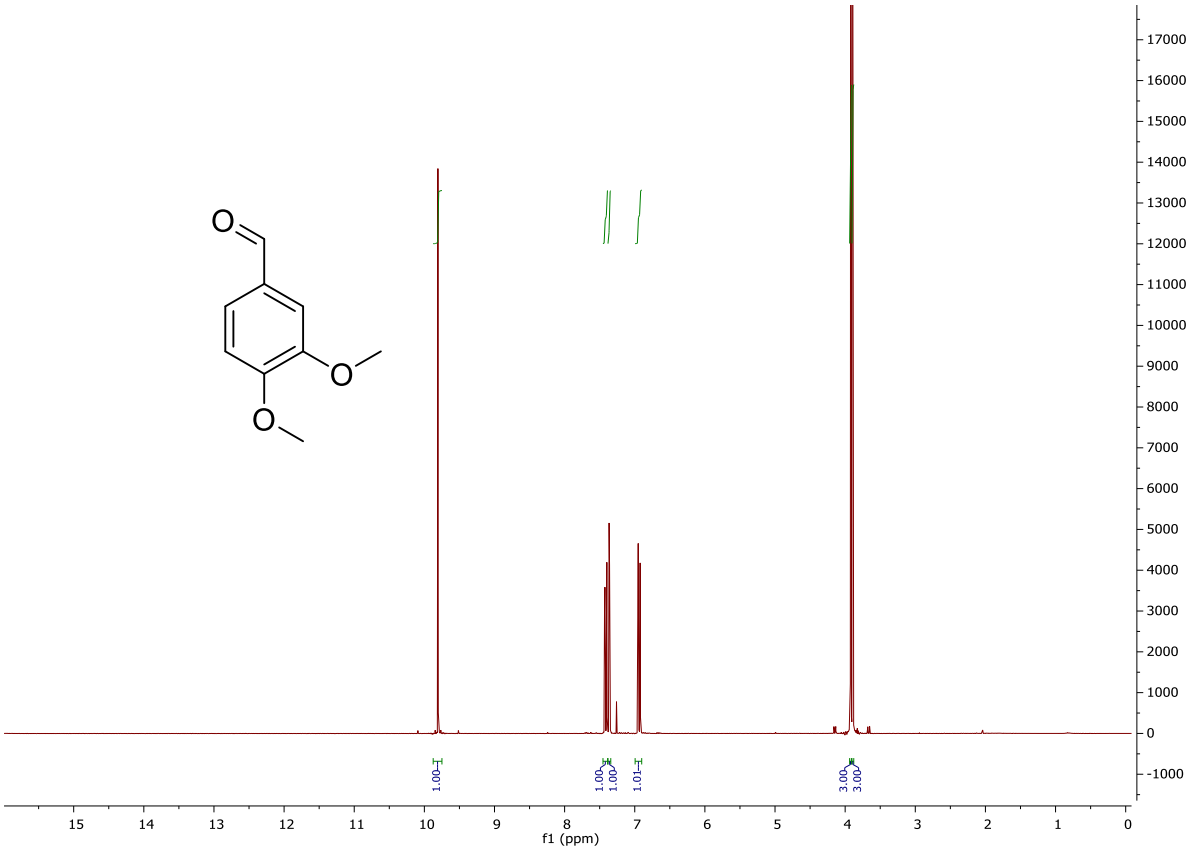

^{1}H NMR spectrum in $CDCl_3$.

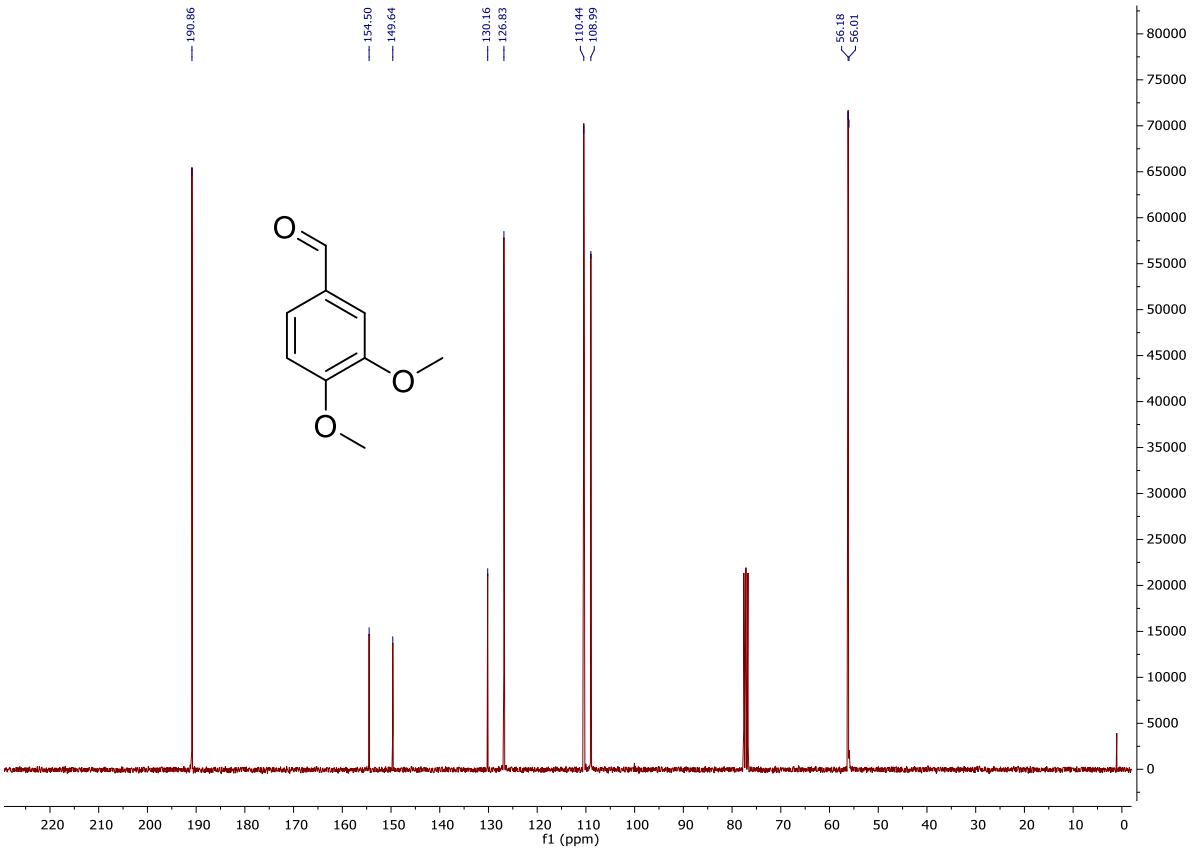

^{13}C NMR spectrum in $CDCl_3$.

62b

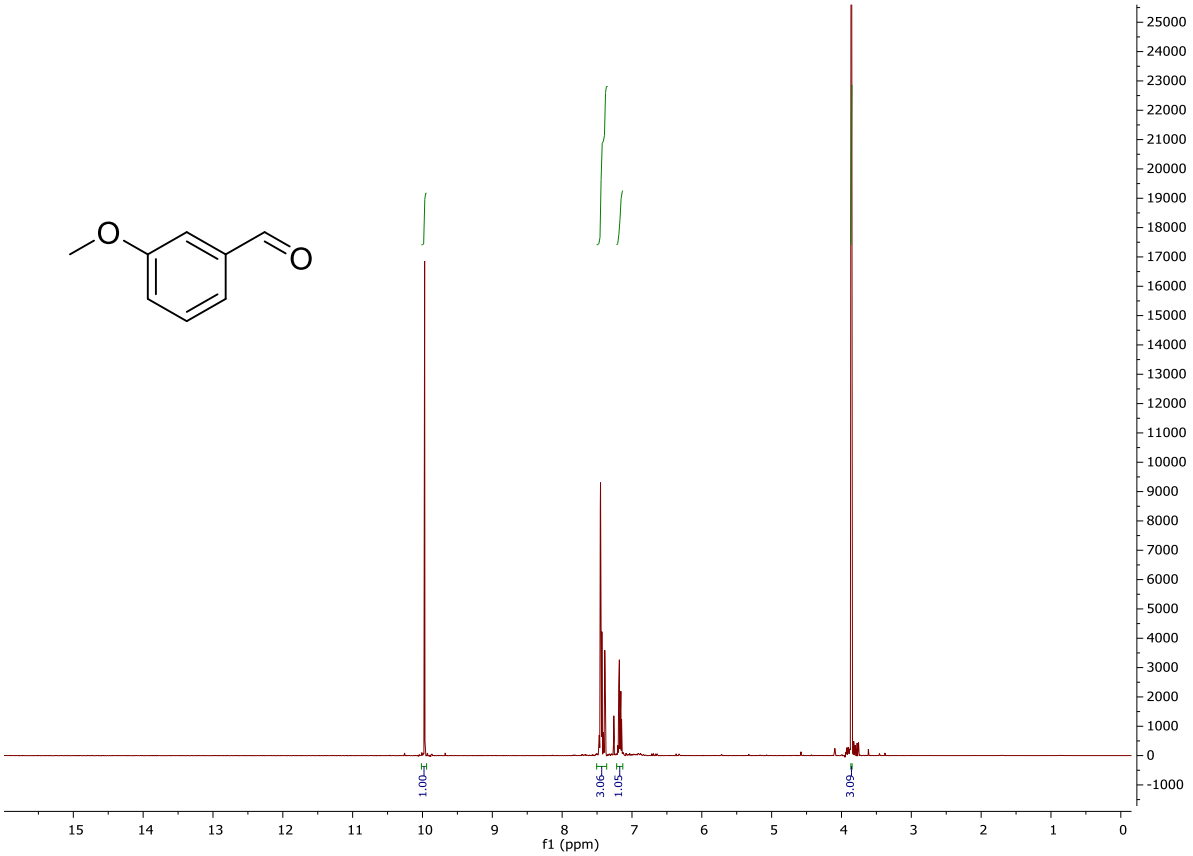

^{1}H NMR spectrum in $CDCl_3$.

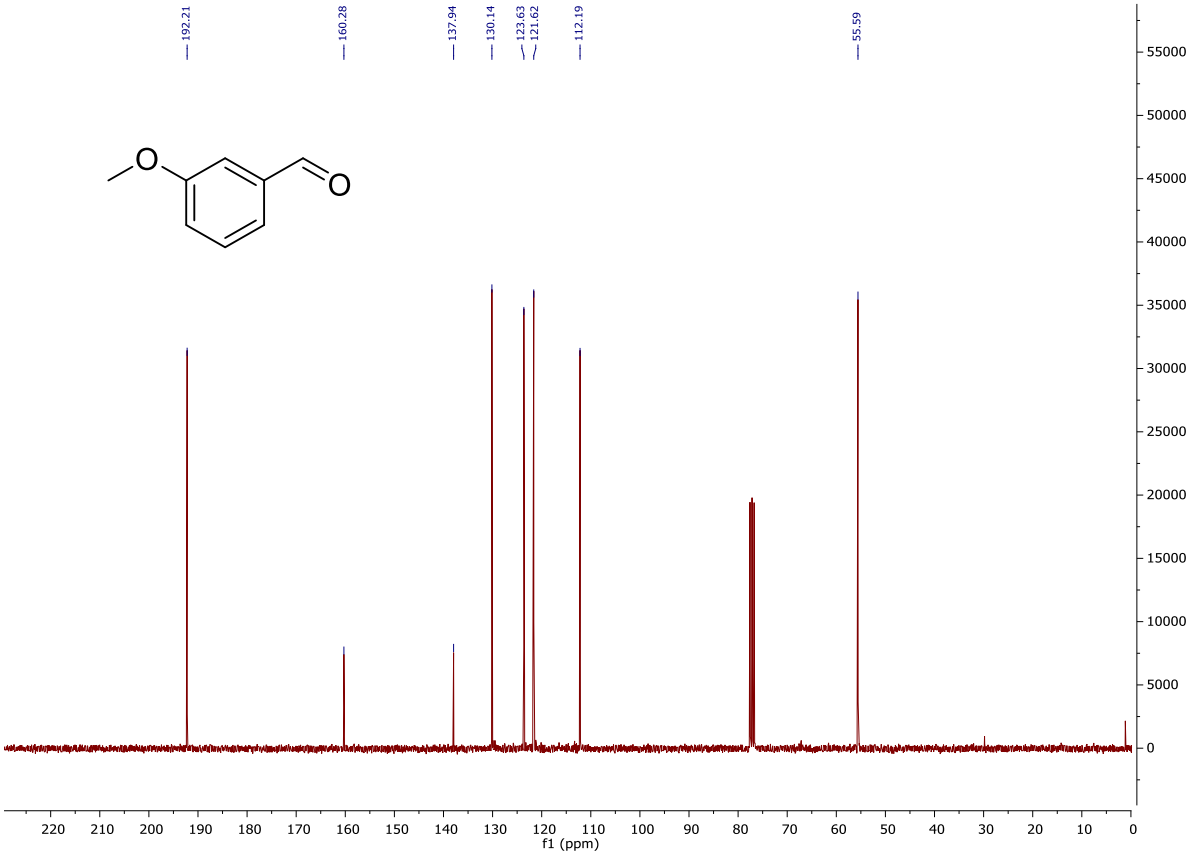

^{13}C NMR spectrum in $CDCl_3$.

63b

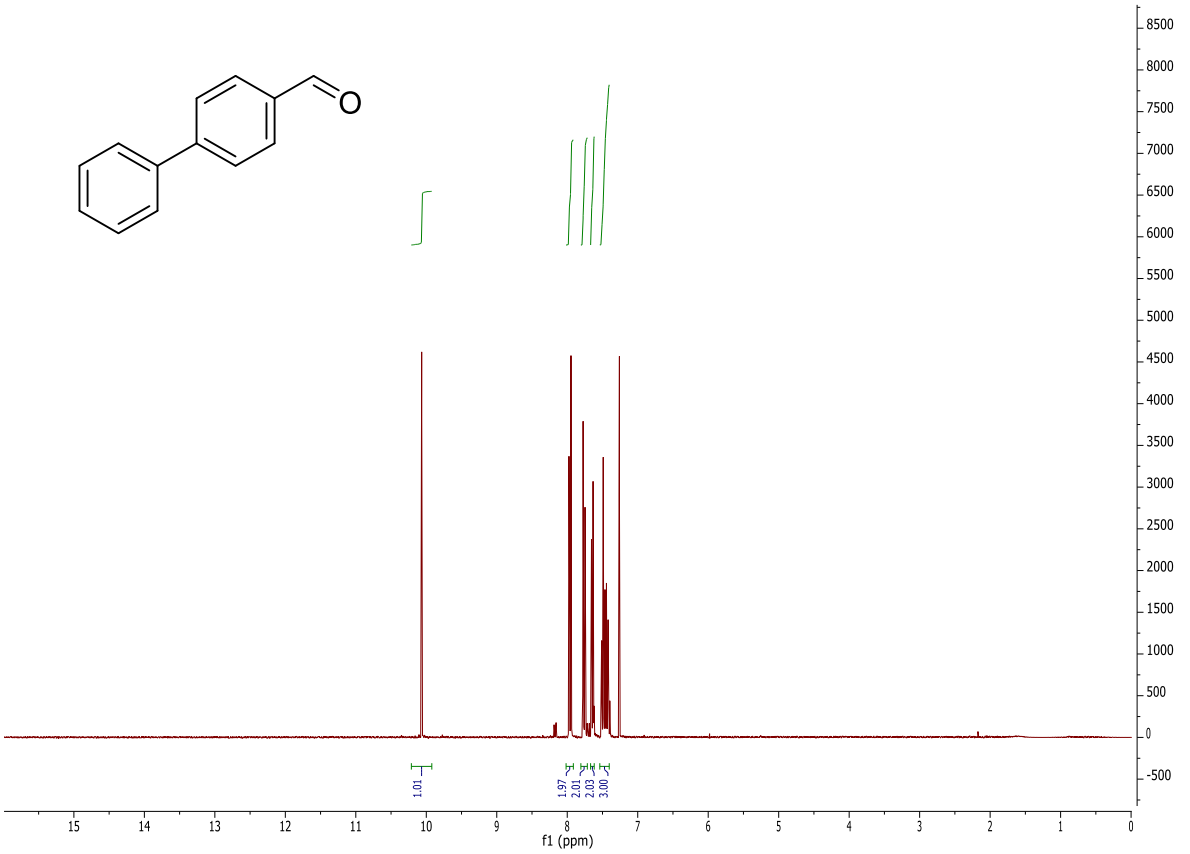

^{1}H NMR spectrum in $CDCl_3$.

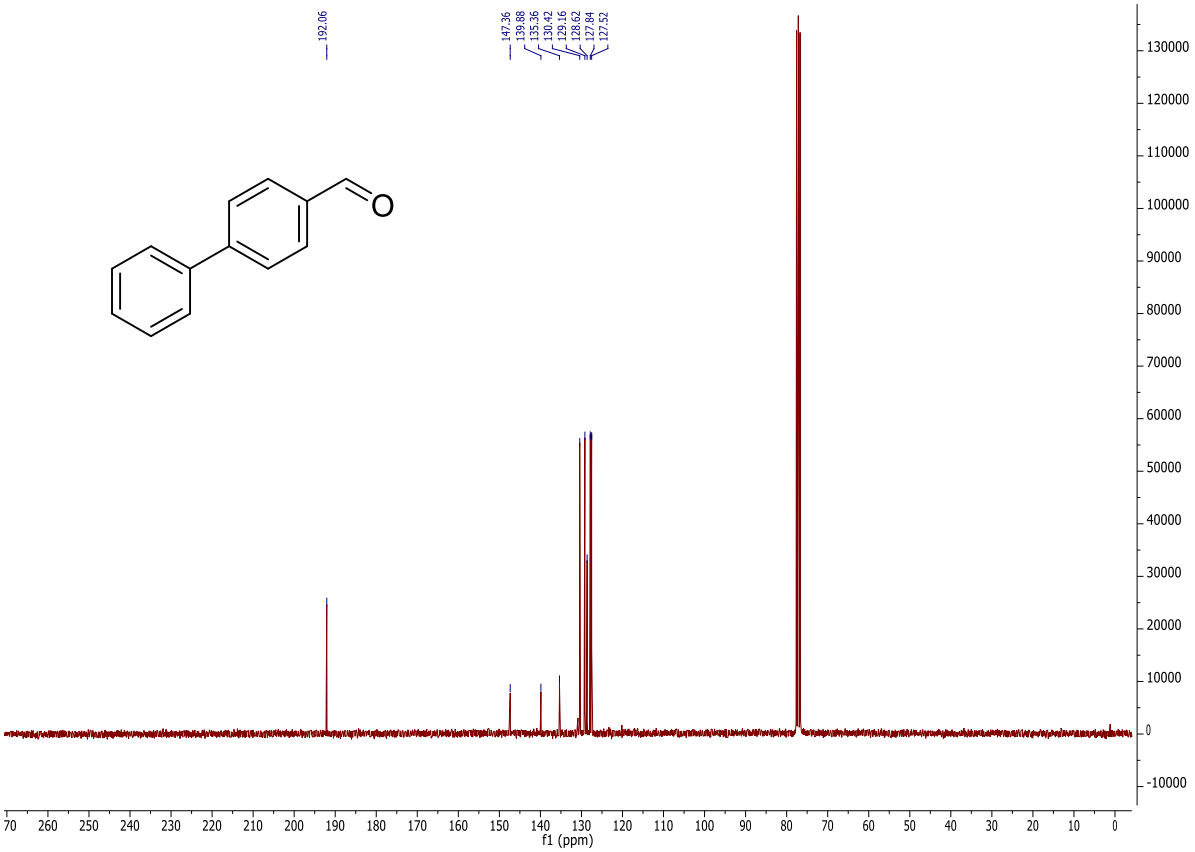

^{13}C NMR spectrum in $CDCl_3$.

64b

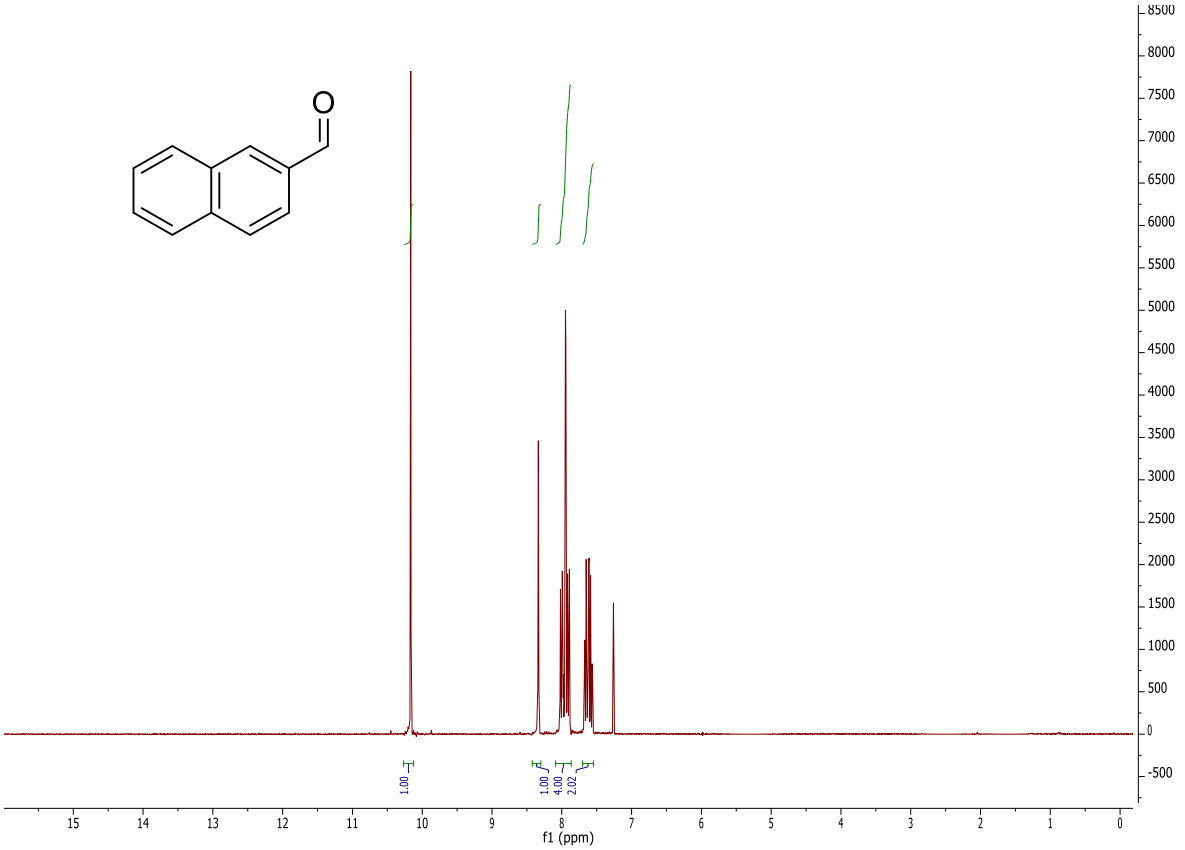

^{1}H NMR spectrum in $CDCl_3$.

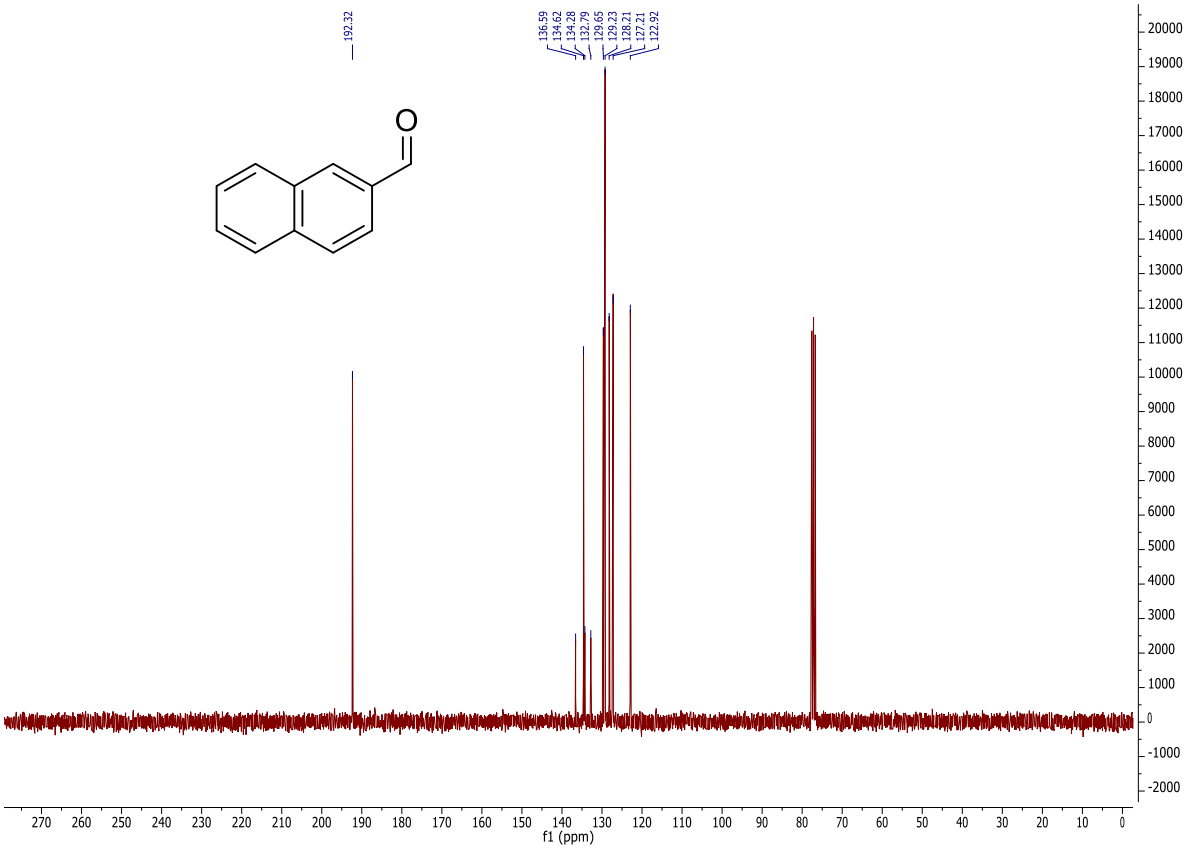

^{13}C NMR spectrum in $CDCl_3$.

65b

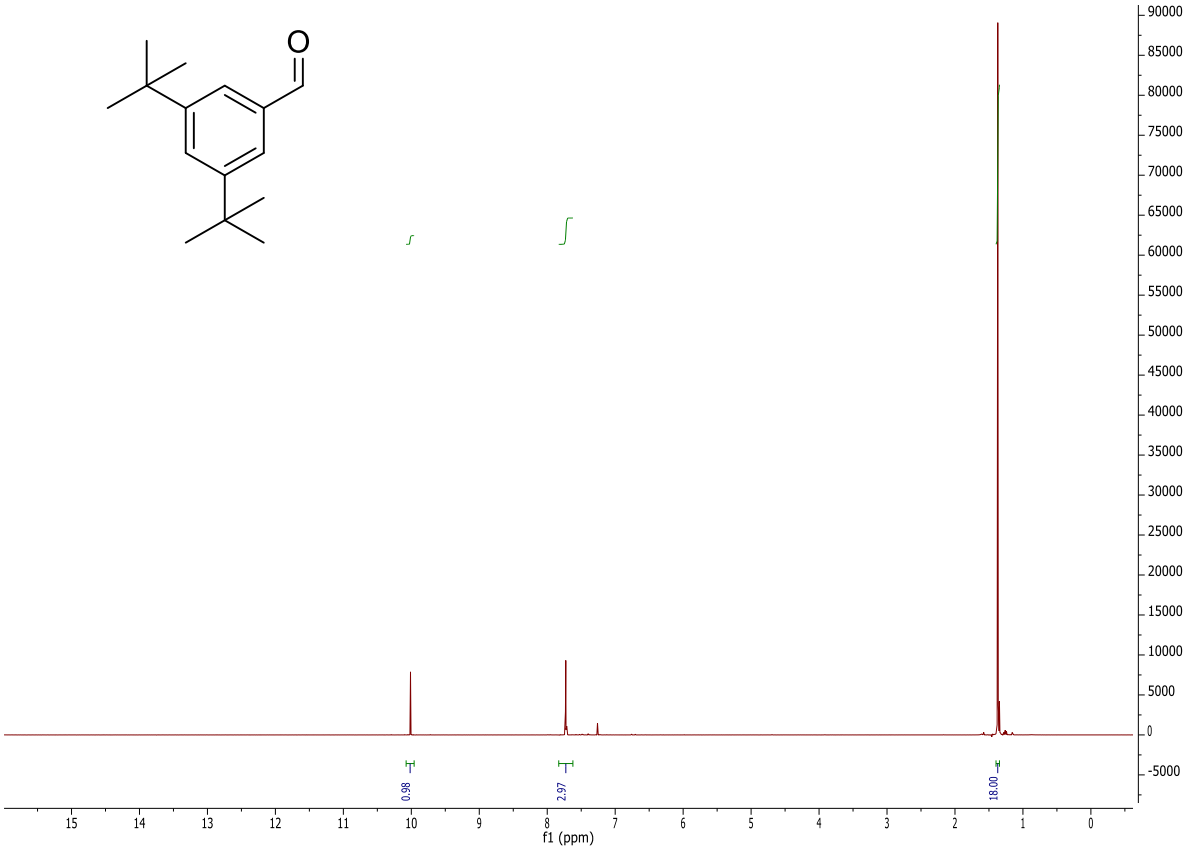

^{1}H NMR spectrum in $CDCl_3$.

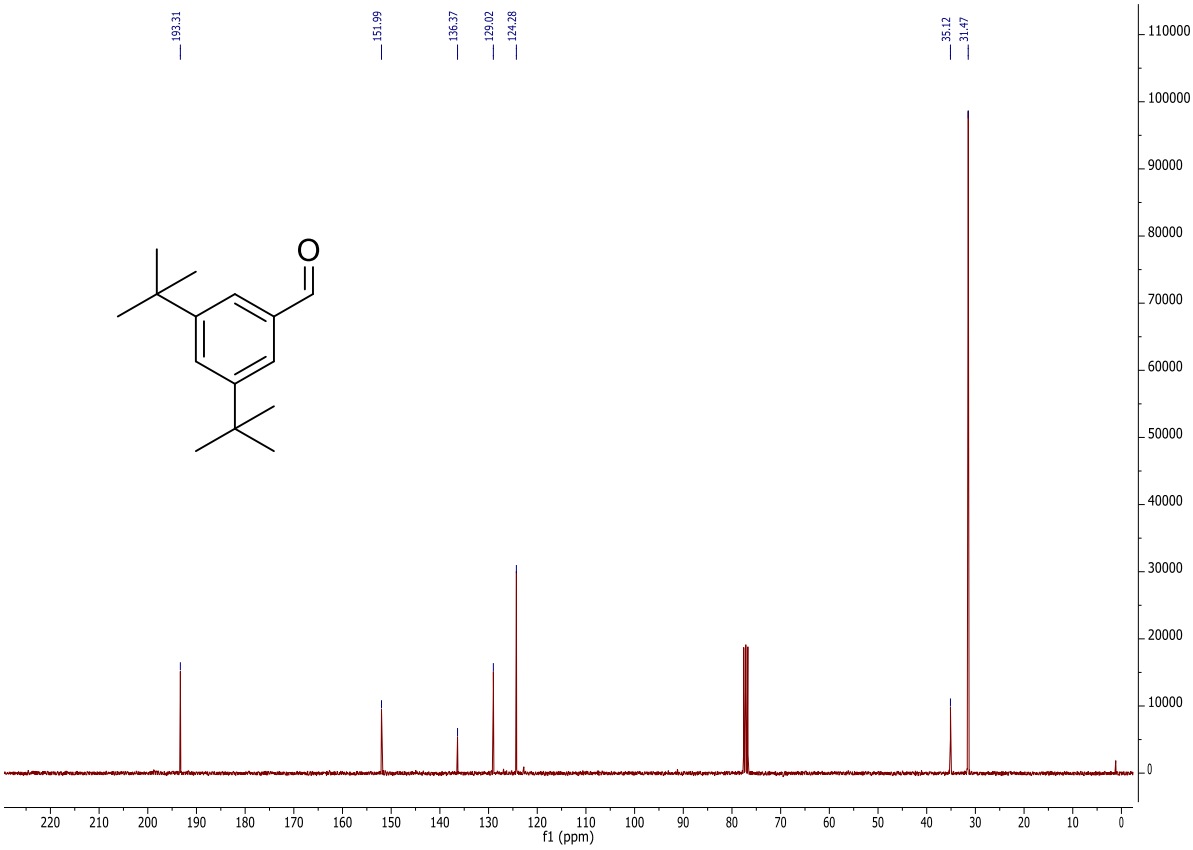

^{13}C NMR spectrum in $CDCl_3$.

66b

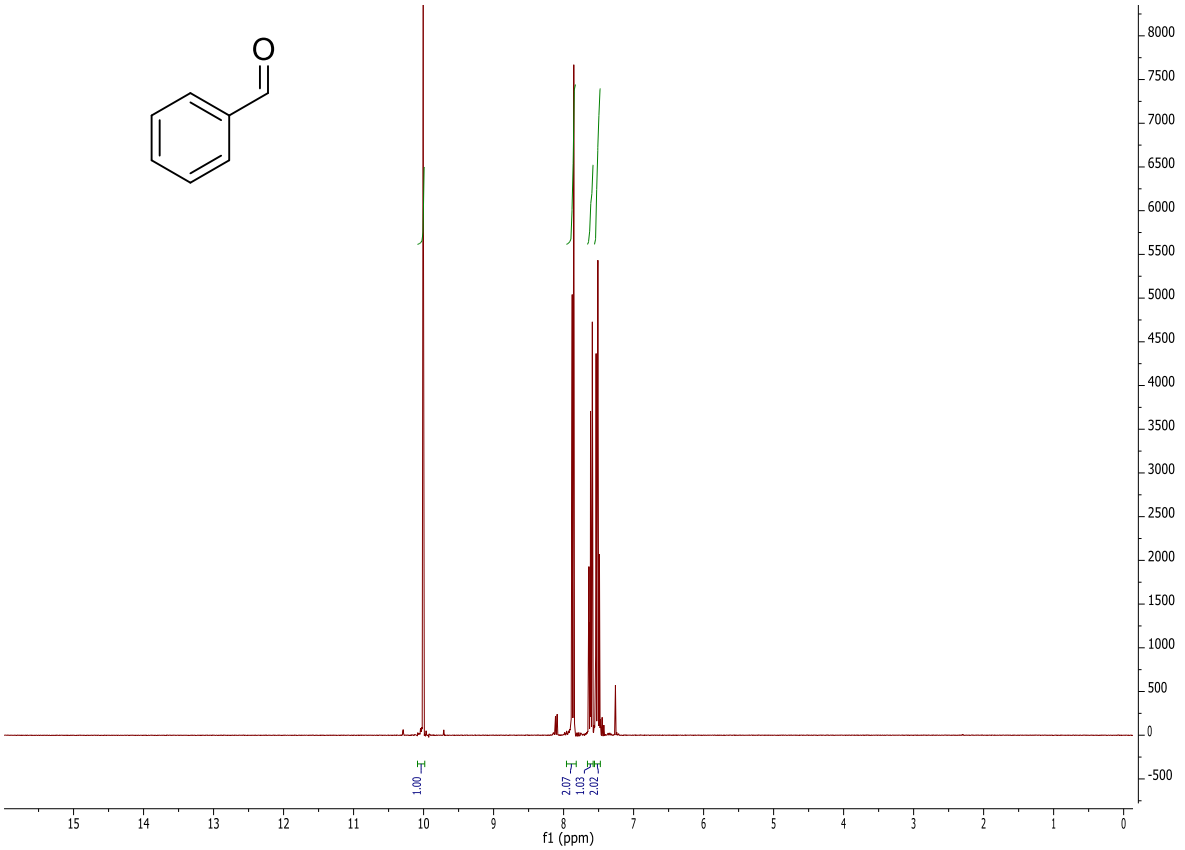

^{1}H NMR spectrum in $CDCl_3$.

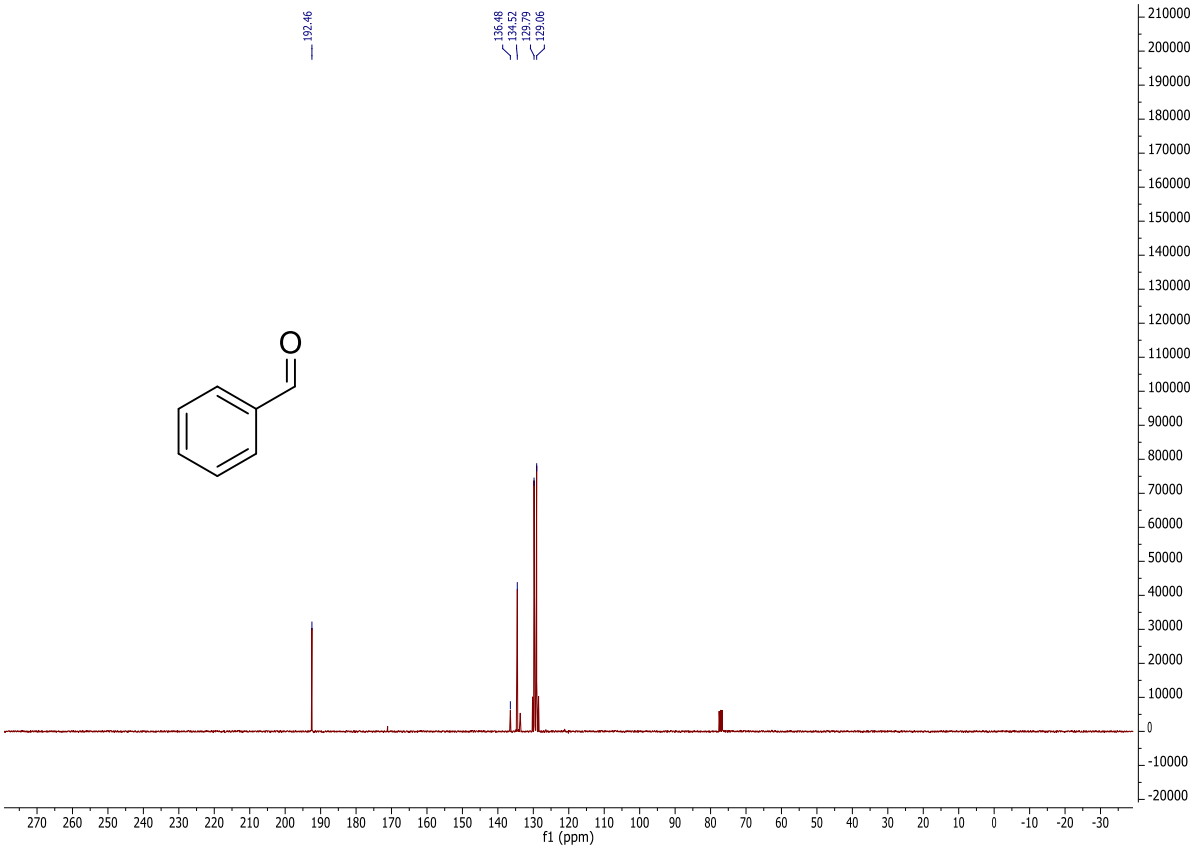

^{13}C NMR spectrum in $CDCl_3$.

67b

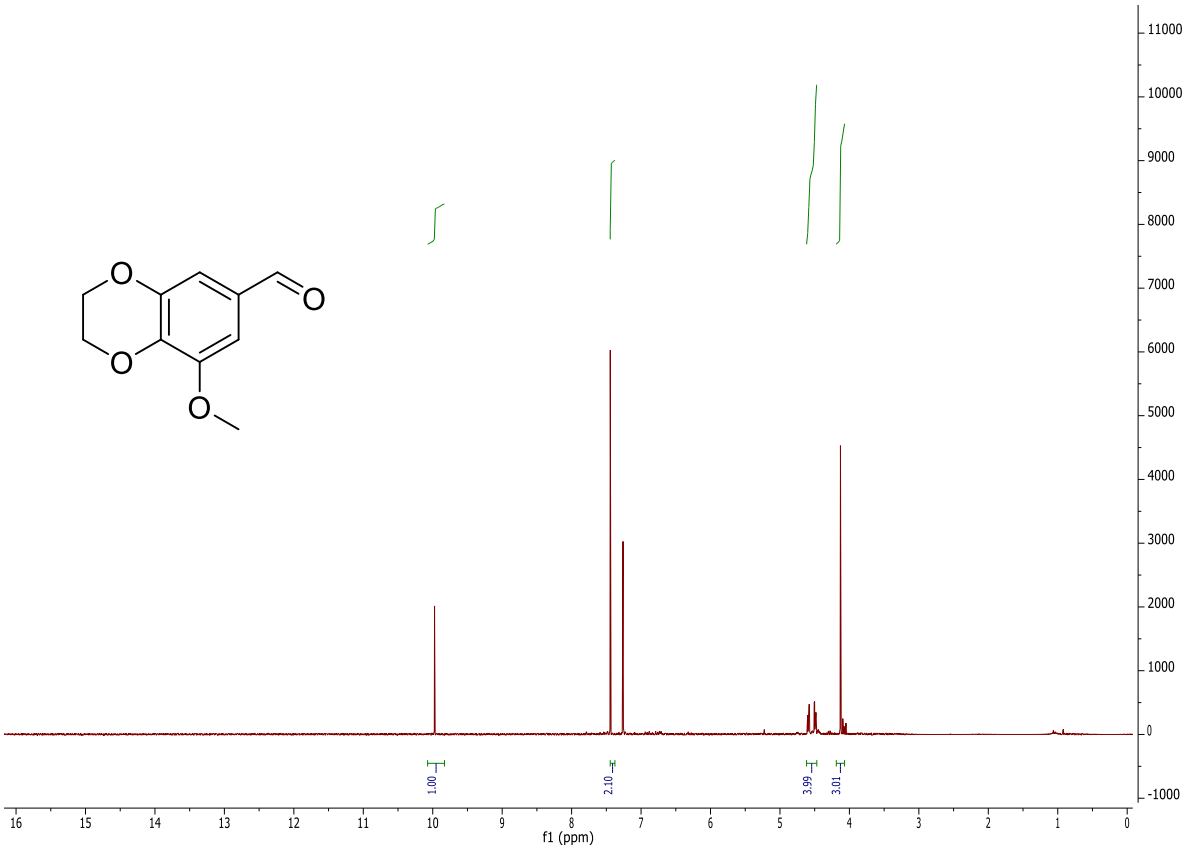

^{1}H NMR spectrum in $CDCl_3$.

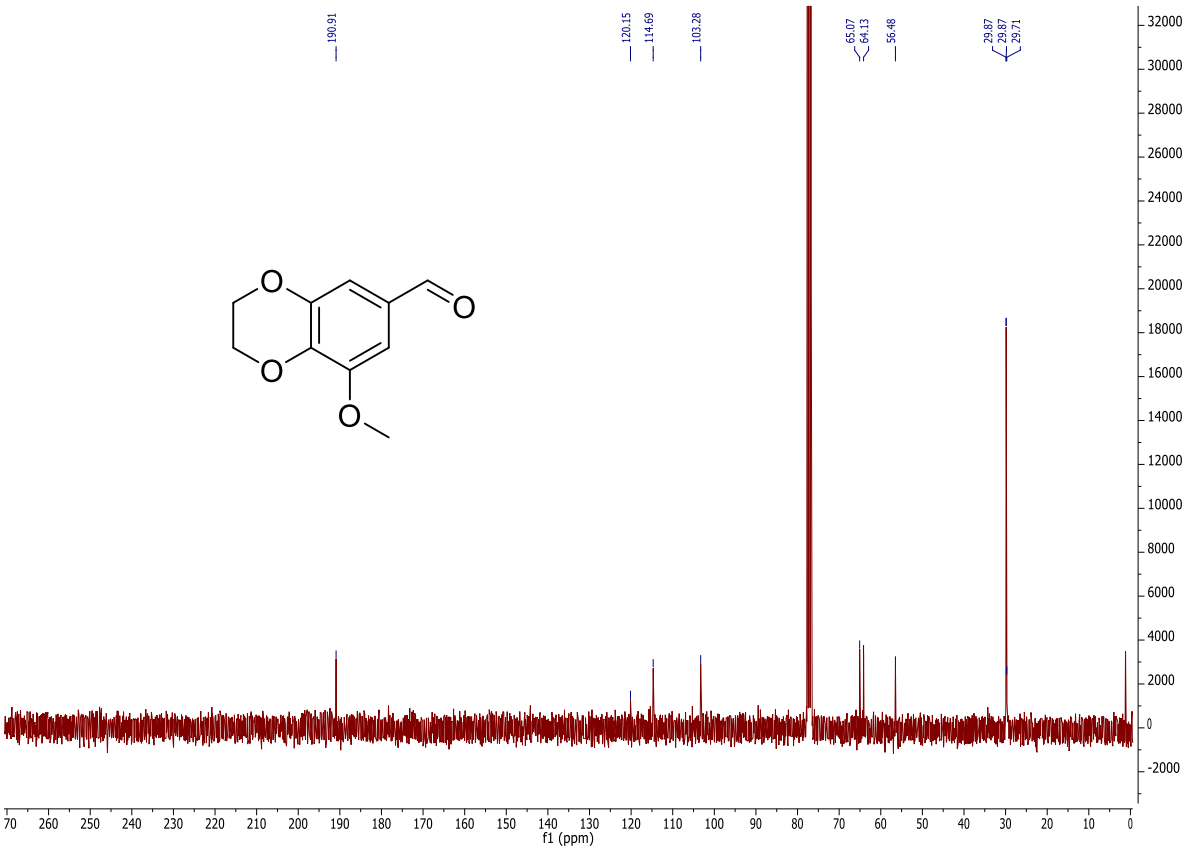

^{13}C NMR spectrum in $CDCl_3$.

68b

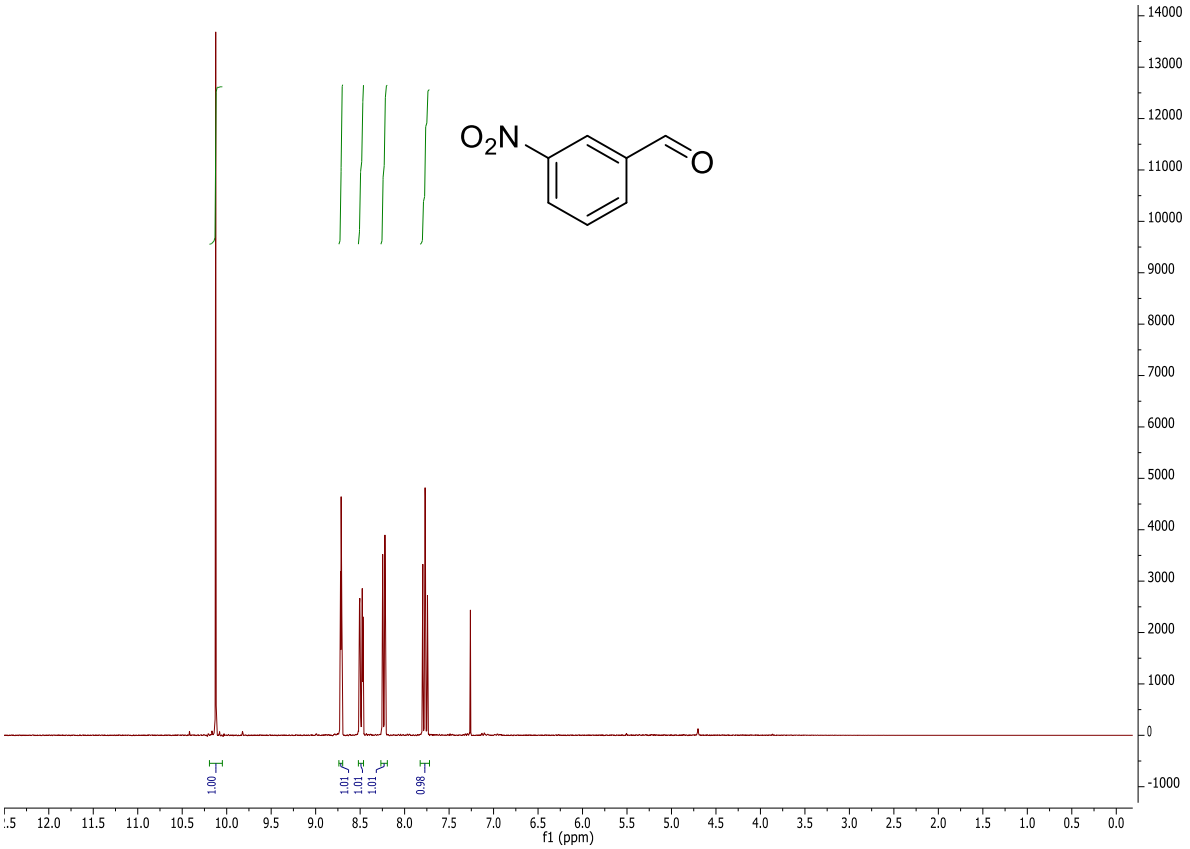

^{1}H NMR spectrum in $CDCl_3$.

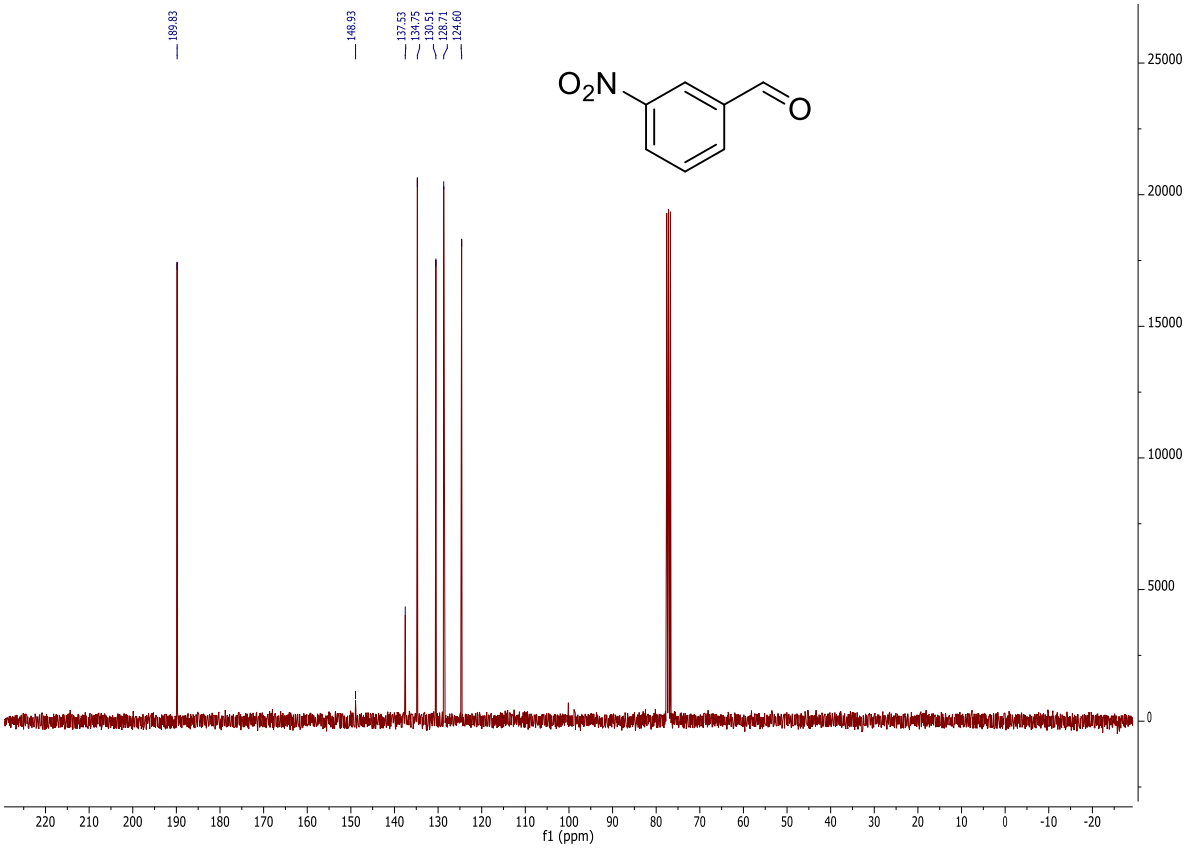

^{13}C NMR spectrum in $CDCl_3$.

69b

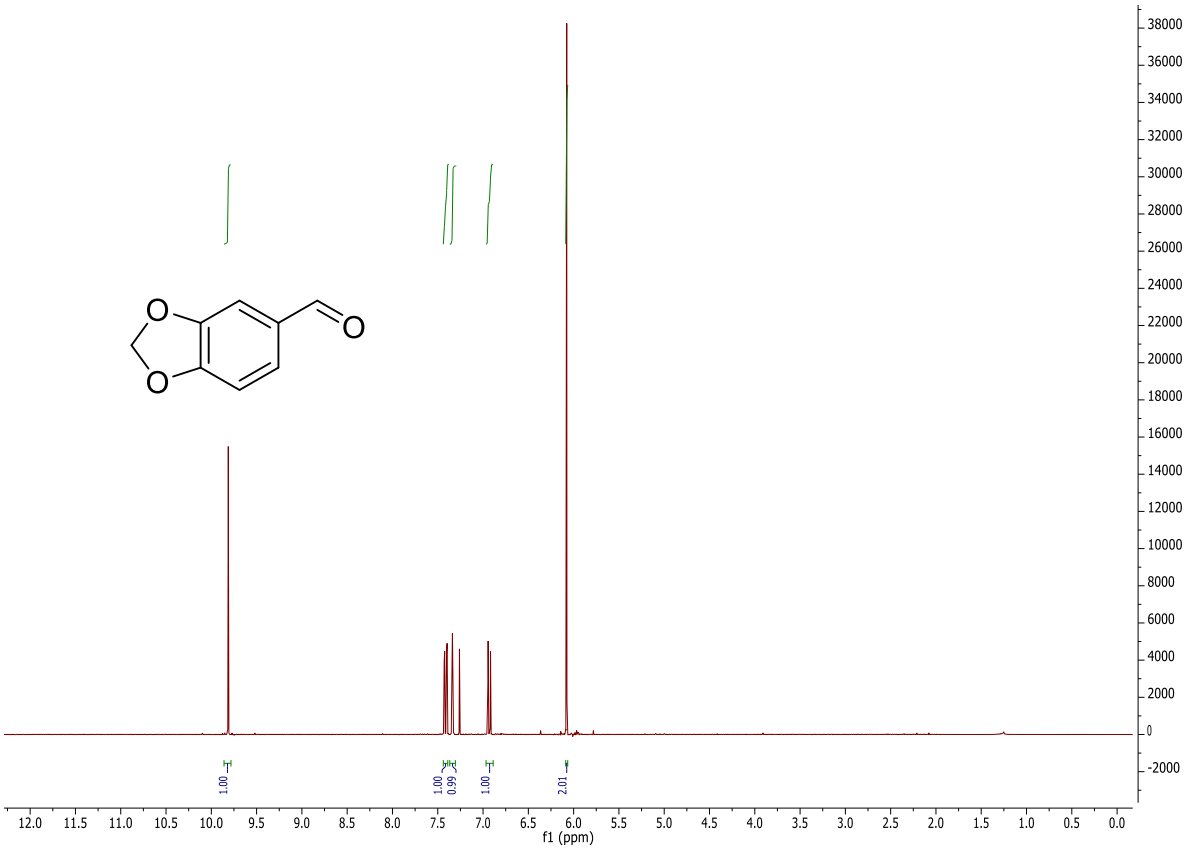

^{1}H NMR spectrum in $CDCl_3$.

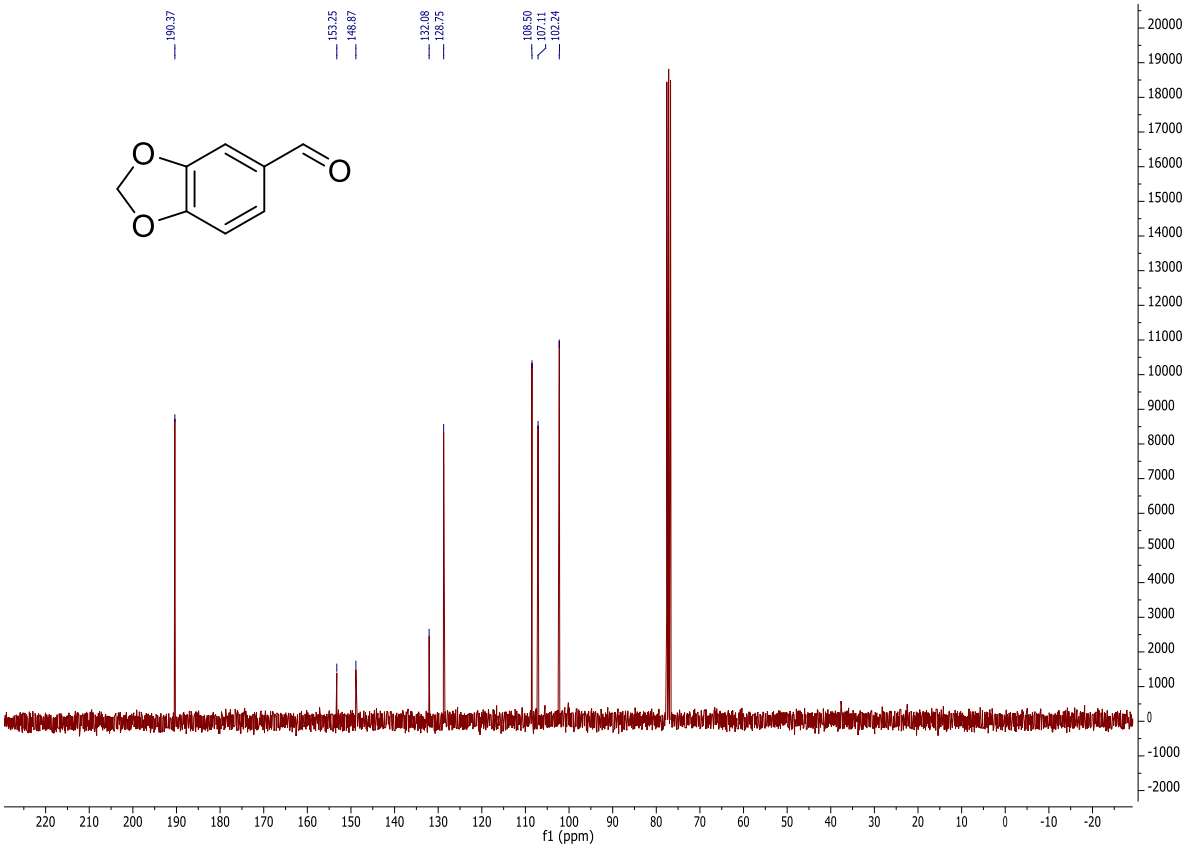

^{13}C NMR spectrum in $CDCl_3$.

71b

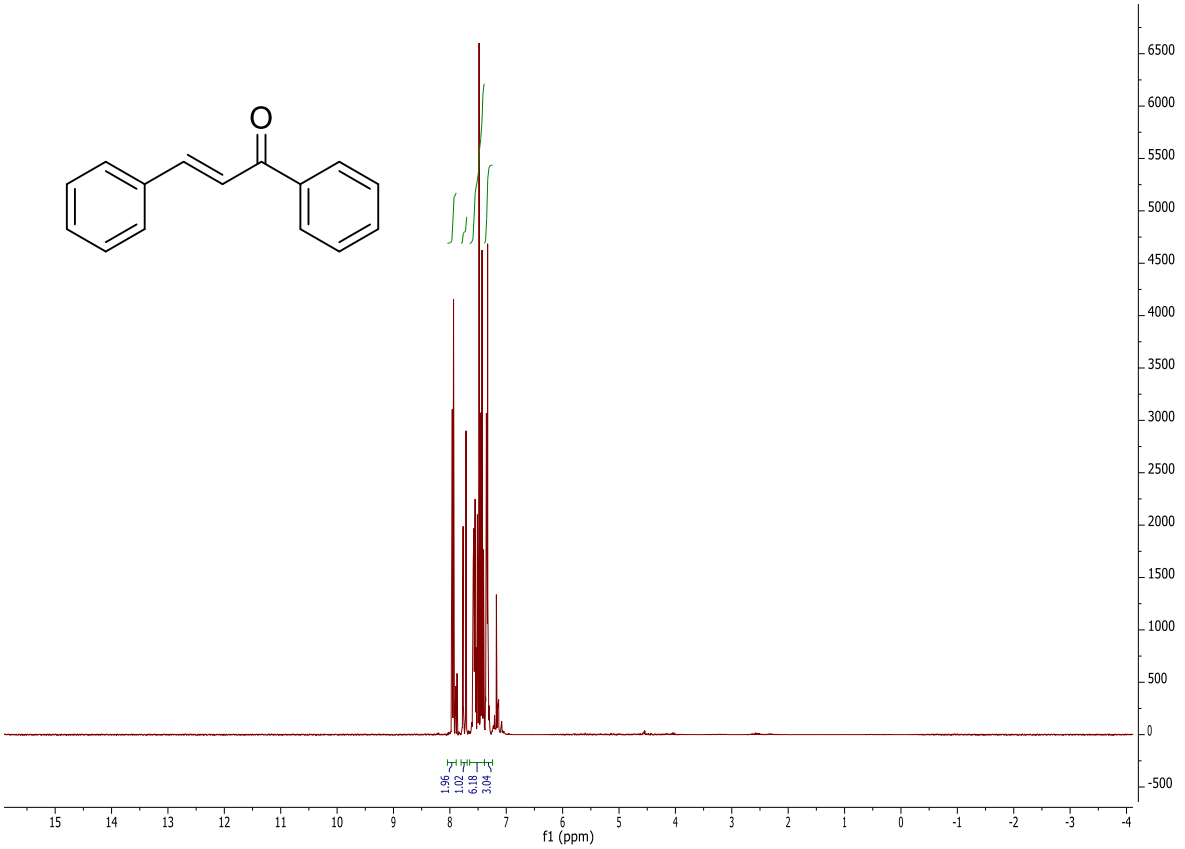

^{1}H NMR spectrum in $CDCl_3$.

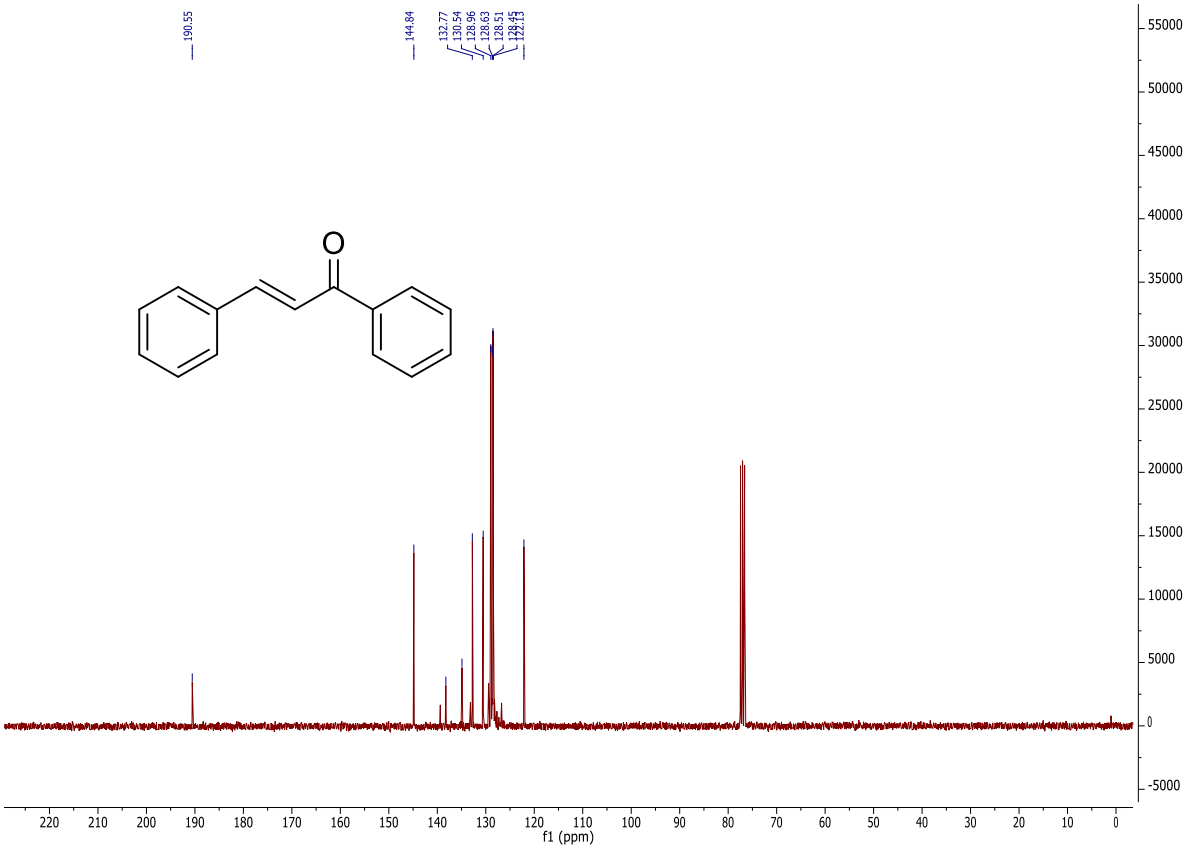

^{13}C NMR spectrum in $CDCl_3$.

72b

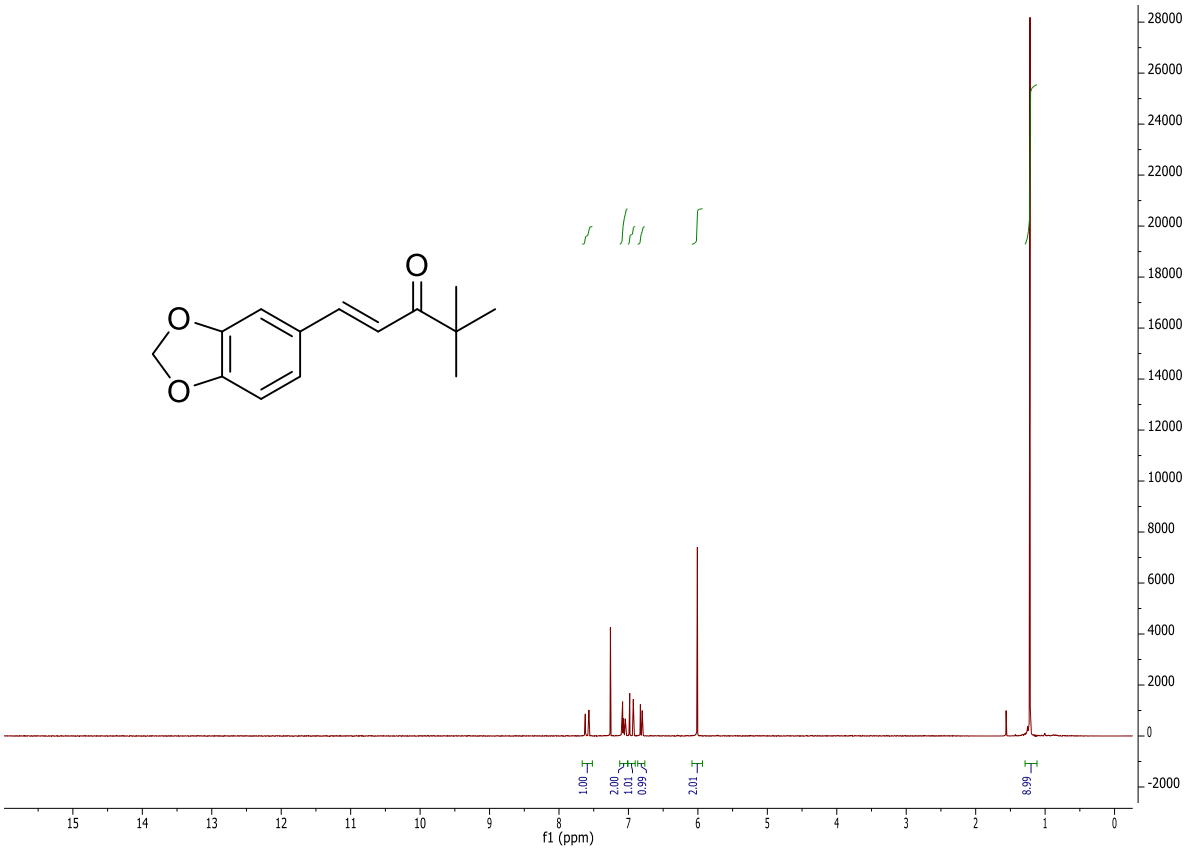

^{1}H NMR spectrum in $CDCl_3$.

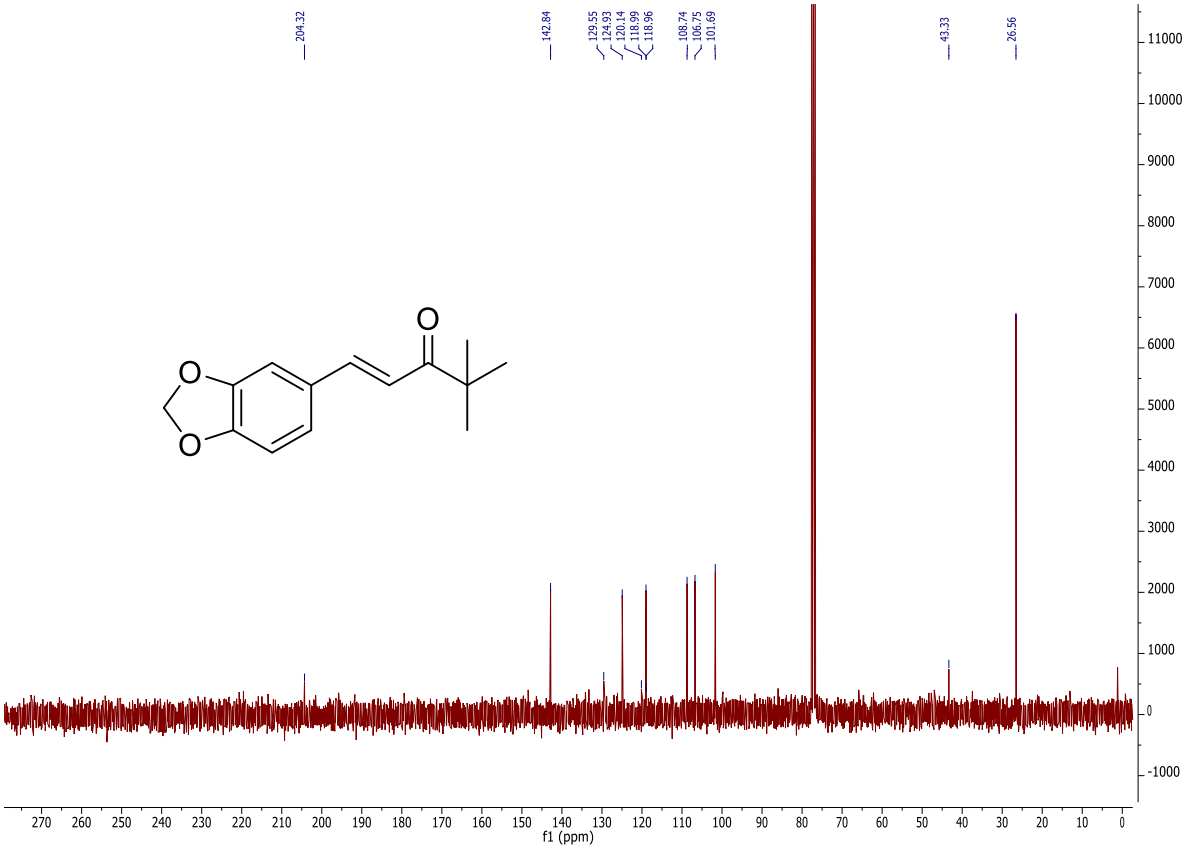

^{13}C NMR spectrum in $CDCl_3$.

73b

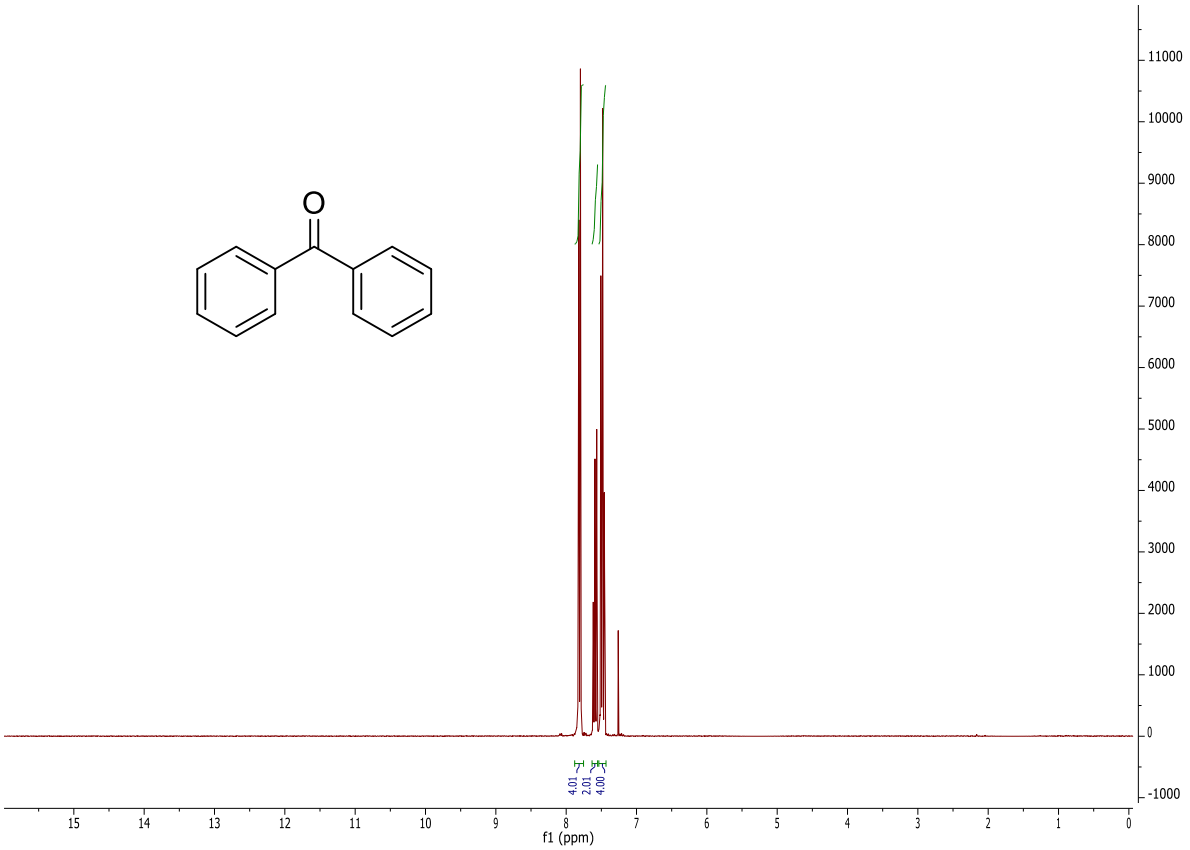

^{1}H NMR spectrum in $CDCl_3$.

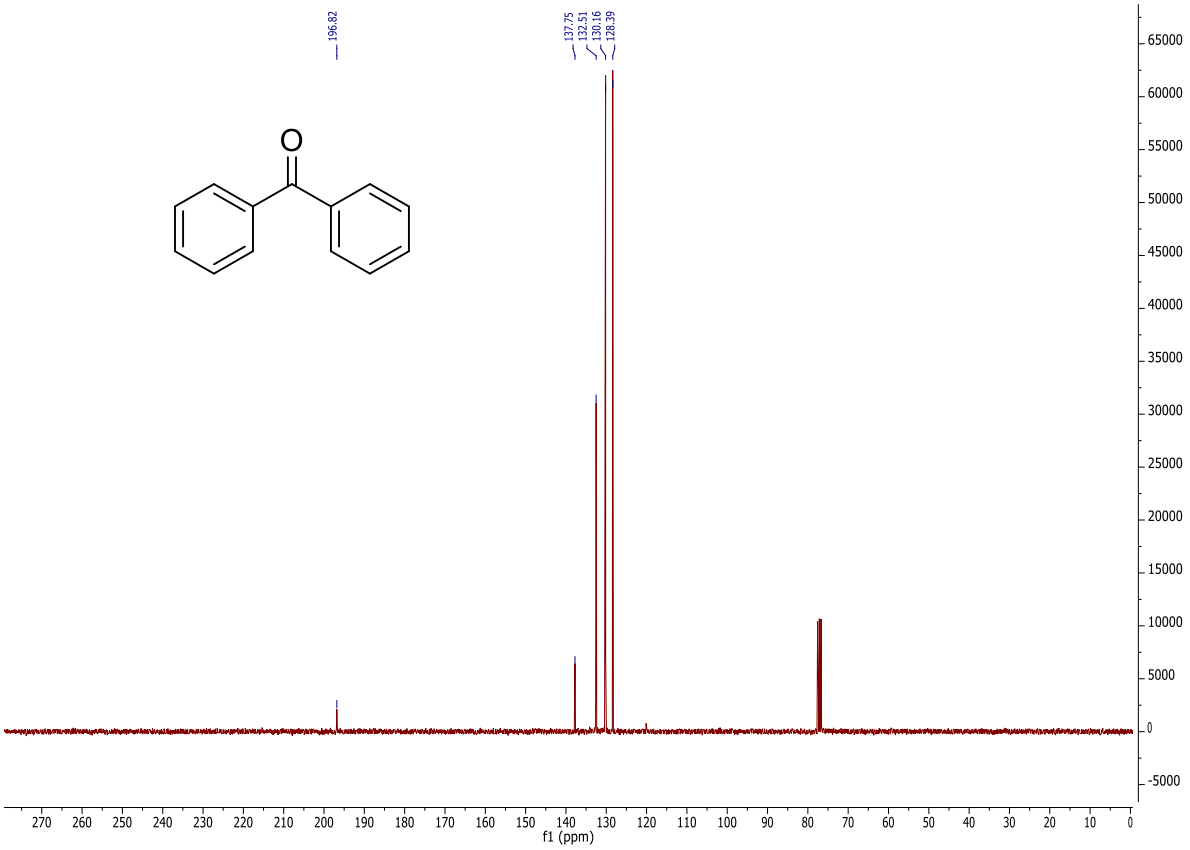

^{13}C NMR spectrum in $CDCl_3$.

74b

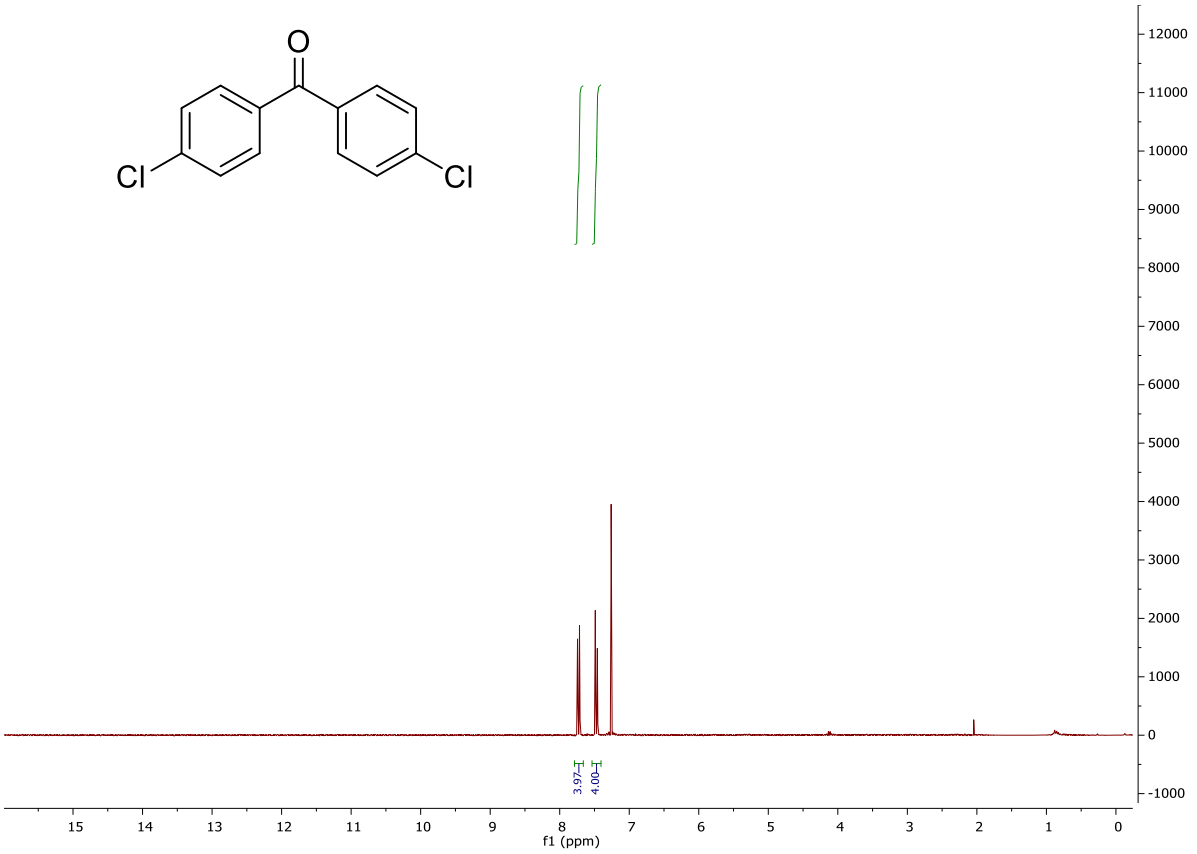

^{1}H NMR spectrum in $CDCl_3$.

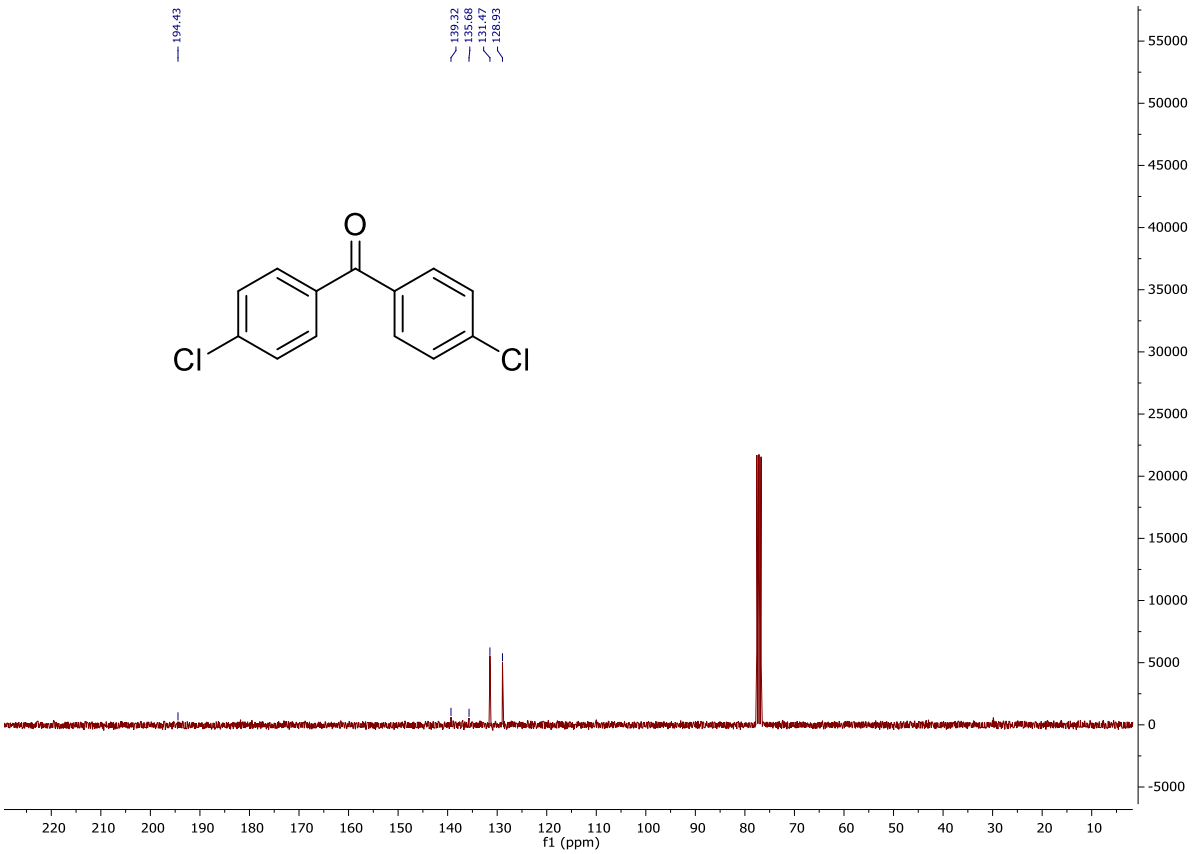

^{13}C NMR spectrum in $CDCl_3$.

75b

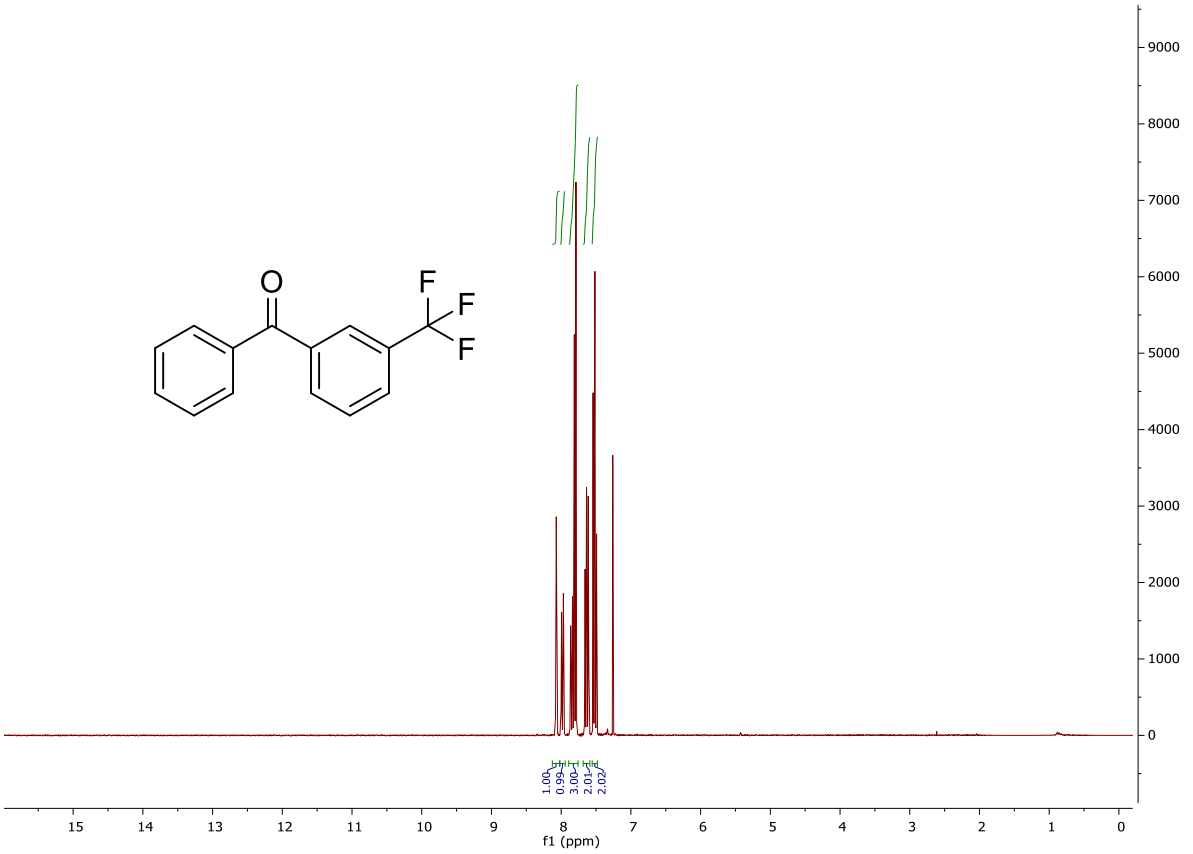

^{1}H NMR spectrum in $CDCl_3$.

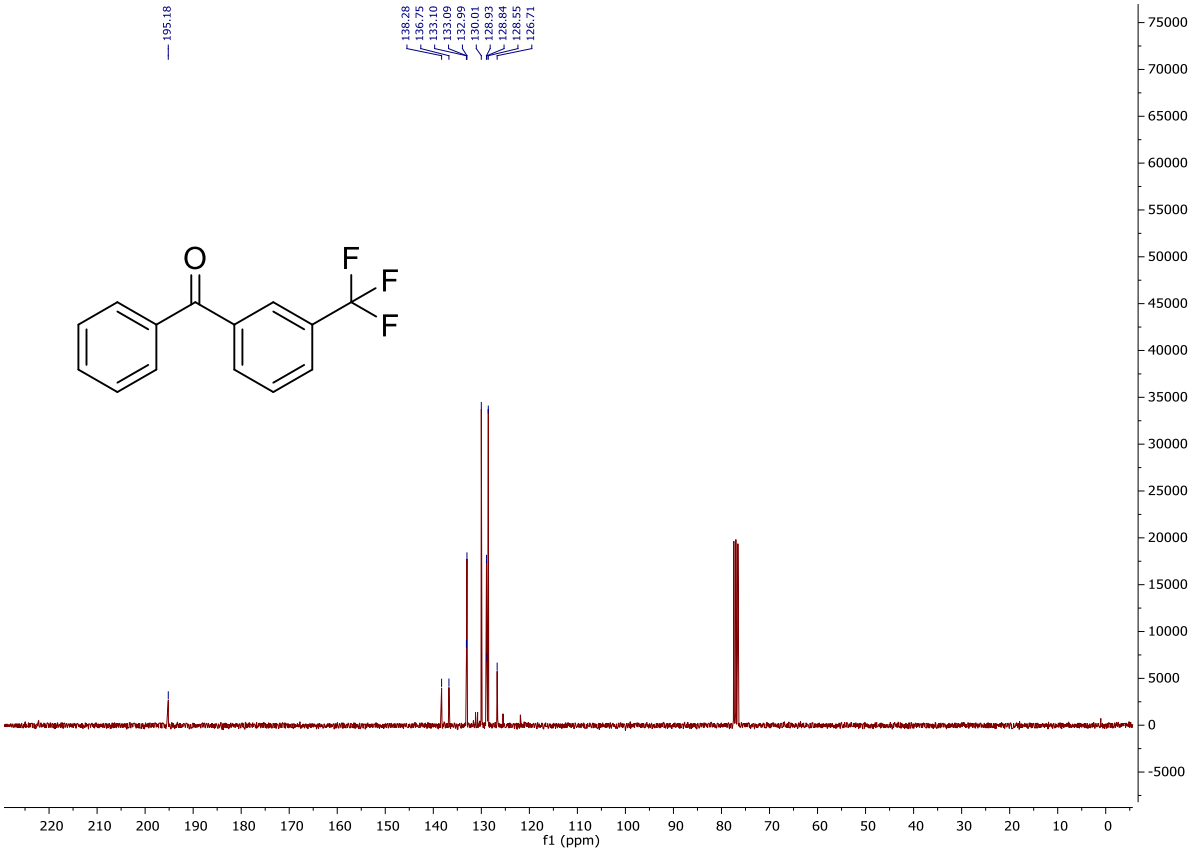

^{13}C NMR spectrum in $CDCl_3$.

76b

^{1}H NMR spectrum in $CDCl_3$.

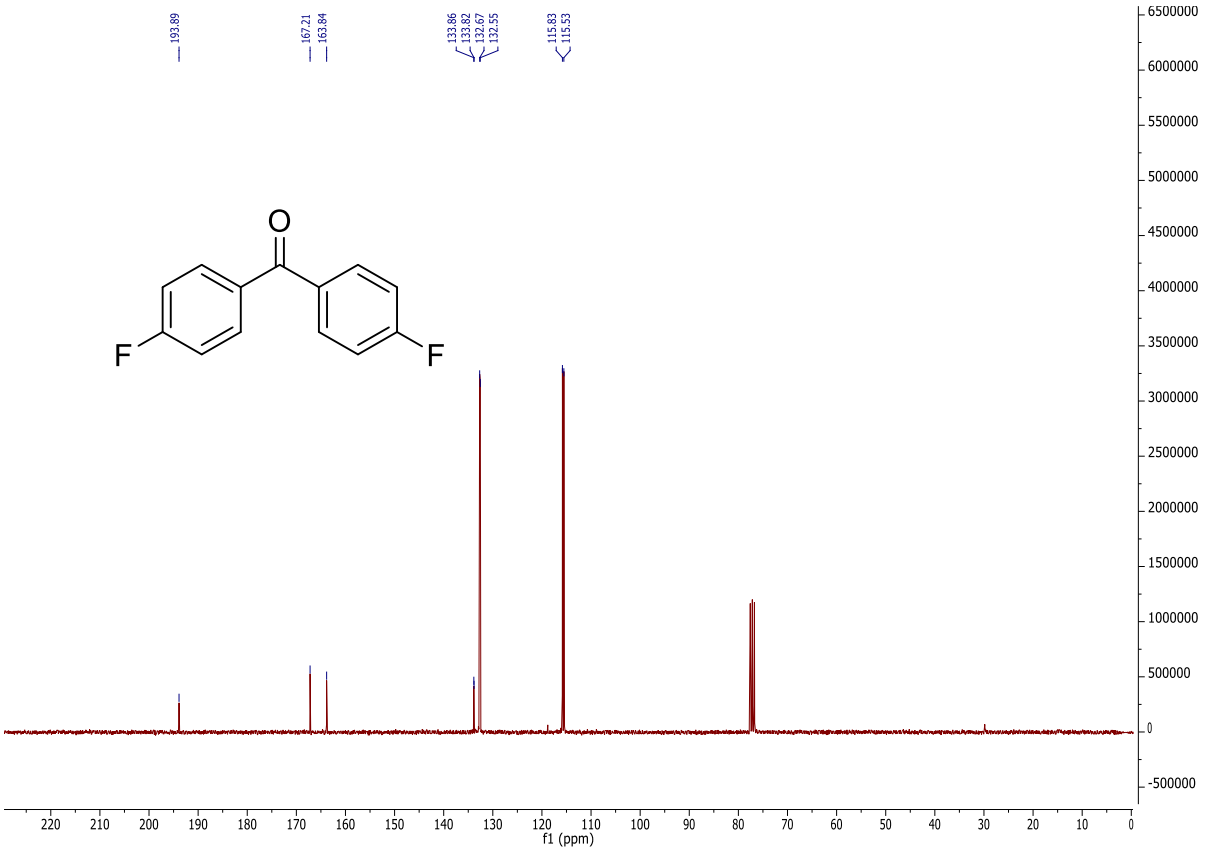

^{13}C NMR spectrum in $CDCl_3$.

77b

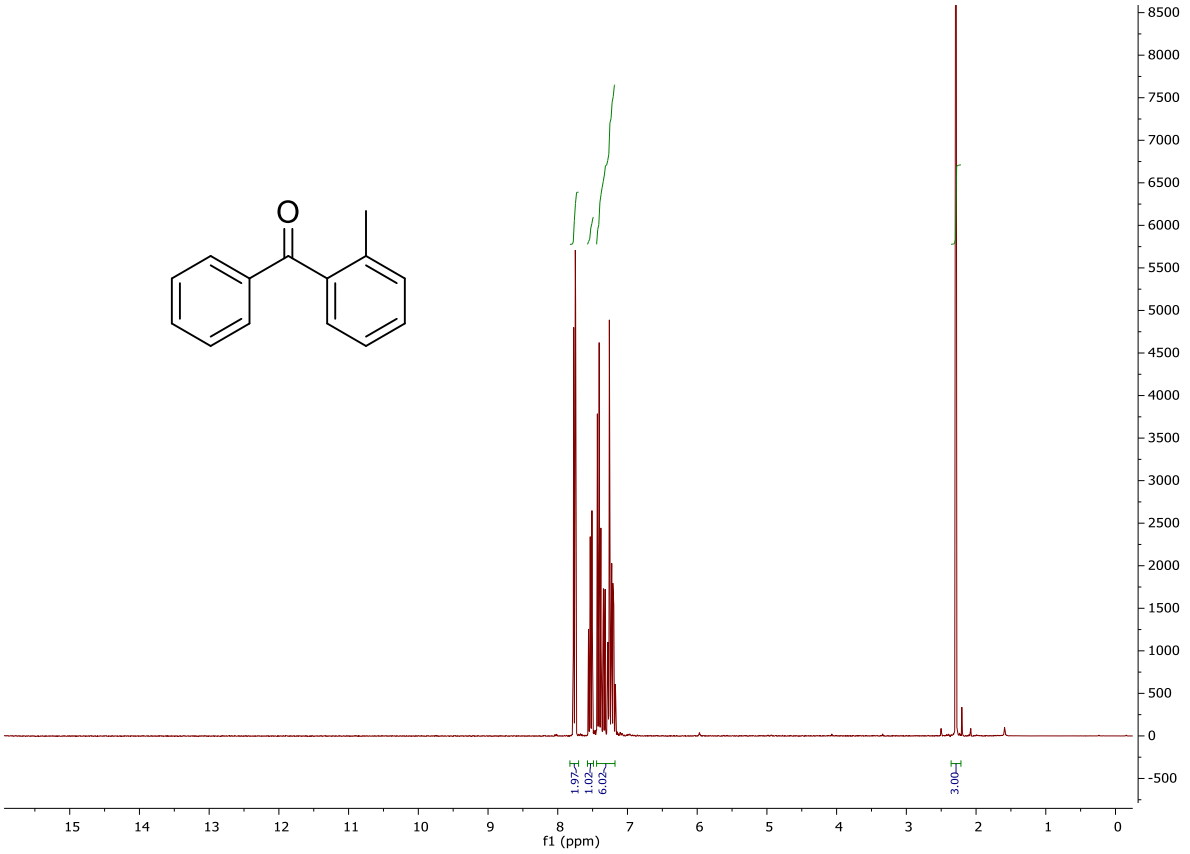

^{1}H NMR spectrum in $CDCl_3$.

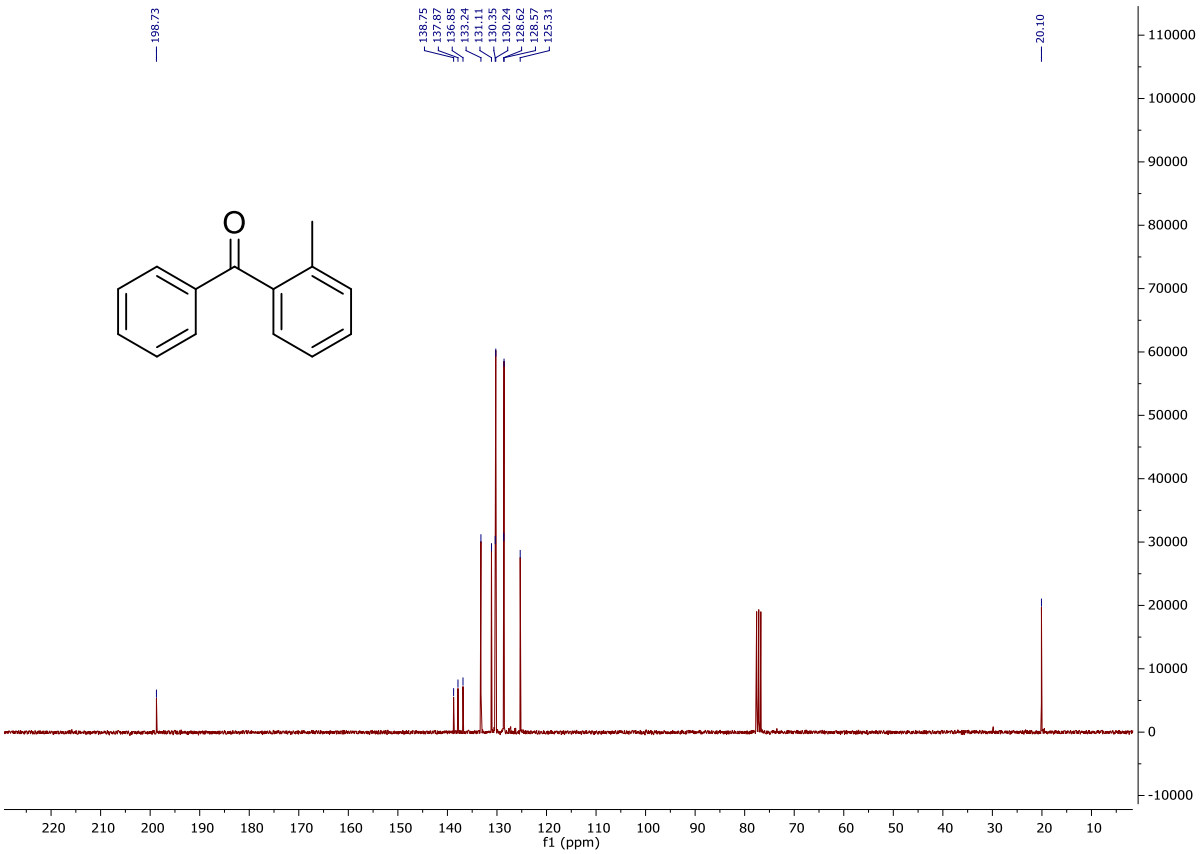

^{13}C NMR spectrum in $CDCl_3$.

78b

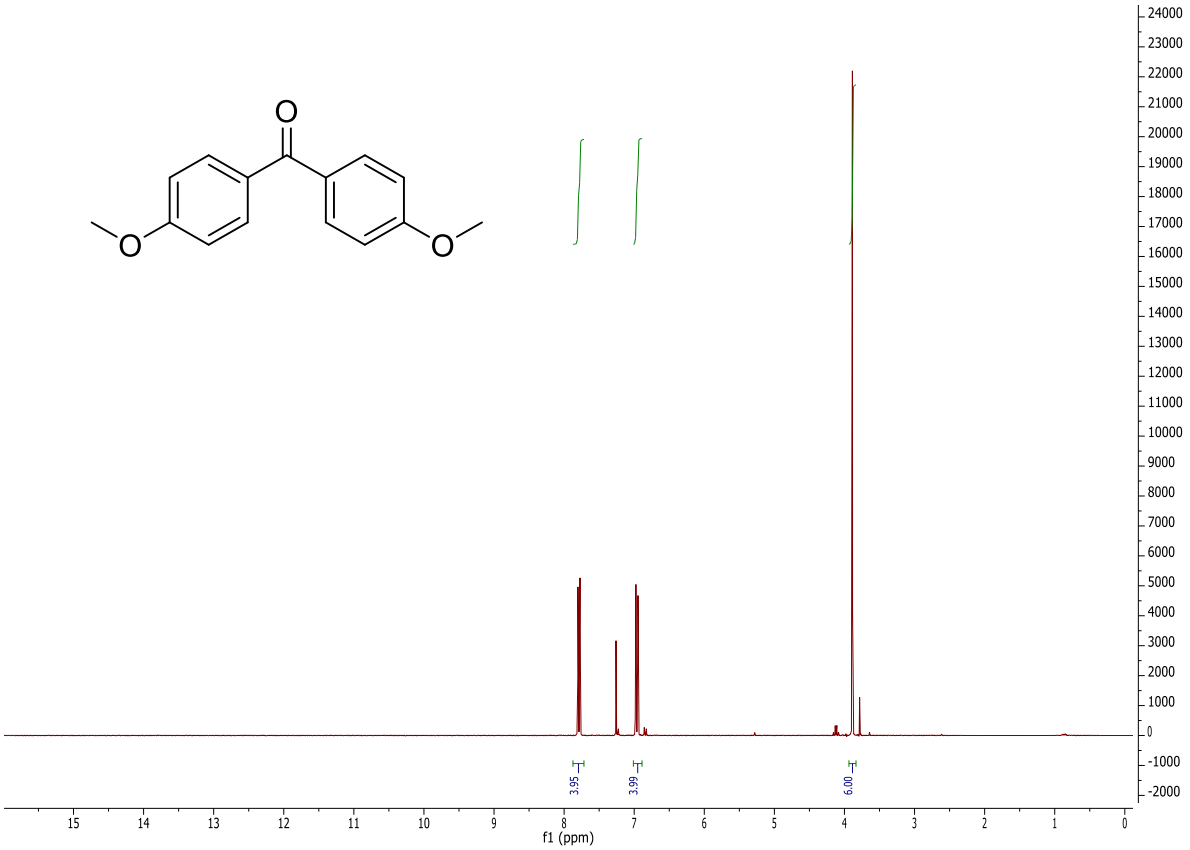

^{1}H NMR spectrum in $CDCl_3$.

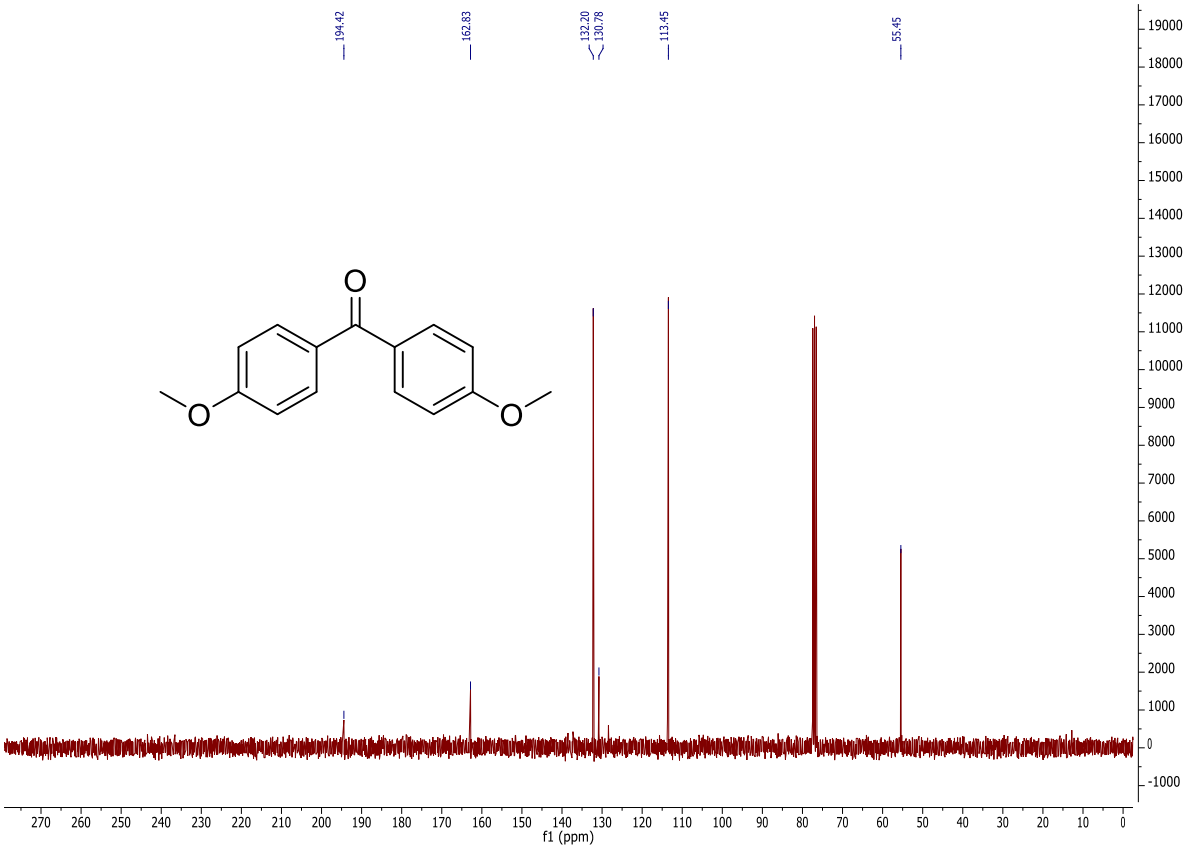

^{13}C NMR spectrum in $CDCl_3$.

79b

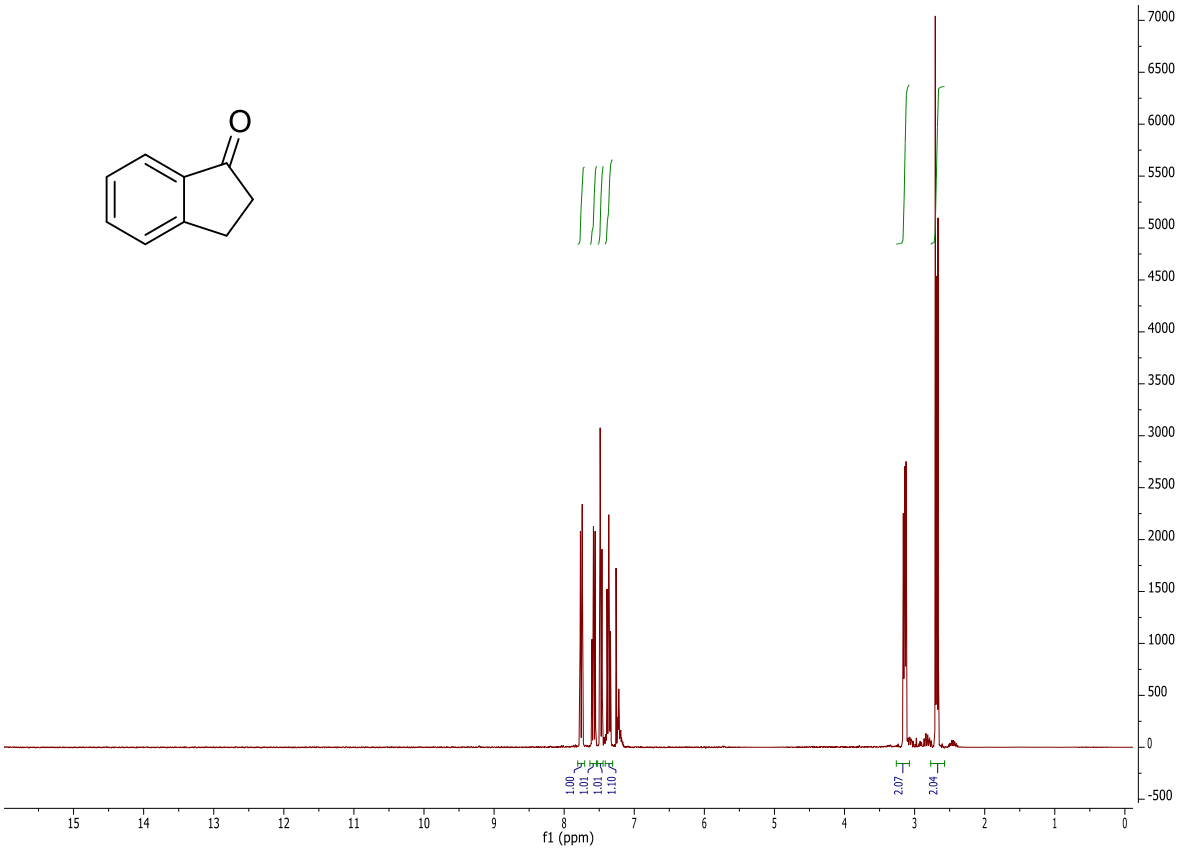

^{1}H NMR spectrum in $CDCl_3$.

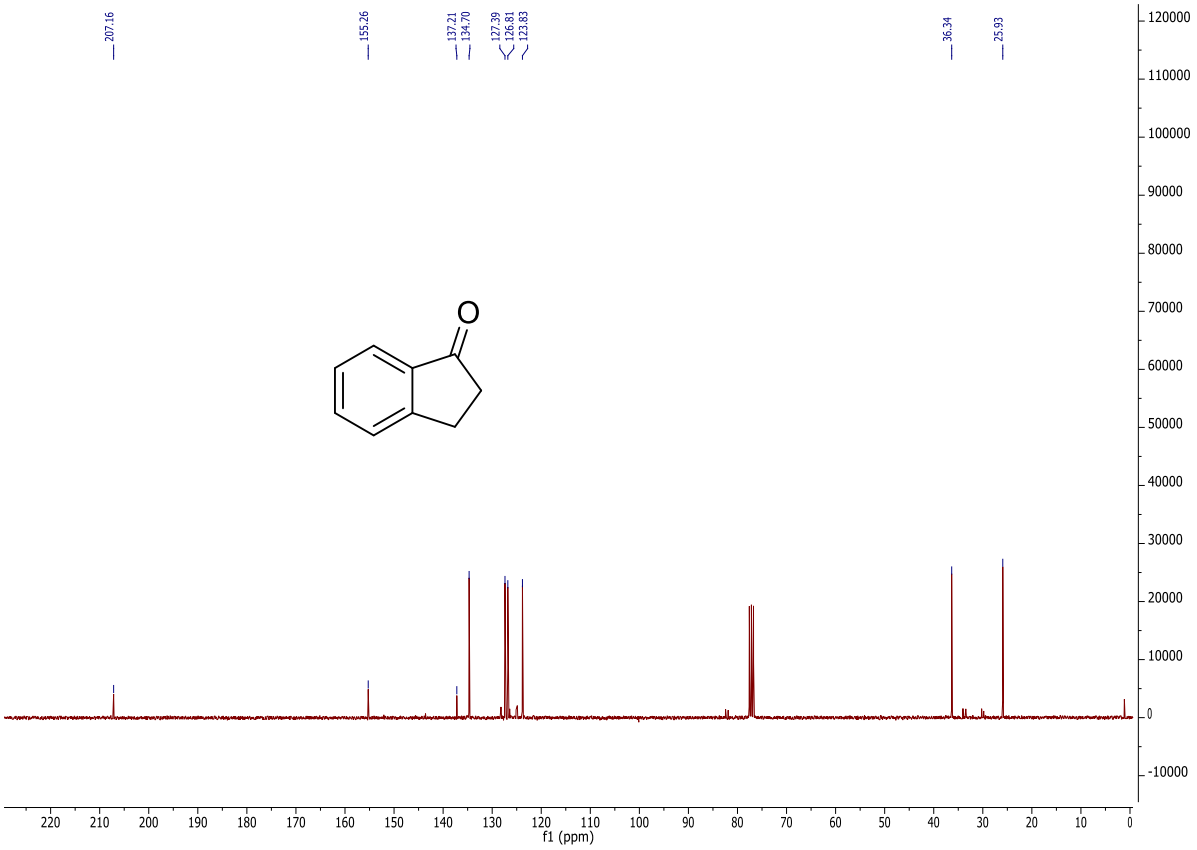

^{13}C NMR spectrum in $CDCl_3$.

80b

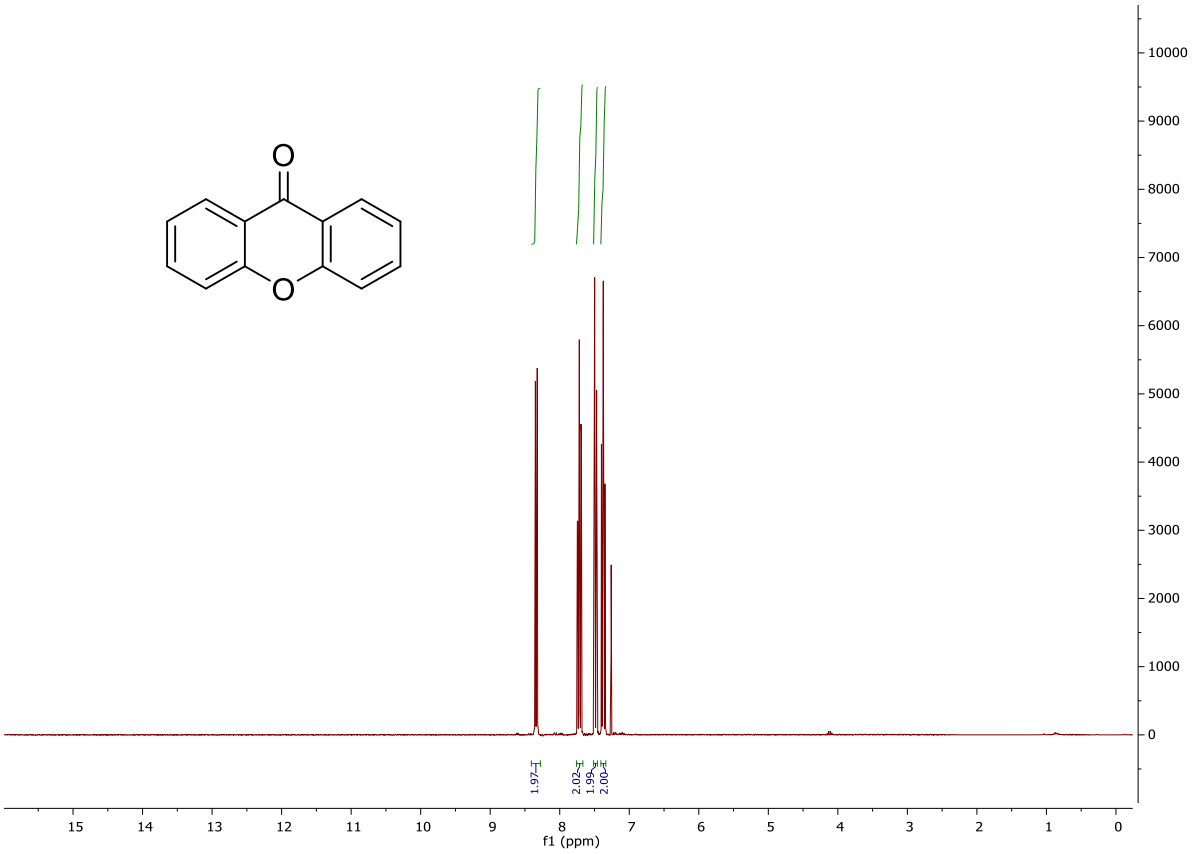

^{1}H NMR spectrum in $CDCl_3$.

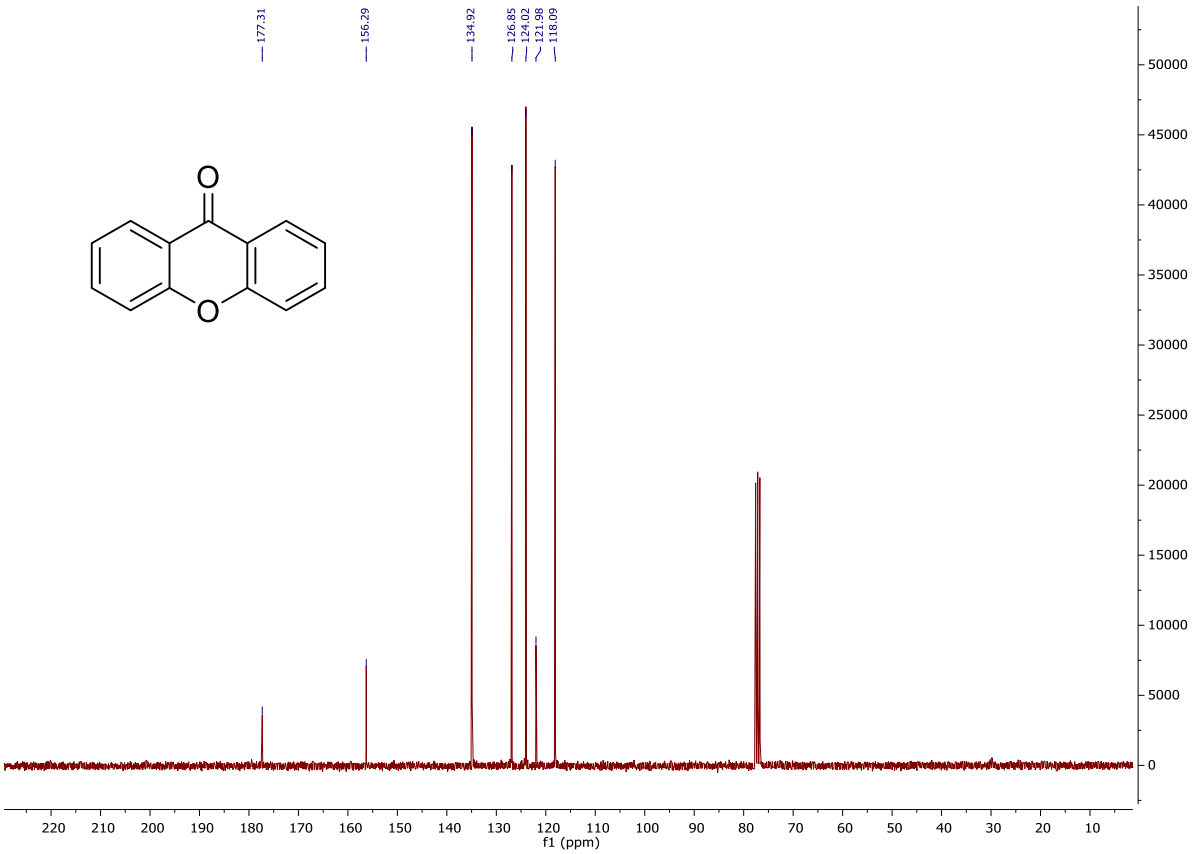

^{13}C NMR spectrum in $CDCl_3$.

81b

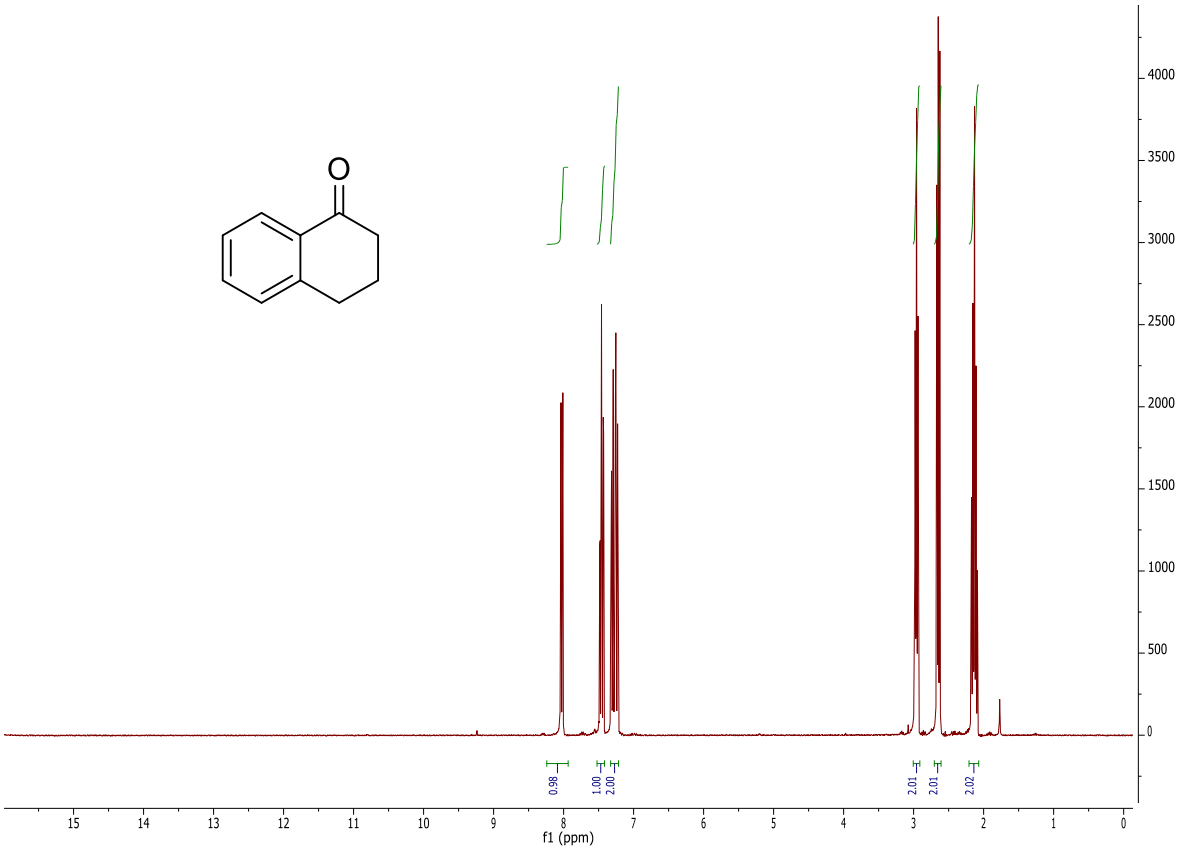

^{1}H NMR spectrum in $CDCl_3$.

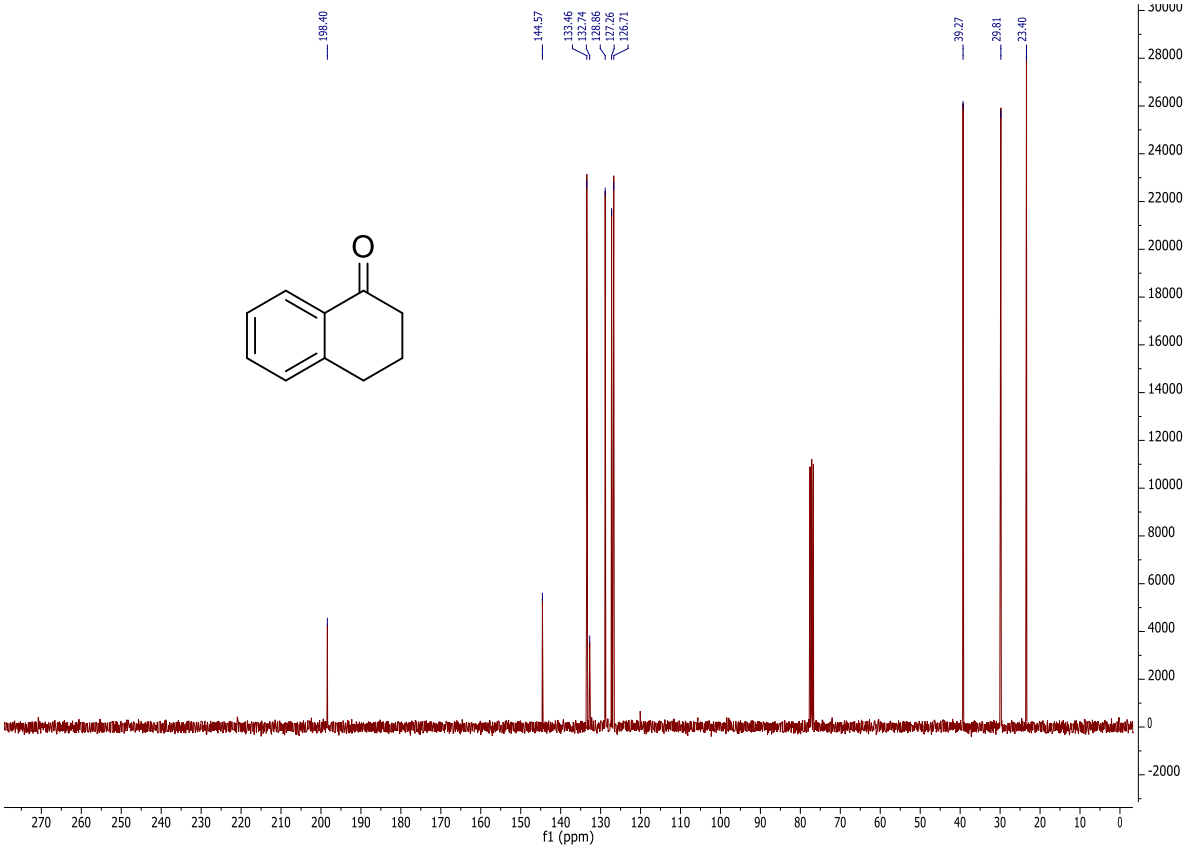

^{13}C NMR spectrum in $CDCl_3$.

82b

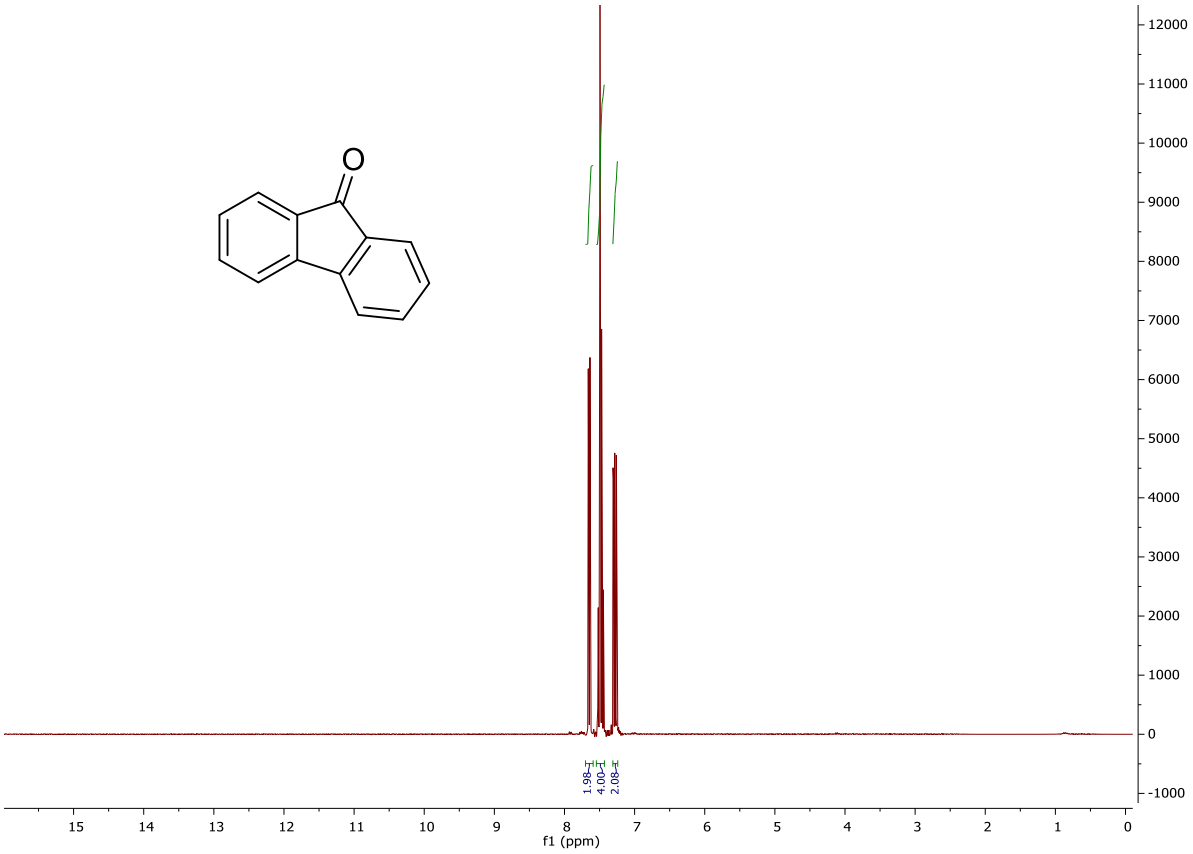

^{1}H NMR spectrum in $CDCl_3$.

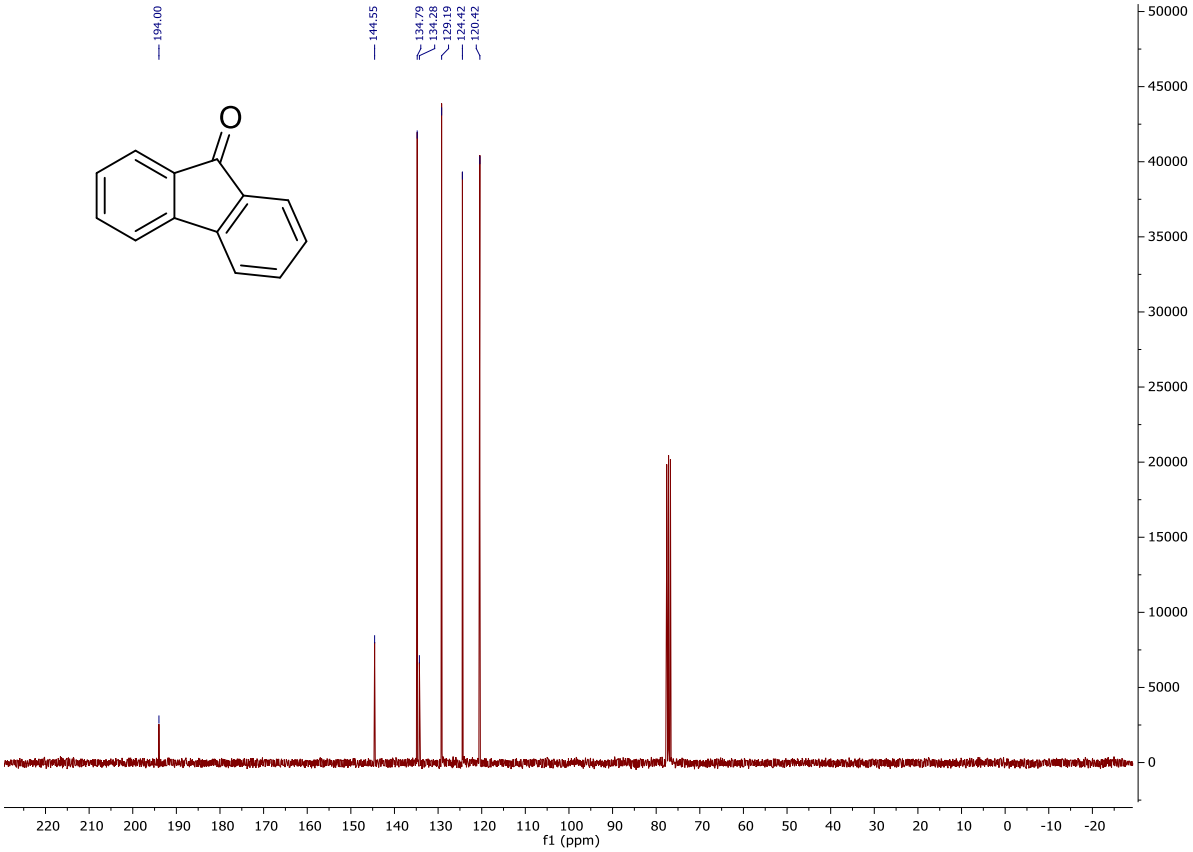

^{13}C NMR spectrum in $CDCl_3$.

83b

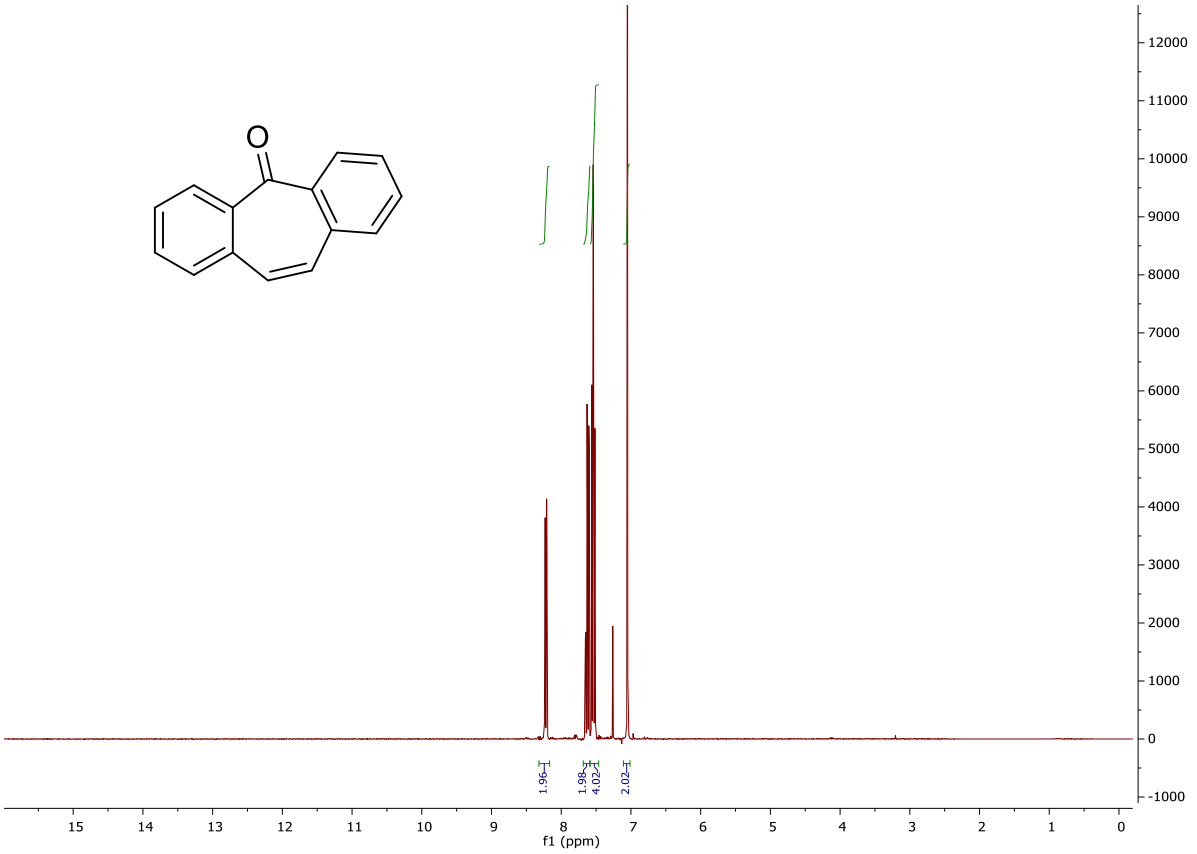

^{1}H NMR spectrum in $CDCl_3$.

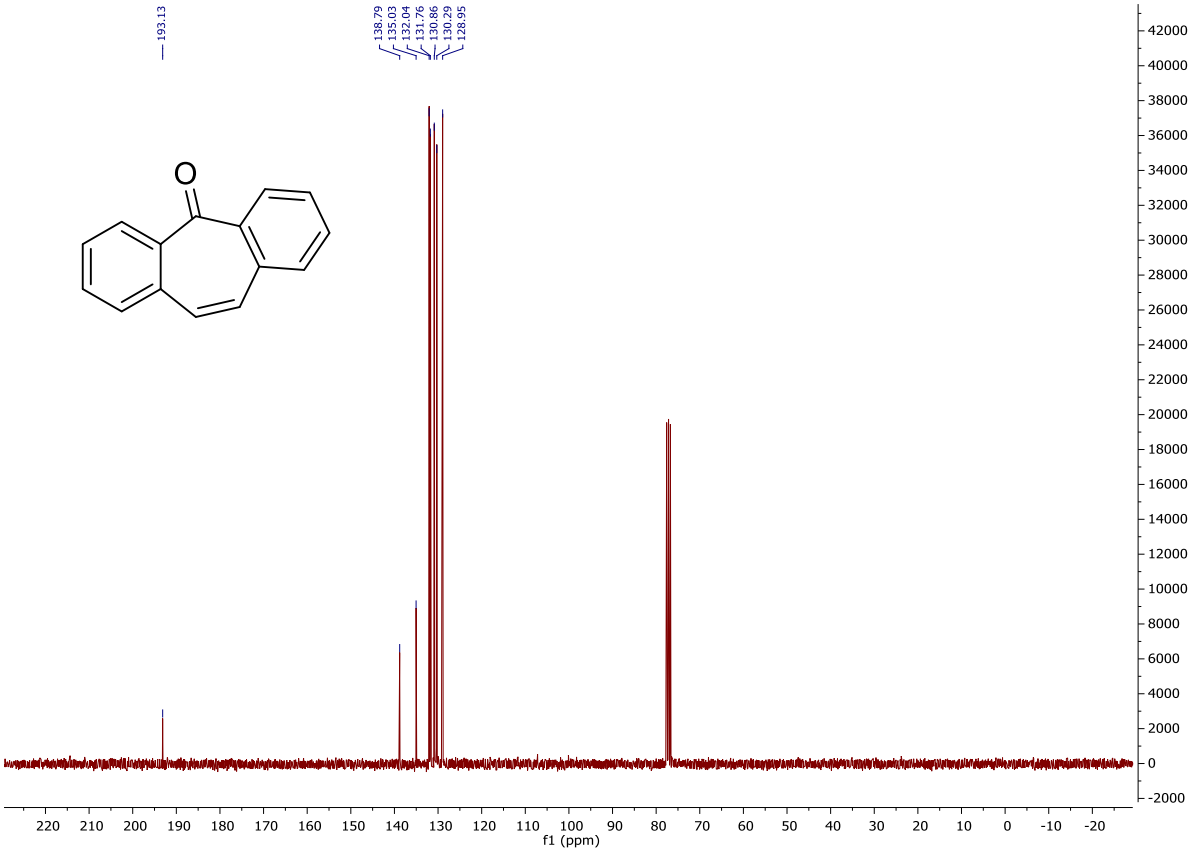

^{13}C NMR spectrum in $CDCl_3$.

84b

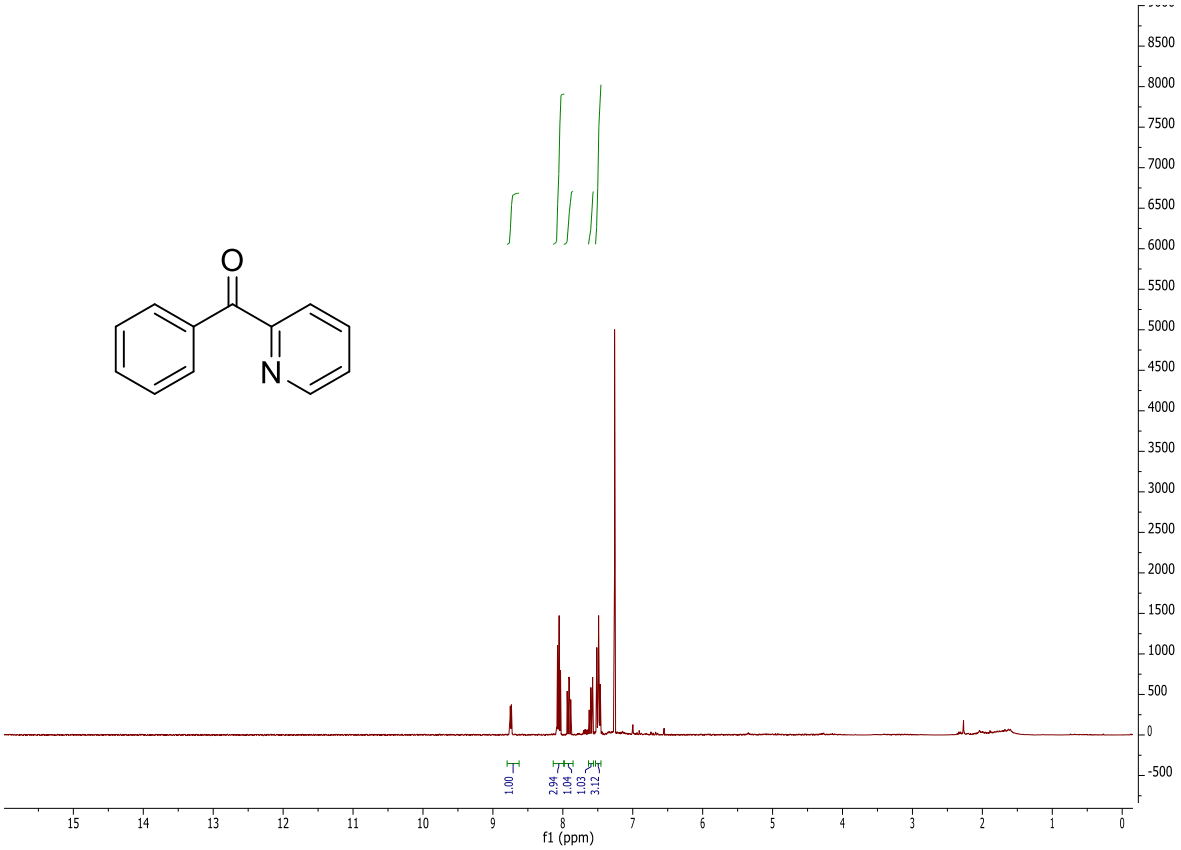

^{1}H NMR spectrum in $CDCl_3$.

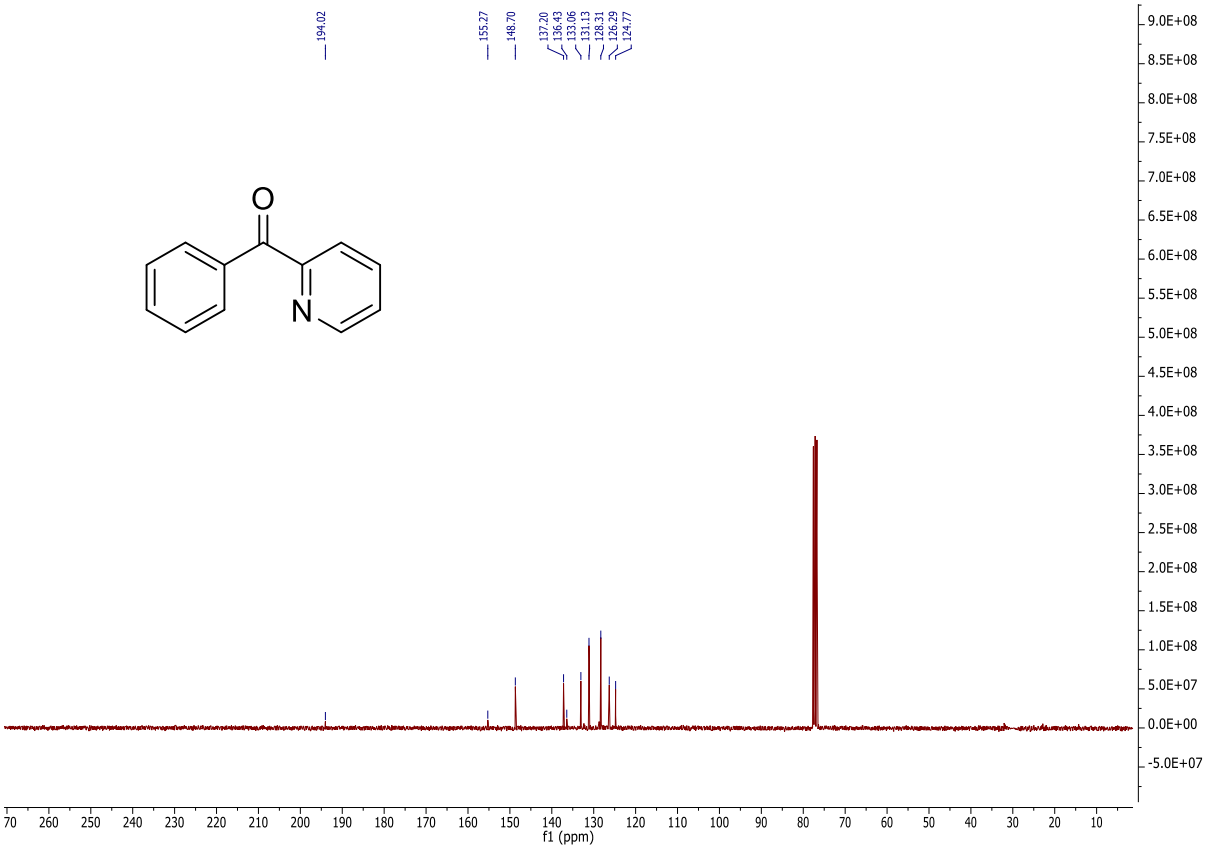

^{13}C NMR spectrum in $CDCl_3$.

85b

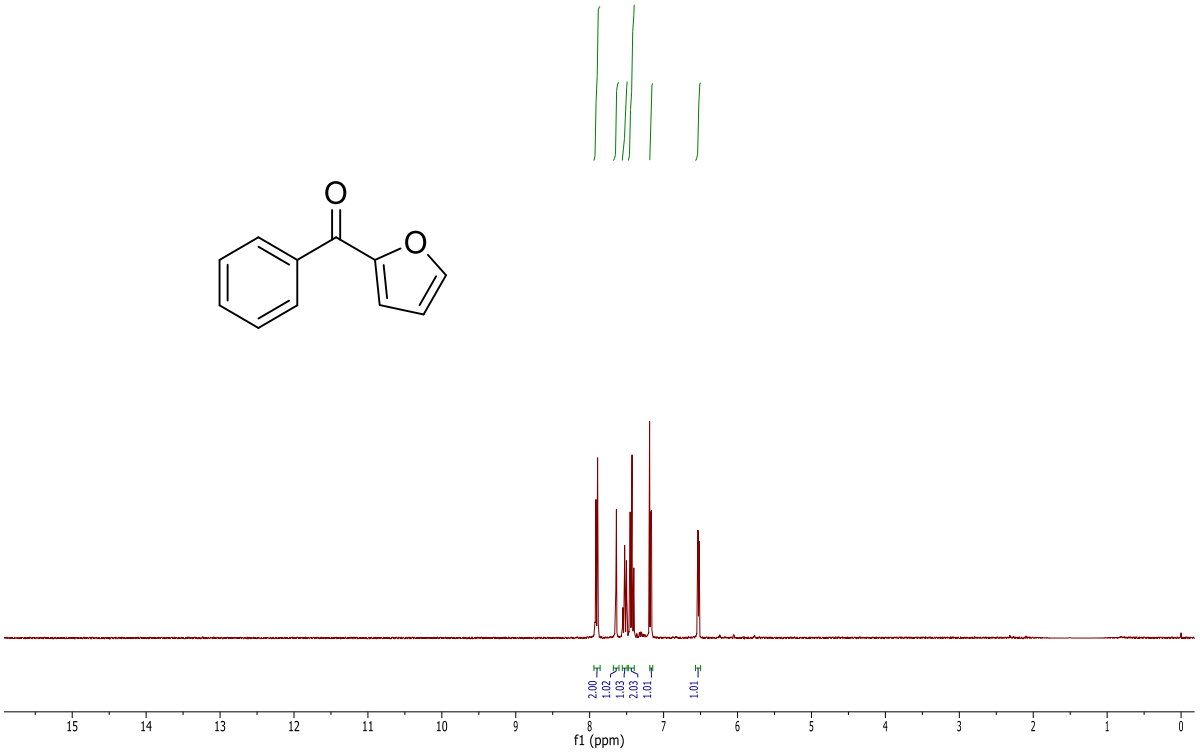

^{1}H NMR spectrum in $CDCl_3$.

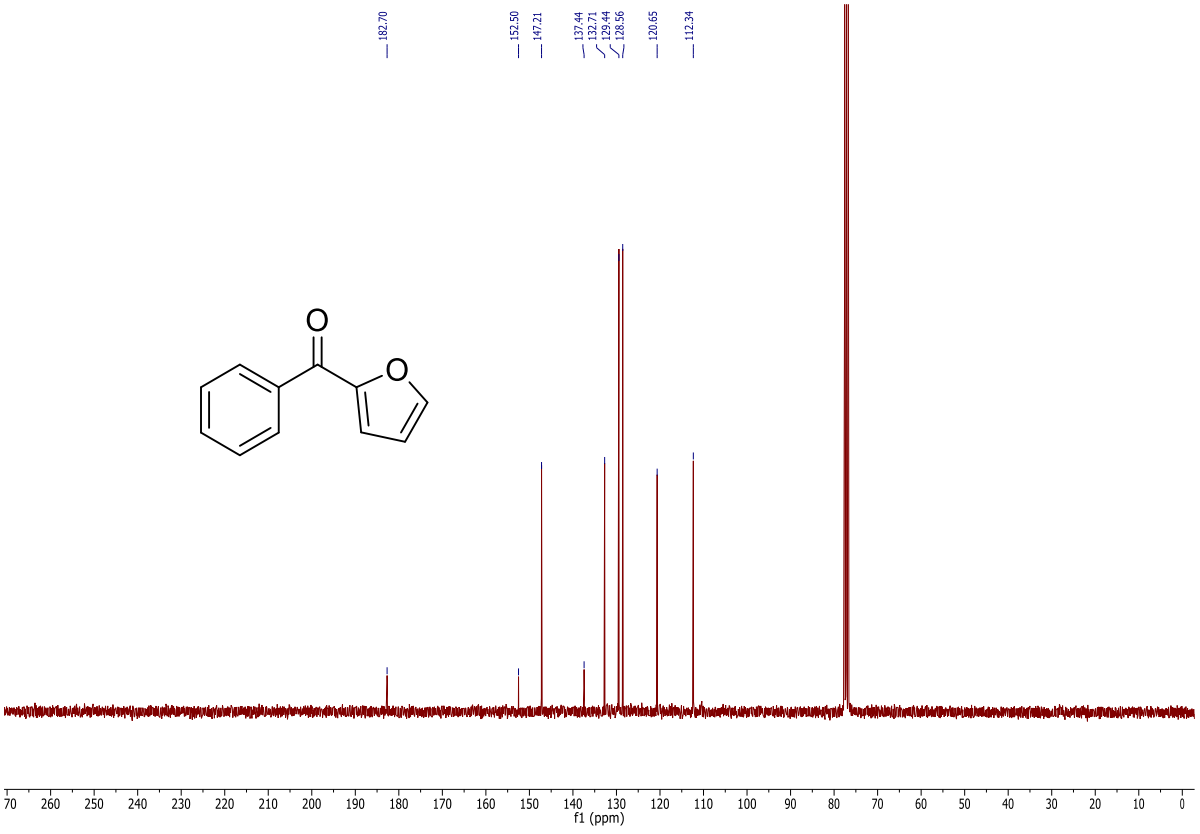

^{13}C NMR spectrum in $CDCl_3$.

86b

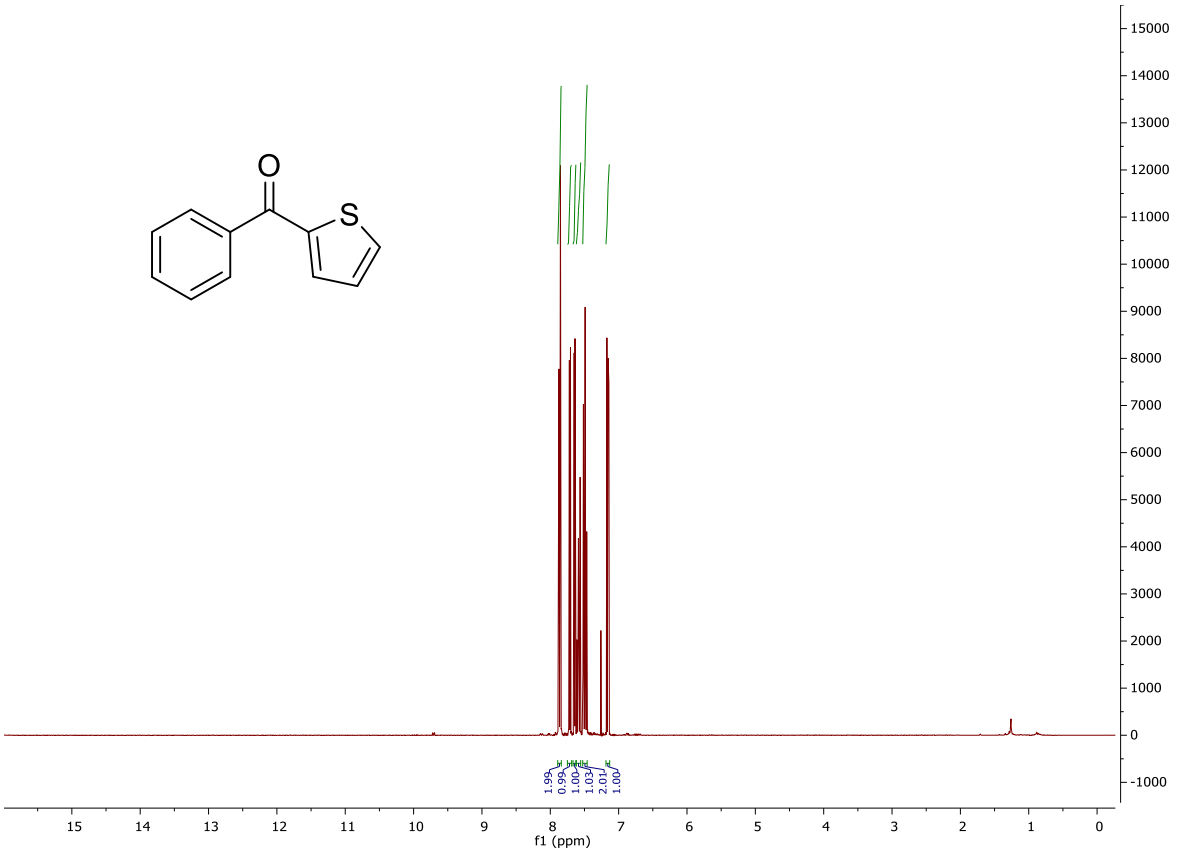

^{1}H NMR spectrum in $CDCl_3$.

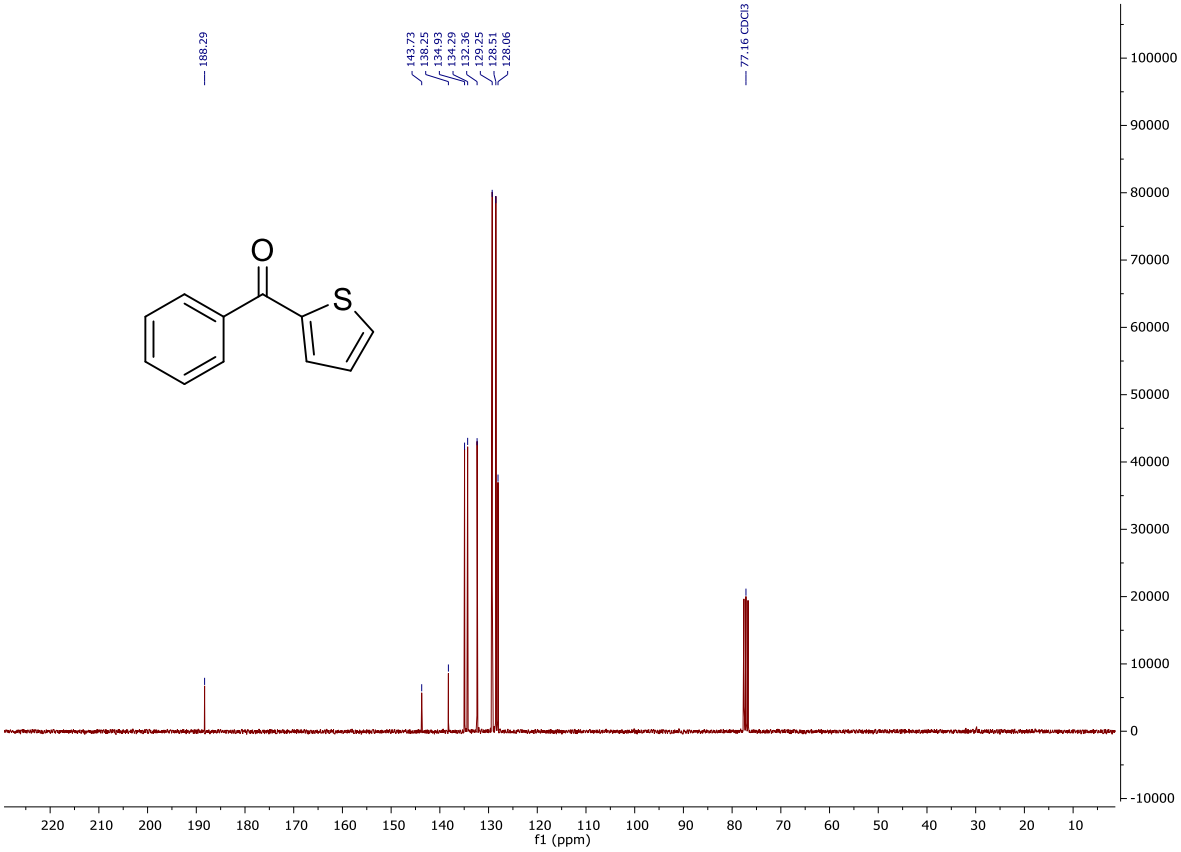

^{13}C NMR spectrum in $CDCl_3$.

87b

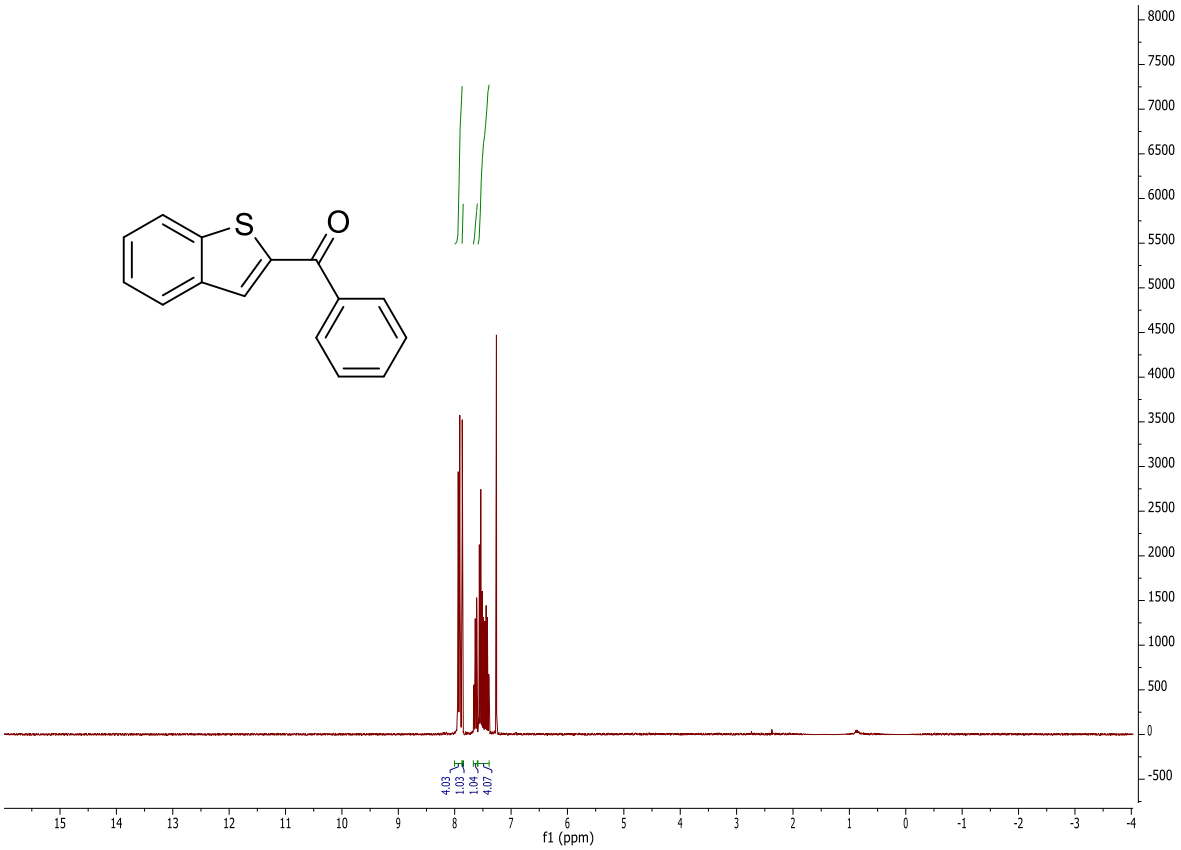

^{1}H NMR spectrum in $CDCl_3$.

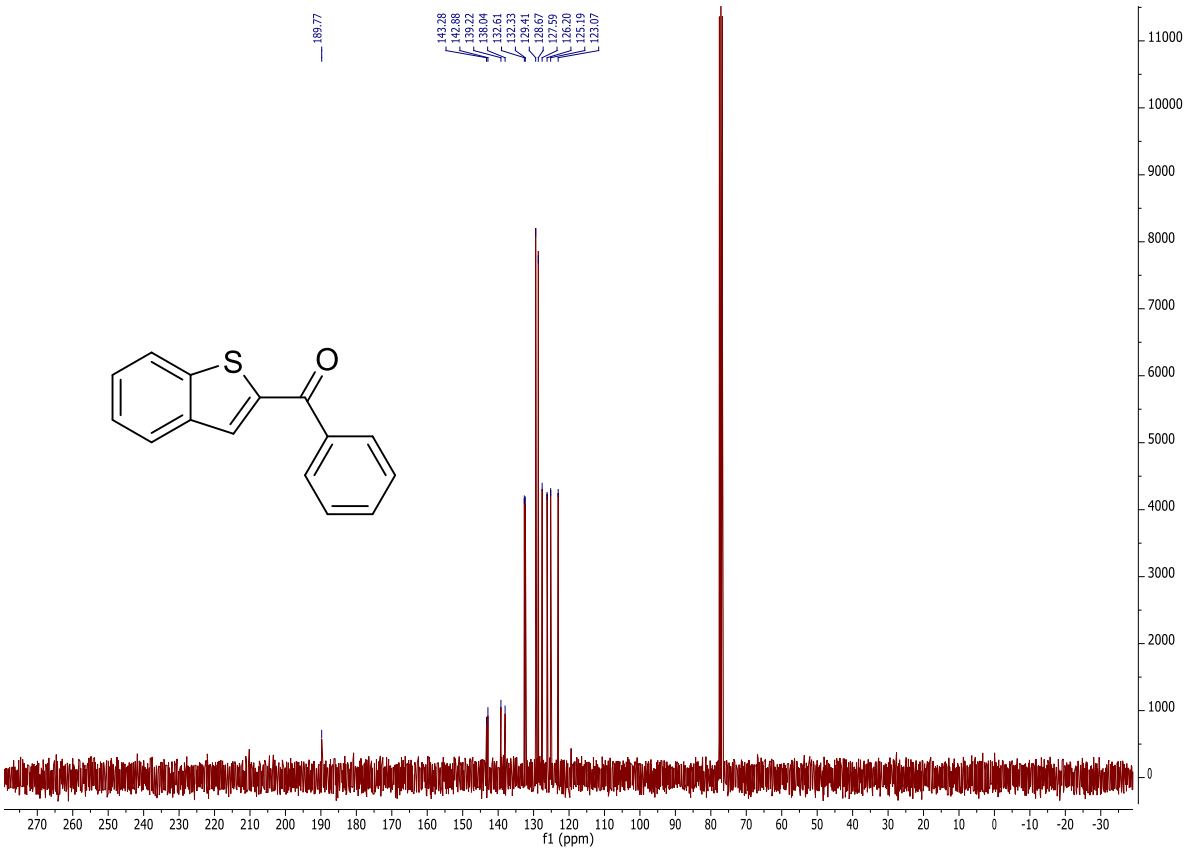

^{13}C NMR spectrum in $CDCl_3$.

88b

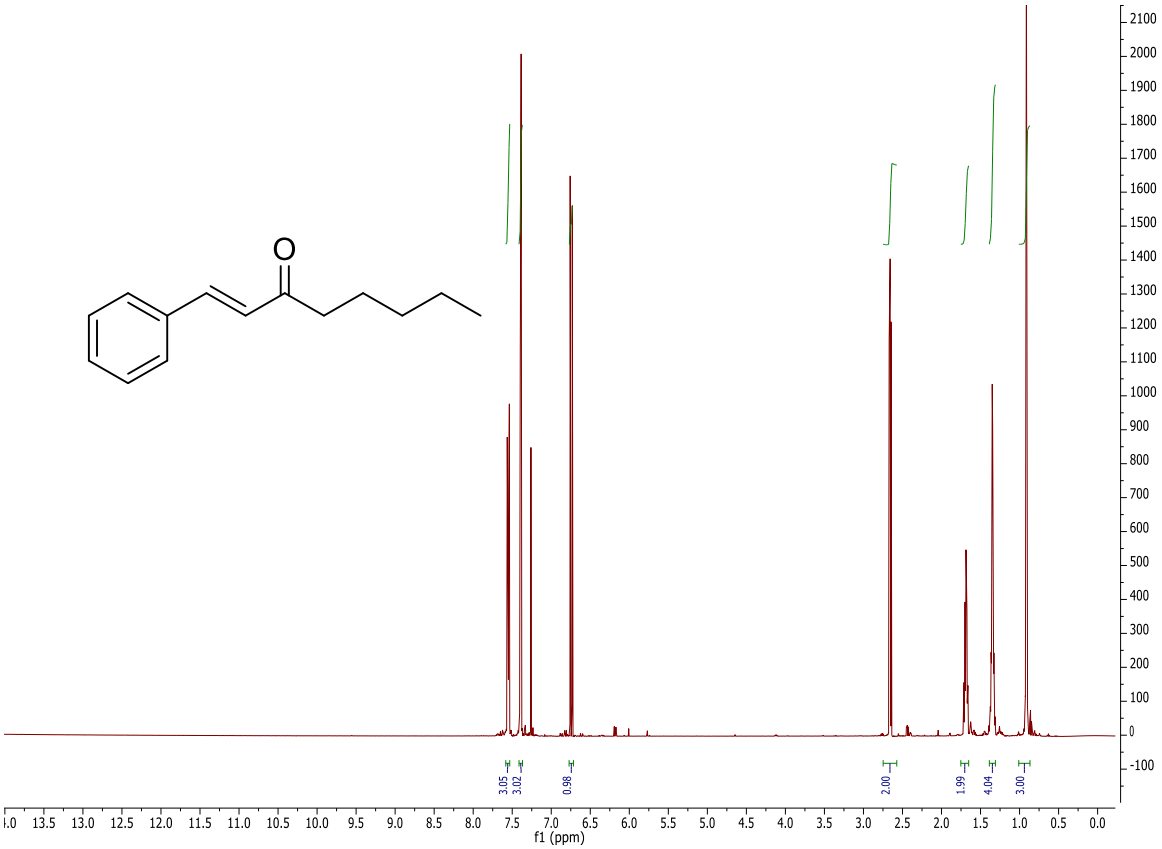

^{1}H NMR spectrum in $CDCl_3$.

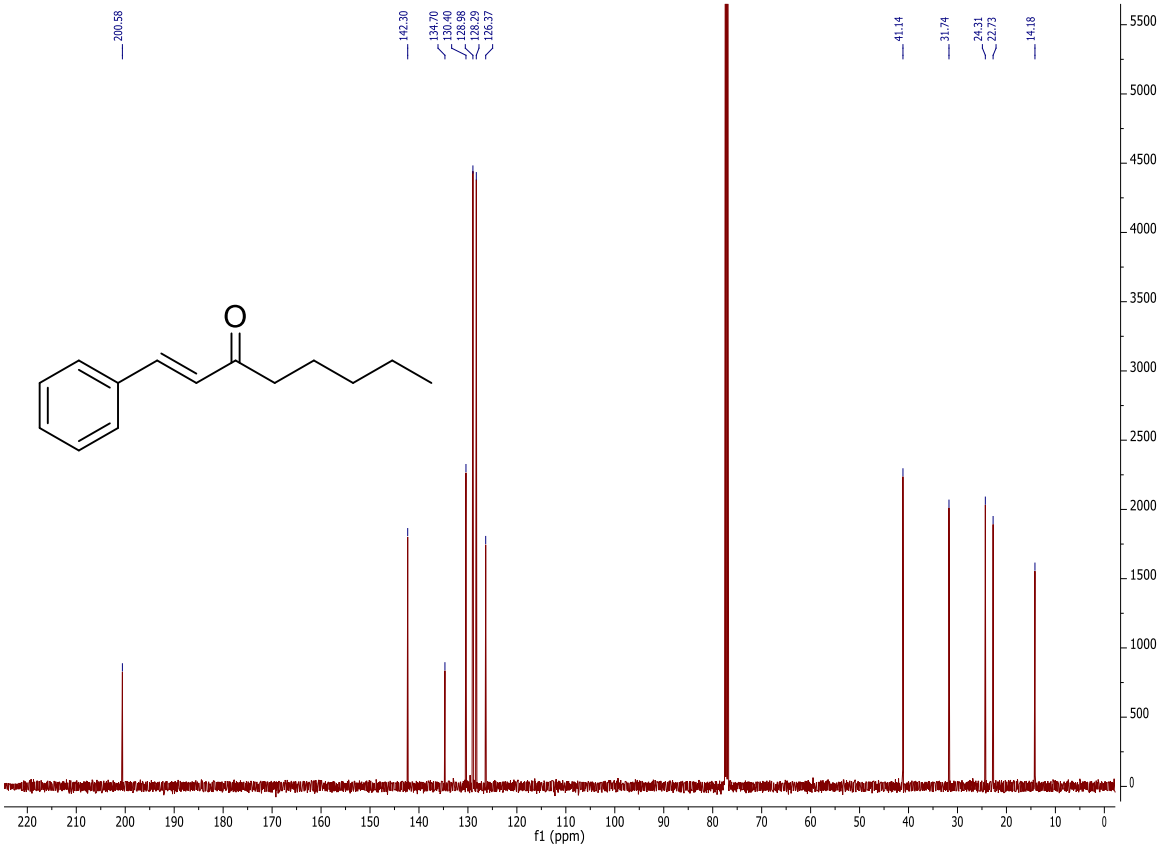

^{13}C NMR spectrum in $CDCl_3$.

89b

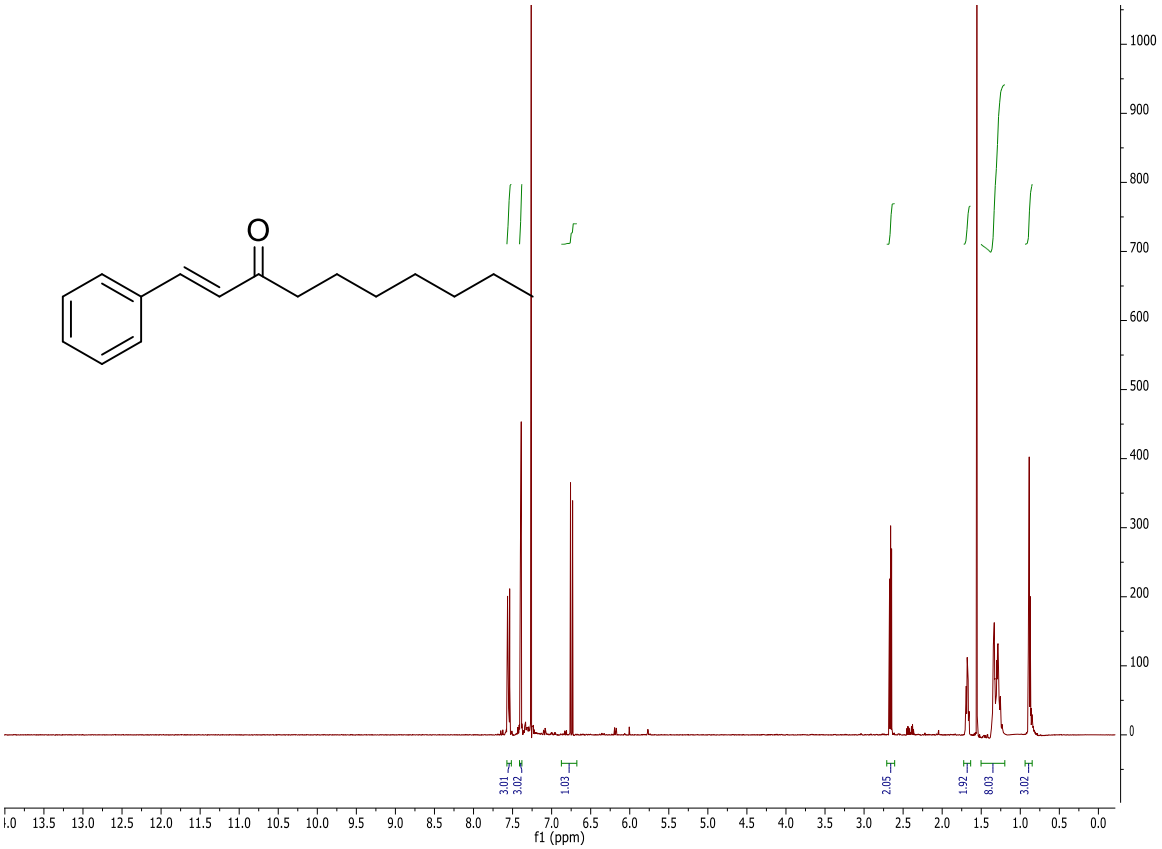

^{1}H NMR spectrum in $CDCl_3$.

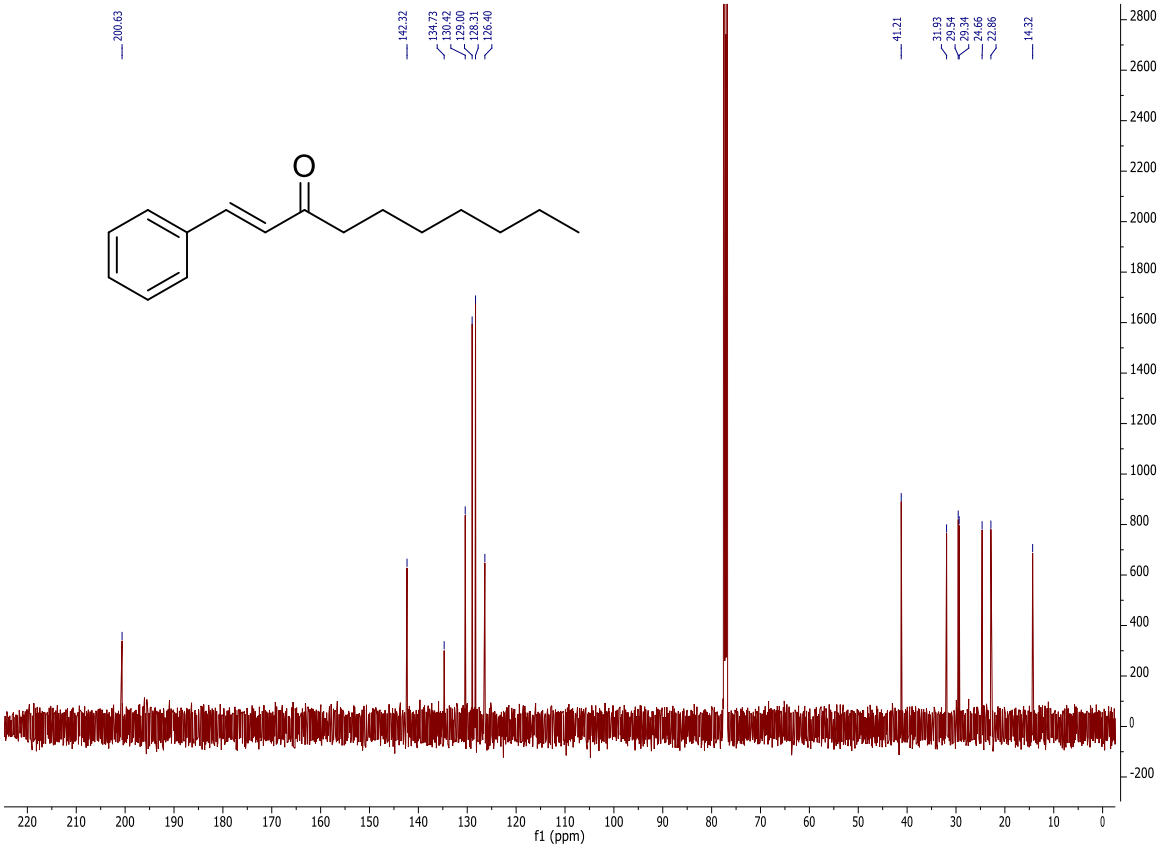

^{13}C NMR spectrum in $CDCl_3$.

98b

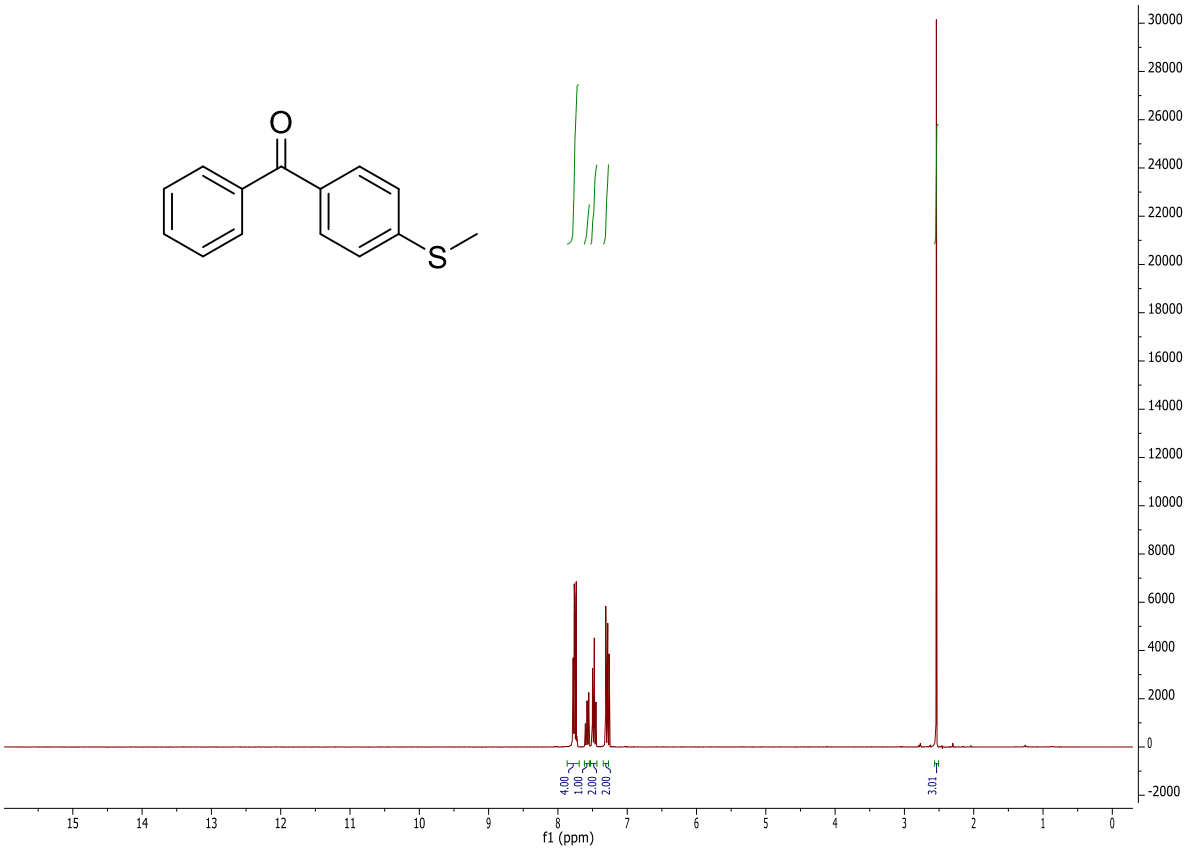

^{1}H NMR spectrum in $CDCl_3$.

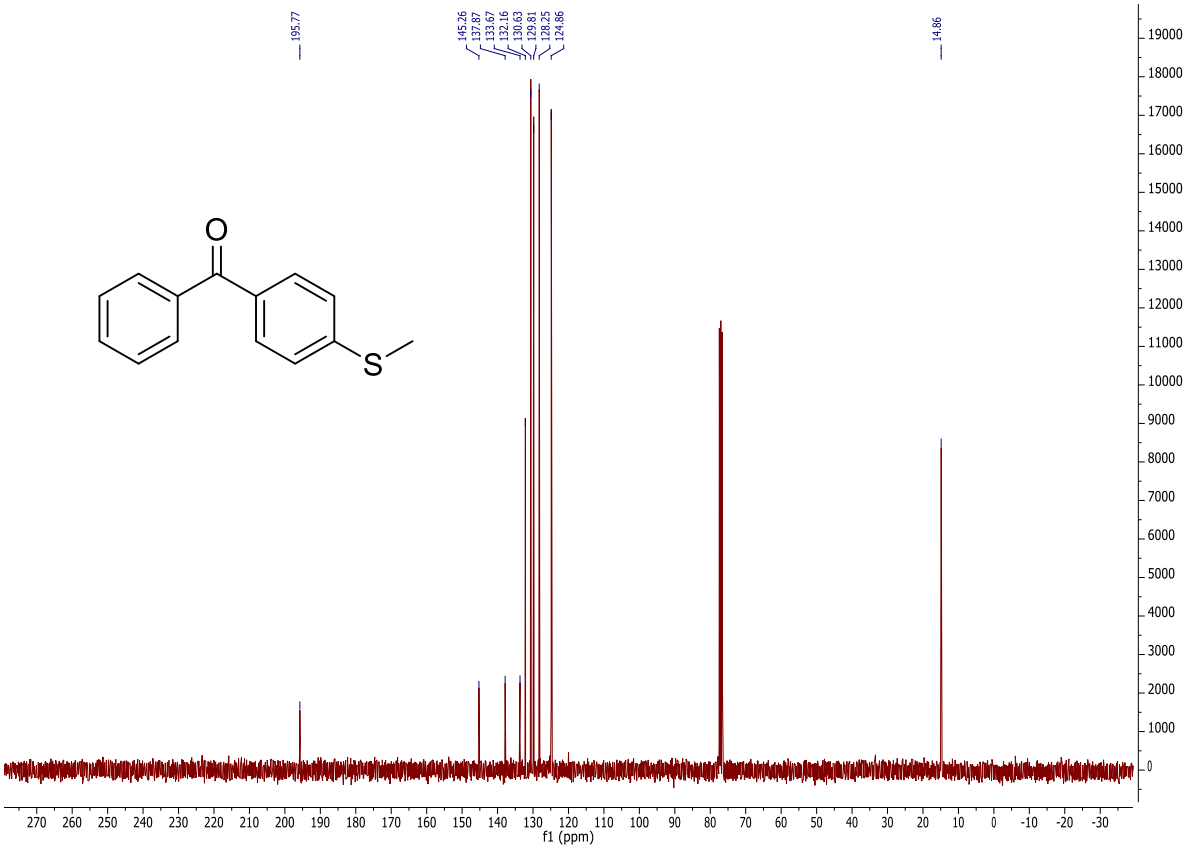

^{13}C NMR spectrum in $CDCl_3$.

99b

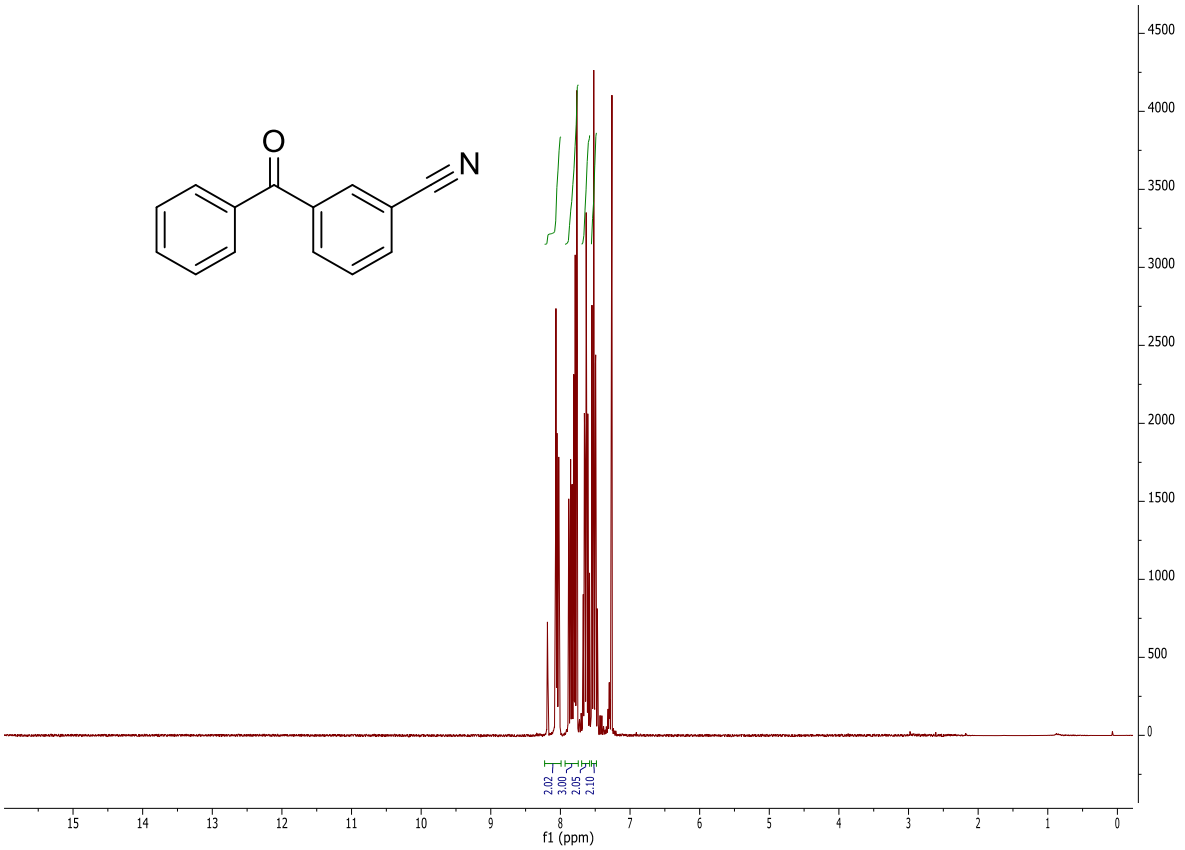

^{1}H NMR spectrum in $CDCl_3$.

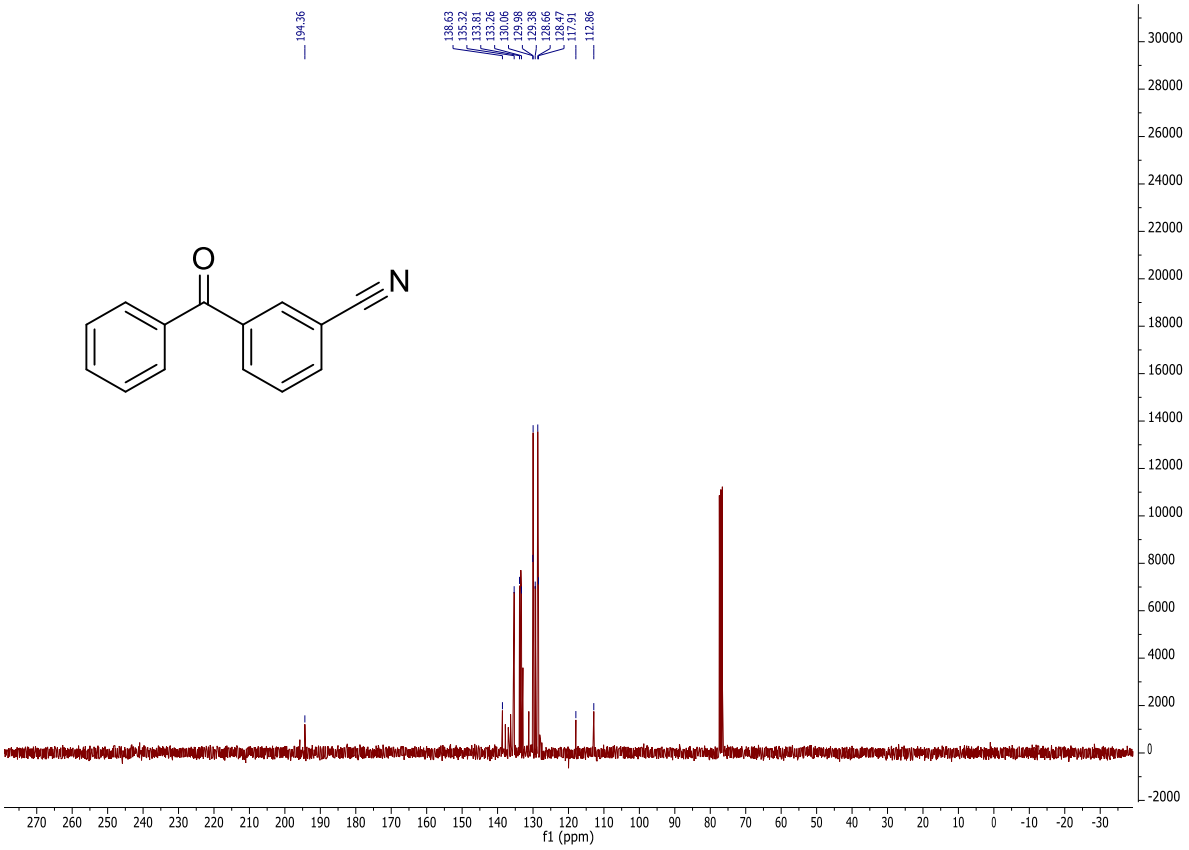

^{13}C NMR spectrum in $CDCl_3$.

100b

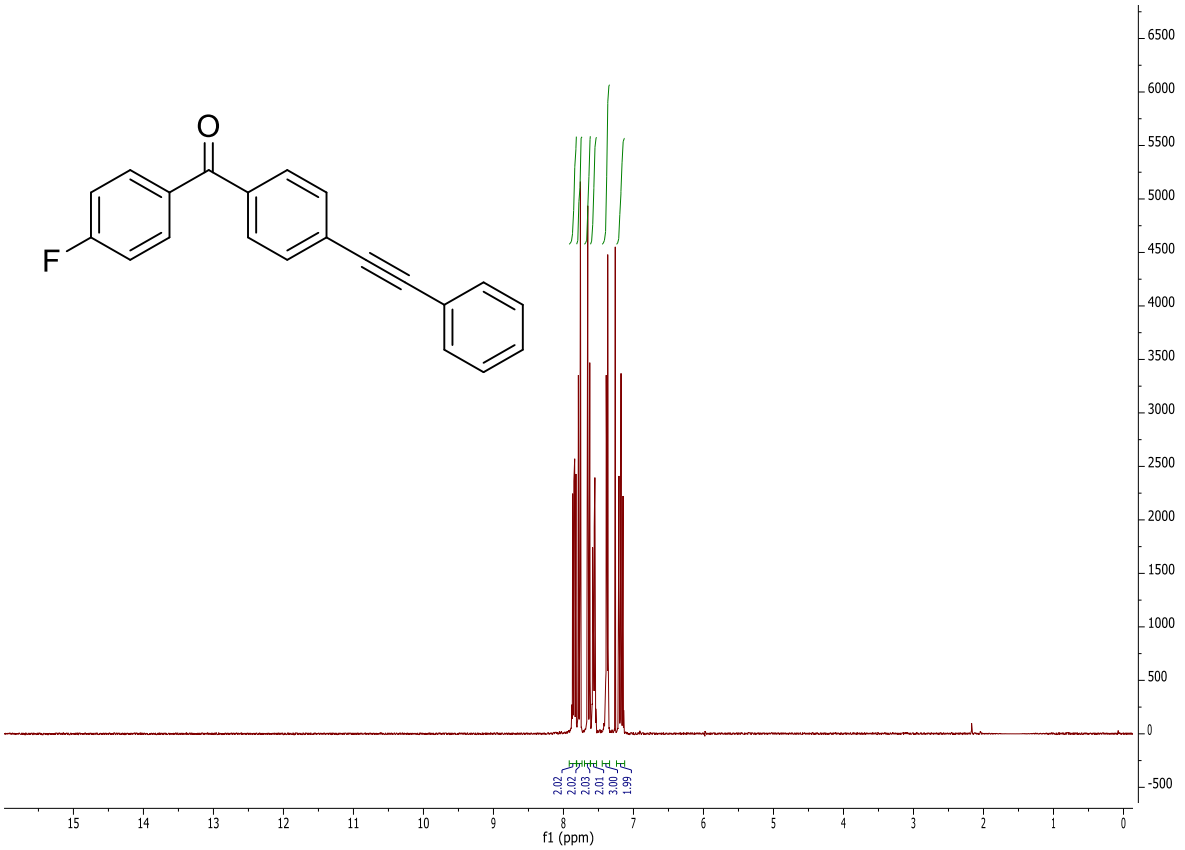

^{1}H NMR spectrum in $CDCl_3$.

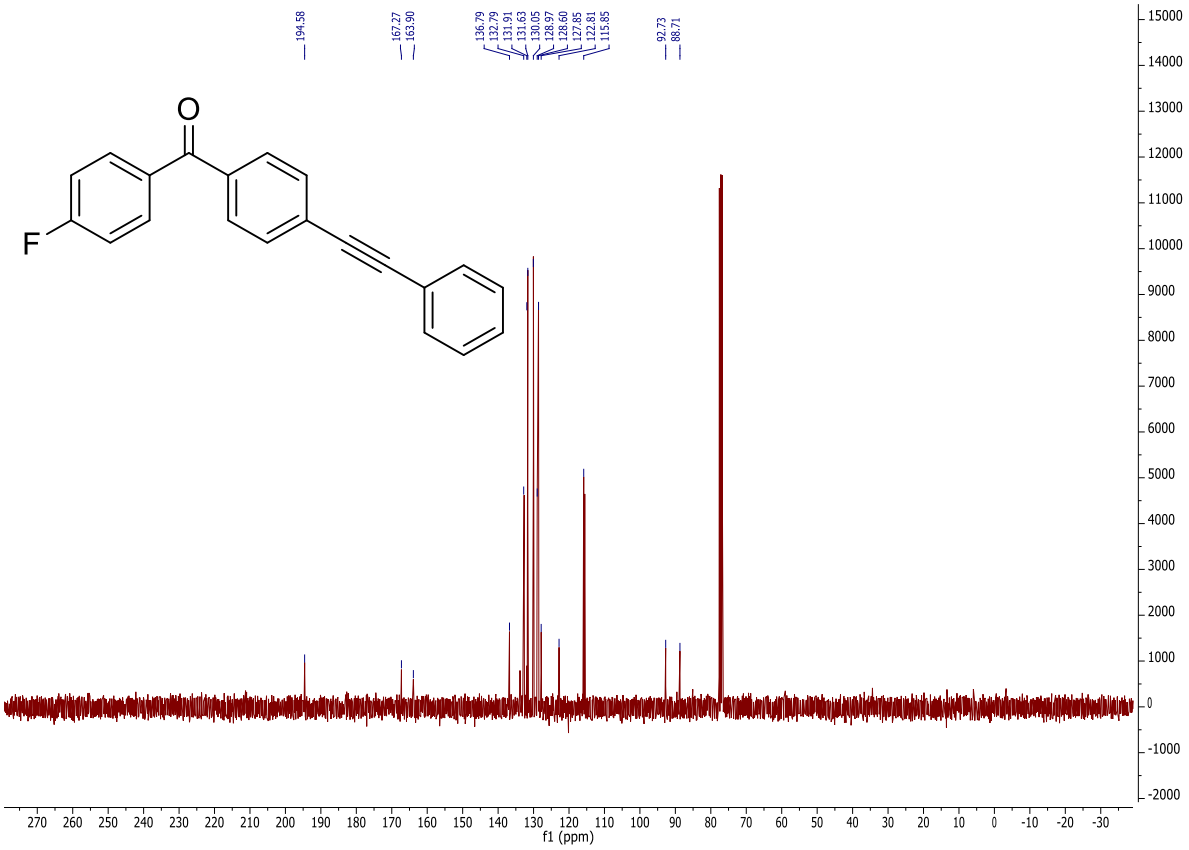

^{13}C NMR spectrum in $CDCl_3$.

101b

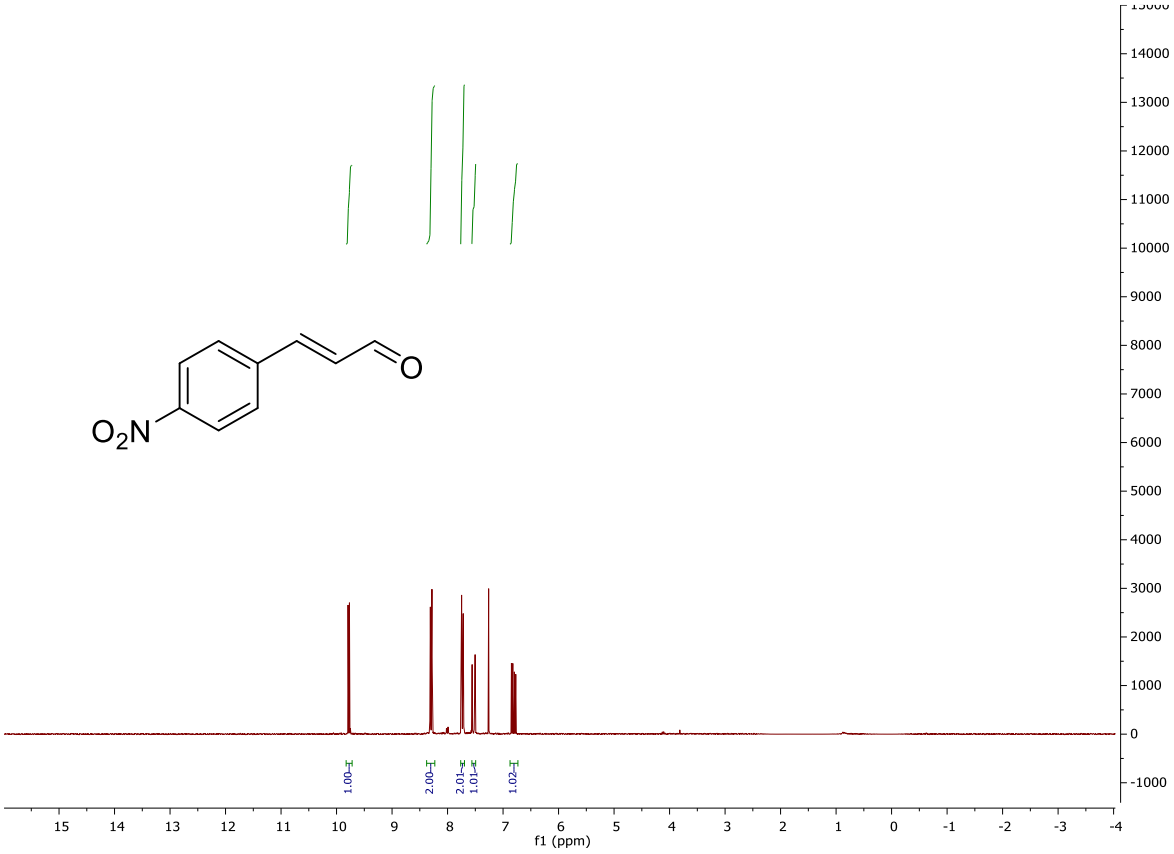

^{1}H NMR spectrum in $CDCl_3$.

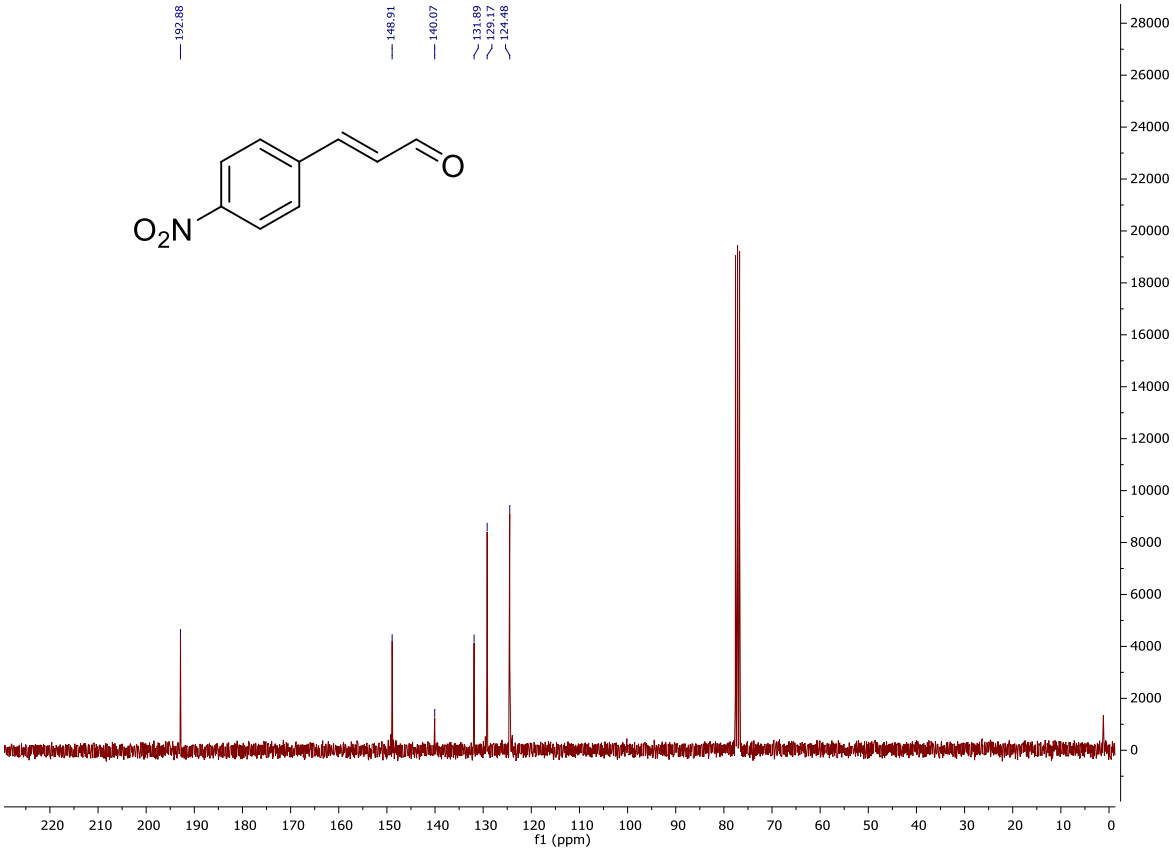

^{13}C NMR spectrum in $CDCl_3$.

102b

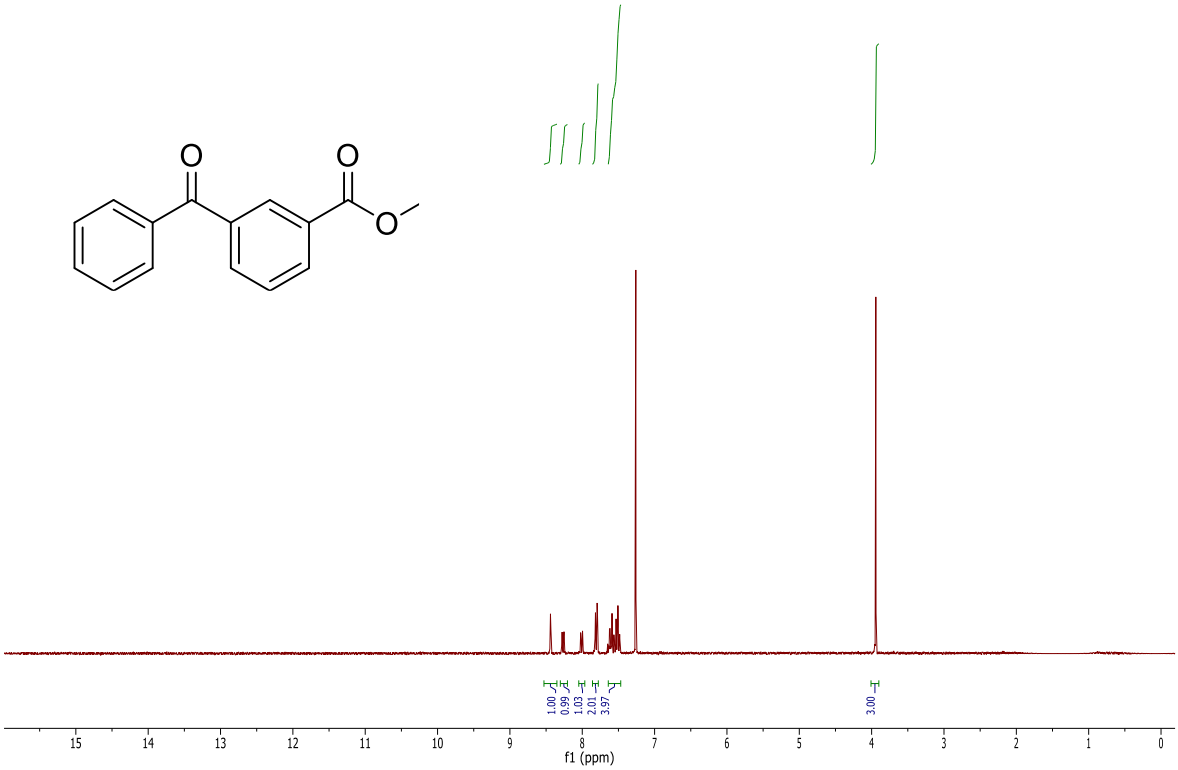

^{1}H NMR spectrum in $CDCl_3$.

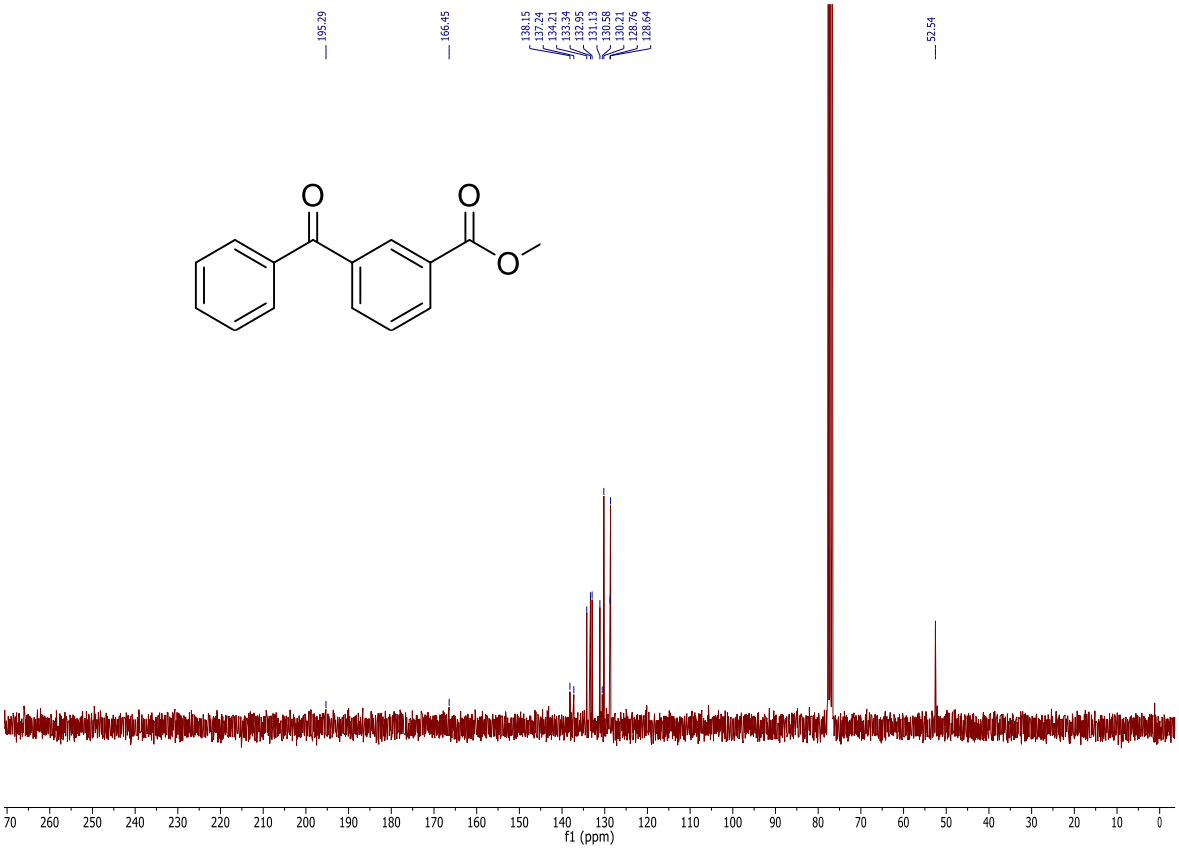

^{13}C NMR spectrum in $CDCl_3$.

103b

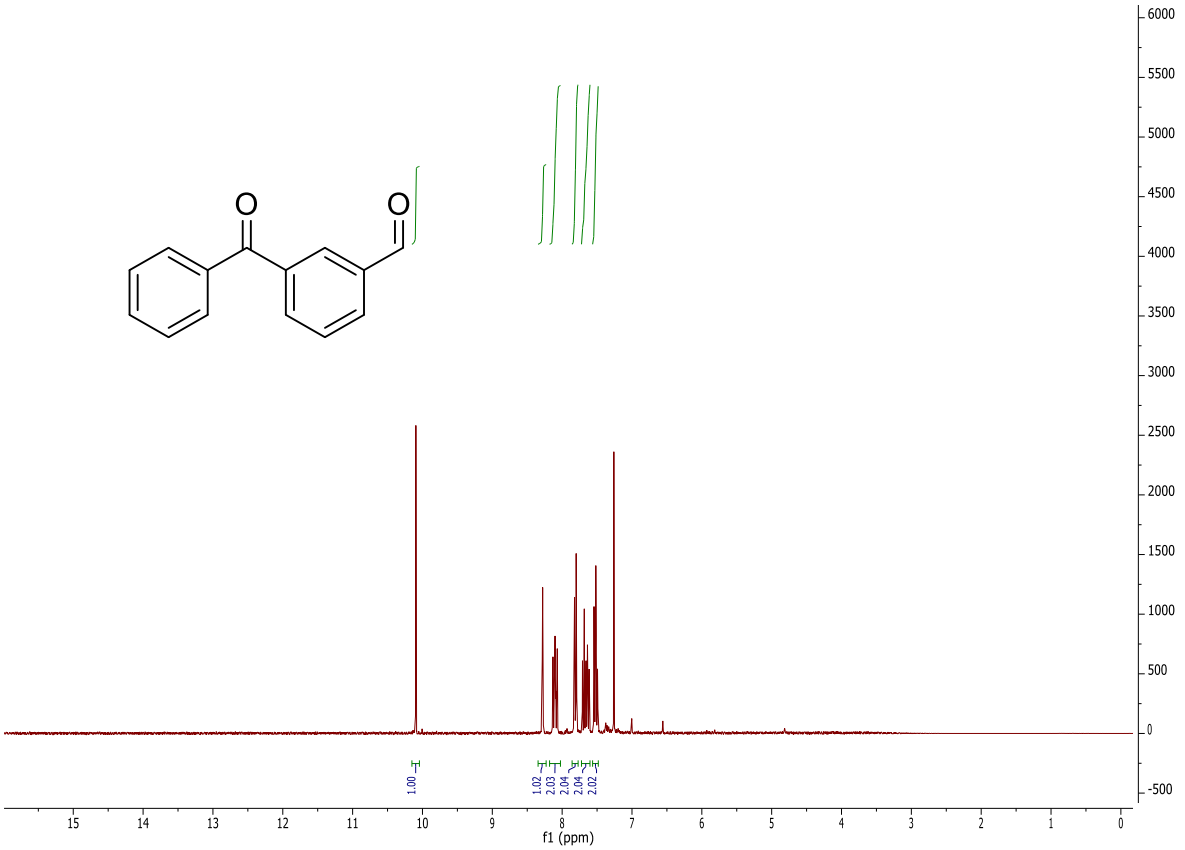

^{1}H NMR spectrum in $CDCl_3$.

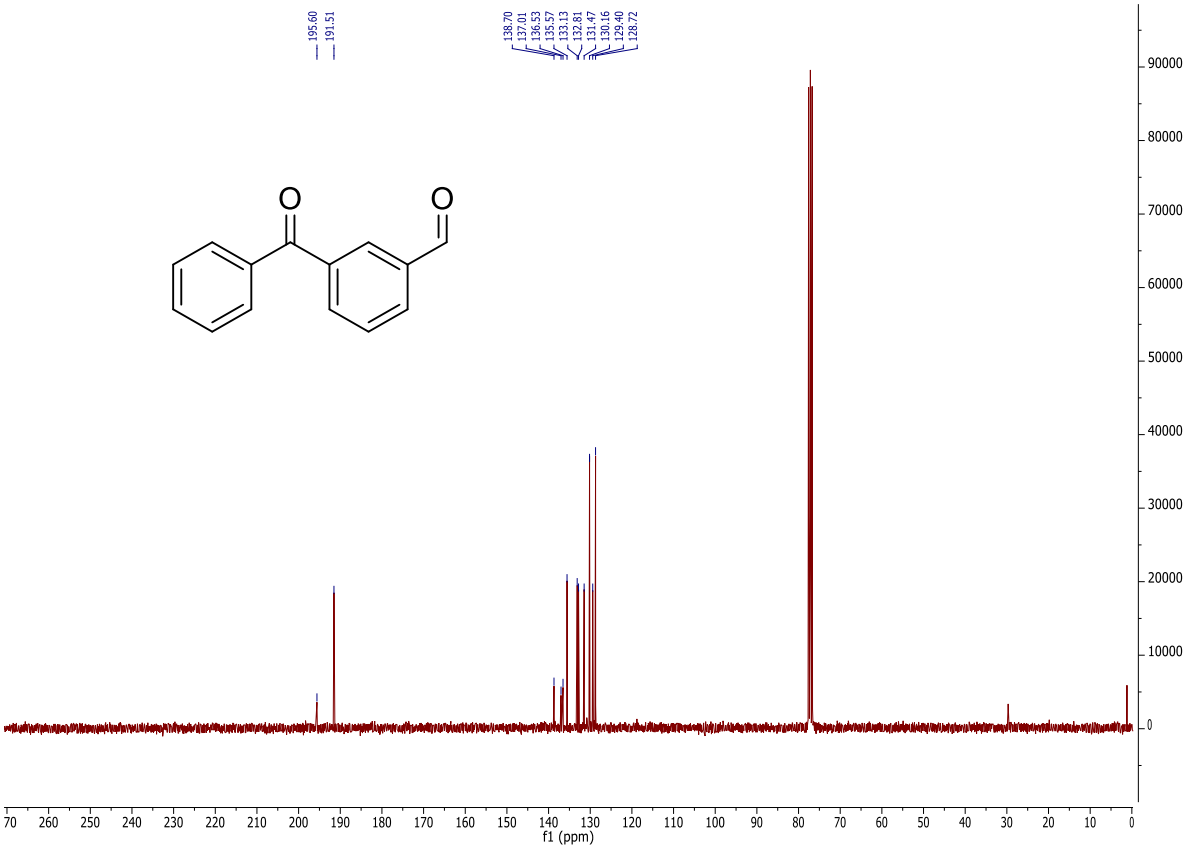

^{13}C NMR spectrum in $CDCl_3$.

190b

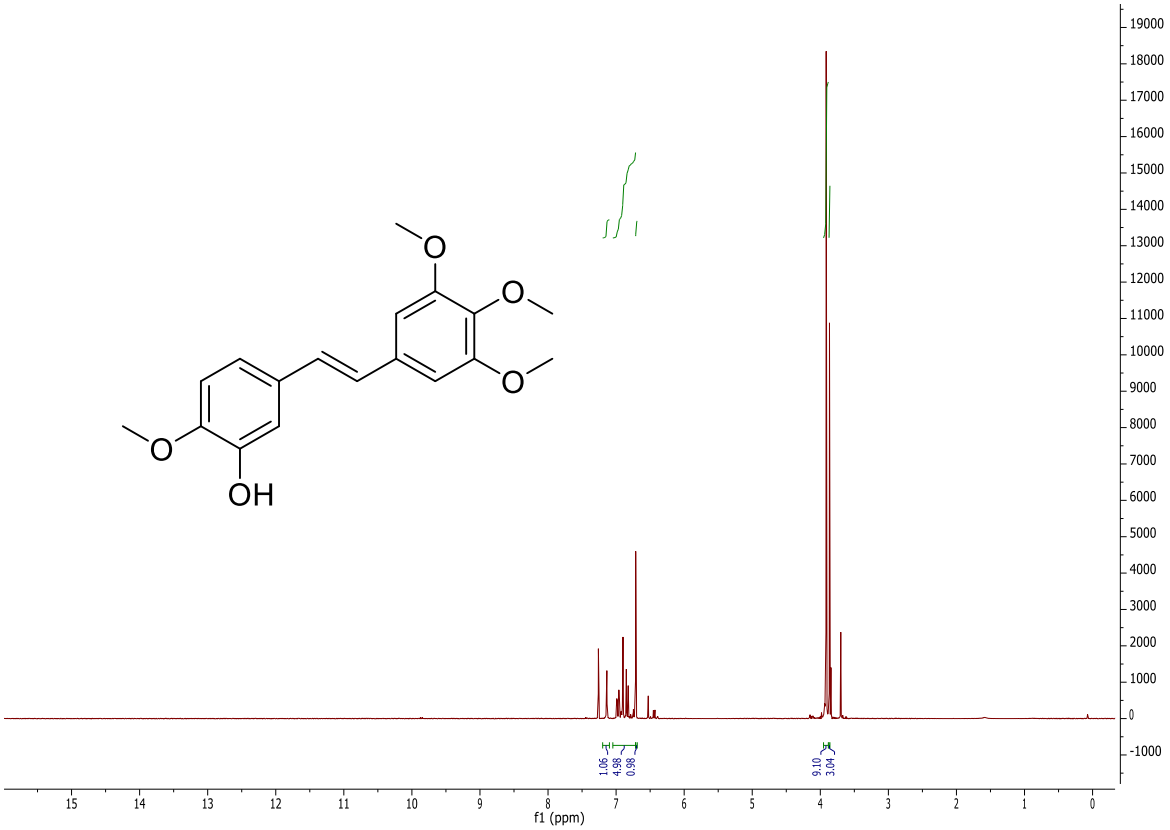

^{1}H NMR spectrum in $CDCl_3$.

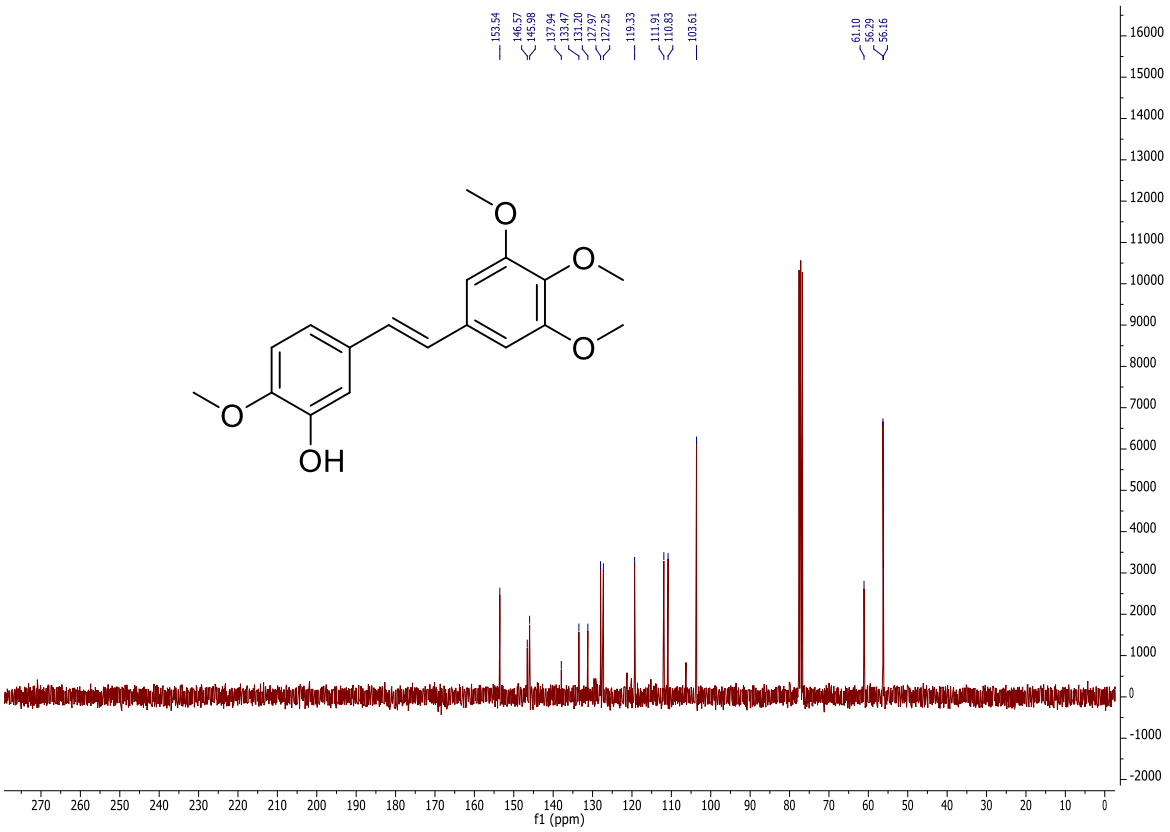

^{13}C NMR spectrum in $CDCl_3$.

191b

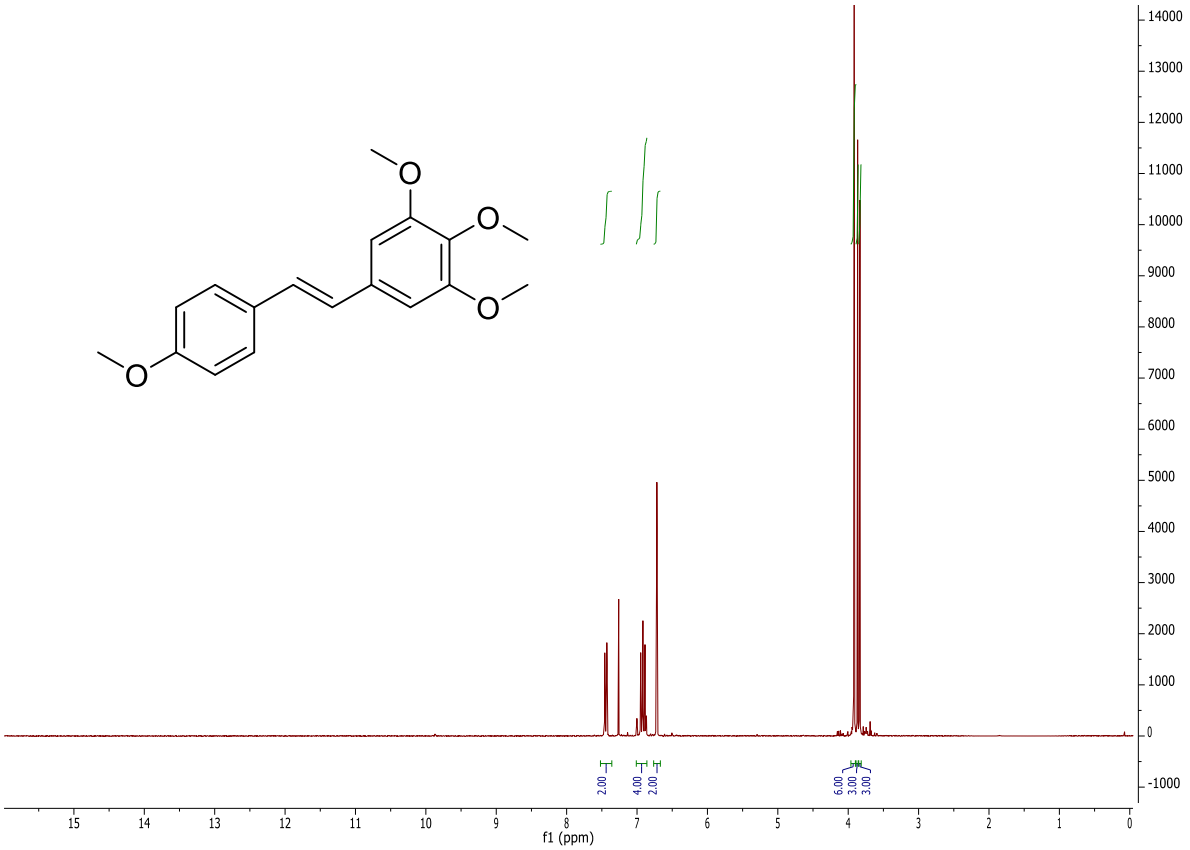

^{1}H NMR spectrum in $CDCl_3$.

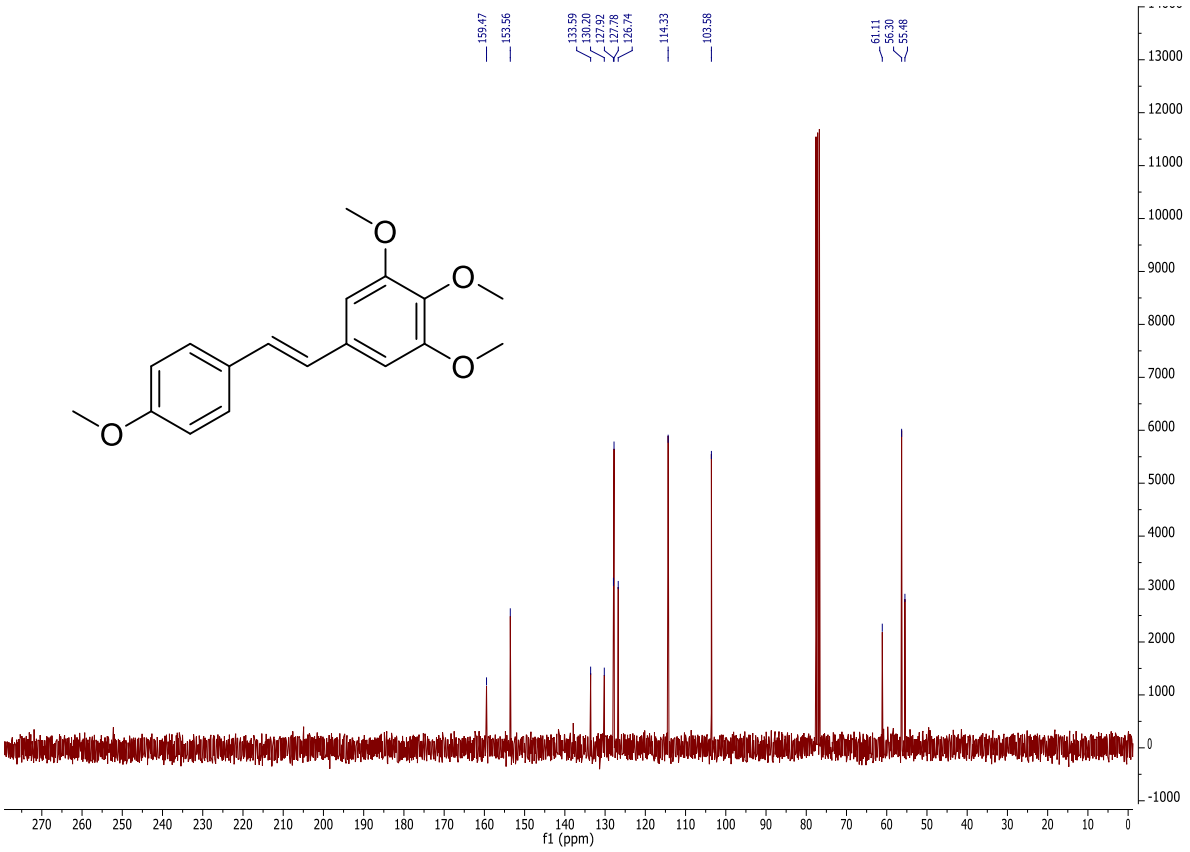

^{13}C NMR spectrum in $CDCl_3$.

192b I

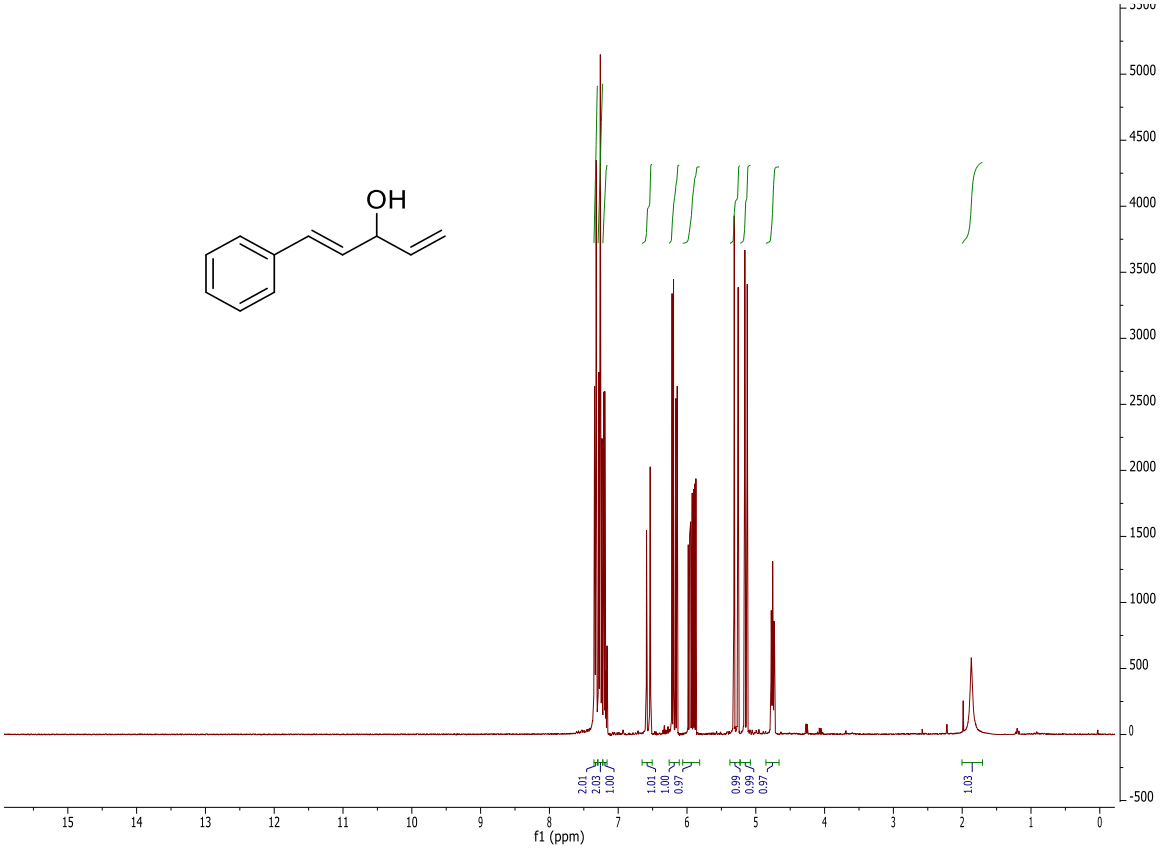

^{1}H NMR spectrum in $CDCl_3$.

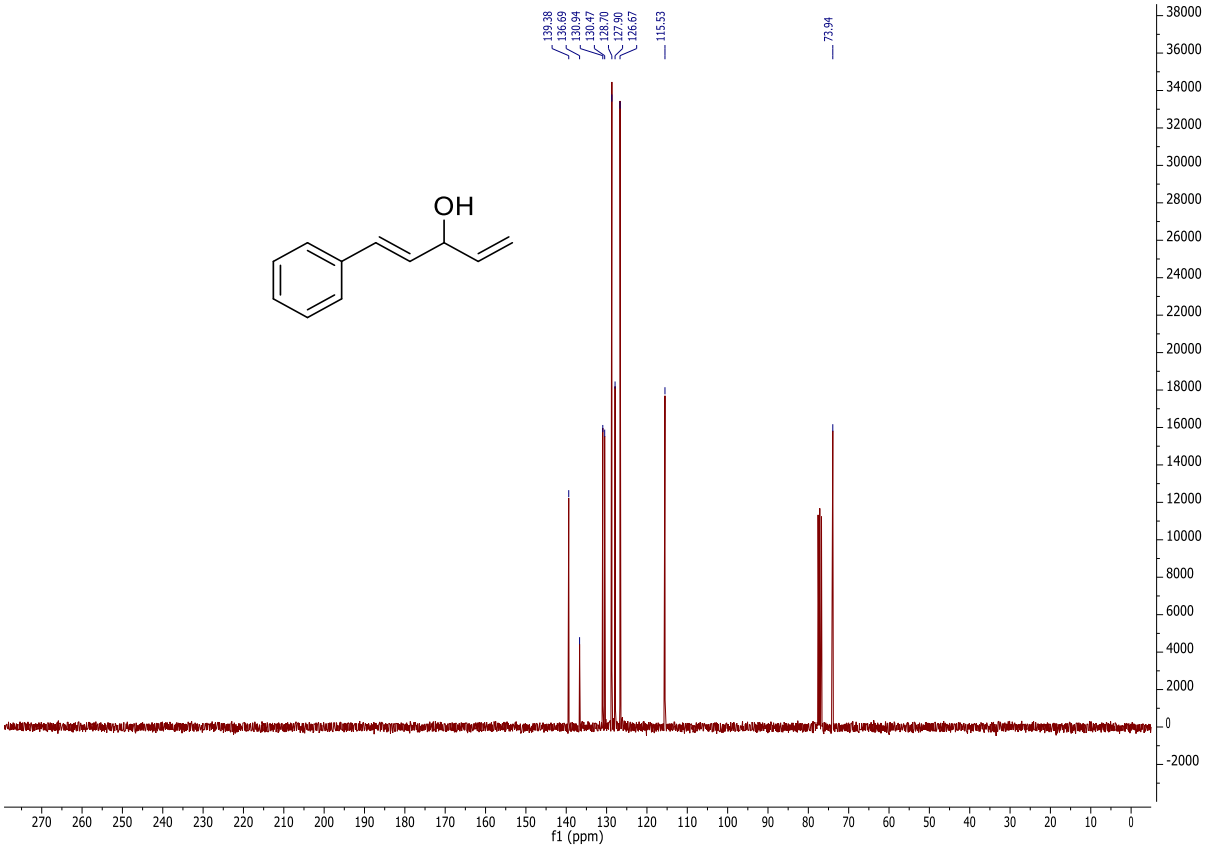

^{13}C NMR spectrum in $CDCl_3$.

192b II

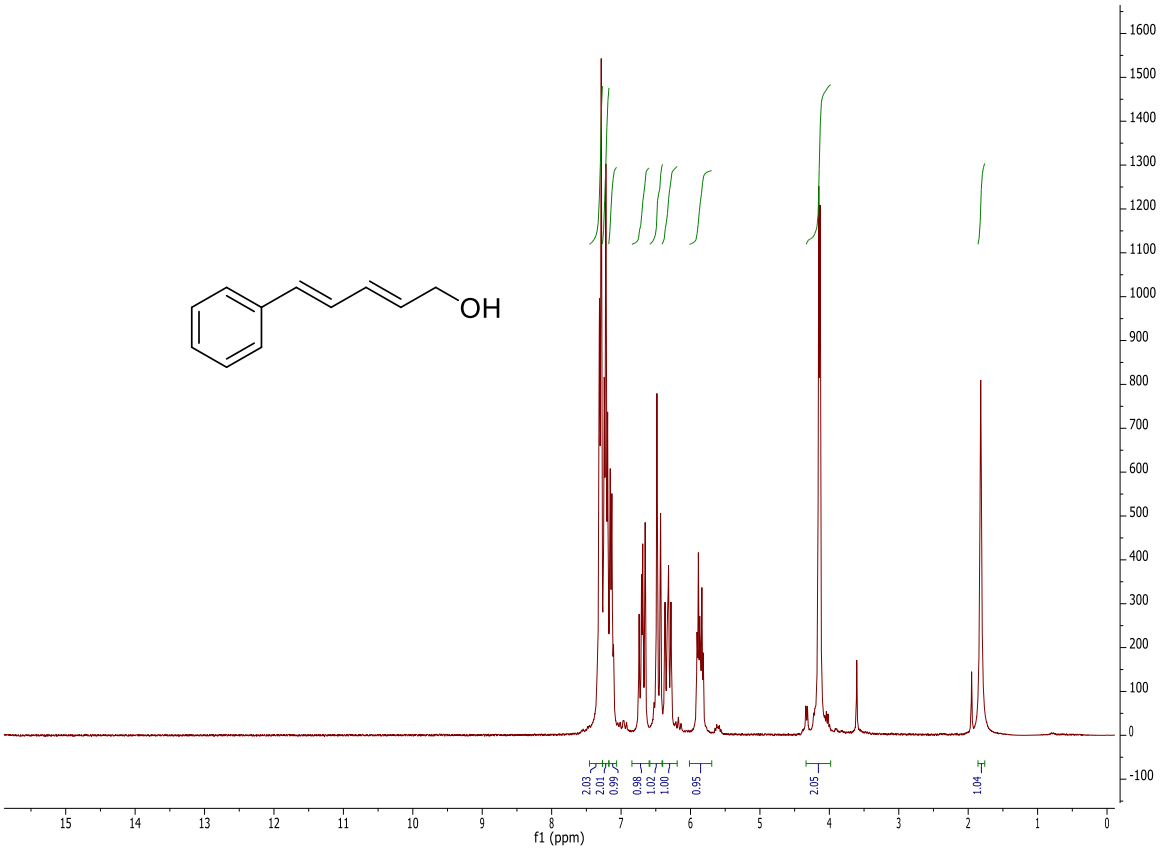

^{1}H NMR spectrum in $CDCl_3$.

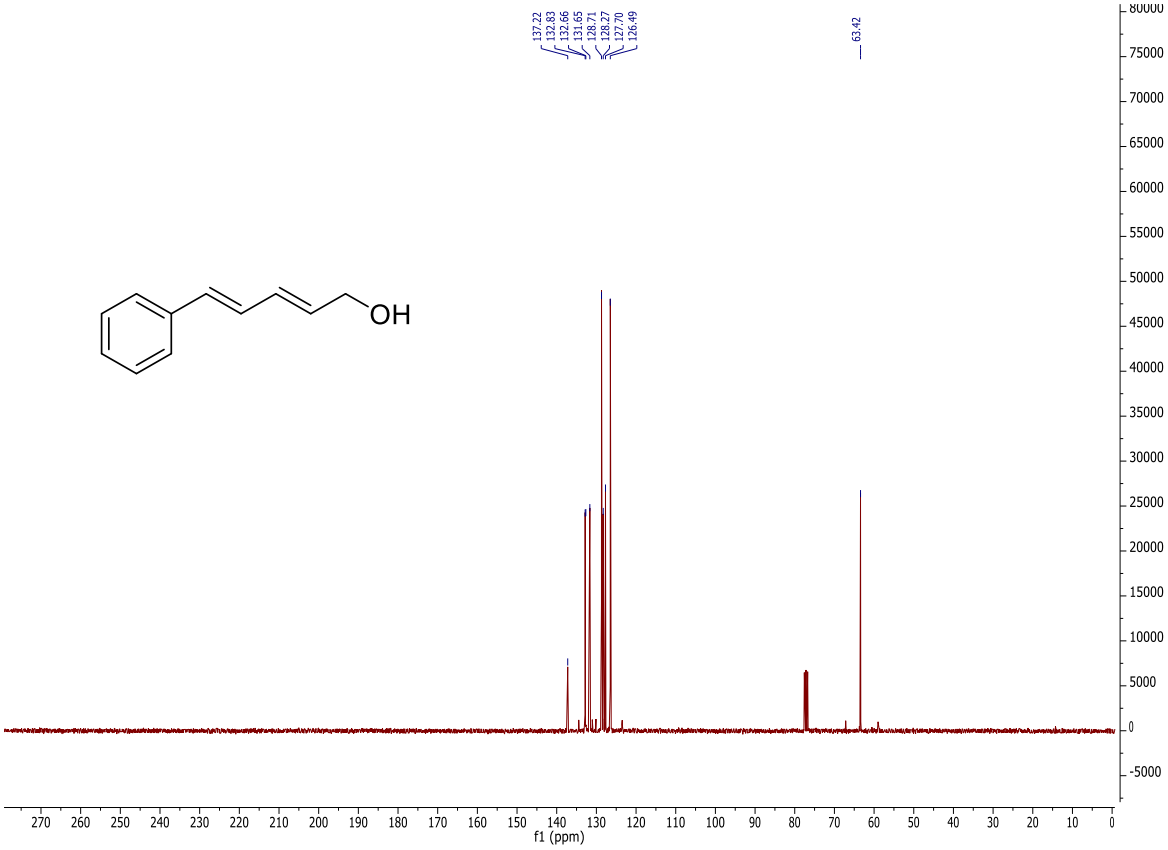

^{13}C NMR spectrum in $CDCl_3$.

192b

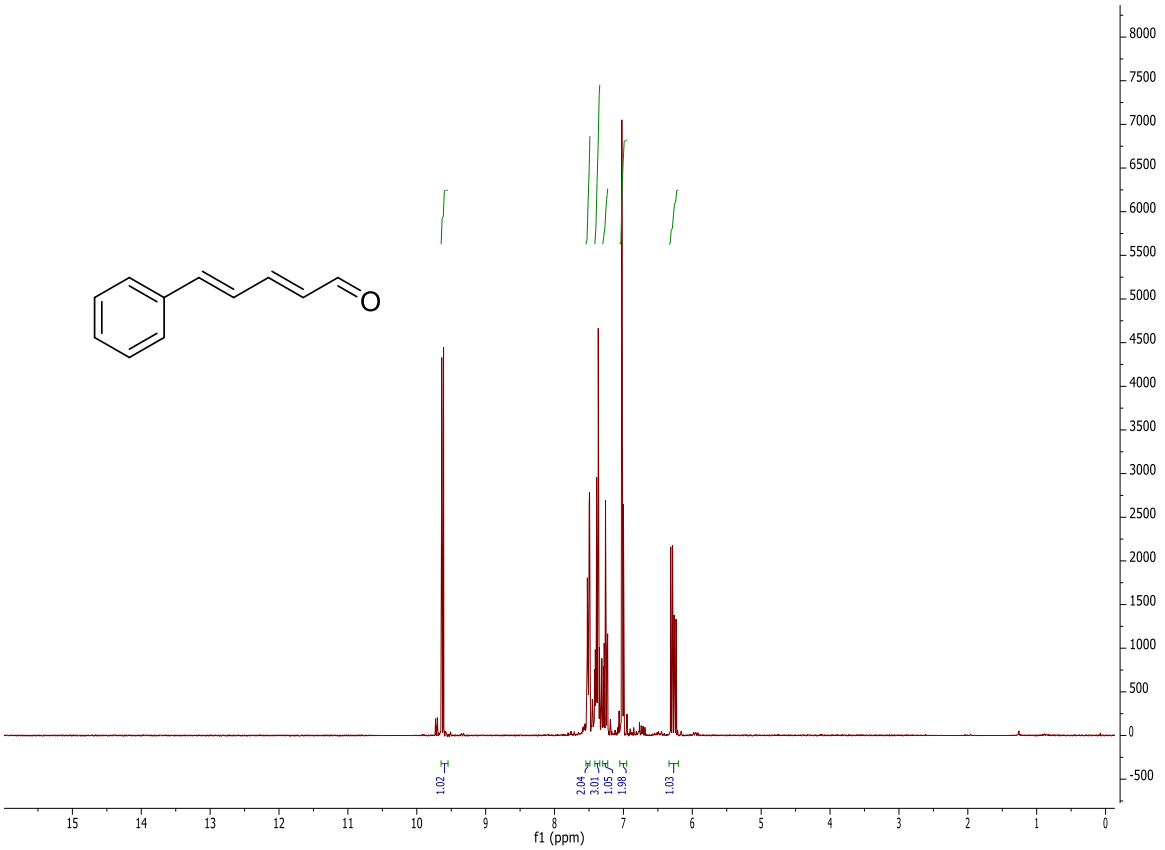

^{1}H NMR spectrum in $CDCl_3$.

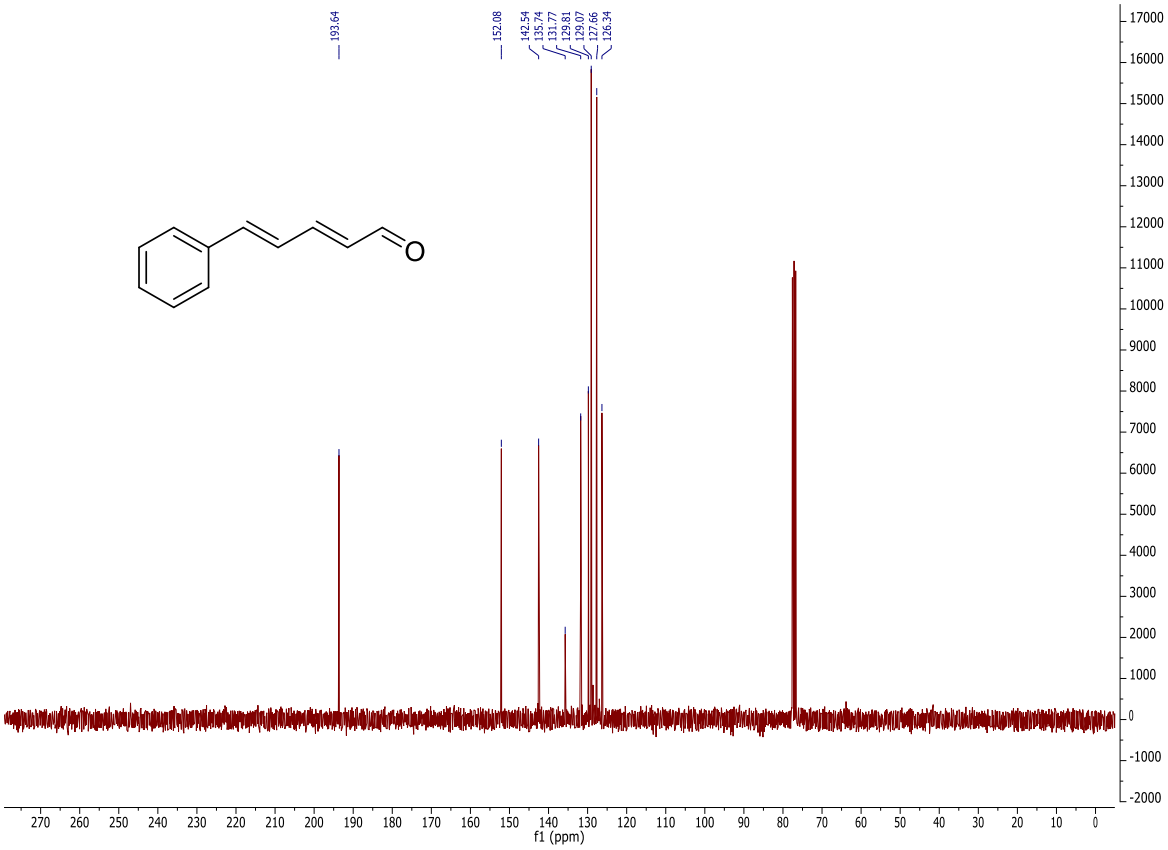

^{13}C NMR spectrum in $CDCl_3$.

193b

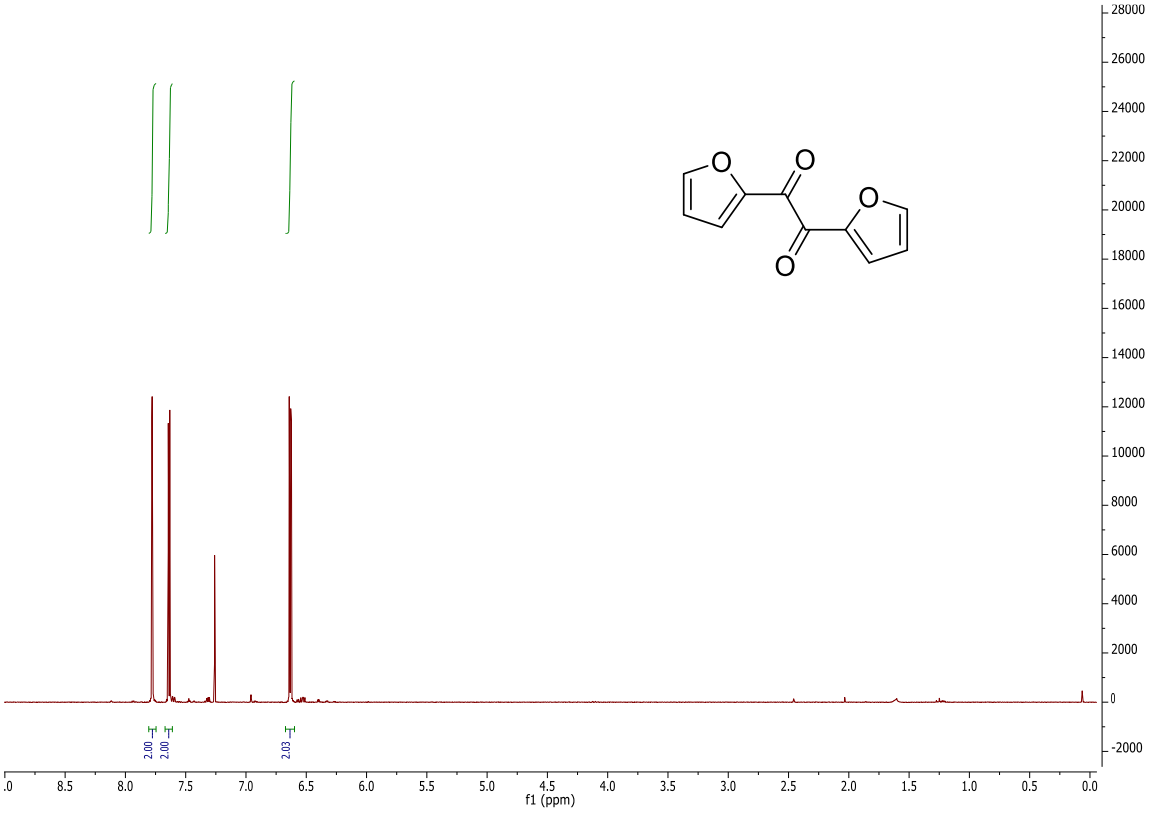

^{1}H NMR spectrum in $CDCl_3$.

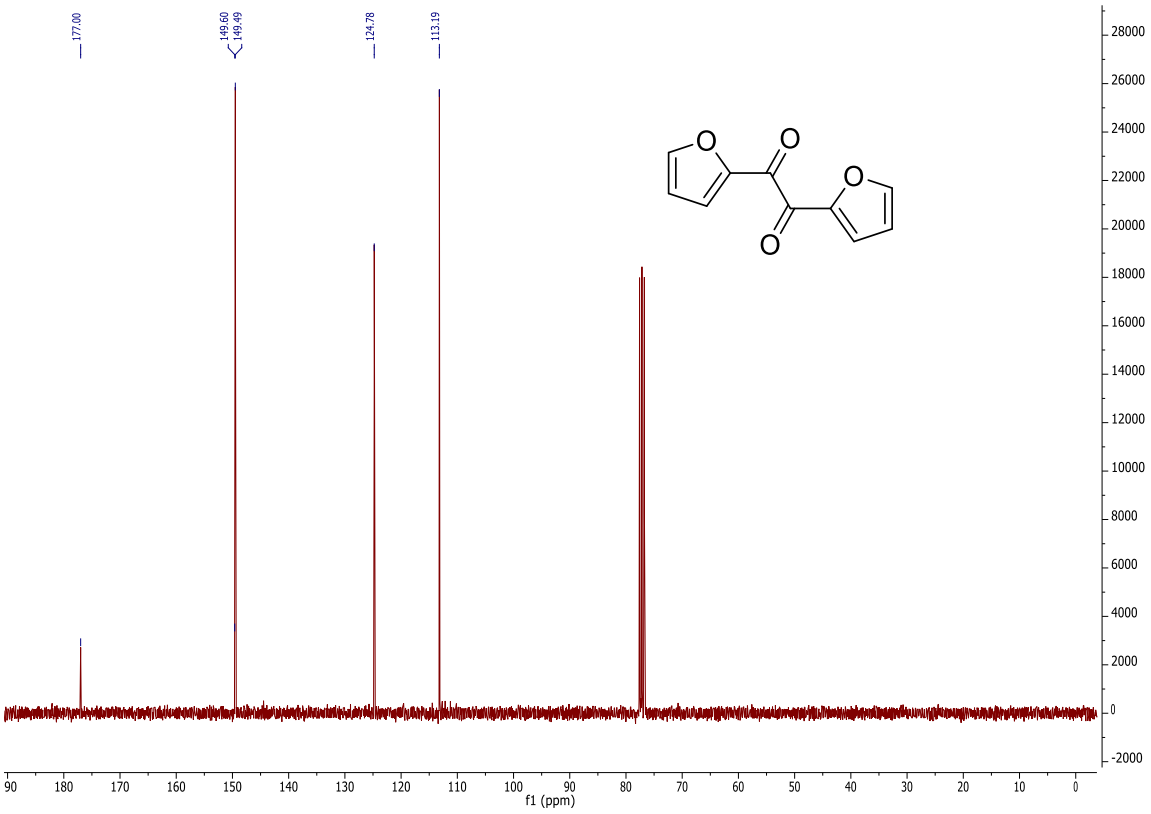

^{13}C NMR spectrum in $CDCl_3$.

194b

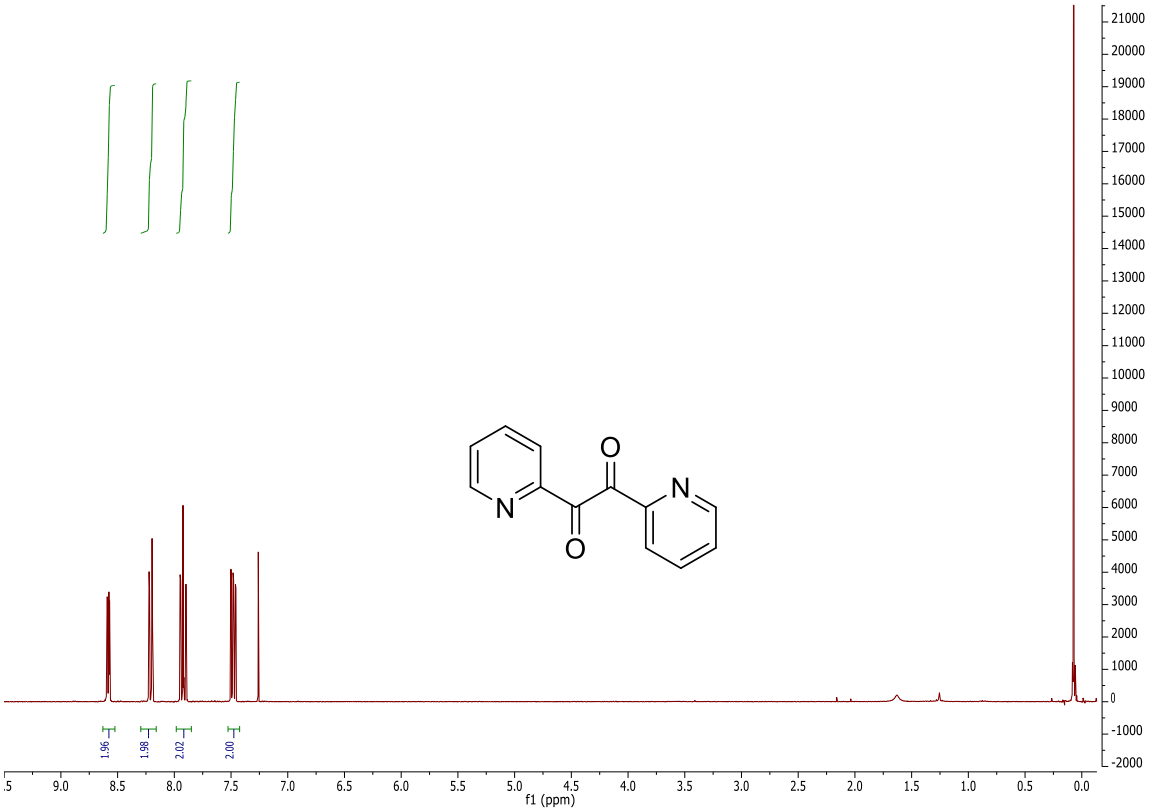

^{1}H NMR spectrum in $CDCl_3$.

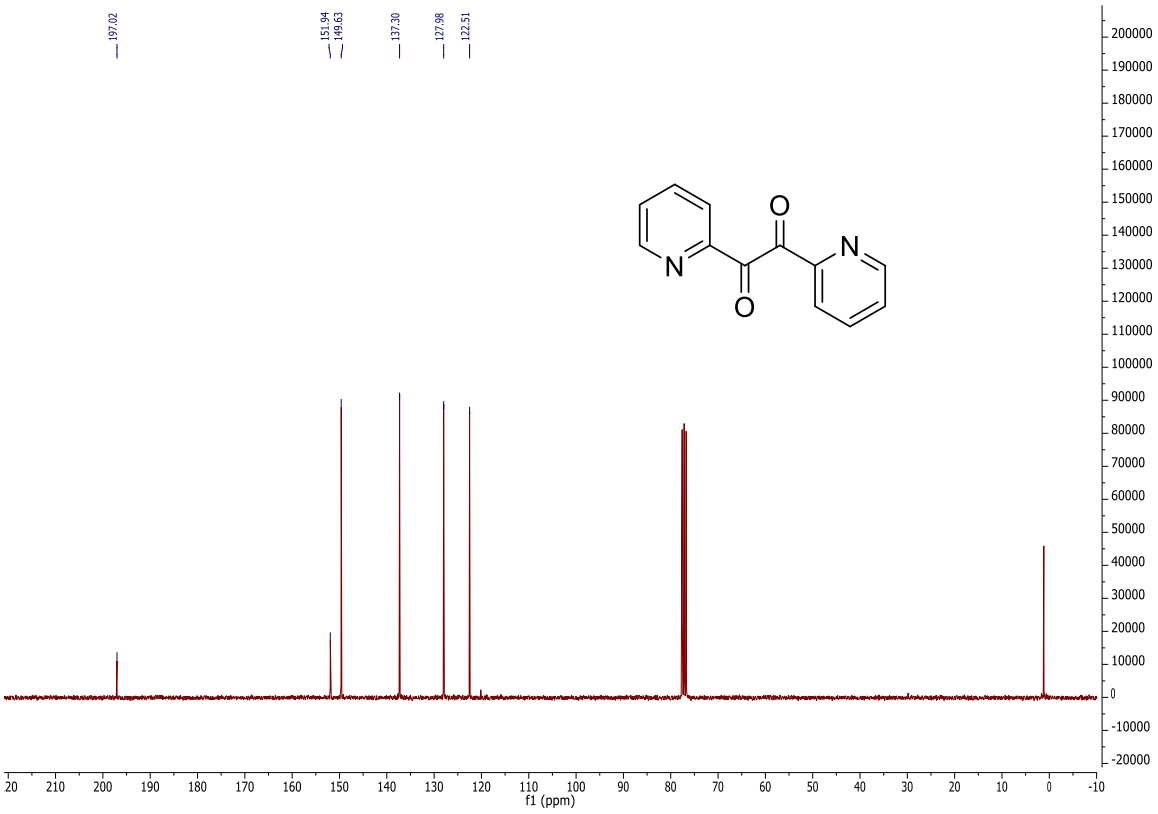

^{13}C NMR spectrum in $CDCl_3$.

195b

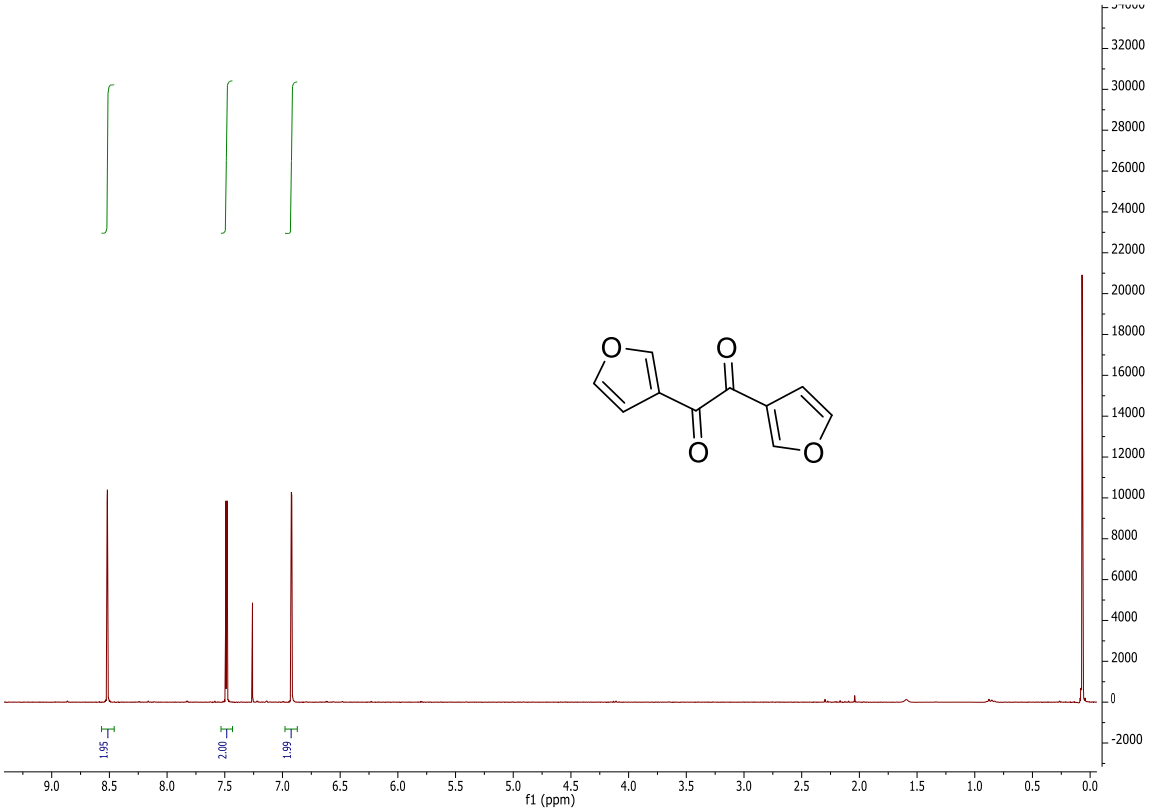

^{1}H NMR spectrum in $CDCl_3$.

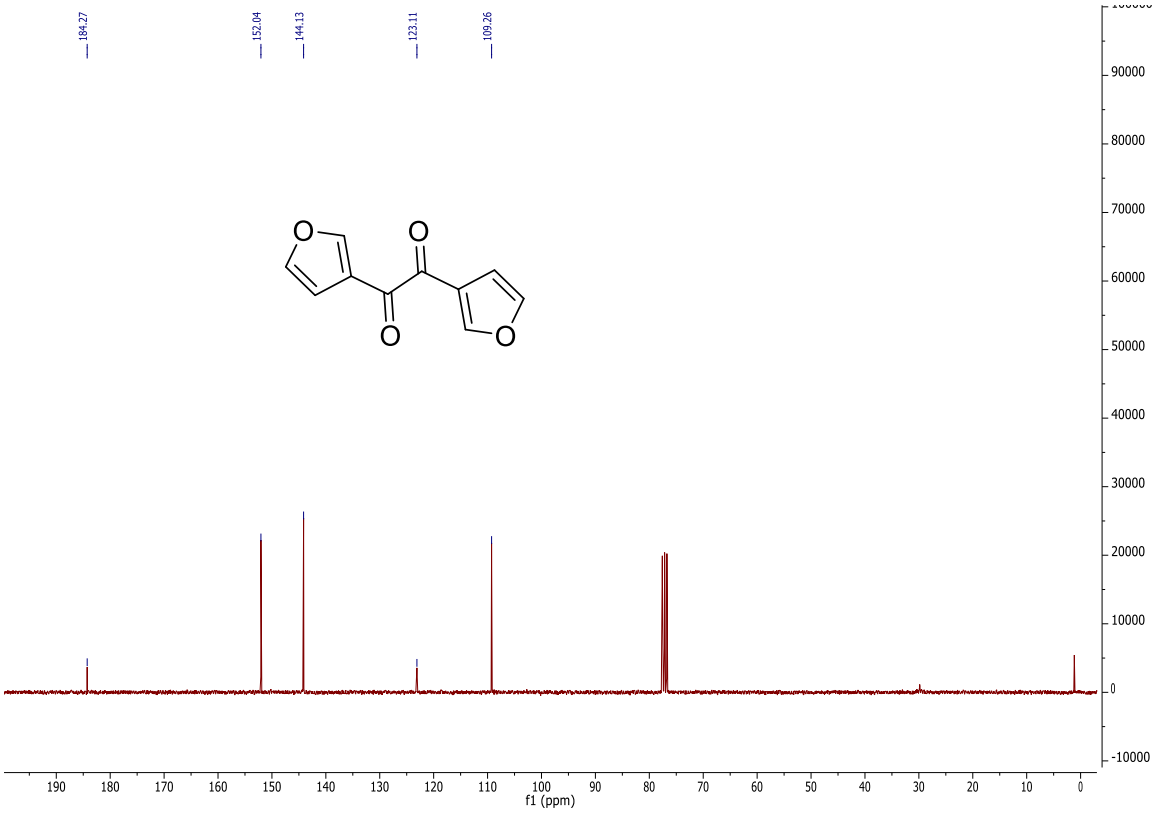

^{13}C NMR spectrum in $CDCl_3$.

196b

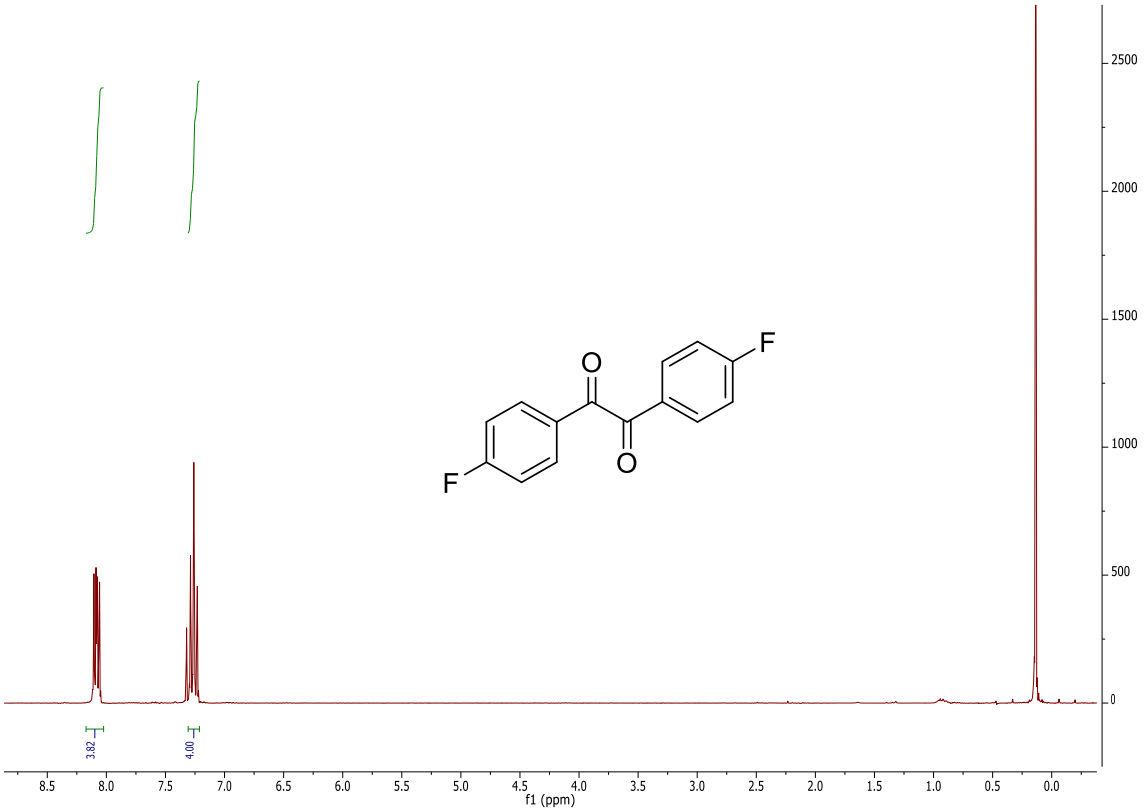

^{1}H NMR spectrum in $CDCl_3$.

^{13}C NMR spectrum in $CDCl_3$.

197b

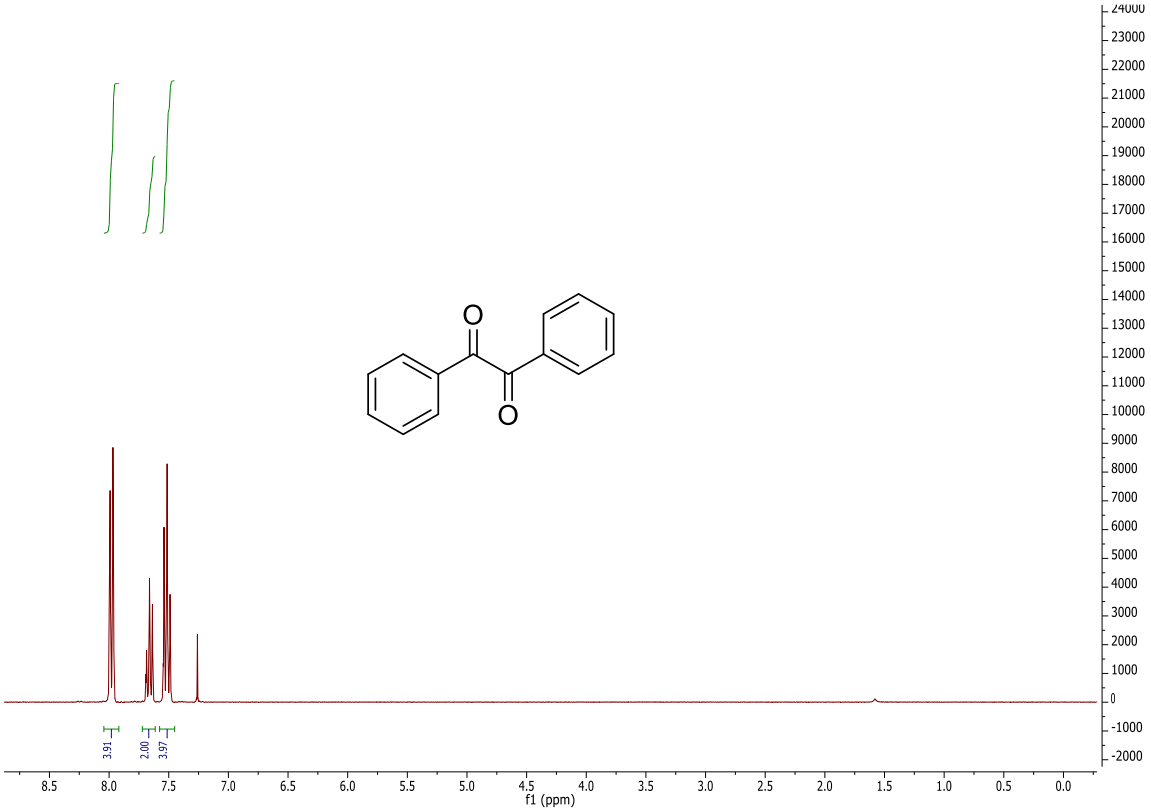

^{1}H NMR spectrum in $CDCl_3$.

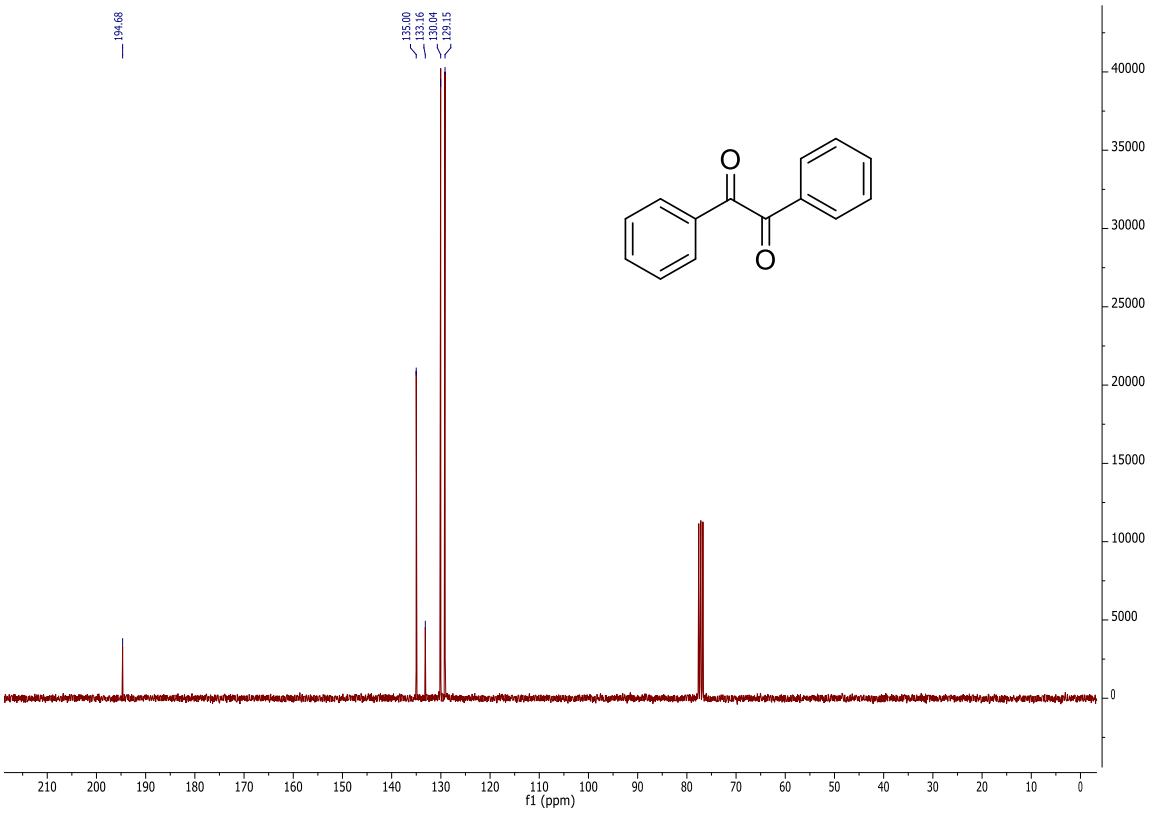

^{13}C NMR spectrum in $CDCl_3$.

198b

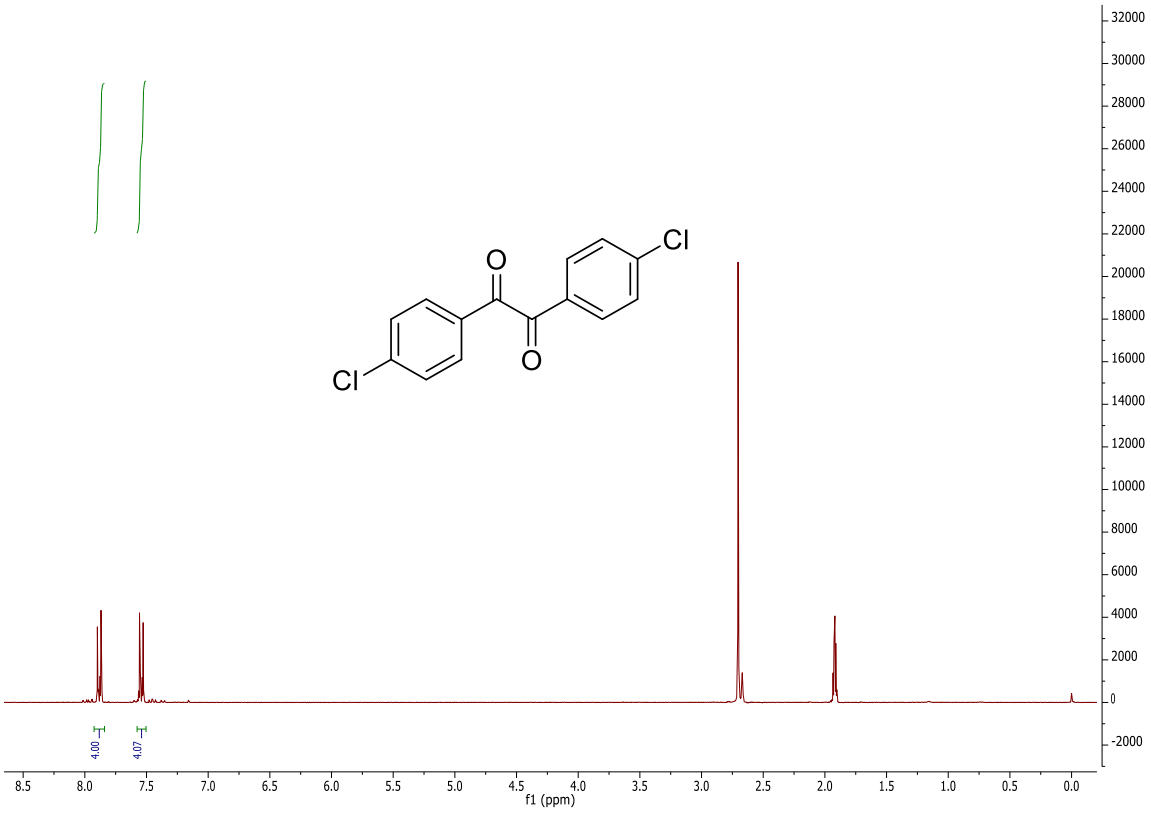

^{1}H NMR spectrum in Acetone-d_6.

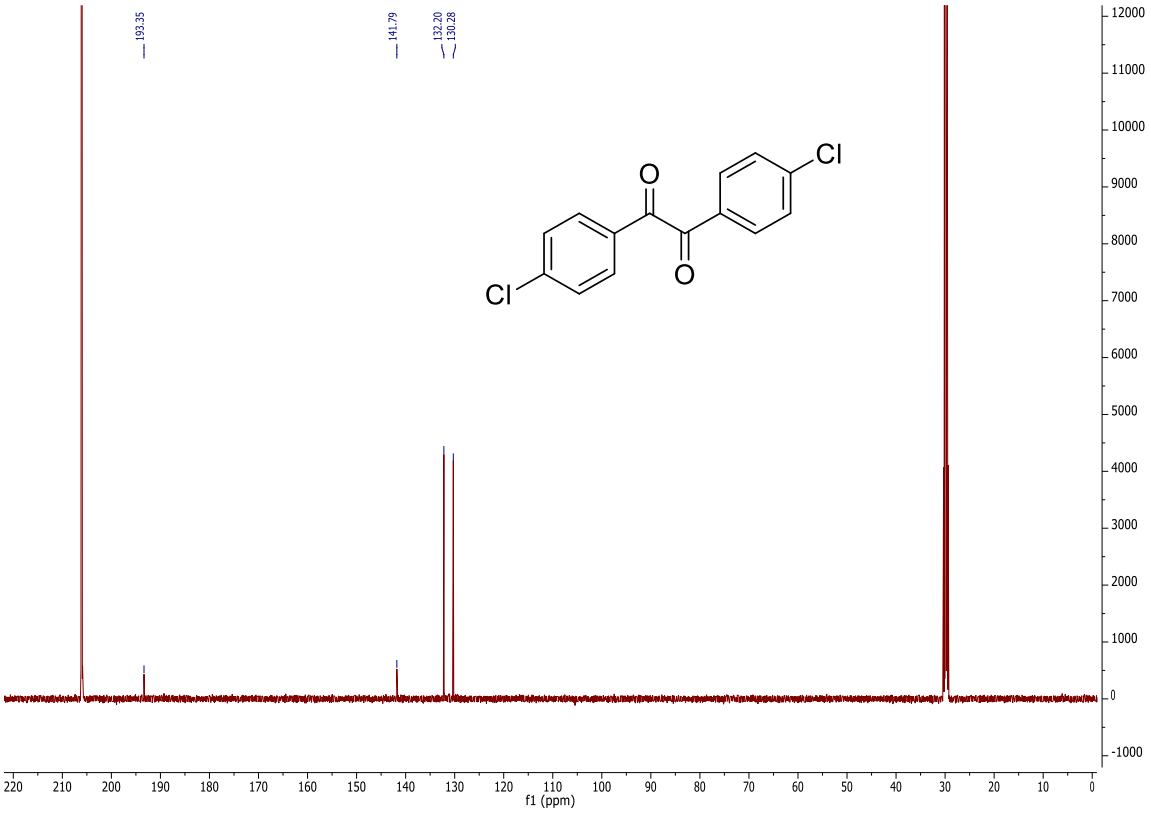

^{13}C NMR spectrum in Acetone-d_6.

199b

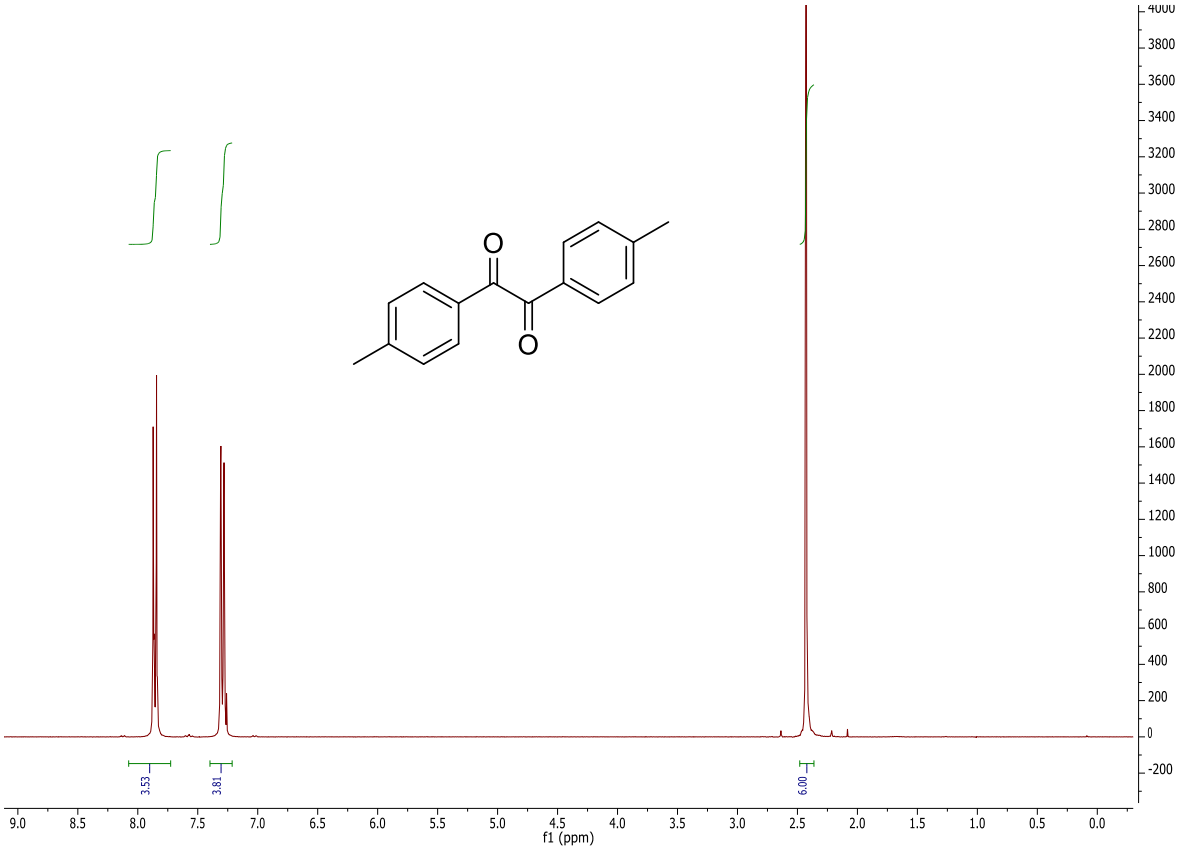

^{1}H NMR spectrum in $CDCl_3$.

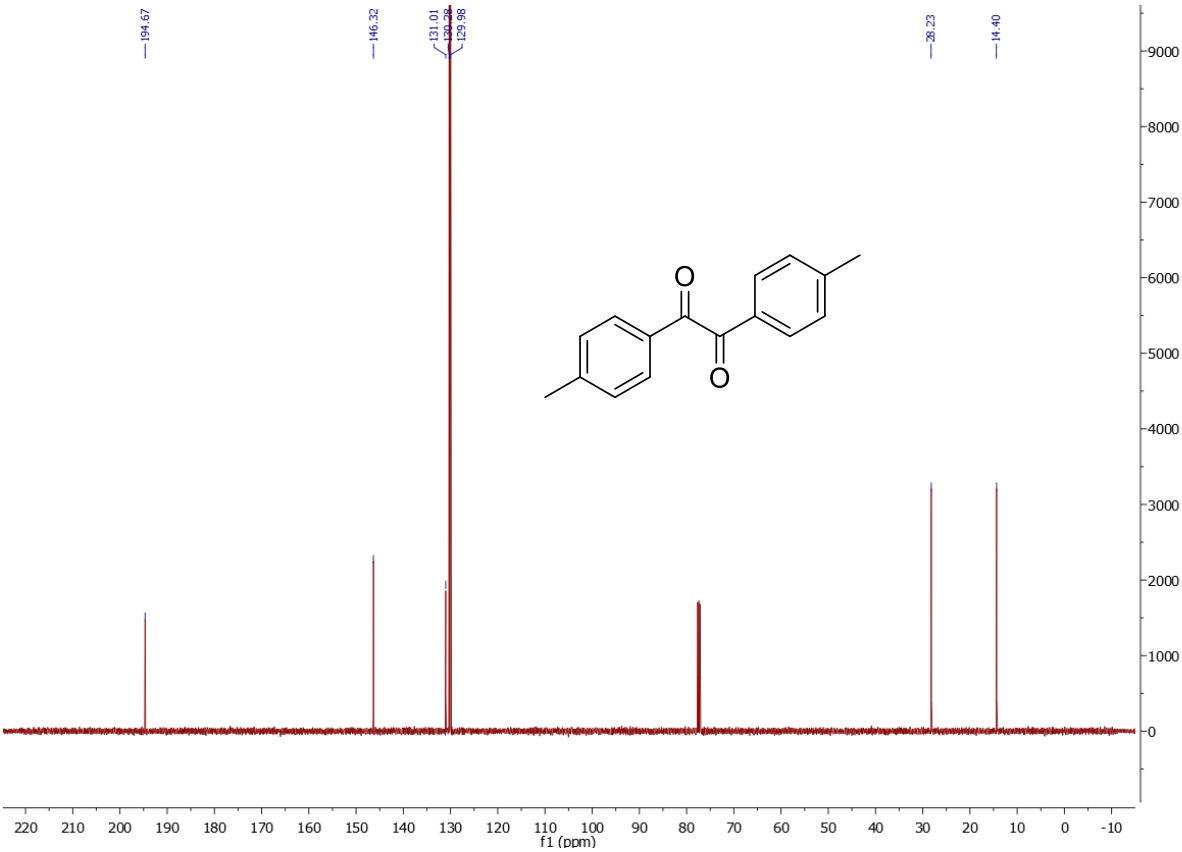

^{13}C NMR spectrum in $CDCl_3$.

200b

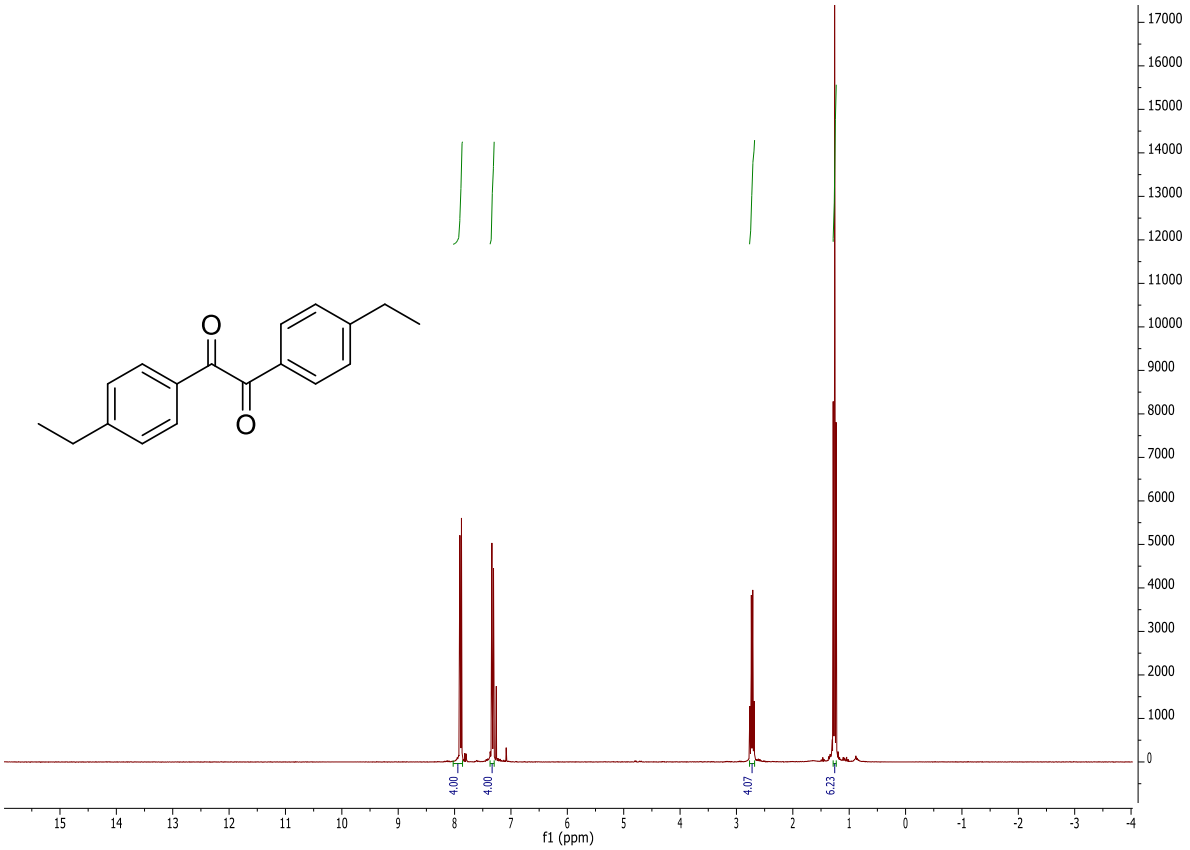

^{1}H NMR spectrum in $CDCl_3$.

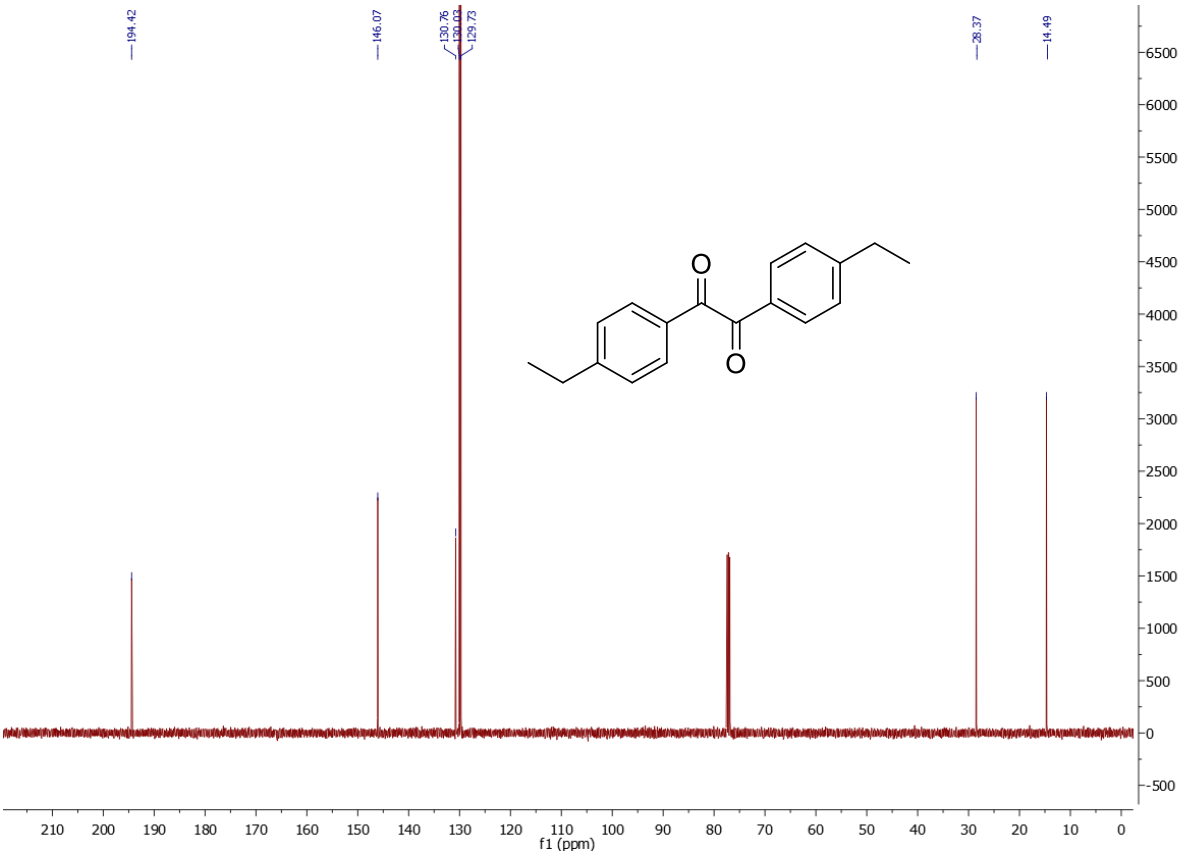

^{13}C NMR spectrum in $CDCl_3$.

201b

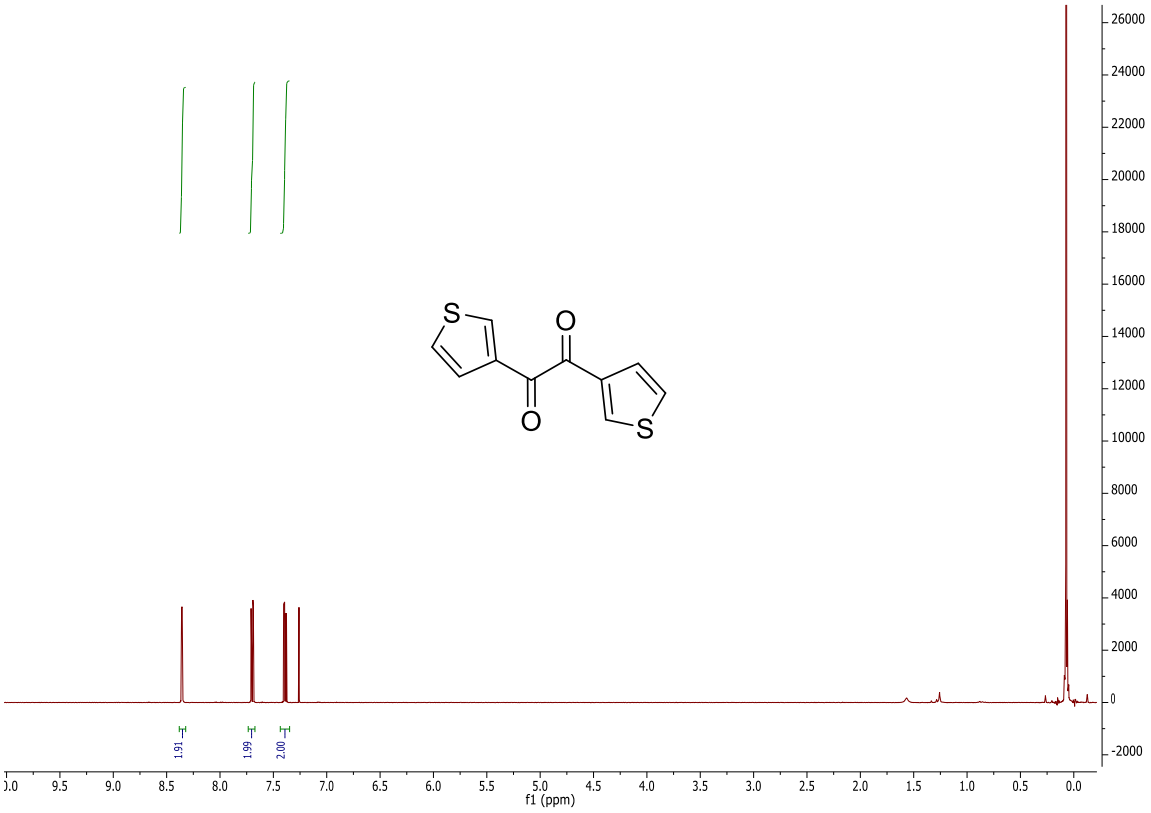

^{1}H NMR spectrum in $CDCl_3$.

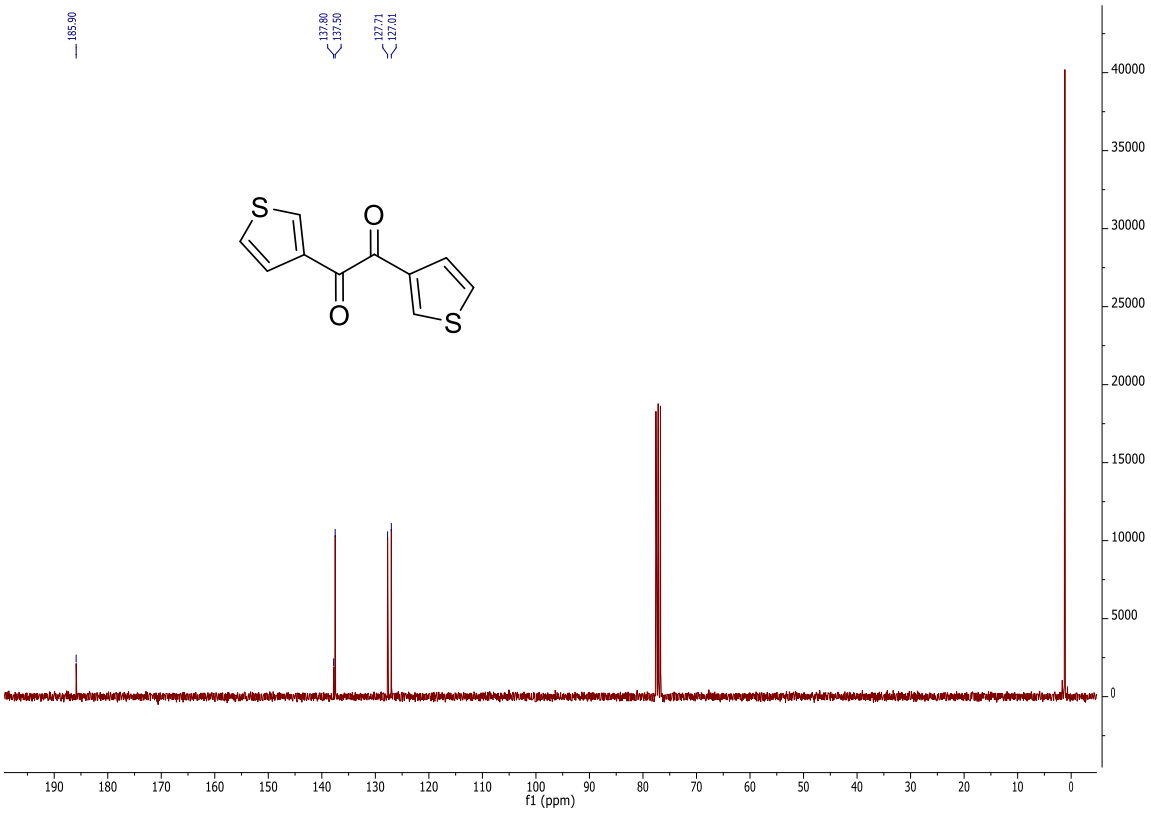

^{13}C NMR spectrum in $CDCl_3$.

202b

^{1}H NMR spectrum in $CDCl_3$.

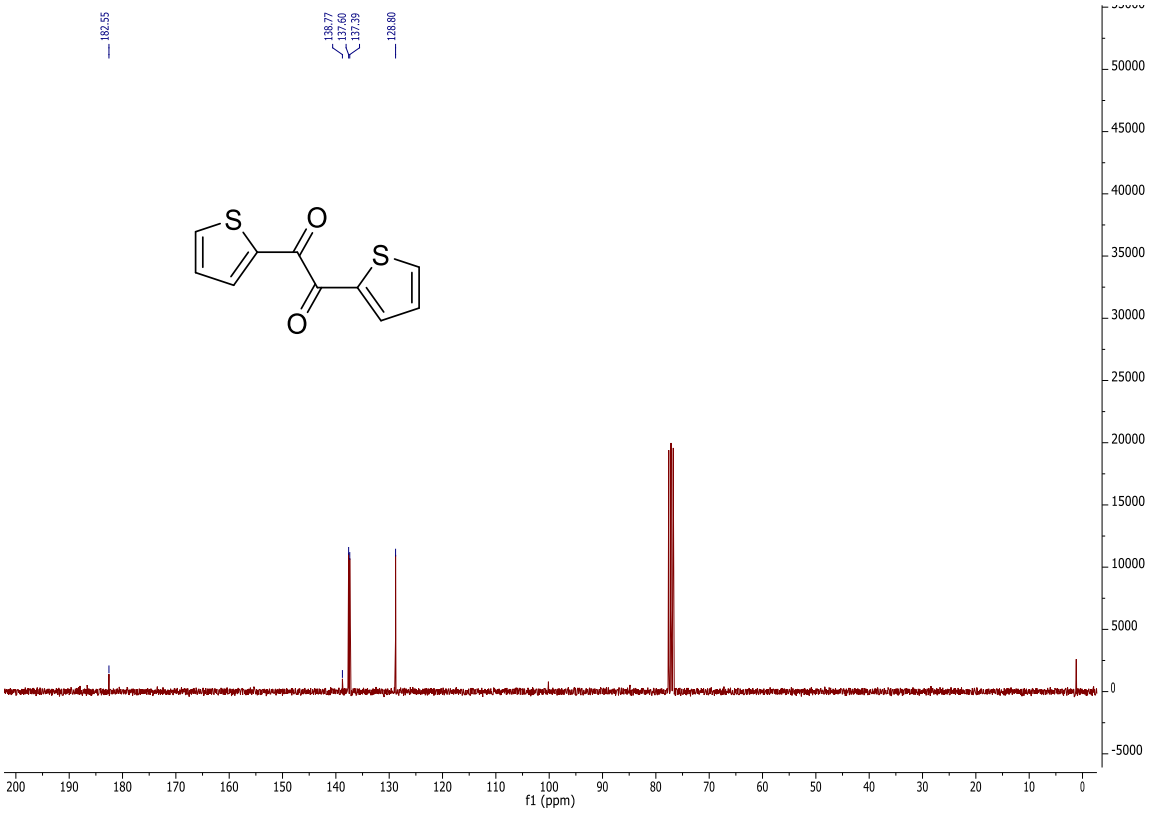

^{13}C NMR spectrum in $CDCl_3$.

203b

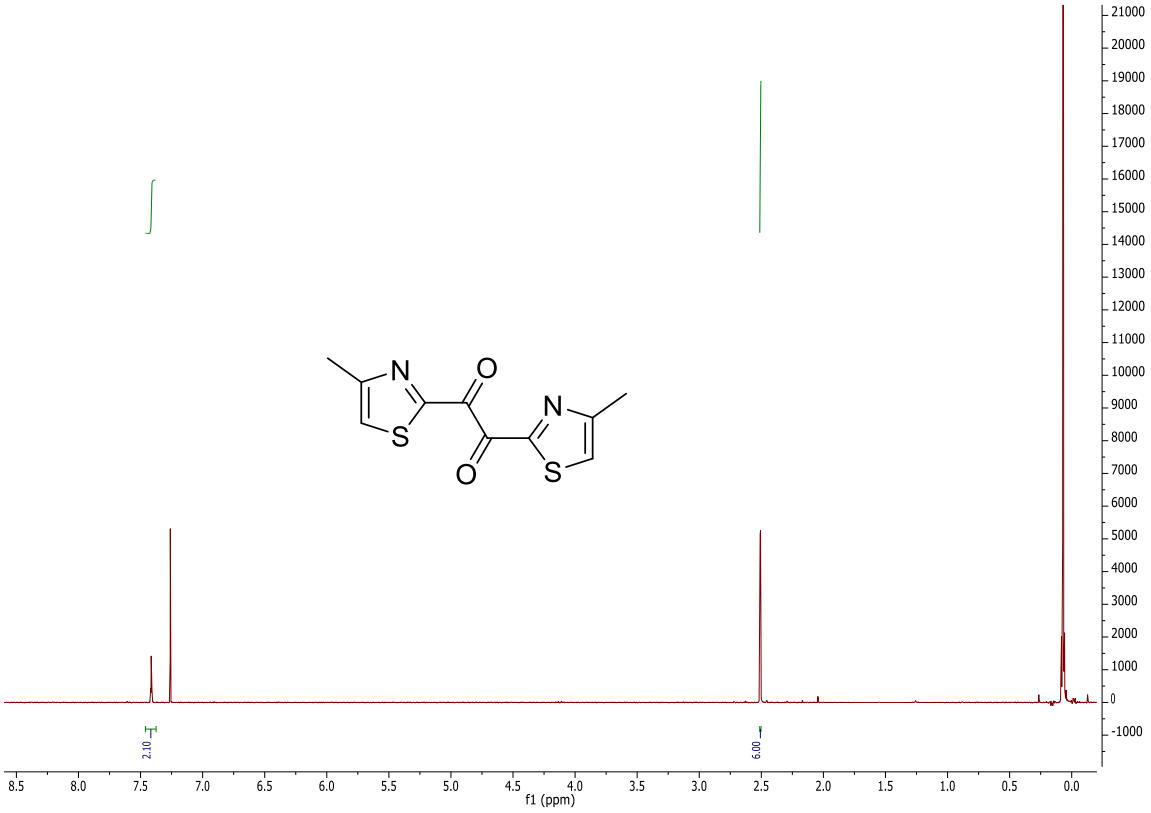

^{1}H NMR spectrum in $CDCl_3$.

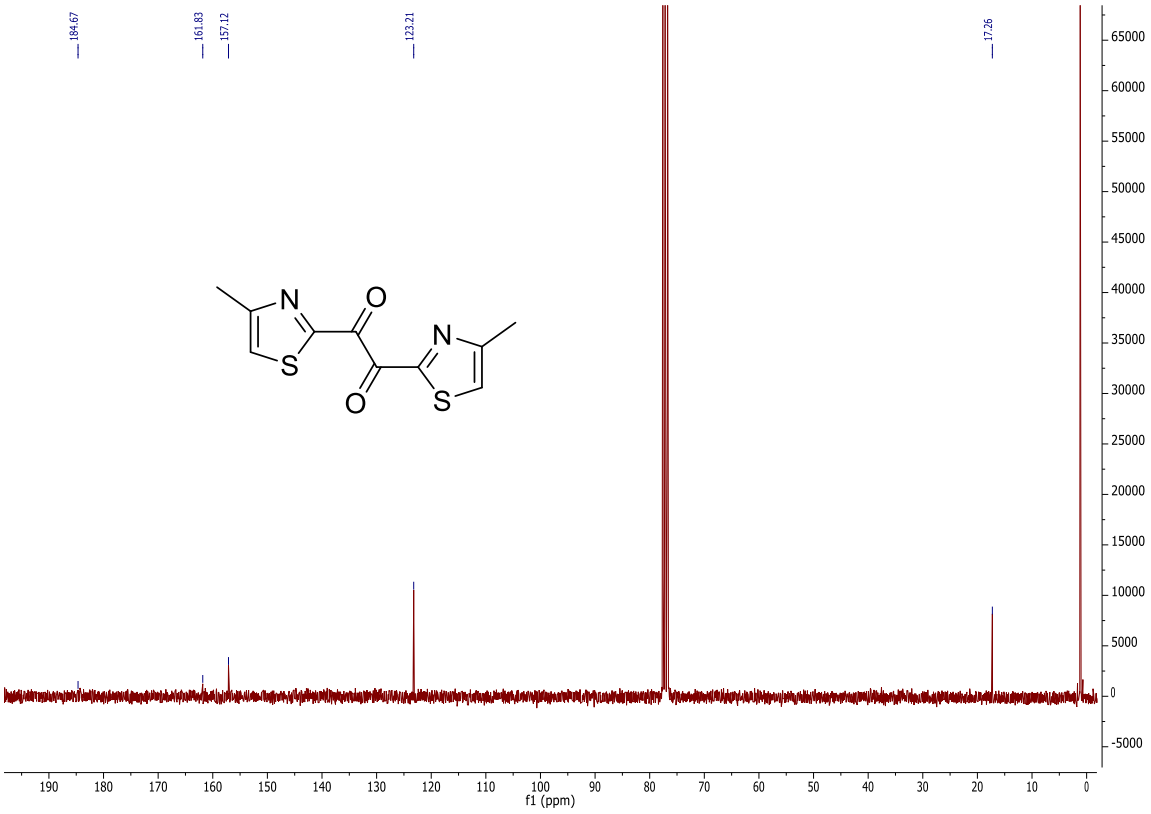

^{13}C NMR spectrum in $CDCl_3$.

204b

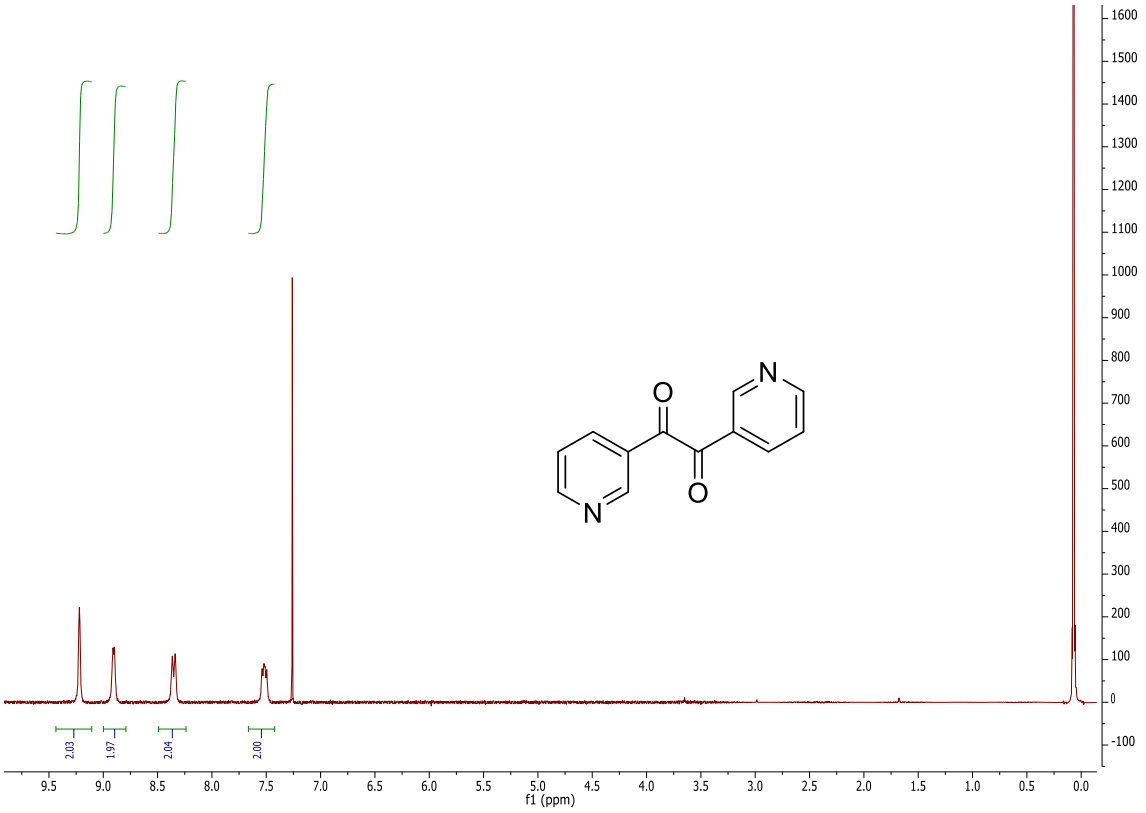

^{1}H NMR spectrum in $CDCl_3$.

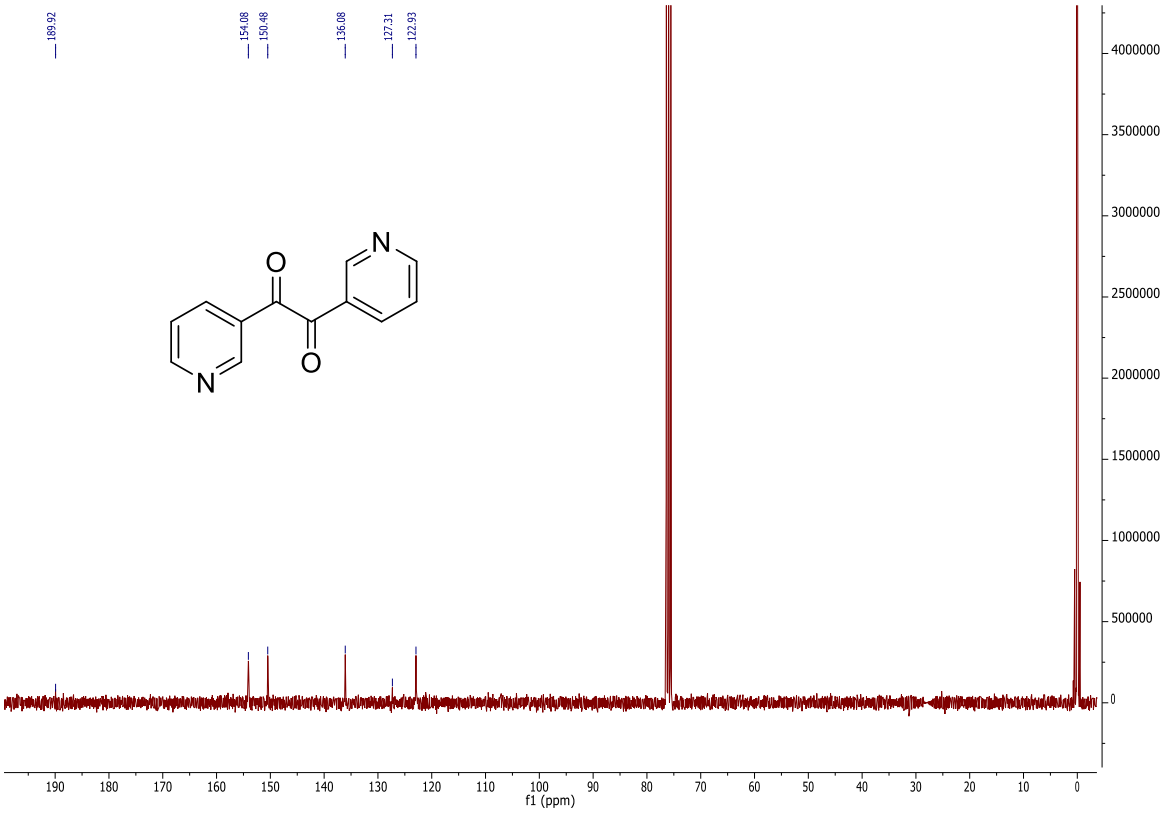

^{13}C NMR spectrum in $CDCl_3$.

205b

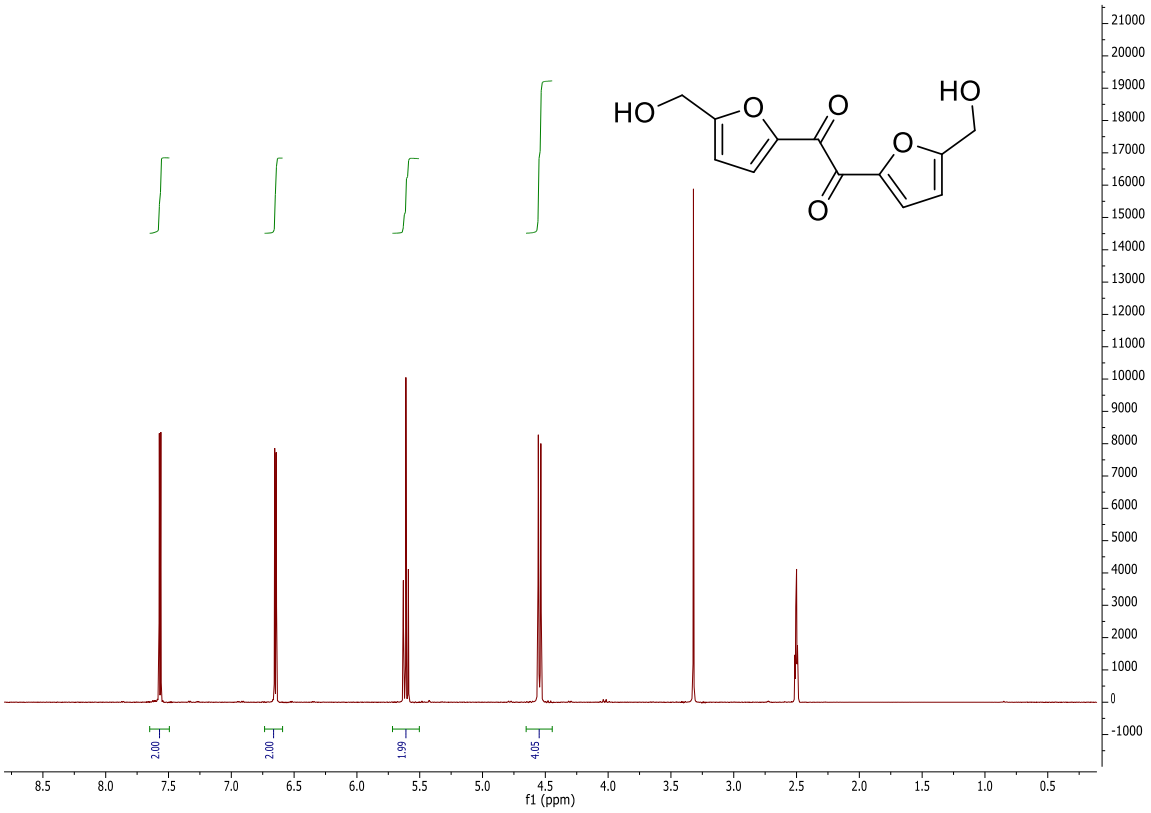

^{1}H NMR spectrum in DMSO-d_6.

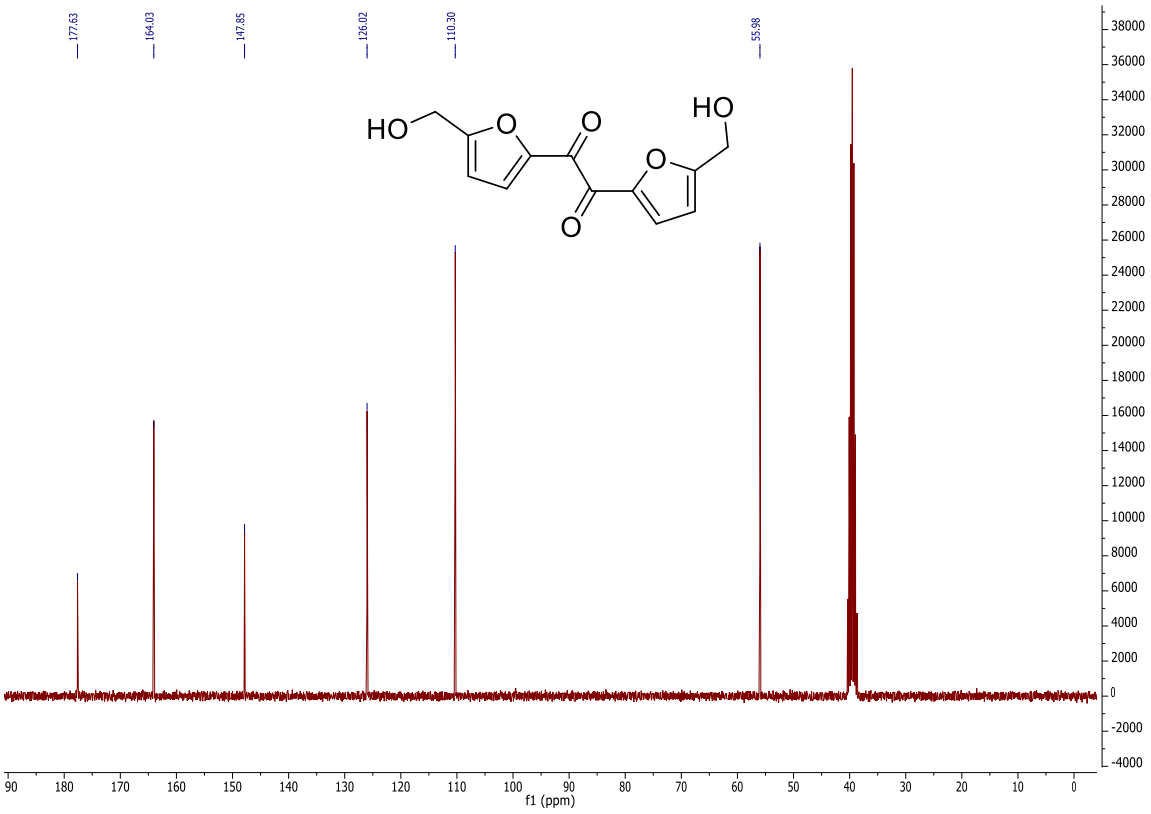

^{13}C NMR spectrum in DMSO-d_6.

206b

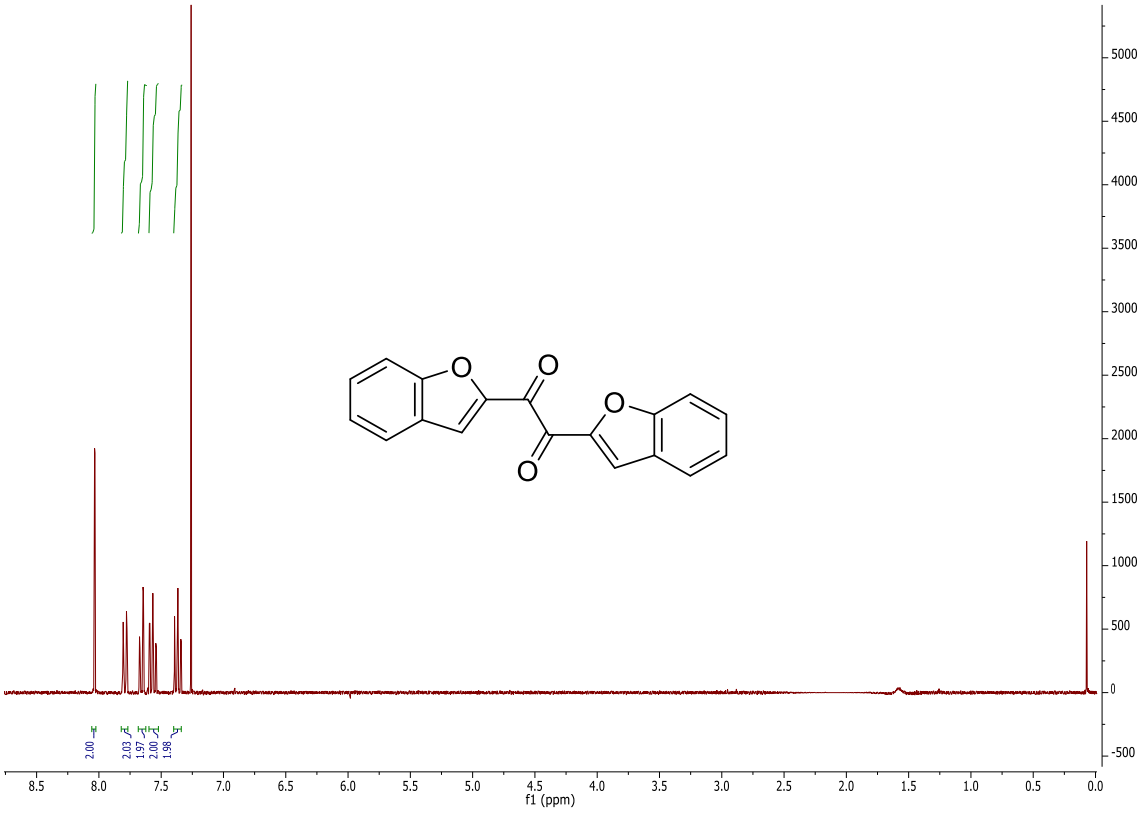

^{1}H spectrum in $CDCl_3$.

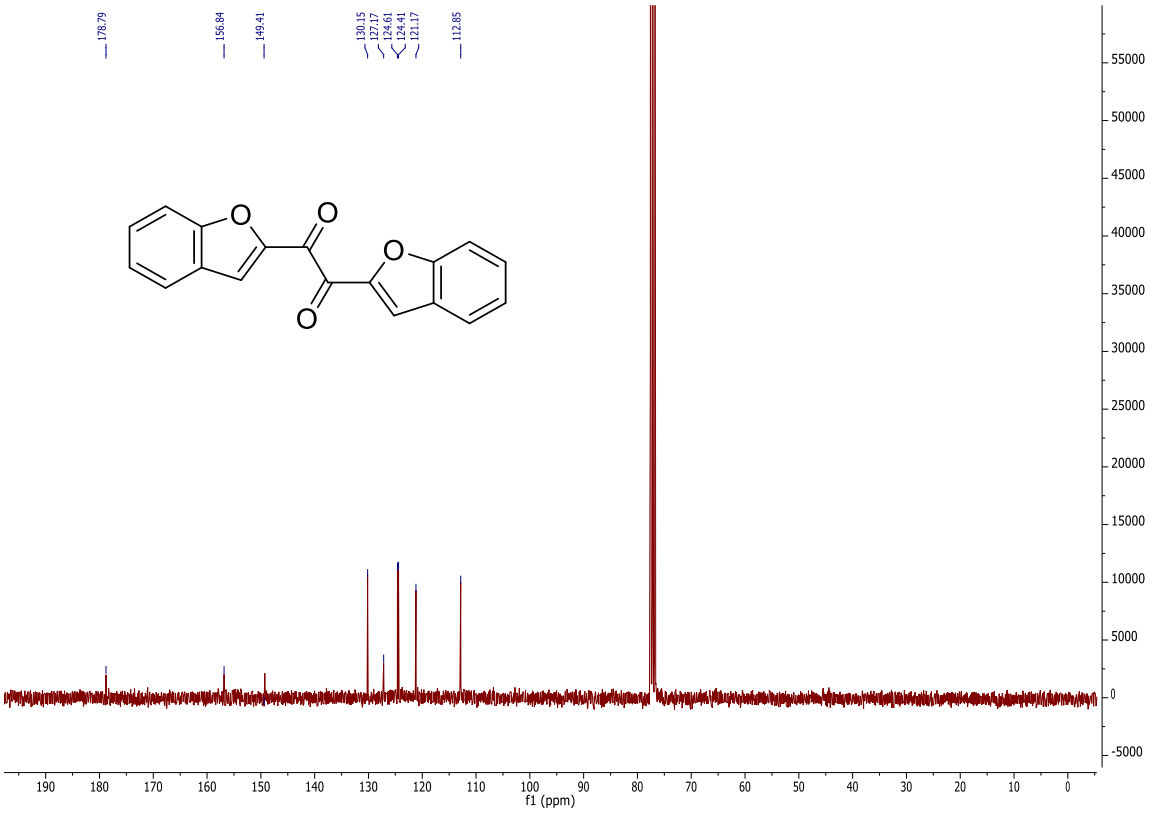

^{13}C NMR spectrum in $CDCl_3$.

207b

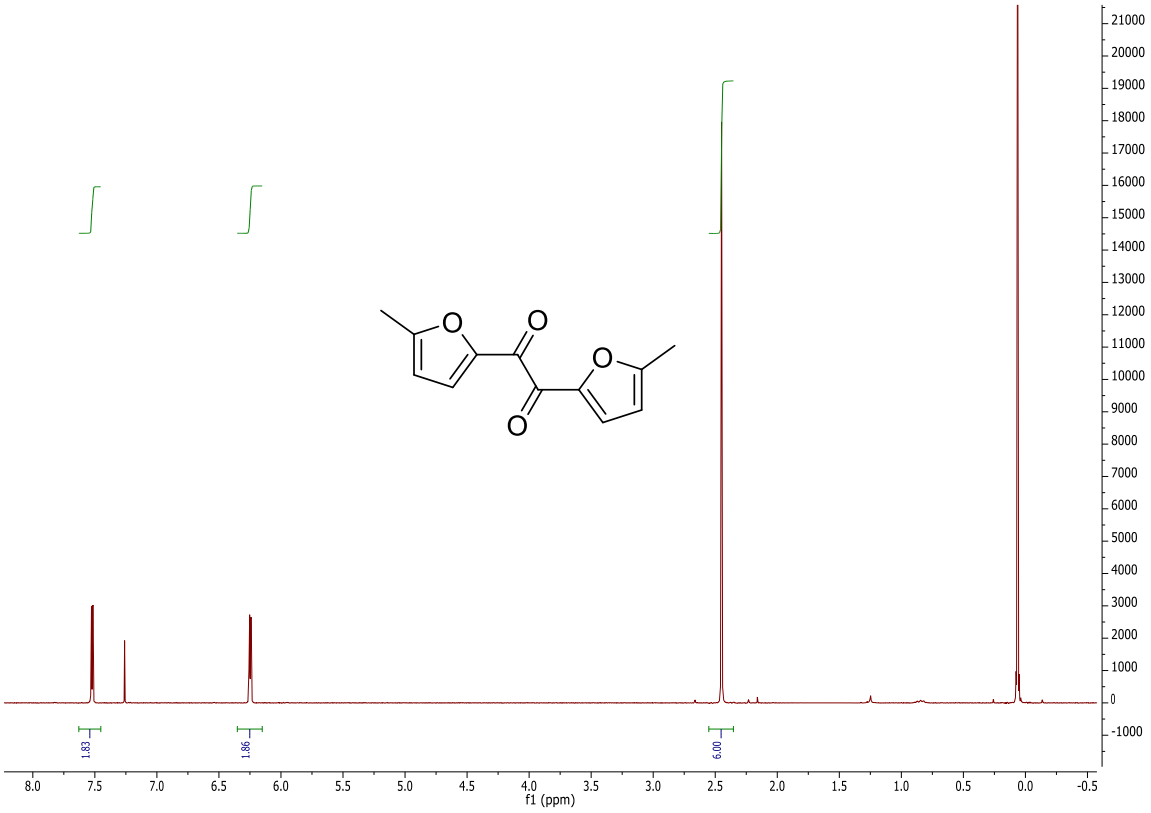

^{1}H spectrum in $CDCl_3$.

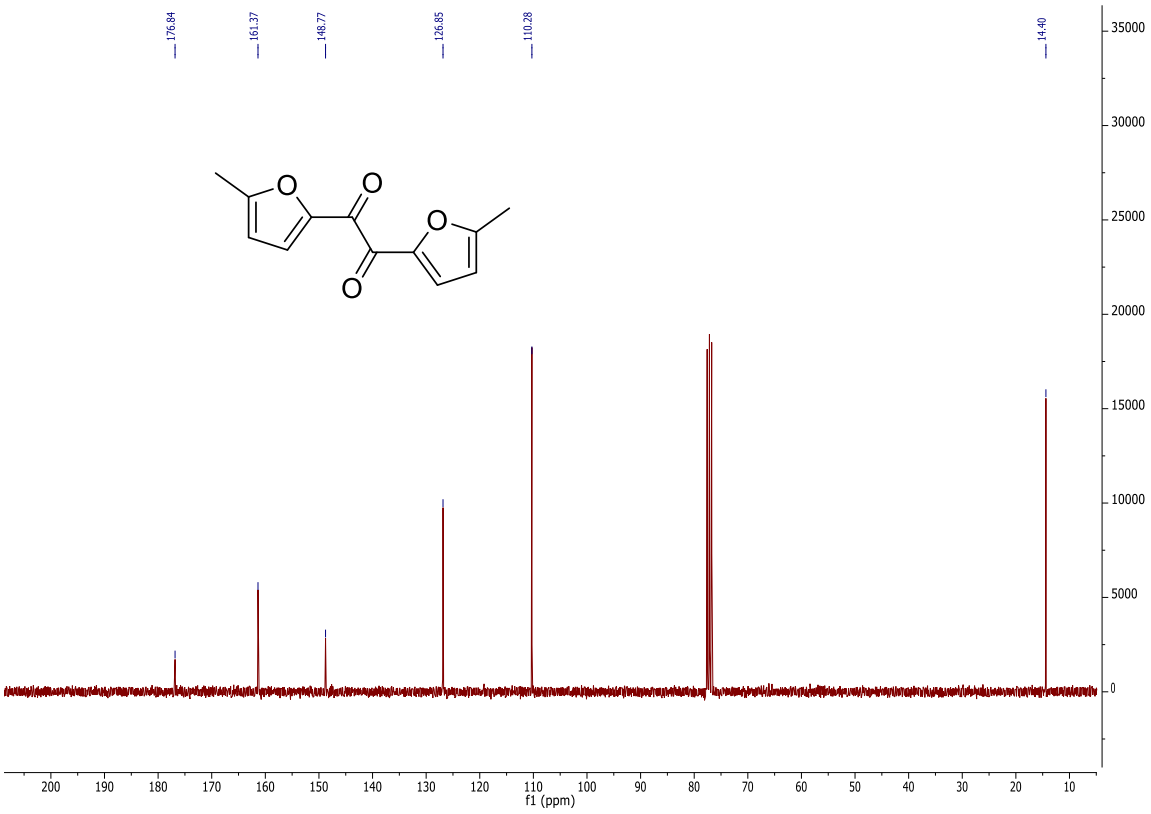

^{13}C NMR spectrum in $CDCl_3$.

208b

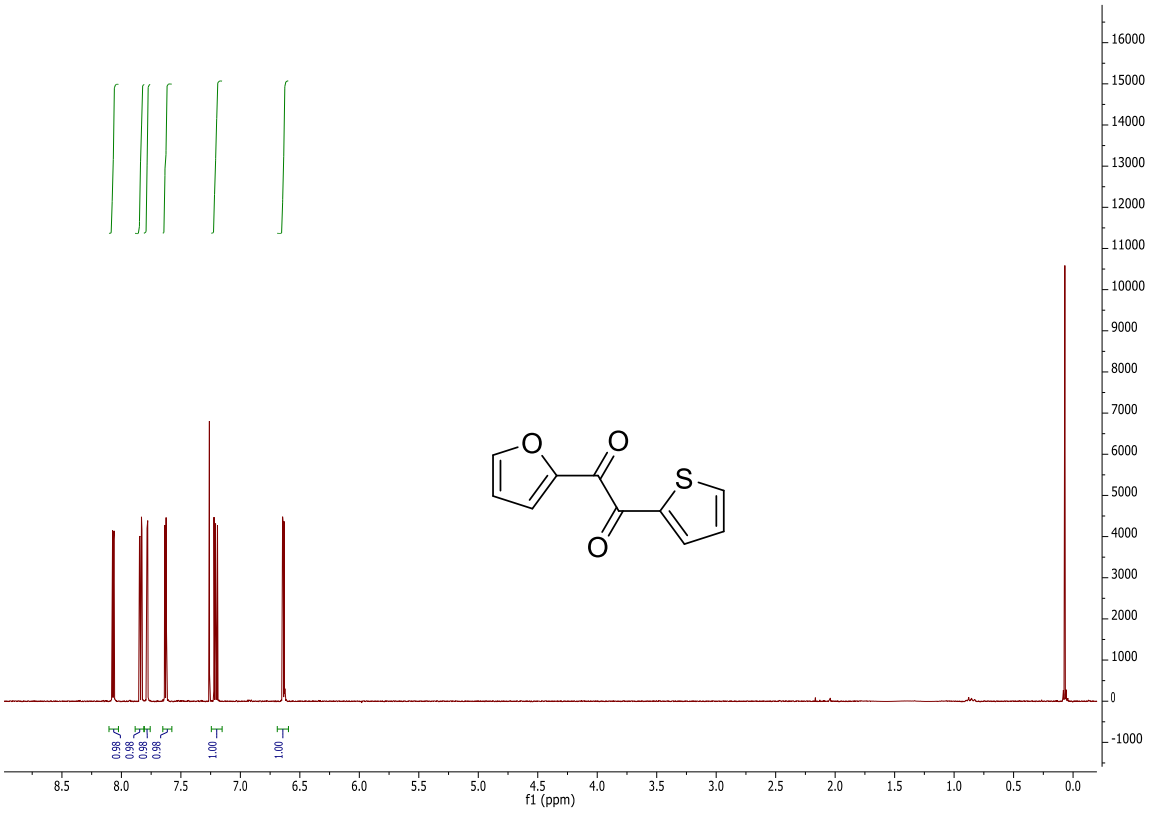

^{1}H spectrum in $CDCl_3$.

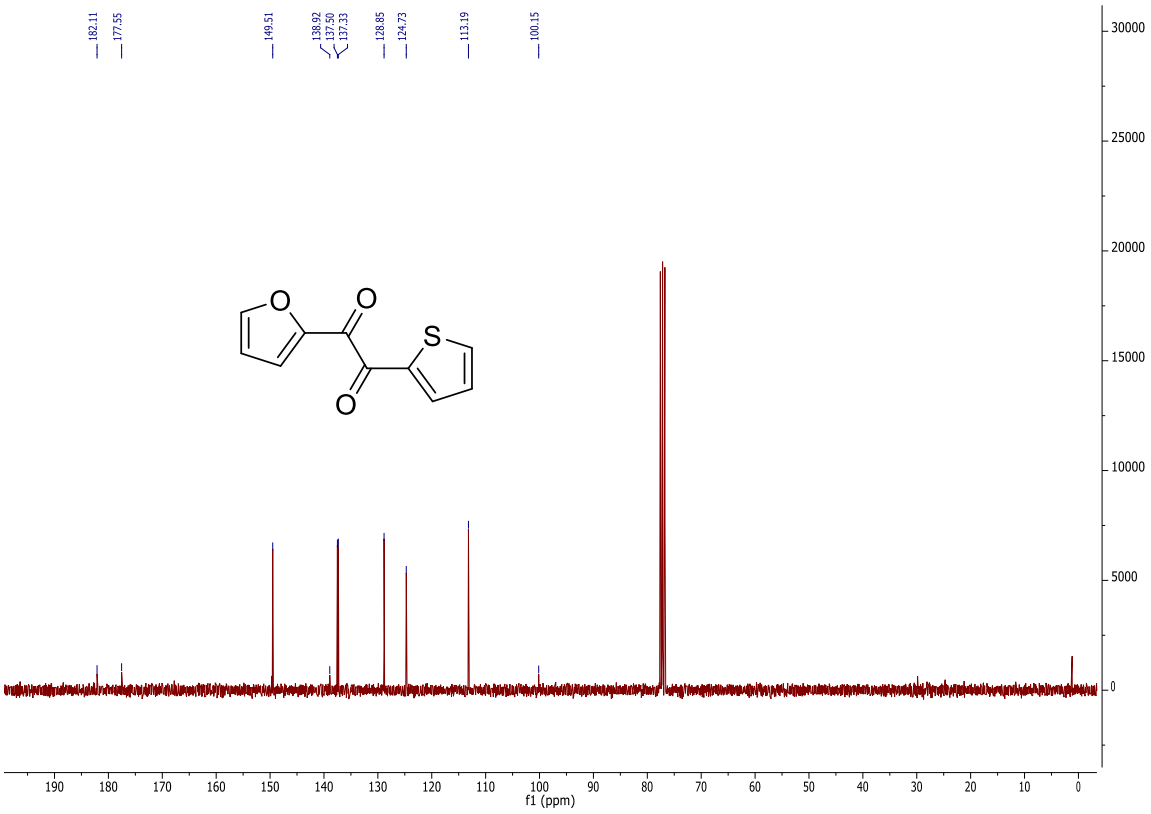

^{13}C NMR spectrum in $CDCl_3$.

209b

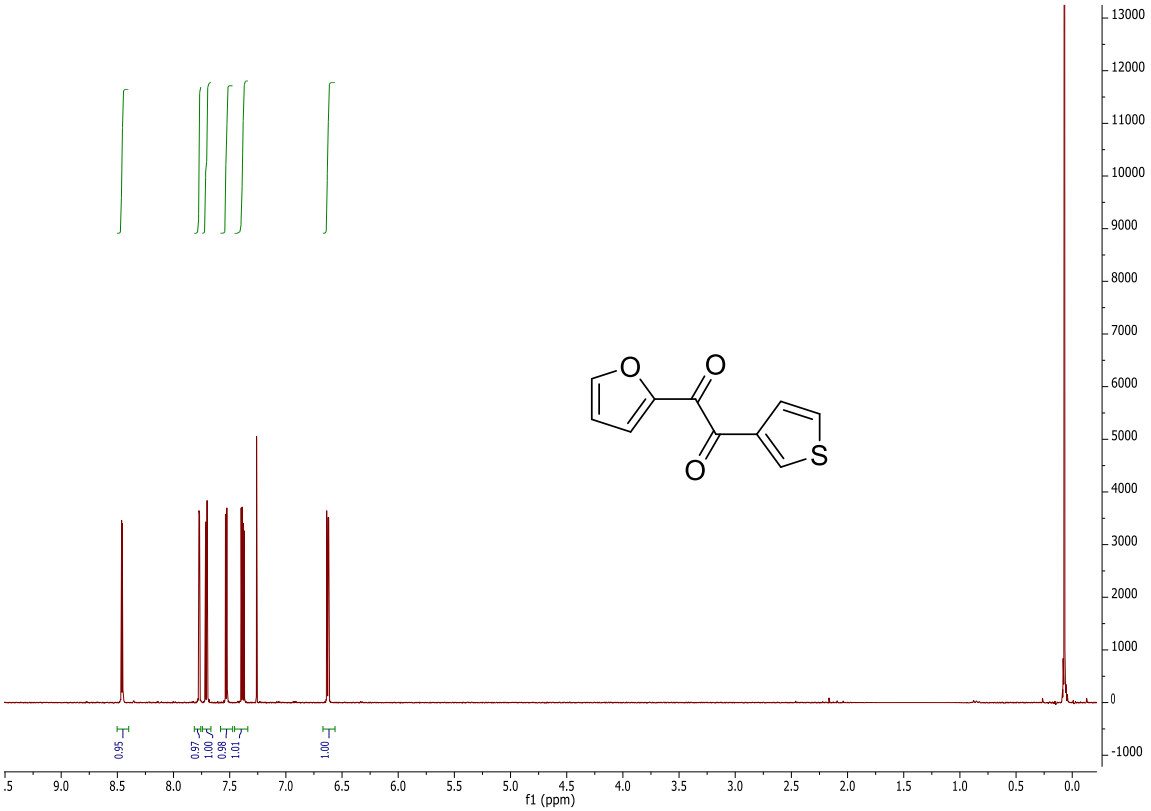

^{1}H spectrum in $CDCl_3$.

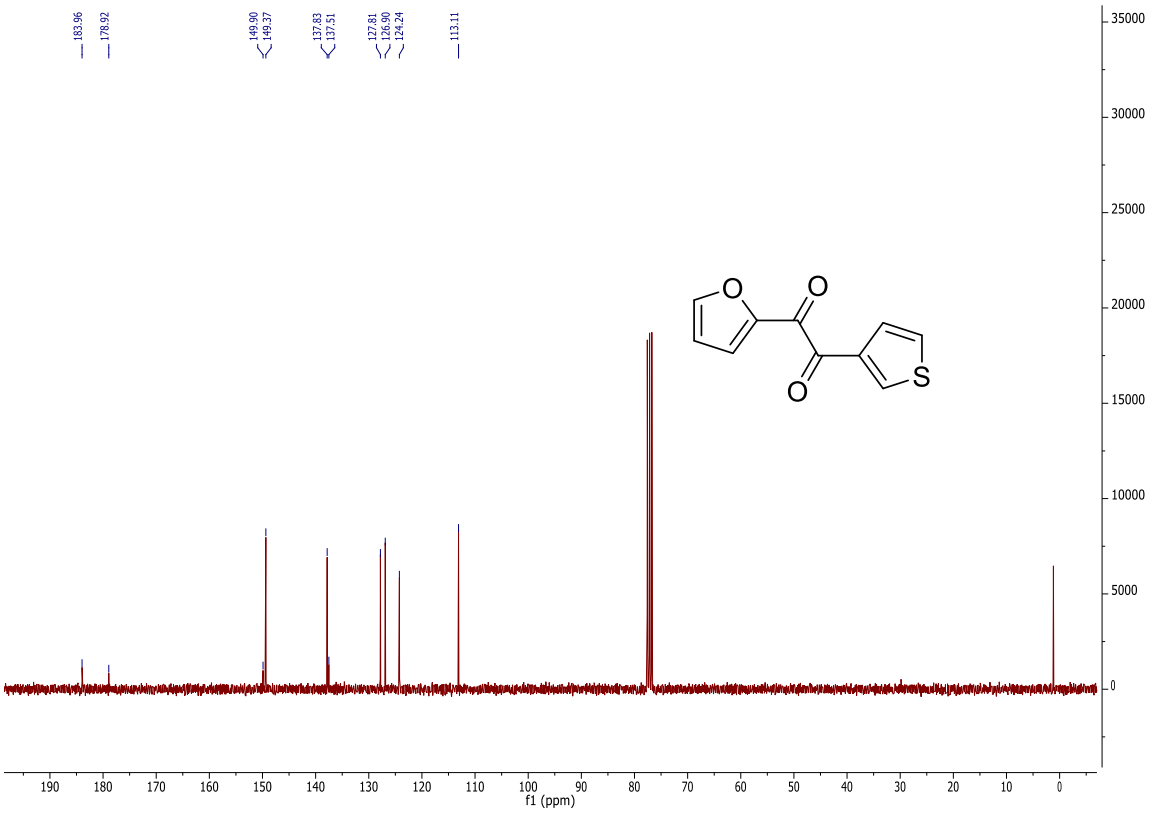

^{13}C NMR spectrum in $CDCl_3$.

210b

^{1}H spectrum in $CDCl_3$.

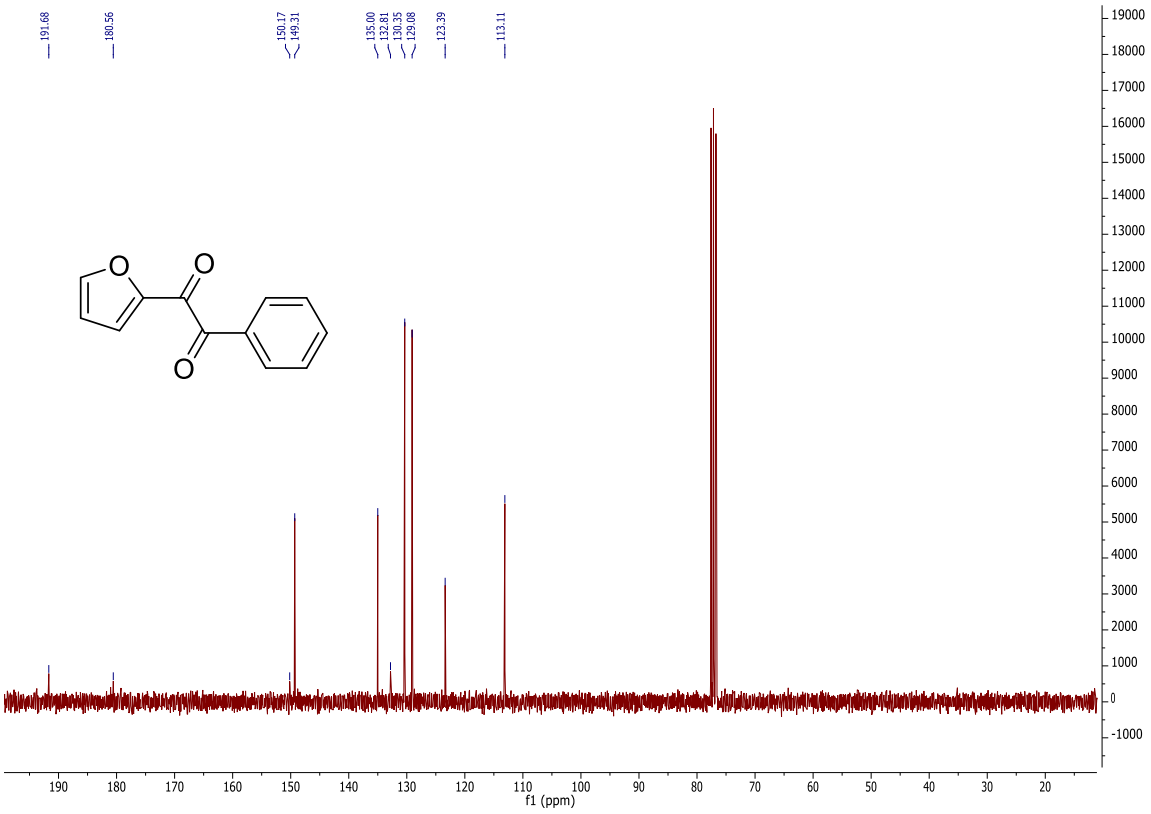

^{13}C NMR spectrum in $CDCl_3$.

211b

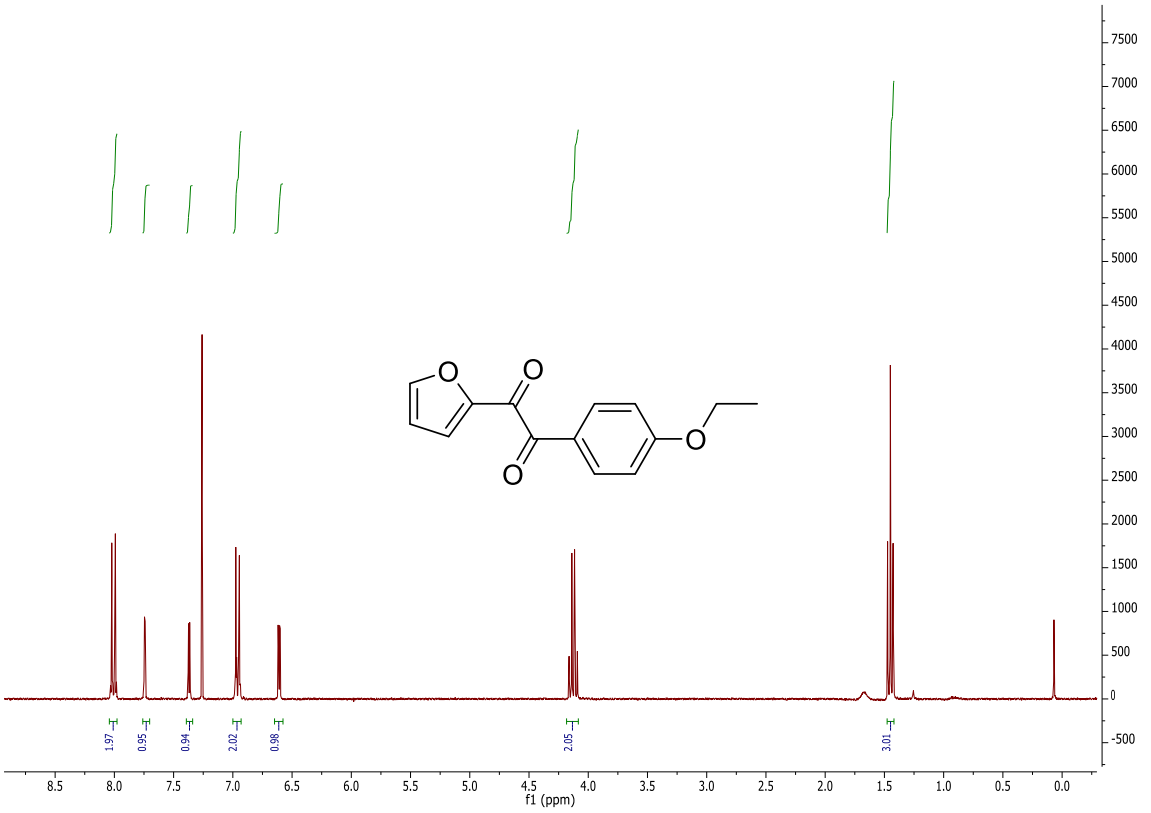

^{1}H spectrum in $CDCl_3$.

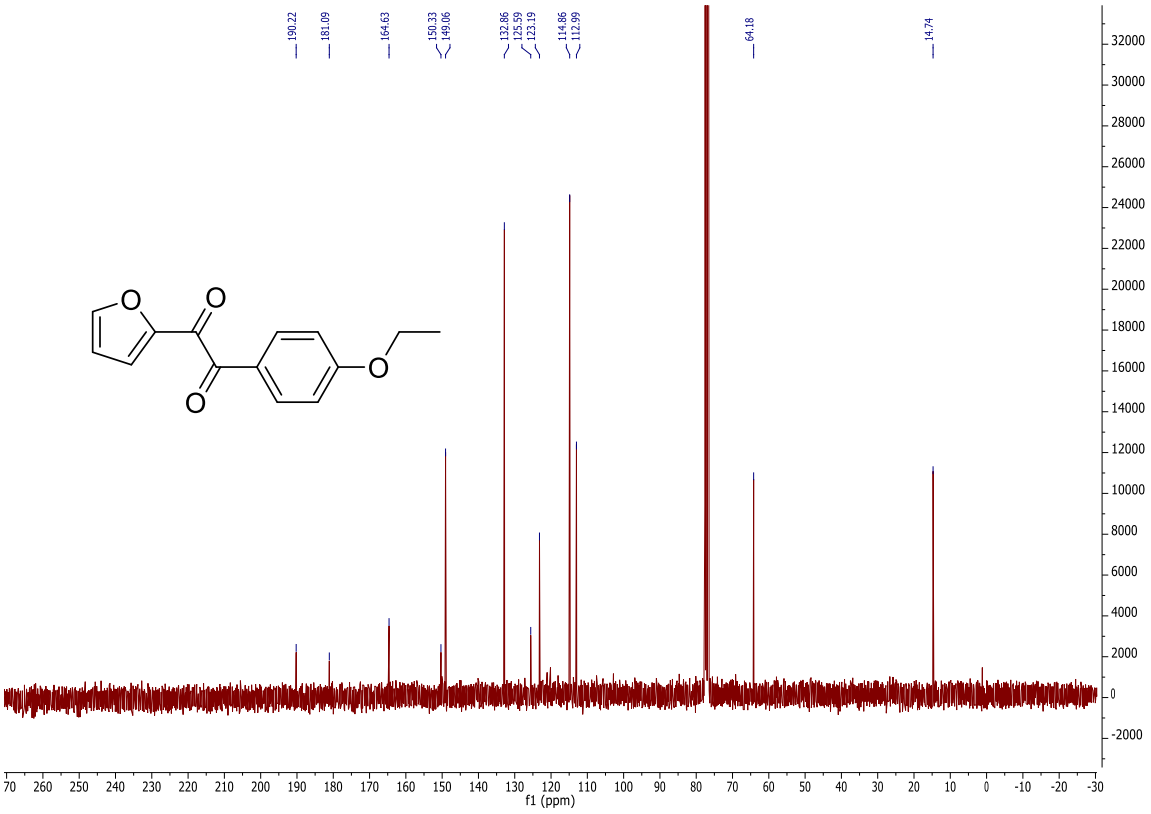

^{13}C NMR spectrum in $CDCl_3$.

212b

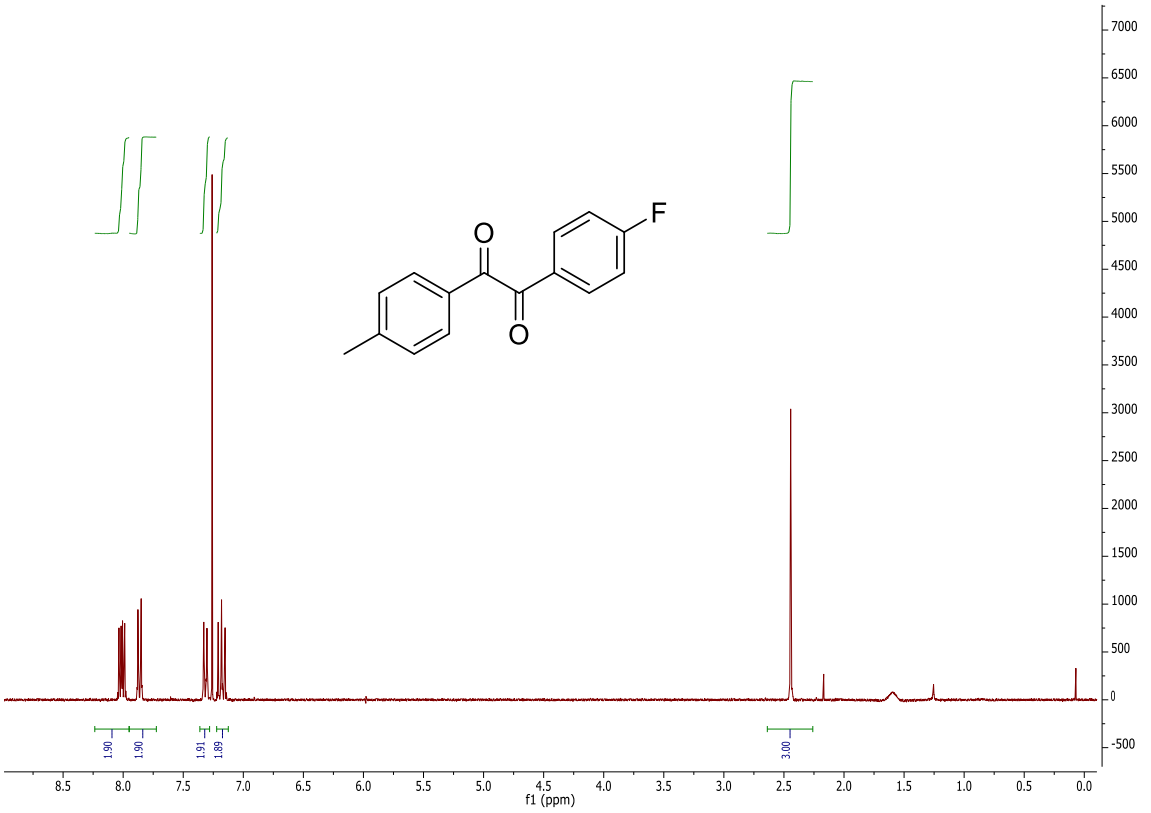

^{1}H spectrum in $CDCl_3$.

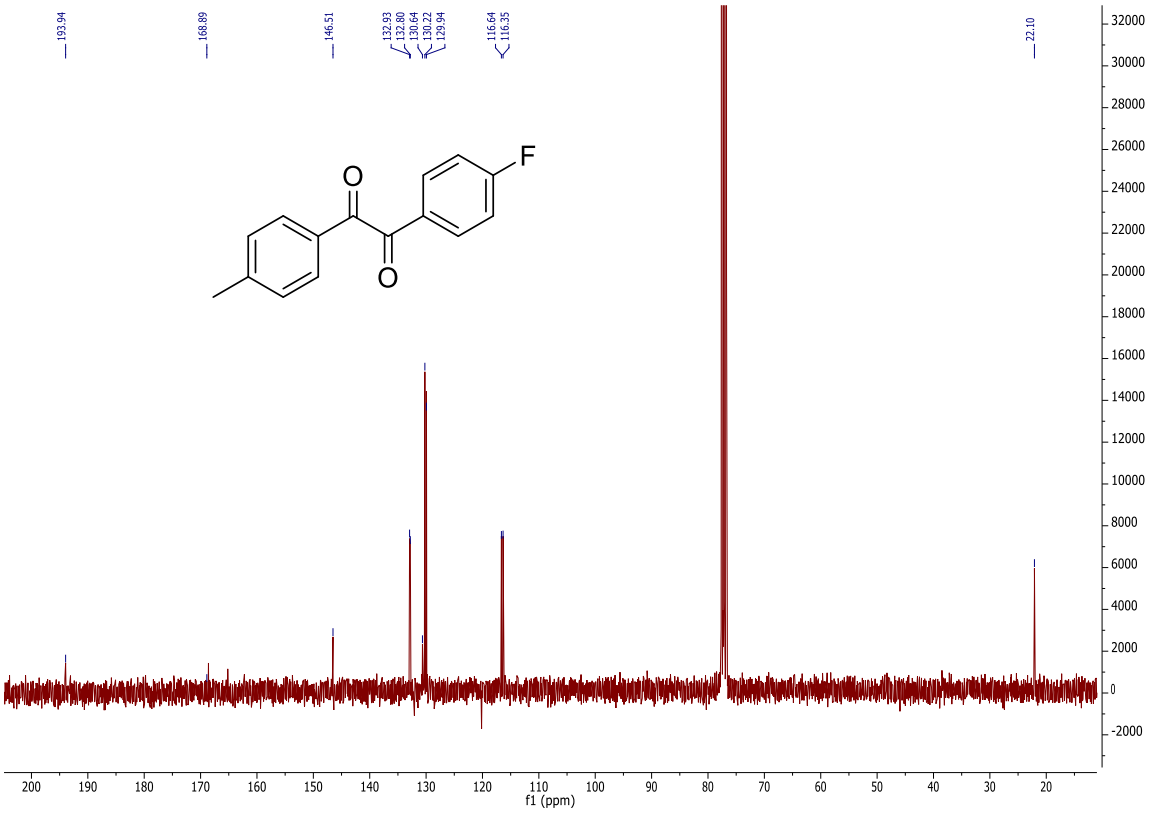

^{13}C NMR spectrum in $CDCl_3$.

213b

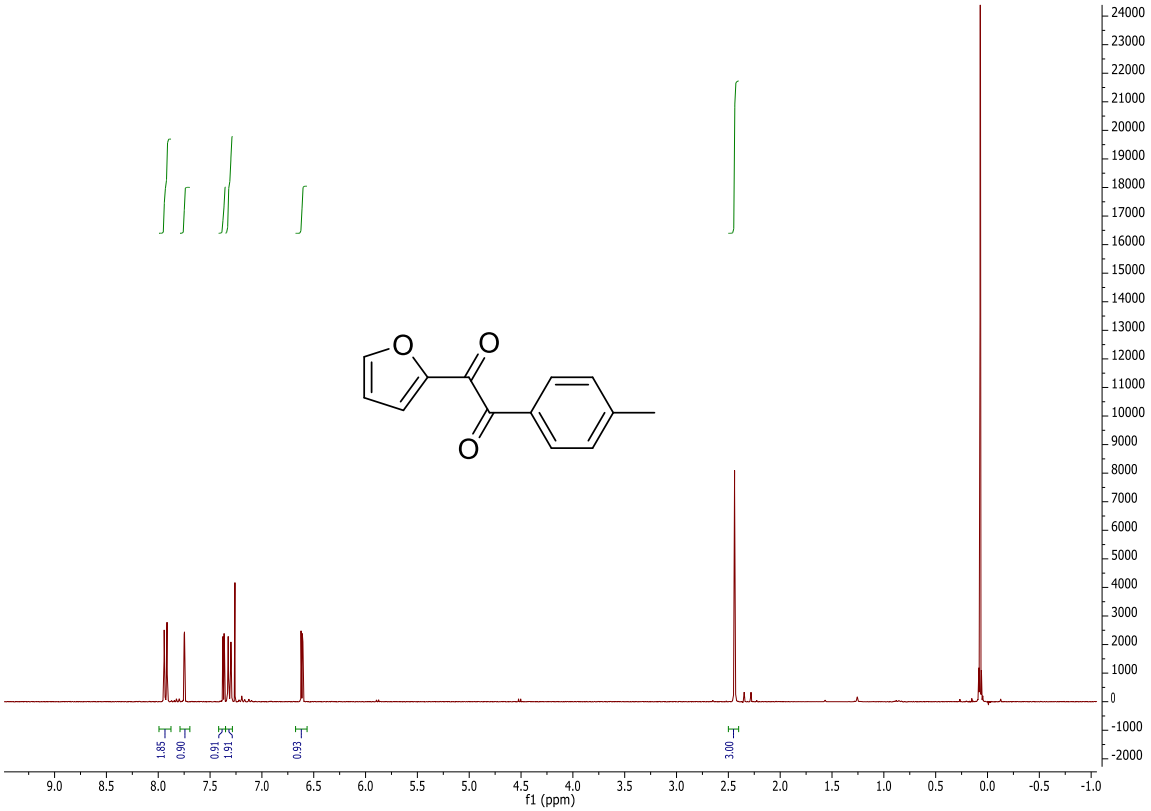

^{1}H spectrum in $CDCl_3$.

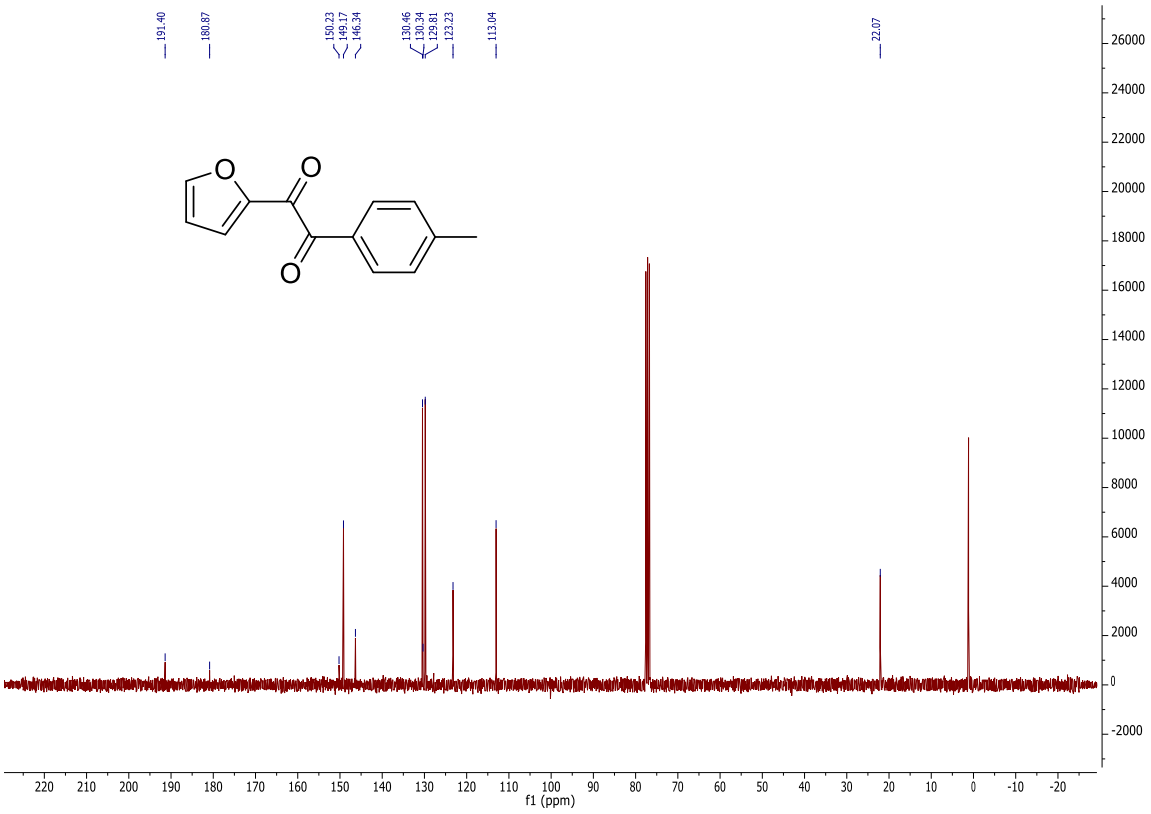

^{13}C NMR spectrum in $CDCl_3$.

214b

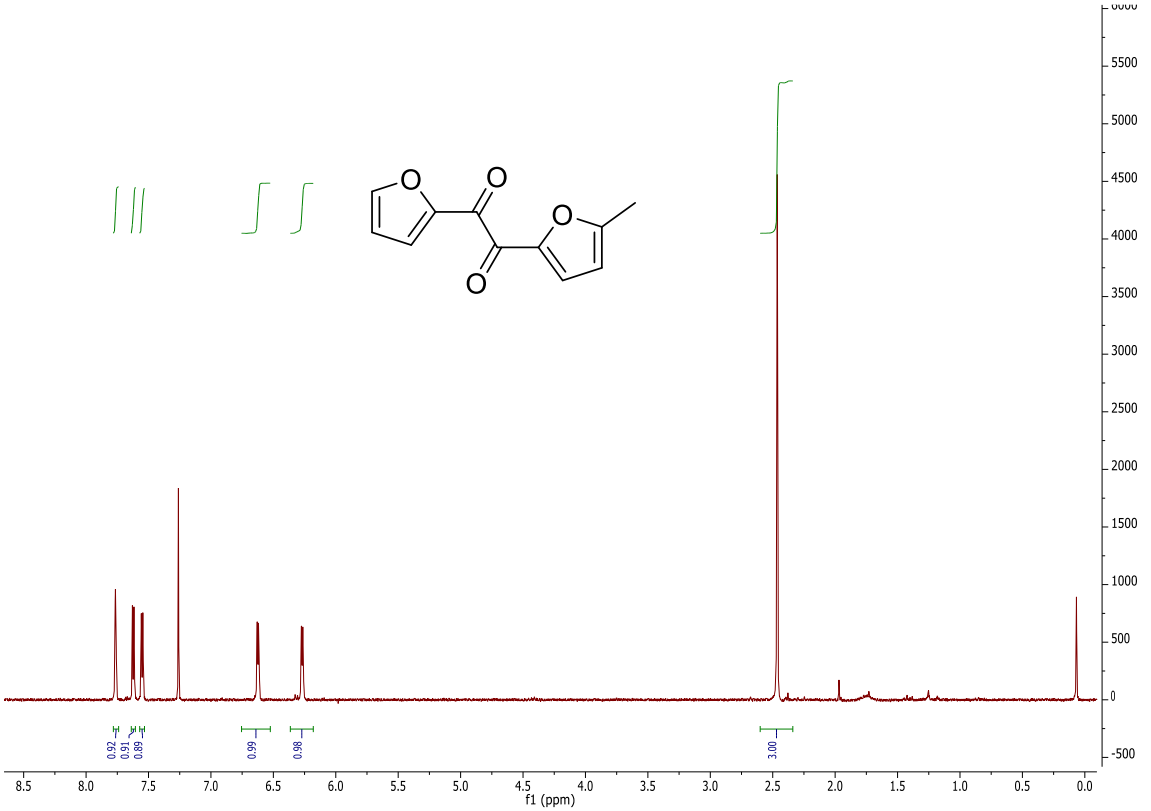

^{1}H spectrum in $CDCl_3$.

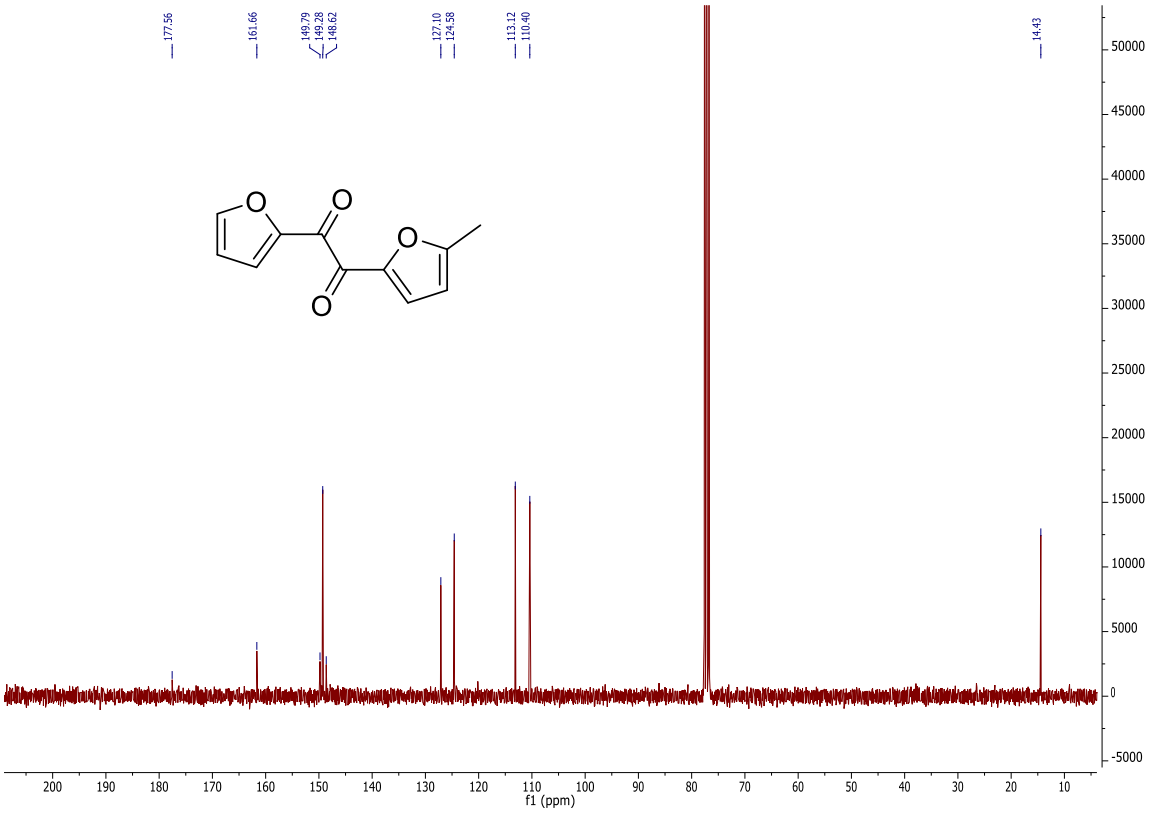

^{13}C NMR spectrum in $CDCl_3$.

215b

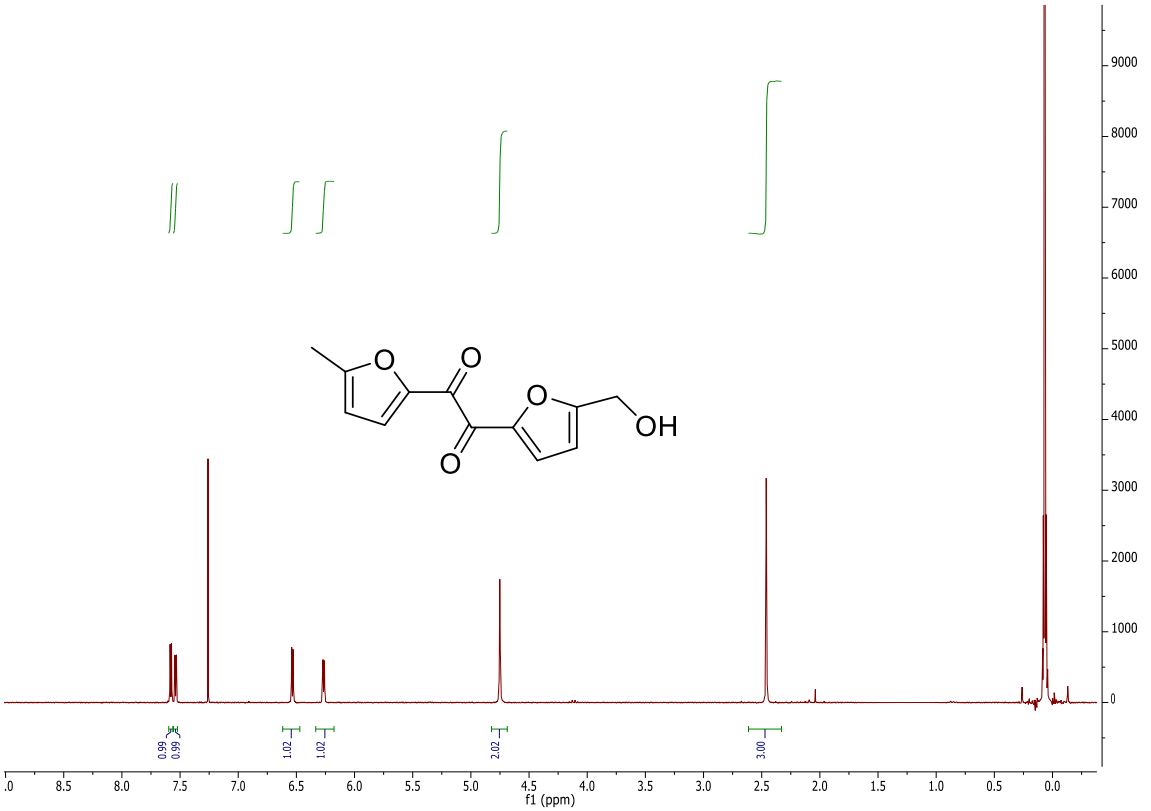

^{1}H spectrum in $CDCl_3$.

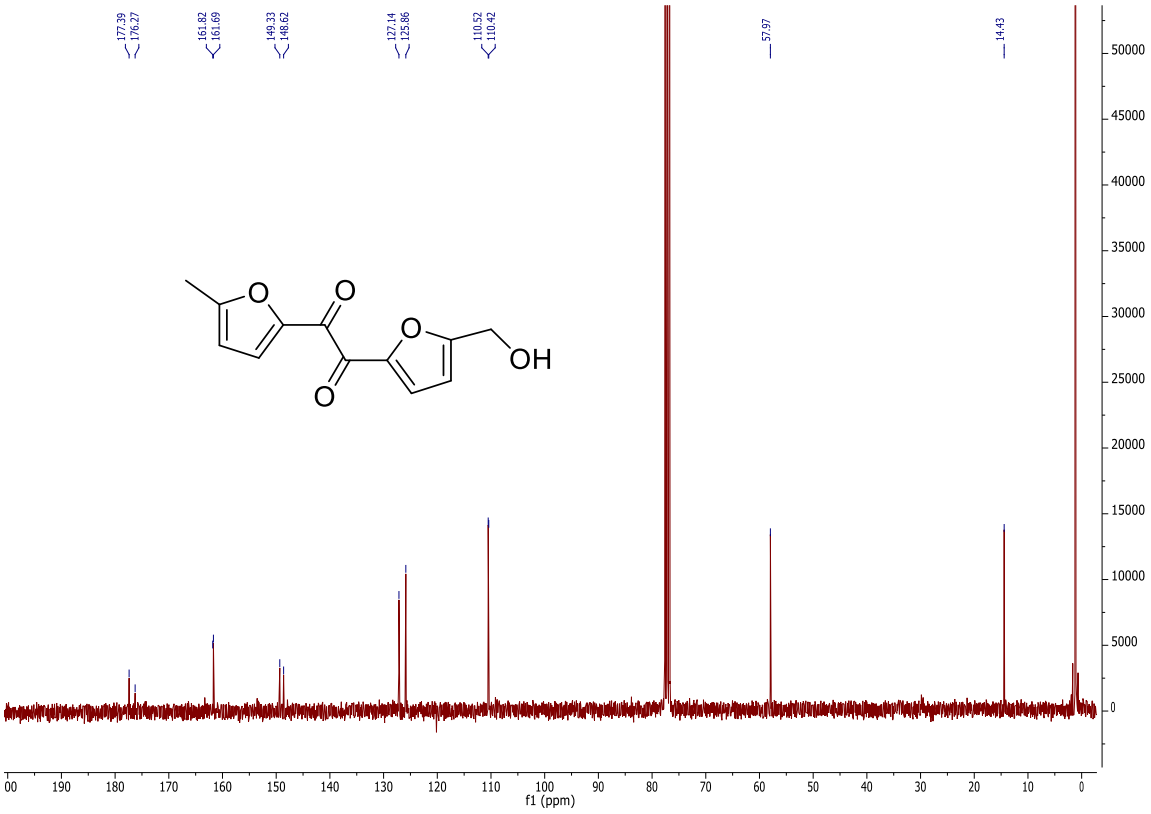

^{13}C NMR spectrum in $CDCl_3$.

216b

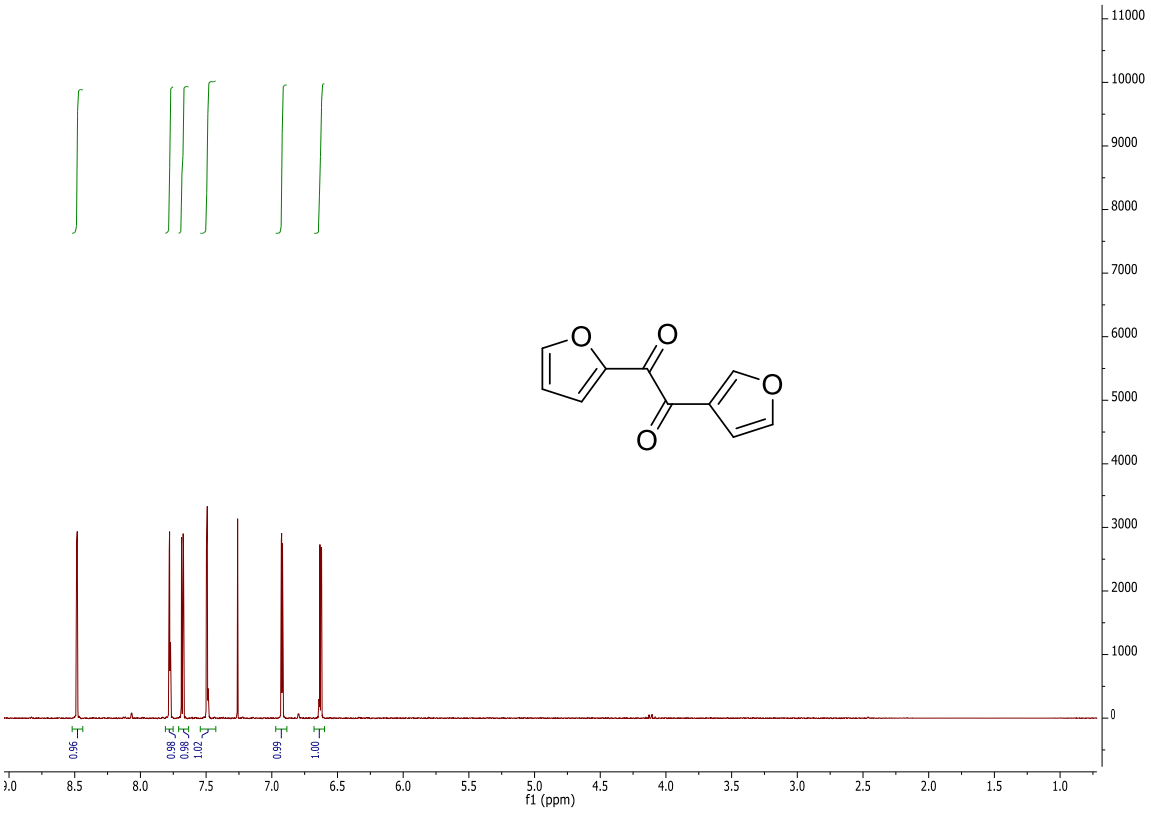

^{1}H spectrum in $CDCl_3$.

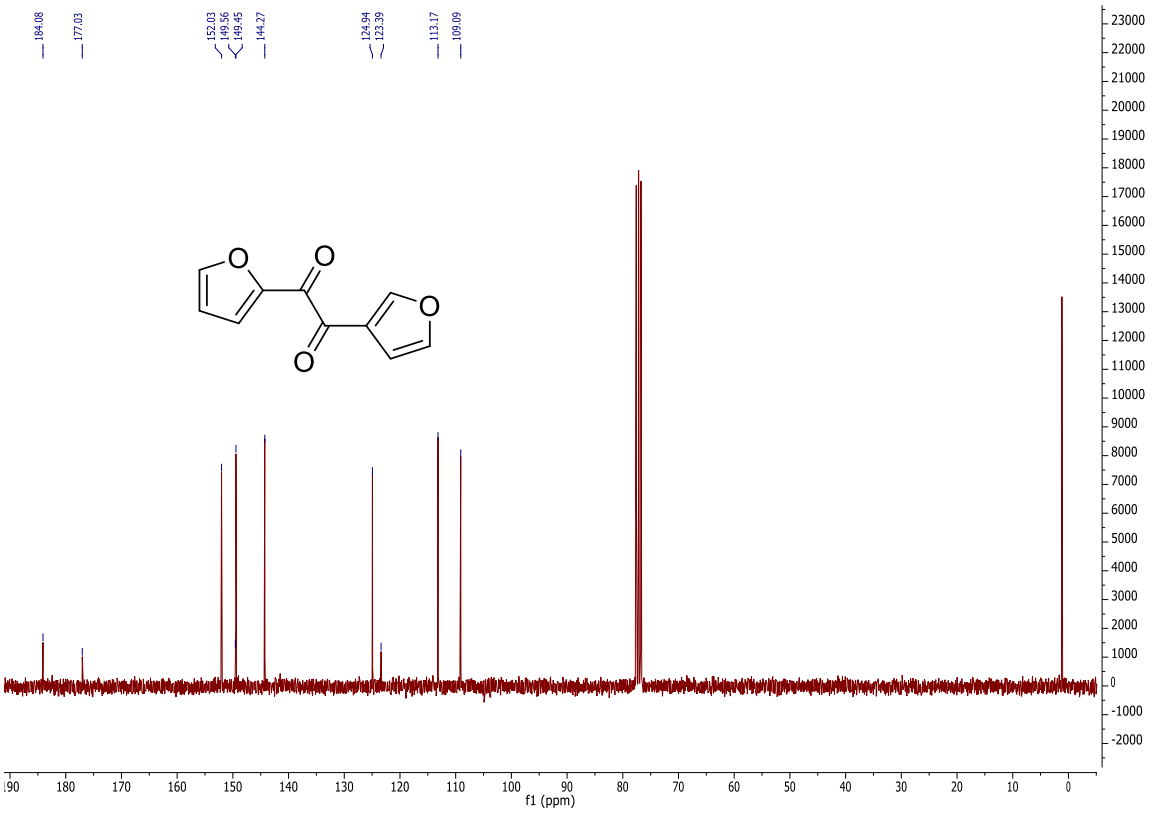

^{13}C NMR spectrum in $CDCl_3$.

217b

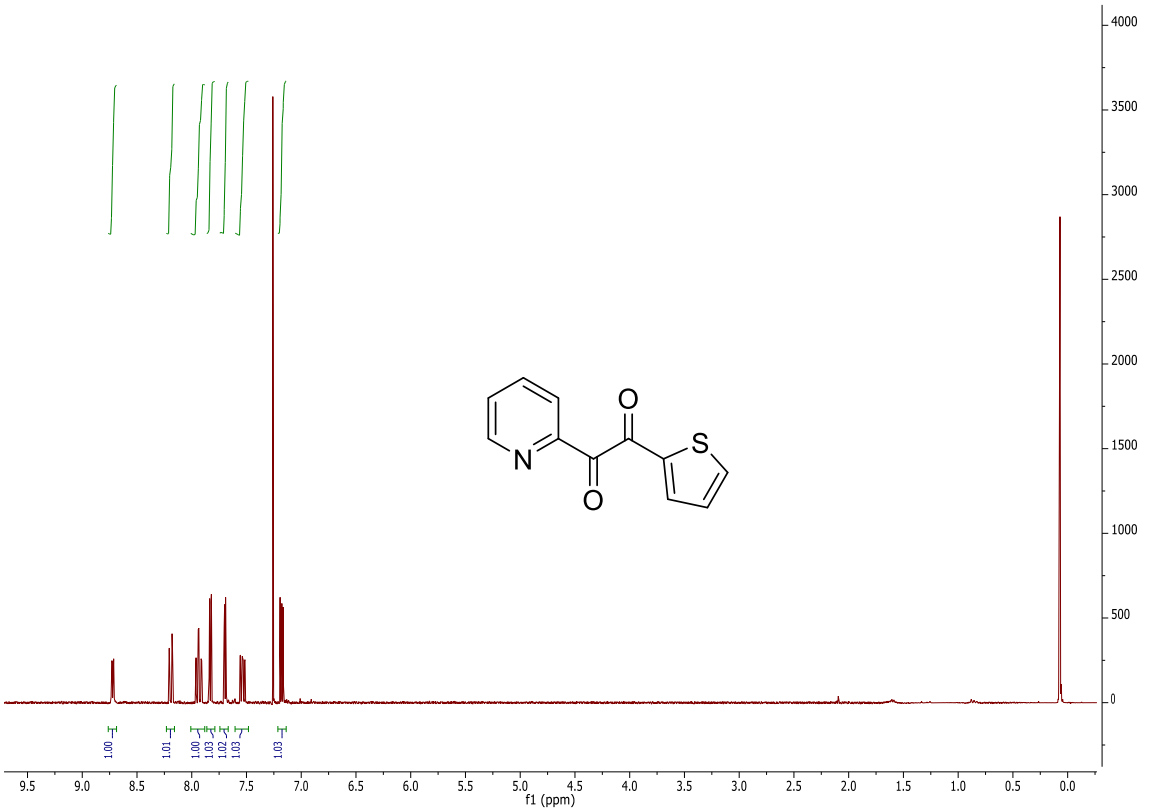

^{1}H spectrum in $CDCl_3$.

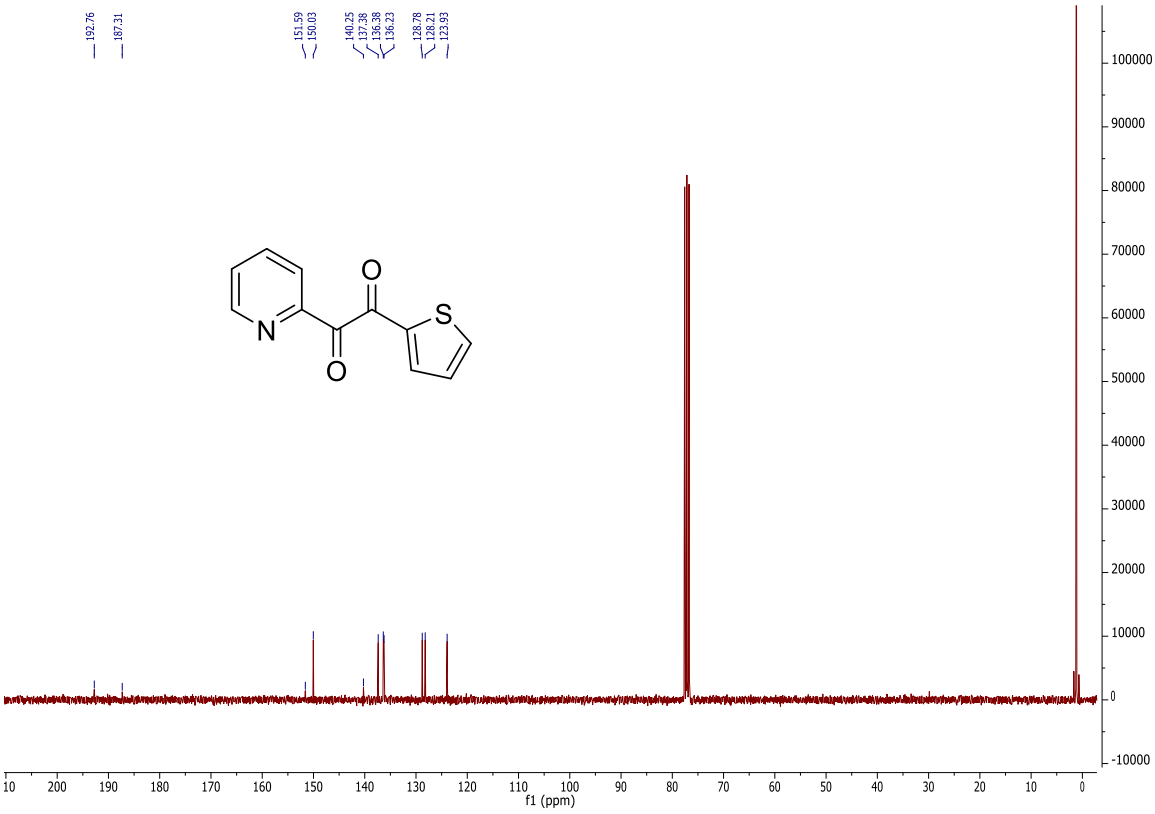

^{13}C NMR spectrum in $CDCl_3$.

218b

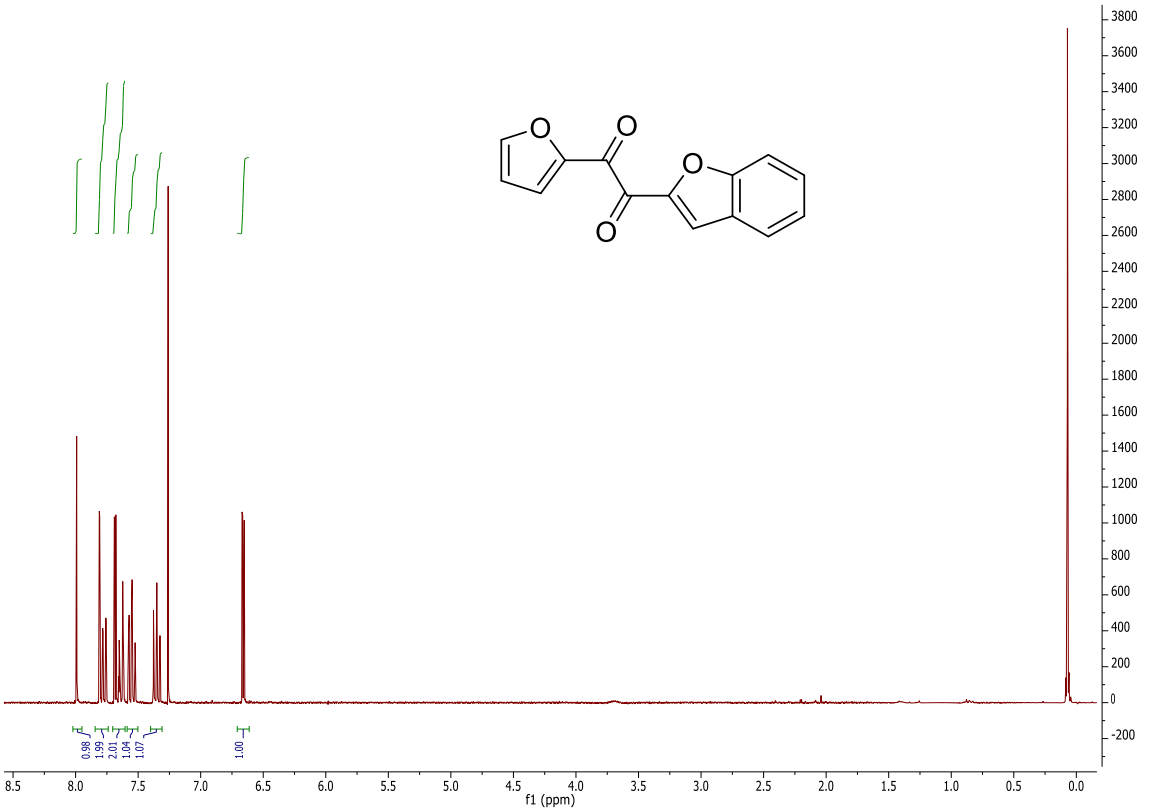

^{1}H spectrum in $CDCl_3$.

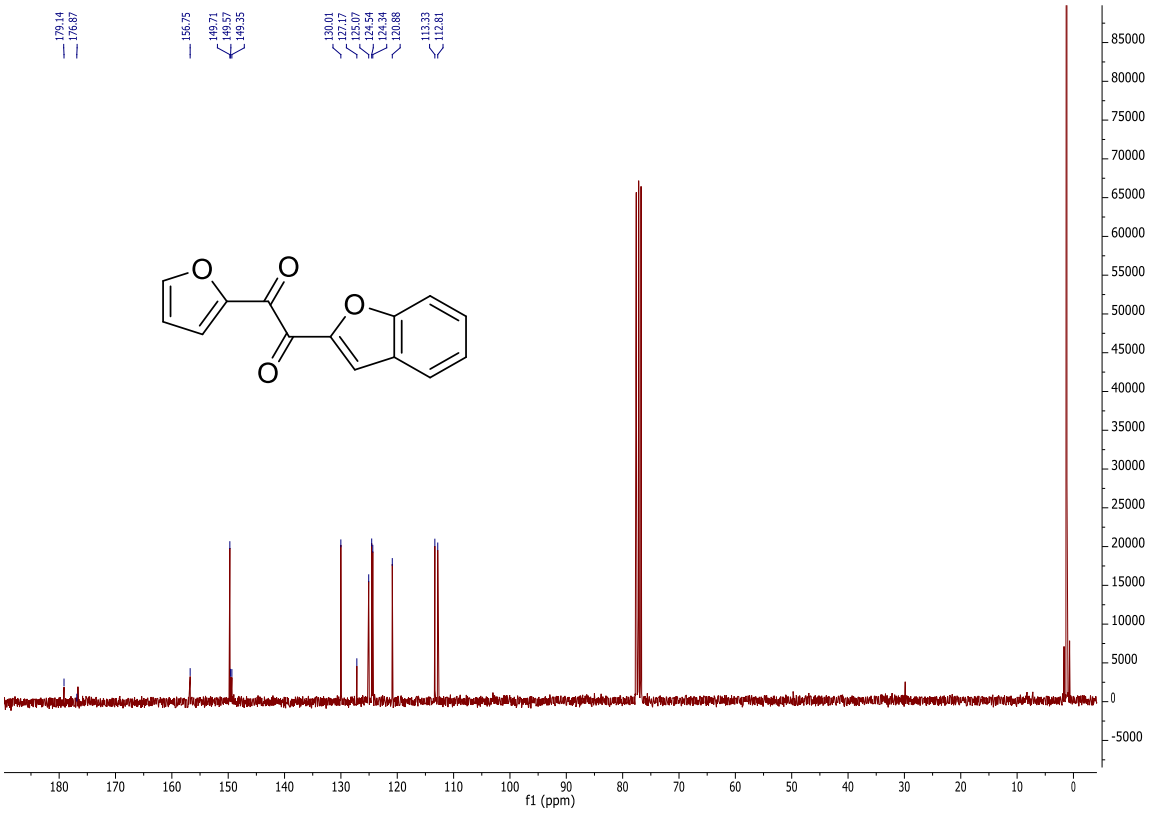

^{13}C NMR spectrum in $CDCl_3$.

219b

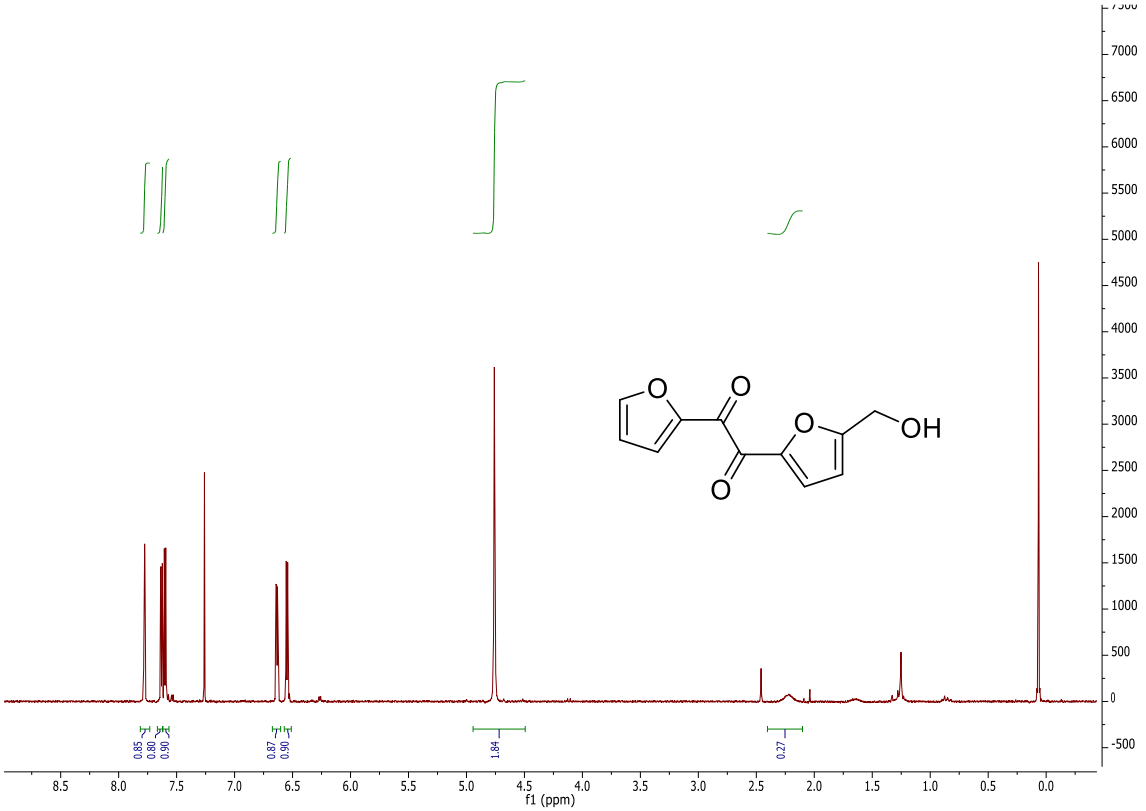

^{1}H spectrum in $CDCl_3$.

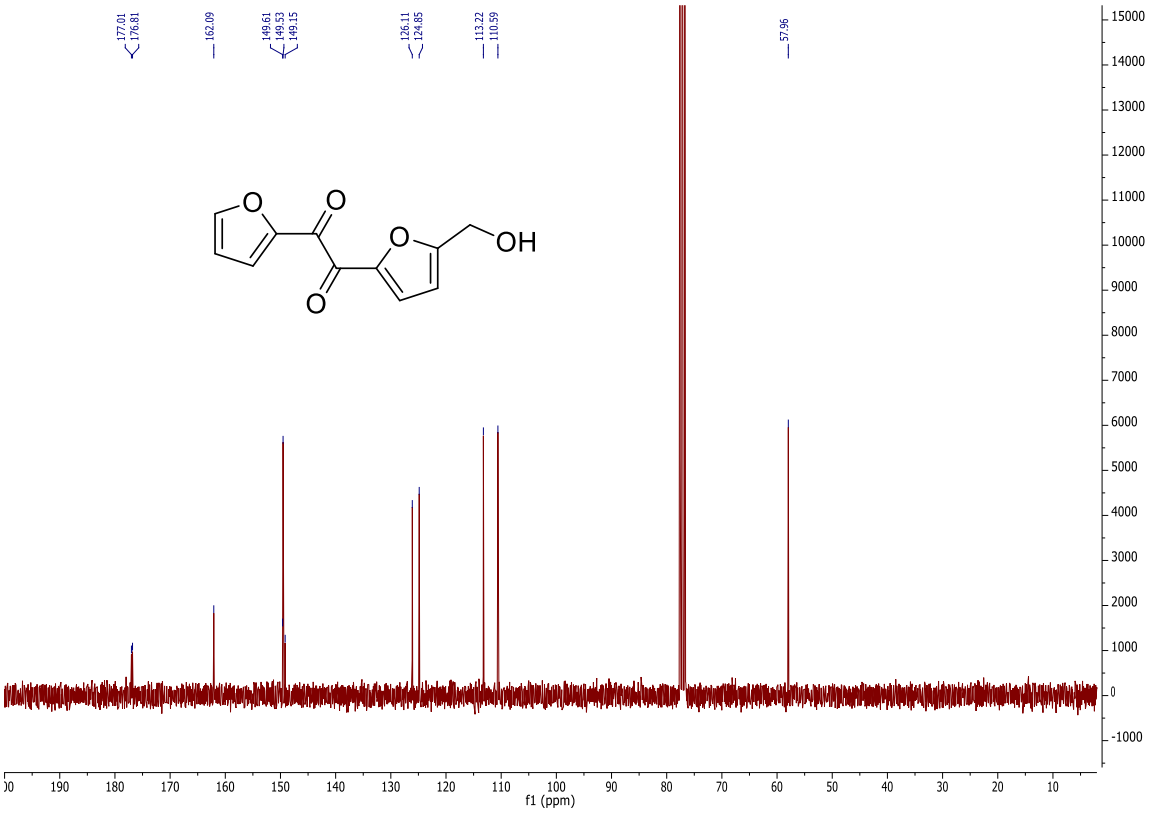

^{13}C NMR spectrum in $CDCl_3$.

258b

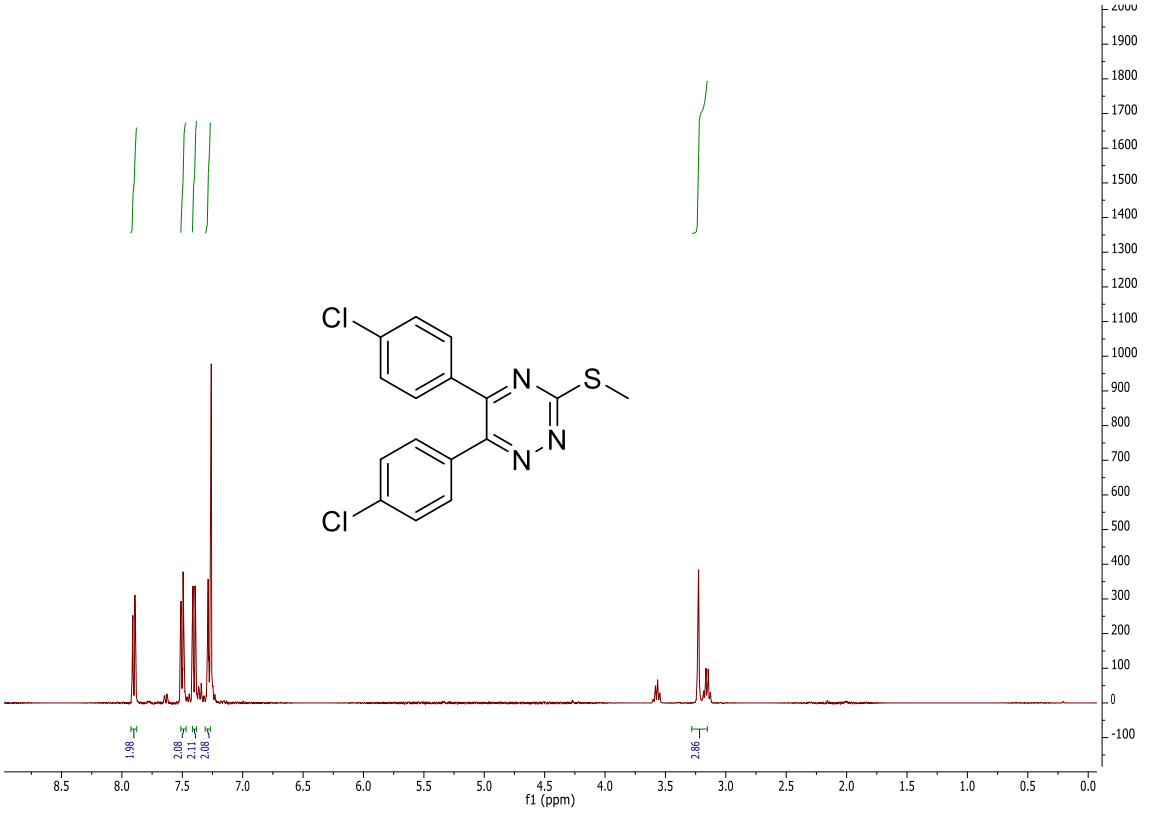

^{1}H spectrum in $CDCl_3$

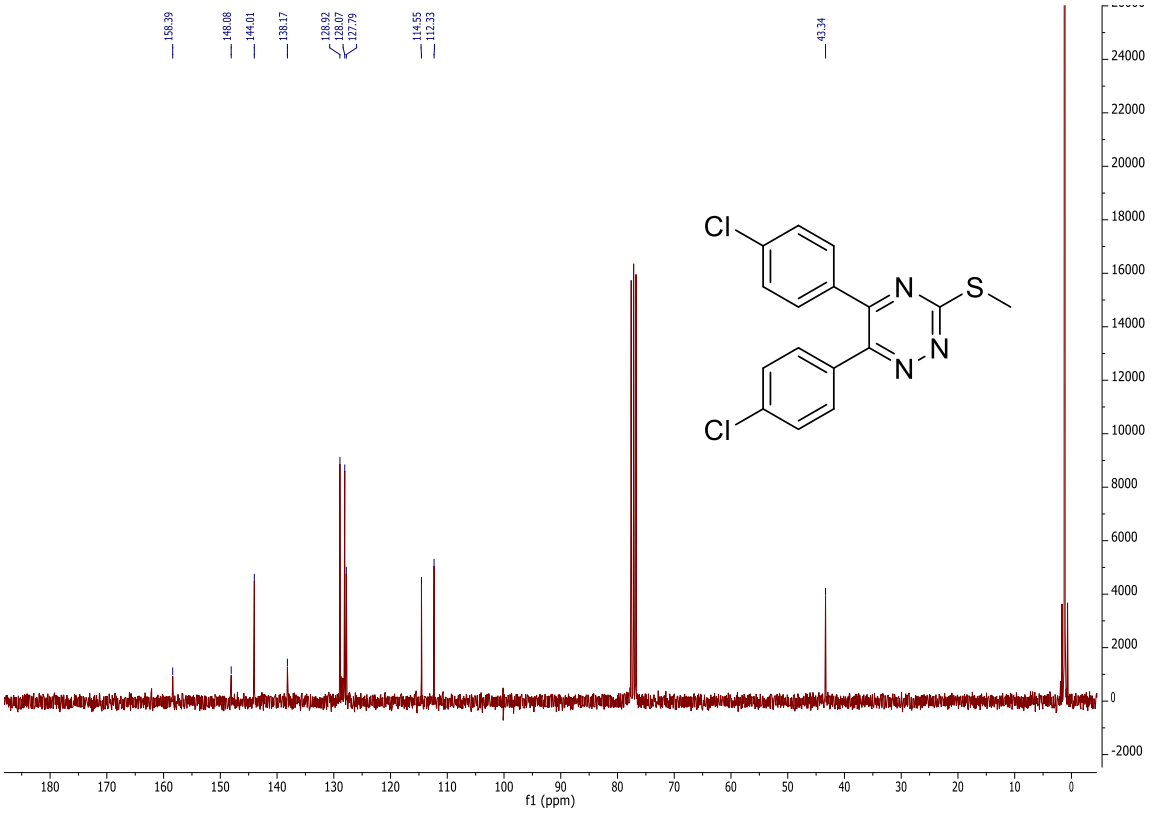

^{13}C NMR spectrum in $CDCl_3$.

259b

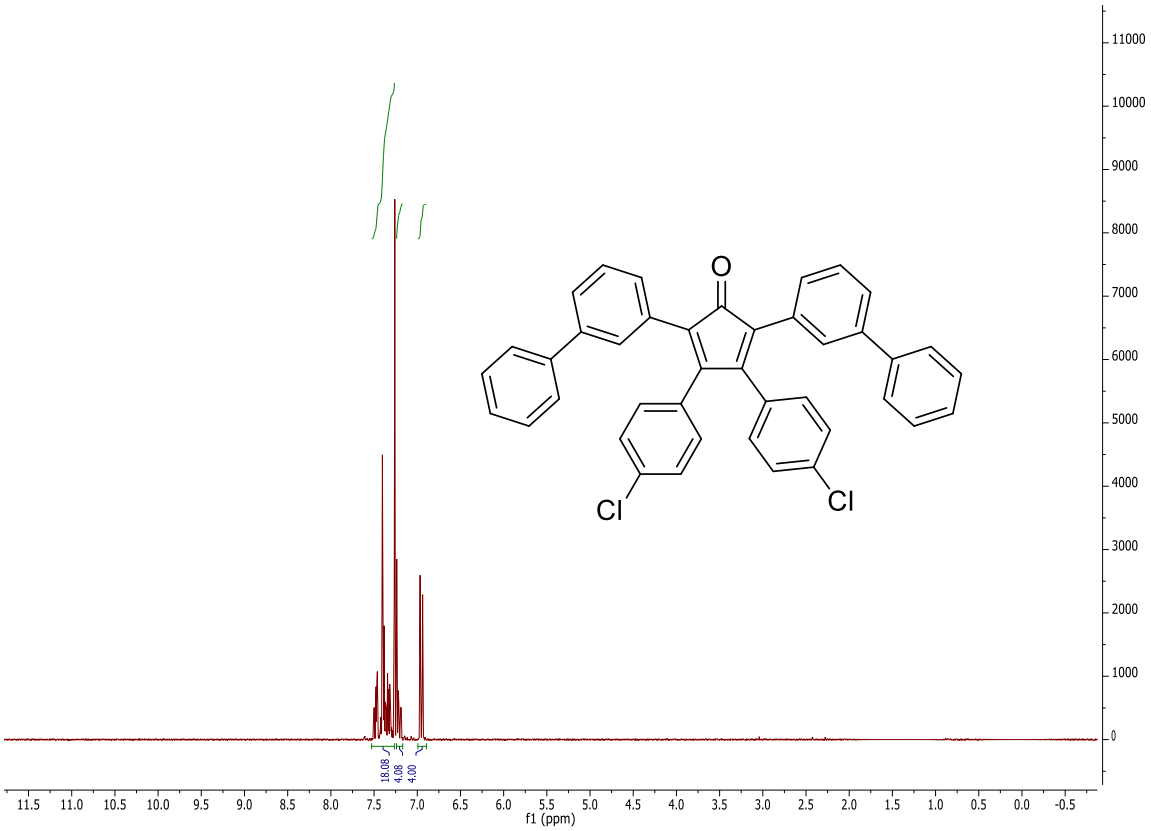

^{1}H spectrum in $CDCl_3$.

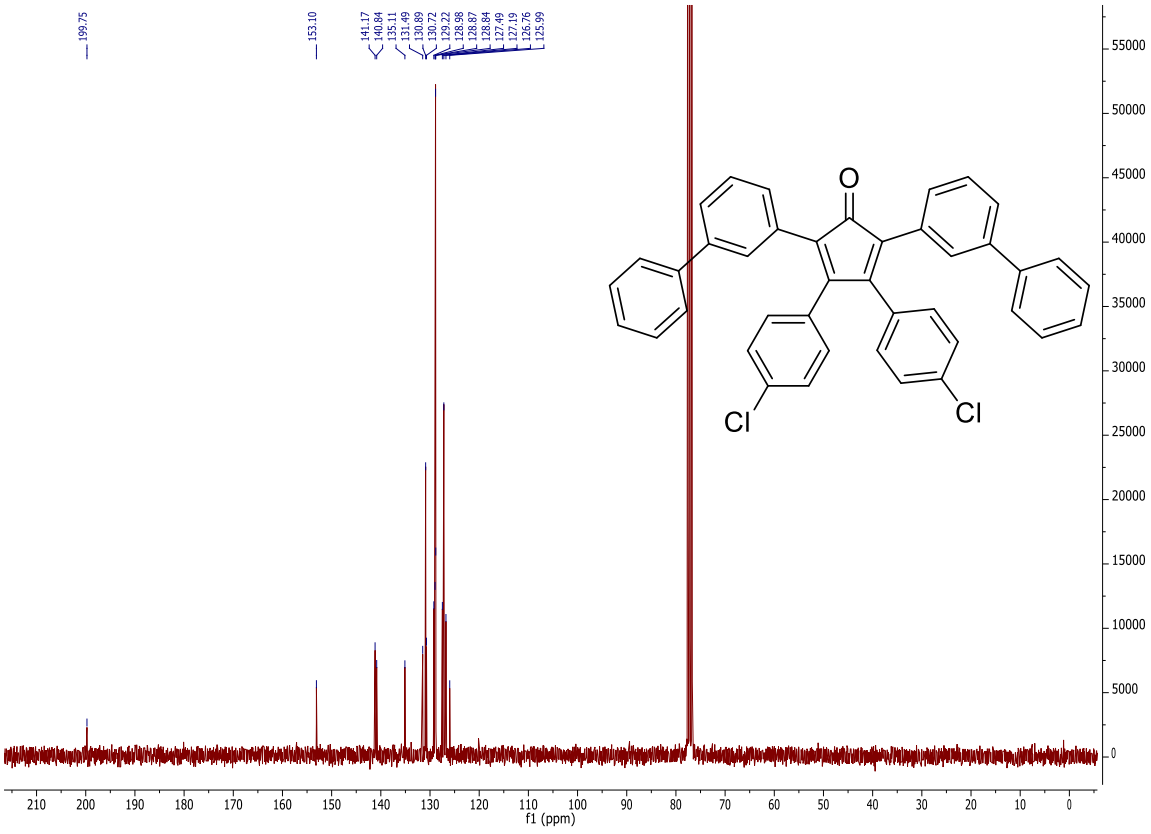

^{13}C NMR spectrum in $CDCl_3$.

260b

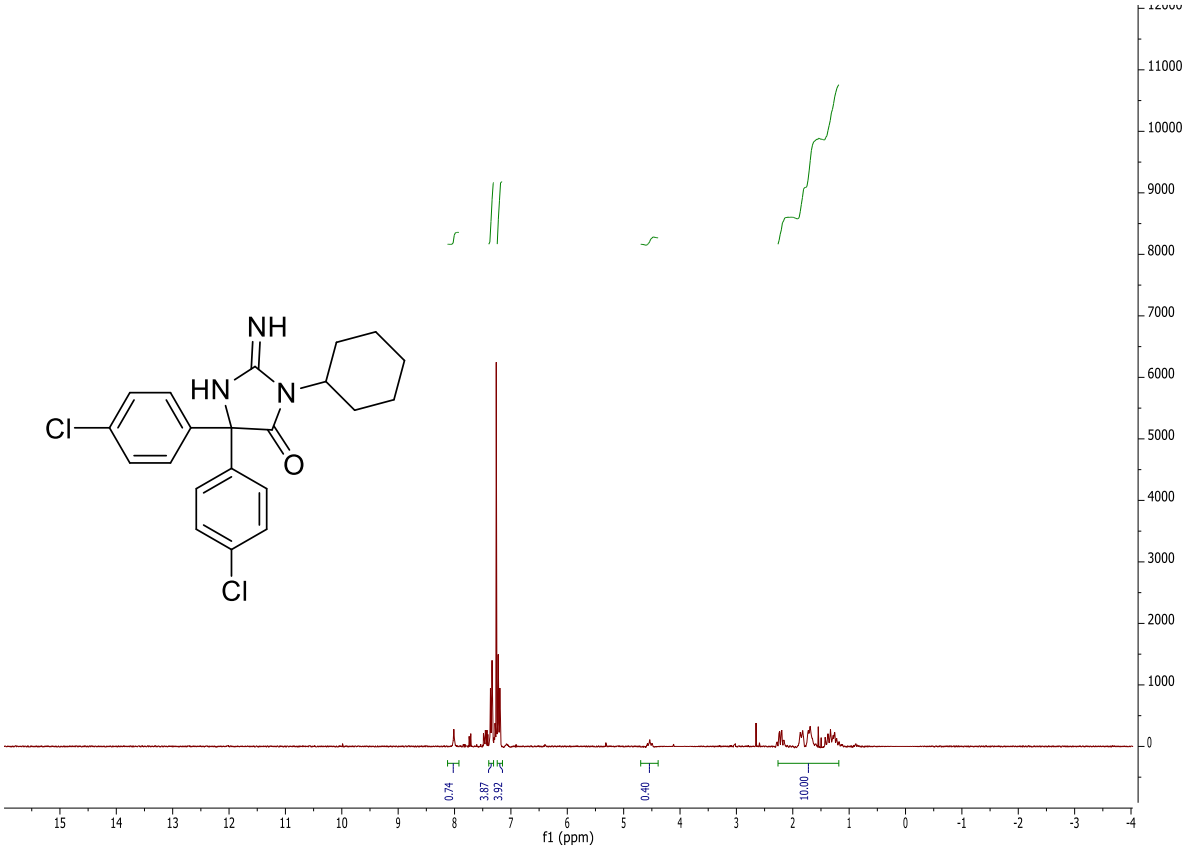

^{1}H spectrum in $CDCl_3$.

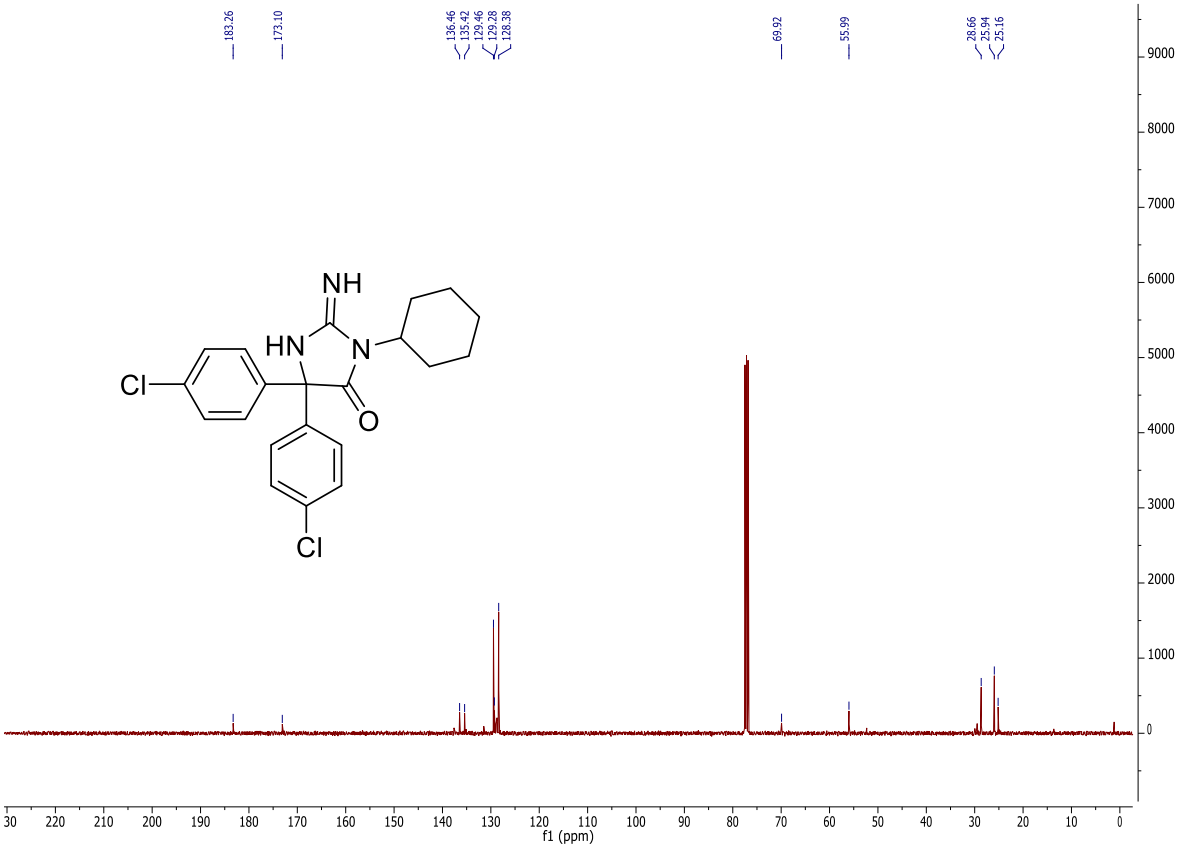

^{13}C NMR spectrum in $CDCl_3$.

261b

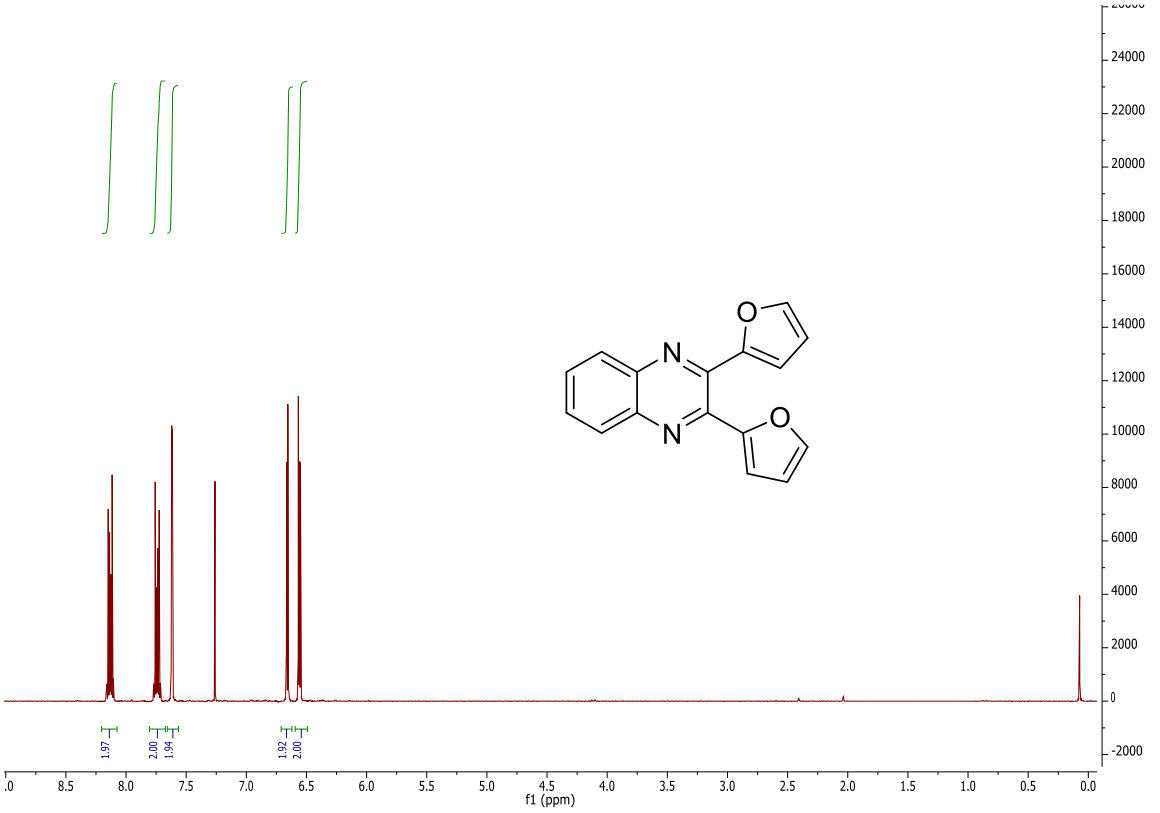

^{1}H spectrum in $CDCl_3$.

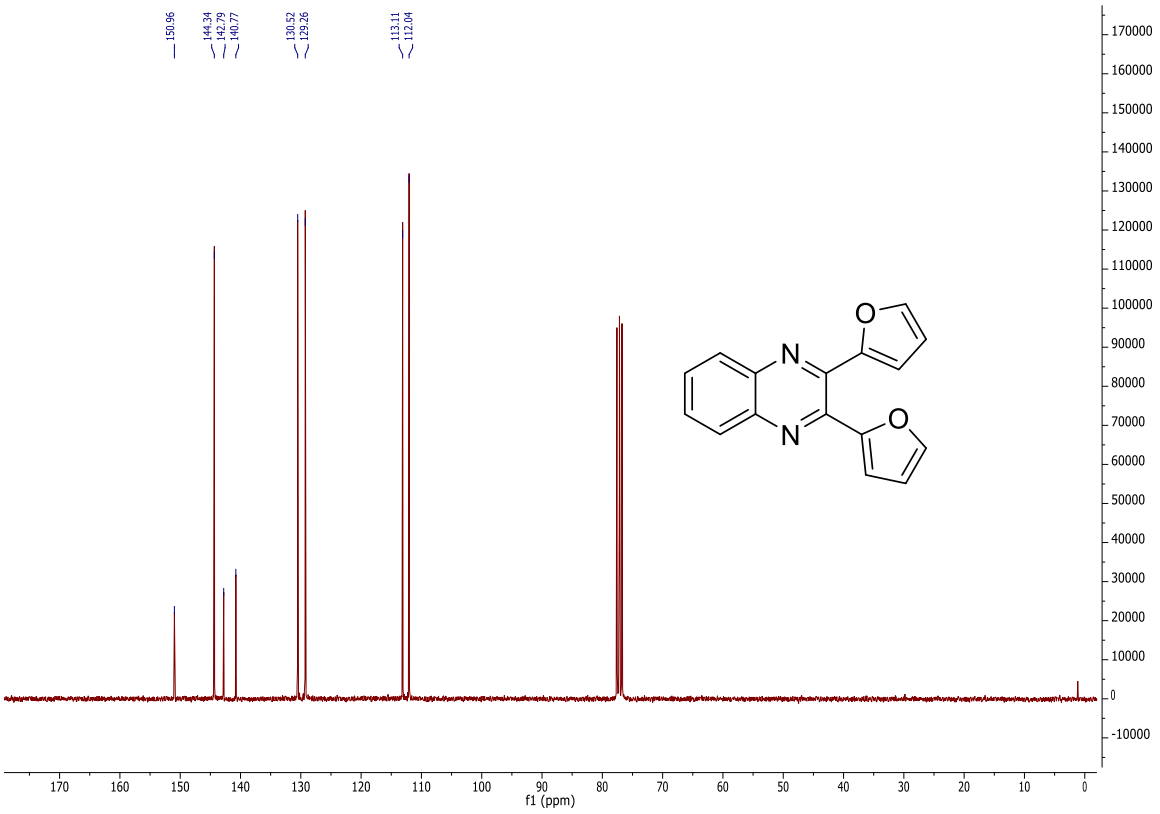

^{13}C NMR spectrum in $CDCl_3$.

262b

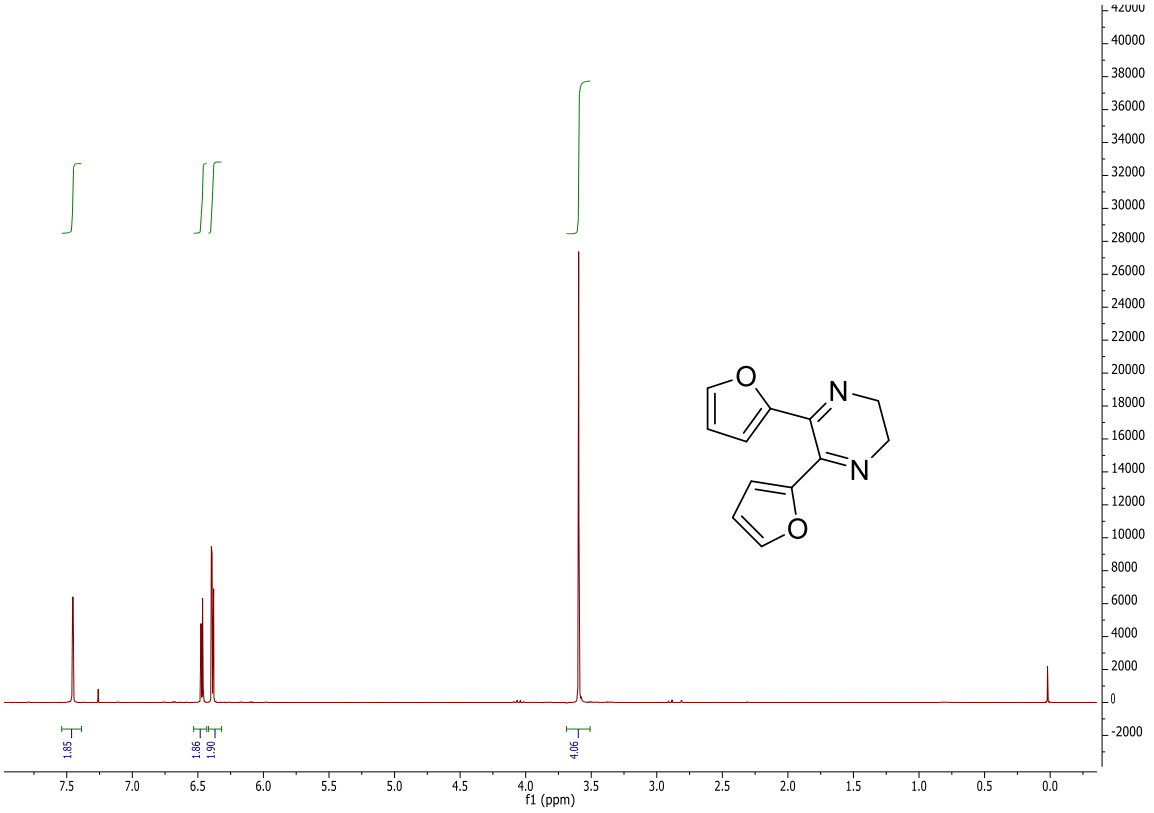

^{1}H spectrum in $CDCl_3$.

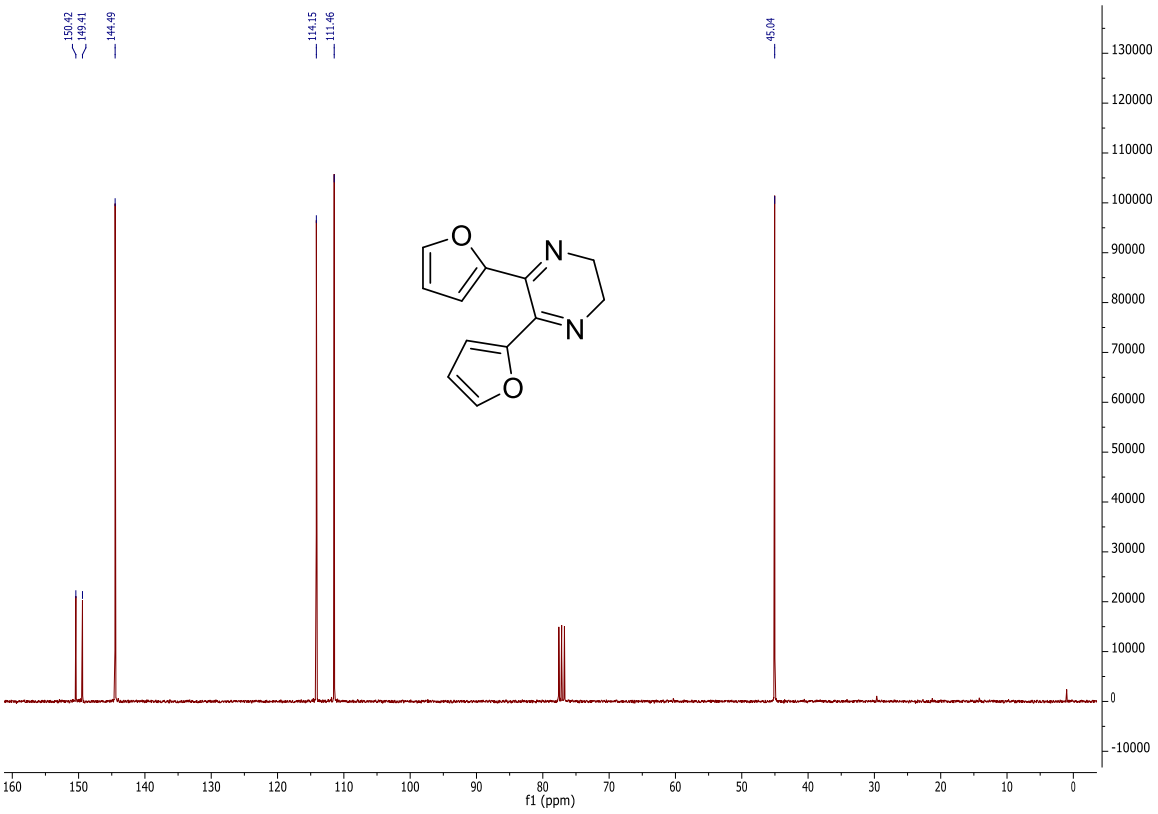

^{13}C NMR spectrum in $CDCl_3$.

263b

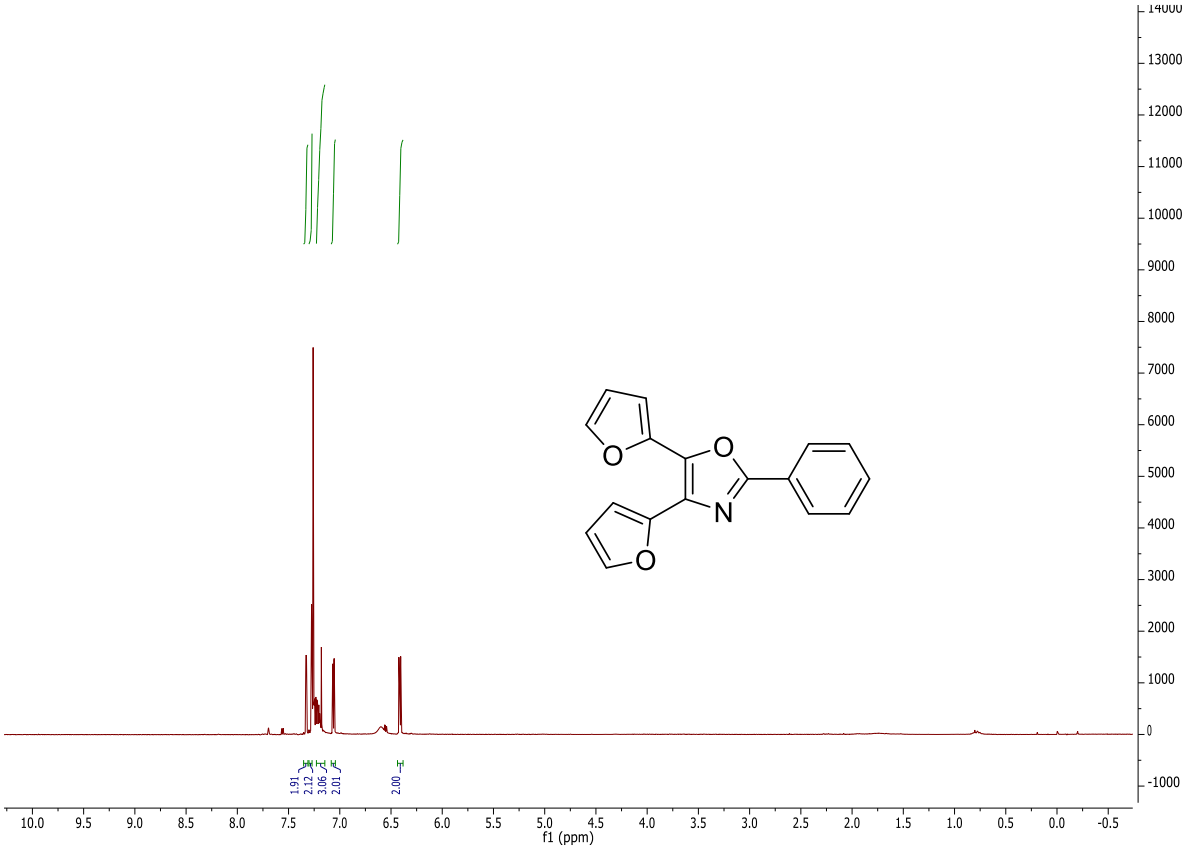

^{1}H spectrum in $CDCl_3$.

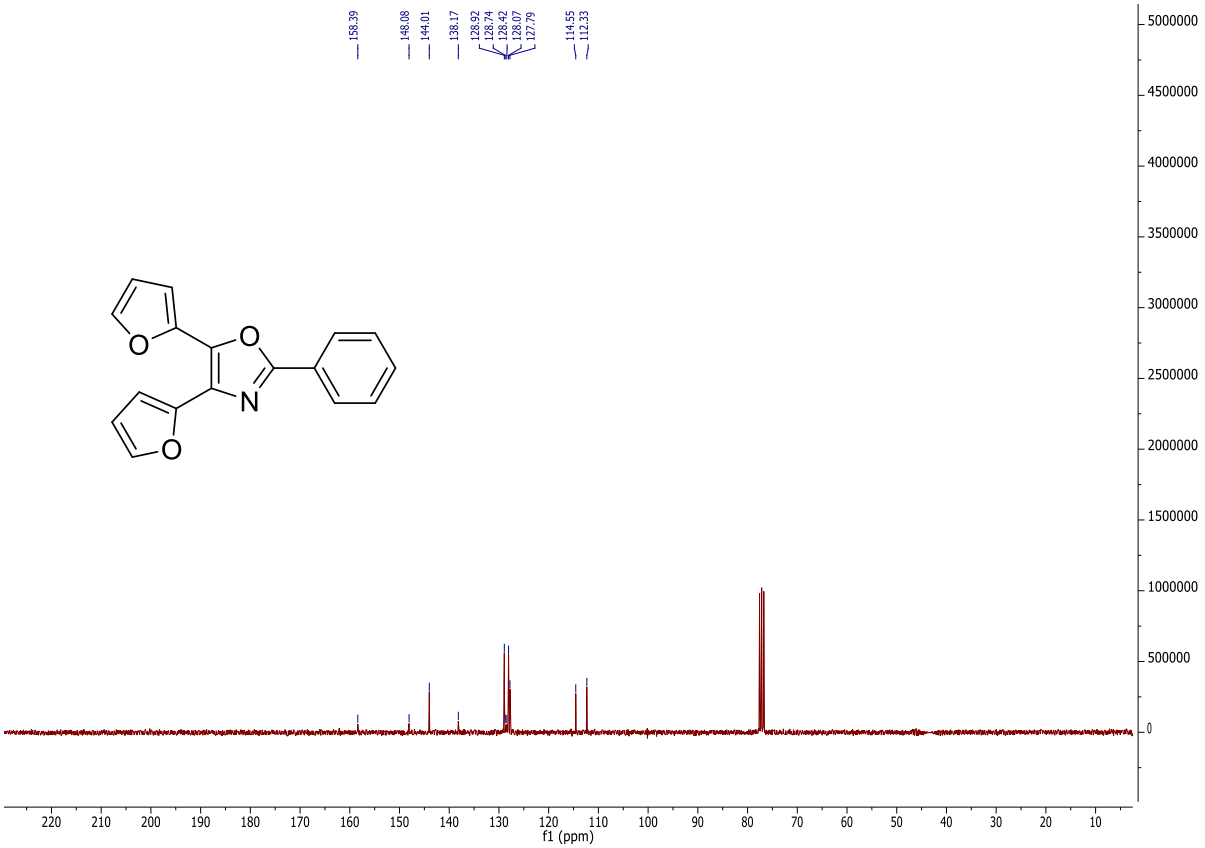

^{13}C NMR spectrum in $CDCl_3$.

264b‘

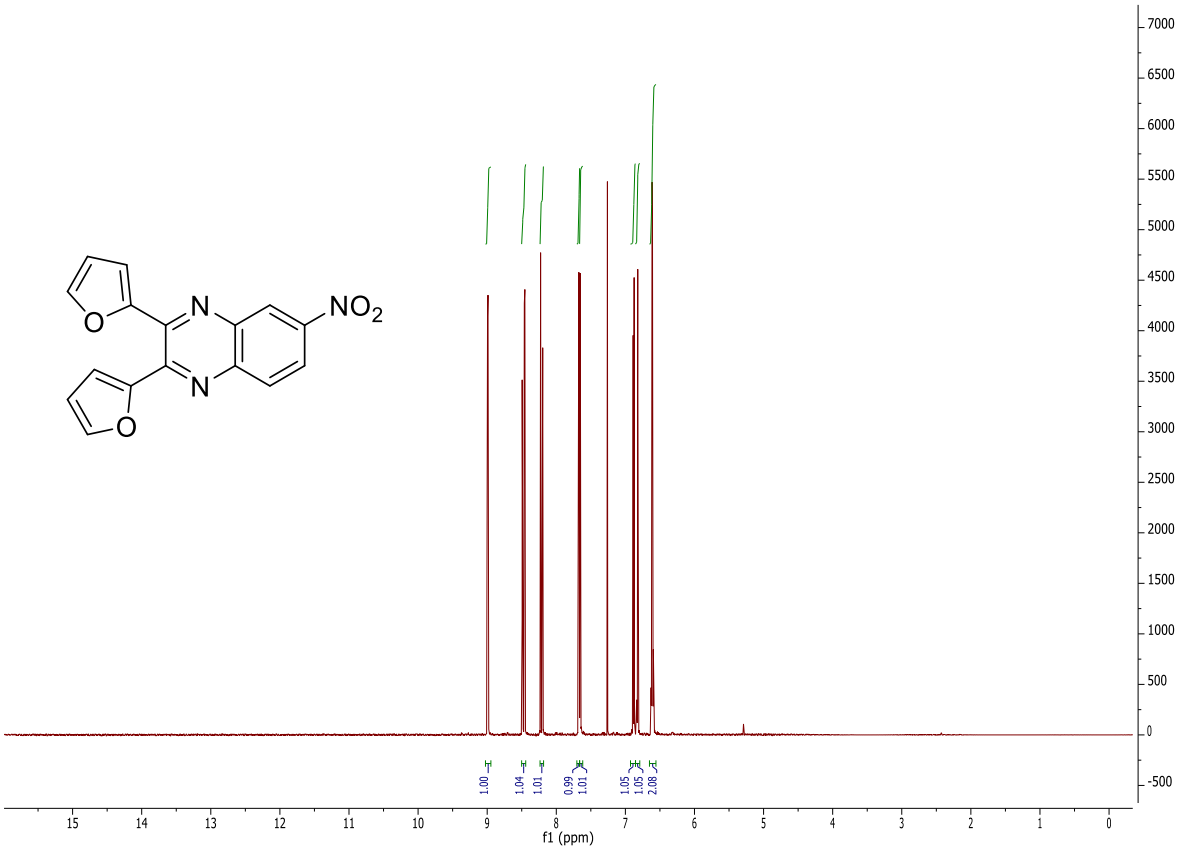

^{1}H spectrum in $CDCl_3$.

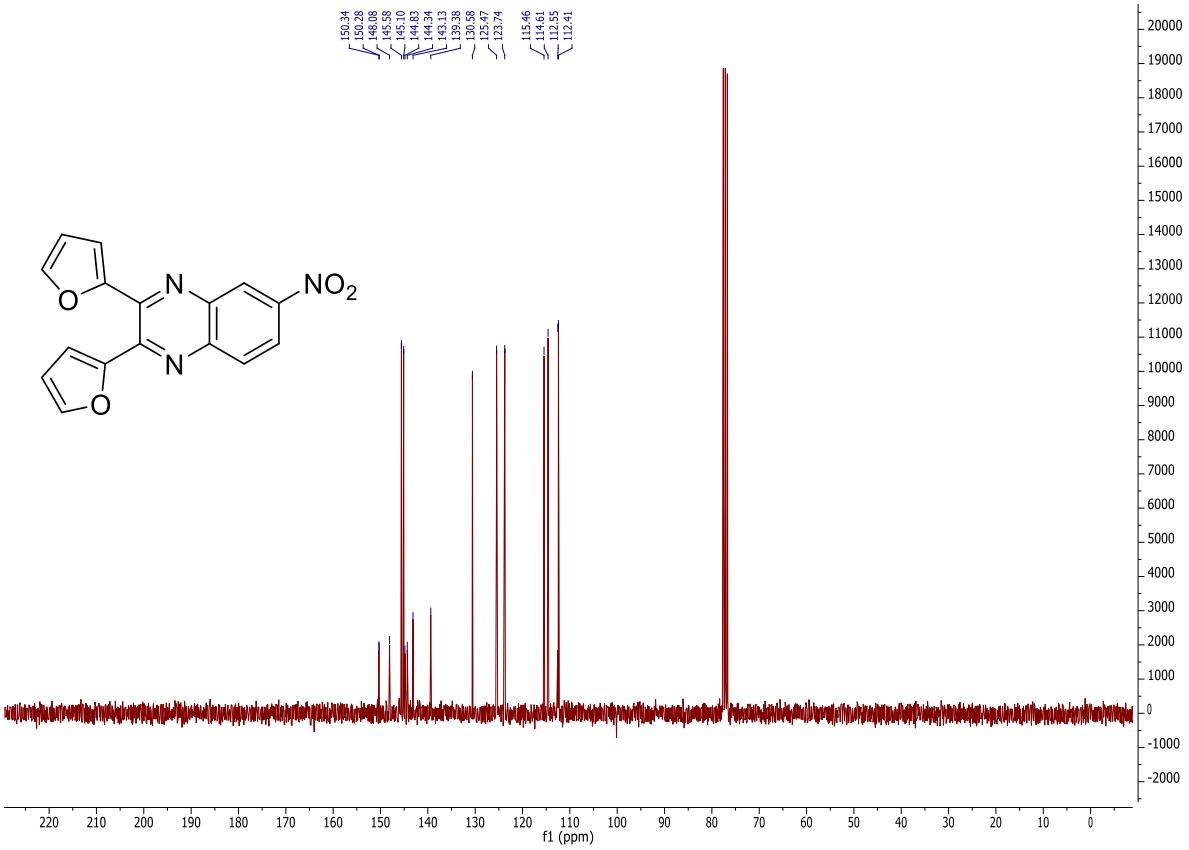

^{13}C NMR spectrum in $CDCl_3$.

264b

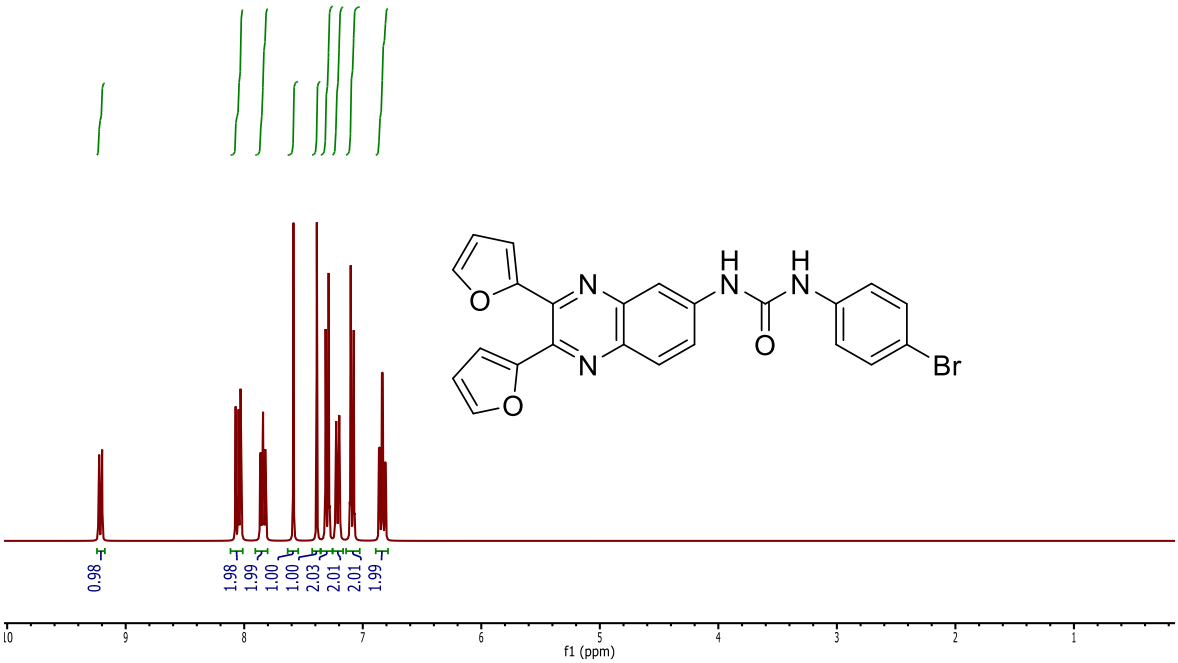

^{1}H spectrum in Benzene-*d*$_6$.

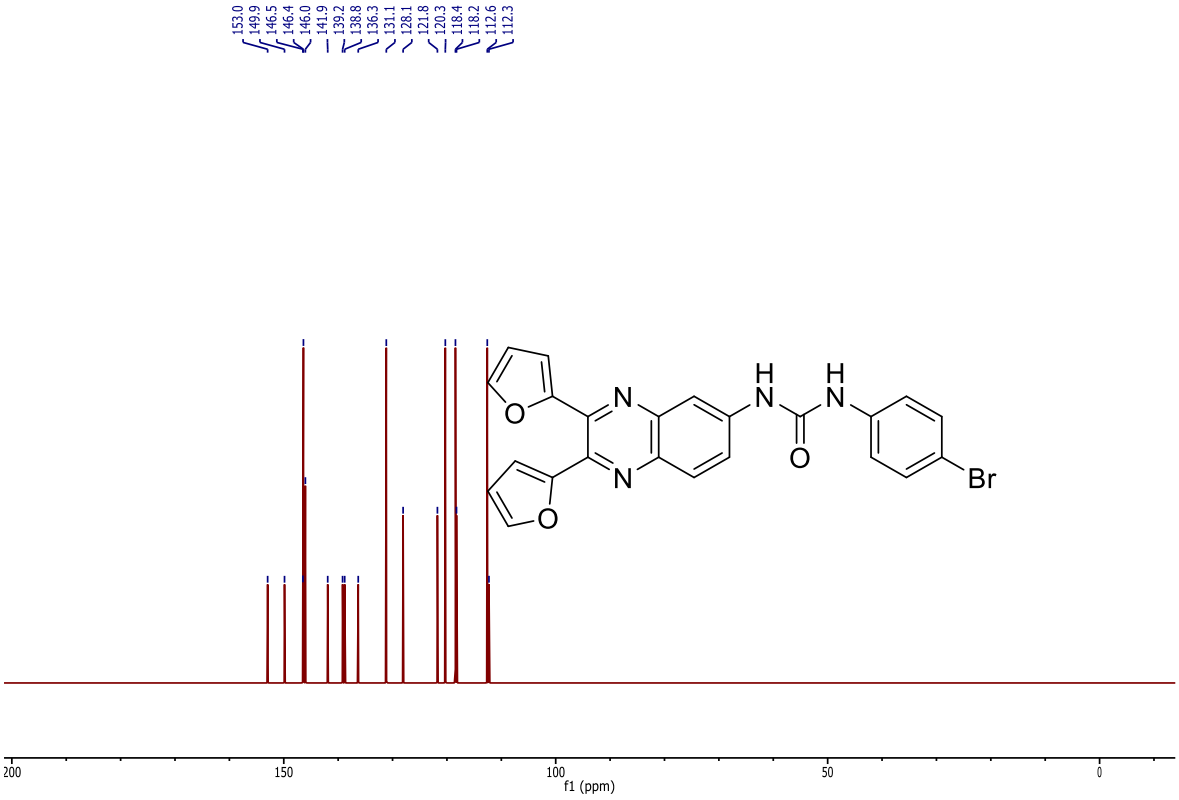

^{13}C NMR spectrum in Benzene-*d*$_6$.

265b

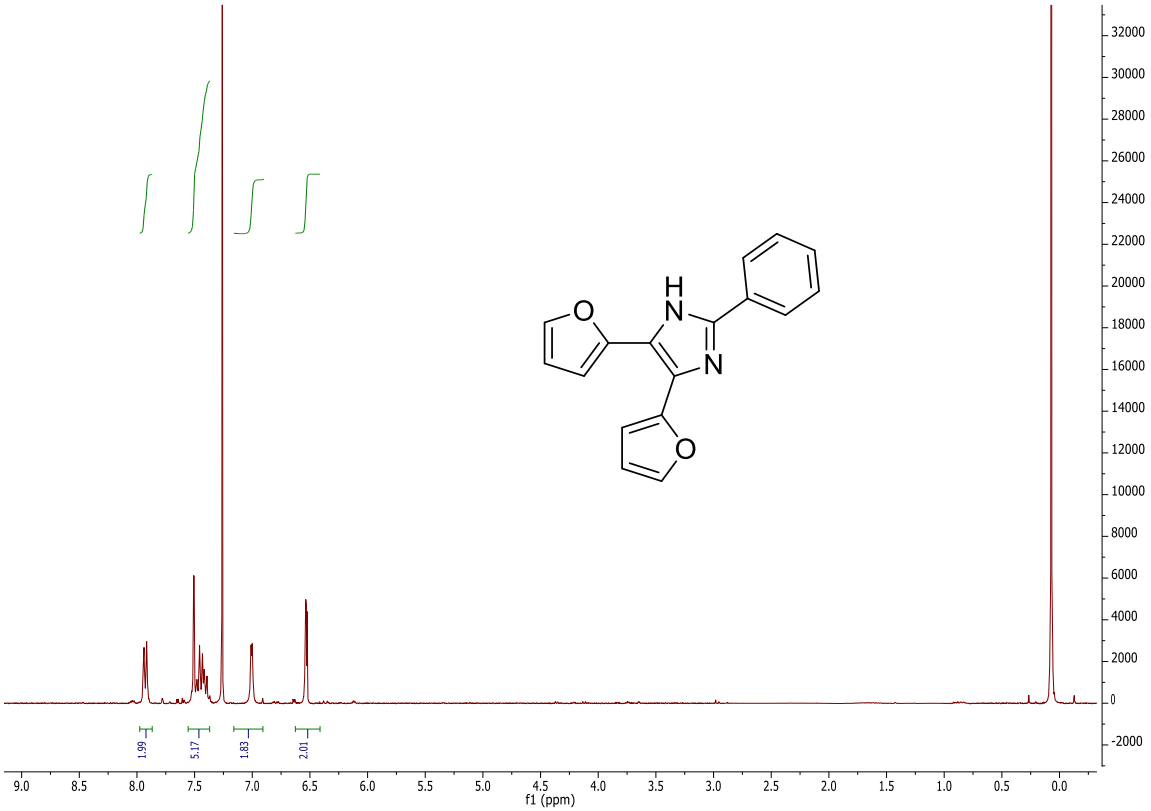

^{1}H spectrum in $CDCl_3$.

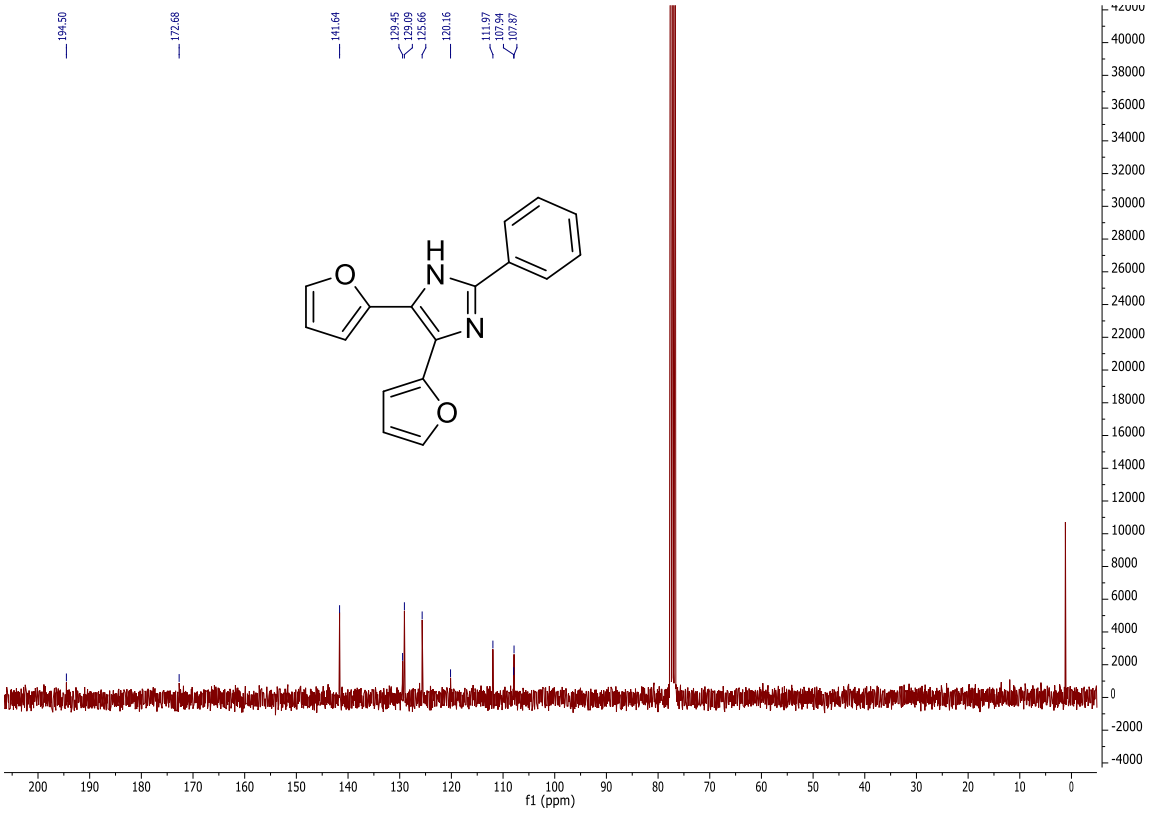

^{13}C NMR spectrum in $CDCl_3$.

266b

^{1}H NMR spectrum in $CDCl_3$.

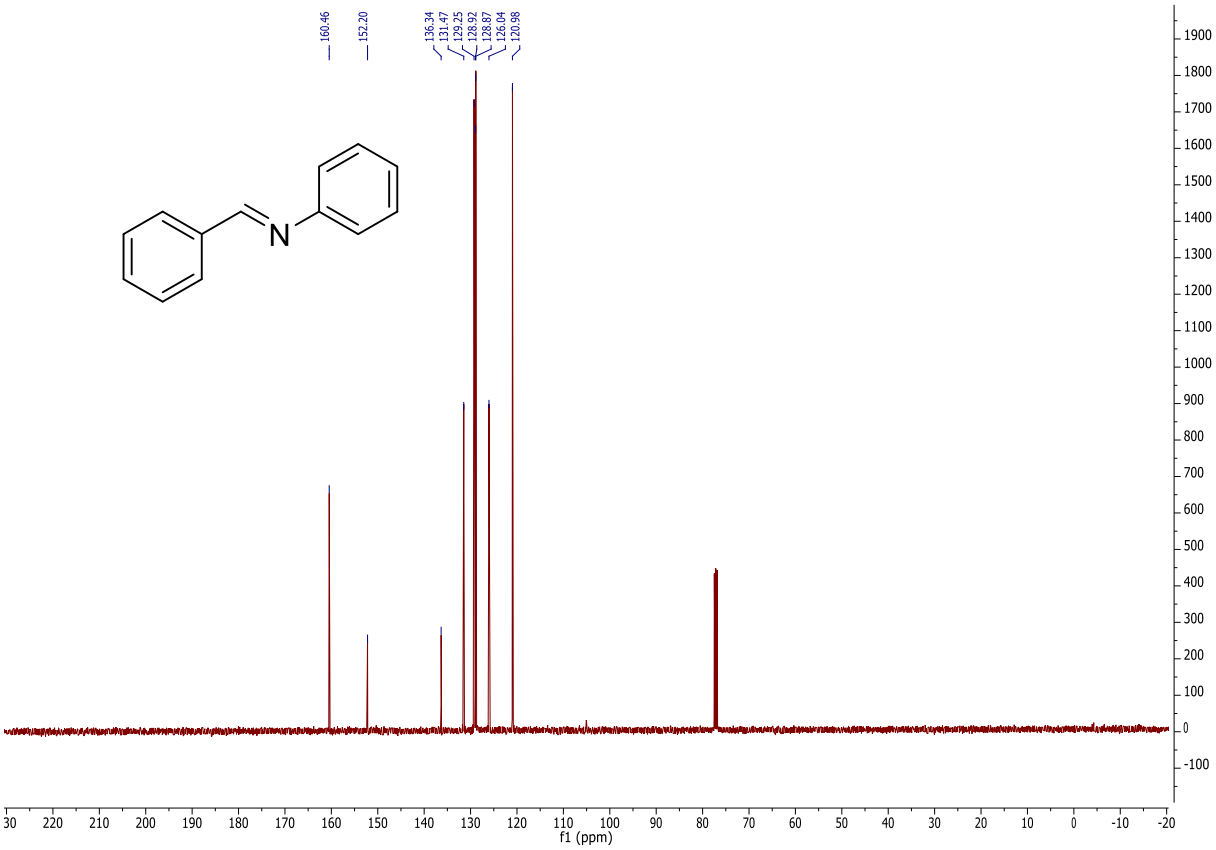

^{13}C NMR spectrum in $CDCl_3$.

267b

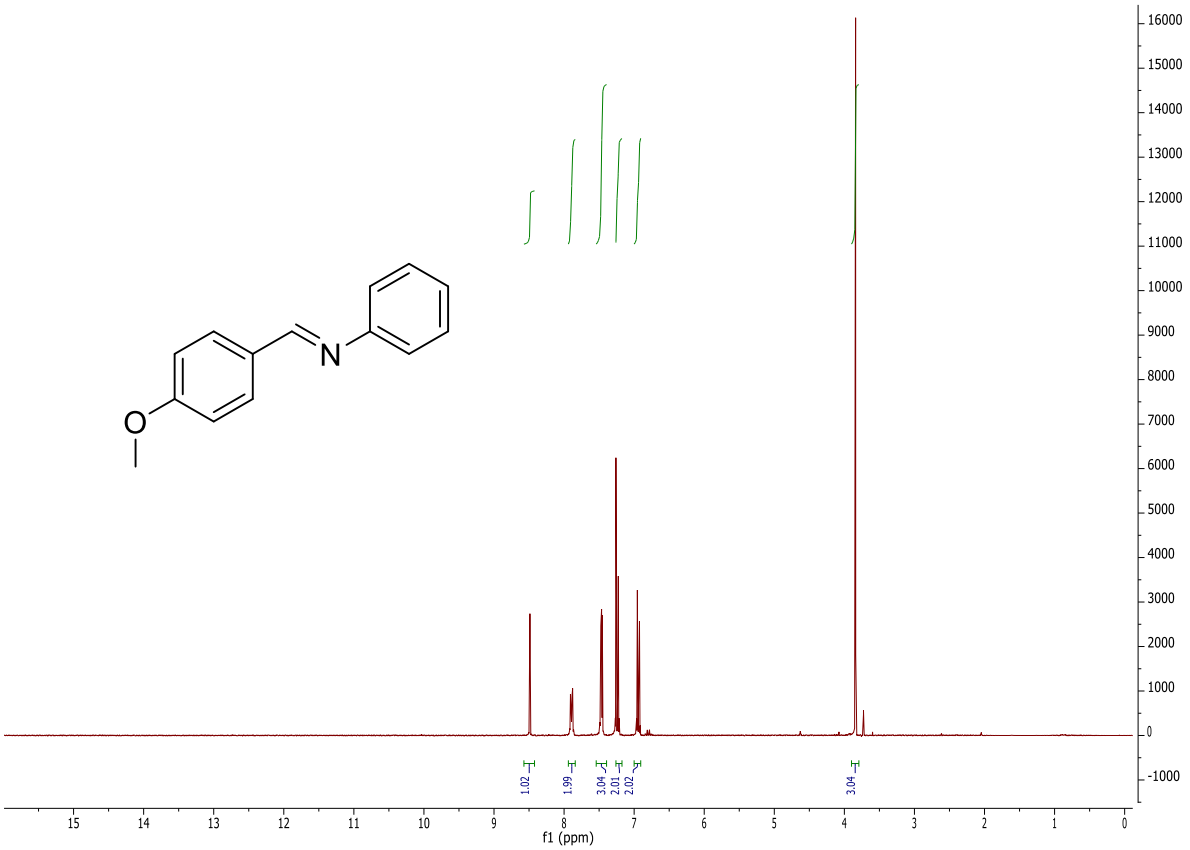

^{1}H NMR spectrum in $CDCl_3$.

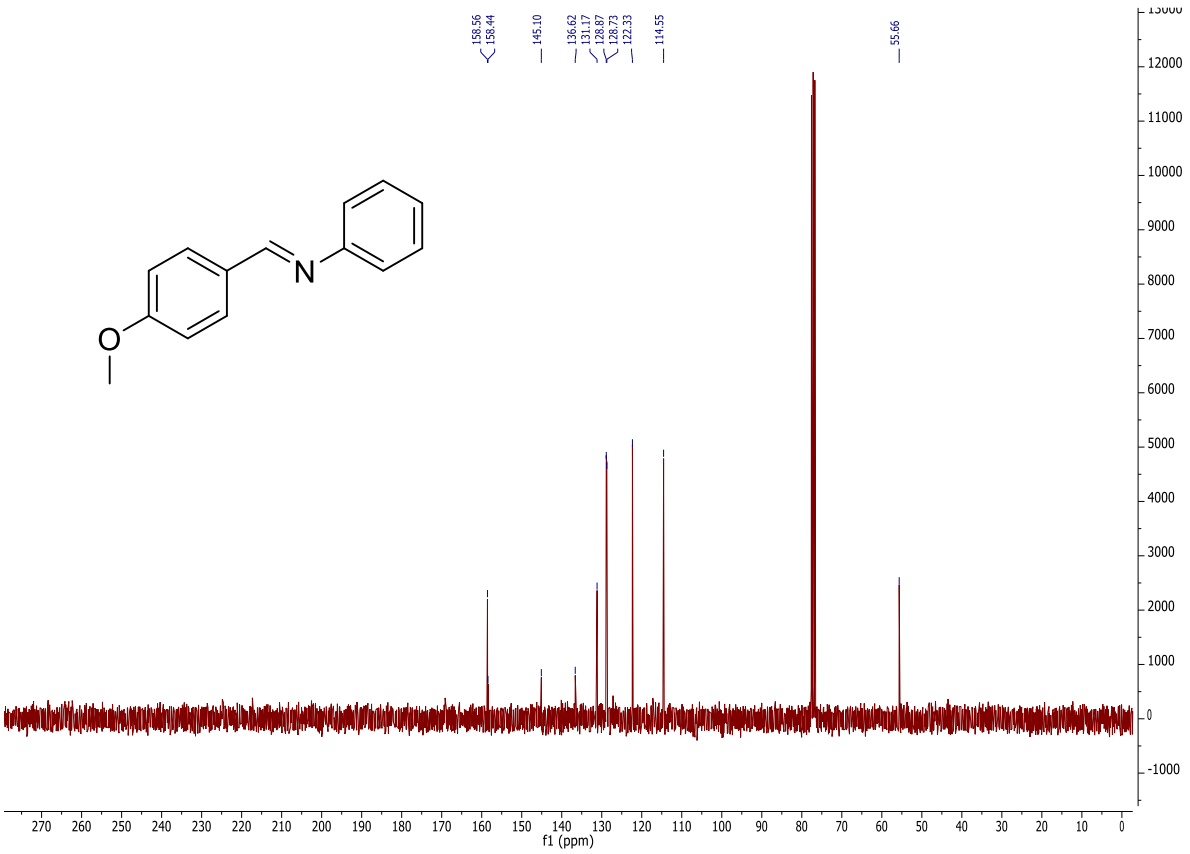

^{13}C NMR spectrum in $CDCl_3$.

268b

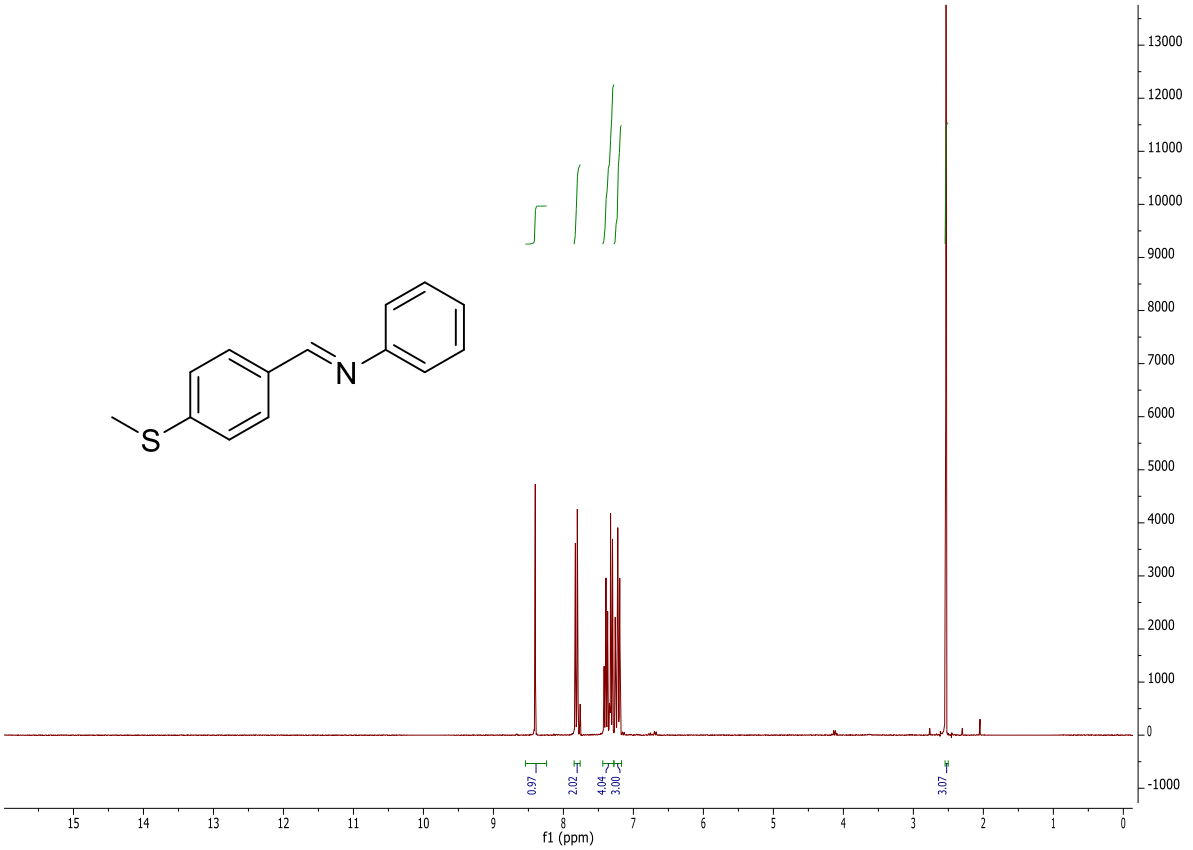

^{1}H NMR spectrum in $CDCl_3$.

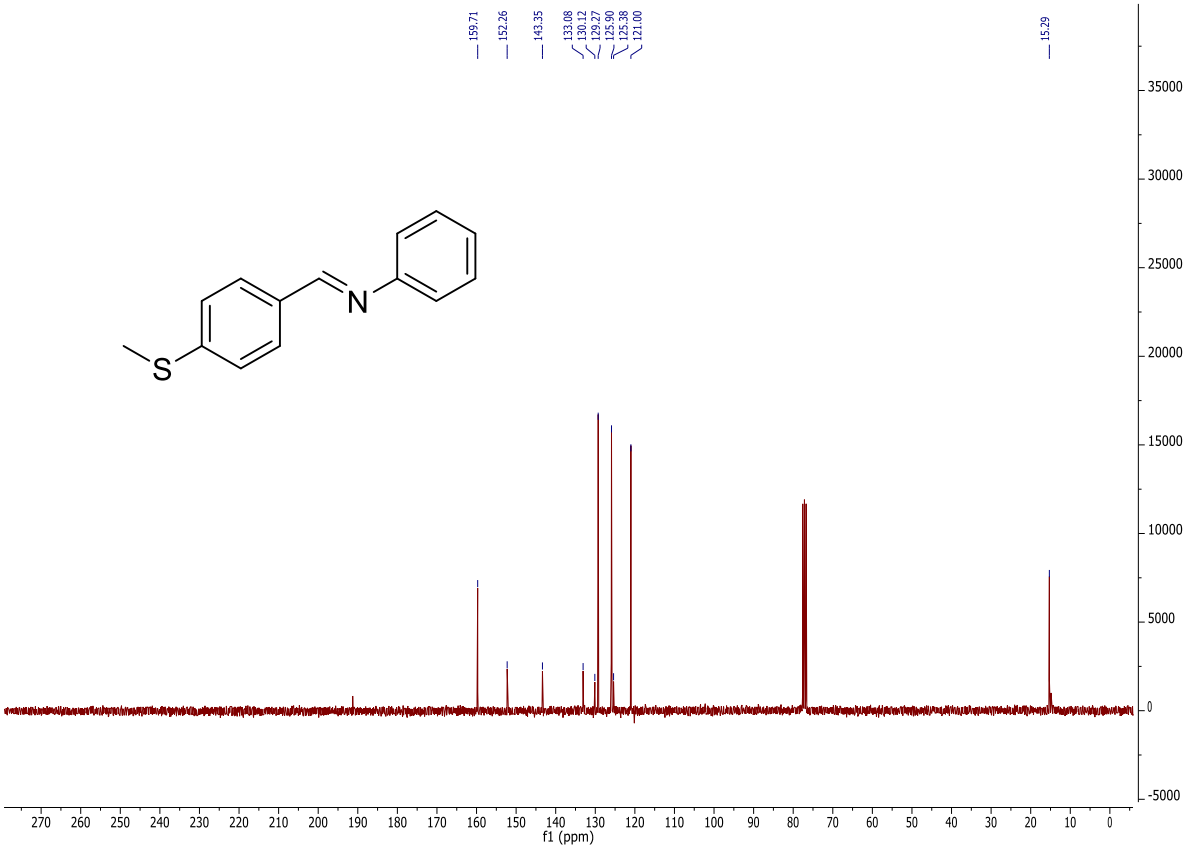

^{13}C NMR spectrum in $CDCl_3$.

269b

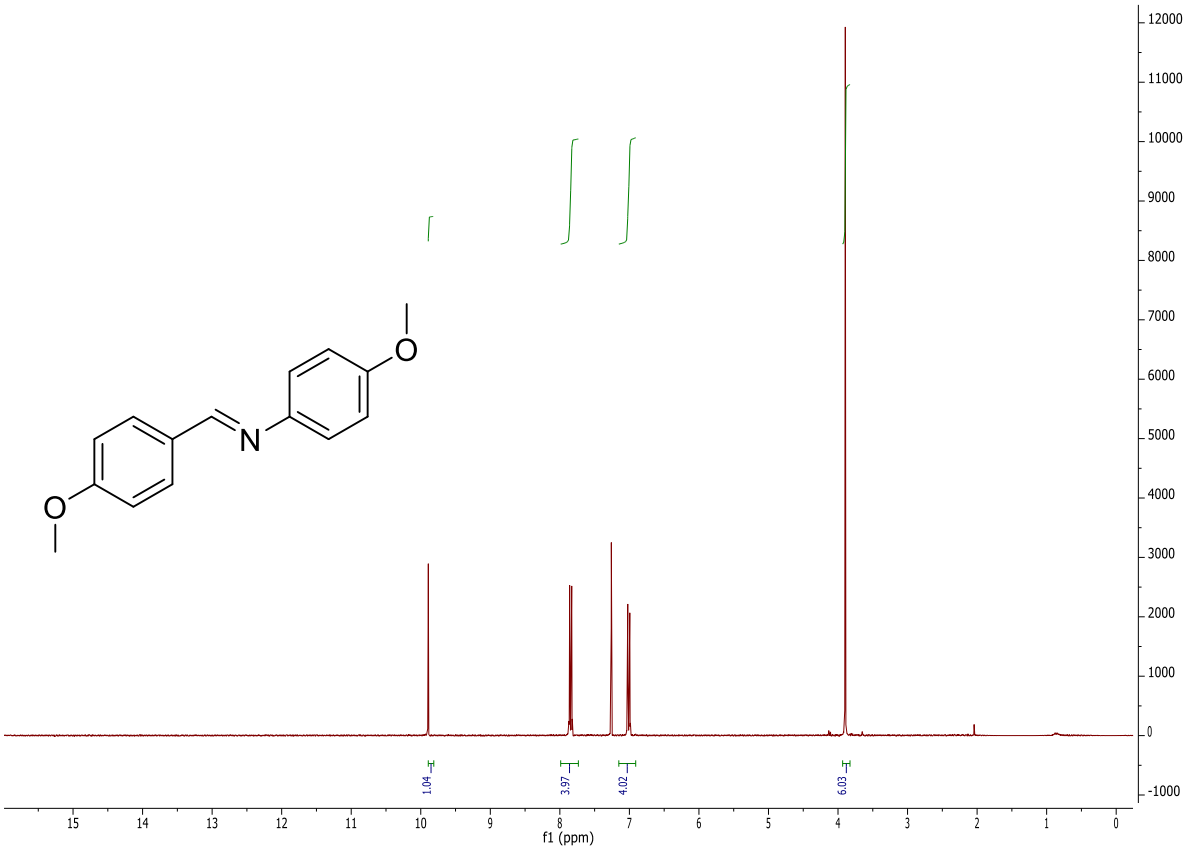

^{1}H NMR spectrum in $CDCl_3$.

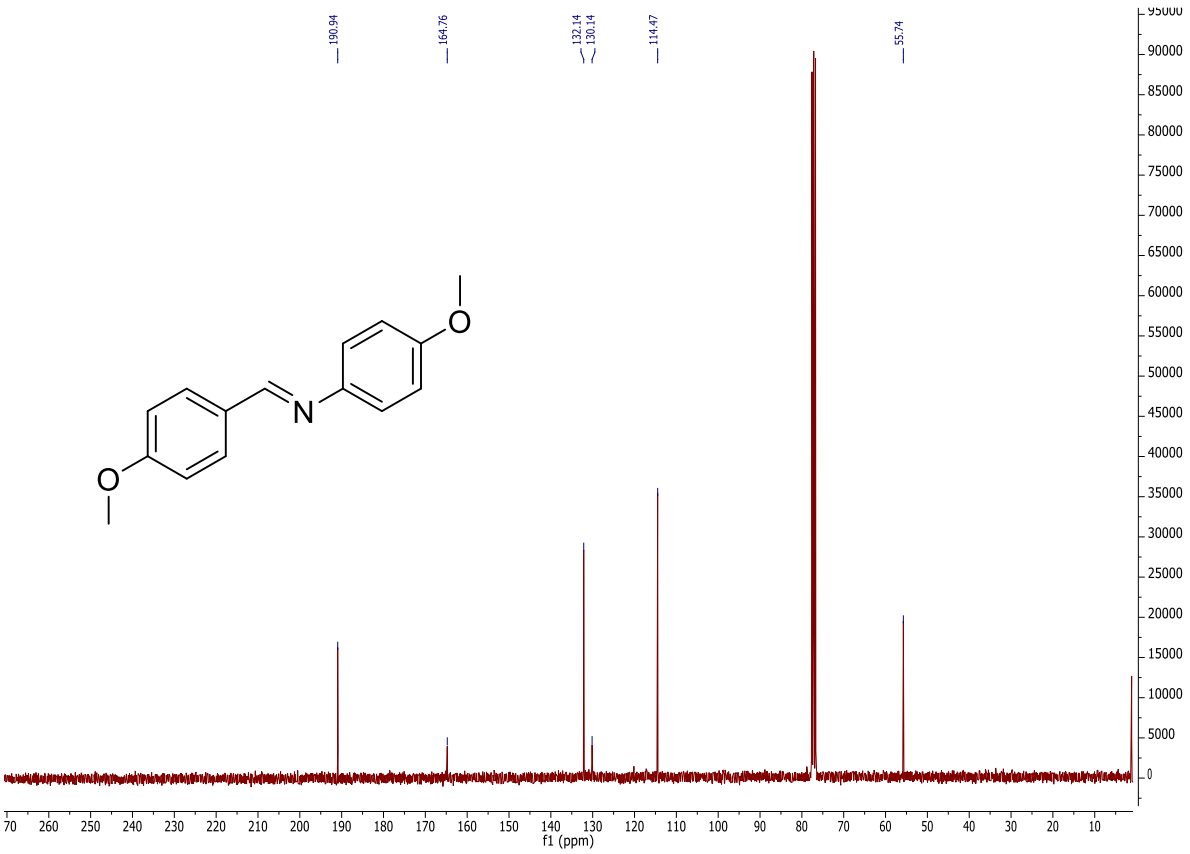

^{13}C NMR spectrum in $CDCl_3$.

270b

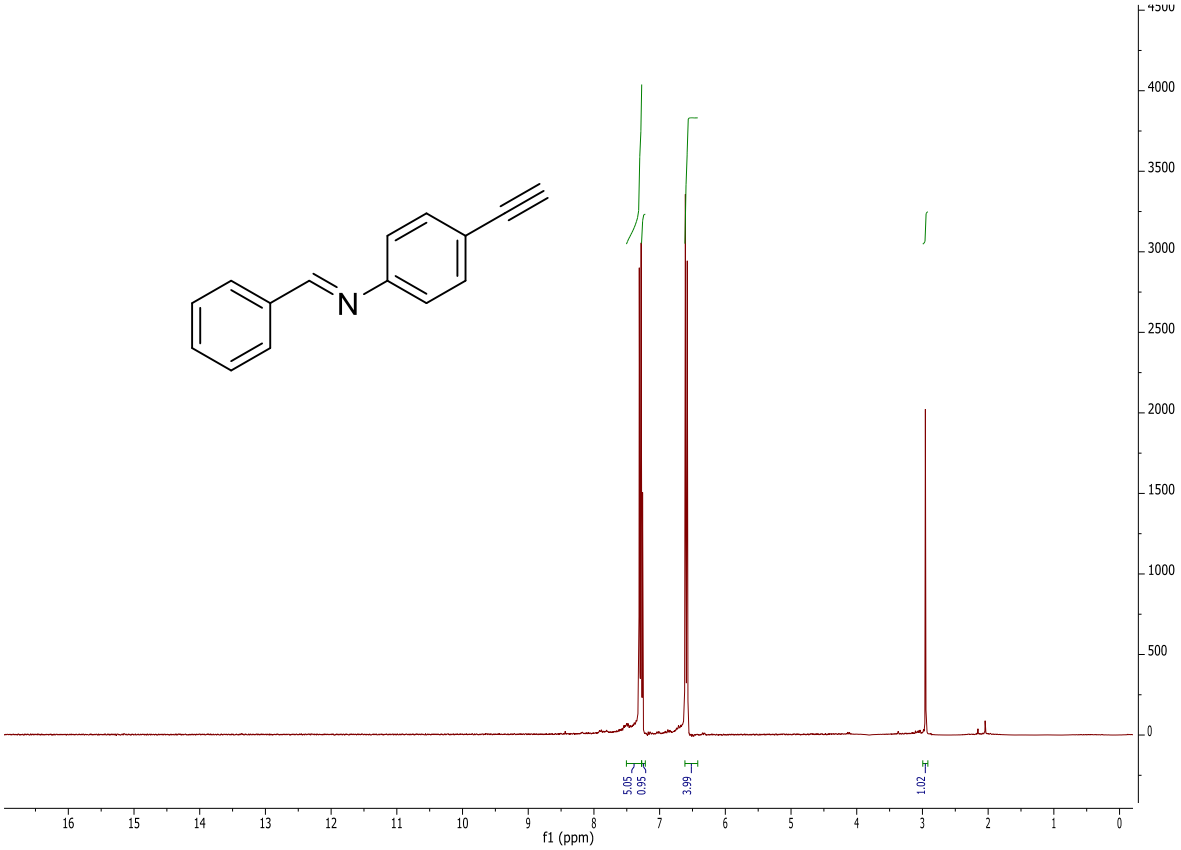

^{1}H NMR spectrum in $CDCl_3$.

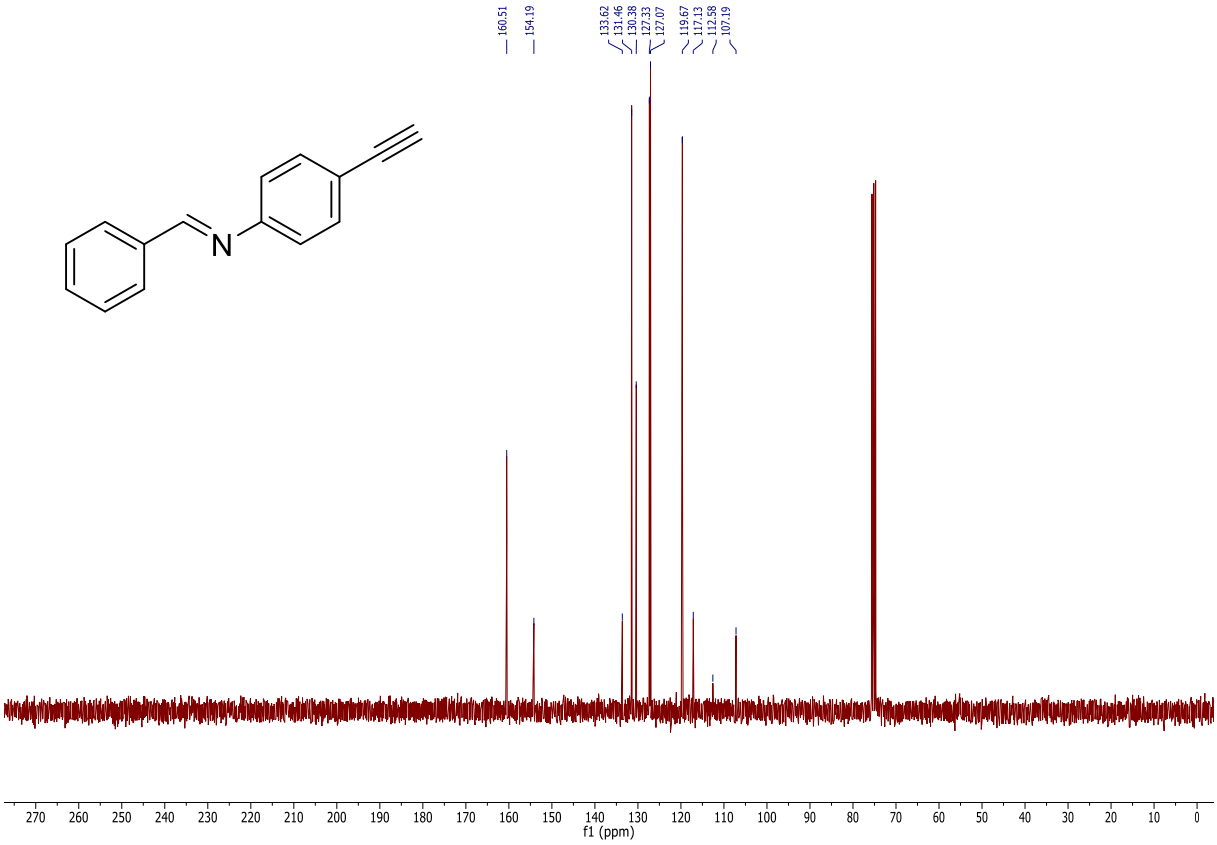

^{13}C NMR spectrum in $CDCl_3$.

271b

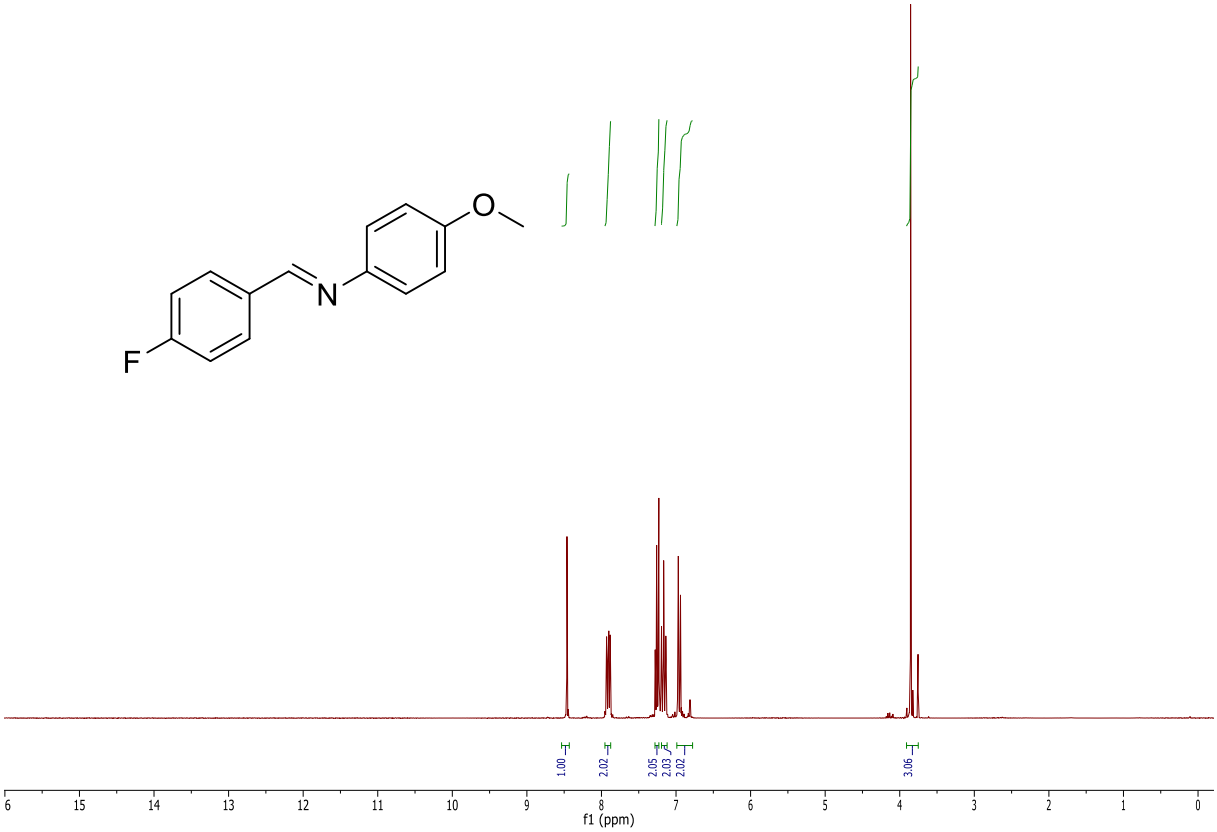

^{1}H NMR spectrum in $CDCl_3$.

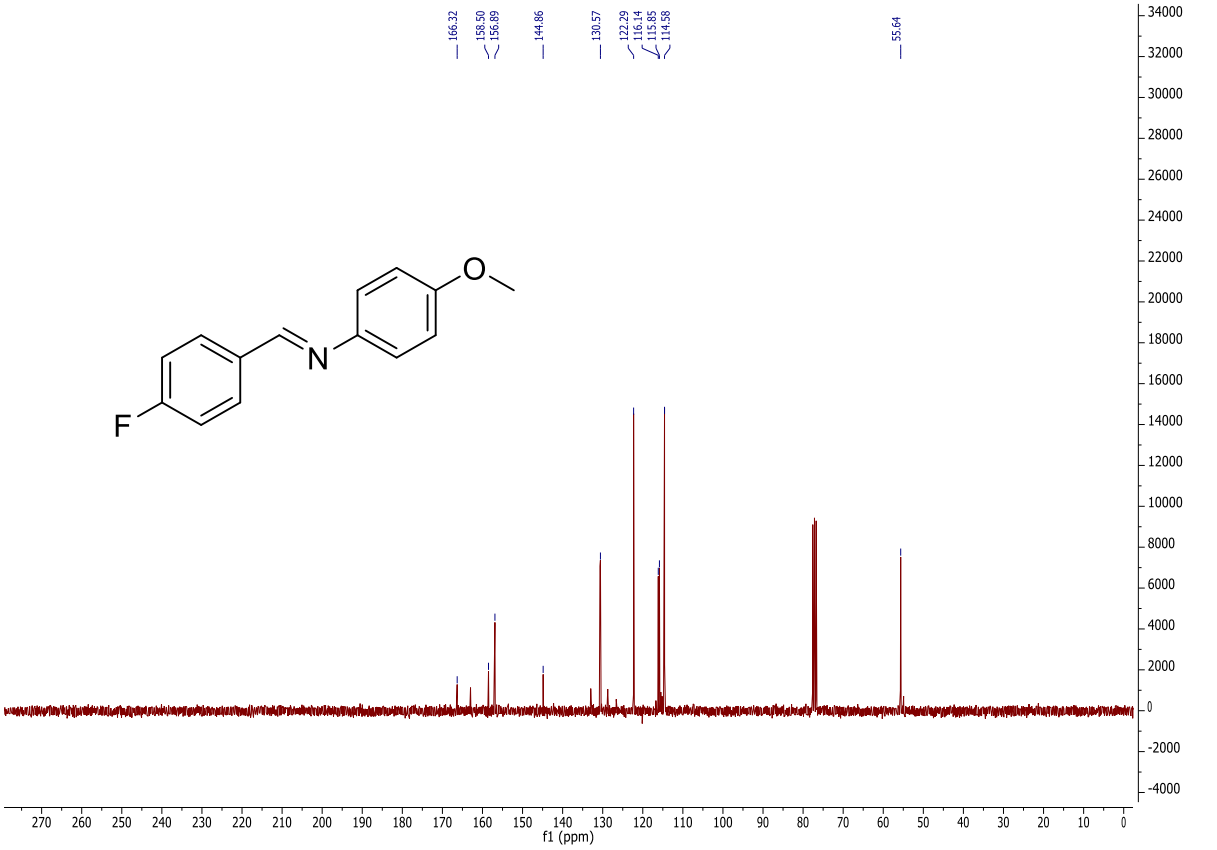

^{13}C NMR spectrum in $CDCl_3$.

272b

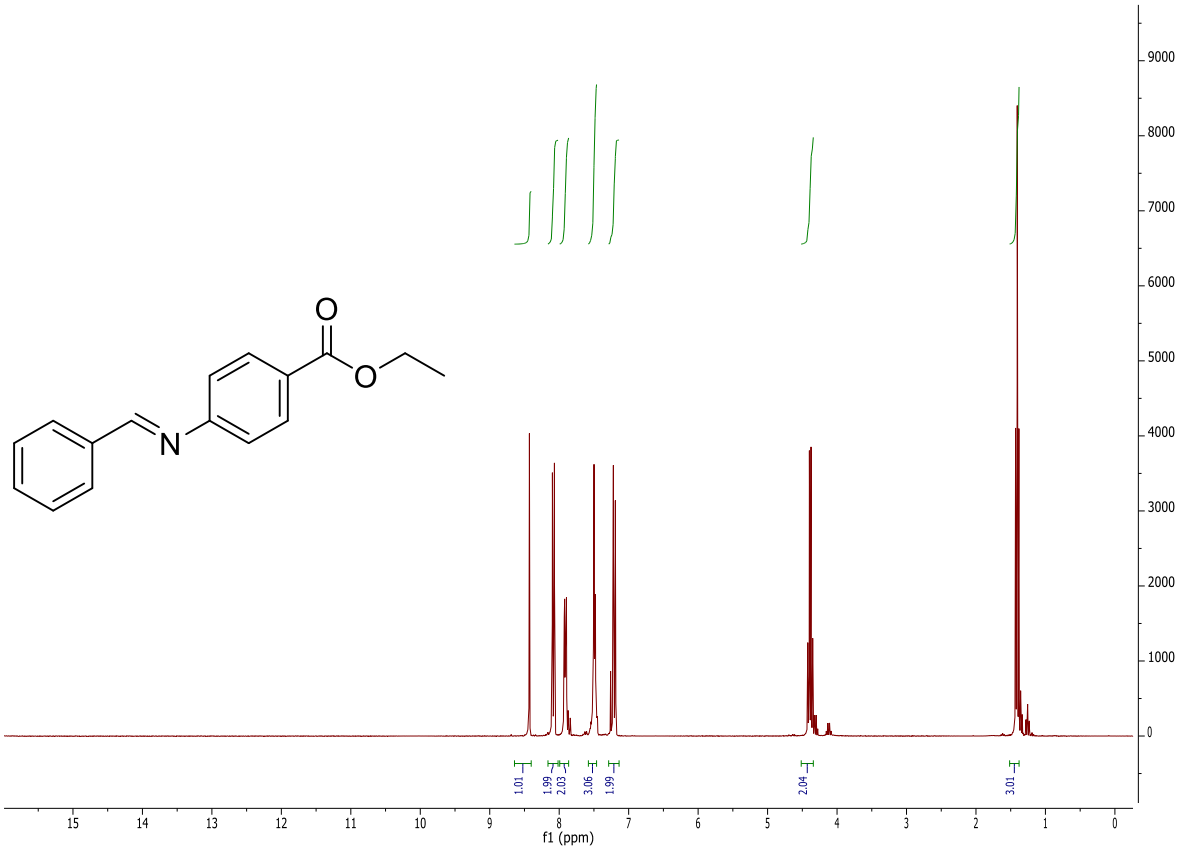

^{1}H NMR spectrum in $CDCl_3$.

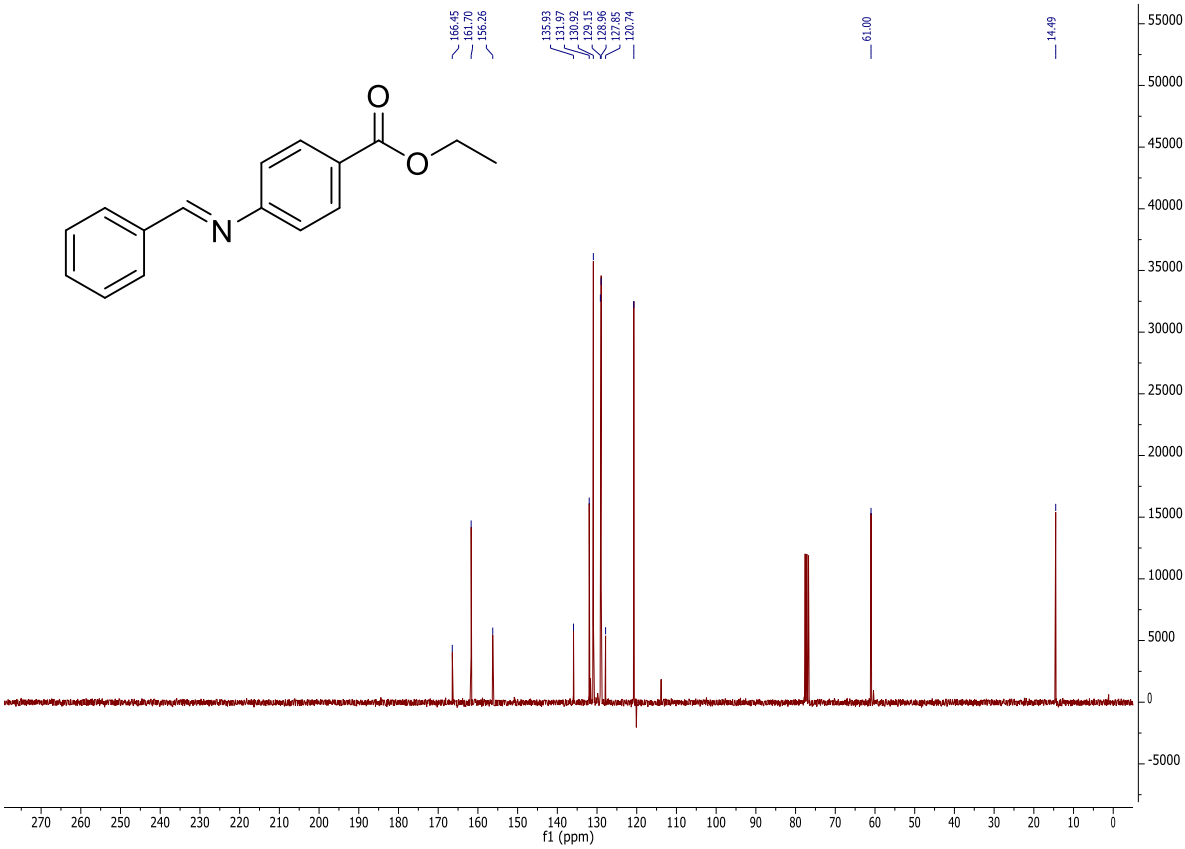

^{13}C NMR spectrum in $CDCl_3$.

273b

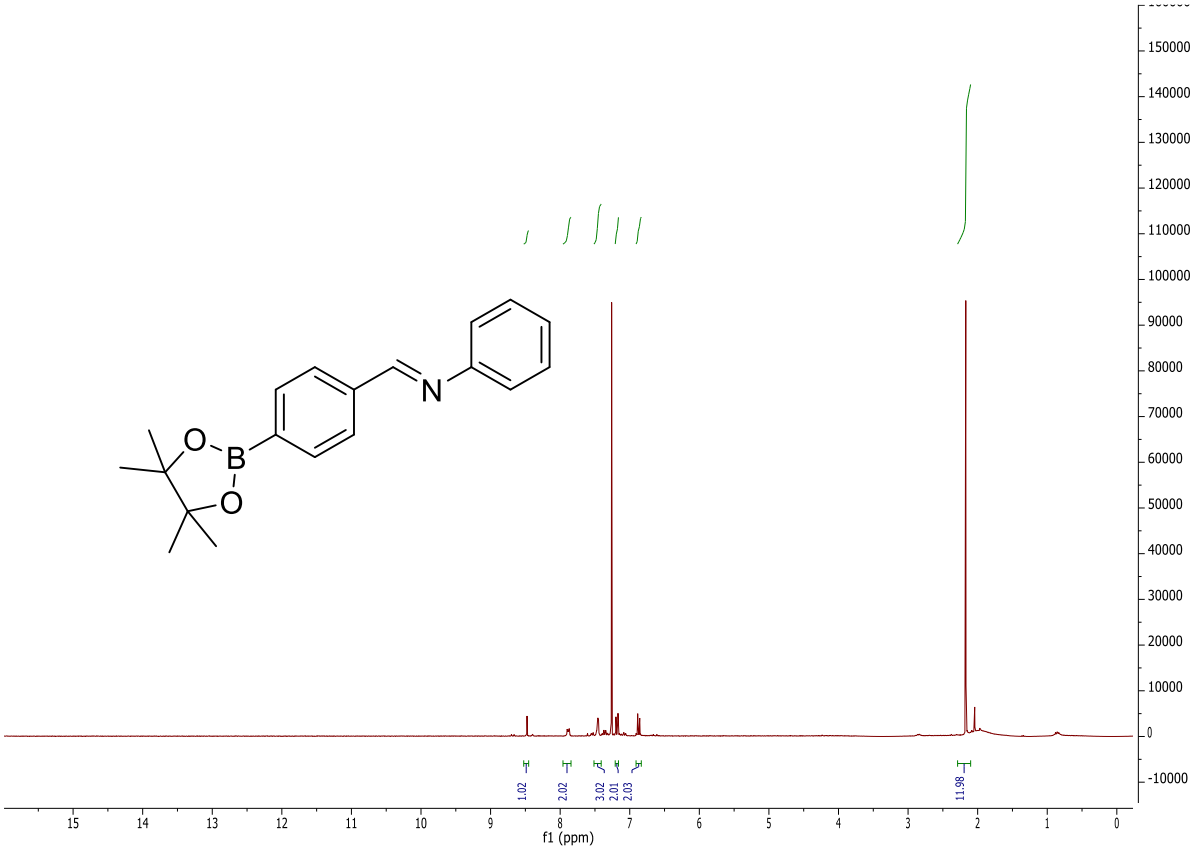

^{1}H NMR spectrum in $CDCl_3$.

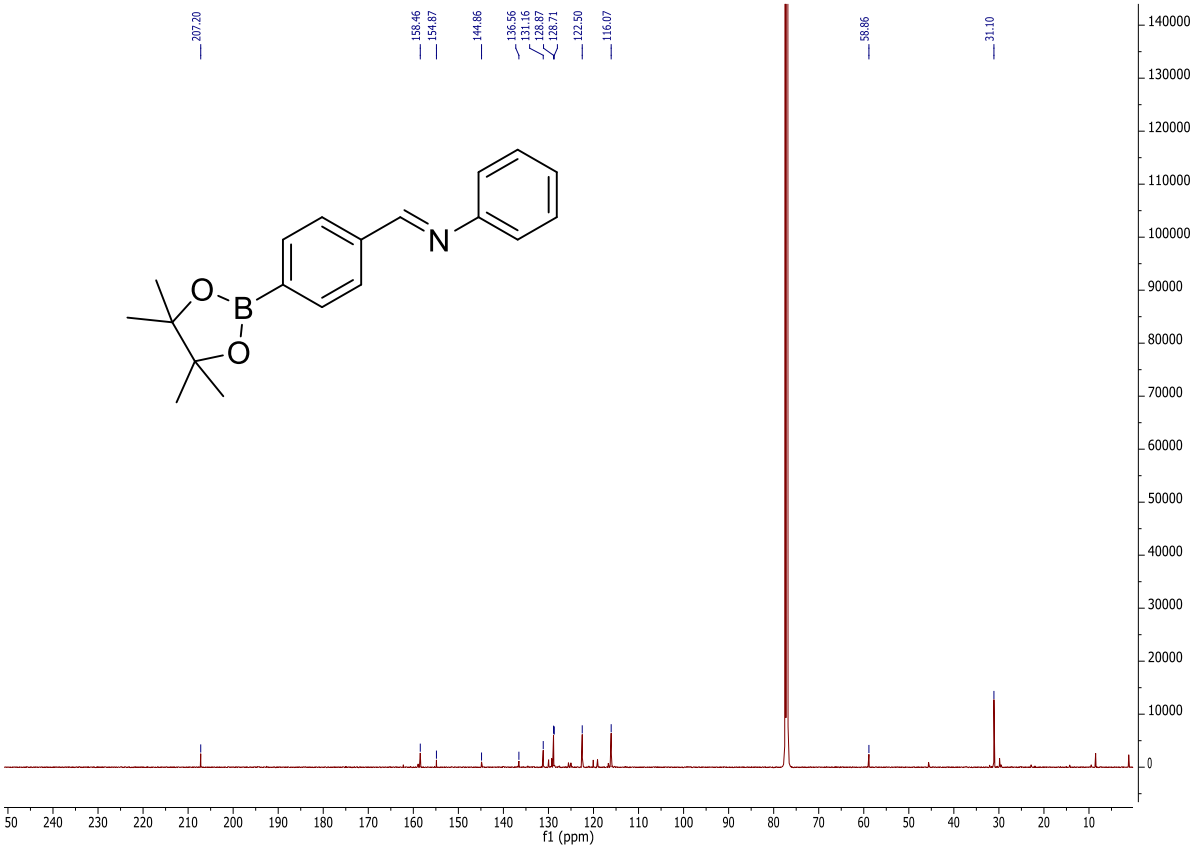

^{13}C NMR spectrum in $CDCl_3$.

274b

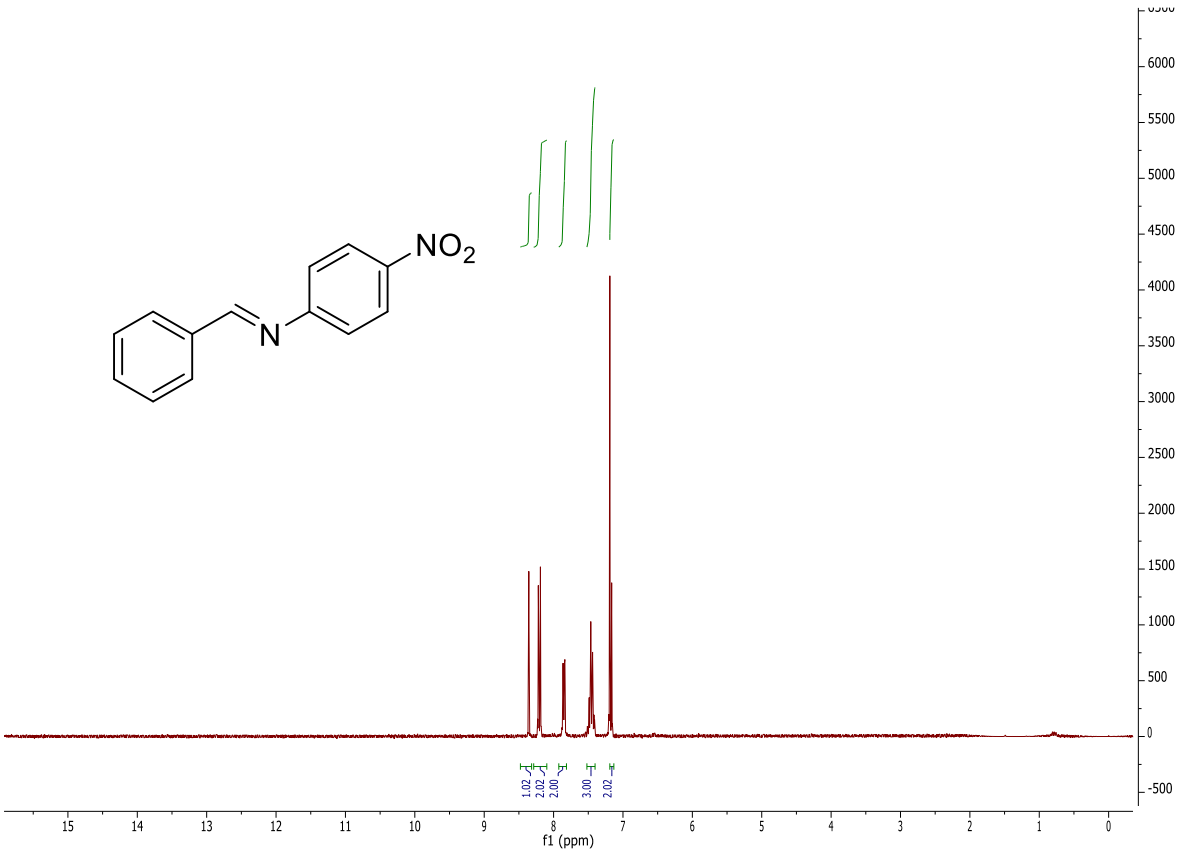

^{1}H NMR spectrum in $CDCl_3$.

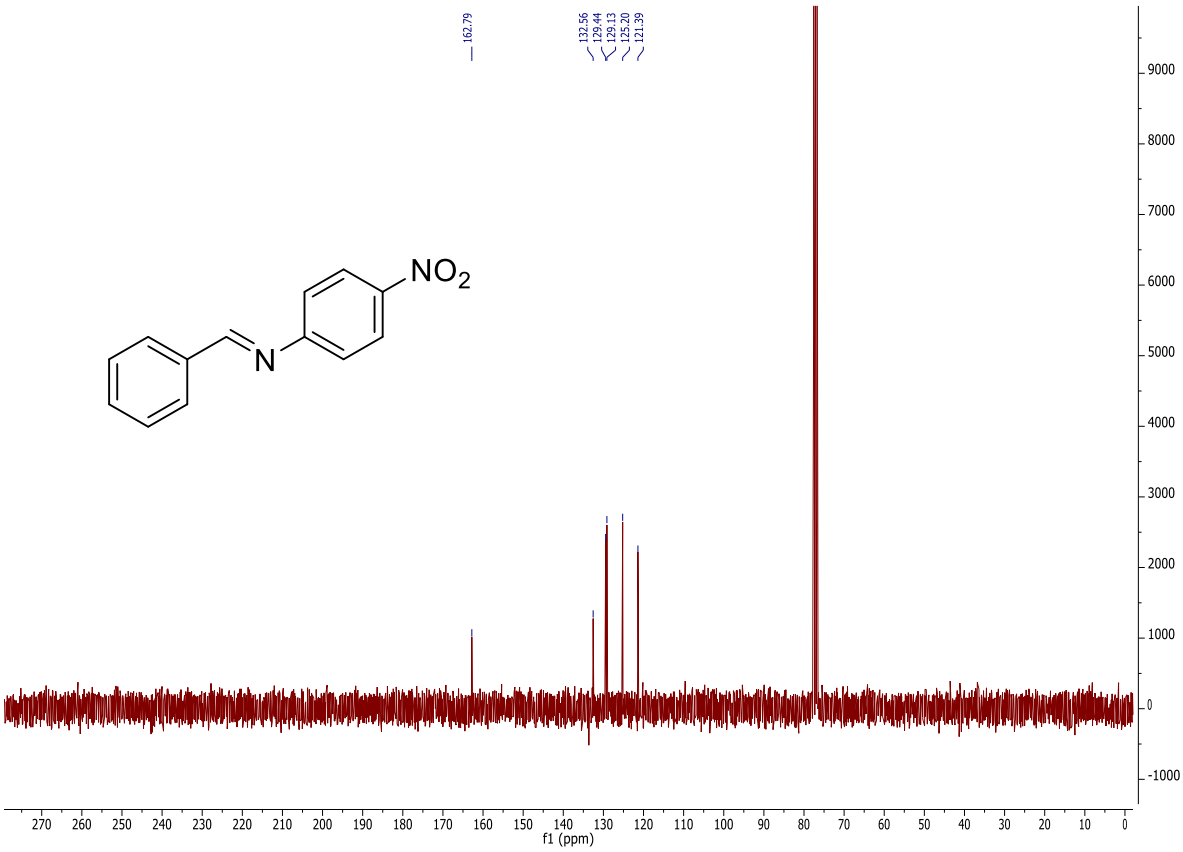

^{13}C NMR spectrum in $CDCl_3$.

275b

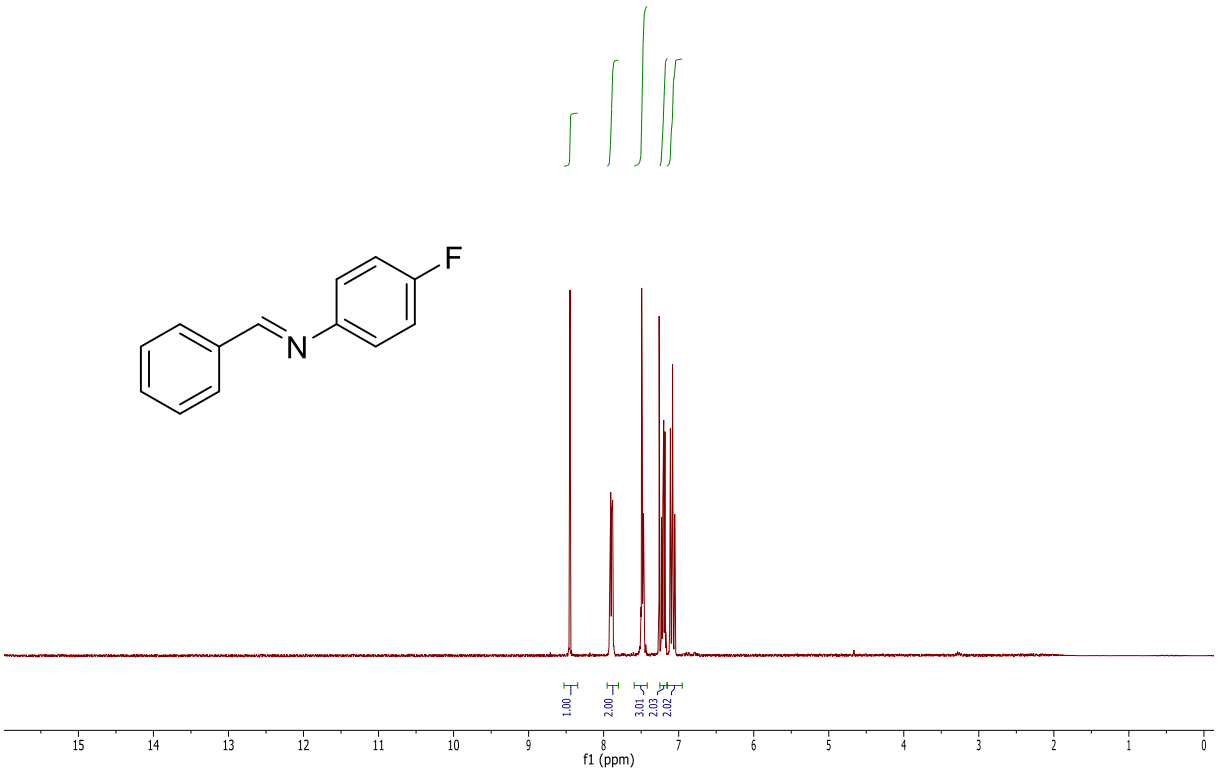

^{1}H NMR spectrum in $CDCl_3$.

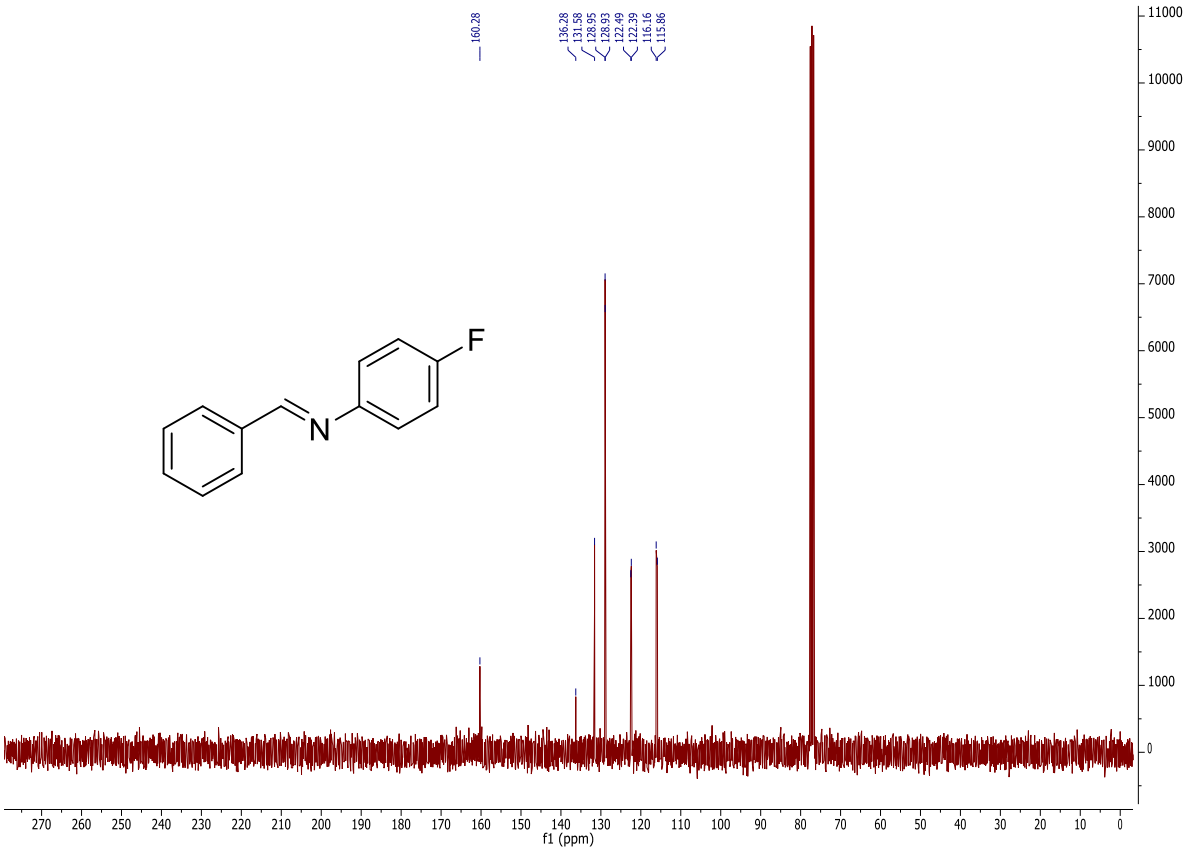

^{13}C NMR spectrum in $CDCl_3$.

276b

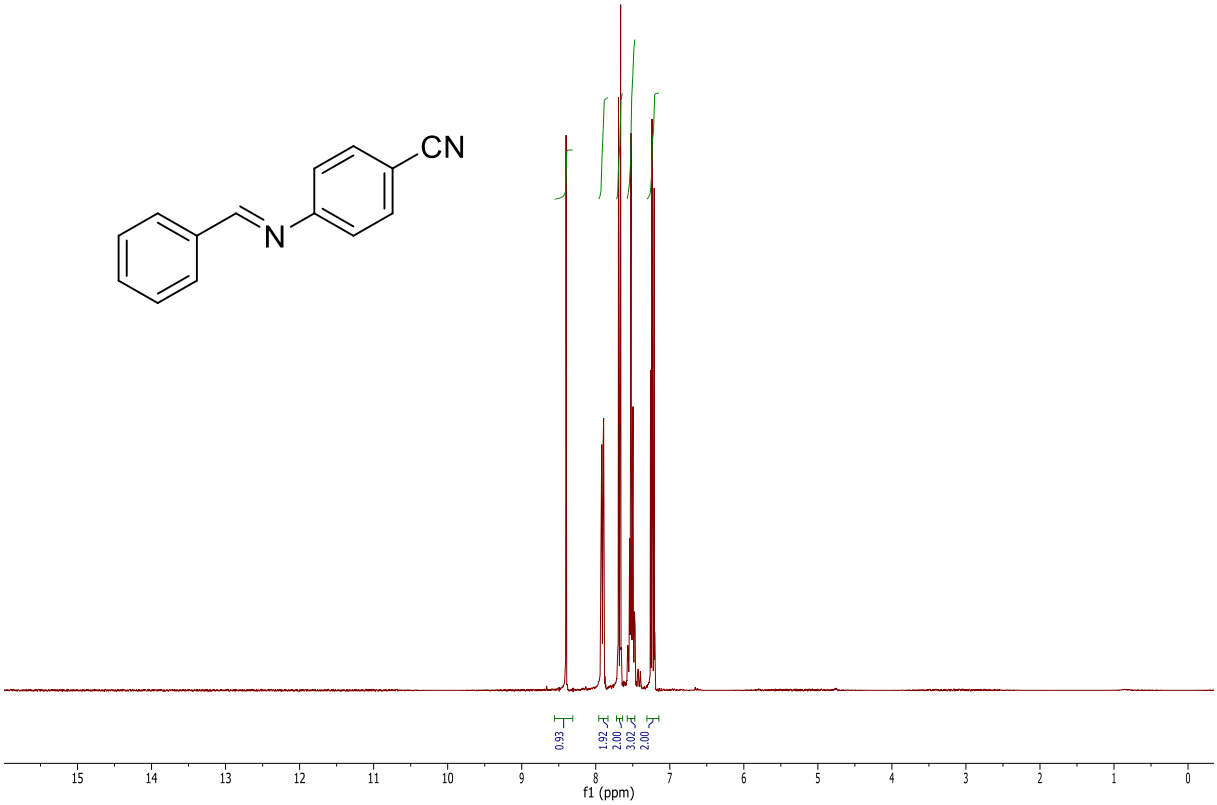

^{1}H NMR spectrum in $CDCl_3$.

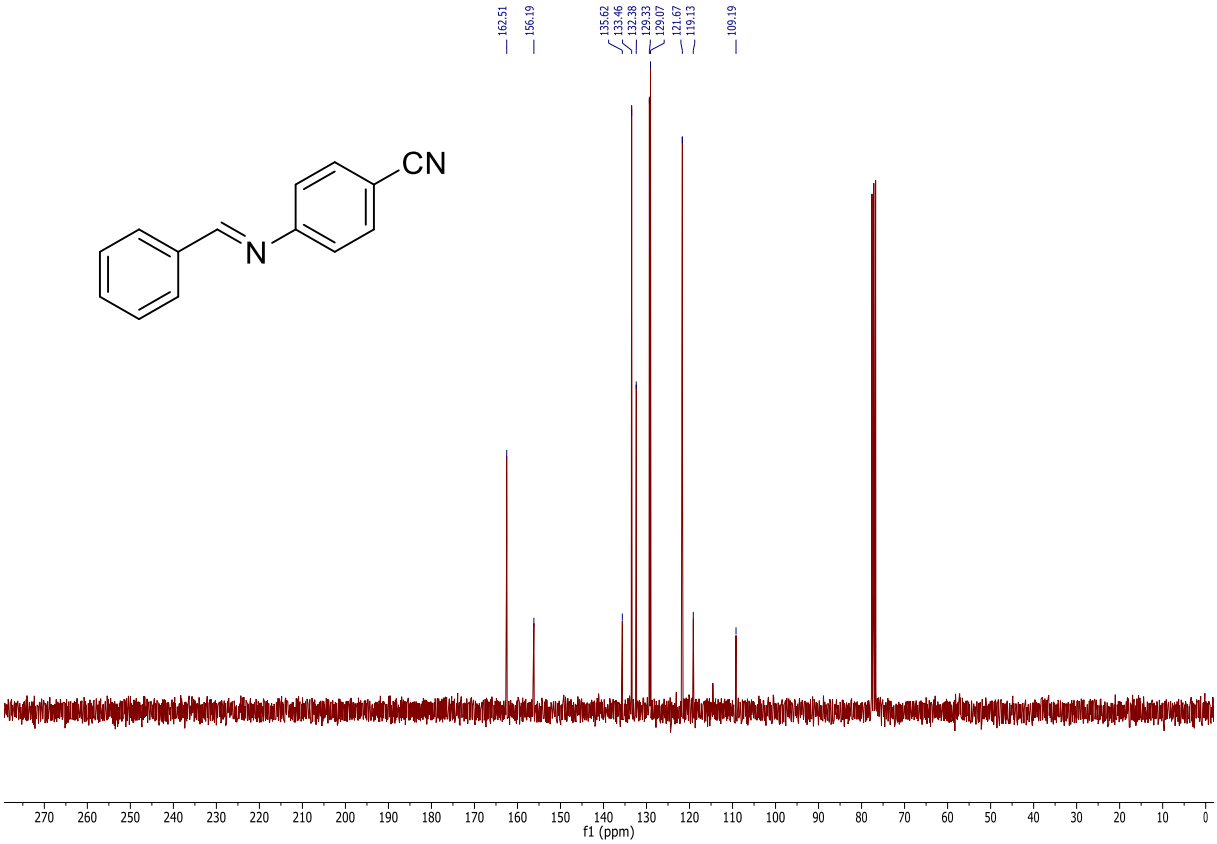

^{13}C NMR spectrum in $CDCl_3$.

277b

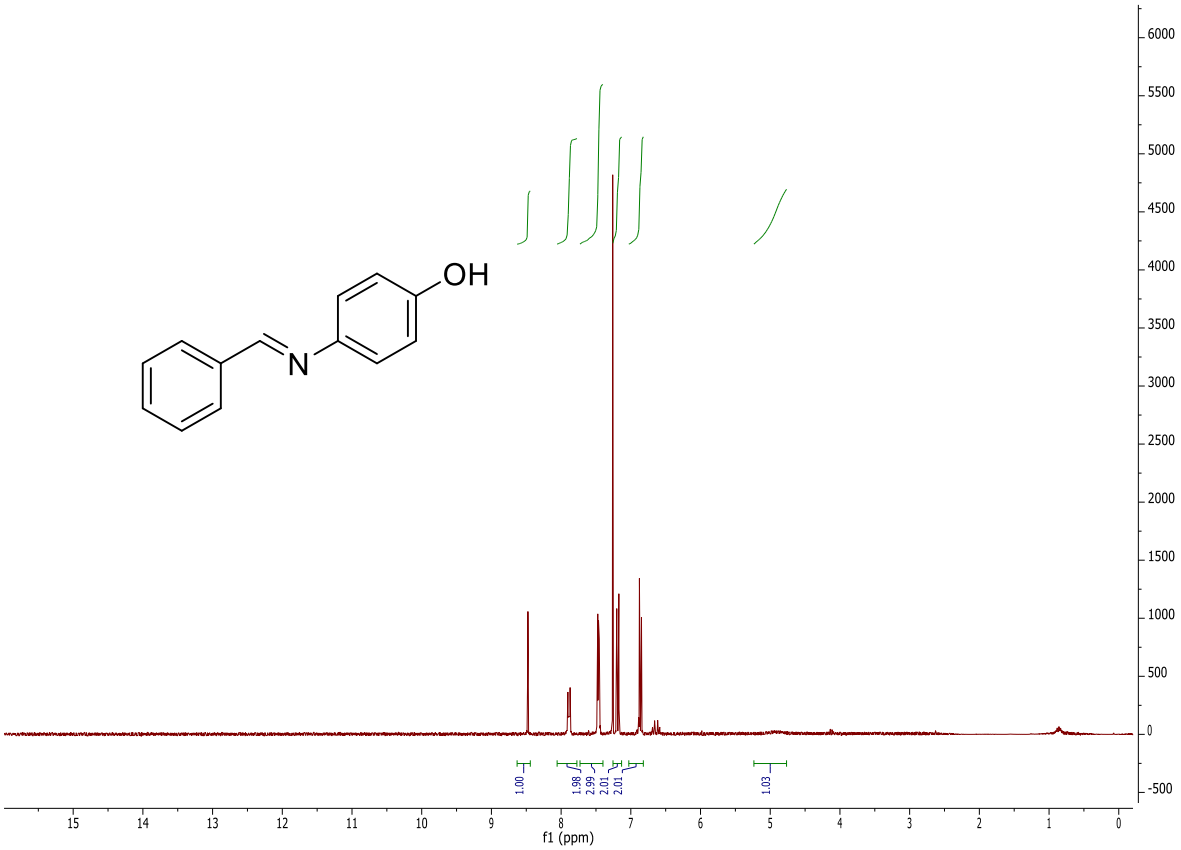

^{1}H NMR spectrum in $CDCl_3$.

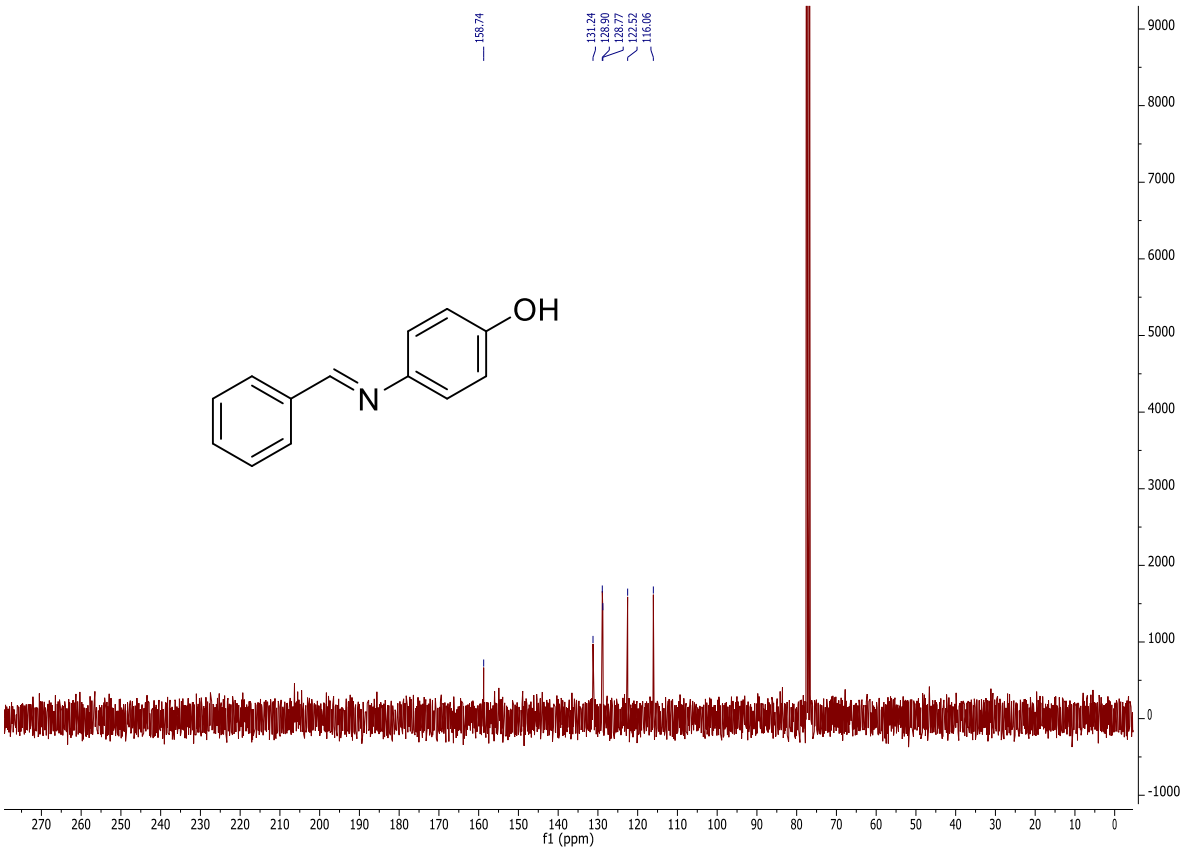

^{13}C NMR spectrum in $CDCl_3$.

278b

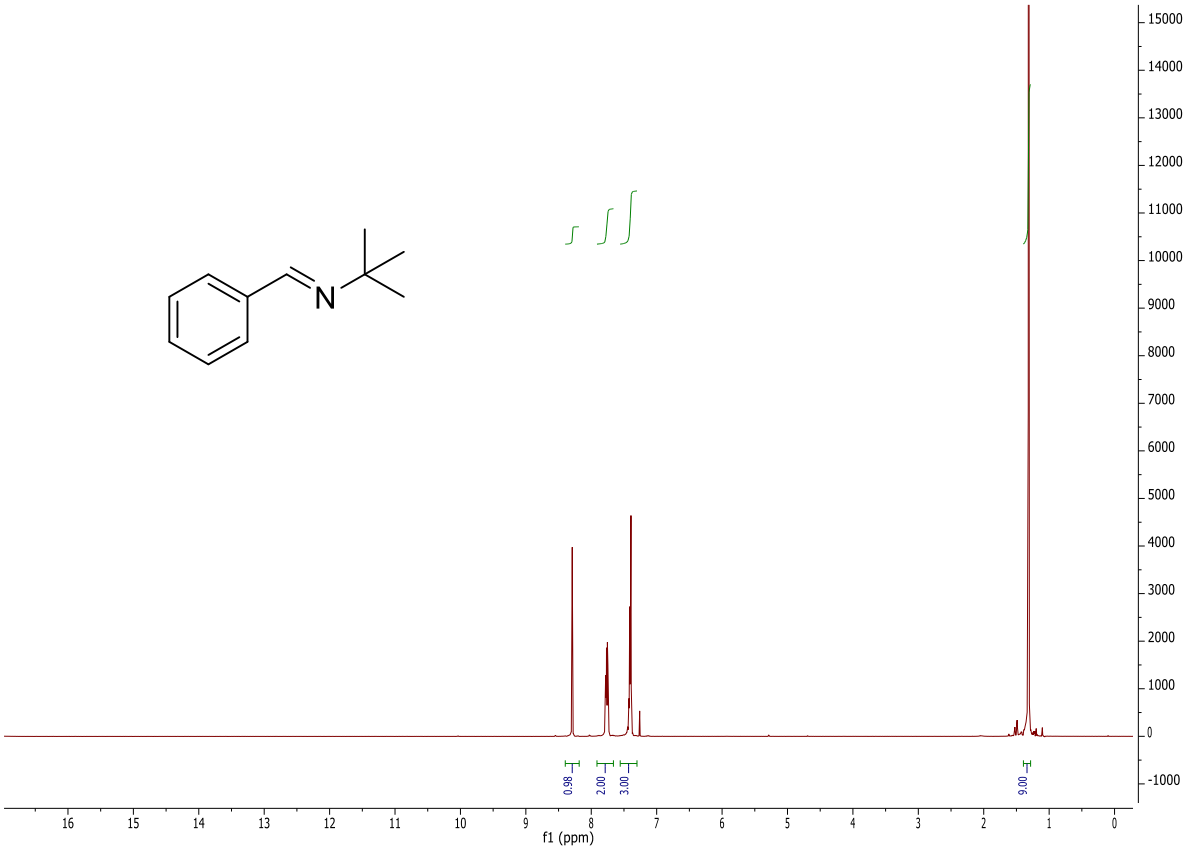

^{1}H NMR spectrum in $CDCl_3$.

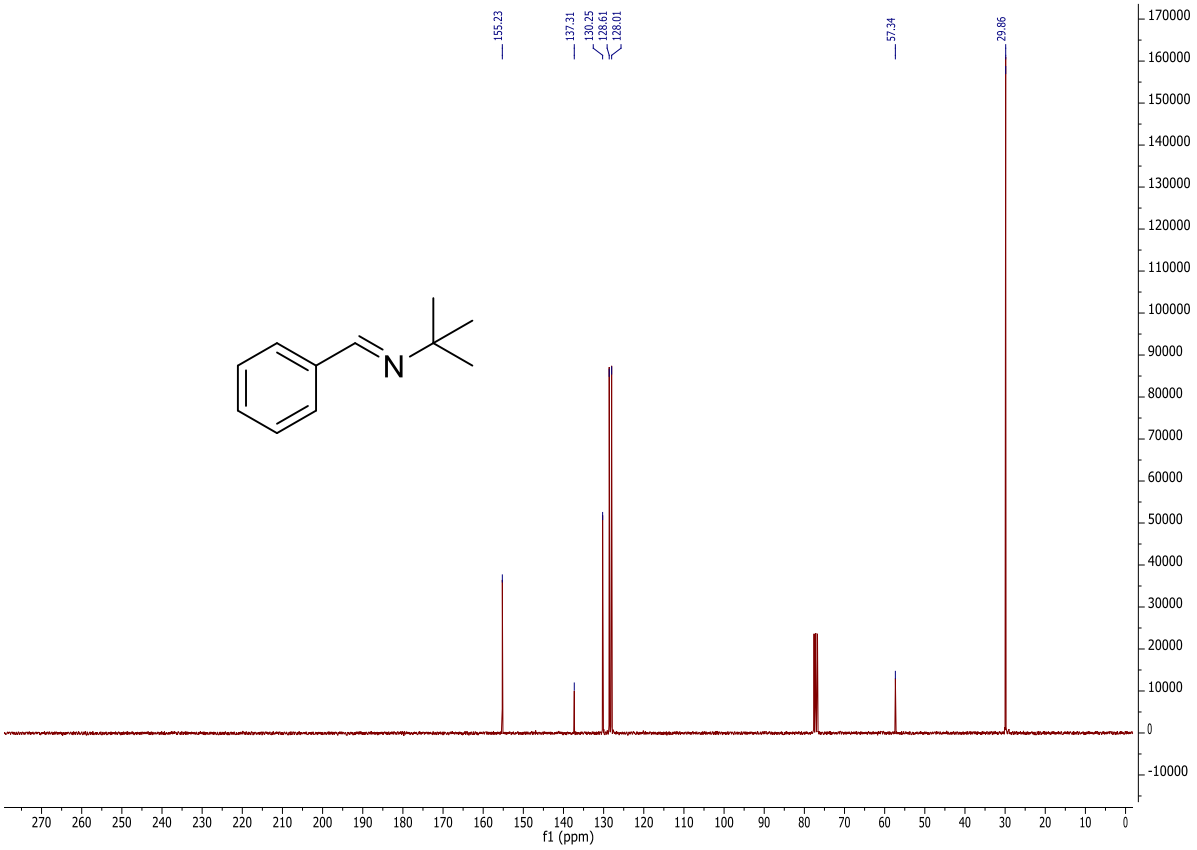

^{13}C NMR spectrum in $CDCl_3$.

279b

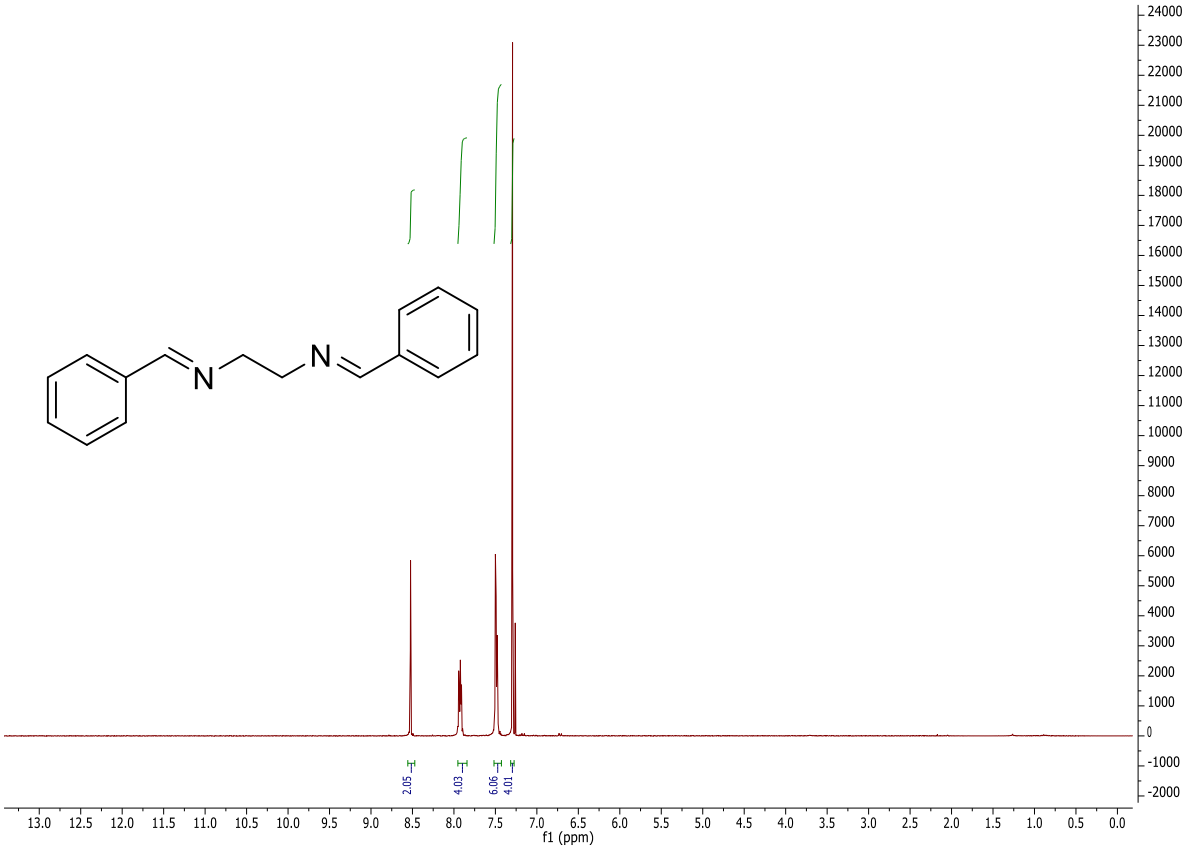

^{1}H NMR spectrum in $CDCl_3$.

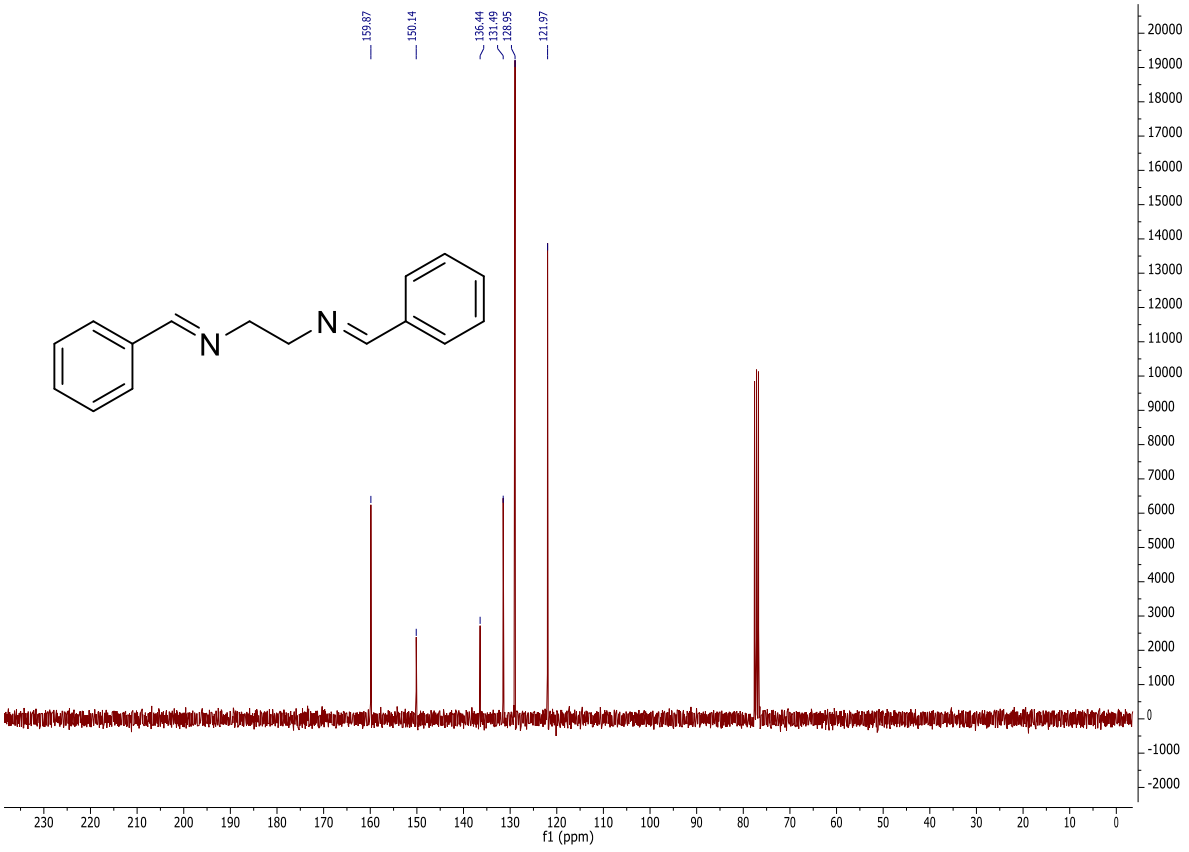

^{13}C NMR spectrum in $CDCl_3$.

280b

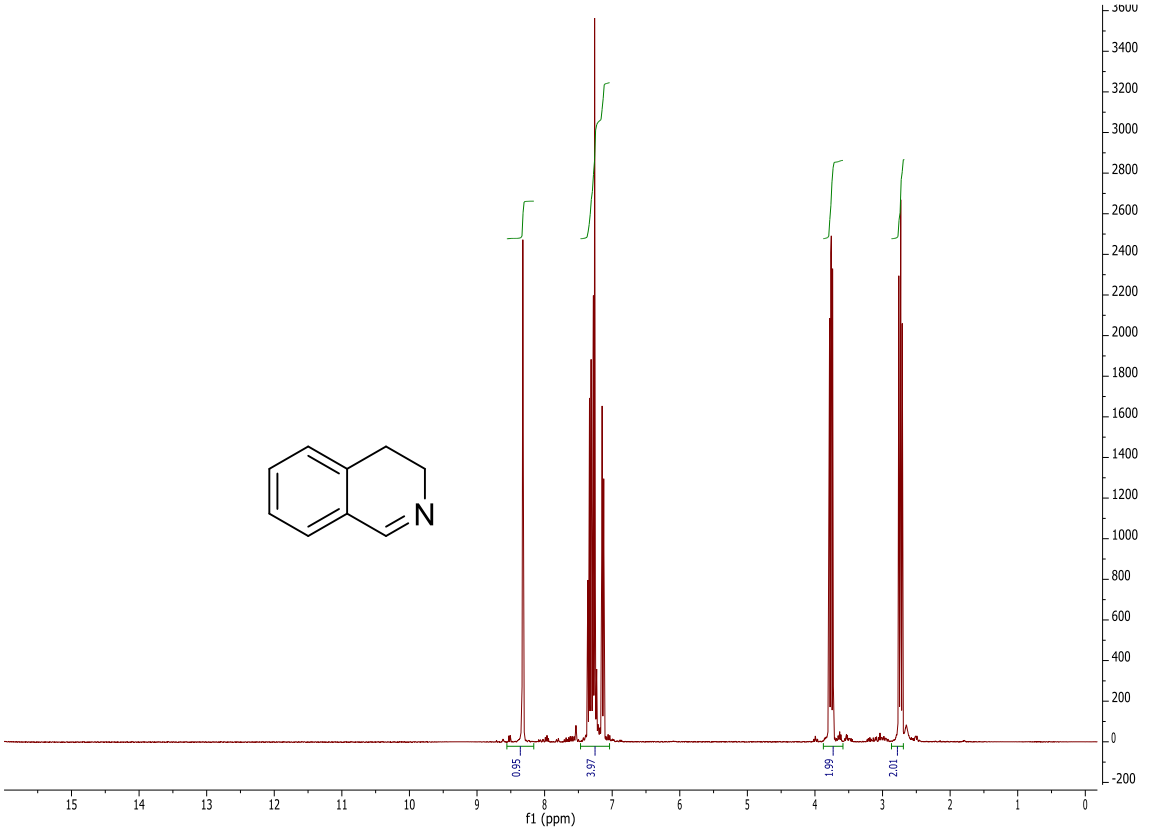

^{1}H NMR spectrum in $CDCl_3$.

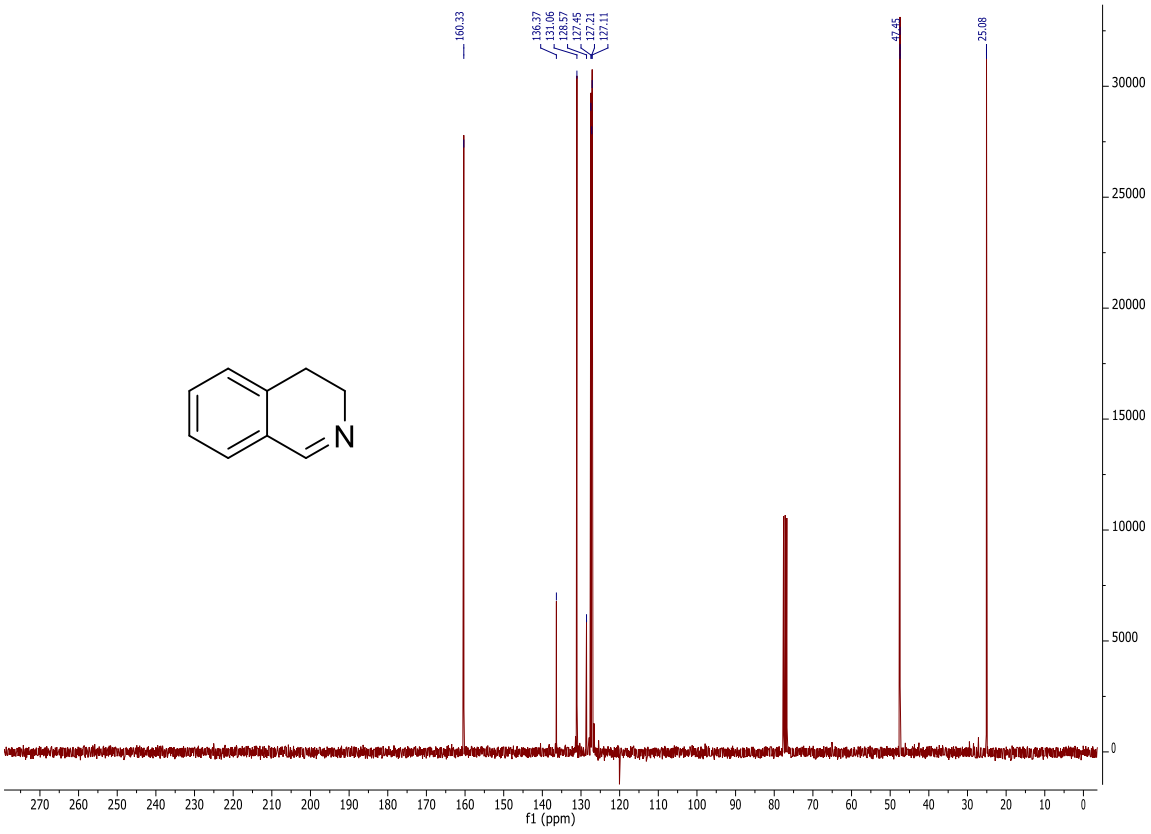

^{13}C NMR spectrum in $CDCl_3$.

281b

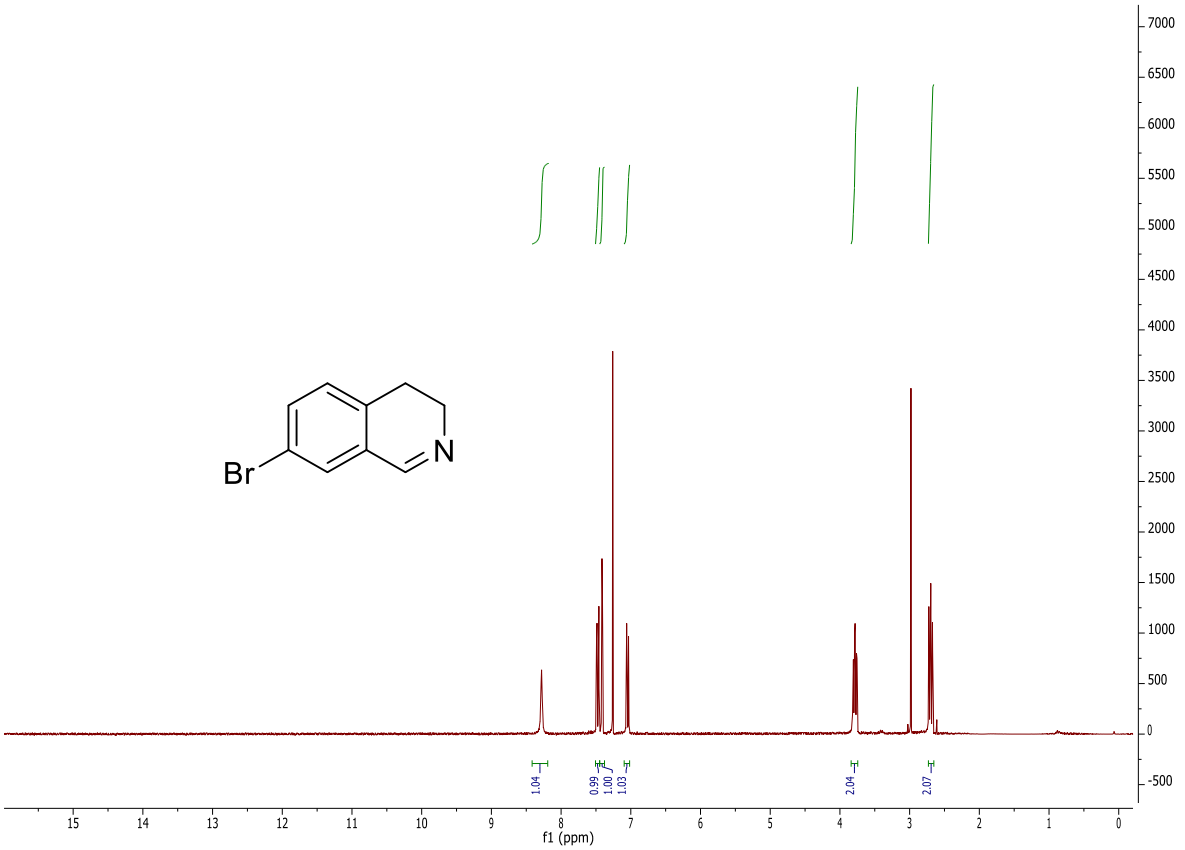

^{1}H NMR spectrum in $CDCl_3$.

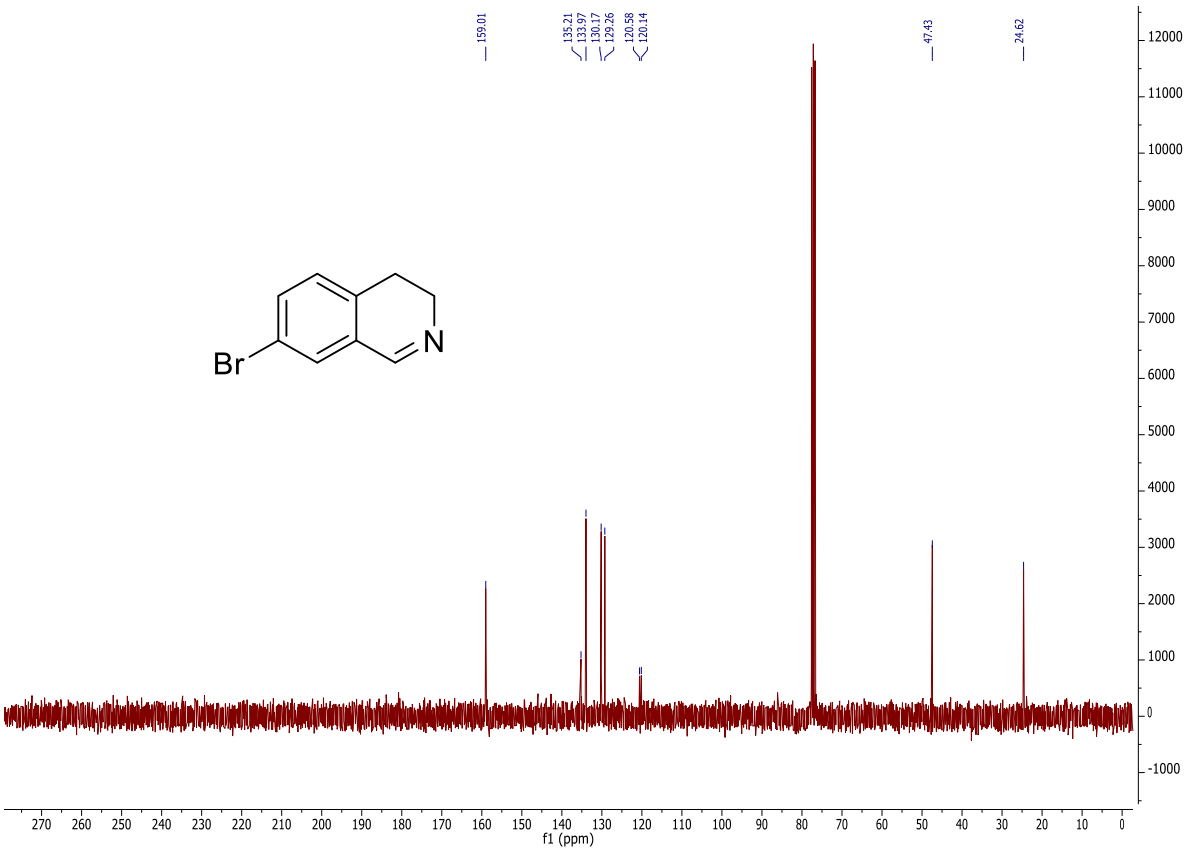

^{13}C NMR spectrum in $CDCl_3$.

282b

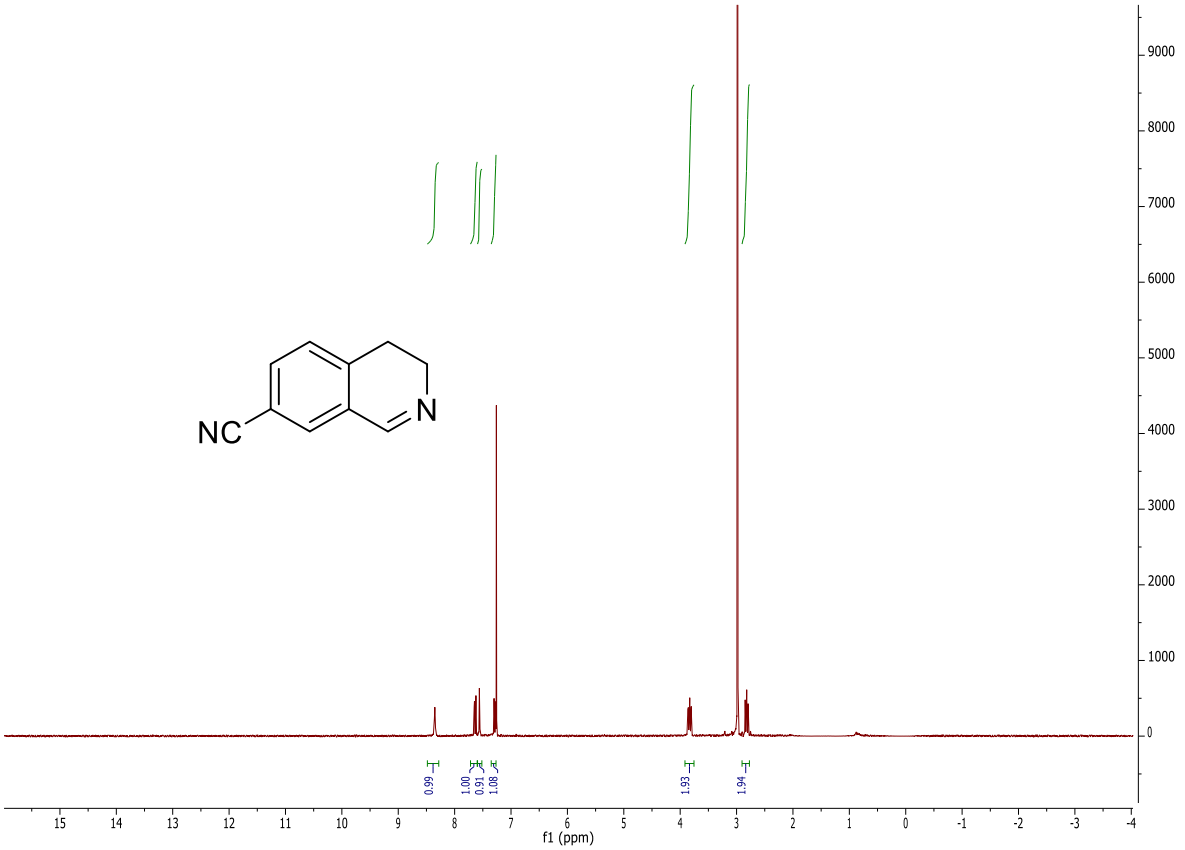

^{1}H NMR spectrum in $CDCl_3$.

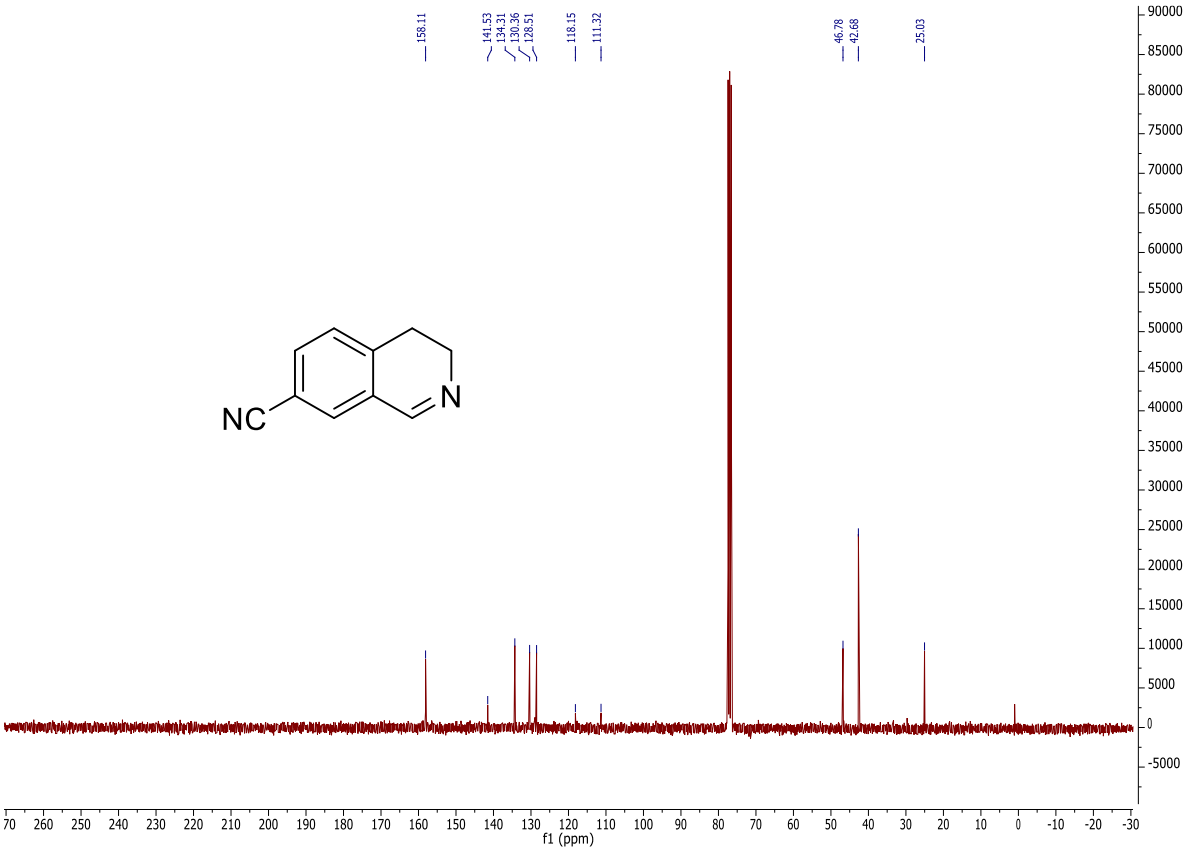

^{13}C NMR spectrum in $CDCl_3$.

283b

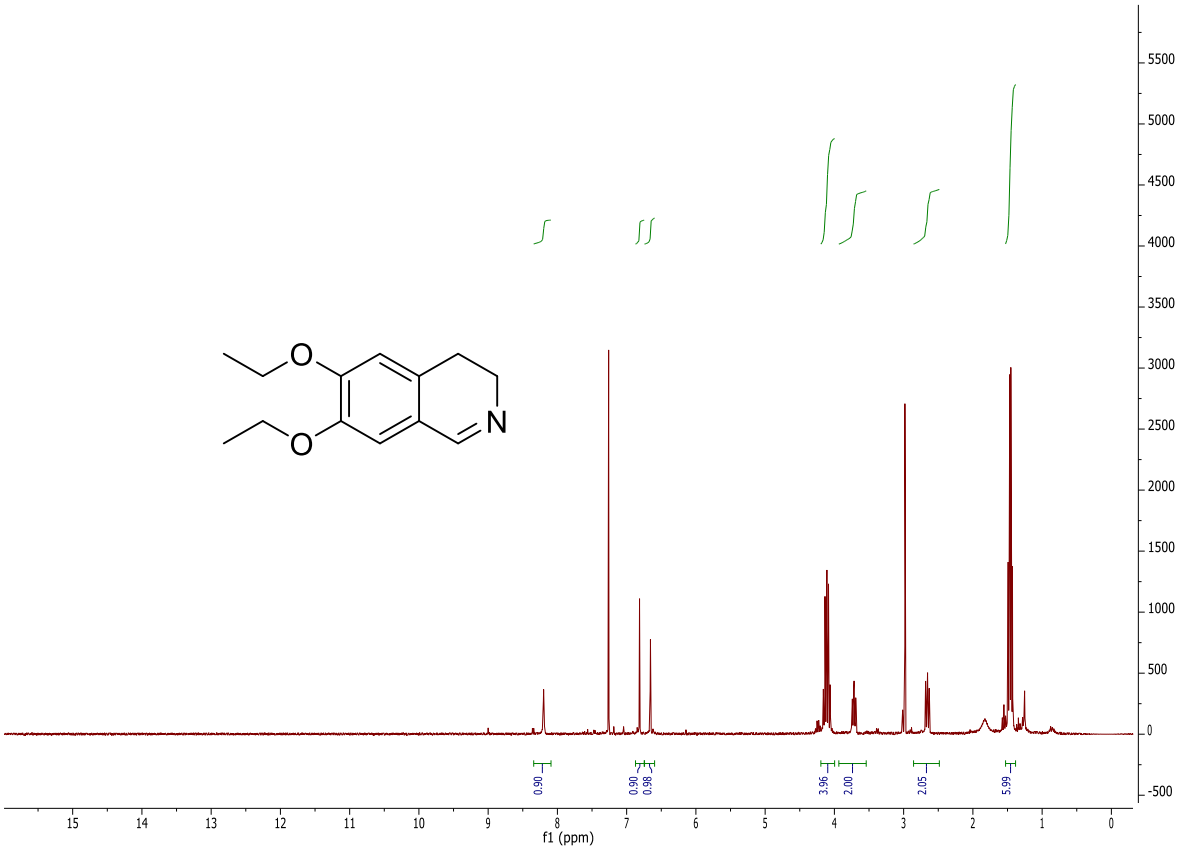

^{1}H NMR spectrum in $CDCl_3$.

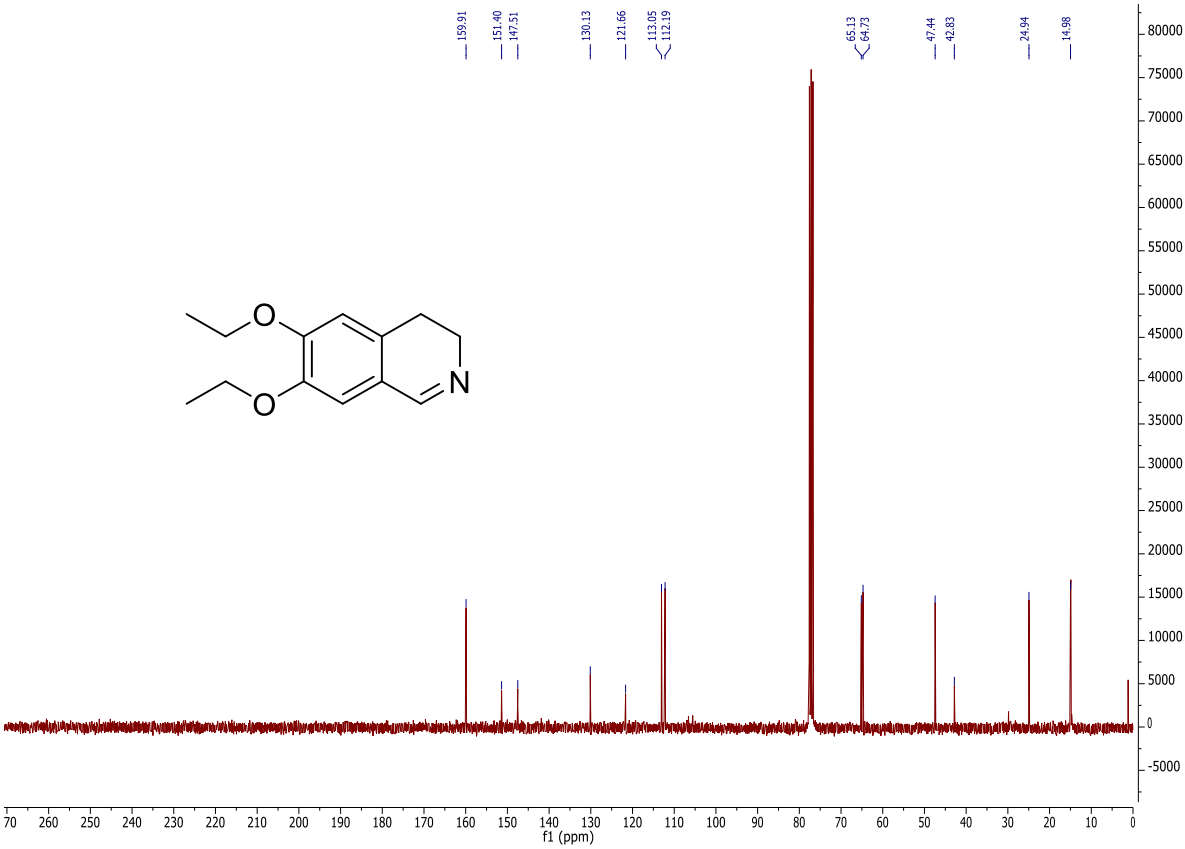

^{13}C NMR spectrum in $CDCl_3$.

284b

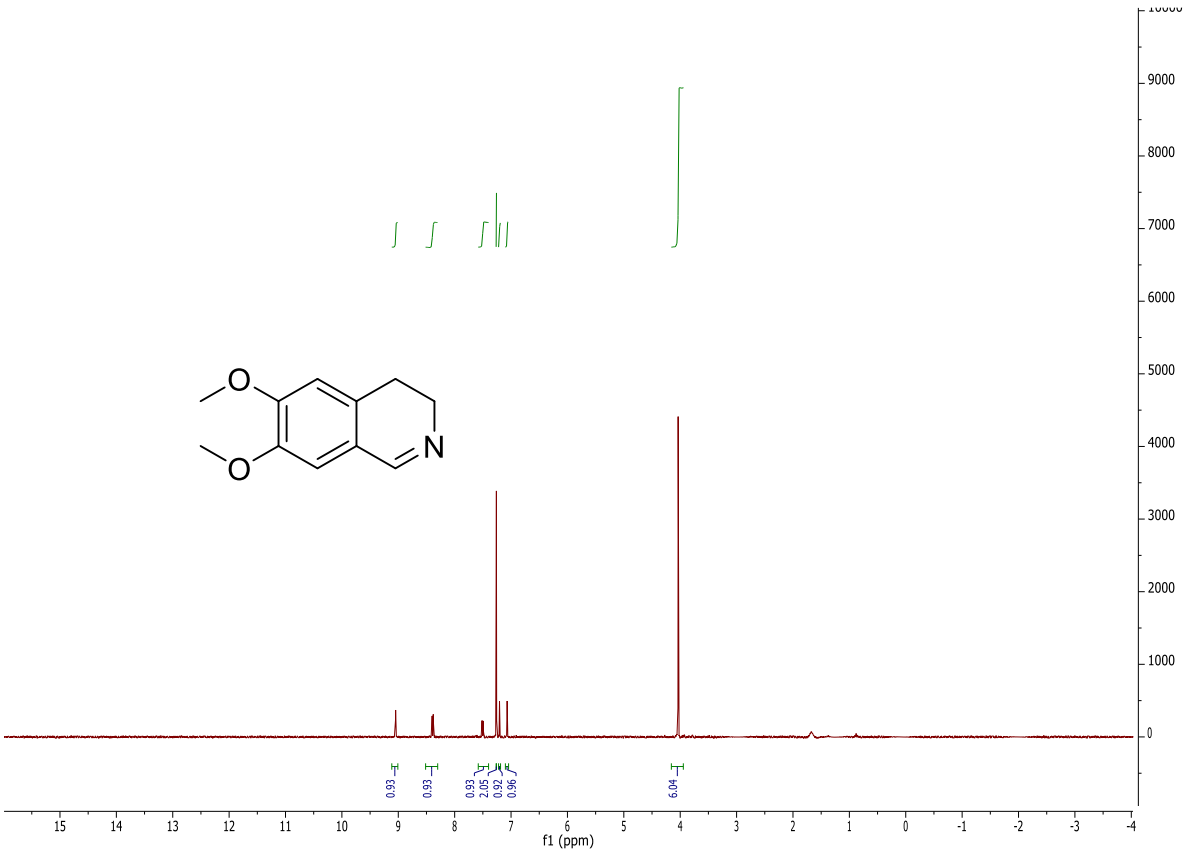

^{1}H NMR spectrum in $CDCl_3$.

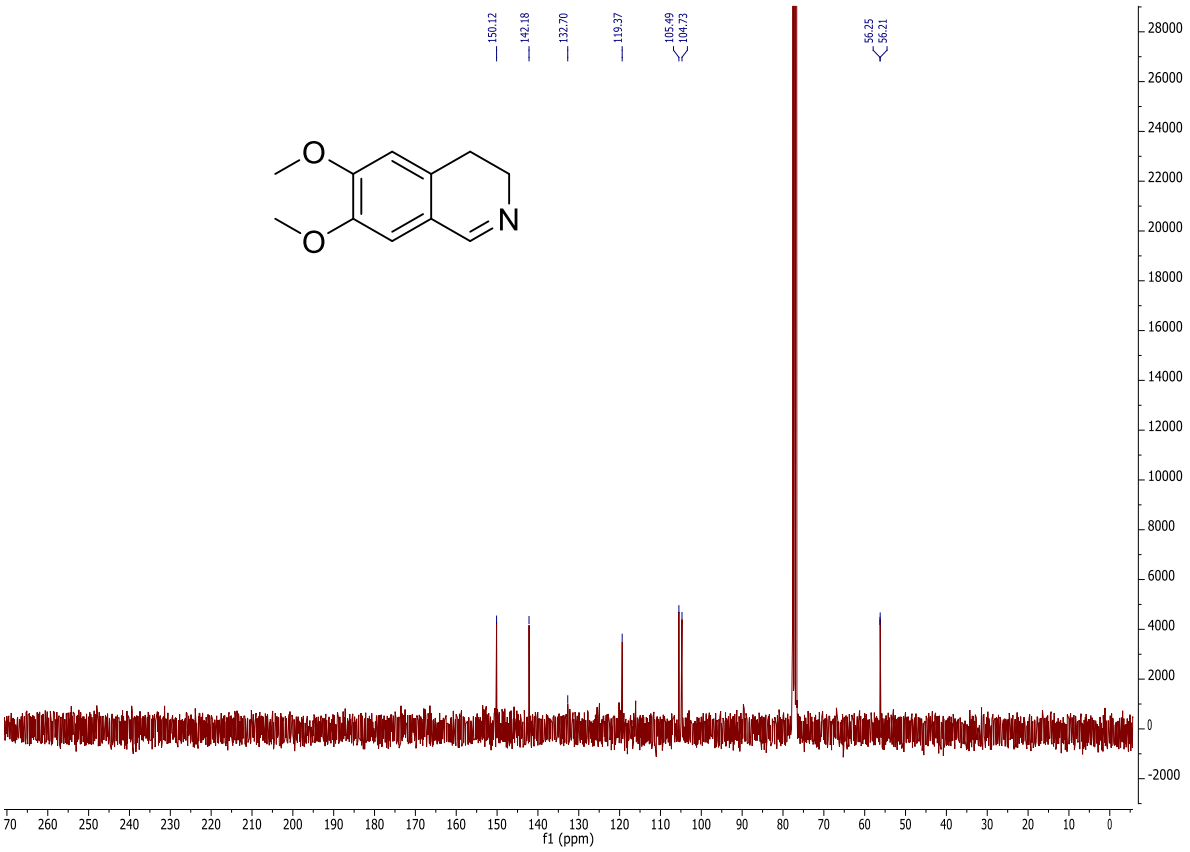

^{13}C NMR spectrum in $CDCl_3$.

285b

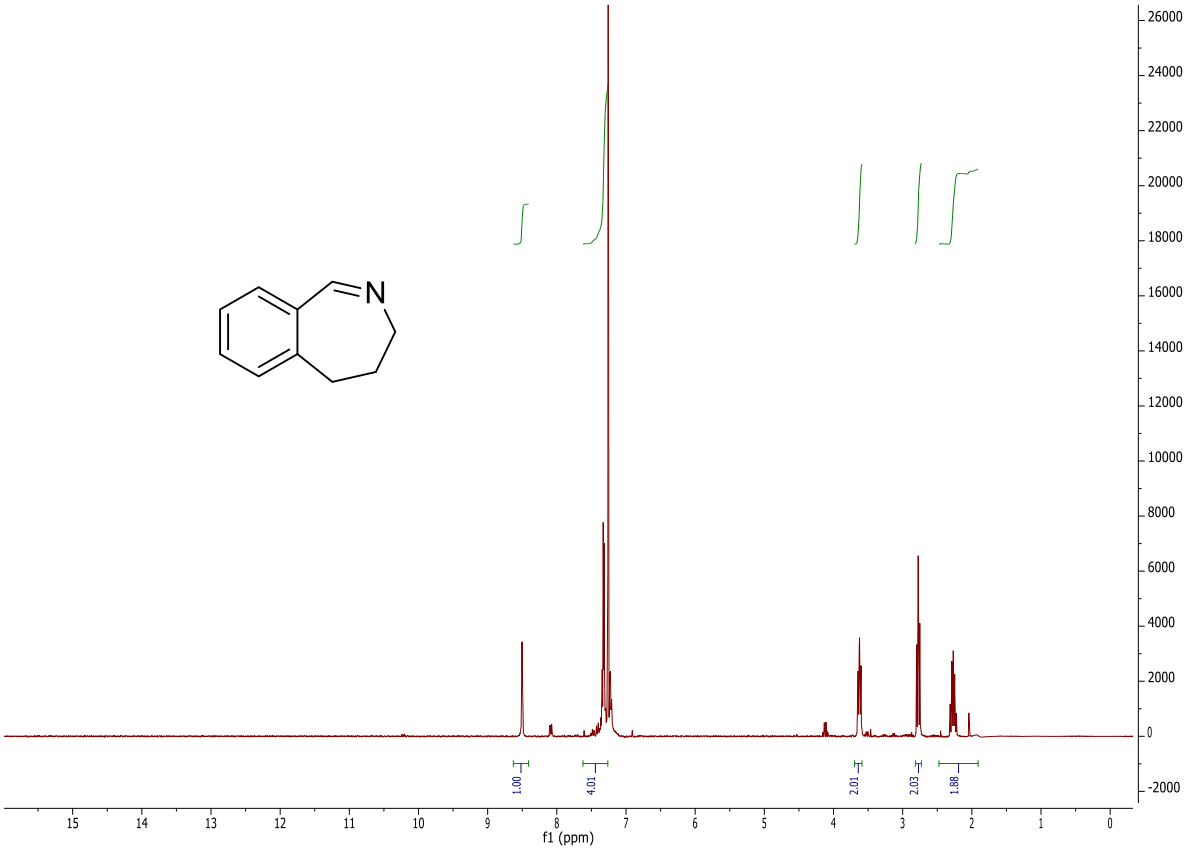

^{1}H NMR spectrum in $CDCl_3$.

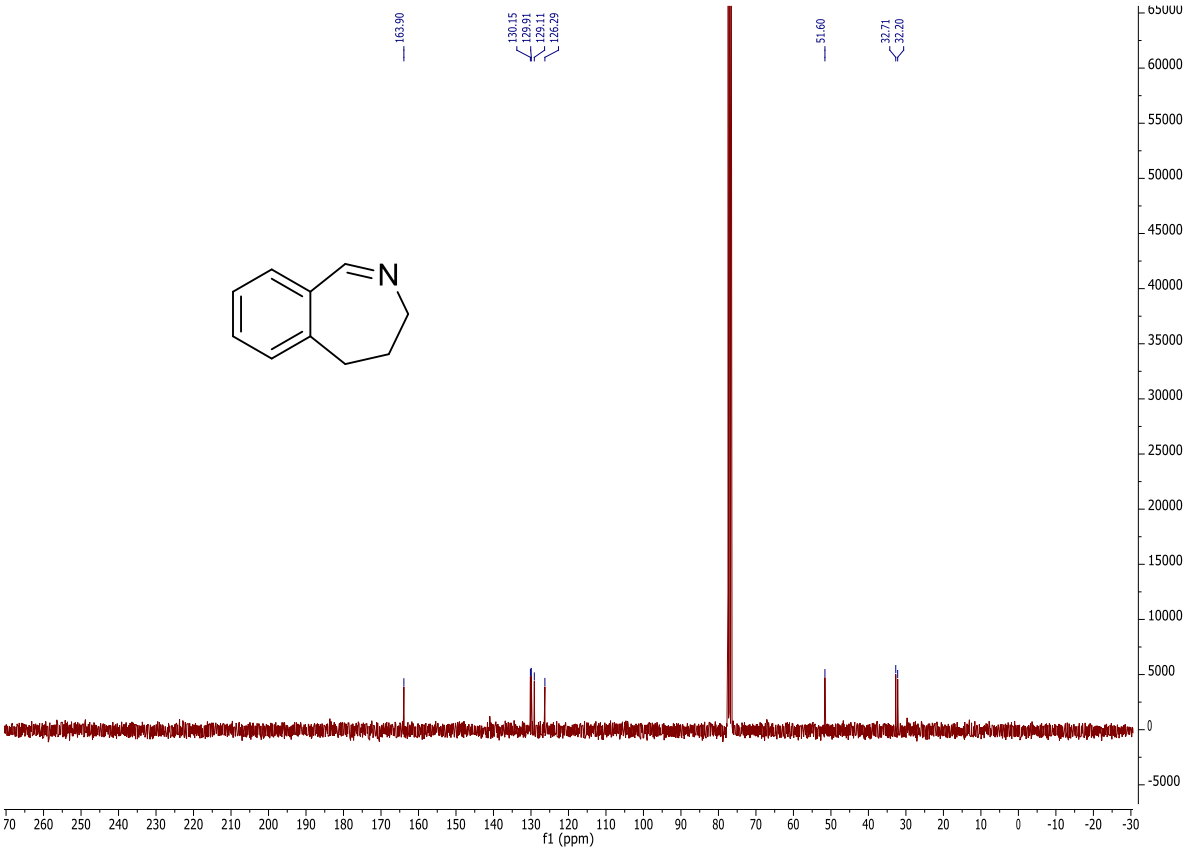

^{13}C NMR spectrum in $CDCl_3$.

286b

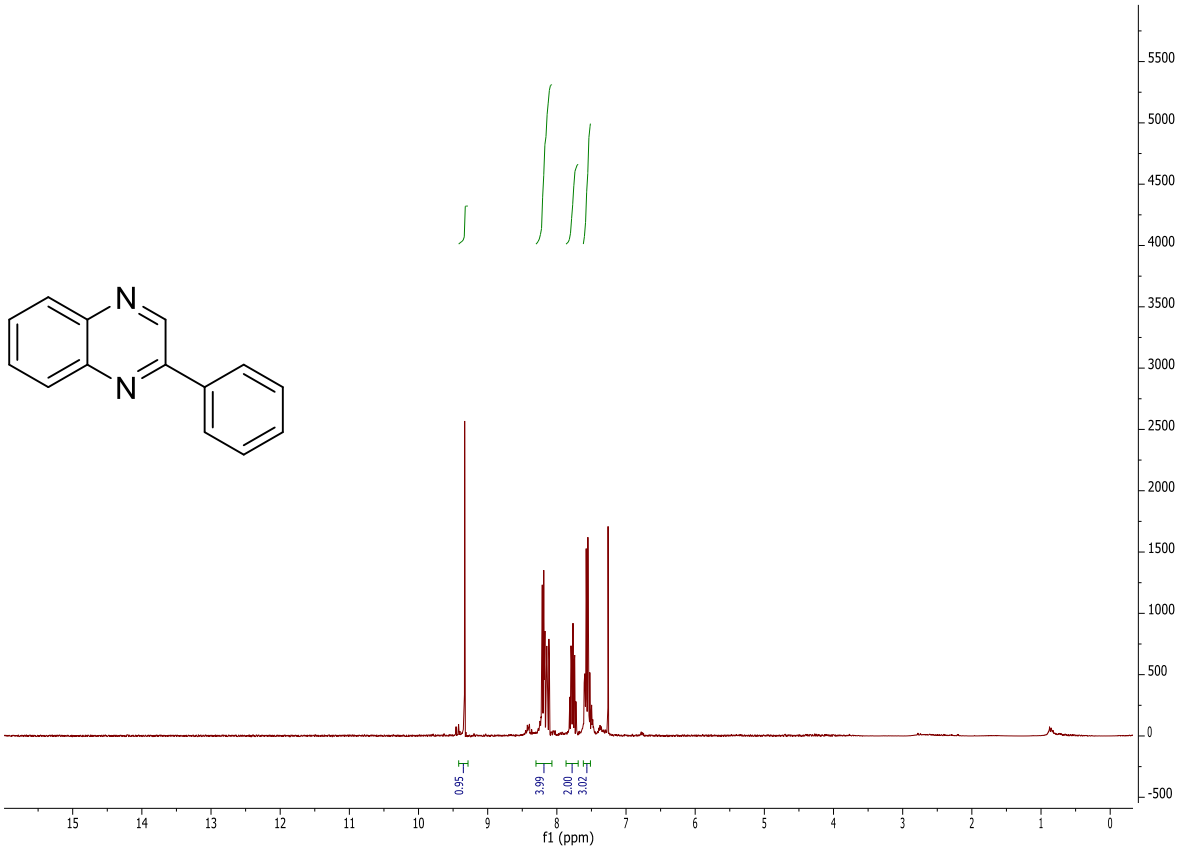

^{1}H NMR spectrum in $CDCl_3$.

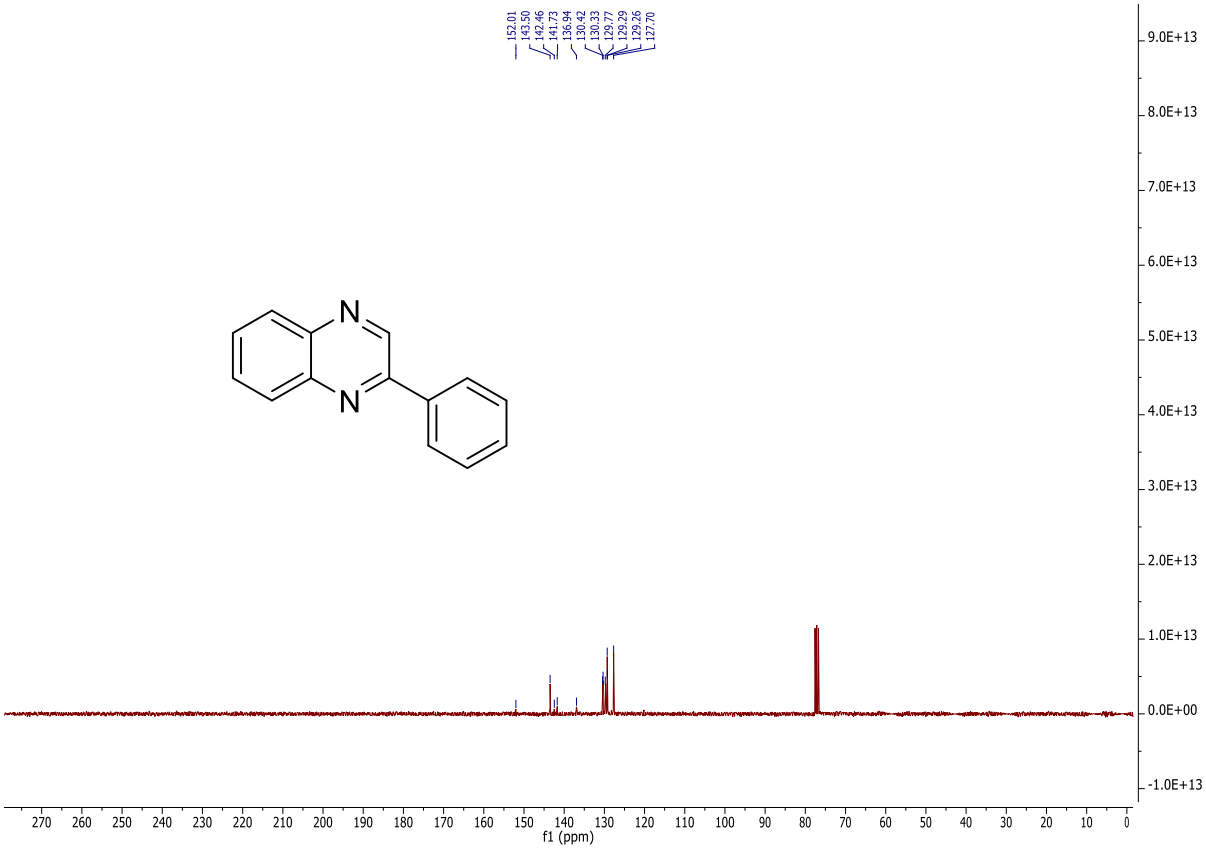

^{13}C NMR spectrum in $CDCl_3$.

287b

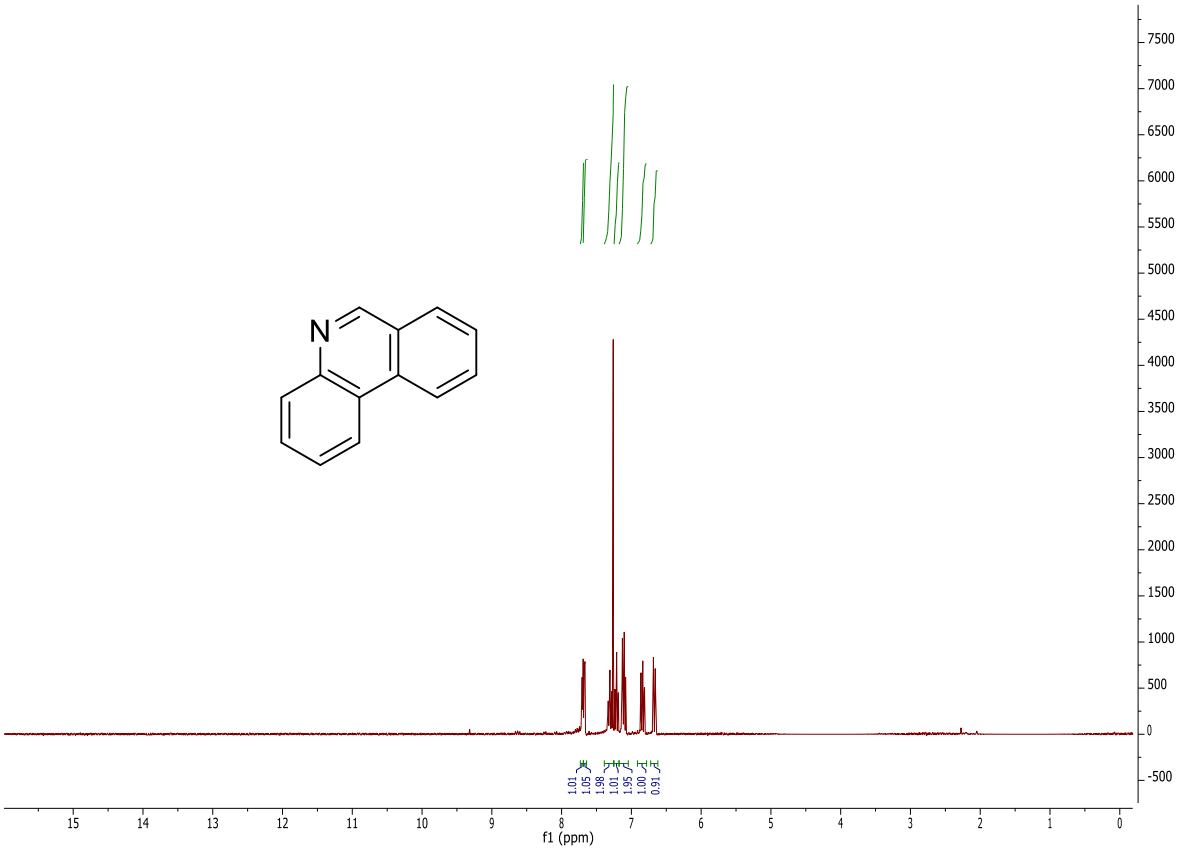

^{1}H NMR spectrum in $CDCl_3$.

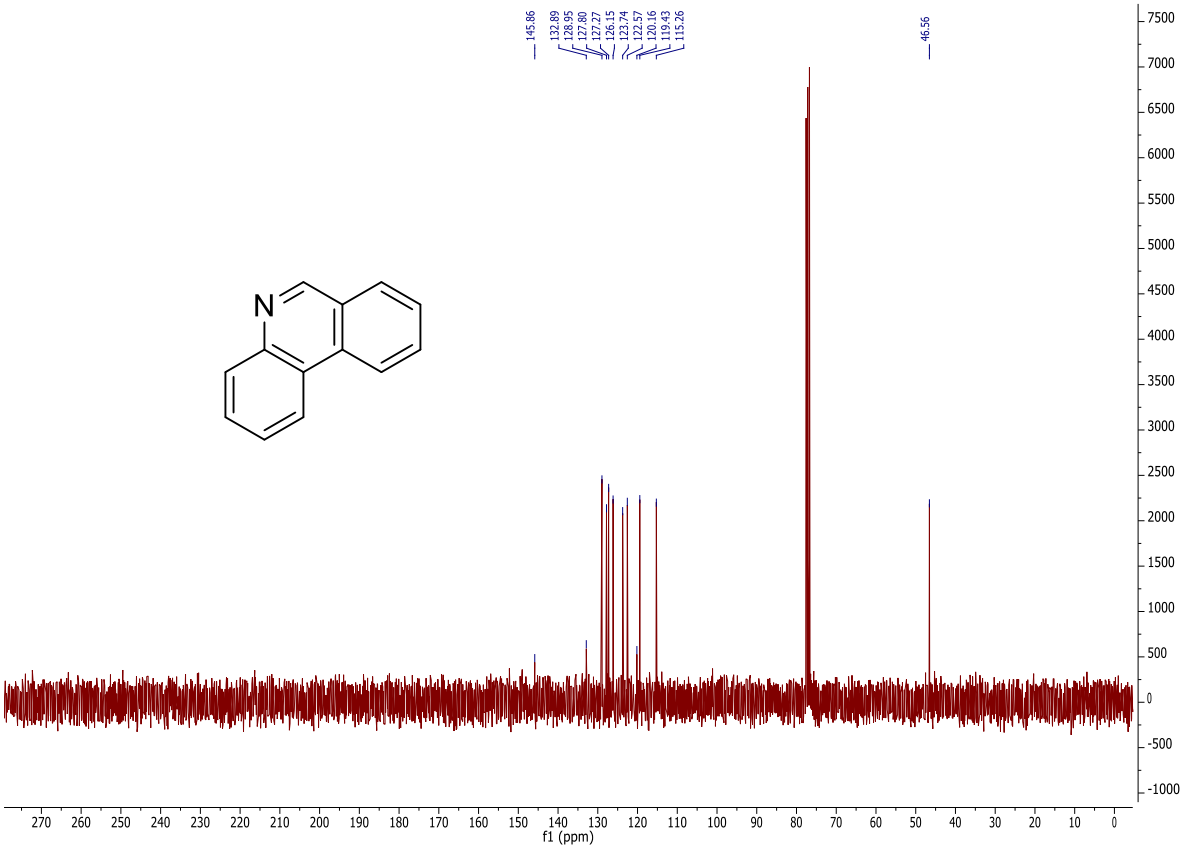

^{13}C NMR spectrum in $CDCl_3$.

288b

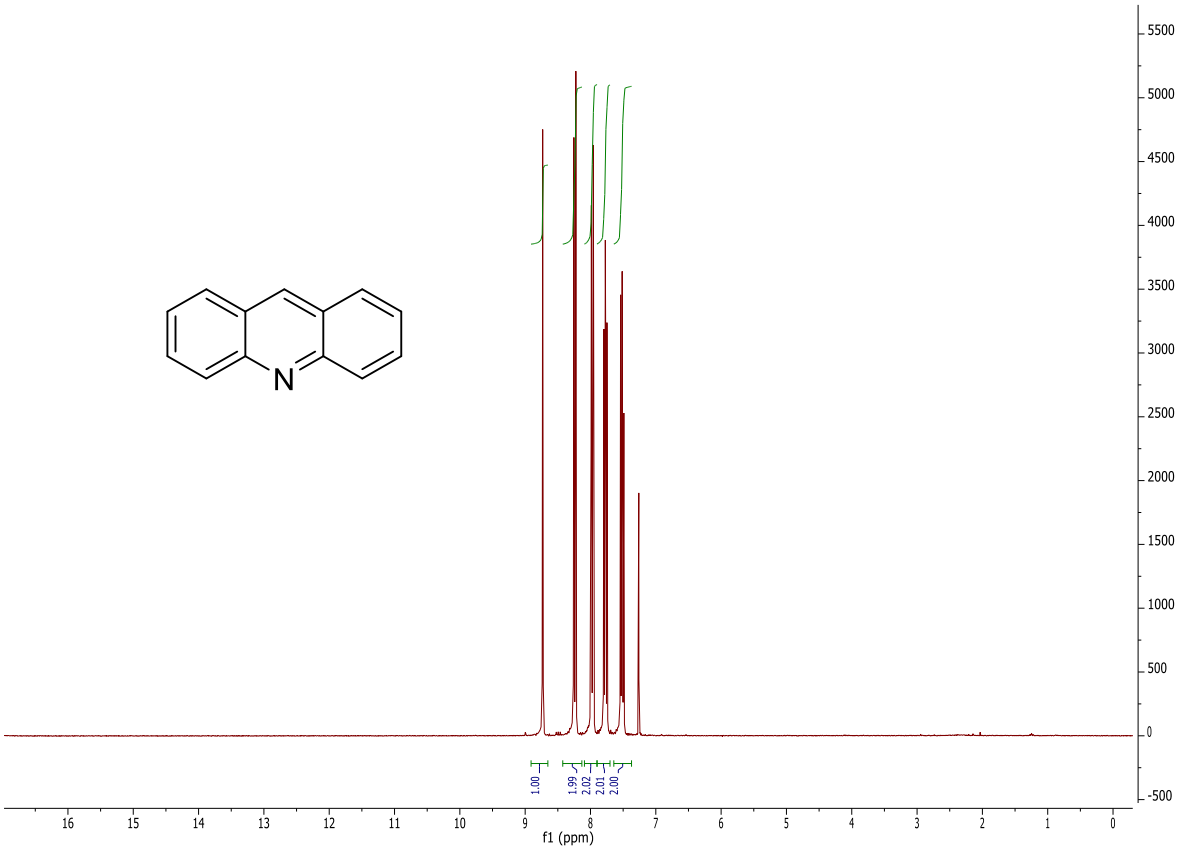

^{1}H NMR spectrum in $CDCl_3$.

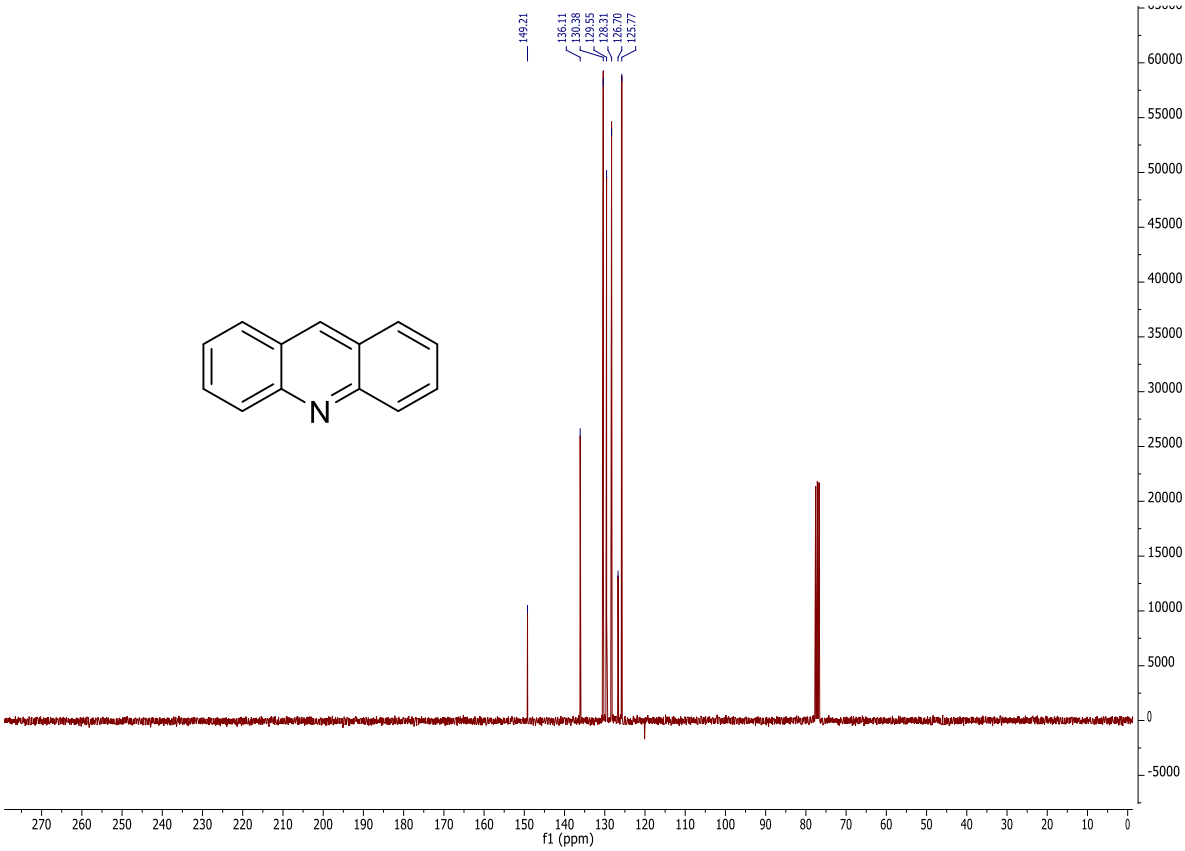

^{13}C NMR spectrum in $CDCl_3$.

289b

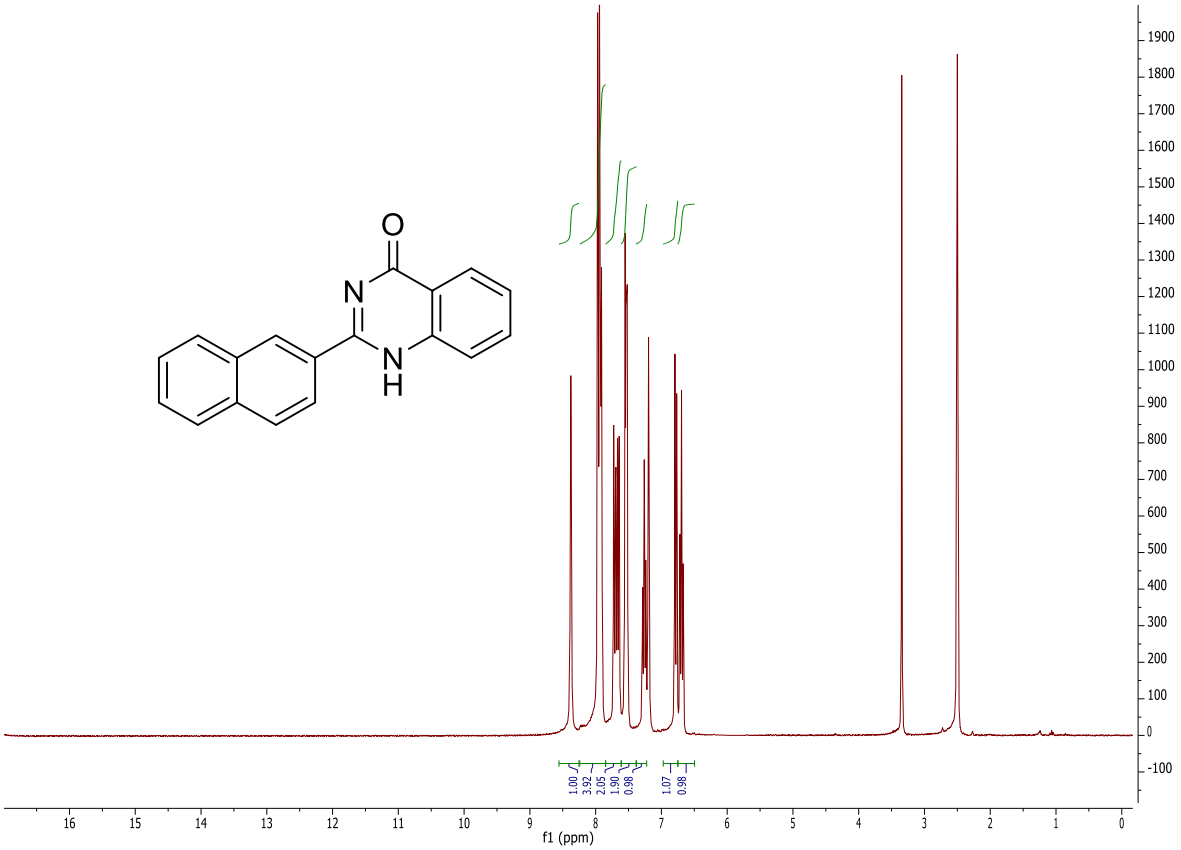

^{1}H NMR spectrum in DMSO-*d*$_6$.

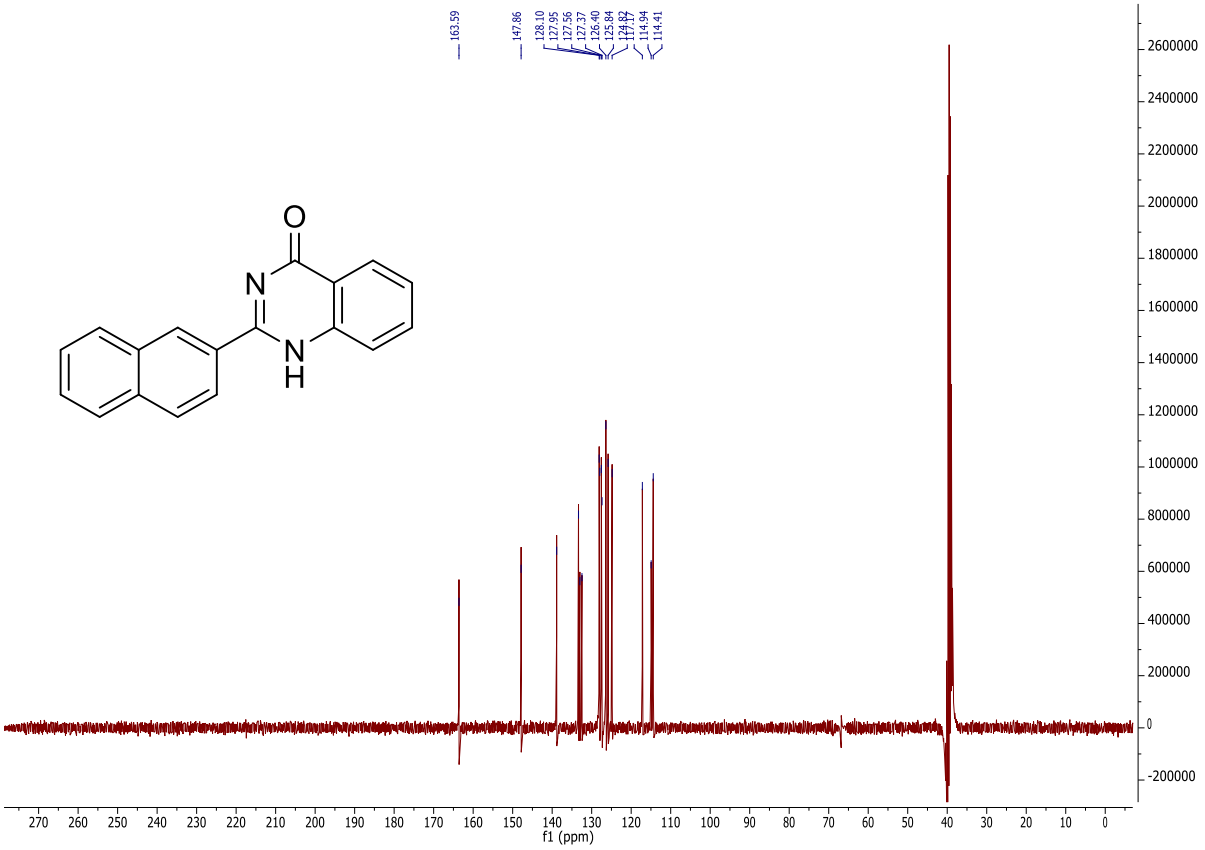

^{13}C NMR spectrum in DMSO-*d*$_6$.

290b

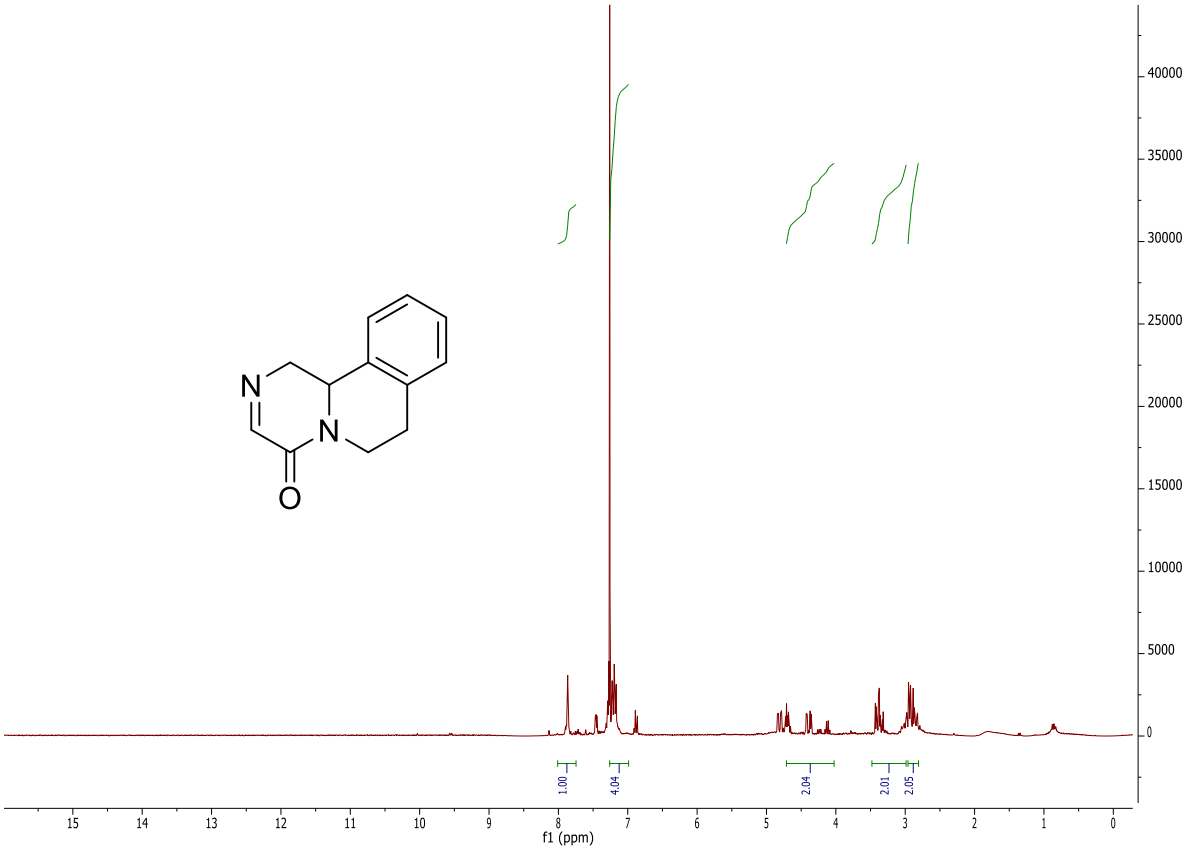

^{1}H NMR spectrum in $CDCl_3$.

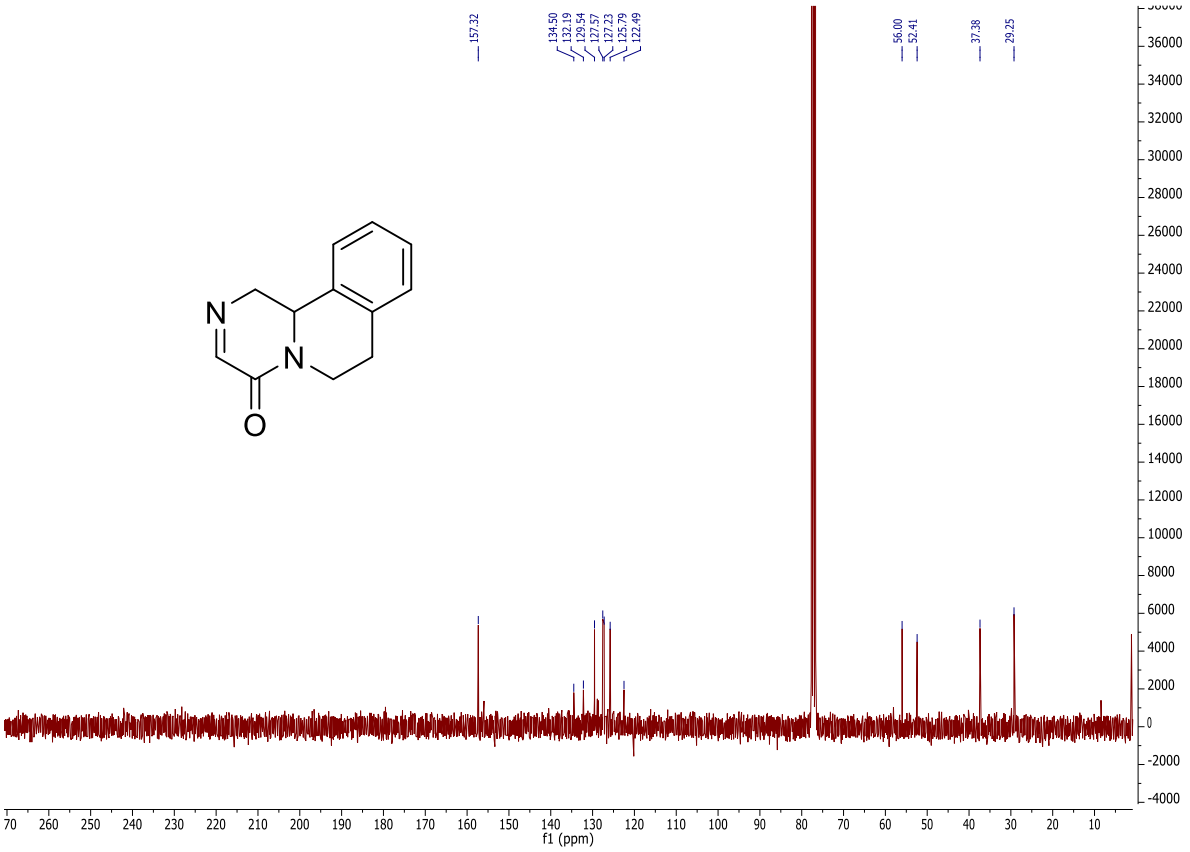

^{13}C NMR spectrum in $CDCl_3$.

291b

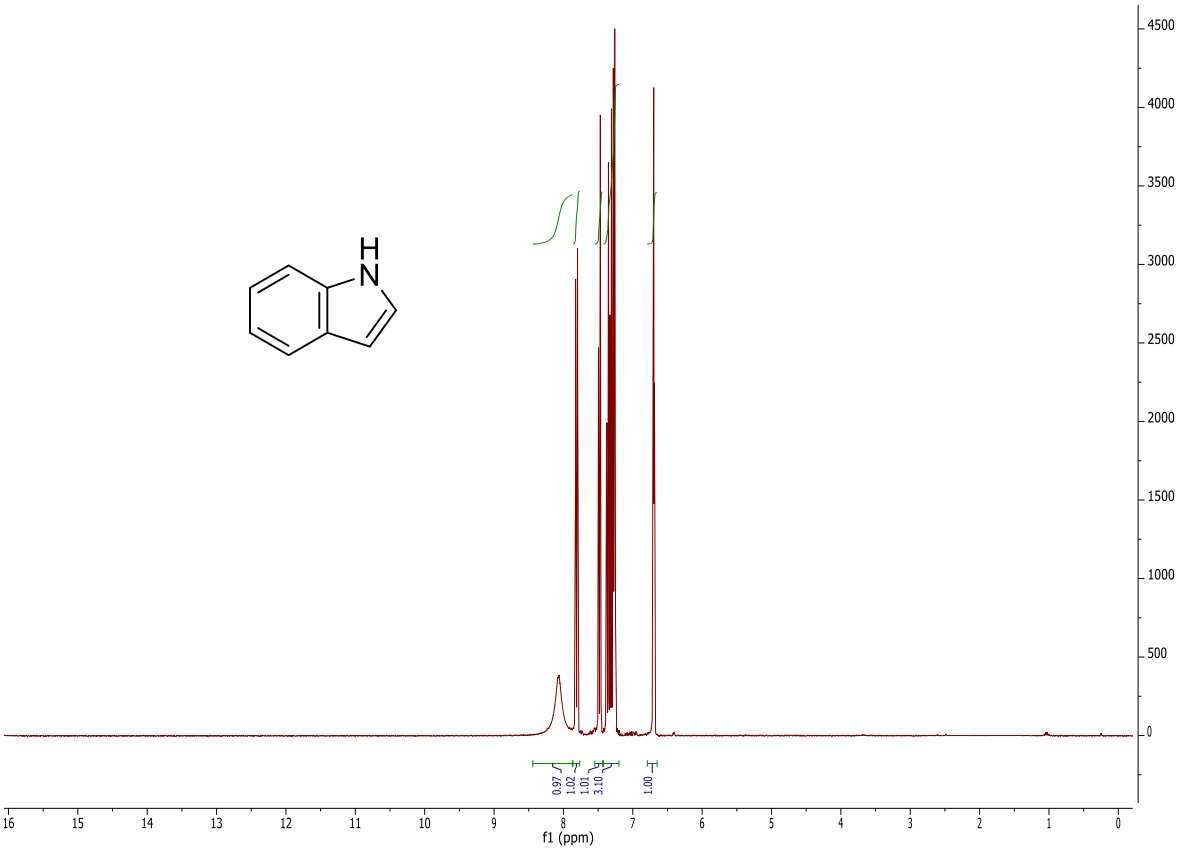

^{1}H NMR spectrum in $CDCl_3$.

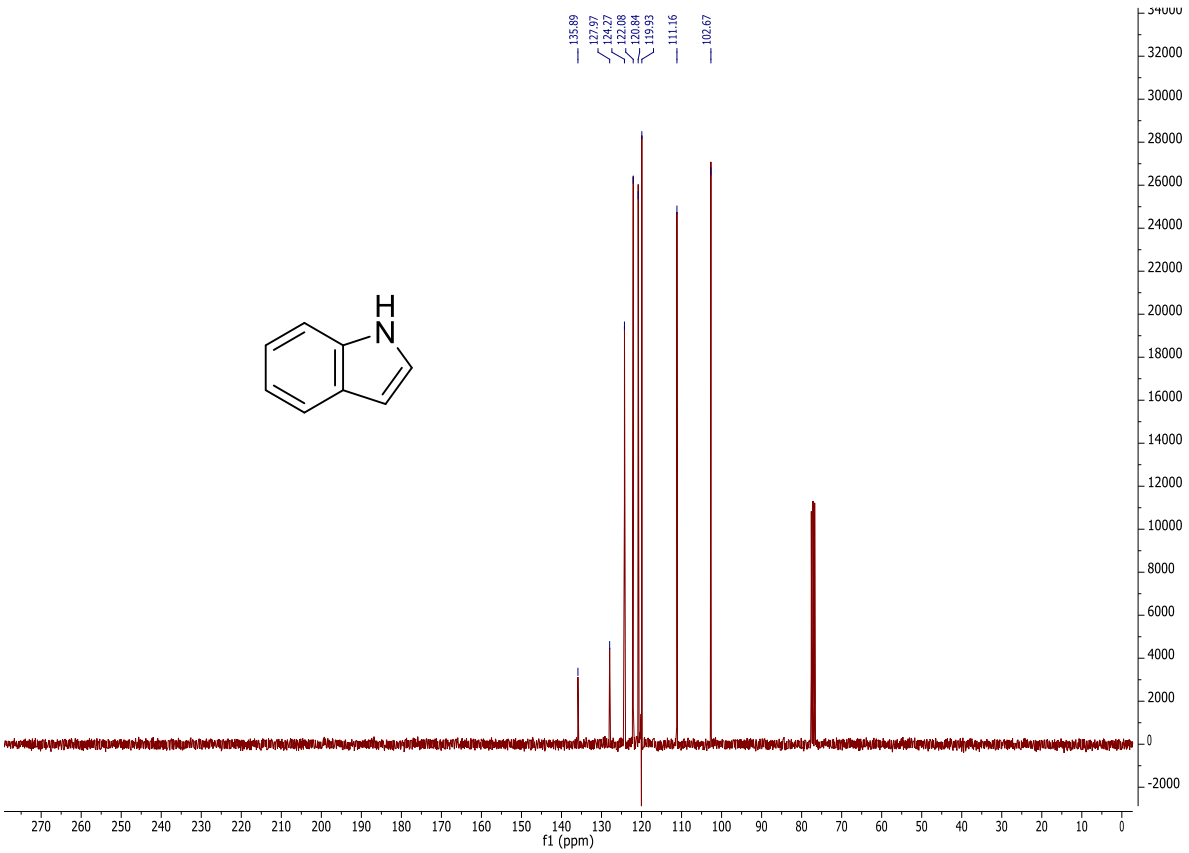

^{13}C NMR spectrum in $CDCl_3$.

292b

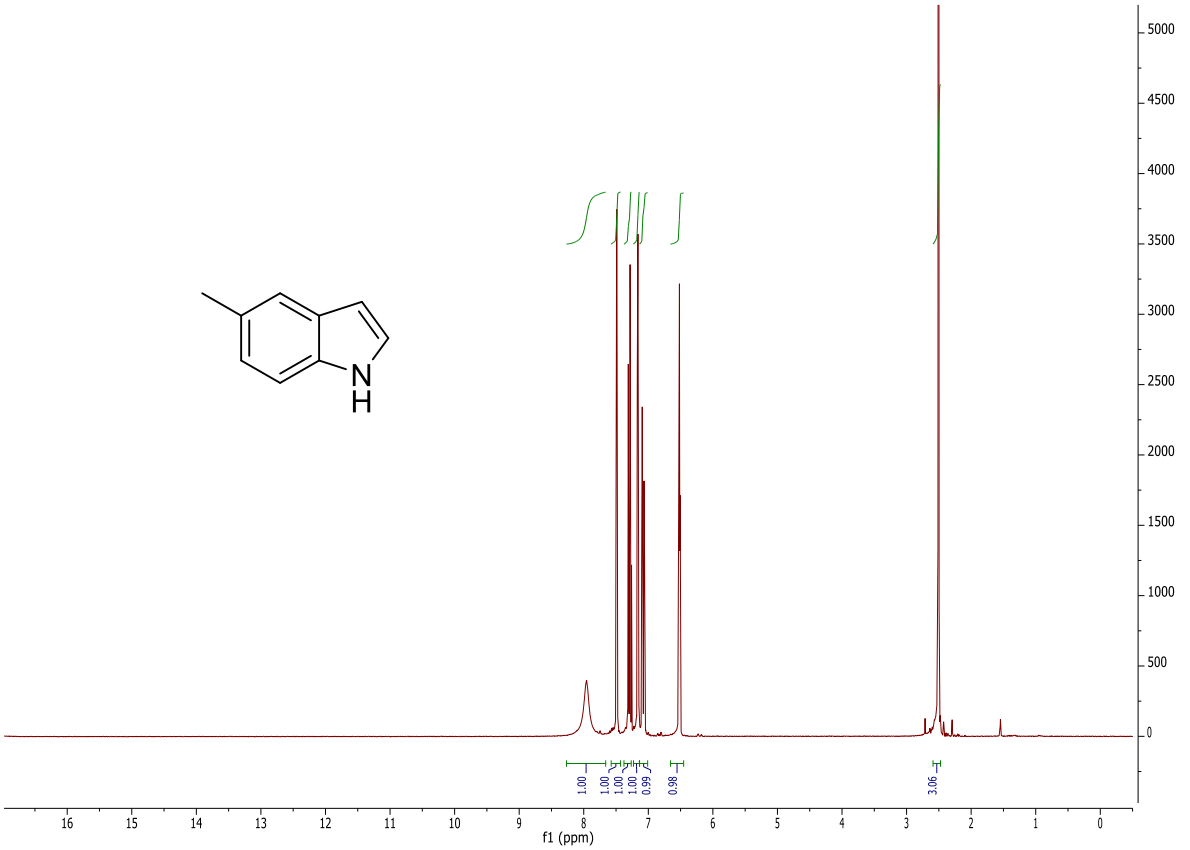

^{1}H NMR spectrum in $CDCl_3$.

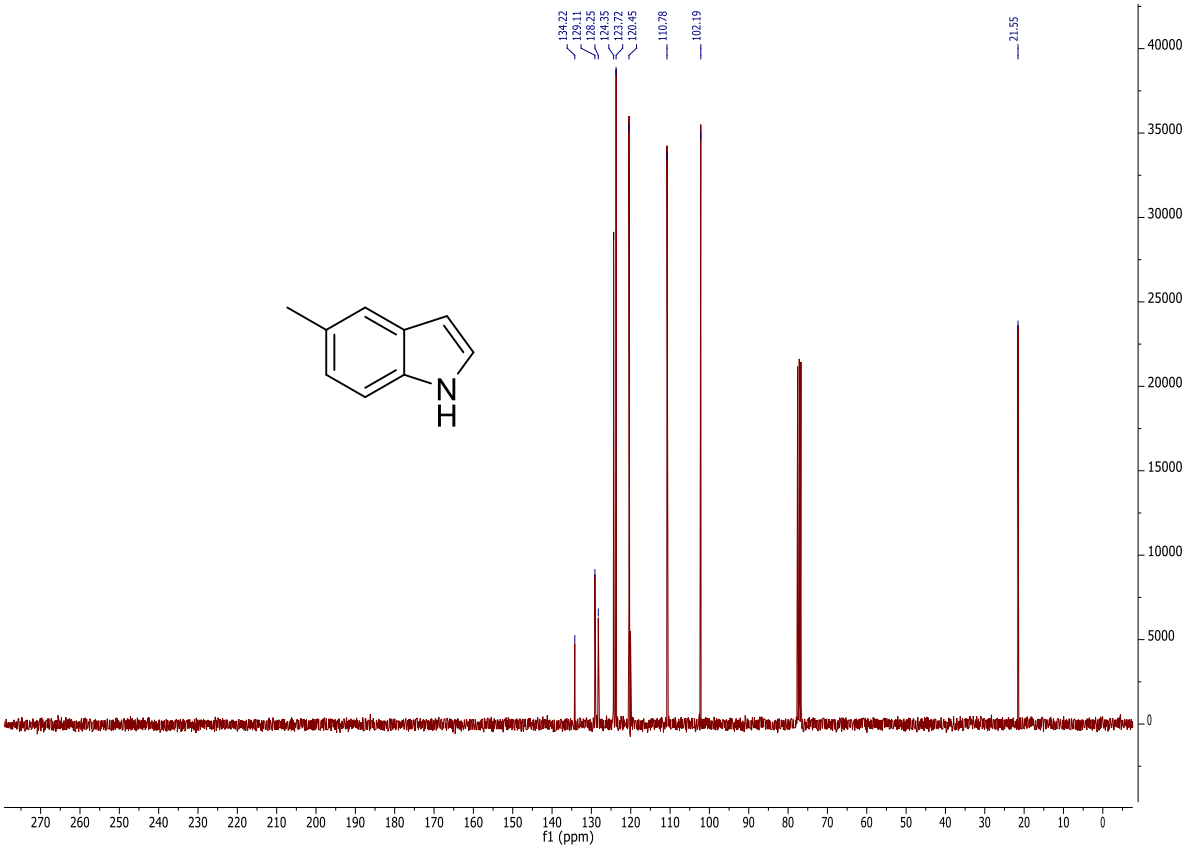

^{13}C NMR spectrum in $CDCl_3$.

293b

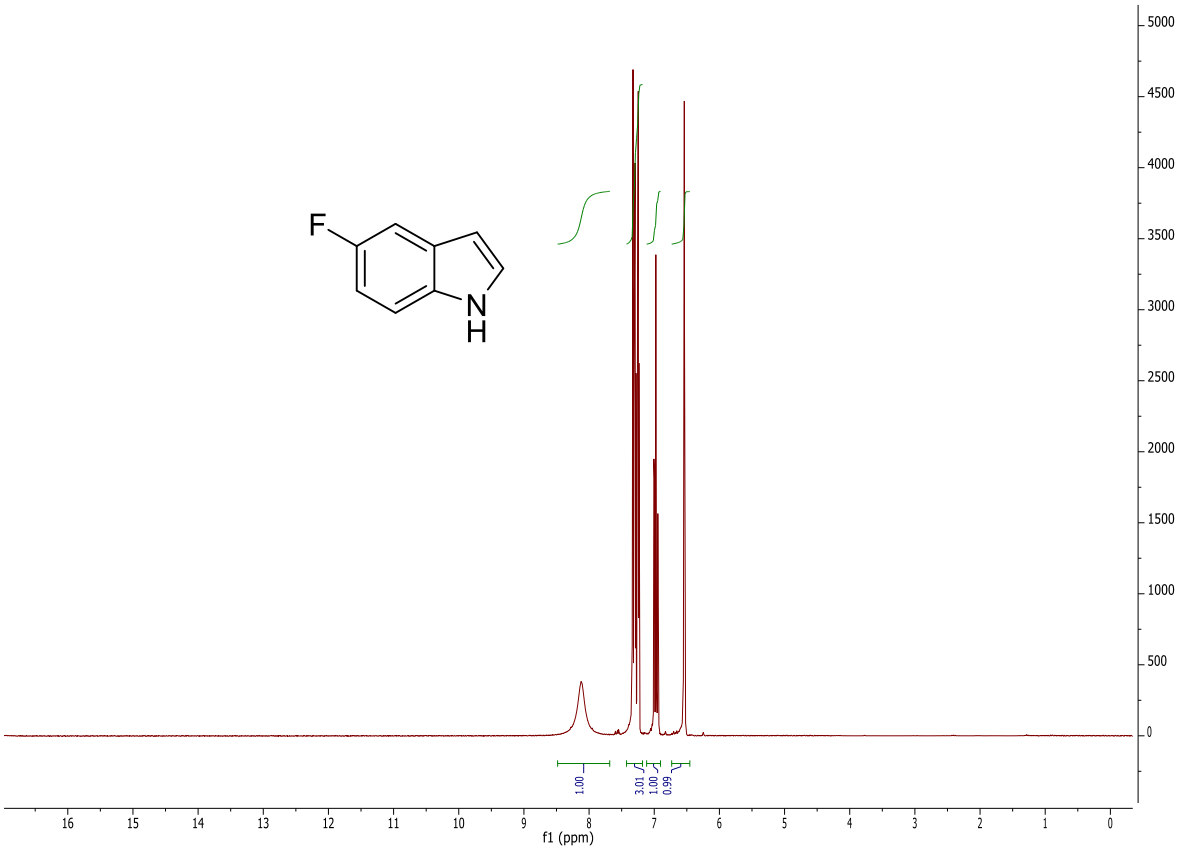

^{1}H NMR spectrum in $CDCl_3$.

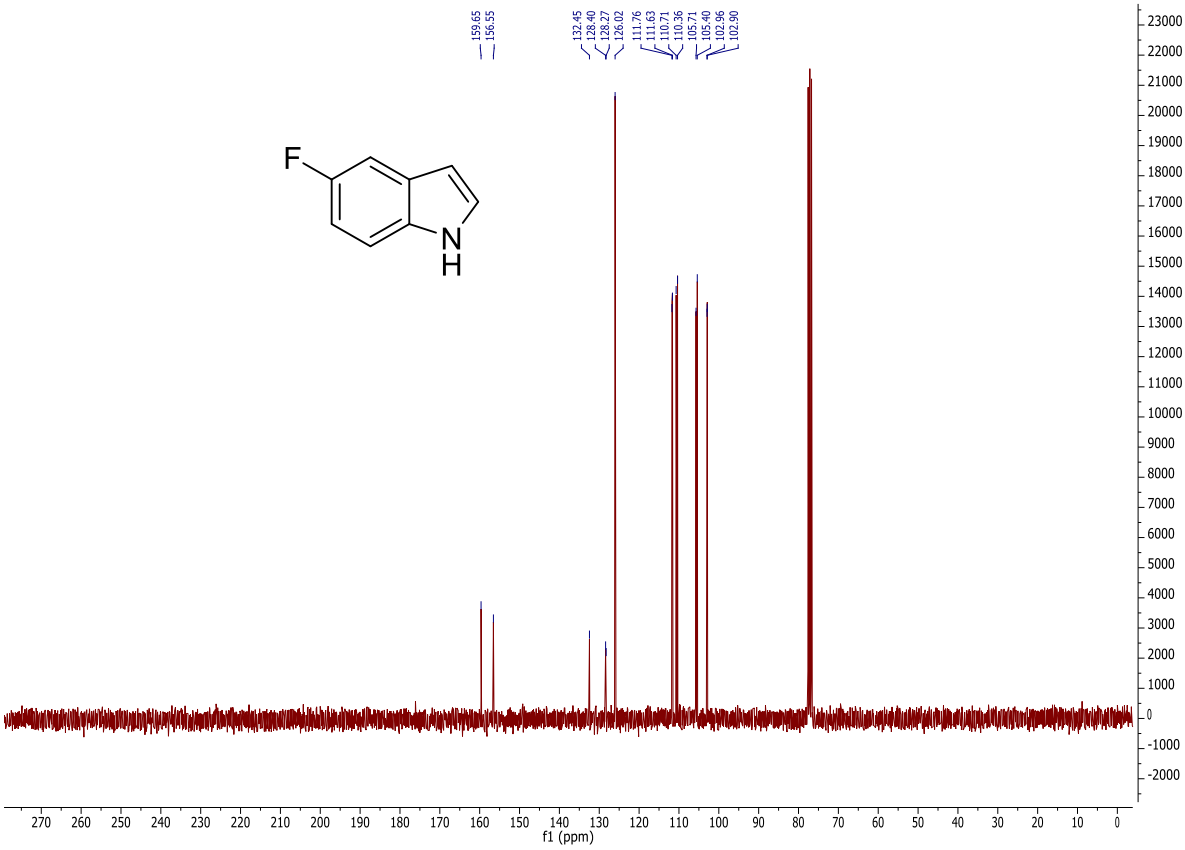

^{13}C NMR spectrum in $CDCl_3$.

294b

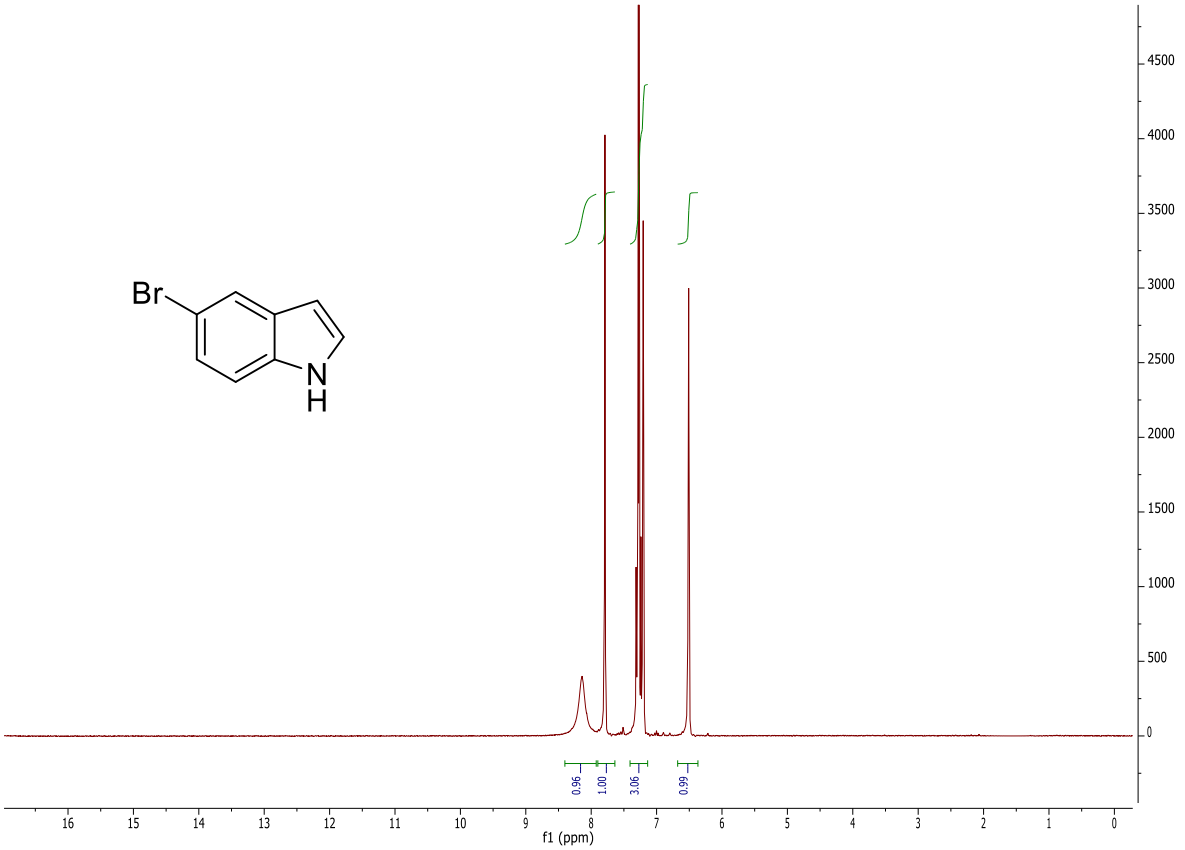

^{1}H NMR spectrum in $CDCl_3$.

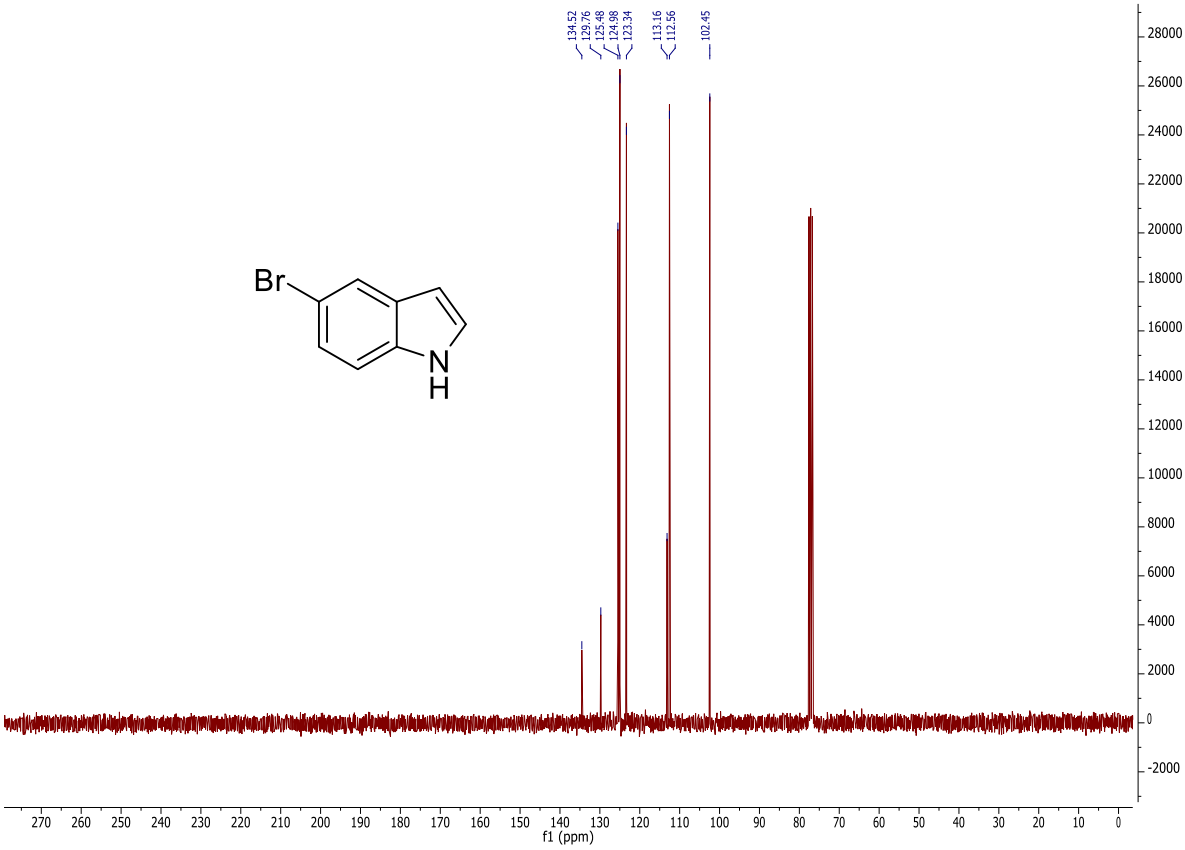

^{13}C NMR spectrum in $CDCl_3$.

295b

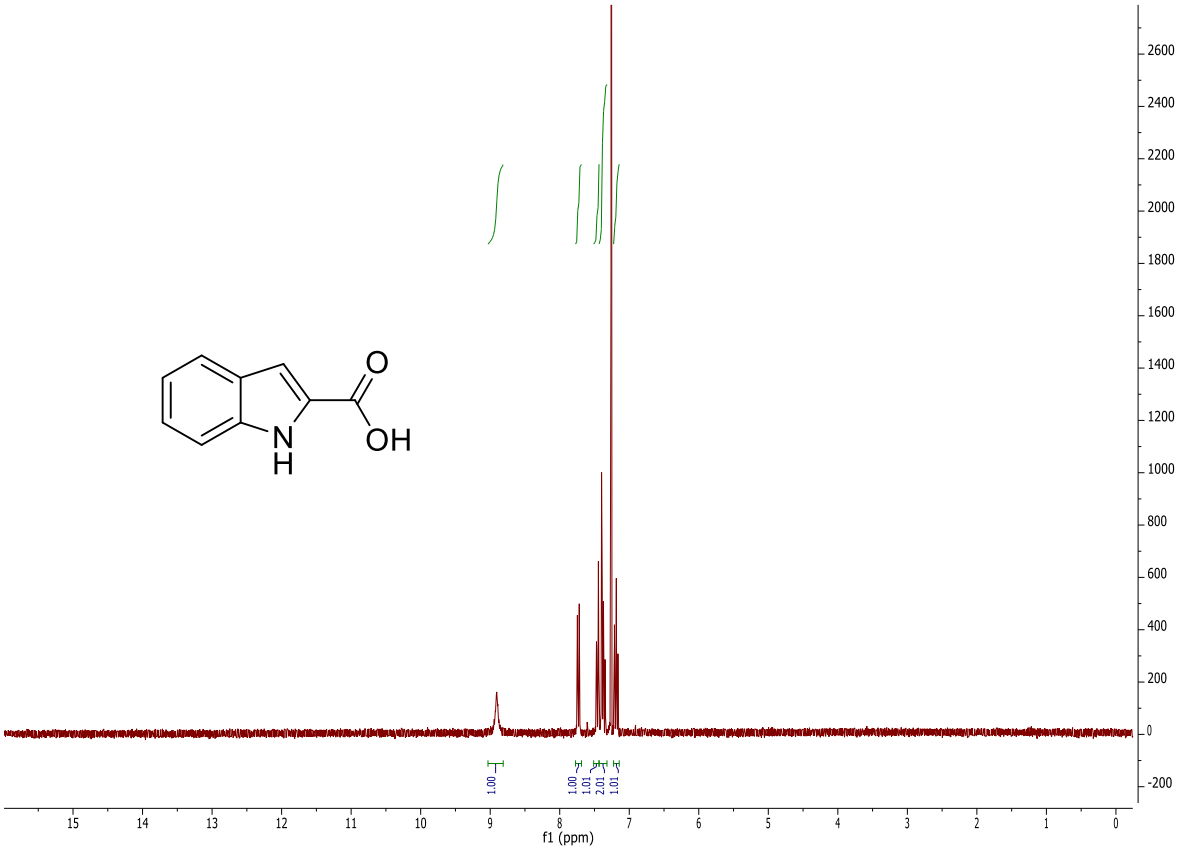

^{1}H NMR spectrum in $CDCl_3$.

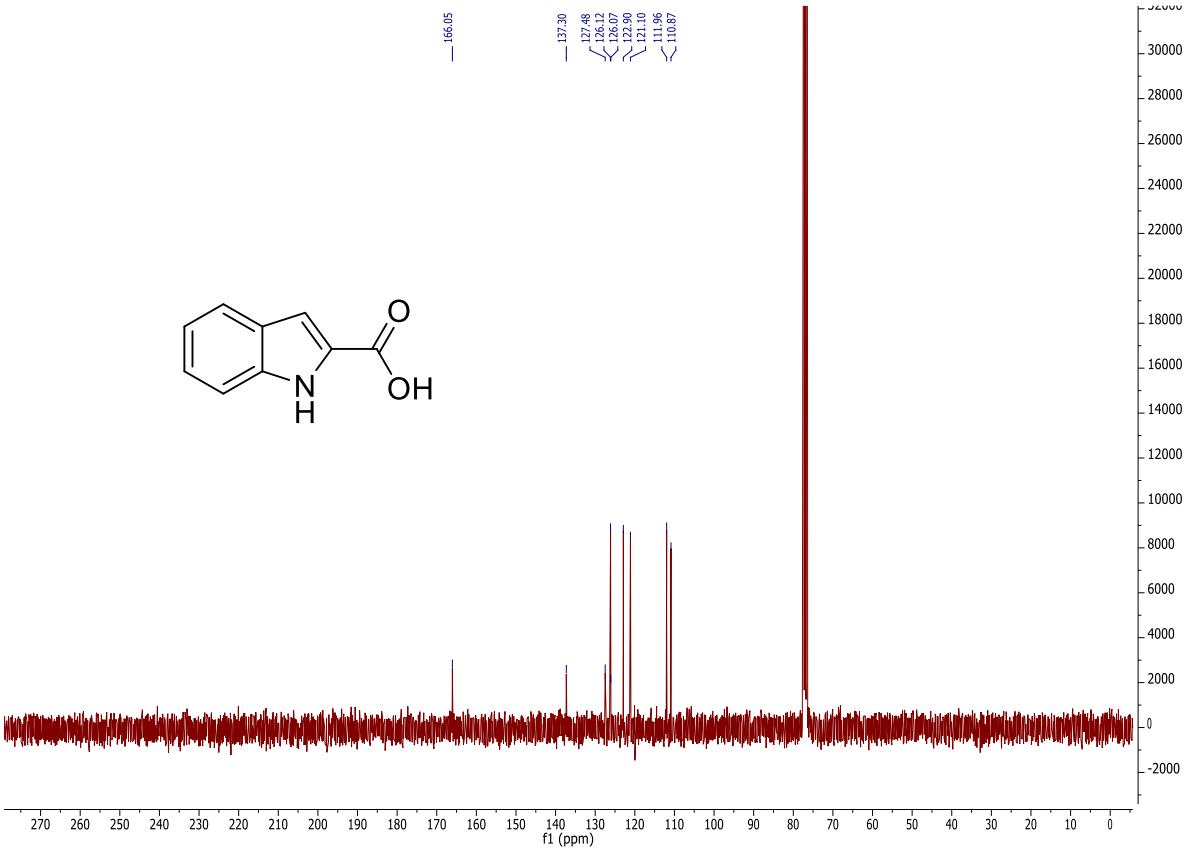

^{13}C NMR spectrum in $CDCl_3$.

296b

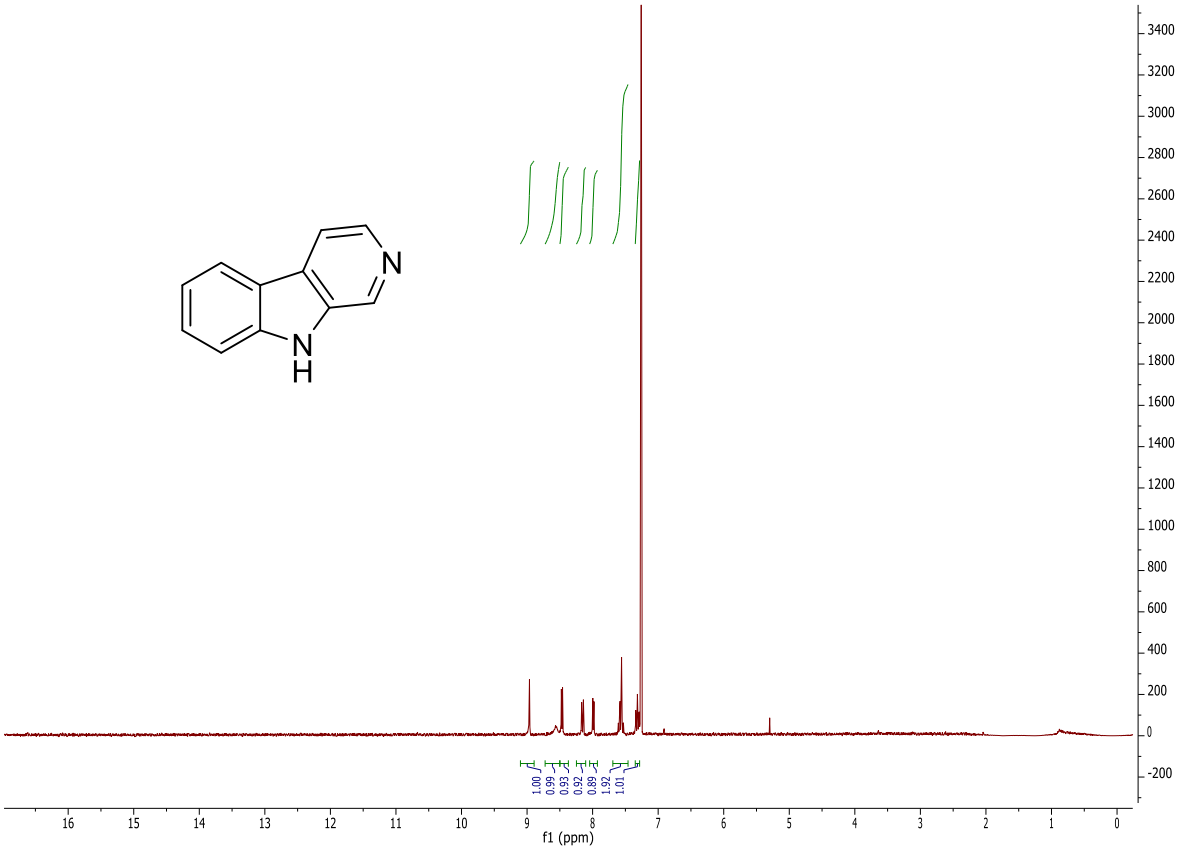

^{1}H NMR spectrum in $CDCl_3$.

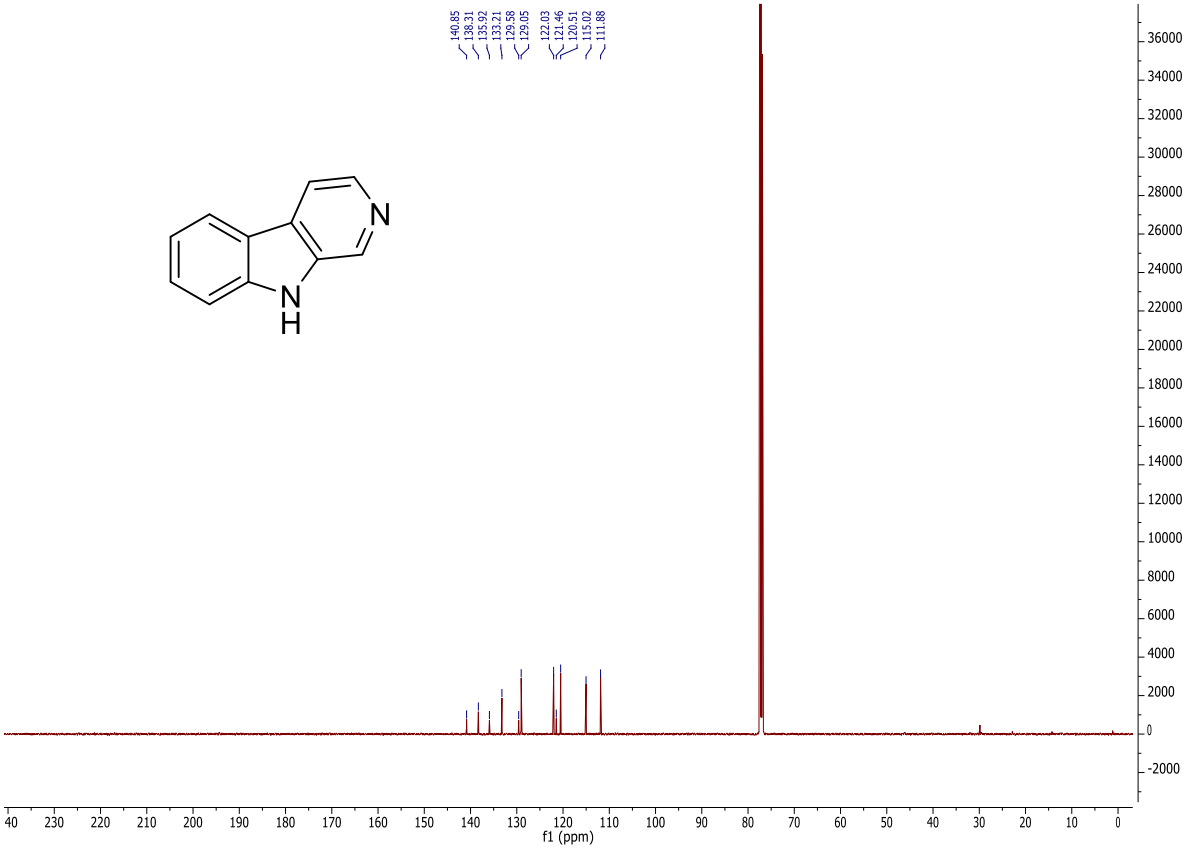

^{13}C NMR spectrum in $CDCl_3$.

297b

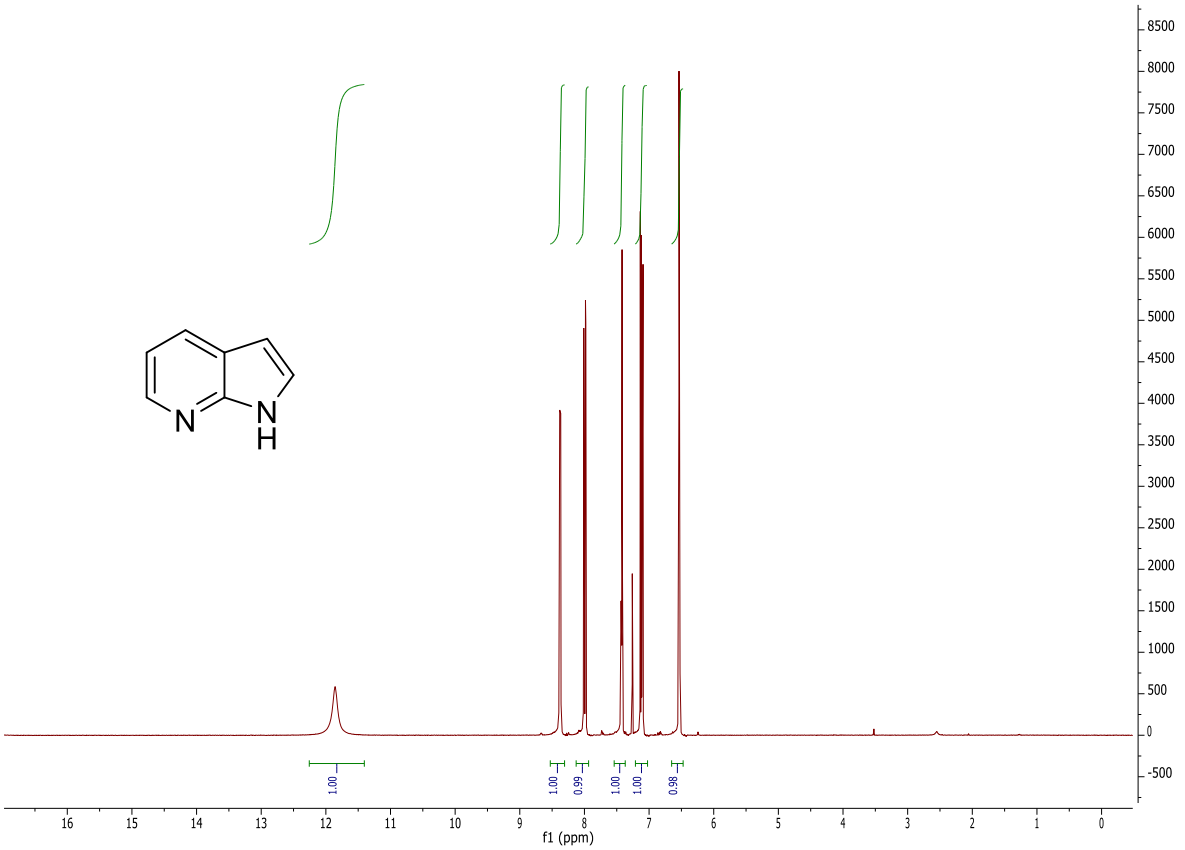

^{1}H NMR spectrum in $CDCl_3$.

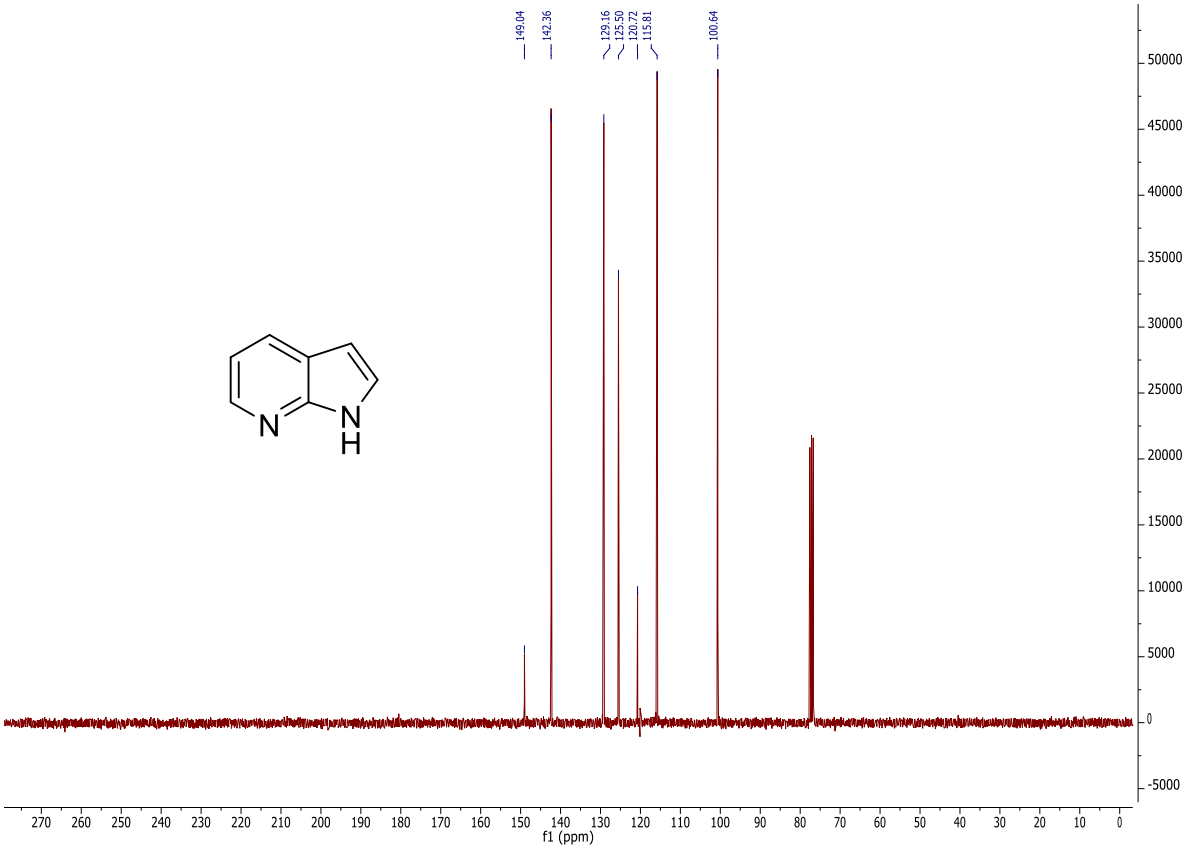

^{13}C NMR spectrum in $CDCl_3$.

298b

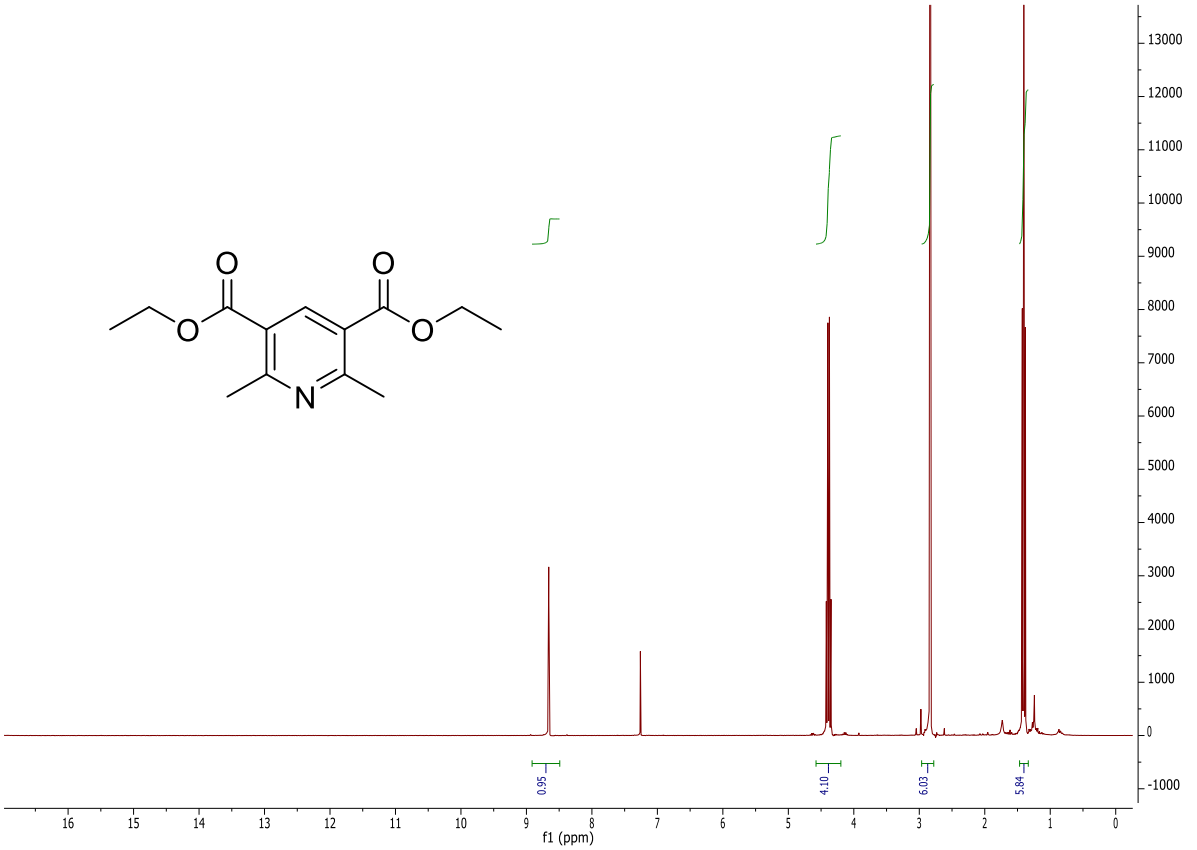

^{1}H NMR spectrum in $CDCl_3$.

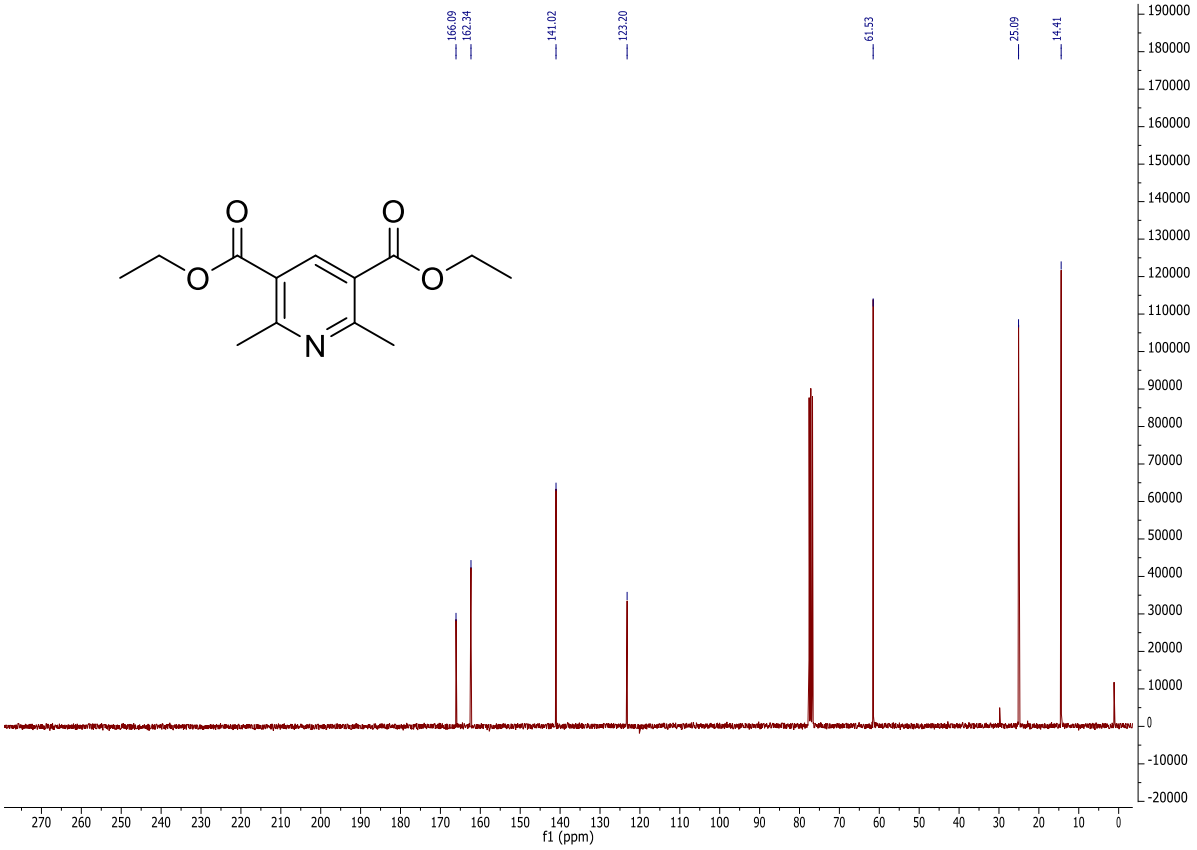

^{13}C NMR spectrum in $CDCl_3$.

299b

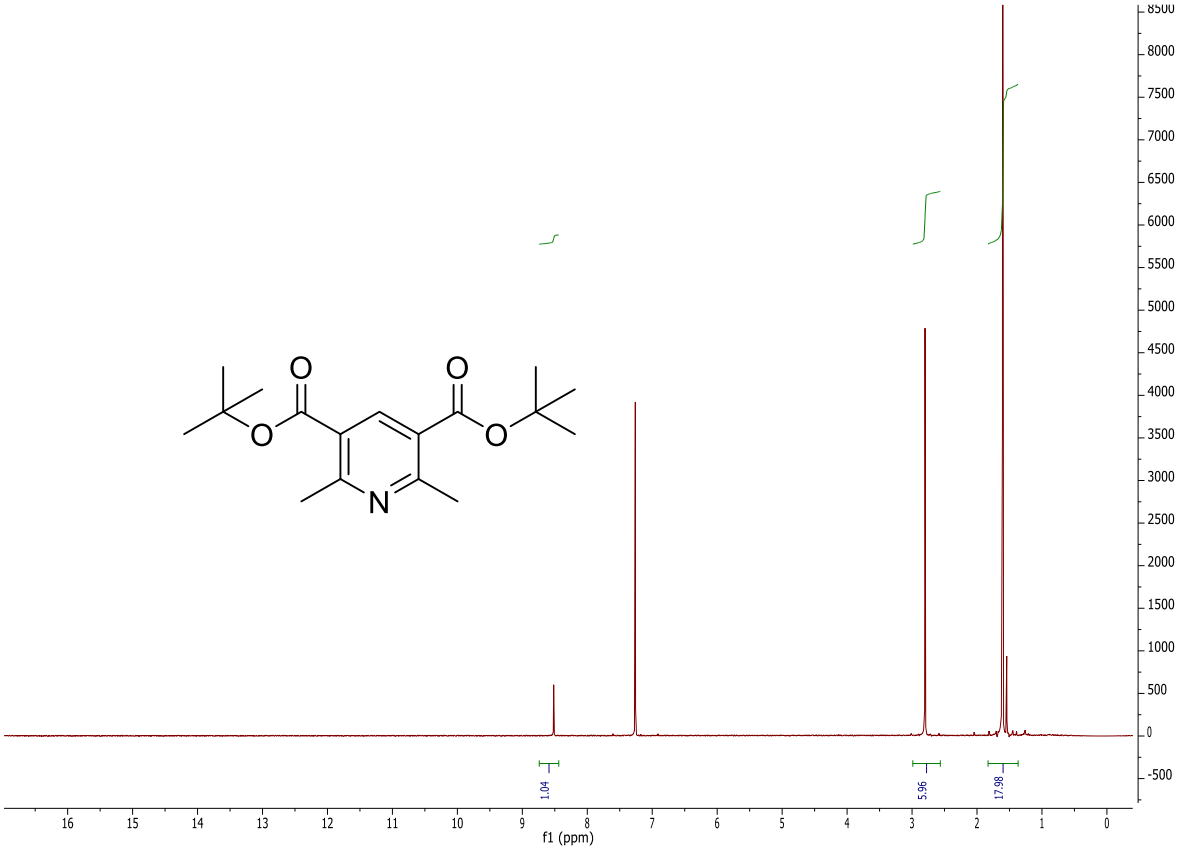

^{1}H NMR spectrum in $CDCl_3$.

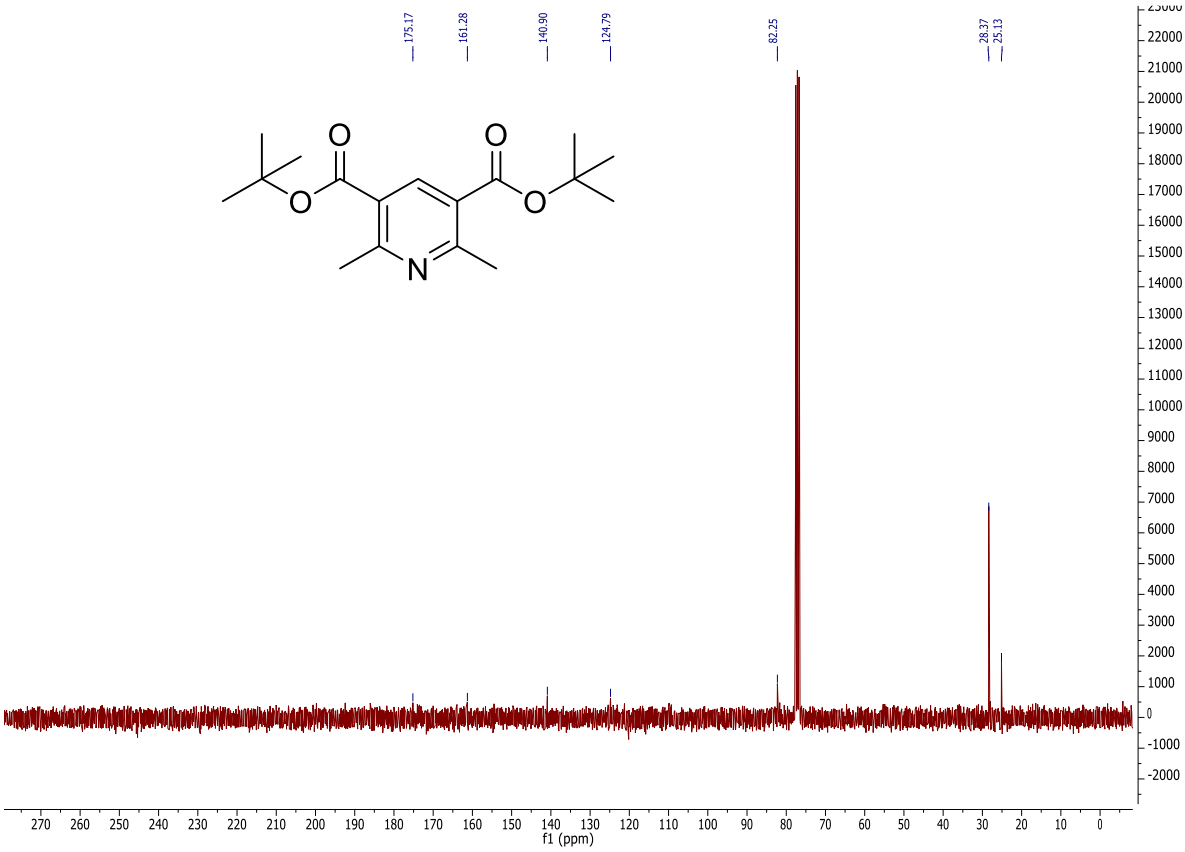

^{13}C NMR spectrum in $CDCl_3$.

300b

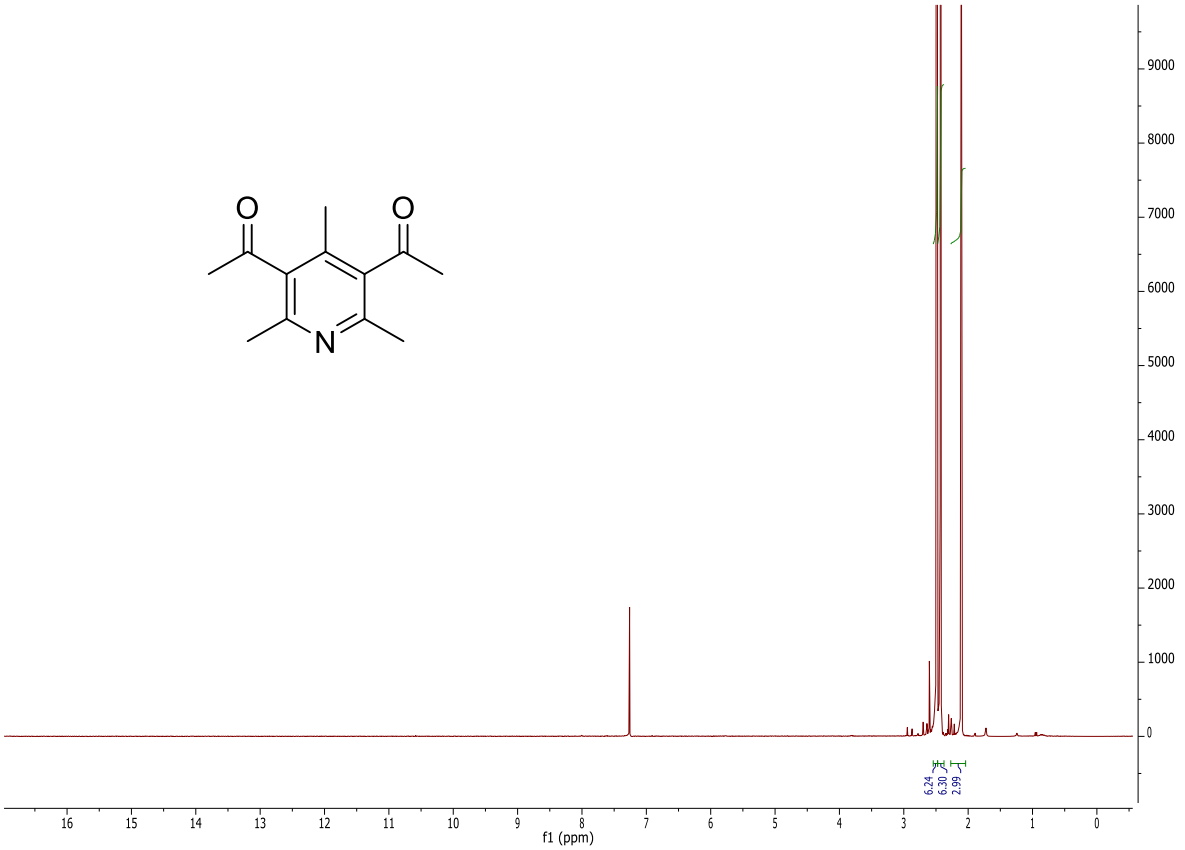

^{1}H NMR spectrum in $CDCl_3$.

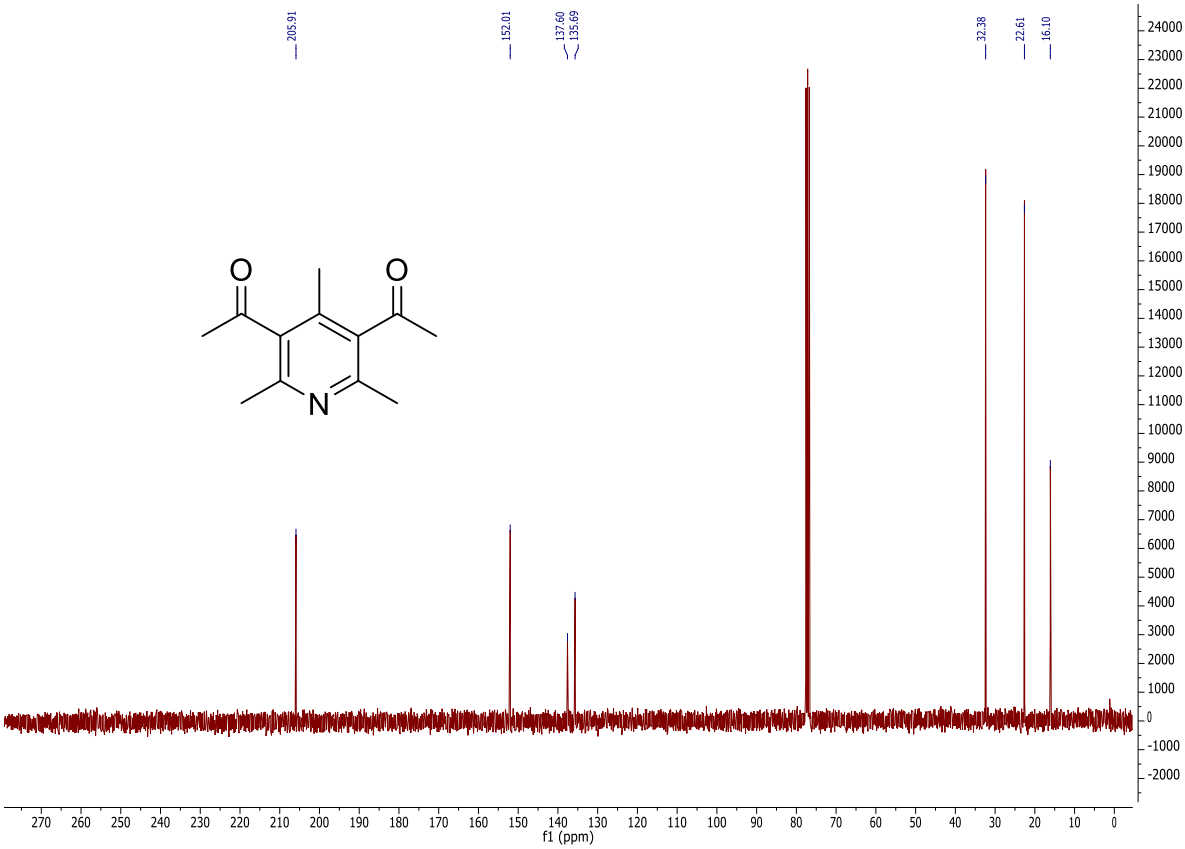

^{13}C NMR spectrum in $CDCl_3$.

301b

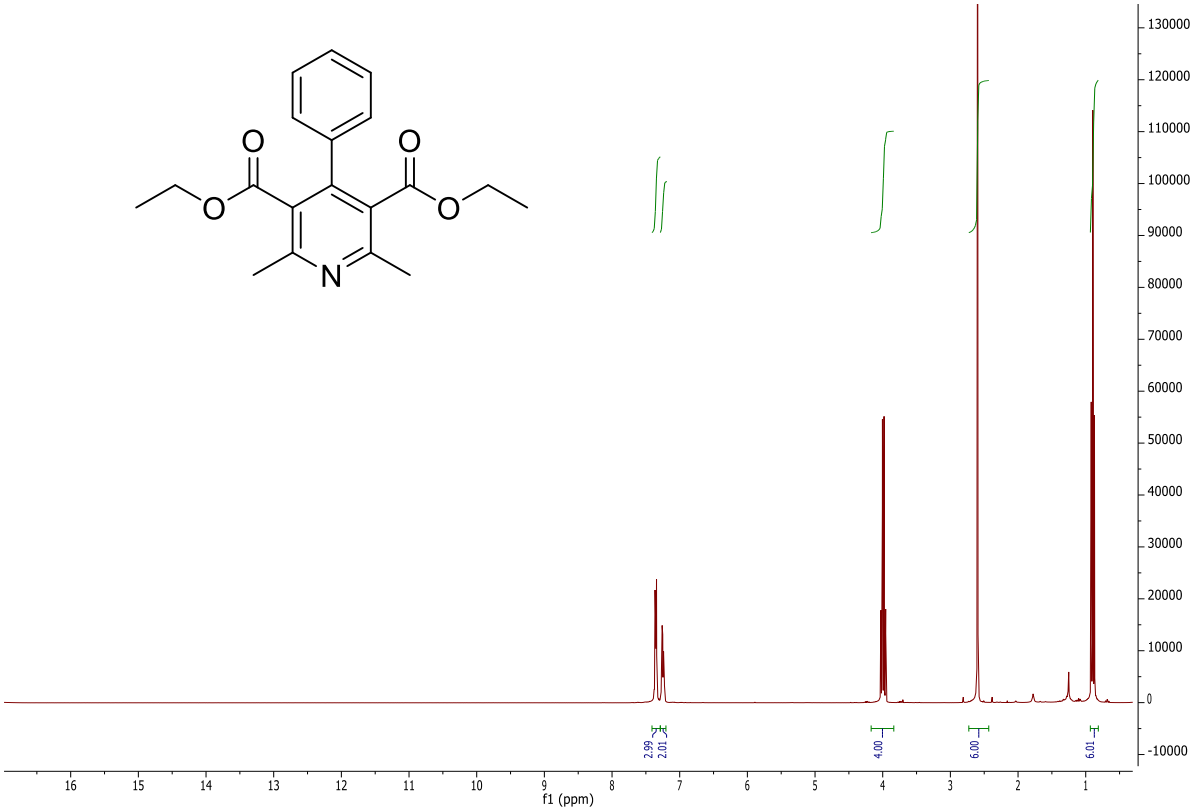

^{1}H NMR spectrum in $CDCl_3$.

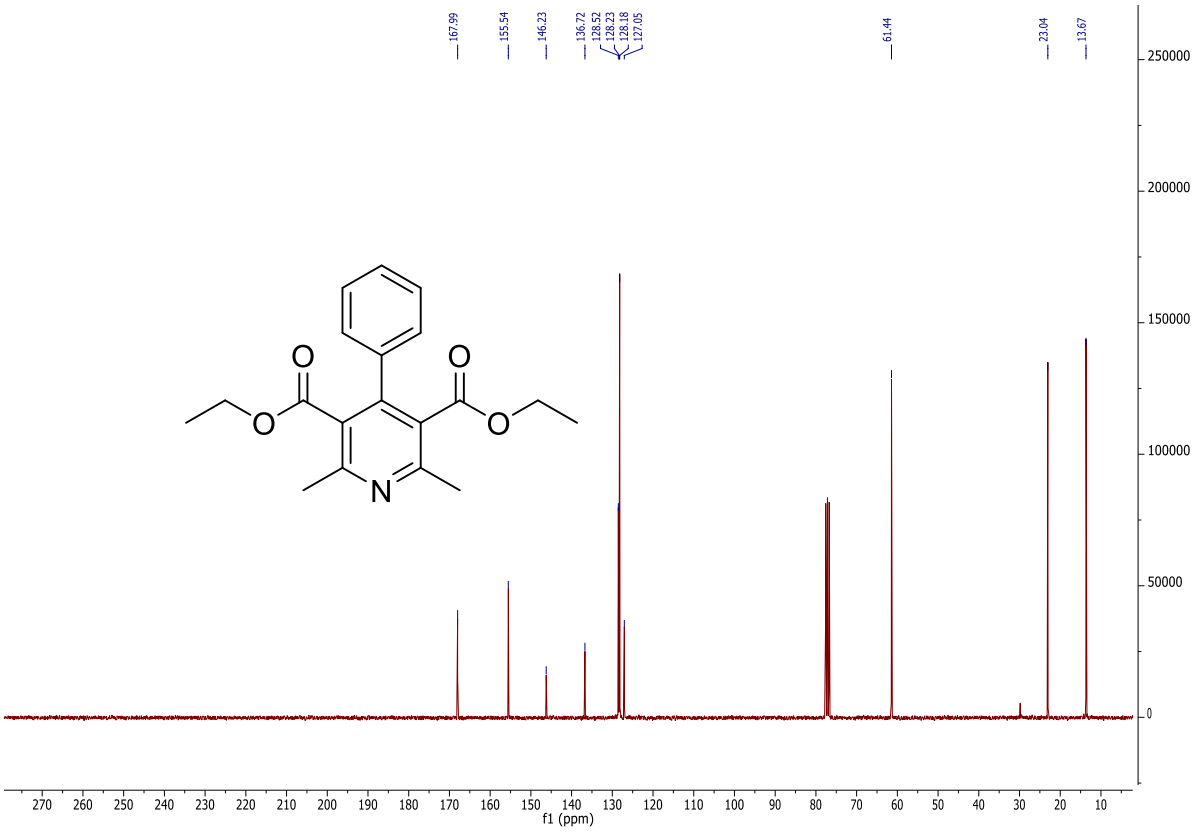

^{13}C NMR spectrum in $CDCl_3$.

329b

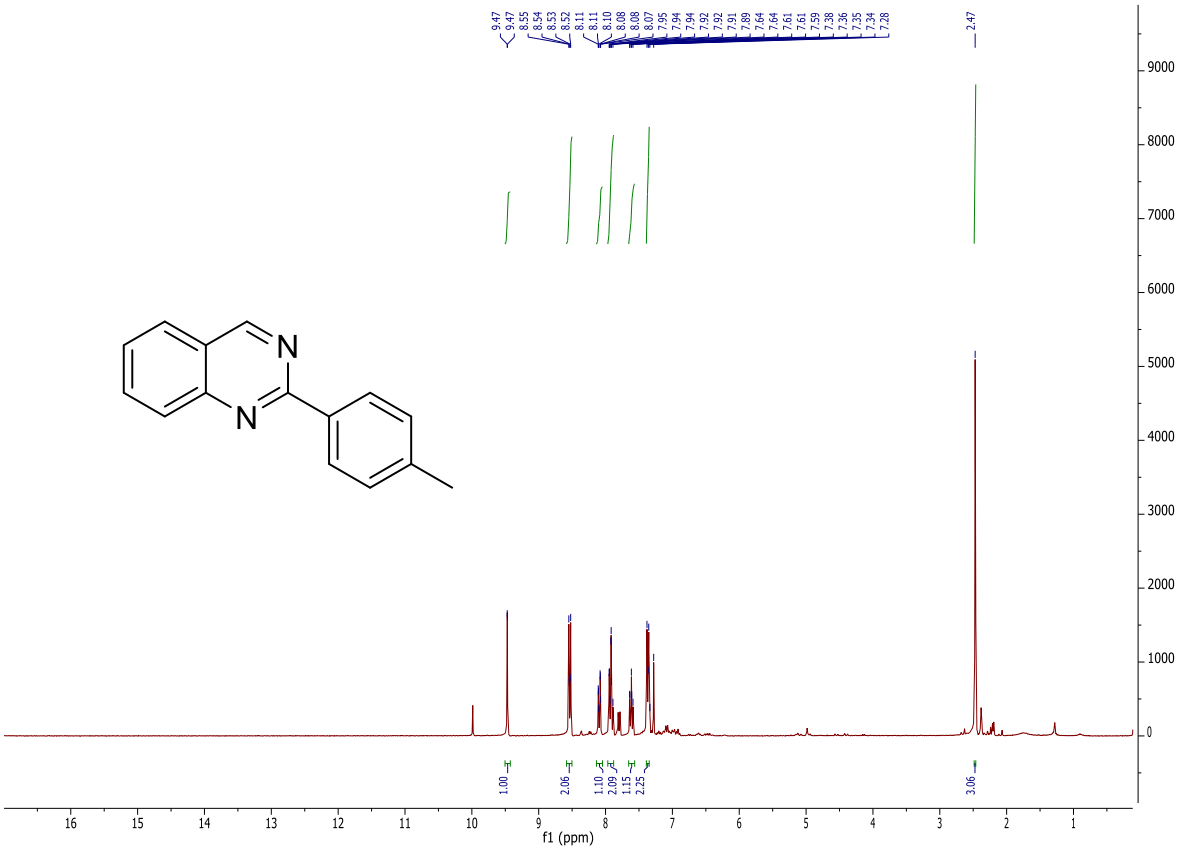

^{1}H NMR spectrum in $CDCl_3$.

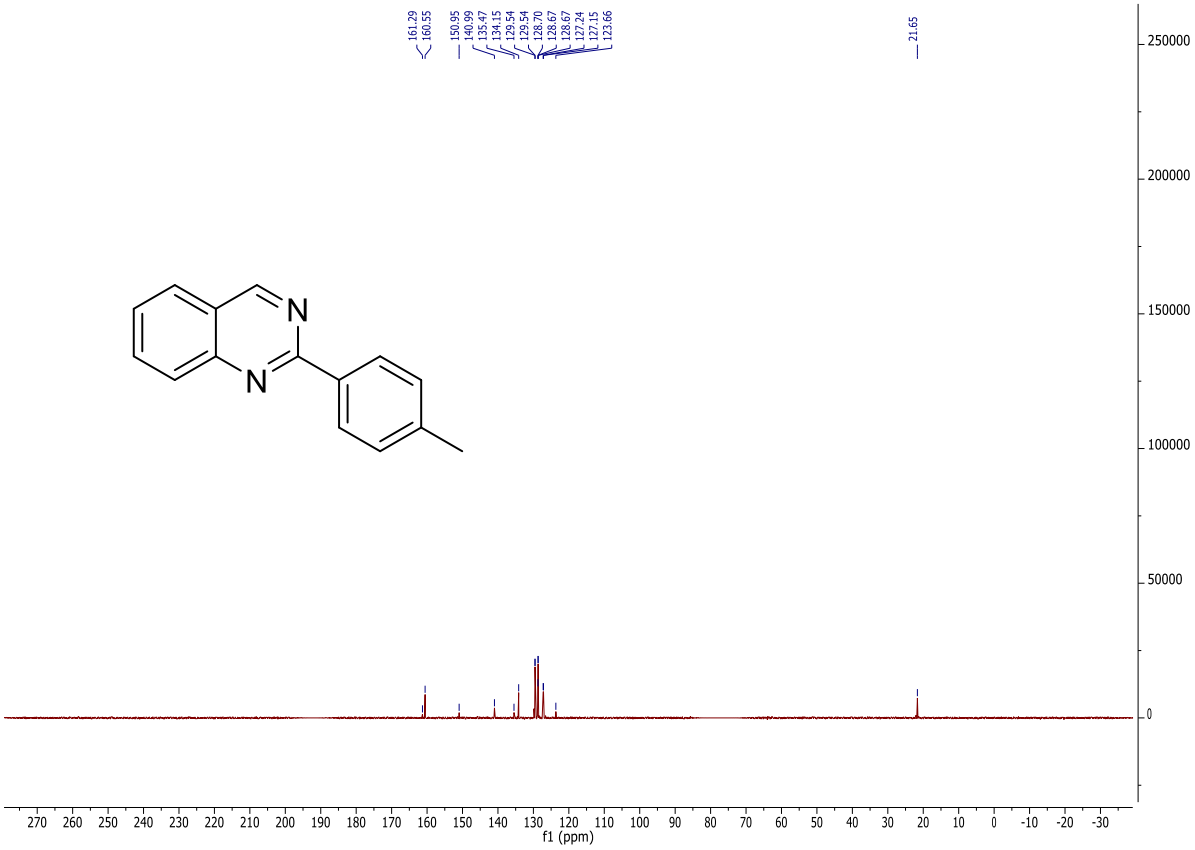

^{13}C NMR spectrum in $CDCl_3$.

330b

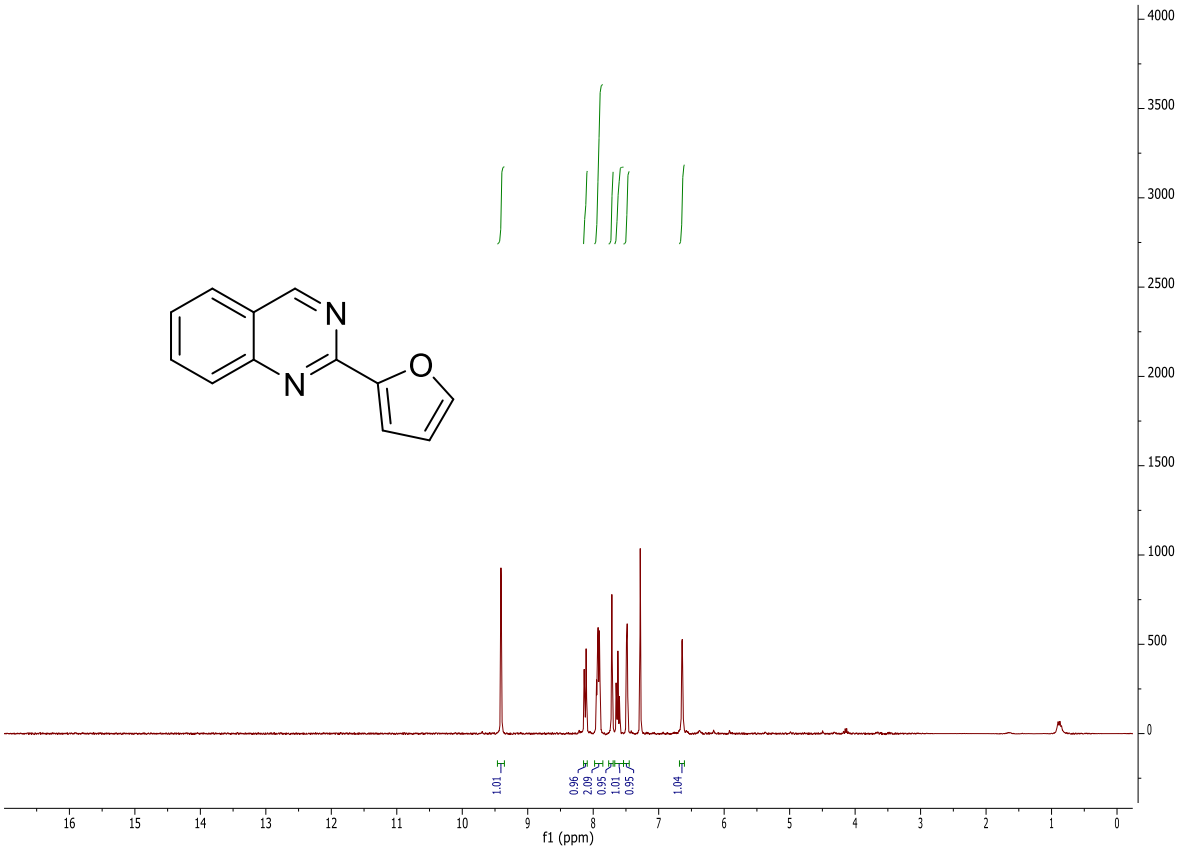

^{1}H NMR spectrum in $CDCl_3$.

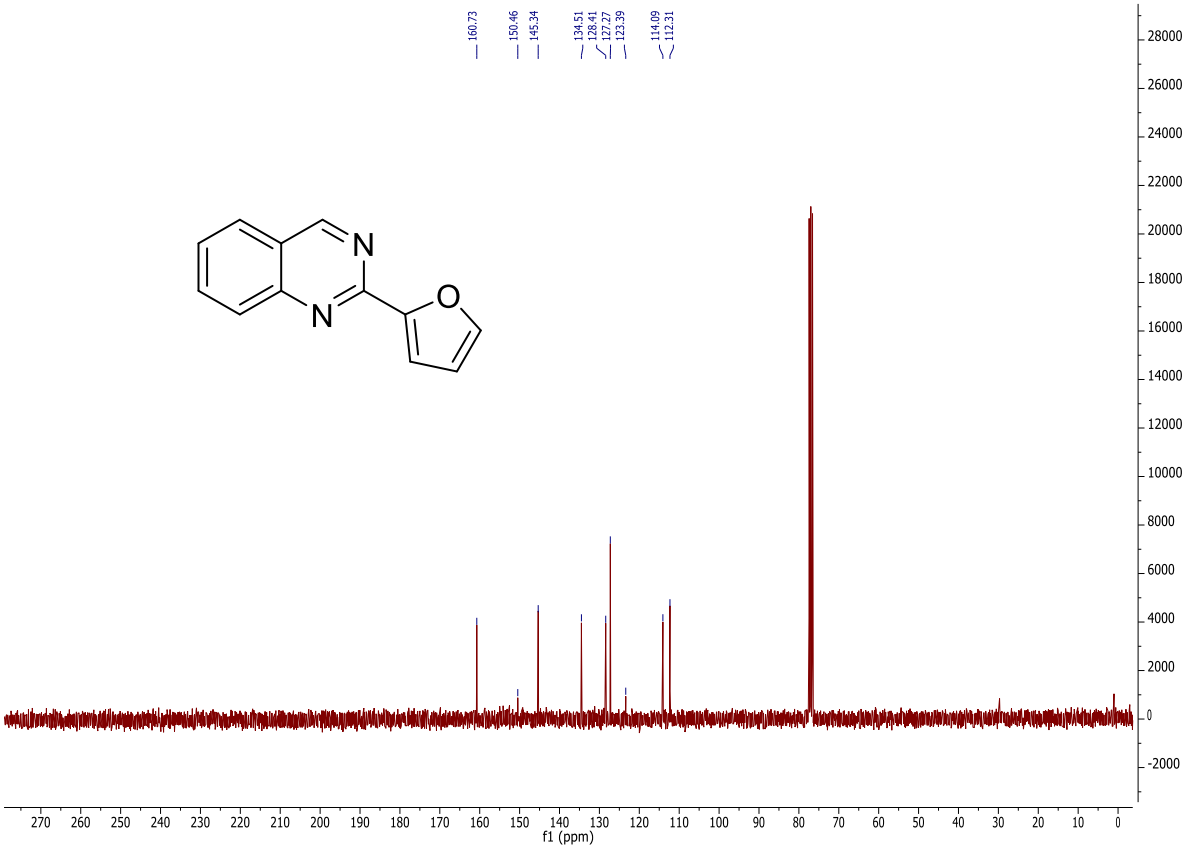

^{13}C NMR spectrum in $CDCl_3$.

331b

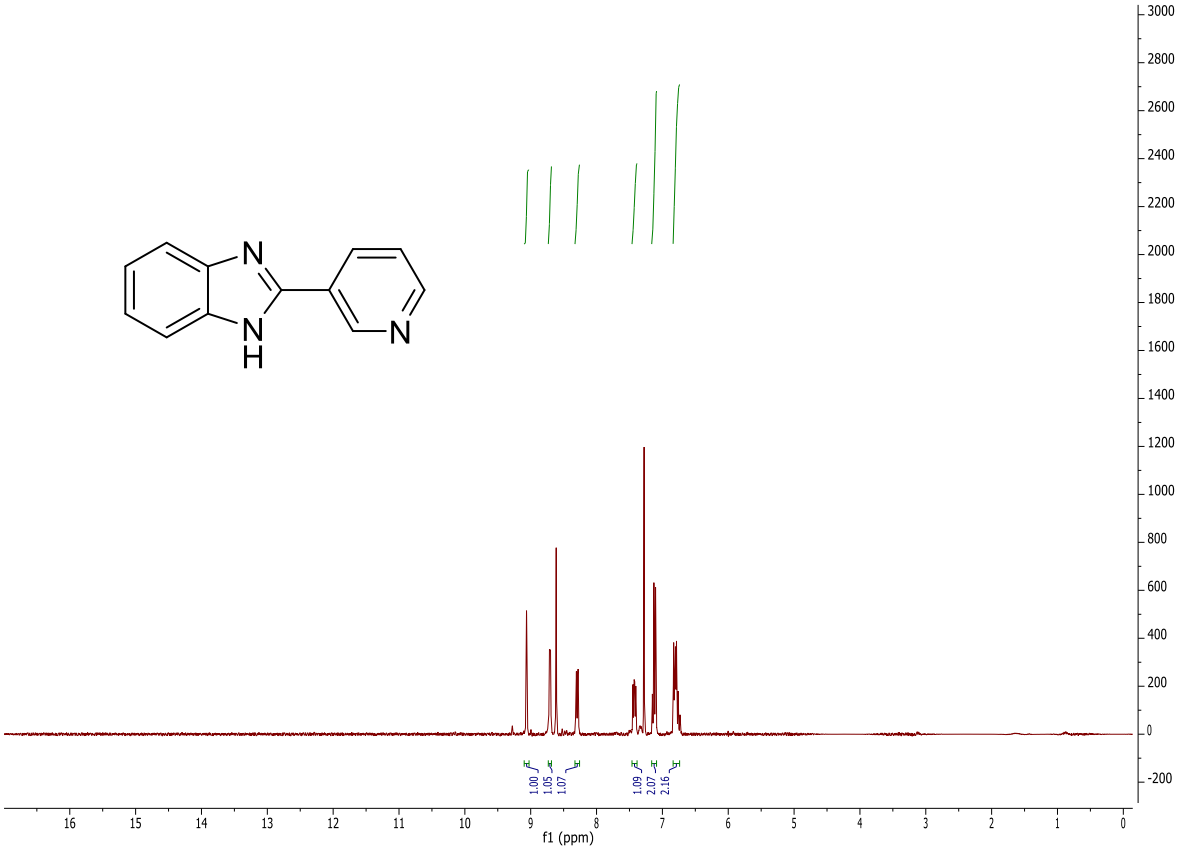

^{1}H NMR spectrum in $CDCl_3$.

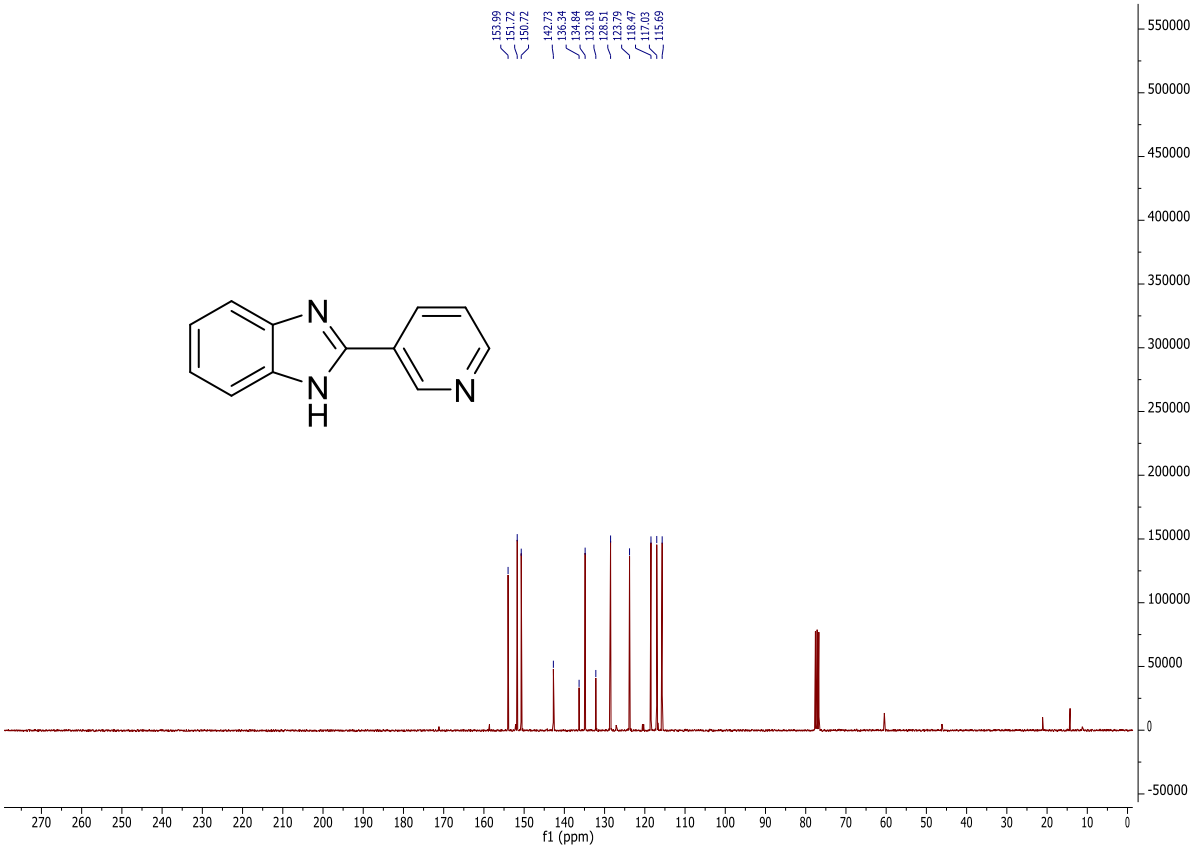

^{13}C NMR spectrum in $CDCl_3$.

332

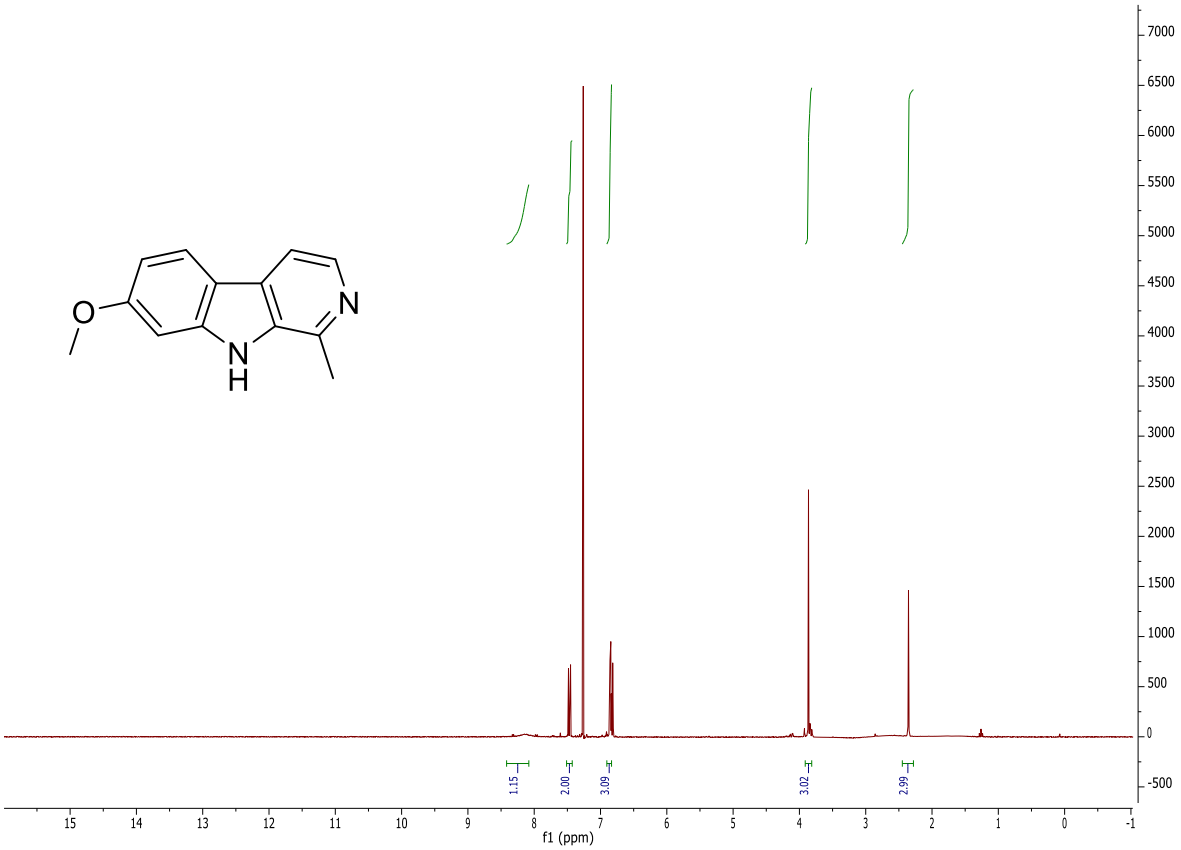

^{1}H NMR spectrum in $CDCl_3$.

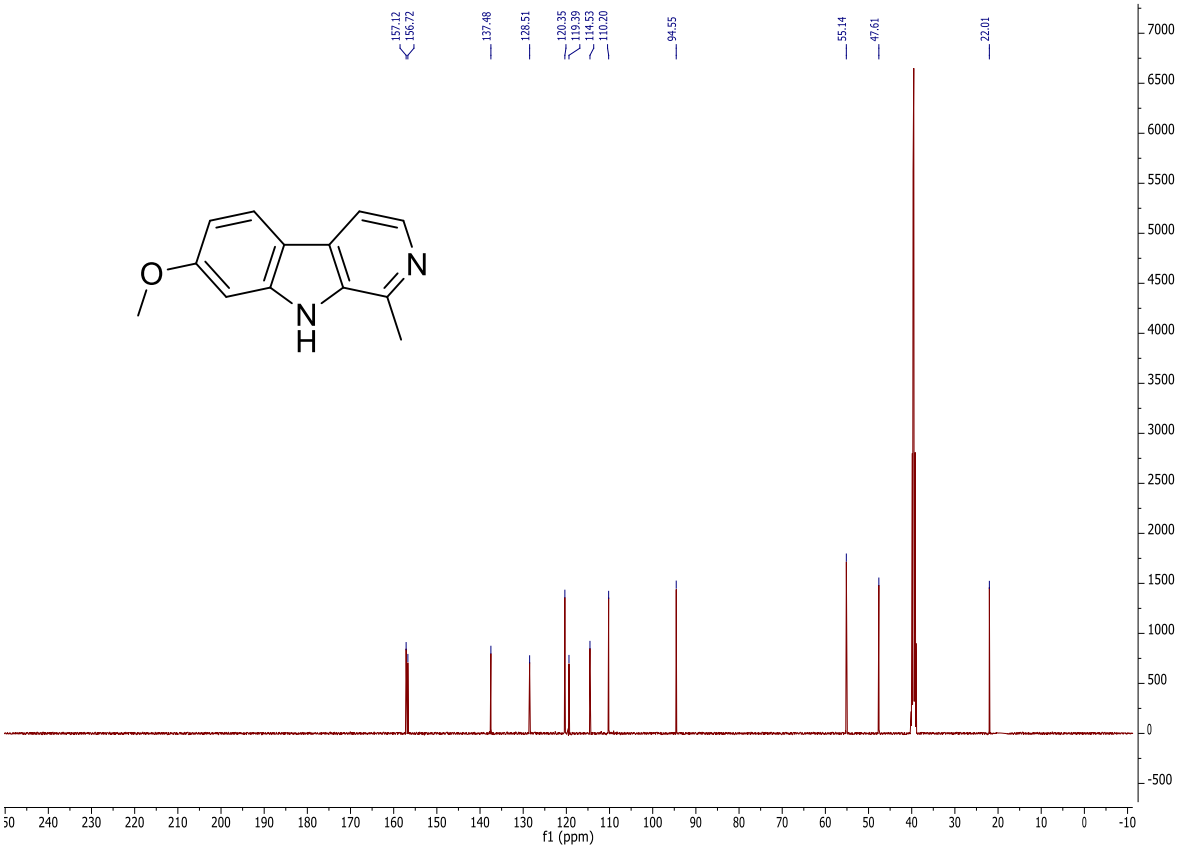

^{13}C NMR spectrum in DMSO-d_6.

333b

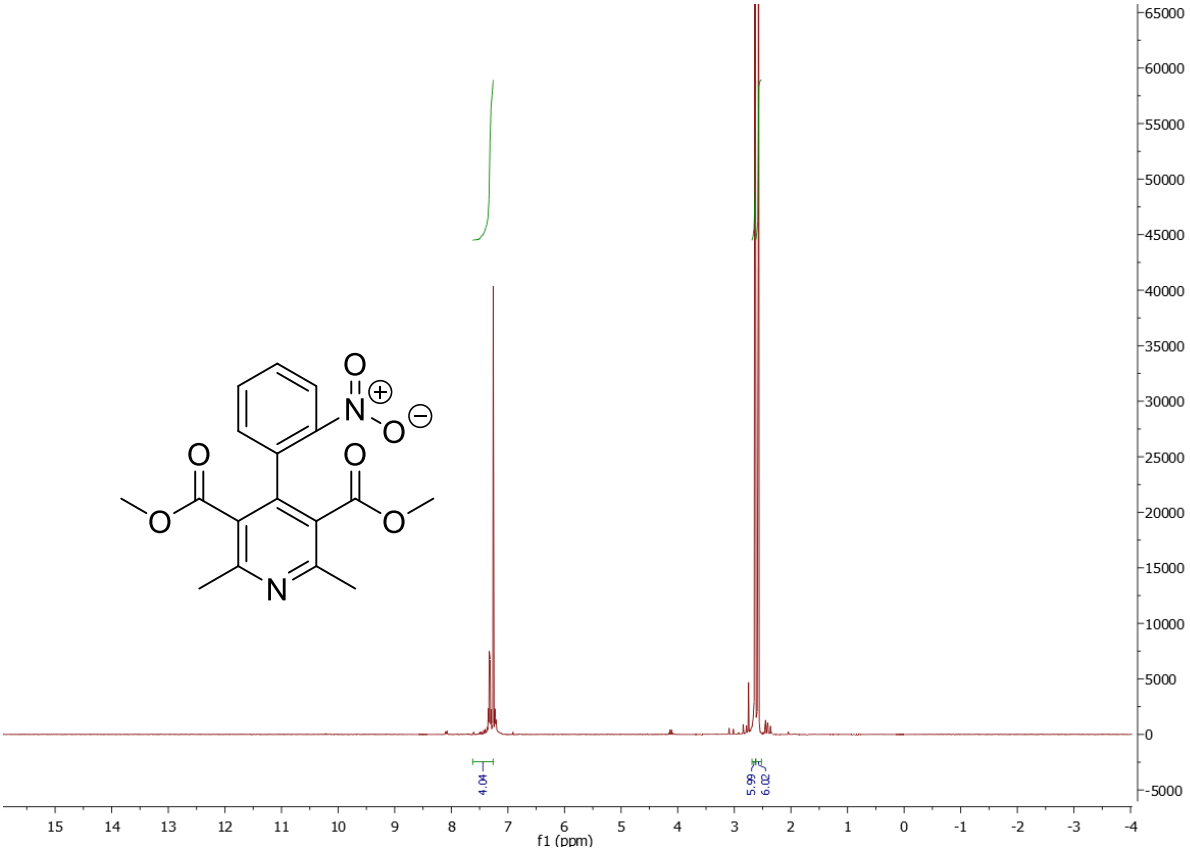

^{1}H NMR spectrum in $CDCl_3$.

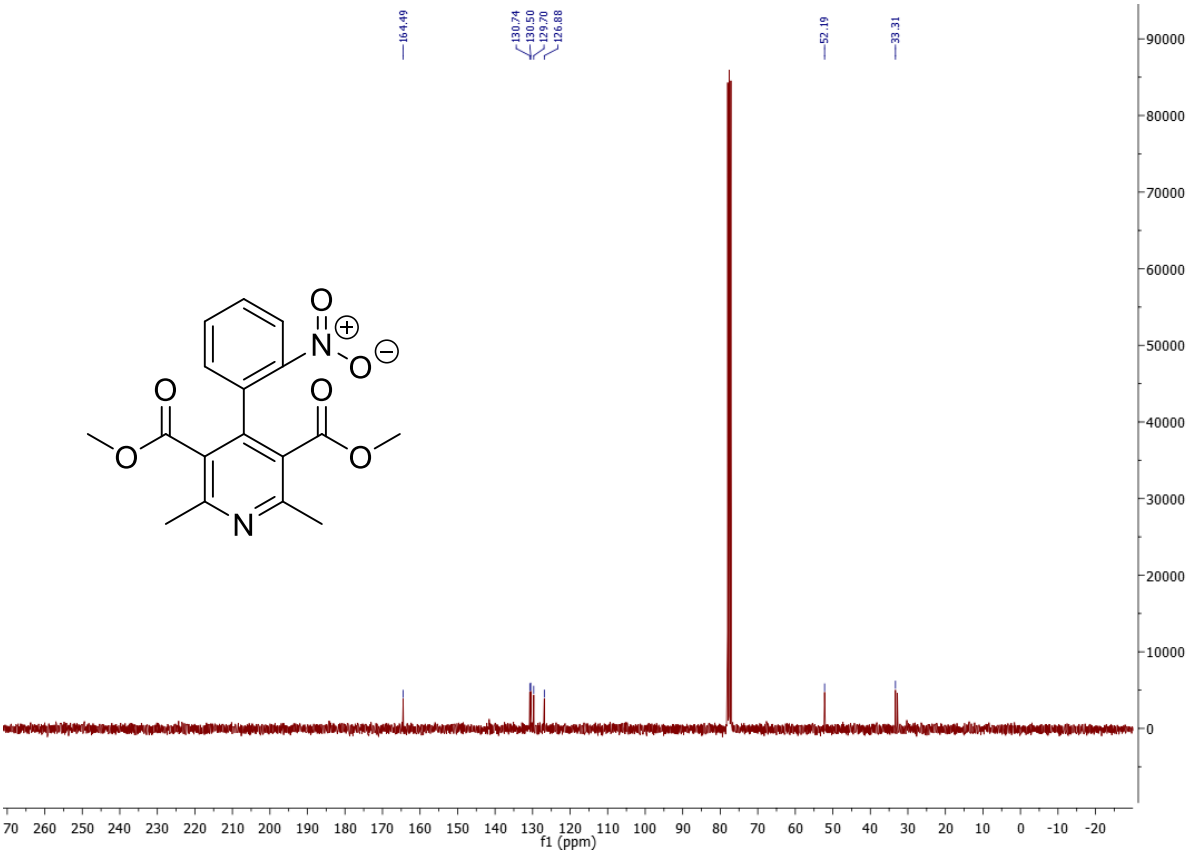

^{13}C NMR spectrum in $CDCl_3$.

6 References

[1] a) R. A. Sheldon, *Green Chem*. **2005**, *7*, 267; b) D. Prat, O. Pardigon, H.-W. Flemming, S. Letestu, V. Ducandas, P. Isnard, E. Guntrum, T. Senac, S. Ruisseau, P. Cruciani, P. Hosek, *Org. Process Res. Dev.* **2013**, *17*, 1517.

[2] C. Wiles, P. Watts, *Green Chem.* **2014**, *16*, 55.

[3] a) Green separation processes, Fundamentals and applications, eds.: C. A. M. Afonso, J. G. Crespo, *Wiley-VCH*, Weinheim **2005**; b) Industrial catalysis, A practical approach, 2nd ed., ed.: J. Hagen, *Wiley-VCH*, Weinheim **2006**; c) B. A. de Marco, B. S. Rechelo, E. G. Tótoli, A. C. Kogawa, H. R. N. Salgado, *Saudi Pharm. J.* **2019**, *27*, 1; d) P. Anastas, N. Eghbali, *Chem. Soc. Rev.* **2010**, *39*, 301; e) C. Wiles, P Watts, *Green Chem.* **2012**, *14*, 38; f) R. A. Sheldon, *ACS Sustainable Chem. Eng.* **2017**, *6*, 32; g) B. Trost, *Science* **1991**, *254*, 1471; h) Green Metrics, Handbook of Green Chemistry, 1st ed., eds.: D. J. C. Constable, J. Gonzalez, *Wiley-VCH*, Weinheim **2018**; i) K. J. M. Matus, W. C. Clark, P. T. Anastas, J. B. Zimmerman, *Environ. Sci. Technol.* **2012**, *46*, 10892.

[4] The greenhouse effect and ozone layer, P. Neal, *Dryad*, London **1989**.

[5] a) M. Mikkelsen, M. Joergensen, F. C. Krebs, *Energy Environ. Sci.* **2010**, *3*, 43; b) A. Dhakshinamoorthy, S. Navalon, A. Corma, H. Gerci, *Energy Environ. Sci.* **2012**, *5*, 9217; c) R. F. Keeling, S. J. Walker, S. C. Piper, A. F. Bollenbacher, Mauna Loa Observatory, Hawaii (Scripps Institution of Oceanography, **2020**), https://scrippsco2.ucsd.edu/data/atmospheric_co2/mlo.html, access on 14.07.2020.

[6] a) M. Bui, C. S. Adjiman, A. Bardow, E. J. Anthony, A. Boston, S. Brown, P. S. Fennell, S. Fuss, A. Galindo, L. A. Hackett, J. P. Hallett, H. J. Herzog, G. Jackson, J. Kemper, S. Krevor, G. C. Maitland, M. Matuszewski, I. S. Metcalfe, C. Petit, G. Puxty, J. Reimer, D. M. Reiner, E. S. Rubin, S. A. Scott, N. Shah, B. Smit, J. P. M. Trusler, P. Webley, J. Wilcox, N. Mac Dowell, *Energy Environ. Sci.* **2018**, *11*, 1062; b) J. Tollefson, *Nature* **2018**, *558*, 173.

[7] a) Q. Liu, L. Wu, R. Jackstell, M. Beller, *Nat. Commun.* **2015**, *6*, 1; b) F. D. Bobbink, P. J. Dyson, *J. Catal.* **2016**, *343*, 52; c) P. G. Jessop, S. M. Mercer, D. J. Heldebrant, *Energy Environ. Sci.* **2012**, *5*, 7240; d) N. Eghbali, C.-J. Li, *Green Chem.* **2007**, *9*, 213; e) M. Peters, B. Köhler, W. Kuckshinrichs, W. Leitner, *ChemSusChem* **2011**, *4*, 1216; f) T. G. Ostapowics, M. Schmitz, M. Krystof, J. Klankermayer, W. Leitner, *Angew. Chem. Int. Ed.* **2013**, *52*, 12119; g) M. Aresta in Carbon Dioxide as Chemical Feedstock, *Wiley-VCH*, Weinheim **2010**; h) A. Decortes, A. M. Castilla, A. W. Kleij, *Angew. Chem. Int. Ed.* **2010**, *49*, 9822; i) A. Dibenedetto, A. Angelini, P. Stufano, *Chem. Technol. Biotechnol.* **2014**, *89*, 334; j) R. M. Cuéllar-Franca, A. Azapagic, *J. CO2 Util.* **2015**, *9*, 82; k) W. Desens, T. Werner, *Adv. Synth. Catal.* **2016**, *358*, 622; l) C. Kohrt, T. Werner, *ChemSusChem* **2015**, *8*, 2031; m) S. Das, S.; F. D. Bobbink, A. Gopakumar, P. J. Dyson, *Chimia* **2015**, *69*, 76.

[8] a) J. Artz, T. E. Müller, K. Thenert, J. Kleinekorte, R. Meys, A. Sternberg, A. Bradow, W. Leitner, *Chem. Rev.* **2018**, *118*, 434; b) M. Aresta, A. Dibenedetto, A. Angelini, *Chem. Rev.* **2014**, *114*, 1709; c) J. Klankermayer, S. Wesselbaum, K. Beydoun, W. Leitner, *Angew. Chem. Int. Ed.* **2016**, *55*, 7296; d) Y. Li, X. Cui, K. Dong, K. Junge, M. Beller, *ACS Catal.* **2017**, *7*, 1077; e) F. D. Bobbink, P. J. Dyson, *J. Catal.* **2016**, *343*, 52; f) D. J. Darensbourg, *Chem. Rev.* **2007**, *107*, 2388.

[9] a) J.-R. Li, Y. Ma, M. C. McCarthy, J. Sculley, J. Yu, H.-K. Jeong, P. B. Balbuena, H.-C. Zhou, *Coord. Chem. Rev.* **2011**, *255*, b) K. Huang, C. L. Sun, Z. J. Shi, *Chem. Soc. Rev.* **2011**, *40*, 2435; c) Supercritical Fluids, Fundamentals and Applications, eds.: E. Kiran, P. G. Debenedetti, C. J. Peters, *Springer*, Dordrecht **2000**.

[10] H. Kolbe, *J. prakt. Chem.* **1874**, *10*, 89.

[11] a) C. Bosch, W. Meiser, US1429483A, **1920**; b) N. W. Krase, V. L. Gaddy, *J. Ind. Eng. Chem.* **1922**, *14*, 611.

[12] S. Fukuoka, M. Kawamura, K. Komiya, M. Tojo, H. Hachiya, K. Hasegawa, M. Aminaka, H. Okamoto, I. Fukawa, S. Konno, *Green Chem.* **2003**, *5*, 497.

[13] a) G. Fiorani, W. Guo, A. W. Kleij, *Green Chem.* **2015**, *17*, 1375; b) C. D. N. Gomes, O. Jacquet, C. Villiers. P. Thuery, M. Ephritikhine, T. Cantat, *Angew. Chem. Int. Ed.* **2012**, *51*, 187; c) D. Riemer, P. Hirapara, S. Das, *ChemSusChem* **2016**, *9*, 1916; d) M. Hulla, S. A. M. Chama, G. Laurenczy, S. Das, P. J. Dyson, *Angew. Chem. Int. Ed.* **2017**, *56*, 10559; e) M. Hulla, F. D. Bobbink, S. Das, P. J. Dyson, *ChemCatChem* **2016**, *8,* 3338; f) F. D. Bobbink, S. Das, P. J. Dyson, *Nat. Protocol* **2017**, *12,* 417; g) S. Das, F. D. Bobbink, G. Laurenczy, P. J. Dyson, *Angew. Chem. Int. Ed.* **2014**, *53*, 12876; h) W. Dai, S. Luo, S. Yin, C. Au, *Applied Catal. A: General* **2009**, *366*, 2; i) D. J. Darensbourg, R. M. Mackiewicz, A. L. Phelps, D. R. Billodeaux, *Acc. Chem. Res.* **2004**, *37*, 836; j) S. N. Riduan, Y. Zhang, *Dalton Trans.* **2010**, *39*, 3347.

[14] a) C. Maeda, Y. Miyazaki, T. Ema, *Catal. Sci. Technol.* **2014**, *4*, 1482; b) M. Mikkelsen, M. Jørgensen, F. C. Krebs, *Energy Environ. Sci.* **2010**, *3*, 43; c) J. Ma, N. Sun, X. Zhang, N. Zhao, F. Xiao, W. Wie, Y. Sun, *Catal. Today* **2009**, *148*, 221.

[15] a) J. Luo, I. Larrosa, *ChemSusChem* **2017**, *10*, 3317; b) I. Tommasi, *Catalysts* **2017**, *7*, 380; c) M. Börjesson, T. Moragas, D. Gallego, R. Martin, *ACS Catal.* **2016**, *6*, 6739; d) L. Ackermann, *Angew. Chem. Int. Ed.* **2011**, *50*, 3842; e) K. Sasano, J. Takaya, N. Iwasawa, *J. Am. Chem. Soc.* **2013**, *135*, 10954; f) H. Mizuno, J. Takaya, J. Iwasawa, *J. Am. Chem. Soc.* **2011**, *133*, 1251; g) Y. Masuda, N. Ishida, M. Murakami, *J. Am. Chem. Soc.* **2015**, *137*, 14063; h) Q. Meng, S. Wang, B. König, *Angew. Chem. Int. Ed.* **2017**, *56*, 13426; i) H. Seo, M. H. Katcher, T. F. Jamison, *Nat. Chem.* **2017***, 9*, 453; j) K. Michigani, T. Mita, Y. Sato, *J. Am. Chem. Soc*. **2017**, *139*, 6094; k) A. Banerjee, G. R. Dick, T. Yoshino, M. W. Kanan, *Nature* **2016**, *531*, 215.

[16] a) L. Wu, Q. Liu, I. Fleischer, R. Jackstell, M. Beller, *Nat. Commun.* **2014**, *5*, 3091; b) S. Das, F. D. Bobbink, S. Bulut, K. Soudani, P. J. Dyson, *Chem. Commun.* **2016**, *52*, 2497; c) C. M. Williams, J. B. Johnson, T. Rovis, *J. Am.*

Chem. Soc. **2008**, *130*, 14396; d) S. Gaillard, C. S. J. Cazin, S. P. Nolan, *Acc. Chem. Res.* **2012**, *45,* 778; e) I. I. F. Boogaerts, S. P. Nolan, *J. Am. Chem. Soc.* **2010**, *132*, 8858; f) X. Wang, M. Nakajima, R. Martin, *J. Am. Chem. Soc.* **2015**, *137*, 8924; g) M. Hulla, F. D. Bobbink, S. Das, P. J. Dyson, *ChemCat-Chem* **2016**, *8*, 3338; h) S. Fenner, L. Ackermann, *Green. Chem.* **2016**, 18, 3804; i) M. Alvaro, C. Baleizao, D. Das, E. Carbonell, H. García, *J. Catal.* **2004**, *228*, 254.

[17] a) M. Aresta, C. Fragale, E. Quaranta, I. Tommasi, *J. Chem. Soc., Chem. Commun.* **1992**, 315; b) M. Aresta, I. Tommasi, E. Quaranta, C. Fragale, J. Mascetti, M. Tranquille, F. Galan, M. Fouassier, *Inorg. Chem*. **1996**, *35*, 4254.

[18] M. B. Ansari, S.-E. Park, *Energy Environ. Sci.* **2012**, *5*, 9419.

[19] E. F. Lutz, US3518310A, **1968**.

[20] a) Y. Sugawara, W. Yamada, S. Yoshida, T. Yamada, *J. Am. Chem. Soc.* **2007**, *129*, 12902; b) R. Ma, A.-H. Liu, C.-B. Huang, X.-D. Li, L. N. He, *Green Chem.* **2013**, *15*, 1274; c) H. He, C. Qi, X. Hu, Y. Guan, H. Jiang, *Green Chem.* **2014**, *16*, 3729; d) R. Lee, J. Harris, P. Champagne, P. G. Jessop, *Green Chem.* **2016**, *18*, 6305; e) G. Pupo, R. Properzi, B. List, *Angew. Chem. Int. Ed.* **2016**, *55*, 6099; f) M. Kapoor, D. Liuz, M. C. Young, *J. Am. Chem. Soc.* **2018**, *140*, 6818; g) W. Schilling, S. Das, *Tetrahedron Lett.* **2018**, *59*, 3821.

[21] S. B. Long, T. M. Locascio, J. A. Tunge, *Org. Lett.* **2014**, *16*, 4308.

[22] R. Lee, J. R. Vanderveen, P. Champagne, P. G. Jessop, *Green Chem.* **2016**, *18*, 5118.

[23] G. Ciamician, *Science* **1912**, *36*, 385.

[24] a) E. Paternò, G. Chieffi, *Gazz. Chim. Ital*. **1909**, *39*, 341; b) G. Büchi, C. G. Inman, E. S. Lipinsky, *J. Am. Chem. Soc.* **1954**, *76*, 4327.

[25] Design of Advanced Photocatalytic Materials for Energy and Environmental Applications, ed.: R. Portela, Springer, *London* **2013**

[26] a) A. Ajmal, I. Majeed, R. N. Malik, H. Idriss, M. A. Nadeem, *RSC Adv.* **2014**, *4*, 37003; b) I. Ani, U. Akpan, M. Olutoye, B. Hameed, *J. Clean Prod.* **2018**, *205*, 930; c) C. Gambarotti, C. Punta, F. Recupero, T. Caronna, L. Palmisano, *Curr. Org. Chem.* **2010**, *14*, 1153.

[27] C. Li, Y. Xu, W. Tu, G. Chen, R. Xu, *Green Chem.* **2017**, *19*, 882.

[28] a) J. W. Tucker, C. R. J. Stephenson, *J. Org. Chem.* **2012**, *77*, 1617; b) J. M. R. Narayanam, C. R. J. Stephenson, *Chem. Soc. Rev.* **2011**, *40*, 102; c) T. P. Yoon, M. A. Ischay, J. Du, *Nat. Chem.* **2010**, *2*, 527; d) M. Fagnoni, D. Dondi, D. Ravelli, A. Albini, *Chem. Rev.* **2007**, *107*, 2725.

[29] a) C. Bottecchia, R. Martin, I. Abdiaj, E. Crovini, J. Alcazar, J. Orduna, M. J. Blesa, J. R. Carrillo, P. Prieto, T. Noel, *Adv. Synth. Catal.* **2019**, *361*, 945; b) L. Marzo, S. K. Pagire, O. Reiser, B. König, *Angew. Chem. Int. Ed.* **2018**, *57*, 10034; c) S. P. Pitre, C. D. McTiernan, J. C. Scaiano, *Acc. Chem. Res.* **2016**, *49*, 1320; d) V. Srivastava, P. P. Singh, *RSC Adv.* **2017**, *7*, 31377.

[30] a) N. A. Romero, D. A. Nicewicz, *Chem. Rev.* **2016**, *116*, 10075; b) L. M. Kreis, S. Krautwald, N. Pfeiffer, R. E. Marin, E. M. Carreira, *Org. Lett.* **2013**, *15*, 1634; c) F. Yang, J. Koeller, L. Ackermann, *Angew. Chem. Int. Ed.* **2016**,

55, 4759; d) Y.-F. Liang, R. Steinbock, L. Yang, L. Ackermann, *Angew. Chem. Int. Ed.* **2018**, *57*, 10625; e) Y. Qiu, A. Scheremetjew, L. H. Finger, L. Ackermann, *Chem. Eur. J.* **2020**, *26*, 3241.

[31] a) T. Suga, H. Mizuno, J. Takaya, N. Iwasawa, *Chem. Commun.* **2014**, *50*, 14360; b) S. Gaillard, A. M. Z. Slawin, S. P. Nolan, *Chem. Commun.* **2010**, *46*, 2742; c) L. Zang, J. Cheng, T. Ohishi, Z. Hou, Angew. Chem. Int. Ed. 2010, 49, 8670; d) I. I. F. Boogaerts, G. C. Fortman, M. R. L. Furst, C. S. J. Cazin, S. P. Nolan, *Angew. Chem. Int. Ed.* **2010**, *49*, 8674; e) X. Wang, Y. Liu, R. Martin, *J. Am. Chem. Soc.* **2015**, *137*, 6476; f) Y. Li, I. Sorribes, T. Yan, K. Junge, M. Beller, *Angew. Chem. Int. Ed.* **2013**, *52*, 12156; g) K. Beydoun, T. vom Stein, J. Klankermayer, W. Leitner, *Angew. Chem. Int. Ed.* **2013**, *52*, 9554; h)) K. Beydoun, G. Ghattas, K. Thenert, J. Klankermayer, W. Leitner, *Angew. Chem. Int. Ed.* **2014**, *53*, 11010; i) X. Cui, X. Dai, Y. Zhang, Y. Deng. F. Shi, *Chem. Sci.* **2014**, *5*, 649; j) O. Jacquet, X. Frogneux, C. D. N. Gomes, T. Cantat, *Chem. Sci.* **2013**, *4*, 2127; k) C. D. N. Gomes, O. Jacquet, C. Villiers, P. Thuery, M. Ephritikhine, T. Cantat, *Angew. Chem. Int. Ed.* **2012**, *51*, 187; l) Z. Yang, B. Yu, H. Zhang, Y. Zhao, G. Ji, Z. Ma, X. Gao, Z. Liu, *Green Chem.* **2015**, *17*, 4189; m) E. Blondiaux, J. Pouessel, T. Cantat, *Angew. Chem. Int. Ed.* **2014**, *53*, 12186; n) T. V. Q. Nguyen, W. Yoo, S. Kobayashi, *Angew Chem. Int. Ed.* **2015**, *54*, 9209; o) O. Jacquet, C. D. N. Gomes, M. Ephritikhine, T. Cantat, *J. Am. Chem. Soc.* **2012**, *134*, 2934.

[32] a) W. Guo, J. González-Fabra, N. A. G. Bandeira, C. Bo, A. W. Kleij, *Angew. Chem. Int. Ed.* **2015**, *54*, 11686; b) W. Guo, V. Laserna, E. Martin, E. C. Escudero-Adan, A. Kleij, *Chem. Eur. J.* **2016**, *22*, 1722; c) M. Shimizu, M. Sodeoka, Org. Lett. 2007, 9, 5231.

[33] a) A. K. Ghosh, M. Brindisi, *J. Med. Chem.* **2015**, *58*, 2895; b) J. Vagner, H. Qu, V. J. Hurby, *Curr. Opin. Chem. Biol.* **2008**, *12*, 292; c) A. Conradi, A. R. Hilgers, P. S. Burton, *Pharm. Res.* **1992**, *9*, 435.

[34] a) N. Squillace, D. Trabattoni, A. Muscatello, F. Sabbatini, A. Maloberti, C. Giannattasio, M. Masetti, C. Fenizia, A. Soria, M. Clerici, A. Gori, A. Bandera, *J. Antimicrob. Chemother.* **2018**, *73*, 2162–2170; b) B. Cao, Y. Wang, D. Wen, W. Liu, J. Wang, G. Fan, L. Ruan, B. Song, Y. Cai, M. Wei, X. Li, J. Xia, N. Chen, J. Xiang, T. Yu, T. Bai, X. Xie, L. Zhang, C. Li, Y. Yuan, H. Chen, Huadong Li, H. Huang, S. Tu, F. Gong, Y. Liu, Y. Wei, C. Dong, F. Zhou, X. Gu, J. Xu, Z. Liu, Y. Zhang, Hui Li, L. Shang, K. Wang, K. Li, X. Zhou, X. Dong, Z. Qu, S. Lu, X. Hu, S. Ruan, S. Luo, J. Wu, L. Peng, F. Cheng, L. Pan, J. Zou, C. Jia, Juan Wang, X. Liu, S. Wang, X. Wu, Q. Ge, J. He, H. Zhan, F. Qiu, L. Guo, C. Huang, T. Jaki, F.G. Hayden, P.W. Horby, D. Zhang, C. Wang, *N. Engl. J. Med.* **2020**, *382*, 1787.

[35] J. L. Roberts, A. Poklepovic, L. Booth, Laurence, P. Dent, *Cell. Signal.* **2020**, *70*, 109573.

[36] S. Shi, J. Li, F. Sun, Y. Chen, C. Pang, Y. Geng, J. Qi, S. Guo, X. Wang, H. Zhang, Y. Zhan, H. An, *J. Membr. Biol.* **2020**, *253*, 167.

[37] a) J. P. Mayer, G. S. Lewis, M. J. Curtius, J. Zhang, *Tetrahedron Lett.* **1997**, *38*, 8445; b) H. P. Buchstaller, *Tetrahedron* **1998**, *54*, 3465; c) P. T. Holte, L. Thijs, B. Zwanenburg, *Tetrahedron Lett.* **1998**, *39*, 7404.

[38] a) P. Adams, F. A. Baron, *Chem. Rev.* **1965**, *65*, 567; b) S. Ozaki, *Chem. Rev.* **1972**, *72*, 457; c) R. A. Batey, V. Santhakumar, C. Y. Ishii, S. D. Taylor, *Tetrahedron Lett.* **1998**, *39*, 6267; d) T. Kihliberg, F. Karimi, B. Langstrom, *J. Org. Chem.* **2002**, *67*, 3687.

[39] a) F. Kojima, T. Aida, S. Inoue, *J. Am. Chem. Soc.* **1986**, *108*, 391; b) R. Mahe, Y. Sasaki, C. Bruneau, P. H. Dixneuf, *J. Org. Chem.* **1989**, *54*, 1520; c) M. Abla, J. Choi, T. Sakakura, *Chem. Commun.* **2001**, 2238; d) Y. Sasaki, P. H. Dixneuf, J*. Chem. Soc. Chem. Commun.* **1986**, 790; e) J. Shang, X. Guo, Z. Li, Y. Deng, *Green Chem.* **2016**, *18*, 3082.

[40] a) M. Aresta, E. Quaranta, *Tetrahedron* **1992**, *48*, 1515; b) K. N. Singh, Synth. Commun. 2007, 37, 2651.

[41] a) W. Xiong, C. Qi, H. He, L. Ouyang, M. Zhang, H. Jiang, *Angew. Chem. Int. Ed.* **2015**, *54*, 3084; b) A. Ion, V. Parvulescu, P. Jacobs, D. De Vos, *Green Chem.* **2007**, *9*, 158; c) A. Ion, C. V. Doorslaer, P. Jacobs, D. De Vos, *Green Chem.* **2008**, *10*, 111; d) S. L. Peterson, S. M. Stucka, C. J. Dinsmore, *Org. Lett.* **2010**, *12*, 1340; e) W. McGhee, D. Riley, K. Christ, Y. Pan, B. Parnas, *J. Org. Chem.* **1995**, *60*, 2820; f) R. N. Salvatore, S. Shin, A. S. Nagle, K. W. Jung, *J. Org. Chem.* **2001**, *66*, 1035; g) W. Xiong, C. Qi, Y. Peng, T. Guo, M. Zhang, H. Jiang, *Chem, Eur. J.* **2015**, *21*, 14314.

[42] Y. Yoshida, S. Ishii, T. Yamashita, *Chem. Lett.* **1984**, 1571.

[43] Y. Yoshida, S. Ishii, M. Watanabe, T. Yamashita, *Bull. Chem. Soc. Jpn.* **1989**, *62*, 1534.

[44] B. Zhao, S. Yao, H. An, X. Zhao, Y. Wang, *J. Chem. Technol. Biotechnol.* **2014**, *89*, 1553.

[45] Y. Ren, S. A. L. Rousseaux, *J. Org. Chem.* **2018**, *83*, 913.

[46] A. Sudo, Y. Morioka, F. Sanda, T. Endo, *Tetrahedron Lett.* **2004**, *45*, 1363.

[47] L. Zhang, Z. Wu, N. C. Nelson, A. D. Sadow, I. I. Slowing, S. H. Overbury, *ACS Catal.* **2015**, *5*, 6426.

[48] a) L. Gu, Y. Zhang, *J. Am. Chem. Soc.* **2010**, *132*, 914; b) V. Nair, V. Varghese, R. R. Paul, A. Jose, C. R. Sinu, R. S. Menon, *Org. Lett.* **2010**, *12,* 2653.

[49] a) Modern Oxidation Methods, Ed.: J.-E. Bäckvall, *Wiley-VCH*, New York **2004**; b) Oxidation of Alcohols to Aldehydes and Ketones, Eds.: G. Tojo, M. Fernández, , Springer, *London* **2006**; c) R. A. Sheldon, I. W. C. E. Arends, G.-J. T. Brink, A. Dijksman, *Acc. Chem. Res.* **2002**, *35*, 774; d) D. Lenoir, *Angew. Chem. Int. Ed.* **2006**, *45*, 3206; e) T. Punniyamurthy, S. Velusamy, J. Iqbal, *Chem. Rev.* **2005**, *105*, 2329.

[50] a) N. Umierski, G. Manolikakes, *Org. Lett.* **2013**, *15*, 188; b) S. M. Roopan, J. Palaniraja, *Res. Chem. Intermed*. **2015**, *41*, 8111; c) Y. Dong, M. I. Lipschutz, T. D. Tilley, *Org. Lett.* **2016**, *18*, 1530; d) C. E. Garrett, K. Prasad, *Adv. Synth. Catal.* **2004**, *346*, 889; e) V. W. Rosso, D. A. Lust, P. J. Bernot, J. A. Grosso, S. P. Modi, A. Rusowicz, T. C. Sedergran, J. H. Simpson, S. K. Srivastava,

M. J. Humora, N. G. Anderson, *Org. Process Res. Dev.* **1997**, *1*, 311; f) Z. Zhang, L.-L. Liao, S.-S. Yan, L. Wang, Y.-Q. He, J.-H. Ye, J. Li, Y.-G. Zhi, D.-G. Yu, *Angew. Chem.* **2016**, *128*, 7184; g) C.-L. Sun, Z.-J. Shi, *Chem. Rev.* **2014**, *114*, 9219.

[51] a) A. Das, S. S. Stahl, *Angew. Chem. Int. Ed.* **2017**, *56*, 8892; b) L. B. Ryland, S. S. Stahl, *Angew. Chem. Int. Ed.* **2014**, *53*, 8824; c) K. Schröder, K. Junge, B. Bitterlich, M. Beller, *Topics in Organometal. Chem.* **2011**, *33*, 83; d) Y. Yuan, N. Yan, P. J. Dyson, *Inorg. Chem.* **2011**, *50*, 11069; e) B. Guan, D. Xing, G. Cai, X. Wann, N. Yu, Z. Fang, L. Ying, Z. Shi, *J. Am. Chem. Soc.* **2005**, *127*, 18004; f) D. Könning, T. Olbrisch, F. D. Sypaseuth, C. C. Tzschucke, M. Christmann, *Chem. Commun.* **2014**, *50*, 5014; g) R. V. Jagadeesh, H. Junge, M. M. Pohl, J. Radnik, A. Brückner, M. Beller, *J. Am. Chem. Soc.* **2013**, *135*, 10776; h) S. Gowrisankar, H. Neumann, D. Goerdes, K. Thurow, H. Jiao, M. Beller, *Chem. Eur. J.* **2013**, *19*, 15979; i) D. S. Mannel, M. S. Ahmed, T. W. Root, S. S. Stahl, *J. Am. Chem. Soc.* **2017**, *139*, 1690; j) J. E. Steves, S. S. Stahl, *J. Org. Chem.* **2015**, *80*, 11184.

[52] H. Nagashima, K. Sato, J. Tsuji, *Tetrahedron* **1985**, *41*, 5645.

[53] a) K. P. Peterson, R. C. Larock, *J. Org. Chem.* **1998**, *63*, 3185; b) B. A. Steinhoff, S. R. Fix, S. S. Stahl, *J. Am. Chem. Soc.* **2002**, *124*, 766.

[54] a) O. Bortolini, V. Conte, F. Di Furia, G. Modena, *J. Org. Chem.* **1985**, *51*, 2661; b) K. Sato, M. Aoki, J. Takagi, R. Noyori, *J. Am. Chem. Soc.* **1997**, *119*, 12386.

[55] S. Samanta, P. Biswas, *RSC Adv.* **2015**, *5*, 84328.

[56] W. Schilling, D. Riemer, Y. Zhang, N. Hatami, S. Das, *ACS Catal.* **2018**, *8*, 5425.

[57] W. Huang, B. C. Ma, H. Lu, R. Li, L. Wang, K. Landfester, K. A. I. Zhang, *ACS Catal.* **2017**, *7*, 5438.

[58] R. Ray, S. Chandra, D. Maiti, G. K. Lahiri, *Chem. Eur. J.* **2016**, *22*, 8814.

[59] B.-Z. Zhan, M. A. White, T.-K. Sham, J. A. Pincock, R. J. Doucet, K. V. R. Rao, K. N. Robertson, T. S. Cameron, *J. Am. Chem. Soc.* **2003**, *125*, 2195.

[60] I. E. Markó, A. Gautier, R. Dumeunier, K. Doda, F. Philippart, S. M. Brown, C. J. Urch, *Angew. Chem. Int. Ed.* **2004**, *43*, 1588.

[61] P. D. Lokhande, S. R. Waghmare, H. Gaikward, P. P. Hankare, *J. Korean Chem. Soc.* **2012**, *56*, 539.

[62] B. Betzemeier, M. Cavazzini, S. Quici, P. Knochel, *Tetrahedron Lett.* **2000**, *41*, 4343.

[63] a) J. M. Hoover, S. S. Stahl, *J. Am. Chem. Soc.* **2011**, *133*, 16901; b) J. M. Hoover, B. L. Ryland, S. S. Stahl, *J. Am. Chem. Soc.* **2013**, *135*, 2357.

[64] S. Velusamy, A. Srinivasan, T. Punniyamurthy, *Tetrahedron Lett.* **2006**, *47*, 923.

[65] A. Cecchetto, F. Fontana, F. Miniscia, F. Recuperoa, *Tetrahedron Lett.* **2001**, *42*, 6651.

[66] R. Liu, X. Liang, C. Dong, X. Hu, *J. Am. Chem. Soc.* **2004**, *126*, 4112.

[67] R. Liu, C. Dong, X. Liang, X. Wang, X. Hu, *J. Org. Chem.* **2005**, *70*, 729.

[68] N. Wang, R. Liu, J. Chen, X. Liang, *Chem. Commun.* **2005**, 5322.

[69] X. Wang, R. Liu, Y. Jin, X. Liang, *Chem. Eur. J.* **2008**, *14*, 2679.
[70] X. He, Z. Shen, W. Mo, N. Sun, B. Hu, X. Hu, *Adv. Synth. Catal.* **2009**, *351*, 89.
[71] a) B. Karimi, A. Biglari, J. H. Clark, V. Budarin, *Angew. Chem. Int. Ed.* **2007**, *46*, 7210; b) W. Adam, C. R. Saha-Möller, P. A. Ganeshpure, *Chem. Rev.* **2001**, *101*, 3499; c) X. Zhang, X. Fu, Y. Zhang, Y. Zhu, J. Yang, *Catal. Lett*. **2016**, *146*, 945; d) H. Watanabe, S. Asano, S. Fujita, H. Yoshida, M. Arai, *ACS Catal.* **2015**, *5*, 2886.
[72] a) K. Alfonsi, J. Colberg, P. J. Dunn, T. Fevig, S. Jennings, T. A. Johnson, H. P. Kleine, C. Knight, M. A. Nagy, D. A. Perry, M. Stefaniak, *Green Chem.* **2008**, *10*, 31; b) K. Omura, D. Swern, *Tetrahedron* **1978**, *34*, 1651; c) L. Gorini, A. Caneschi, S. Menichetti, *Synlett* **2006**, *6*, 948.
[73] a) K. E. Pfitzner, J. G. Moffatt, *J. Am. Chem. Soc.* **1963**, *85*, 3027; b) J. R. Parikh, W. v. E. Doering, *J. Am. Chem. Soc.* **1967**, *89*, 5505; c) J. D. Albright, L. Goldman *J. Am. Chem. Soc.* **1965**, *87*, 4214.
[74] a) E. Franco-Luesma, M.-P. Sáenz-Navajas, D. Valentin, J. Ballester, H. Rodrigues, V. Ferreira, *Food Res. Int.* **2016**, *87*, 152; b) H. Jang, M. A. Hossain, S. C. Sutradhar, F. Ahmed, K. Choi, T. Ryu, K. Kim, W. Kim, *Int. J. Hydrogen Energy* **2017***, 42,* 12759; c) K. Li, X. Lei, CN105984848, **2016**; d) R. J. Herschler, US3023074, **1962**; e) H. D. Wellman, US3236046, **1966**; f) G. Zhu, Z. Xiao, N. Rujuan, Y. Niu, CN104643004, **2016**.
[75] C.-J. Li, B. M. Trost, *Proc. Natl. Acad. Sci. USA* **2008**, *105*, 13197.
[76] a) X. Wang, Y. N. Lam, C. Lee, M. Ji, E. J. Kang, H. Jang, *RSC Adv.* **2013**, *3*, 24922; b) P.-C. Chiang, J. W. Bode, *Org. Lett.* **2011**, *13*, 2422.
[77] a) K. C. Nicolaou, D. L. F. Gray, J. Tae, *J. Am. Chem. Soc.* **2004**, *126*, 613; b) X. Hui, J. Desrivot, C. Bories, P. M. Loiseau, X. Franck, R. Hocquemiller, B. Figadère, *Bioorg. Med. Chem.* **2006**, *6*, 815; c) G. R. Boyce, J. S. Johnson, *Angew. Chem. Int. Ed.* **2010**, *49*, 8930.
[78] a) C. A. Buehler, J. O. Harris, W. F. Arendale, *J. Am. Chem. Soc.* **1950**, *72*, 4953; b) G. L. Southard, B. R. Zaborowsky, J. M. Pettee, *J. Am. Chem. Soc.* **1971**, *93*, 3303; c) S. Chen, Z. Liu, E. Shi, L. Chen, W. Wei, H. Li, Y. Cheng, X. Wan, *Org. Lett.* **2011**, *13*, 2274; d) Y. Xu, X. Wan, *Tetrahedron Lett.* **2013**, *54*, 642; e) M. S. Yusybo, V. D. Filimonov, *Synthesis* **1991**, 131; f) W.-X. Lv, Y.-F. Zeng, S.-S. Zhang, Q. Li, H. Wang, *Org. Lett.* **2015**, *17*, 2972; g) Z. Wan, C. D. Jones, D. Mitchell, J. Y. Pu, T. Y. Zhang, *J. Org. Chem.* **2006**, *71*, 826; h) W. Ren, Y. Xia, S.-J. Ji, Y. Zhang, X. Wan, J. Zhao, *Org. Lett.* **2009**, *11*, 1841; i) W. Ren, J. Liu, L. Chen, X. Wan, *Adv. Synth. Catal.* **2010**, *352*, 1424; j) C.-F. Xu, M. Xu, Y.-X. Jia, C.-Y. Li, *Org. Lett.* **2011**, *13*, 1556; k) A. Gao, F. Yang, J. Li, Y. Wu, *Tetrahedron* **2012**, *68*, 4950; l) J. Muzart, *J. Mol. Catal. A: Chem.* **2011**, *338*, 7; m) X. Zhu, P. Li, Q. Shi, L. Wang, *Green Chem.* **2016**, *18*, 6373; n) E. J. Steves, S. S. Stahl, *J. Am. Chem. Soc.* **2013**, *135*, 15742; o) Y. Yu, C. Lin, B. Li, P. Zhao, S. Zhang, *Green Chem.* **2016**, *18*, 3647; p) G. Urgoitia, R. SanMartin, M. T. Herrero, E. Domínguez, *Green Chem.* **2011**, *13*, 2161; q) T. Bhattacharya, T. K. Sarma, S. Samanta, *Catal. Sci. Tech.* **2012**, *2*, 2216; r) T. A. Alsalim, J. S. Hadi, O. N. Ali, H. S. Abbo, S. J. Titinchi,

Chem. Central J. **2013**, *7*, 3; s) M. Kirihara, Y. Ochiai, S. Takizawa, H. Takahata, H. Nemoto, *Chem. Commun.* **1999**, 1387; t) M. Mahyari, M. S. Laeini, A. Shabani, *Chem. Commun.* **2014**, *50*, 7855; u) A. Shaabani, M. Boroujeni, M. Laeini, *Appl. Organometal. Chem.* **2016**, *30*, 154; v) X.-F. Zhao, C. Zhang, *Synthesis* **2007**, 551.

[79] a) L. Huang, K. Cheng, B. Yao, Y. Xie, Y. Zhang, *J. Org. Chem.* **2011**, *76*, 5732; b) A. Stergiou, A. Bariotaki, D. Kalaitzakis, I. Smonou, *J. Org. Chem.* **2013**, *78*, 7268; c) Z. Li, J. Yin, G. Wen, T. Li, X. Shen, *RSC Adv.* **2014**, *4*, 32298.

[80] a) J. von Liebig, F. Wöhler, *Ann. Pharm.* **1832**, *3*, 249; b) A. Lapworth, *J. Chem. Soc., Trans.* **1904**, *85*, 1206.

[81] R. Breslow, *J. Am. Chem. Soc.* **1958**, *80*, 3719.

[82] a) X. Bugaut, F: Glorius*, Chem. Soc. Rev.* **2012**, **41**, 3511; b) R. S. Menon, A. T. Biju, V. Nair, *Beilstein J. Org. Chem.* **2016**, *12*, 444.

[83] L. Baragwanath, C. A. Rose, K. Zeitler, S. J. Connon, *J. Org. Chem.* **2009**, *74*, 9214.

[84] L. Myles, N. Gathergood, S. J. Connon, *Chem. Commun.* **2013**, *49*, 5316.

[85] X. Bi, L. Wu, C. Yan, X. Jing, H. Zhu, *J. Chil. Chem. Soc.* **2011**, 56, F663.

[86] Z. Kelemen, O. Hollóczki, J. Nagyc, L. Nyulászi, *Org. Biomol. Chem.* **2011**, *9*, 5362.

[87] Y. Shimakawa, T. Morikawa, S. Sakaguchi, *Tetrahedron Lett.* **2010**, *51*, 1786.

[88] a) R. W. Layer, *Chem. Rev.* **1963**, *63*, 489; b) R. D: Patil. S. Adimurthy, *Asian. J. Org. Chem.* **2013**, *2*, 726; c) S. F. Martin, *Pure Appl. Chem.* **2009**, *81*, 195; d) M. E. Belowich, J. F. Stoddart, *Chem. Soc. Rev.* **2012**, *41*, 2003; e) L. Dai, Y. Lin, X. Hou, Y. Zhou, *Pure Appl. Chem.* **1999**, *71*, 1033; f) S. Zhou, S. Fleischer, K. Junge, S. Das, D. Addis, M. Beller. *Angew. Chem. Int. Ed.* **2010**, *49*, 8121.

[89] J. Clayden, N. Greeves, S. Warren, Organic chemistry, 2nd ed., *Oxford Univ. Press*, Oxford, **2012**.

[90] D. A. Black, B. A. Arndtsen, *Org. Lett.* **2004**, *6*, 1107.

[91] C. E. Mortimer, U. Müller, J. Beck, Chemie, Das Basiswissen der Chemie, 12th ed., *Georg Thieme Verlag*, Stuttgart, New York, **2015**.

[92] a) M. T. Schümperli, C. Hammond, I. Hermans, *ACS Catal.* **2012**, *2*, 1108; b) X. Ji, Z. Su, P. Wang, G. Ma, S. Zhang, *Small* **2016**, *12*, 4753; c) S. K. Kuk, R. K. Singh, D. H. Nam, R. Singh, J.-K. Lee, C. B. Park, *Angew. Chem. Int. Ed.* **2017**, *56*, 3827; d) A. V. Iosub, S. S. Stahl, *Org. Lett.* **2015**, *17*, 4404−4407; e) H. Choi, M. P. Doyle, *Chem. Commun.* **2007**, 745–747

[93] J.-R. Wang, Y. Fu, B.-B. Zhang, X. Cui, L. Liu, Q.-X. Guo, *Tetrahedron Lett.* **2006**, *47*, 8293.

[94] a) M.-H. So, Y. Lui, C.-M. Ho, C.-M. Che, *Chem. Asian J.* **2009**, *4*, 1551; b) A. F. Holleman, E. Wiberg, N. Wiberg, Lehrbuch der anorganischen Chemie, 101st ed., *de Gruyter*, Berlin, **1995**.

[95] J. S. M. Samec, A. H. Éll, J.-E. Bäckvall, *Chem. Eur. J.* **2005**, *11*, 2327.

[96] A. Kamal, V. Devaiah, K. L. Reddy, N. Shankaraiah, *Adv. Synth. Catal.* **2006**, *348*, 249.

[97] T. Sonobe, K. Oisaki, M. Kanai, *Chem. Sci.* **2012**, *3*, 3249.
[98] M. Hirano, S. Yakabe, H. Chikamori, J. H. Clark, T. Morimoto, *J. Chem. Res.* **1998**, 770.
[99] K. Gopalaiah, A. Saini, Catal. Lett. **2016**, *146*, 1648.
[100] A. E. Wendlandt, S. S. Stahl, *Org. Lett.* **2012**, *14*, 2850.
[101] J. Zhang, S. Chen, F. Chen, W. Xu, G.-J. Deng, H. Gong, *Adv. Synth. Catal.* **2017**, *359*, 2358.
[102] a) M. A. Mohamed, K.-I. Yamada, K. Tomioka, *Tetrahedron Lett.* **2009**, *50*, 3436; b) D. Chen, G. Xu, Q. Zhou, L. W. Chung, W. Tang, *J. Am. Chem. Soc.* **2017**, *139*, 9767.
[103] a) A. Rosas-Hernández, H. Junge, M. Beller, *ChemCatChem* **2015**, *7*, 3316; b) Y. Izumi, *Coord. Chem. Rev.* **2013**, *257*, 171; c) K. Li, B. Peng, T. Peng, *ACS Catal.* **2016**, *6*, 7485; d) M. F. Kuehnel, K. L. Orchard, K. E. Dalle, E. Reisner, *J. Am. Chem. Soc.* **2017**, *139*, 7217; e) W: Zhang, Y. Hu, L. Ma, G. Zhu, Y. Wang, X. Xue, R. Chen, S. Yang, Z. Jin. *Adv. Sci.* **2018**, *5*, 1700275; f) J. Shen, R. Kortlever, R. Kas, Y. Y. Birdja, O. Diaz-Morales, Y. Kwon, I. Ledezma-Yanez, K. J. P. Schouten, G. Mul, M. T. M. Koper, *Nature Commun*. **2015**, *6*, 8177; g) T. Tachikawa, S. Tojo, M. Fujitsuka, T. Majima, *Langmuir* **2004**, *20*, 9441; h) S: N. Habisreutinger, L. Schmidt-Mende, J. K. Stolarczyk, *Angew. Chem. Int. Ed.* **2013**, *52*, 7372; i) T. Kai, M. Zhou, Z. Duan, G. A. Henkelman, A. J. Bard, *J. Am. Chem. Soc.* **2017**, *139*, 18552; j) R. Zhou, M. I. Guzman, *J. Phys. Chem. C.* **2014**, *118*, 11649; k) T. W. Schneider, M. Z. Ertem, J. T. Muckerman, A. M. Angeles-Boza, *ACS Catal.* ***2016****, 6*, 5473; l) B. Zhang, T.-J. Zhao, W.-J. Feng, Y.-X. Liu, H.-H. Wang, H. Su, L.-B. Lv, X.-H. Li, J.-S. Chen, *Nano Res.* **2018**, *11*, 2450
[104] J. Hou, J.-S. Li, J. Wu, *Asian J. Org. Chem.* **2018**, *7*, 1439.
[105] D. A. Morgenstern, R. E. Wittrig, P. E. Fanwick, C. P. Kubiak, *J. Am. Chem. Soc.* **1993**, *115*, 6470.
[106] N. Ishida, Y. Masuda, S. Uemoto, M. Murakami, *Chem. Eur. J.* **2016**, *22*, 6524.
[107] H. Seo, A. Liu, T. F. Jamison, *J. Am. Chem. Soc.* **2017**, *139*, 13969.
[108] Q.-Y. Meng, S. Wang, G. S. Huff, B. König, *J. Am. Chem. Soc.* **2018**, *140*, 3198.
[109] a) T. Ito, H. Hatta, S. Nishimoto, *Int. J. Rad. Biology* **2000**, *76*, 683; b) A. B. Ross, W. G. Mallard, W. P. Helman, G. V. Buxton, R. E. Huie, P. Neta, *J. Phys. Org. Chem.* **2001**, *14*, 300; c) A. L. J. Beckwith, R. O. C. Norman, *J. Chem. Soc. B* **1969**, 400; d) E. Hayon, M. Simic, *J. Am. Chem. Soc.* **1973**, *95*, 2433; e) G. V. Buxton, R. M. Sellers, *J. Chem. Soc., Faraday Trans. 1* **1973**, *69*, 555; f) K.-D. Asmus, A. Wigger, A. Henglein, *Ber. Bunsenges. Phys. Chem.* **1966**, *70*, 966; g) K.-D. Asmus, G. Beck. A. Henglein, A. Wigger, *Ber. Bunsenges. Phys. Chem*. **1966**, *70*, 869; h) S. Solar, N. Getoff, J. Holcman, K. Sehested, *J. Phys. Chem.* **1995**, *99*, 9425; i) M. B. Ansari, B.-H. Min, Y.-H. Mo, S.-E. Park, *Green Chem.* **2011**, *13*, 1416; j) J. A. Rosso, S. G. Bertolotti, A. M. Braun, D. O. Martire, M. C. Gonzalez, *J. Phys. Org. Chem.* **2001**, *14*, 300; k) Z. D. Draganic, A. Negron-Mendoza, K. Sehested, S. I. Vulosevic, R.

Navarro-Gonzalez, M. G. Albarran-Sanchez. I. G. Draganic, *Radiat. Phys. Chem.* **1991**, *38*, 317; l) J. Lilie, R. J. Hanrahan, A. Henglein, *Radiat. Phys. Chem.* **1978**, *11*, 225.

[110] a) H. S. Kim, K. Yu, P. Puthiaraj, W.-S. Ahn, *Microporous Mesoporous Mater.* **2020**, 110432; b) S. N. Talapaneni, O. Buyukcakir, S. H. Je, S. Srinivasan, Y. Seo, K. Polychronopoulou, A. Coskun, *Chem. Mater.* **2015**, *27*, 6818; c) H. Zhou, W.-Z. Zhang, C.-H. Liu, J.-P. Qu, X.-B. Lu, *J. Org. Chem.* **2008**, *73*, 8039.

[111] a) Y.-B. Wang, Y.-M. Wang, W.-Z. Zhang, X.-B. Lu, *J. Am. Chem. Soc.* **2013**, *135*, 11996; b) H. Zhou, Y.-M. Wang, W.-Z. Zhang, J.-P. Qu, X.-B. Lu, *Green Chem.* **2011**, *13*, 644.

[112] Y. Yuan, C. Chen, C. Zeng, B. Mousavi, S. Chaemchuen, F. Verpoort, *ChemCatChem* **2017**, *9*, 882.

[113] H. Lv, W. Wang, F. Li, *Chem. Eur. J.* **2018**, *24*, 16588.

[114] a) G. Maier, J. Endres, H. P. Reisenauer, *Angew. Chem.* **1997**, *109*, 1788; b) A. Tudose, A. Demonceau, L. Delaude, *J. Organomet. Chem.* **2006**, *691*, 5356; c) Z. Kelemen, B. Péter-Szabó, E. Székely, O. Hollóczki, D. S. Firaha, B. Kirchner, J. Nagy, L. Nyulászi, *Chem. Eur. J.* **2014**, *20*, 13002; d) I. Tommasi, F. Sorrentino, *Tetrahedron Lett.* **2006**, *47*, 6453; e) J. D. Holbrey, W. M. Reichert, I. Tkatchenko, E. Bouajila, O. Walter, I. Tommasid, R. D. Rogers, *Chem. Commun.* **2003**, 28; f) H. A. Duong, T. N. Tekavec, A. M. Arif, J. Louie, *Chem. Commun.* **2004**, 112; g) J. Pinaud, J. Vignolle, Y. Gnanou, D. Taton, *Macromolecules* **2011**, *44*, 1900.

[115] Q. Zhou, Y. Li, *J. Am. Chem. Soc.* **2015**, *137*, 10182.

[116] a) O. Vechorkin, N. Hirt, X. Hu, *Org. Lett.* **2010**, *12*, 3567; b) W. Yoo, M. G. Capdevila, X. Du, S. Kobayashi, *Org. Lett.* **2012**, *14*, 5326.

[117] a) R. Rajasingam, L. Lioe, Q. T. Pham, F. P. Lucien, *J. Supercrit. Fluids* **2004**, *31*, 227; b) L. Hua, *Phys. Chem. Liq.* **2009**, 47, 296.

[118] M. Shokouhi, H. Farahani, M. Hosseini-Jenab, *Fluid Phase Equilib.* **2014**, *367*, 29.

[119] a) D. H. Aue, H. M. Webb, M. T. Bowers, *J. Am. Chem. Soc.* **1976**, *98*, 318; b) H. Lv, Q. Xing, C. Yue, Z. Lei, F. Li, *Chem. Commun.* **2016**, *52*, 6545.

[120] J. Rautio, H. Kumpulainen, T. Heimbach, R. Oliyai, D. Oh, T. Järvinen, J. Savolainen, *Nature Rev.* **2008**, *7*, 255.

[121] U. Farooq, A. Ali, R. Patel, N. A. Malik, *J. Mol. Liq.* **2017**, *233*, 310.

[122] L.-H. Ni, C. Yuan, K.-Y. Song, X.-C. Wang, S.-J. Chen, L.-T. Wang, Y.-X. Zhang, H. Liu., B.-C. Liu, R.-N. Tang, *Ann. Transl. Med.* **2019**, *7*, 322.

[123] J. Cui, J. Hao, O. A. Ulanovskaya, J. Liang, S. A. Kozmi, *Proc. Nat. Acad. Sci.* **2011**, *108*, 6763.

[124] a) A. R. King, A. Duranti, A. Tontini, S. Rivara, A. Rosengarth, J. R. Clapper, G. Astarita, J. A. Geaga, H. Luecke, M. Mor, G. Tarzia, D. Piomelli, *Chem. and Biol.* **2007**, *14*, 1357; b) M. Szabo, M. Agostino, D. T. Malone, E. Yuriev, B. Capuano, *Bioorg. Med. Lett.* **2011**, *21*, 6782.

[125] S. Vandevoorde, K. Jonsson, G. Labar, E. Persson, D. M. Lambert, C. J. Fowler, *British J. Pharmacology* **2007**, *150*, 186.

[126] A. Isidro-Llobet, M. Álvarez, F. Albericio, *Chem. Rev.* **2009**, *109*, 2455.
[127] D. Riemer, B. Mandaviya, W. Schilling, A. C. Götz, T. Kühl, M. Finger, S. Das, *ACS Catal.* **2018**, *8*, 3030.
[128] Y. Oda, K. Hirano, T. Satoh, S. Kuwabata, M. Miura, *Tetrahedron Lett.* **2011**, *52*, 5392.
[129] N. Polkam, B. Kummari, P. Rayam, U. Brahma, V. G. M. Naidu, S. Balasubramanian, J. S. Anireddy, *ChemistrySelect* **2017**, *2*, 5492.
[130] J. D. Conklin, R. D. Hollifield, *Eur. J. Pharmacol.* **1970**, *10*, 360.
[131] H. Su, X. Song, H. Yan, *J. Liaoning Univ. Petr. Chem. Technol.* **2006**, *26*, 51.
[132] M. S. von Wittenau, T. F. Brewer, *Pharmacology* **1971**, *6*, 173.
[133] M. González-Lozano, M. E. Trujillo-Ortega, M. Alonso-Spilsbury, A. M. Rosales, R. Ramírez-Necoechea, A. González-Maciel, R. Martínez-Rodríguez, M. Becerril-Herrera, D. Mota-Rojas, *Theriogenology* **2012**, *78*, 455.
[134] A. Aykac, A. Ö. Şehirli, M. Z. Gören, *J. Mol. Neurosci.* **2020**, DOI: 10.1007/s12031-020-01518-7.
[135] G. Cocco, D. Chu, C. Strozzi, *Clin. Cardiol.* **1979**, *2*, 131.
[136] B.-S. Li, Y. Wang, R. S. J. Proctor, Y. Zhang, R. D. Webster, S. Yang, B. Song, Y. R. Chi, *Nat. Commun.* **2016**, *7*, 12933.
[137] S. Tang, J. He, Y. Sun, L. He, X. She, *J. Org. Chem.* **2010**, *75*, 1961.
[138] a) D. P. Hruszkewycz, K. C. Miles, O. R. Thiel, S. S. Stahl, *Chem. Sci.* **2017**, *8*, 1282; b) B. H. Lipshutz, M. Hageman, J. C. Fennewald, R. Linstadt, E. Slack, K. Voigtritter, *Chem. Commun.* **2014**, *50*, 11378; c) S. Das, D. Addis, S. Zhou, K. Junge, M. Beller, *J. Am. Chem. Soc.* **2010**, *132*, 1770; d) A. Karakulina, A. Gopakumar, I. Akcok, B. L. Roulier, T. LaGrange, S. Katsyuba, S. Das, P. J. Dyson, *Angew. Chem. Int. Ed.* **2016**, *55*, 292; e) S. Das, Y. Li, C. Bornschein, S. Pisiewicz, K. Kiersch, D. Michalik, F. Gallou, K. Junge, M. Beller, *Angew. Chem. Int. Ed.* **2015**, *54*, 12389; f) D. Addis, S. Zhou, S. Das, K. Junge, H. Kosslick, J. Harloff, H. Lund, A. Schulz, M. Beller, *Chem. Asian J.* **2010**, *5*, 2341.
[139] D. Cao, B. Yu, S. Zhang, L. Cui, J. Zhang, W. Cai, *Appl. Catal. A Gen.* **2016**, *528*, 59.
[140] A. Rahimi, A. Ulbrich, J. J. Coon, S. S. Stahl, *Nature* **2014**, *515*, 249.
[141] Y.-Q. Yang, M.-C. Ji, Z. Lu, M. Jiang, W.-W. Huang, X.-Z. He, *Synth. Commun.* **2016**, 977.
[142] R. Ramesh, K. De, S. Chandrasekaran, *Tetrahedron*, **2007**, *63*, 10534.
[143] Y. Kuwahara, N. Shimizu, T. Tanabe, *J. Chem. Ecol.* **2011**, *37*, 232.
[144] Olga Bortolini, G. Fantin, V. Ferretti, M. Fogagnolo, P. P. Giovannini, A. Massi, S. Pacifico, D. Ragnoa, *Adv. Synth. Catal.* **2013**, *355*, 3244.
[145] Y.-J. Kim, N. Y. Kim, C.-H. Cheon, *Org. Lett.* **2014**, *16*, 2514.
[146] a) Z. S. Seddigi, M. S. Malik, A. P. Saraswati, S. A. Ahmed, A. O. Babalghith, H. A. Lamfon, A. Kamal, *Med. Chem. Commun.* **2017**, *8*, 1592; b) T. C. Wang, L. P. Cheng, X. Y. Huang, L. Zhao, W. Pang, *RSC Adv.* **2017**, *7*, 38479; c) Y. Fang, Y. Luo, X. Ma, *Monatsh. Chem.* **2017**, *148*, 1823. d) V. Sherbet, *Cancer Lett.* **2017**, *403*, 289.

[147] a) V. P. Androutsopoulos, I. Fragiadaki, A. Tosca, *Exp. Dermatol.* **2015**, *24*, 630; b) M. Cichocki, W. Baer-Dubowska, M. Wierzchowski, M. Murias, *Mol. Cell. Biochem.* **2014**, *391*, 27; c) H. Piotrowska, K. Myszkowski, J. Abraszek, E. Kwiatkowska-Borowczy, R. Amarowicz, M. Murias, M. Wierzchowski, J. Jodynis-Liebert, J. Jodynis-Liebert, *Biomed. Pharmacother.* **2014**, *68*, 397; d) Y.-M. Miao, L.-Q. Cui, Z.-Q. Chen, L. Zhang, *Pharm. Biol.* **2016**, *54*, 660; e) L.-K. Chen, P.-F. Qiang, Q.-P. Xu, Y.-H. Zhao, F. Dai, L. Zhang, *Acta Pharmacol. Sin.* **2013**, *34*, 1174.

[148] a) J. McNulty, P. Das, *Eur. J. Org. Chem.* **2009**, 3041; b) X. Guo, D. Zhang, Z. Yu, T. Liu, D. Li, C. Li, *J. Chem. Res.* **2011**, 229.

[149] a) S. BouzBouz, C. Roche, J. Cossy, *Synlett* **2009**, *5*, 803; b) B. Crousse, M. Mladenova, P. Ducept, M. Alami, G. Linstrumelle, *Tetrahedron* **1999**, *55*, 4353; c) M. Sakakibara, M. Matsui, *Agric. Biol. Chem.* **1979**, *43*, 117; d) H. L. Sleeper, V. J. Paul, W. Fenical, *J. Chem. Ecol.* **1980**, *6*, 57; e) K. Hemming, R. J. K. Taylor, *J. Chem. Soc., Chem. Commun.* **1993**, 1409; f) D. Soullez, Y. Ramondenc, G. Ple, L. Duhamel, *Nat. Prod. Lett.* **1994**, *4*, 203; g) G. Solladié, F. Colobert, G. B. Stone, *Synlett* **1995**, 1135; h) S. J. Lee, T. M. Anderson, M. D. Burke, *Angew. Chem. Int. Ed.* **2010**, *49*, 8860; i) S. D. Rychnovsky, *Chem. Rev.* **1995**, *95*, 2021; j) S. Fujii, S. Y. Chang, M. D. Burke, *Angew. Chem. Int. Ed.* **2011**, *50*, 7862.

[150] R. Stradi, A. Bertelli, E. Pini, WO03/095403A1, **2002**.

[151] P.-F. Li, H.-L. Wang, J. Qu, *J. Org. Chem.* **2014**, *79*, 3955.

[152] R. R. Leleti, B. Hu, M. Prashad, O. Repič, *Tetrahedron Lett.* **2007**, *48*, 8505.

[153] S. J. Lee, K. C. Gray, J. S. Paek, M. D. Burke, *J. Am. Chem. Soc.* **2008**, *130*, 466.

[154] L. Wang, X. Zhang, L. Yang, C. Wang, H. Wang, *Catal. Sci. Technol.* **2015**, *5*, 4800.

[155] a) X. Wu, K. Natte, *Adv. Synth. Catal.* **2016**, *358*, 336; b) J. Zou, W. Huang, L. Li, Z. Xu, Z. Zheng, K. Yang, L. Xu, *RSC Adv.* **2015**, *5*, 30389; c) T. Tidwell, *Synthesis* **1990**, *10*, 857; d) J. H. Song, M. J. Sailor, *Inorg. Chem.* **1998**, *37*, 3355.

[156] P. Hirapara, D. Riemer, N. Hazra, J. Gajera, M. Finger, S. Das, *Green Chem*. **2017**, *19*, 5356.

[157] Y. He, Y. Xue, *J. Phys. Chem. A* **2010**, *114*, 9222.

[158] A. Kabro, E. C. Escudero-Adán, V. V. Grushin, P. W. N. M. van Leeuwen, *Org. Lett.* **2012**, *14*, 4014.

[159] P. Gallezot, *Chem. Soc. Rev.* **2012**, *41*, 1538.

[160] S. M. Langdon, M. M. D. Wilde, K. Thai, M. Gravel, *J. Am. Chem. Soc.* **2014**, *136*, 7539.

[161] a) W. S. Ide, J. S. Buck, *Org. React.* **1948**, *4*, 269; b) H. Stetter, G. Dämbkes, *Synthesis* **1977**, *403*; c) H. Stetter, G. Dämbkes, *Synthesis* **1980**, 309.

[162] C. A. Rose, S. Gundala, S. J. Connon, K. Zeitler, *Synthesis* **2011**, *2*, 0190.

[163] a) H. Irannejad, M. Amini, F. Khodagholi, N. Ansari, S. Tusi, M. Sharifzadeh, A. Shafiee, *Bioorg. Med. Chem.* **2010**, *18*, 4224; b) M. J. Meyers, M. D. Tortorella, J. Xu, L. Qin, Z. He, X. Lang, W. Zeng, W. Xu, L. Qin, M. J. Prinsen, F.

M. Sverdrup, C. S. Eickhoff, D. W. Griggs, J. Oliva, P. G. Ruminski, E. J. Jacobsen, M. A. Campbell, D. C. Wood, D. E. Goldberg, X. Liu, Y. Lu, X. Lu, Z. Tu, X. Lu, K. Ding, X. Chen*, ACS Med. Chem. Lett.* **2014**, *5*, 89; c) M. Gemayel, A. Narita, L. Dössel, R. Sundaram, A. Kiersnowski, W. Pisula, M. Hansen, A. Ferrari, E. Orgiu, X. Feng, K. Müllen, P. Samori, *Nanoscale* **2014**, *6*, 6301.

[164] J. Saranya, M. Sowmiya, P. Sounthary, K. Parameswari, S. Chitra, K. Senthilkumar, *J. Mol. Liq.* **2016**, *216*, 42.

[165] T. Kanbara, T. Yamamoto, *Chem. Lett.* **1993**, 1459.

[166] P. Ghosh, A. Mandal, *Green Chem. Lett. Rev.* **2012**, *5*, 127.

[167] P. Hu, Q. Wang, Y. Yan, S. Zhang, B. Zhang, Z. Wang, *Org. Biomol. Chem.* **2013**, *11*, 4304.

[168] Q. Chen, V. Bryant, H. Lopez, D. Kelly, X. Luo, A. Natarajan, *Bioorg. Med. Chem. Lett.* **2011**, *21*, 1929.

[169] S. Khaskar, M. Alipour, M.; *Montash. Chem.* **2013**, *144*, 395.

[170] D. Riemer, W. Schilling, A. C. Götz, Y. Zhang, S. Gehrke, I. Tkach, O. Hollóczki, S. Das, *ACS Catal.* **2018**, *8*, 11679.

[171] a) A. Akhgarnusch, R. F. Höckendorf, Q. Hao, K. P. Jäger, C. Siu, M. K. Beyer, *Angew. Chem. Int. Ed.* **2013**, *52*, 9327; b) E. R. Perez, R. H. A. Santos, M. T. P. Gambardella, L. M. de Macedo, U. P. Rodrigues-Filho, J.-C. Launay, D. W. Franco, *J. Org. Chem.* **2004**, *69*, 8005; c) D. J. Heldebrant, P. G. Jessop, C. A. Thomas, C. A. Eckert, C. L. Liotta, *J. Org. Chem.* **2005**, *70*, 5335; d) M. Lessio, E. A. Carter, *J. Am. Chem. Soc.* **2015**, *137*, 13248.

[172] a) A. Pictet, T. Spengler, *Ber. Dtsch. Chem. Ges.* **1911**, *44*, 2030; b) A. Yokoyama, T. Ohwada, K. Shudo, *J. Org. Chem.* **1999**, *64*, 611.

[173] a) M. Kojima, M. Kanai, *Angew. Chem. Int. Ed.* **2016**, *55*, 12224; b) X. Cui, Y. Li, S. Bachmann, M. Scalone, A.-E. Surkus, K. Junge, C. Topf, M. Beller, *J. Am. Chem. Soc.* **2015**, *137*, 10652.

[174] A. Bischler, B. Napieralski, *Ber. Dtsch. Chem. Ges.* **1893**, *26*, 1903.

[175] a) S. L. Capim, G. M. Gonçalves; G. C. M. dos Santos, B. G. Marinho, *Bioorg. Med. Chem.* **2013**, *21*, 6003; b) M. Arisawa, Y. Kasaya, T. Obata, T. Sasaki, M. Ito, H. Abe, Y. Ito, A. Yamano, S. Shto, *ACS Med. Chem. Lett.* **2011**, *2*, 353; c) M. Milen, P. Ábrányi-Balogh, *Chem. Heterocycl. Compd.* **2016**, *52*, 996; d) D. S. C. Black, *Synlett* **1992**, 246; e) S. Hibino, T. Choshi, *Nat. Prod. Rep.* **2001**, *18*, 66.

[176] a) M. Balogh, I. Hermecz, Z. Mészáros, P. Laszlo, *Helv. Chim. Acta* **1984**, *67*, 2270; b) B. Khadilkar, S. Borkar, *Synth. Commun.* **1998**, *28*, 207.

[177] a) J.-J. Xia, G.-W. Wang, *Synthesis* **2005**, *14*, 2379; b) J.-J. Vanden Eynde, R. D'Orazio, Y. V. Haverbeke, *Tetrahedron* **1994**, *50*, 2479.

[178] A. Hantzsch, *Ber. Dtsch. Chem. Ges.* **1881***, 14*, 1637.

[179] T. Mani, D. Liu, D. Zhou, L. Li, W. E. Knabe, F. Wang, K. Oh, S. O. Meroueh, *ChemMedChem* **2013**, *8*, 1963.

[180] A. A. Sathe, D. R. Hartline, A. T. A Radosevich, *Chem. Commun.* **2013**, *49*, 5040.

[181] a) S. Agarwal, O. Kataeva, U. Schmidt, H.-J. Knölker, *RSC Adv.* **2013**, *3*, 1089; b) N. Sasamoto, C. Dubs, Y. Hamashima, M. Sodeoka, *J. Am. Chem. Soc.* **2006**, *128*, 14010; c) T. Itoh, M. Miyazaki, H. Fukuoka, K. Nagata, A. Ohsawa, *Org. Lett.* **2006**, *8*, 1295; d) J. Szawkało, Z. Czarnocki, *Monatsh. Chem.* **2005**, *136*, 1619; e) T. Kanemitsu, Y. Yamashita, K. Nagata, T. Itoh, *Synlett* **2006**, *10*, 1595; f) T. R. Hoye, M. Chen, *Tetrahedron Lett.* **1996**, *37*, 3099; g) L. Liu, *Synthesis* **2003**, *11*, 1705.

[182] J. Zhang, S. Chen, F. Chen, W. Xu, G.-J. Deng, H. Gong, *Adv. Synth. Catal.* **2017**, *359*, 2358.

[183] R. S. Kusurkar, S. K. Goswami, *Tetrahedron* **2004**, *60*, 5315.

[184] a) J.-S. Choi, J.-S. Choi, D.-H. Choi, *Biopharm. Drug Dispos.* **2014**, *35*, 382; b) T. D. Ardizzone, X.-H. Lu, D. S. Dwyer, *Am. J. Phiosol. Cell Phiosol.* **2002**, *283*, C579; c) B. Zeynizadeh, K. A. Dilmaghani, A. Roozijoy, *J. Chem. Res.* **2005**, 657; d) J. Lemay, B. S. Tea, P. Hamet, D. deBlois, J. Vasc. Res. 2001, 38, 462; e) T. Ago, Y. Yang, P. Zhai, J. Sadoshima, *J. Cardiovasc. Transl. Res.* **2010**, *3*, 304.

[185] a) S. Eagon, M. O. Anderson, *Eur. J. Org. Chem.* **2014**, 1653; b) J. Wu, D. Talwar, S. Johnston, M. Yan, J. Xiao, *Angew. Chem. Int. Ed.* **2013**, *52*, 6983.

[186] a) J. Wang, H. Du, N. Li, H. Gu, B. Liu, CN104557916A1, **2014**; b) J. Wang, H. Du, N. Li, H. Gu, W. Qin, CN104497012A1, **2014**.

[187] K. C. Patki, L. L. von Moltke, D. J. Greenblatt, *Drug Metab. Dispos.* **2003**, *31*, 938.

[188] a) X. Wei, L. Wang, W. Jia, S. Du, L. Wu, Q. Liu, *Chin. J. Chem.* **2014**, *32*, 1245; b) C.-K. Lee, J.-S. Choi, D.-H. Choi, *Pharm. Chem. J.* **2017**, *51*, 748; c) A. C. Chaikh, C. Chen, *Bioorg. Med. Chem. Lett.* **2010**, *20*, 3664.

[189] F. A. Villamena, E. J. Locigno, A. Rockenbauer, C. M. Hadad, J. L. Zweier, *J. Phys. Chem. A* **2006**, *110*, 13253.

[190] a) H. Tanigushi, K.P. Madden, *J. Radiat. Res.* **2000**, *153*, 447; b) Y. Kirino, T. Ohkuma, T. Kwan, *Chem. Pharm. Bull.* **1981**, *29*, 29.

[191] S. P. Pitre, C. D. McThiernan, J. C. Scaiano, *Acc. Chem. Res.* **2016**, *49*, 1320.

[192] a) D. Basavaiah, B. S. Reddy, S. S. Badsara, *Chem. Rev.* **2010**, *110*, 5447; b) G. Masson, C. Housseman, J. Zhu, *Angew. Chem. Int. Ed.* **2007**, *46*, 4614; c) D. Basavaiah, G. Veeraraghavaiah, *Chem. Soc. Rev*. **2012**, *41*, 68; d) V. Declerck, J. Martinez, F. Lamaty, *Chem. Rev.* **2009**, *109*, 1; e) D. Basavaiah, A. J. Rao, T. Satyanarayana, *Chem. Rev.* **2003**, *103*, 811.

[193] I. Bughun, D. Lexa, J.-M.Savéant, *J. Am. Chem. Soc.* **1996**, *118*, 1769.

[194] P. M. Brian, P. Musau, *Indones. J. Chem.* **2016**, *16*, 53.

[195] J. Saranya, M. Sowmiya, P. Sounthari, K. Parameswari S. Chitra, K. Senthilkumar, *J. Mol. Liq.* **2016**, *216*, 42.

[196] a) S. N. Murthy, B. Madhav, Y. V. D. Nageswar, *Tetrahedron Lett.* **2010**, *51*, 5252; b) S. Khaksar, M. Alipour, *Monatsh. Chem.* **2013**, *144*, 395.

[197] M. Łukomska, A. J. Rybarczyk-Pirek, M. Jabłoński, M. Palusiak, *Phys. Chem. Chem. Phys.* **2015**, *17*, 16375.

[198] TURBOMOLE V7.0 2015, a development of University of Karlsruhe and Forschungszentrum Karlsruhe GmbH, 1989-2007, TURBOMOLE GmbH, since **2007**; available from http://www.turbomole.com.
[199] A. D. Becke, *J. Chem. Phys.* **1993**, *98*, 5648; b) C. Lee, W. Yang, R. G. Parr, *Phys. Rev. B* **1988**, *37*, 785.
[200] a) S. Grimme, J. Antony, S. Ehrlich, H. Krieg, *J. Chem. Phys.* **2010**, *132*, 154104; b) S. Grimme, S. Ehrlich, L. Goerigk *J. Comput. Chem.* **2011**, *32*, 1456.
[201] a) F. Weigend, R. Ahlrichs, *Phys. Chem. Chem. Phys.* **2005**, *7*, 3297; b) F. Weigend, M. Häser, H. Patzelt, R. Ahlrichs, *Chem. Phys. Lett.* **1998**, *294*, 143.
[202] a) O. Treutler, R. Ahlrichs, *J. Chem. Phys.* **1995**, *102*, 346; b) K. Eichkorn, O. Treutler, H. Öhm, M. Häser, R. Ahlrichs, *Chem. Phys. Lett.* **1995**, *240*, 283; c) K. Eichkorn, O. Treutler, H. Öhm, M. Häser, R. Ahlrichs, *Chem. Phys. Lett.* **1995**, *242*, 652; d) K. Eichkorn, F. Weigend, O. Treutler, R. Ahlrichs, *Theo. Chem. Acc.* **1997**, *97*, 119.
[203] L. Chen, L. Zhang, J. Lv, J.-P. Cheng, S. Luo, *Chem. Eur. J.* **2012**, *18*, 8891.
[204] S. Stoll, A. Schweiger, *J. Magn. Resonan.* **2006**, *178*, 42.
[205] a) F. Neese, *WIREs: Comp. Mol. Sci.* **2012**, *2*, 73; b) F. Neese, *WIREs: Comp. Mol. Sci.* **2018**, *8*, e1327.
[206] Y. Zhao, D. G. Truhlarm, *Theor. Chem. Acc.* **2008**, *120*, 215.
[207] V. Barone, M. Cossi, *J. Phys. Chem. A* **1998**, *102*, 1995.
[208] a) C. Riplinger, B. Sandhoefer, A. Hansen, F. Neese, *J. Chem. Phys.* **2013**, *139*, 134101; b) D. G. Liakos, M. Sparta, M. K. Kesharwani, J. M. Martin, F. Neese, *J. Chem. Theory Comput.* **2015**, *11*, 1525; c) D.G. Liakos, F. Neese, *J. Chem. Theory Comput.* **2015**, *11*, 4054; d) D. G. Liakos, F. Neese, *J. Phys. Chem. A* **2012**, *116*, 4801.
[209] a) A. Klamt, *J. Phys. Chem.* **1995**, *99*, 2224; b) A. Klamt, *J. Phys. Chem. A* **1998**, *102*, 5074.
[210] a) F. Eckert, A. Klamt, *AIChE J.* **2002**, *48*, 369; b) A. Klamt, *WIRes: Comp. Mol. Sci.* **2018**, *8*, e1338.
[211] R. Ahlrichs, M. Bär, M. Häser, H. Horn, C. Kölmel, *Chem. Phys. Lett.* **1989**, *162*, 165.
[212] A. Schäfer, H. Horn, R. Ahlrichs, *J. Chem. Phys.* **1992**, *97*, 2571.
[213] J. Li, C. Fisher, J. Chen, D. Bashford, L. Noodleman, *Inorg. Chem.* **1996**, *35*, 4694.
[214] IUPAC. Compendium of Chemical Terminology, 2nd ed. (the "Gold Book").
[215] G. Sandford, *Sci. Synt.* **2007**, *31a*, 21.
[216] R. Haridharan, K. Muralirajan, C.-H. Cheng, *Adv. Synth. Catal.* **2015**, *357*, 366.
[217] A. Ion, C. Van Doorslaer, V. Parvulescu, P. Jacobs, D. De Vos, *Green Chem.* **2008**, *10*, 111.
[218] U. Hess, C. O. Bluemcke, *Zeitschr. Chem.* **1988**, *28*, 144.
[219] S. M. Yakout, S. H. Abd-Alrahman, M. M. Salem-Bekhit, A. Mostafa, *J. Pure Appl. Microbiol.* **2013**, *7*, 1373.

[220] K. Zhang, Z. Chen, L. Feng, J. Zhang, C. Yao, H. Zhu, Z. Guo, *Faming Zhuanli Shenqing*, **2013**, CN 103113290 A 20130522.
[221] U. Jacquemard, V. Beneteau, M. Lefoix, S. Routier, J.-Y. Merour, G. Coudert, *Tetrahedron* **2004**, *60*, 10039.
[222] a) P. Wang, Y. Ma, S. Liu, F. Zhou, B. Yang, Y. Deng, *Green Chem.* **2015**, *17*, 3964; b) D. L. Cheney, J. M. Bozarth, W. J. Metzler, P. E. Morin, L. Mueller, J. A. Newitt, A. H. Nirschl, A. R. Rendina, J. K. Tamura, A. Wei, X. Wen, N. R. Wurtz, D. A. Seiffert, R. R. Wexler, S. Priestley, *J. Med. Chem.* **2015**, *58*, 2799.
[223] M.-N. Belzile, A. A. Neverov, R. S. Brown, *Inorg. Chem.* **2014**, *53*, 7916.
[224] N. Okamoto, M. Ishikura, R. Yanada, *Org. Lett.* **2013**, 15, 2571.
[225] S. Witek, J. Bielawski, A. Bielawska, *J. Prakt. Chem.* **1979**, *321*, 804.
[226] D. F. Niu, L. Zhang, L. P. Xiao, Y. W. Luo, J. X. Lu, *Appl. Organomet. Chem.* **2007**, *21*, 941.
[227] Y. Iwakura, S. Izawa, *Yuki Gosei Kagaku Kyokaishi* **1966**, *24*, 60.
[228] A. M. Shur, N. V. Ivanov, N. A. Barba, I. L. Pogrebnoi, I. D. Korzha, R. I. Ishchenko, R. I. Vinnitskaya, I. A. Gershkovich, *Sb. Nauch. Statei, Kishinev. Gos. Univ., Estestv. Mat. Nauki* **1969**, 118.
[229] E. Pop, B. Kovacs, M. Sclifos, R. T. Miloia, M. Peterlecean, O. Pirosca, **1981**, RO 76340 A2 19810530.
[230] R. Suffis, D. E. Dean, *Anal. Chem.* **1962**, *34*, 480.
[231] D. S. W. Lim, T. T. S. Lew, Y. Zhang, *Org. Lett.* **2015**, *17*, 6054.
[232] W. Mahy, P. K. Plucinski, C. G. Frost, *Org. Lett.* **2014**, *16*, 5020.
[233] H. Liu, L. Chang, C. Bai, L. Chen, R. Luque, Y. Li, *Angew. Chem. Int. Ed.* **2016**, *55*, 5019.
[234] C. B. Kelly, J. M. Ovian, R. M. Cywar, T. R. Gosselin, R. J. Wiles, N. E. Leadbeater, *Org. Biomol. Chem.* **2015**, *13*, 4255.
[235] R. Vadakkekara, A. K. Biswas, T. Sahoo, P. Pal, B. Ganguly, S. C. Ghosh, A. B. Panda, *Chem. Asian J.* **2016**, *11*, 3084.
[236] I. Y. El-Deeb, T. Funakoshi, Y. Shimomoto, R. Matsubara, M. Hayashi, *J. Org. Chem.* **2017**, *82*, 2630.
[237] D.-D. Quin, W. Chen, Y. Tang, W. Yu, A.-A. Wu, Y. Liao, H.-B. Chen, *Asian J. Org. Chem.* **2016**, *5*, 1345.
[238] L. Li, R. Matsuda, I. Tanaka, H. Sato, P. Kanoo, H. J. Jeon, M. L. Foo, A. Wakamiya, Y. Murata, S. Kitagawa, *J. Am. Chem. Soc.* **2014**, *136*, 7543.
[239] S. Gu, J. Du, J. Huang, Y. Guo, L. Yang, W. Xu, W. Chen, *Dalton Trans.* **2017**, *46*, 586.
[240] E. Buxaderas, M. Graziano-Mayer, M. A. Volpe, G. Radivoy, *Synthesis* **2017**, *49*, 1387.
[241] P. D. Giorgi, N. Elizarov, S. Antoniotti, *ChemCatChem* **2017**, *9*, 1830.
[242] S. Hashemian, A. Sedrpoushan, F. H. Eshbala, *Catal. Lett.* **2017**, *147*, 196.
[243] C. Ebner, C. A. Müller, C. Markert, A. Pfaltz, *J. Am. Chem. Soc.* **2011**, *133*, 4710.
[244] Mo. E. Assal, M. Kuniyil, M. R. Shaik, M. Khan, A. Al-Warthan, M. R. H. Siddiqui, S. F. Adil, *J. Chem.* **2017**, 2937108.

[245] J.-J. Zhong, W.-P. To, Y. Liu, W. Lu, C.-M. Che, *Chem. Sci.* **2019**, *10*, 4883.
[246] I. Dip, C. Gethers, T. Rice, T. S. Straub, *Tetrahedron Lett.* **2017**, *58*, 2720.
[247] Z. Czakó, L. Juhász, T. Docsa, P. Gergely, S. Antus, *Pharmazie* **2010**, *65*, 235.
[248] C.-K. Chan, Y.-L. Tsai, M.-Y. Chang, *Tetrahedron* **2017**, *73*, 3368.
[249] P. Gautam, M. Dhiman, V. Polshettiwar, B. M. Bhanage, *Green Chem.* **2016**, *18*, 5890.
[250] J.-S. Li, F. Yang, Q. Yang, Z.-W. Li, G.-Q. Chen, Y.-D. Da, P.-M. Huang, C. Chen, Y. Zhang, L.-Z. Huang, *Synlett* **2017**, *28*, 994.
[251] W. Hao, H. Liu, L. Yin, M. Cai, *J. Org. Chem.* **2016**, *81*, 4244.
[252] A. Rérat, C. Michon, F. Agbossou-Niedercorn, C. Gosmini, *Eur. J. Org. Chem.* **2016**, *26*, 4554.
[253] P. Lei, G. Meng, M. Szostak, *ACS Catal.* **2017**, *7*, 1960.
[254] A. Shaabani, H. Afaridoun, S. Shaabani, M. K. Nejad, *RSC Adv.* **2016**, *6*, 97367.
[255] M. M. Hossain, S.-G. Shyu, *Tetrahedron* **2016**, *72*, 4252.
[256] B. Karimi, S. Vahdati, H. Vali, *RSC Adv.* **2016**, *6*, 63717.
[257] S. Kawasaki, K. Kamata, M. Hara, *ChemCatChem* **2016**, *8*, 3247.
[258] C. McTiernan, S. P. Pitre, J. C. Scaiano, *ACS Catal.* **2014**, *4*, 4034.
[259] M. Kamitani, M. Ito, M. Itazaki, H. Nakazawa, *Chem. Commun.* **2014**, *50*, 7941.
[260] B. Xin, Y. Zhang, K. Cheng, *J. Org. Chem.* **2006**, *71*, 5725.
[261] P. Gautam, R. Gupta, B. M. Bhanage, *Eur. J. Org. Chem.* **2017**, *24*, 3431.
[262] M. Kuriyama, N. Hamaguchi, K. Sakata, O. Onomura, *Eur. J. Org. Chem.* **2013**, 3378.
[263] M. Lemhadri, Y. Fall, H. Doucet, M. Santelli, *Synthesis* **2009**, *6*, 1021.
[264] S.-I. Inaba, R. D. Rieke, *J. Org. Chem.* **1984**, 1373.
[265] P. H. Tran, P. E. Hansen, H. M. Hoang, D.-K. N. Chau, T. N. Le, *Tetrahedron Lett.* **2015**, *56*, 2187.
[266] X. Liu, Z. Yi, M. Yi, J. Wang, G. Liu, *Tetrahedron* **2015**, *71*, 4635.
[267] M. L. Keshtov, A. L. Rusanov, S. V. Keshtova, P. V. Petrovskii, A. A. Shchegolikhin, *Russ. Chem. Bull.* **2002**, *51*, 117.
[268] J. C. Lee, I.-G. Song, J. Y. Park, *Synth. Commun.* **2002**, *32*, 2209.
[269] Y. Lin, L. Zhu, Y. Lan, Y. Rao, *Chem. Eur. J.* **2015**, *21*, 14937.
[270] D. J. Wardrop, J. P. Komenda, *Org. Lett.* **2012**, *14*, 1548.
[271] F. Alonso, P. Riente, M. Yus, *Eur. J. Org. Chem.* **2009**, 6034.
[272] M. Baranac-Stojanović, R. Marković, M. Stojanović *Tetrahedron* **2011**, *67,* 8000.
[273] A. Saha, S. Payra, S. Banerjee, *New J. Catal.* **2017**, *41*, 13377.
[274] E. Cho, A. Jayaraman, J. Lee, K. C. Ko, S. Lee, *Adv. Synth Catal.* **2019**, *361*, 1846.
[275] S.-S. Meng, L.-R. Lin, X. Luo, J.-J. Lv, J.-L. Zhao, A. S. C. Chan, *Green Chem.* **2019**, *21*, 6187.
[276] A. Y. Dubovtsev, N. V. Shcherbakov, D. V. Dar'in, V. Y. Kukushkin, *J. Org. Chem.* **2020**, *85*, 745.

[277] A. Ziarati, A. Badiei, G. M. Ziarani, H. Eskandarloo, *Catal. Commun.* **2017**, *95*, 77.
[278] M. Liu, J. Wang, X. Yuan, R. Jiang, N. Fu, *Synth. Commun.* **2017**, *47*, 2369.
[279] T. Stemmler, A. E. Surkus, M. M. Pohl, K. Junge, M. Beller, *ChemSusChem* **2014**, *7*, 3012.
[280] S. Saranya, R. Ramesh, J. G. Malecki, *Eur. J. Org. Chem.* **2017**, 6726.
[281] F. I. López, F. N. de la Cruz, J. López, J. M. Martínez, Y. Alcaraz, F. Delgado, A. Sánches-Recillas, S. Estrada-Soto, M. A. Vázquez, *Med. Chem. Res.* **2017**, *26*, 1325.
[282] U. Kuppuswamy, K. Krishnakumar, A. Bhat, *J. Pharm. Res.* **2012**, *5*, 3096.
[283] I. Solic, D. Reich, J. Lim, R. W. Bates, *Asian J. Org. Chem.* **2017**, *6*, 658.
[284] B. Bananezhad, M. R. Islami, *Synlett* **2017**, *28*, 1453.
[285] J. L. García Ruano, J. Alemán, I. Alonso, A. Parra, V. Marcos, J. Aguirre, *Chem. Eur. J.* **2007**, *13*, 6179.
[286] G. Chen, W. Gao, X. Wang, H. Huo, W. Li, L. Zhang, R. Li, Z. Li, *RSC Adv.* **2016**, *63*, 58805.
[287] F. Ji, J. Li, X. Li, W. Guo, W. Wu, H. Jiang, *J. Org. Chem.* **2018**, *83*, 104.
[288] Y. Fang, Z. Wang, Y. Li, Y. Quan, Y. Cheng, *Analyst* **2018**,*143*, 2405.
[289] M. L. Deb, C. D. Pegu, P. J. Borpatra, P. J. Saikia, P. K. Baruah, *Green Chem.* **2017**, *19*, 4036.
[290] P. Barta, I. Szatmári, F. Fülöp, M. Hexdenreich, A. Koch, E. Kleinpeter, *Tetrahedron* **2016**, *72*, 2402.
[291] S. D. Pardeshi, P. A. Sathe, K. S. Vadagaonkar, A. C. Chaskar, *Adv. Synth. Catal.* **2017**, *359*, 4217.
[292] C. J. Evoniuk, G. dos Passos Gomes, S. P. Hill, S. Fujita, K. Hanson, I. V. Alabugin, *J. Am. Chem. Soc.* **2017**, *139*, 16210.
[293] M. Wang, Q. Fan, X. Jiang, *Org. Lett.* **2018**, *20*, 216.
[294] Z. Yang, X. Guo, S. Xu, H. Jiao, Z. Tan, F. Zhang, *Heterocycles* **2017**, *94*, 122.
[295] P. J. Llabres-Campaner, R. Ballesteros-Garrido, R. Ballesteros, B. Abarca, *J. Org. Chem.* **2018**, *83*, 521.
[296] T. Jiang, N. Liu, Y.-W. Jiang, P.-P. Ye, W.-M. Xu, *Org. Prep. Proced. Int.* **2017**, *49*, 476.
[297] M. K. Sahoo, G. Jaiswal, J. Rana, E. Balaraman, *Chem. Eur. J.* **2017**, *23*, 14167.
[298] S. D. Durham, B. Sierra, M. J. Gomez, J. K. Tran, M. O. Anderson, N. A. Whittington-Davis, S. Eagon, *Tetrahedron Lett.* **2017**, *58*, 2747.
[299] M. J. D. Pires, D. L. Poeira, S. I. Purificacao, M. M. B. Marques, *Org. Lett* **2016**, *18*, 3250.
[300] L. Buzzetti, A. Prieto, S. R. Roy, P. Melchiorre, *Angew. Chem. Int. Ed.* **2017**, *56*, 15039.
[301] Y. Yan, H. Li, Z. Li, B. Niu, M. Shi, M. Liu, *J. Org. Chem.* **2017**, *82*, 8628.
[302] Z. Lu, Y.-Q. Yang, H.-X. Li, *Synthesis* **2016**, *48*, 4221.
[303] C. Wang, Z. Lu, *Org. Lett.* **2017**, *19*, 5888.

[304] J. Ma, Y. Wan, C. Hong, M. Li, X. Hu, W. Mo, B. Hu, N. Sun, L. Jin, Z. Shen, *Eur. J. Org. Chem.* **2017**, 3335.
[305] T. B. Nguyen, L. Ermolenko, A. Al-Mourabit, *Green Chem.* **2013**, *15*, 2713.

Affidavit

I hereby confirm that my thesis entitled *Transition Metal-Free Catalytic Systems for the Utilization of CO_2 to Achieve Valuable Chemicals* is the result of my own work I did not receive any help or support from commercial consultants. All sources and materials applied are listed and specified in the thesis.

Furthermore, I confirm that this thesis has not yet been submitted as part of another examination process neither in identical nor in similar form.

Göttingen, 07.10.2020